Using *Saccharomyces cerevisiae* to characterise the *in vivo* effects of exposure to the prion-curing drug Tacrine and the fungal metabolite gliotoxin

Jennifer O'Brien B.Sc.

A thesis submitted to the
National University of Ireland
for the degree of
Doctor of Philosophy
May 2012

Supervisor
Dr. Gary Jones
Department of Biology
National University of Ireland
Maynooth
Co. Kildare

Head of Department
Prof. Kay Ohlendieck
Department of Biology
National University of Ireland
Maynooth
Co. Kildare

Acknowledgements

Firstly, I would like to sincerely thank Dr. Gary Jones for giving me the opportunity to work in the Yeast Genetics lab and for his support, guidance and advice over the last three years. I would like to thank Professor Marc Blondel and Dr. Cecile Voisset for reagents and strains and Dr. David Fitzpatrick for help with bioinformatics analysis. Thanks to Grainne and the girls from Muscle Biology, Lisa and Edel who helped me with protein work and to Eoin for his patience when I bombarded him with qPCR questions.

I feel so lucky to have worked with great people during my PhD and to have made such good friends. Thanks to Ciara, Sarah and Emma for showing me the ropes, answering my constant questions and being such good craic, you girls made settling in so easy! Ste and Naushie, you two did a brilliant job taking over, really enjoyed working and drinking coffee with you, keep up the good work! I want to thank members of the Biotechnology and Medical Mycology labs for advice on experiments and laughs in the coffee room. A special thanks to Niamhio for being a great friend over the years, inside and outside college.

I would like to thank my three best friends Amanda, Fi and Ash for their constant encouragement even though they regularly didn't really have a clue what I was talking about. A massive thanks to my three parents and Dave for supporting me through this process, for being professionals at feigning interest and saying all the right things. I really appreciate everything you have done for me. Nuno, I could not have done this without you, thank you so much for being patient, supportive and encouraging and for being the first person there when I needed to moan or rant!

Declaration of Authorship

This thesis has not previously been submitted in part to this or any other university and is the sole work of the author.

_____

Jennifer O’Brien, B.Sc.

List of abbreviations

AB	Ammonium bicarbonate
ABD	ATPase-binding domain
ABPA	Allergic bronchopulmonary aspergillosis
ACh	Acetylcholine
AChR	Acetylcholine receptor
ACN	Acetonitrile
AdoMet	S-adenosyl-methionine
A. fumigatus	*Aspergillus fumigatus*
Amp	Ampicillin
6AP	6-aminophenanthridine
APP	Amyloid precursor proteins
APS	Ammonium persulfate
ARE	AP-1 recognition element
BSA	Bovine serum albumin
BSE	Bovine spongiform encephalopathy
[^{14}C]	Carbon-14
CJD	Creutzfeldt–Jakob disease
CWD	Chronic wasting disease
CuZnSOD	Copper- and zinc-containing SOD
dH_2O	Distilled water
Da	Dalton
DTT	Dithiothreitol
EB	Elution buffer
E. coli	*Escherichia coli*
EDTA	Ethylenediaminetetraacetic acid
eRF	Eukaryotic release factor
ETP	Epipolythiodioxopiperazine
FSE	Feline spongiform encephalopathy
FeSOD	Iron-containing SOD
GA	Guanabenz
GdnHCl	Guanidine Hydrochloride
GFP	Green fluorescent protein
Grx	Glutaredoxin
GSH	Reduced glutathione
GSS	Gerstmann–Straussler–Sheinker disease
GSSG	Oxidised glutathione
GT	Gliotoxin
HPLC	High-performance liquid chromatography
Hr	Hour(s)
HSP	Heatshock protein
H_2O	Water
H_2O_2	Hydrogen peroxide
IA	Invasive aspergillosis
IEF	Isoelectric focusing
kDA	Kilodalton
L	Litre
LB	Luria broth
LC-MS	Liquid Chromatography Mass Spectrometry
M	Molar
mA	Milliamps

Min	Minute(s)
ml	Millilitre
mM	Millimolar
MnSOD	Manganese-containing SOD
NEF	Nucleotide exchange factor
NiSOD	Nickel-containing SOD
NRPS	Nonribosomal peptide synthetase
OD	Optical density
OH	Hydroxyl radical
OS	Oxidative stress
O_2^-	Superoxide anion
PBD	Peptide-binding domain
PCR	Polymerase chain reaction
PEG	Polyethylene glycol
PMSF	Phenylmethylsulfonyl fluoride
PrD	Prion domain
PSB	Protein sample buffer
RFM	Ribosomal folding modulators
ROS	Reactive oxygen species
RPFA	Ribosome-borne protein folding activity
rpm	Repetitions per minute
RT	Room temperature
S. cerevisiae	*Saccharomyces cerevisiae*
SC	Synthetic complete
SDS-PAGE	Sodium Dodecyl Sulphate Polyacrylamide gel electrophoresis
Sec	Second(s)
SOD	Superoxide dismutase
TA	Tacrine
TBS	Tris buffered saline
TSE	Transmissible spongiform encephalopathy
Trx	Thioredoxin
TrxR	Thioredoxin reductase
YNB	Yeast nitrogen base
YPD	Yeast peptone dextrose
YPGAL	Yeast peptone galactose
V	Volts
v/v	volume/volume
w/v	weight/volume
µm	Micrometer
µl	Microlitre

List of figures

List of tables

Presentations

Oral presentations

As presenting author

Defining drug prion-curing mechanisms in *Saccharomyces cerevisiae*. Jennifer O'Brien, Gary W. Jones. NUIM departmental presentations. May, 2009.

Defining drug prion-curing mechanisms in *Saccharomyces cerevisiae*/Assessing the mode of action of gliotoxin and functional analysis of the *Aspergillus fumigatus GliT* gene using a yeast-based system. Jennifer O'Brien, Sean Doyle, Gary W. Jones. NUIM departmental presentations. June, 2010.

As contributing author

Analysis of inactivating stop codon mutations (ISCMs) in 40 *Saccharomyces cerevisiae* strains: implications for prion-associated phenotypes. David A. Fitzpatrick, Jennifer O'Brien, Ciara Moran, Naushaba Hasin, Elaine Kenny, Paul Cormican, Amy Gates, Derek W. Morris and Gary W. Jones. ICM9 The Biology of Fungi, Edinburgh, UK. August, 2010.

Poster presentations

As presenting author

Assessing the mode of action of gliotoxin and functional analysis of the *Aspergillus fumigatus GliT* gene using a yeast-based system. Jennifer O'Brien, Stephen Hammel, Markus Schrettl, Sean Doyle, Gary W. Jones. British Yeast Group Meeting, Oxford University, Oxfordshire, UK. March, 2010.

Assessing the mode of action of gliotoxin and functional analysis of the *Aspergillus fumigatus GliT* gene using a yeast-based system. Jennifer O'Brien, Stephen Hammel, Markus Schrettl, Sean Doyle, Gary W. Jones. Irish Fungal Society Meeting, University College Cork, Cork. June, 2010.

Using *Saccharomyces cerevisiae* to assess the *in vivo* cellular response to gliotoxin exposure. Jennifer O'Brien, Stephen Hammel, David A. Fitzpatrick, Sean Doyle, Gary W. Jones. British Yeast Group Meeting, Brighton, UK. March, 2011.

As contributing author

Assessment of inactivating stop codon mutations in 40 *Saccharomyces cerevisiae* strains: implication for [*PSI*$^{+}$] prion-mediated phenotypes. David A. Fitzpatrick, Jennifer O'Brien, Ciara Moran, Naushaba Hasin, Gary W. Jones. British Yeast Group Meeting, Brighton, UK. March, 2011.

Using *Saccharomyces cerevisiae* to assess the *in vivo* cellular response to gliotoxin exposure. Stephen Hammel, Jennifer O'Brien, David A. Fitzpatrick, Gary W. Jones. Irish Fungal Society Meeting, Trinity College Dublin, Dublin. June 2011.

Assessment of inactivating stop codon mutations in 40 *Saccharomyces cerevisiae* strains: implication for [*PSI*$^{+}$] prion-mediated phenotypes. David A. Fitzpatrick, Jennifer O'Brien, Ciara Moran, Naushaba Hasin, Gary W. Jones. Irish Fungal Society Meeting, Trinity College Dublin, Dublin. June 2011.

Publications

Self-protection against gliotoxin – a component of the gliotoxin biosynthetic cluster, *GliT*, completely protects *Aspergillus fumigatus* against exogenous gliotoxin. Schrettl M., Carberry S., Kavanagh K., Haas H., Jones G.W., O'Brien J., Nolan A., Stephens J., Fenelon O., Doyle S. *PLoS Pathogens*, 2010, 6, e1000952.

Assessment of inactivating stop codon mutations in 40 *Saccharomyces cerevisiae* strains: implications for [*PSI*$^{+}$] prion-mediated phenotypes. Fitzpatrick D.A., O'Brien J., Moran C., Hasin N., Kenny, E., Cormican, P., Gates, A., Morris D.W., Jones G.W. In *PLoS One* press.

Summary

Gliotoxin is a toxic fungal metabolite that is produced by *Aspergillus fumigatus*, amongst other species. Gliotoxin contains a disulfide bridge that has been significantly implicated in its toxicity. Research has demonstrated that gliotoxin displays immunomodulating capacity and anti-viral activity, and induces apoptosis and necrosis. The *gli* gene cluster responsible for gliotoxin biosynthesis has recently been identified and is continually being further characterised. In this study, evidence is provided that strongly suggests gliotoxin exposure causes conditions of oxidative stress in yeast cells. Additionally, the *GliT* gene, which is part of the said gliotoxin biosynthesis cluster, is shown to confer resistance to gliotoxin in *Saccharomyces cerevisiae*.

Prions are infectious proteins that are known to be responsible for a number of neurodegenerative disorders in mammals, such as Creutzfeldt-Jakob Disease (CJD) and Bovine Spongiform Encephalopathy (BSE). Fungal prions also exist, which provide a useful tool for studying the propagation of these non-mendelian genetic elements. Possibly the most widely-studied *S. cerevisiae* prion is [PSI^+], which is the prion form of Sup35p, a protein that functions in translation termination. In this study, the effects of three prion-curing agents, Tacrine, 6-aminophenanthridine and Guanabenz on [PSI^+] have been studied. The ability of all three drugs to cure [PSI^+] has been demonstrated. From investigating the Tacrine mode of action, it appears that this drug may inhibit Hsp104p, a chaperone that is involved in prion propagation. Differences in the mode of action of Tacrine, compared to 6-aminophenanthridine and Guanabenz have also been highlighted. Additional results suggest that Ltv1p and Yar1p, which contribute to ribosome stability, are important for regular recovery from heatshock, thus potentially implicating them in prion propagation.

Chapter 1 Introduction

Part 1

Part 2

Chapter 2 Materials and methods

Chapter 3 Using *Saccharomyces cerevisiae* as a model organism to investigate the eukaryotic response to the toxic fungal metabolite gliotoxin

Chapter 1 Introduction

Part 1 Using *Saccharomyces cerevisiae* as a model organism to investigate the eukaryotic response to the toxic fungal metabolite gliotoxin

1.1 *Aspergillus fumigatus*, a pathogenic fungus

Aspergillus fumigatus, one of the six *Aspergillus* subgenera, is a ubiquitous, saprophytic fungus described in 1863 by Fresenius following isolation from avian lungs (Pitt, 1994). *Aspergillus* species naturally occur in soil and organic matter undergoing decomposition and their ability to form spores allows for widespread contamination (Hinson *et al.*, 1952). The number of airborne spores has been reported to be more elevated in winter, with increase in water presence from rainfall and decay of plant vegetation being principal causes suggested for this (Mullins *et al.*, 1976).

The fact that *A. fumigatus* spores are just 2.5-3 µm in diameter allows easy access to mammalian hosts via inhalation followed by accumulation due to a high level of spore thermotolerance (Bateman, 1994). Colonisation by this fungus can give rise to a number of different types of host infections (figure 1.1), usually depending on host predisposition. Pulmonary migration leading to allergic bronchopulmonary aspergillosis (ABPA) has been mainly found to occur in those suffering from pulmonary diseases such as cystic fibrosis and prolonged asthma (Bardana *et al.*, 1975, Louridas, 1976, Laufer *et al.*, 1984, Soubani and Chandrasekar, 2002). Aspergillomas, fungal masses composed of mycelia and mucous, were first described by Deve (1938) and are also characteristic of *Aspergillus* infection. These assemblages form in pre-existing pulmonary cavities that are often remnant of tuberculosis infection, sarcoidosis and severe pneumonia (Hinson *et al.*, 1952, Tomlinson and Sahn, 1987). Invasive aspergillosis (IA) has been found to affect the immunocompromised, including those infected with HIV, cancer patients and people who have undergone transplant surgery (Meunier-Carpentier, 1983, Weiland *et al.*, 1983, Trull *et al.*, 1985, Marisavljević *et al.*,

1989, Rodríguez-Arrondo *et al.*, 1991). IA usually occurs following *A. fumigatus* entry though the respiratory tract, damaged skin, operative wounds, the ear or the cornea (Denning, 1998). This is the most deadly form of colonisation and if left untreated can result in a mortality rate of almost 100% (Denning, 1996).

A. fumigatus has the capacity to form biofilm on bronchial epithelial cells and this form of growth displays increased resistance to drug treatment (Seidler *et al.*, 2008, Beauvais and Müller, 2009, Müller *et al.*, 2011).

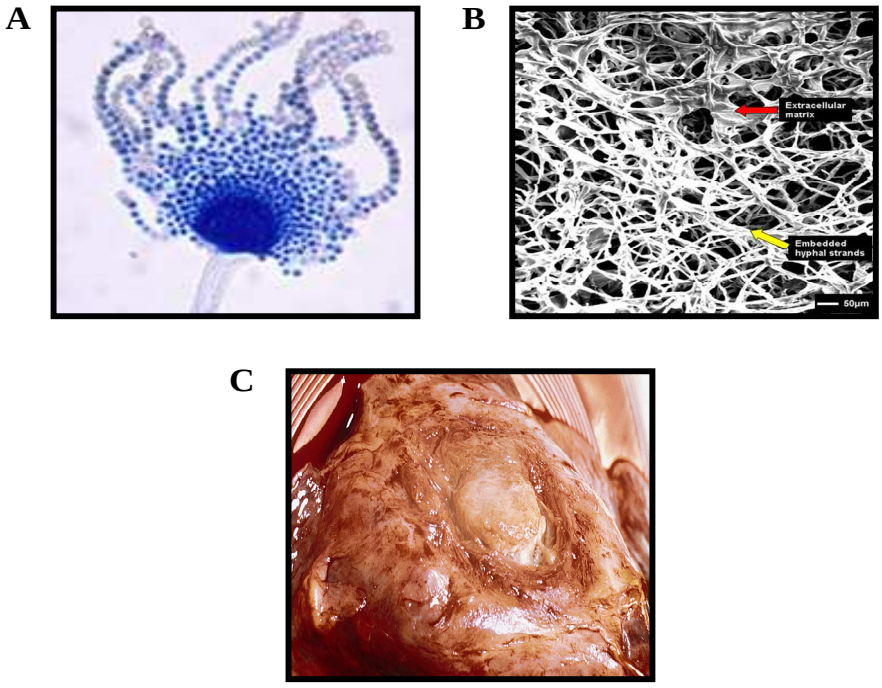

Figure 1.1 A = Image of *A. fumigatus*. B = *A. fumigatus* biofilm on bronchial epithelial cells. C = Aspergilloma in lung of child suffering from leukaemia.
Images from www.aspergillus.org.uk.

A range of secondary metabolites are produced by *A. fumigatus* that are contributory factors to fungal pathogenicity, such as restrictocin, verruculogen, fumagillin, helvolic acid, ergot alkaloids, fumitremorgin and importantly, gliotoxin (Dagenais and Keller, 2009). It is thought that mycotoxins such as these are produced to

assist the fungus in evading the host immune system and facilitating colonisation (Latgé, 1999).

1.2 Gliotoxin

1.2.1 Structure and description

Gliotoxin (figure 1.2) is a 326 Da fungal metabolite produced by *A. fumigatus*, in addition to certain strains of *Trichoderma* and *Gliocladium* and a number of *Penicillium* and *Candida* species (Weindling and Emerson, 1936, Shah and Larsen, 1991, Richard *et al.*, 1994, Kamei and Watanabe, 2005). This highly toxic epipolythiodioxopiperazine (ETP) contains a redox-sensitive disulfide bridge, characteristic of this group of toxins, which is implicated in *A. fumigatus* virulence (Trown and Bilello, 1972, Müllbacher *et al.*, 1986). Diketopiperazines are the smallest cyclic peptides documented, containing a heterocyclic system, and gliotoxin falls into this group (Martins and Carvalho, 2007, Gross *et al.*, 2010). The core ETP moiety amino acids of this toxin are phenylalanine and serine (Suhadolnik and Chenowith, 1958, Winstead and Suhadolnik, 1960, Gardiner *et al.*, 2005).

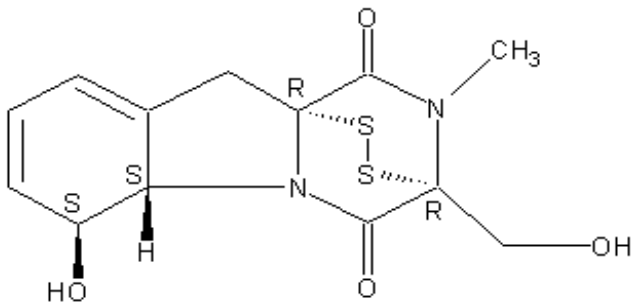

Figure 1.2 Structure of gliotoxin. Image from www.aspergillus.org.uk.

This nonribosomal peptide is just one of at least fourteen ETPs documented to date (Gardiner *et al.*, 2005). Gliotoxin can occur in the oxidised (natural) form, depicted in figure 1.2, or in the reduced (dithiol) form if the disulfide bridge has undergone

reduction by a suitable reducing agent such as glutathione, as discussed later (Trown and Bilello, 1972, Eichner *et al.*, 1988).

1.2.2 Production

In addition to *A. fumigatus*, the species *A. niger*, *A. terrus* and *A. flavus* have been reported to produce gliotoxin, although not all *Aspergillus* species appear to. Of these species *A. fumigatus* was documented as the isolate that consistently produced the highest level of the toxin (Lewis *et al.*, 2005, Kupfahl *et al.*, 2008). Gliotoxin appears to be heavily involved in *A. fumigatus* cytotoxicity due to its high production level, however, in the other strains mentioned above, the low level of the toxin generated is thought to be inadequate to influence cytotoxic effects of the strains (Kupfahl *et al.*, 2008).

During biofilm formation, there is a strong increase in the expression of gliotoxin by *A. fumigatus*, while there is a reduction in the level of metabolic activity (Bruns *et al.*, 2010). A twelve-gene cluster (*gli* cluster) has been identified as being responsible for gliotoxin production in *A. fumigatus*, and has similarity to that culpable for the generation of another ETP, sirodesmin, in *Leptosphaeria maculans* (Gardiner *et al.*, 2004, Gardiner and Howlett, 2005). This cluster, illustrated in figure 1.3, has been predicted to produce a zinc finger transcription factor encoded by *gliZ*, an aminocyclopropane carboxylic acid synthase encoded by *gliI*, a dipeptidase encoded by *gliJ*, a peptide synthetase encoded by *gliP*, two cytochrome P450 monooxygenases encoded by *gliC* and *gliF*, an O-methyl transferase encoded by *gliM*, a glutathione S-transferase encoded by *gliG*, a hypothetical protein encoded by *gliK*, a transporter protein encoded by *gliA*, a methyl transferase encoded by *gliN* and a thioredoxin reductase encoded by *gliT*. Interestingly, gliotoxin presence has been shown to induce

upregulation of genes belonging to this cluster (Cramer *et al.*, 2006, Schrettl *et al.*, 2010).

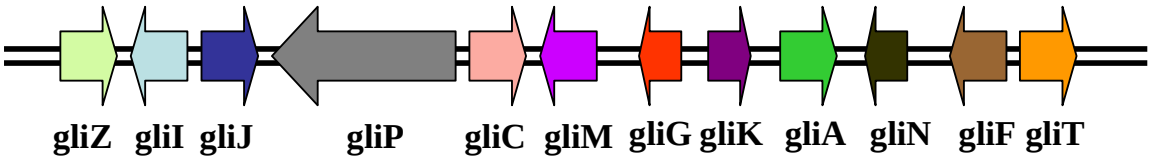

Figure 1.3 12-gene gliotoxin biosynthetic cluster, *gli* cluster. Image reproduced from Gardiner and Howlett (2005).

There is still much to be elucidated on the subject of gliotoxin biosynthesis and release. For gliotoxin to be synthesised in *A. fumigatus*, GliZp must be present, which is responsible for the transcriptional expression of other genes in the *gli* cluster (Bok *et al.*, 2006). GliPp has been determined to be a nonribosomal peptide synthetase (NRPS) involved in the formation of the gliotoxin diketopiperazine scaffold (Balibar and Walsh, 2006, Cramer *et al.*, 2006). A shunt metabolite has been identified by Davis *et al.* (2011) that accumulates in the absence of GliGp and lacks sulfur atoms necessary for disulfide bridge formation. It has been suggested that the glutathione S-transferase GliGp is involved in the addition of sulfur to the precursor of this shunt metabolite, that can subsequently be transformed into gliotoxin (Davis *et al.*, 2011). Disruption of either GliGp or GliPp renders *A. fumigatus* unable to produce gliotoxin (Cramer *et al.*, 2006, Kupfahl *et al.*, 2006, Davis *et al.*, 2011). Schrettl *et al.* (2010) predict that prior to efflux, gliotoxin may undergo importation into intracellular vesicles for storage.

Is has been proposed that another protein, LaeAp, plays an important role in secondary metabolism regulation in *Aspergillus* species, impacting on the ability of the fungus to colonise the host (Bok and Keller, 2004). *A. fumigatus* Δ*laeA* exhibits impaired virulence affiliated with loss of gliotoxin production (Bok *et al.*, 2005).

1.2.3 General effects of gliotoxin

There are two principal ways in which gliotoxin has been shown to cause deleterious effects in the cell. Firstly, the functionally indispensible disulfide bridge can conjugate to proteins that have susceptible thiol residues, leading to protein inactivation e.g. the transcription factor NF-kB which plays a key role in immune response (Pahl *et al.*, 1996, Gardiner *et al.*, 2005). Secondly, upon cellular uptake of gliotoxin, redox cycling can occur, whereby in the presence of a suitable reducing agent the disulfide form of the toxin can be processed into the dithiol form. This can then undergo re-oxidation with the return of the disulfide form (Eichner *et al.*, 1988). One of the main initiators of this redox cycling is glutathione and characteristic of this process is the production of hydrogen peroxide and superoxide (Waring and Beaver, 1996), as illustrated in figure 1.4. Oxidative stress and the generation of reactive oxygen species in the presence of gliotoxin is discussed further in section 1.4.

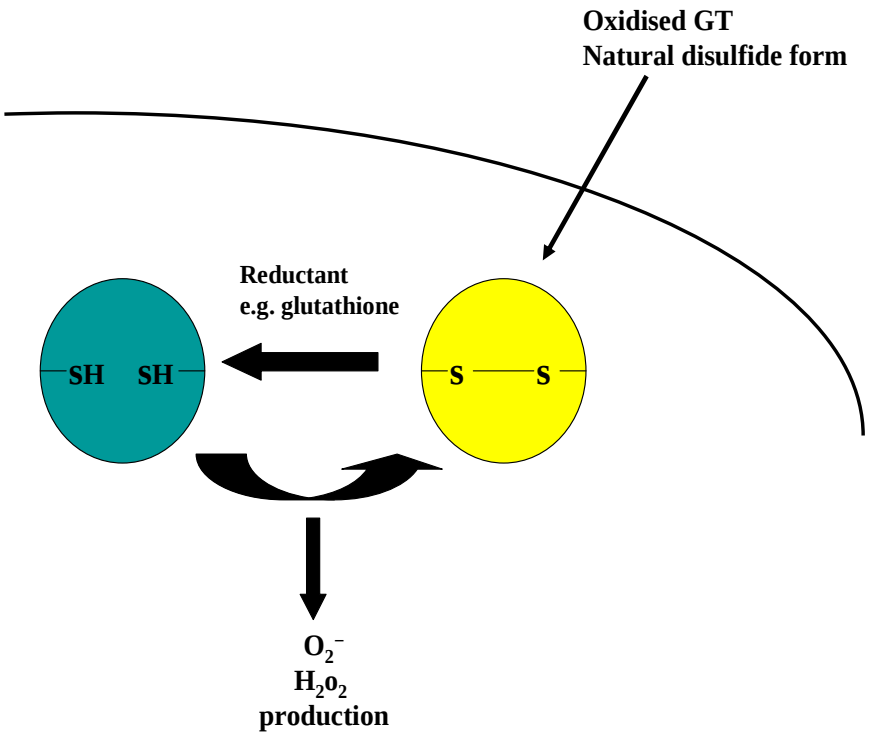

Figure 1.4 Redox cycling of GT within the cell induces ROS production and oxidative stress.

The toxicity of gliotoxin is appears to be heavily influenced by the concentration of glutathione. Within SH-SY5Y cells, glutathione presence heightens the cytotoxicity of gliotoxin (Axelsson *et al.*, 2006).

Interestingly, gliotoxin has been found at nanomolar concentrations to exhibit anti-oxidant and anti-angiogenic activity itself. The metabolite can mimic peroxiredoxin function of the thioredoxin redox system whereby it reduces H_2O_2 to H_2O by accepting electrons from NADPH (Choi *et al.*, 2007). It has since been suggested that gliotoxin is an 'accidental toxin' and that it was originally synthesised to protect *A. fumigatus* against oxidative stress, such as is caused by H_2O_2 (Schrettl *et al.*, 2010).

1.2.4 The effects of gliotoxin on the immune response

Gliotoxin was first shown three decades ago to have immunosuppressive activity, which can aid in host colonisation. This metabolite induces apoptotic cell death in macrophages (Waring *et al.*, 1988, Waring, 1990) and represses macrophage function, such as phagocytosis, adherence, bactericidal activity and induction of alloreactive cytotoxic T cells (Müllbacher and Eichner, 1984, Eichner *et al.*, 1986). Gliotoxin can target and kill antigen-presenting cells such as monocytes and dendritic cells, thus repressing antigen-presentation and appears to actively inhibit T-cell response (Stanzani *et al.*, 2005). NF-kB activation is abrogated in various cell lines under exposure to the toxin, preventing the regulation of inflammatory cytokines, growth factors and receptors and adhesion molecules (Pahl *et al.*, 1996). It has been reported that gliotoxin hinders the ability of polymorphonuclear neutrophils to generate reactive oxygen species and carry out phagocytosis (Orciuolo *et al.*, 2007) and also inhibits Langerhans' cell function and cutanaeous foreign antigen response (McMinn *et al.*, 1990).

Although gliotoxin principally obstructs the host immune response through immunosuppression to prevent fungal eradication, the toxin has also been shown

to induce inflammation. The presence of a low concentration of gliotoxin has been reported to instigate a decrease in host expression of the anti-inflammatory cytokine IL-10 and an increase in production of the pro-inflammatory cytokine TNF-α (Johannessen *et al.*, 2005).

1.2.5 Gliotoxin anti-viral activity

Many researchers have demonstrated gliotoxin toxicity against various bacteria and fungi (McDougall, 1969, Aljofan *et al.*, 2009) but it has long been known that gliotoxin also has anti-viral activity, which is attributed to specific inhibition of viral RNA replication (Rightsel *et al.*, 1964, Larin *et al.*, 1965, Miller *et al.*, 1968). Some of the viruses found to be negatively affected by this toxin are polio virus, herpes simplex virus, influenza virus, coxsackie virus, Sendai virus, Newcastle disease virus and measles virus (Rightsel *et al.*, 1964, Larin *et al.*, 1965, McDougall, 1969, Aljofan *et al.*, 2009). It has been demonstrated that reduction of the toxin or removal of the sulphur atoms renders gliotoxin unable to inhibit viral RNA synthesis like its natural disulfide counterpart (Trown and Bilello, 1972, Rodriguez and Carrasco, 1992).

1.2.6 Gliotoxin-induced apoptosis and necrosis

Beaver and Waring (1994) demonstrated that concentrations of gliotoxin above 10 µM favour induction of thymocyte cell death by necrosis, rather than apoptosis, which is seen during exposure to relatively lower concentrations. It has since been demonstrated that this applies to other cell lines, with hepatic, epithelial, fibroblast and macrophage cells undergoing apoptosis or necrosis in the presence of low or high toxin concentrations respectively (Kweon *et al.*, 2003, DeWitte-Orr and Bols, 2005). Reports have also described how the mode of cell death also may be dependent on the cell type,

as it was observed that gliotoxin preferentially kills fibroblasts and epithelial cells via necrosis and macrophages via apoptosis (DeWitte-Orr and Bols, 2005).

1.3 GliTp

GliTp is a FAD-dependent 36 kDa protein that is encoded by a gene that is part of the *gli* cluster, described above (Gardiner and Howlett, 2005, Scharf *et al.*, 2010, Schrettl *et al.*, 2010). Loss of *GliT* in *A. fumigatus* results in a severe increase in sensitivity to gliotoxin, demonstrating the importance of GliTp in protection against this endogenous toxin (Scharf *et al.*, 2010, Schrettl *et al.*, 2010). The introduction of *GliT* into the non-gliotoxin producing species *Saccharomyces cerevisiae* and *Aspergillus nidulans* conferred resistance to exogenous gliotoxin application (Schrettl *et al.*, 2010). From work with *A. fumigatus*, it appears that GliTp is involved in preventing the depletion of reduced glutathione in the presence of gliotoxin, as glutathione supplementation restored wild-type phenotype in the Δ*gliT* strain (Schrettl *et al.*, 2010). Importantly, another consequence of GliTp absence is the lack of *A. fumigatus* ability to produce gliotoxin (Schrettl *et al.*, 2010). Research has demonstrated that GliTp displays gliotoxin reductase activity and it has been suggested that direct gliotoxin reduction occurs prior to secretion from *A. fumigatus* (Schrettl *et al.*, 2010).

It seems that *GliT* is differentially expressed relative to the other *gli* cluster genes as *GliT* expression is induced by gliotoxin, even in the absence of *GliZ*, encoding the transcriptional regulator of the *gli* cluster. Also, it has been previously shown that loss of GliZp abolishes expression of *gli* cluster genes, except for *GliT* (Bok *et al.*, 2006, Schrettl *et al.*, 2010).

1.4 Oxidative stress

1.4.1 Description

Growth of organisms in oxygen-containing environments results in the generation of reactive oxygen species (ROS) such as the superoxide anion (O_2^-), hydroxyl radical ($OH^\bullet$) and hydrogen peroxide (H_2O_2), which are formed inadvertently when molecular oxygen is reduced during oxidative phosphorylation (Lushchak, 2011). $OH^\bullet$ is more reactive than H_2O_2, which in turn is more reactive than O_2^- (Lushchak, 2011). O_2^- can cause enzyme inactivation through oxidising functional iron clusters and induces aromatic and sulfur-containing amino acid auxotrophy (Flint *et al.*, 1993, Imlay, 2003). H_2O_2 can oxidise sulfur atoms, thereby affecting sulfur-containing amino acids such as cysteine and methionine, while $OH^\bullet$ can oxidise the majority of organic molecules and generate protein and lipid radicals (Slump and Schreuder, 1973, Powell, 2000, Imlay, 2003).

Overall, ROS have been shown to display non-specific mutagenic, protein modification/damage and lipid peroxidation capacities (Farr *et al.*, 1986, Halliwell, 1991, Costa *et al.*, 2007). Consistent damage by ROS, accompanied by cellular inability to successfully control the causative agents is termed oxidative stress (OS) (Halliwell, 1994).

1.4.2 Causative agents

Various compounds, such as metals, have the capacity to impose increased cellular OS. The presence of metal ions facilitates the oxidative modification of proteins by ROS, which is followed by selective degradation by proteases (Stadtman, 1990). Iron can reduce oxygen to O_2^- and catalyse peroxide decomposition resulting in the production of $OH^\bullet$ (Fraga and Oteiza, 2002). Thus, an organisms ability to regulate the separation of iron and molecular oxygen is crucial (Valko *et al.*, 2005). Copper can also

catalyse the generation of $OH^{\bullet}$ and, like iron, can cause DNA damage through strand breaks (Kawanishi *et al.*, 1989, Kadiiska *et al.*, 1993). Cadmium has also been implicated in causing significant levels of cellular OS. The detrimental effects of this heavy metal are mediated by ROS and result in the obstruction of oxidative DNA damage repair (Filipic and Hei, 2004). The ability of lead to induce OS has been well documented and Ercal *et al.* (2001) evaluated the possible mechanisms employed for stress imposition; the effect of the metal on cell membranes, its interaction with haemoglobin, its inhibition of heme synthesis regulation and ROS generation and the metal's effect on cellular antioxidant defence.

There are also non-metal catalysts that exhibit OS-causing capabilities, such as quinones and paraquat. Quinones undergo redox cycling whereby they are reduced by cellular reductases and then reoxidised, and this process is accompanied by the generation of by-products O_2^- and H_2O_2 (Brunmark and Cadenas, 1989). Cellular exposure to paraquat augments the generation of ROS and induces mitochondrial dysfunction (McCarthy *et al.*, 2004).

1.5 *S. cerevisiae* oxidative stress response

Due to the damage that can be caused by OS, organisms continually work to protect cells and maintain redox state, and yeast are no different employing both enzymatic and non-enzymatic processes to do so (Jamieson, 1998). Common yeast responses and individual pathways are discussed below in more detail.

1.5.1 Glutathione

Glutathione (L-γ-glutamyl-L-cysteinylglycine/GSH) is possibly one of the most important molecules produced in response to OS. This tripeptide is a free radical scavenger and reduces oxidising species to prevent them causing damage to cellular

constituents. Upon reaction, peroxide detoxification leads to the formation of GSSG, the oxidised or disulfide form of GSH (Pompella *et al.*, 2003). The GSH sulfhydral or free thiol group is thus functionally essential and its ability to confer stability to the thiol has been recorded (Meister, 1988). Under normal circumstances, less than 1% of the total cellular glutathione content is in the form of GSSG and therefore, measurement of the GSH:GSSG ratio has been used for decades as an indication of the level of OS imposed on cells (Güntherberg and Rost, 1966, Lauterburg *et al.*, 1984). The enzymatic function of NADPH-dependent glutathione reductase is critical for the regeneration of GSH from GSSG, to maintain cellular antioxidant capacity (Meldrum and Tarr, 1935, Conn and Vennesland, 1951). Glutathione reductase is encoded by *GLR1* in *S. cerevisiae* (Grant *et al.*, 1996). In 1951, Mills reported that there is a factor that works in union with GSH to abrogate haemoglobin oxidative breakdown. This factor exhibited peroxidase activity and employed GSH as hydrogen donor (Mills, 1957). The evaluation of glutathione peroxidases has since resulted in the conclusion that these enzymes have cellular protective abilites and prevent membrane and protein oxidation by reducing ROS. This process involves the exploitation of GSH as a cofactor and its oxidation to GSSG (Meister, 1988). Yeast can synthesise three glutathione peroxidases, which are encoded by *GPX1*, *GPX2* and *GPX3* (Inoue *et al.*, 1999). GSH can also form mixed disulfides with cellular protein thiols, a process termed S-glutathionylation, protecting vulnerable proteins from oxidation and irreversible damage (Herrero *et al.*, 2008).

1.5.1.1 Glutathione biosynthesis

The pathway that leads to the production of this important thiol has been well documented to date. Glutathione biosynthesis is dependent on the precursor amino acids glutamate, glycine and cysteine, the latter being a product of the superpathway of sulfur amino acid biosynthesis (Penninckx, 2002).

The sulfur amino acid biosynthesis pathway commences with sulfate assimilation and involves subsequent reduction to sulfide involving the formation of a number of intermediates. This process is regulated in *S. cerevisiae* by proteins encoded by *MET3* (Cherest *et al.*, 1985, Cherest *et al.*, 1987), *MET14* (Masselot and De Robichon-Szulmajster, 1975, Korch *et al.*, 1991), *MET16* (Thomas *et al.*, 1990), *MET5* (Mountain *et al.*, 1991), and *MET10* (Hansen *et al.*, 1994). Sulfide is then implicated in the generation of homocysteine, which is required for methionine and cysteine production. Homoserine, produced from aspartate, is activated through esterification resulting in the generation of O-acetylhomoserine which is then sulfhydralased and sulfide is incorporated into the carbon chain, giving rise to homocysteine (Thomas and Surdin-Kerjan, 1997). This process whereby homoserine and subsequently homocysteine are formed is catalysed by enzymes encoded by *HOM3* (Rafalski and Falco, 1988), *HOM2* (Thomas and Surdin-Kerjan, 1989), *HOM6* (Yumoto *et al.*, 1991, Arévalo-Rodríguez *et al.*, 2004), *MET2* (Masselot and De Robichon-Szulmajster, 1975, Baroni *et al.*, 1986) and *MET17* (Yamagata *et al.*, 1975, D'Andrea *et al.*, 1987, Brzywczy and Paszewski, 1993).

Homocysteine can be metabolised to create methionine, or can act as a key protein in the transsulfuration pathway (Finkelstein, 1998). Biosynthesis of the folate polyglutamate 5-methyltetrahydrofolate is catalysed by *MET7* and prerequisite to methionine biosynthesis (Boyer *et al.*, 1996, Cherest *et al.*, 2000, DeSouza *et al.*, 2000). The *MET6* gene product, methionine synthase, then catalyses the transfer of a methyl group to homocysteine, yielding methionine (Csaikl and Csaikl, 1986, González *et al.*, 1992, Suliman *et al.*, 2005). S-adenosyl-methionine (AdoMet) can be generated from methionine by two synthetases encoded by *SAM1* and *SAM2* (Chiang and Cantoni, 1977, Cherest and Surdin-Kerjan, 1978, Thomas and Surdin-Kerjan, 1991). Both methionine and AdoMet can then negatively regulate enzymes involved in sulfur assimilation and

sulfur amino acid biosynthesis (Cherest *et al.*, 1969). Homocysteine retains a vital function in cysteine biosynthesis, in addition to methionine production. The transsulfuration pathway in *S. cerevisiae* involves the interconversion of homocysteine and cysteine with the generation of the intermediary, cystathionine (Cherest *et al.*, 1993). Cystathionine β-synthase, encoded by *CYS4*, converts homocysteine to cystathionine, which can then be modified to generate cysteine by cystathionine γ-lyase, encoded by *CYS3* (Ono *et al.*, 1988, Cherest and Surdin-Kerjan, 1992, Ono *et al.*, 1992, Ono *et al.*, 1994). The opposing side of the transsulfuration pathway sees the generation of cystathionine from cysteine, catalysed by cystathionine γ-synthase, encoded by *STR2* and the subsequent regeneration of homocysteine by cystathionine β-lyase, encoded by *STR3* (Cherest *et al.*, 1993, Hansen and Johannesen, 2000).

Cysteine and glutamate have the potential to combine to form L-γ-glutamylcysteine, under the catalytic function of the synthetase encoded by *GSH1*, the first step of glutathione biosynthesis (Ohtake and Yabuuchi, 1991, Wu and Moye-Rowley, 1994). Thus, the rate-limiting step of cysteine biosynthesis is in itself required for protection against oxidative damage (Williamson *et al.*, 1982). Glutathione synthetase encoded by *GSH2* mediates the formation of glutathione from L-γ-glutamylcysteine and glycine (Grant *et al.*, 1997, Inoue *et al.*, 1998), facilitating the yeast stress response, as described above.

1.5.2 The thioredoxin system

Thioredoxin is a small protein that can exist in either a reduced or oxidised form, due to a redox active disulfide bridge (Söderberg *et al.*, 1978, Holmgren, 1985). In combination with thioredoxin reductase (TrxR) and NADPH, thioredoxin (Trx) makes up the thioredoxin system, which can act as a hydrogen donor for ribonucleotide reductase (Laurent *et al.*, 1964, Berglund *et al.*, 1969). Yeast thioredoxin is in fact

involved in sulfate assimilation and thus sulfur amino acid biosynthesis (Gonzalez Porqué *et al.*, 1970). TrxR reduces Trx, maintaining it in the sulfhydral state, using NADPH. Trx can then reduce other protein disulfides, including GSSG (Nordberg and Arnér, 2001). Trx also functions in the reduction of Trx peroxidase (peroxiredoxin). Donating electons to Trx peroxidase enables the enzyme to directly reduce peroxides, such as H_2O_2 (Chae *et al.*, 1994, Kang *et al.*, 1998).

Three *S. cerevisiae* genes encode thioredoxin, *TRX1*, *TRX2* (both cytoplasmic thioredoxins) and *TRX3* (a mitochondrial thioredoxin) (Muller, 1991, Muller, 1992, Pedrajas *et al.*, 1999). *TRR1* encodes a yeast cytoplasmic TrxR, which when absent results in hypersensitivity to OS (Chae *et al.*, 1994, Machado *et al.*, 1997). The Trr1p, Trx1p, Trx2p defence system is important not only in protecting against OS but also against reductive stress (Trotter and Grant, 2002). *S. cerevisiae* encodes an additional TrxR, *TRR2*, which makes up the mitochondrial thioredoxin system in combination with *TRX3*. This system plays a role in preservation against respiratory metabolism-generated OS (Pedrajas *et al.*, 1999).

1.5.3 The glutaredoxin system

The glutaredoxin system comprises GSH, glutaredoxin (Grx), NADPH and the already discussed glutathione reductase (Holmgren, 1979). Like thioredoxins, glutaredoxins are heat-stable oxidoreductases and play a glutathione-dependent role in delivering electrons to ribonucleotide reductase (Holmgren, 1976). As stated before, proteins containing cysteine residues are particularly vulnerable to modification during OS. As an OS protection mechanism, Grx can induce reversible glutathionylation through catalysing mixed disulfide formation between GSH and susceptible protein thiols (Yoshitake *et al.*, 1994, Ruoppolo *et al.*, 1997, Shelton *et al.*, 2005). During OS in mammalian cell lines, Grx interaction with the Ask1p can be disrupted, activating

signalling pathways that lead to cell death, demonstrating the role of Grx in redox-sensing in addition to cellular protection (Song *et al.*, 2002). Two genes encoding dithiol glutaredoxin were initially found to be present in *S. cerevisiae*, *GRX1* and *GRX2*, and were reported to be important in protection against OS. The gene with a more prominent role in resisting this stress appears to be *GRX2* (Gan *et al.*, 1990, Luikenhuis *et al.*, 1998). Following this, a further five genes were identified as monocysteinic glutaredoxins, *GRX3*, *GRX4*, *GRX5*, *GRX6* and *GRX7* (Rodríguez-Manzaneque *et al.*, 1999, Pujol-Carrion *et al.*, 2006, Izquierdo *et al.*, 2008, Mesecke *et al.*, 2008, Pujol-Carrion and de la Torre-Ruiz, 2010). An eighth yeast glutaredoxin gene, *GRX8* encoding a third dithiol, has since been documented although it does not appear to protect against OS (Mesecke *et al.*, 2008, Eckers *et al.*, 2009).

1.5.4 Superoxide dismutase

Superoxide dismutases are a group of enzymes that have the capacity to dismutate O_2^- yielding O_2 and H_2O_2 (McCord and Fridovich, 1968, McCord and Fridovich, 1969b). Across eukaryotic and prokaryotic species, four main classes of superoxide dismutase (SOD) have been recorded to date, with differing cofactors. These are manganese-containing SOD (MnSOD), iron-containing SOD (FeSOD), copper- and zinc-containing SOD (CuZnSOD) and nickel-containing SOD (NiSOD) (McCord and Fridovich, 1969a, Carrico and Deutsch, 1970, Keele *et al.*, 1970, Yost and Fridovich, 1973, Youn *et al.*, 1996). *S. cerevisiae* has two SOD genes, *SOD1* and *SOD2* which encode a cytosolic CuZnSOD and a mitochondrial MnSOD respectively (Ravindranath and Fridovich, 1975, van Loon *et al.*, 1986, Bermingham-McDonogh *et al.*, 1988, Chang *et al.*, 1991, Liu *et al.*, 1992).

1.5.5 Catalase

Catalase was described by Loew (1900) as an enzyme which yielded a high level of oxygen under reaction with H_2O_2, and was thus named. The decomposition of H_2O_2 to O_2 and H_2O by catalase has been well documented to date and reaction is broken down into stages, dependent on the type of enzyme (Chelikani *et al.*, 2004). When cells find themselves under conditions of OS, H_2O_2 produced by both redox cycling and the reduction of O_2^- requires detoxification, illustrating the important role of catalase in protection against OS (Roos *et al.*, 1980, Kappus, 1987).

The *S. cerevisiae* genome contains two catalase genes, *CTA1* encoding the yeast peroxisomal catalase A and *CTT1* which encodes the yeast cytoplasmic catalase T (Seah *et al.*, 1973, Susani *et al.*, 1976, Spevak *et al.*, 1983, Cohen *et al.*, 1985, Hartig and Ruis, 1986, Cohen *et al.*, 1988). The functions of Cta1p and Ctt1p in surviving exposure to H_2O_2 overlap to some degree with GSH, as it has been demonstrated that the presence of these proteins is required to a) prevent the formation of excess GSSG and b) provide important resistance against H_2O_2 in Δ*glr1* and Δ*gsh1* (Grant *et al.*, 1998). Peroxisomal proteins and fatty acids have been shown to induce Cta1p production (Veenhuis *et al.*, 1987, Skoneczny *et al.*, 1988), which interestingly, can also scavenge mitochondrial-derived H_2O_2 and undergo mitochondrial importation (Petrova *et al.*, 2004). *CTT1* expression on the other hand is positively regulated by OS, osmotic stress, heat stress, nutrient starvation and heme (Spevak *et al.*, 1986, Bissinger *et al.*, 1989, Belazzi *et al.*, 1991, Schüller *et al.*, 1994).

1.5.6 Yap1p-regulated transcription

Yap1p is a transcription factor involved in the regulation of a number of genes that are significantly implicated in *S. cerevisiae* OS defence. Yap1p or yeast AP-1 is so called due to the fact that it binds to the mammalian AP-1 recognition element (ARE),

and is in fact a homologue of the mammalian protein (Harshman *et al.*, 1988, Moye-Rowley *et al.*, 1988). AP-1 proteins have the ability to regulate the cell cycle and thus mediate cell proliferation and death (Shaulian and Karin, 2001). The yeast Δ*yap1* mutant exhibits increased sensitivity to H_2O_2 (Schnell *et al.*, 1992). In yeast, Yap1p has been shown to regulate the expression of *GSH1* and *GLR1* (Wu and Moye-Rowley, 1994, Grant *et al.*, 1996). It is also known that Yap1p interacts with another transcription factor Skn7p to control *TRX2* and *TRR1* (Kuge and Jones, 1994, Morgan *et al.*, 1997). Yap1p-mediated upregulation of gene assemblages is induced by OS (Hirata *et al.*, 1994, Kuge and Jones, 1994, Kuge *et al.*, 1997, Lee *et al.*, 1999).

1.6 Main objectives of this study

As a unicellular eukaryote, *S. cerevisiae* has long been a useful model organism. With a mean generation time of approximately 2 hr. and a fully sequenced genome, this species was an ideal organism for employment in this study.

We initially wanted to analyse the visible effects of gliotoxin on yeast growth and investigate the capacity of different strains to withstand deleterious effects of the toxin. The principal endeavour was to utilise RNA sequencing technology and proteomics to analyse the global response of *S. cerevisiae* to gliotoxin. From these results, we wanted to assess the efficacy and apply functional genetics to further investigate the said response and compare it to that induced by typical OS-causing agents.

Part 2 Investigation into the mode of action of the prion-curing drug Tacrine

1.7 Mammalian prions

The term prion was first coined by Stanley Prusiner (1982) in naming disease-causing proteinaceous infectious particles. Diseases caused by prions are collectively known as transmissible spongiform encephalopathies (TSEs) and one of the earliest prion diseases to be documented was scrapie, which affects sheep (Detwiler, 1992). It is thought that scrapie, so named due to infected sheep rubbing against stationary objects (figure 1.5), was reported in Europe as far back as 1732 (Plummer, 1946). Other TSEs include Creutzfeldt–Jakob disease (CJD), Gerstmann–Straussler–Sheinker disease (GSS) and Kuru which affect humans, and bovine spongiform encephalopathy (BSE) found in cattle (Gerstmann *et al.*, 1936, Gajdusek *et al.*, 1966, Holt and Phillips, 1988, Prusiner, 1998).

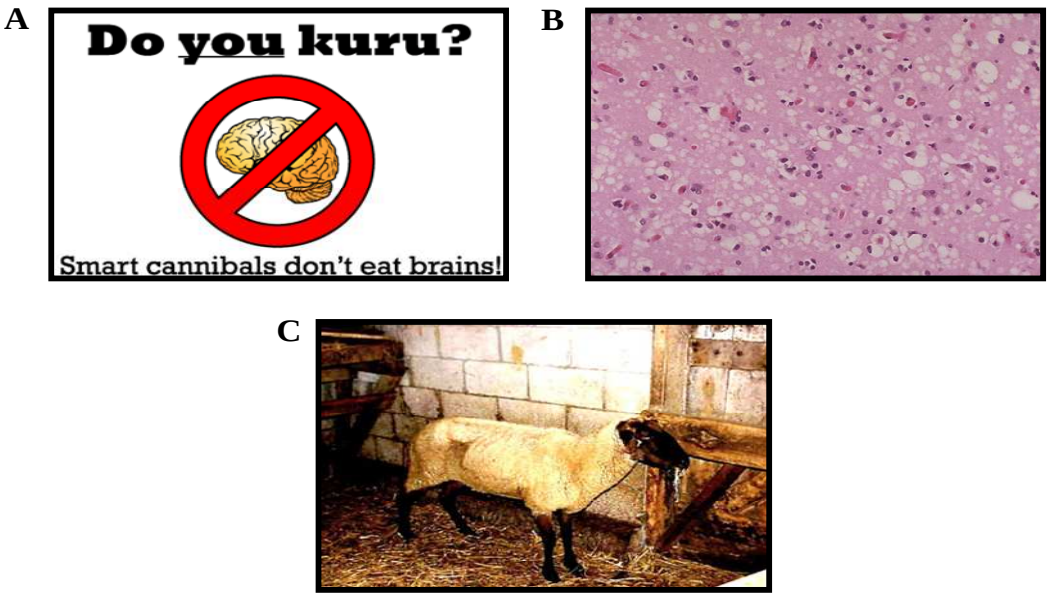

Figure 1.5 A = Comedic advertisement warning against the contraction of Kuru which can be transmitted through brain consumption. Image from www.bizarremedical.com B = Sponge-like legion in the brain tissue of a CJD patient. Image from Centres for Disease Control www.cdc.gov C = Sheep displaying weight loss and behaviour characteristic of scrapie infection. Image from Ohio State University www.ohioline.osu.edu.com

TSEs can also cause chronic wasting disease (CWD) in elk and feline spongiform encephalopathy (FSE) in cats (Williams and Young, 1980, Aldhous, 1990). Prion diseases are characterised by aggregation of prions within the brain, forming amyloid plaques (Prusiner *et al.*, 1983) and lead to fatal neurodegeneration which currently cannot be treated (Trevitt and Collinge, 2006). Amyloid plaques are also implicit in non-infectious amyloid diseases such as Alzheimer's Disease and Parkinson's Disease (Lansbury, 1999) and are therefore of major research interest. Interestingly, Gimbel *et al.* (2010) reported that for transgenic Alzheimer mice to display memory impairment, the mammalian cellular prion protein must be present.

1.7.1 PrP protein

Although prion diseases may be contracted sporadically, by infection or through inheritance, all involve prion protein (PrP) metabolism and accumulation (McKinley *et al.*, 1983, Prusiner, 1991). Prion replication occurs through the cyclic conversion of the normal functional PrP protein (PrP^{C}) into a non-functional, disease-causing form (PrP^{Sc}) (Prusiner, 1998). Devoid of nucleic acid, PrP^{Sc} is the only component of the mammalian prion (McKinley *et al.*, 1983, Prusiner, 1997). The generation of insoluble protease-resistant PrP^{Sc} is characterised by the refolding of α-helical segments into β-sheets, which is a posttranslational event (McKinley *et al.*, 1983, Oesch *et al.*, 1985, Borchelt *et al.*, 1990, Pan *et al.*, 1993). This fully supports the "protein-only hypothesis" first put forward by Griffith (1967), suggesting that prions are self-replicating.

PrP^{C} is encoded by the *PRNP* gene in humans (Kretzschmar *et al.*, 1986). Twenty *PRNP* mutations have been identified that appear to give rise to host prion diseases, thus accounting for the fact that ~10% of CJD cases are familial (Prusiner, 1991, Prusiner, 1997). PrP^{C}, expressed in the brain and spinal chord is a sialoglycoprotein and is thought to adhere to the cell surface by its glycolipid (Bolton *et*

al., 1985, Stahl *et al.*, 1987). It it possible that PrP^C may function in protecting the cell against OS, due to reports that the protein displays superoxide dismutase activity (Brown *et al.*, 1999, Brown *et al.*, 2001). It has been demonstrated that PrP^C also appears to be involved in cell signalling and play a role in cell adhesion (Schmitt-Ulms *et al.*, 2001, Gavín *et al.*, 2005).

1.8 Fungal prions

Prion studies have not been limited to mammals, as fungal prions have also been identified. [Het-s] is a prion found in the filamentous fungus *Podospora anserina* that can induce cell death as a protection mechanism to prevent virus transmission, through mating incompatibility (Coustou *et al.*, 1997, Wickner, 1997). A number of *Saccharomyces cerevisiae* proteins have the ability to form prions, as listed in table 1.1.

Table 1.1 A selection of *S. cerevisiae* prions.

Functional Protein	Function	Prion Form	Reference
Sup35p	Translation termination	[*PSI*$^+$]	(Cox, 1965)
Ure2p	Nitrogen metabolism	[*URE3*]	(Wickner, 1994)
Rnq1p	Unknown	[*PIN*$^+$]	(Derkatch *et al.*, 1997)
Cyc8p	Transcriptional co-repression	[*OCT*$^+$]	(Patel *et al.*, 2009)
Swi1p	Transcription regulation	[*SWI*$^+$]	(Du *et al.*, 2008)
New1p	ATP-binding protein	[*NU*$^+$]	(Santoso *et al.*, 2000)
Sfp1p	Transcription regulation	[*ISP*$^+$]	(Rogoza *et al.*, 2010)

1.8.1 [*PSI*$^+$]

In yeast, two proteins work in conjunction with one another to control the translation termination process. These are Sup35p and Sup45p, which function as eukaryotic release factors eRF3 and eRF1 respectively (Frolova *et al.*, 1994,

Zhouravleva *et al.*, 1995). Sup45p recognises when a stop codon (TAA, TAG or TGA) enters the ribosome, while Sup35p is directly involved in translation termination and binds GTP which is required for polypeptide chain release from peptidyl-tRNA (Beaudet and Caskey, 1971, Frolova *et al.*, 1994, Zhouravleva *et al.*, 1995).

In 1965, Brian Cox discovered a non-mendelian genetic element that was identified about 30 years later as the yeast prion [PSI^+] (Wickner, 1994). [PSI^+] is the prion form of Sup35p, and thus depends on the *SUP35* chromosomal gene (Ter-Avanesyan *et al.*, 1994, Wickner, 1994). In [PSI^+] strains, the spontaneously altered prion protein induces the conformation of soluble, functional Sup35p to the prion form, resulting in [PSI^+] aggregation (Patino *et al.*, 1996). This aggregation and reduction in functional Sup35p, leads to suppression of nonsense codons, characteristic of the [PSI^+] phenotype (Tuite *et al.*, 1987, Cox *et al.*, 1988). [PSI^+] confers strength to weak nonsense suppressor tRNAs and lethality to strong suppressors (Cox, 1965, Cox, 1971).

Sup35p is a multidomain protein, containing N-, middle- and C-terminal domains (Kushnirov *et al.*, 1988), as illustrated in figure 1.6.

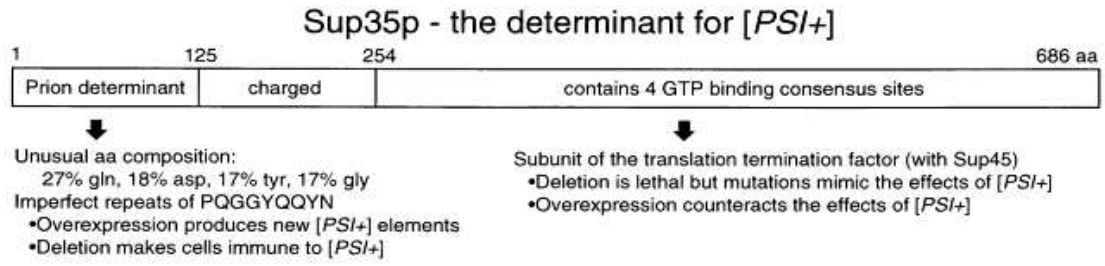

Figure 1.6 Structure of the *S. cerevisiae* Sup35p. The prion determinant is the N-terminal domain. The charged middle-domain is situated between the N- and C-domains. The C-terminal domain responsible for translation termination retains the GTP-binding capacity. Image from Lindquist (1997).

The aminoterminal N-domain retains prion activity and is thus referred to as the prion domain (PrD) (Derkatch *et al.*, 1996, King *et al.*, 1997). The C-terminal domain is responsible for the Sup35p translation termination function and is essential for cell

viability (Ter-Avanesyan *et al.*, 1994). The highly charged middle-domain assists in maintaining Sup35p solubility and enabling prion and non-prion state interconversion (Liu *et al.*, 2002). Like other yeast prions, [*PSI*$^+$] is inherited by daughter cells in a non-Mendelian cytoplasmic manner (Lindquist, 1997). [*PIN*$^+$] ([*PSI*$^+$] inducible) creates a scaffold that must pre-exist to allow the appearance of [*PSI*$^+$], as the spontaneous generation of [*PSI*$^+$] was observed in [*PIN*$^+$] cells, but not [*pin*$^-$] (Derkatch *et al.*, 1997). [*PIN*$^+$] is the prion form of Rnq1p, of which the function is not yet clear.

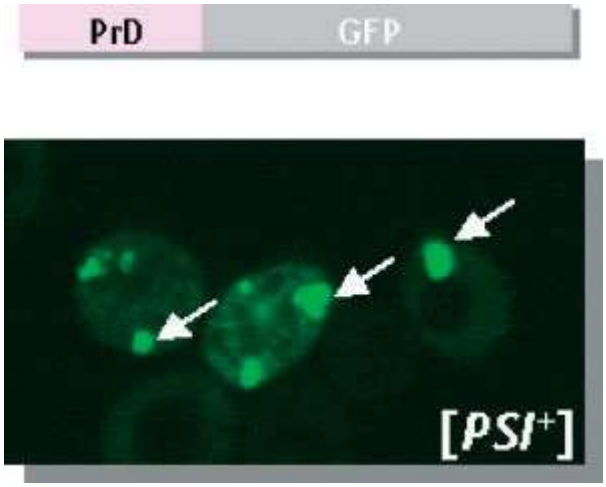

Figure 1.7 Illustration of aggregated yeast PrD fused to GFP to enable detection in a [*PSI*$^+$] strain. Aggregates are indicated by arrows. Image from Jones and Tuite (2005).

Simple colour assays are often used to monitor the presence of [*PSI*$^+$] in *S. cerevisiae*. The introduction of aberrant stop mutations such as *ade2-1* and *ade1-14* confer adenine auxotrophy to cells. These cells subsequently display a red colour which represents the build-up of by-products from the adenine biosynthesis pathway. [*PSI*$^+$] can partially suppress the nonsense mutation in the presence of the serine-inserting, weak UAA suppressor tRNA *SUQ5*. This facilitates cellular growth in the absence of adenine and eradicates the red pigmentation, allowing growth of white colonies (Cox,

1965, Liebman *et al.*, 1975, Ono *et al.*, 1979). This creates an easy way for the presence of [*PSI*$^+$] to be monitored; red cells are [*psi*$^-$], white cells are [*PSI*$^+$].

1.8.2 [*PSI*$^+$] propagation and the importance of chaperone proteins

As briefly stated above, [*PSI*$^+$] yeast cells typically contain a large amount of aggregated insoluble non-functional Sup35p. As opposed to this, the Sup35p in [*psi*$^-$] cells is soluble and functional. The structural change of α-helical content to β-sheets characteristic of [*PSI*$^+$] means protein-folding is inherently associated with prion propagation (Glover *et al.*, 1997). In order for the prion to be maintained and passed to daughter cells, [*PSI*$^+$] must be able to propagate efficiently and chaperone proteins play a key role in this process. Hsp104p (heat-shock protein 104) is essential for prion propagation and maintenance of [*PSI*$^+$] within a yeast cell line (Chernoff *et al.*, 1995). However, close cooperation with other heat-shock proteins, Hsp70p and Hsp40p is required for Hsp104p-mediated activity (Glover and Lindquist, 1998).

1.8.2.1 Hsp104p

Hsp104p is a heat-shock protein that functions in induced cellular thermotolerance, enabling yeast cells to survive at high temperatures (Sanchez and Lindquist, 1990). It has been shown to play a role in the disaggregation of proteins that are heat-damaged (Parsell *et al.*, 1994). Overproduction or absence of Hsp104p chaperone activity abolishes [*PSI*$^+$] (Chernoff *et al.*, 1995). This is because wild-type levels of Hsp104p are required for [*PSI*$^+$] cleavage, leading to the production of prion "seeds" which can be passed to daughter cells, enabling prion propagation (Paushkin *et al.*, 1996).

Recent work has raised the possibility that Hsp104p may regulate the transmission of propagons to daughter cells. Erjavec *et al.* (2007) demonstrated that

during mitosis, Hsp104p is involved in segregating damaged proteins, preventing them from being passed to daughter cells, through a Sir2p-dependent process. This group also found that overexpression of Hsp104p improves the retention of damaged proteins. Liu *et al.* (2010) have proposed that rather than simply retaining damaged proteins in the mother cell, aggregates are transported to the emerging bud but subsequently translocate back to the mother cell, prior to cytokinesis completion. The polarisome machinery has been identified as essential for partitioning of damaged proteins and it has been shown that this process requires actin cables to act as a scaffold for Hsp104p and associated aggregates (Liu *et al.*, 2010). As prions are essentially damaged aggregated proteins, it is quite likely that the [*psi*$^-$] phenotype resulting from Hsp104p overexpression occurs due to lack of prion inheritance through retention of aggregates in the mother cells.

Hsp104p overexpression leads to maintenance of soluble Sup35p, while lack of this chaperone activity results in reduced prion forming capacity (Paushkin *et al.*, 1996, Wegrzyn *et al.*, 2001). Thus a balance of Hsp104p activity level is essential for prion maintenance. [*PSI*$^+$] curing mediated by Hsp104p overexpression is dependent upon the N-terminal domain of the chaperone, although this domain is not required for normal levels of [*PSI*$^+$] propagation (Hung and Masison, 2006). It has also been demonstrated that the presence of Sti1p, a Hsp70p and Hsp90p co-chaperone (discussed below), is critical for successful [*PSI*$^+$] curing by excess Hsp104p (Moosavi *et al.*, 2010, Reidy and Masison, 2010).

1.8.2.2 Hsp70 protein family

Hsp70, a 70 kDa protein family comprises a complex key molecular chaperone group (Ingolia *et al.*, 1982). These proteins have a number of different roles in the cell, from folding nascent polypeptide chains to preventing the aggregation of and refolding misfolded proteins (Bukau and Horwich, 1998). The Ssa (stress seventy subclass A) and

Ssb (stress seventy subclass B) proteins make up cytosolic subfamilies of the Hsp70 proteins and are themselves composed of Ssa1-4p and Ssb1-2p respectively (Craig *et al.*, 1993). In addition to these six cytosolic Hsp70 proteins, a further three, Sse1p, Sse2p and Ssz1p exist (Ingolia *et al.*, 1982, Craig and Jacobsen, 1984, Craig and Jacobsen, 1985, Werner-Washburne *et al.*, 1987, Mukai *et al.*, 1993, Gautschi *et al.*, 2001). Three mitochondrial Hsp70 proteins Ssc1p, Ssq1p and Ecm10p have also been identified (Craig *et al.*, 1987, Craig *et al.*, 1989, Schilke *et al.*, 1996, Baumann *et al.*, 2000), in addition to two endoplasmic reticulum-associated Hsp70 proteins Kar2p and Lhs1p (Rose *et al.*, 1989, Craven *et al.*, 1996). With reference to yeast prions, the Ssa and Ssb proteins are of great interest.

The presence of at least one Ssa protein is essential for cell viability (Werner-Washburne *et al.*, 1989). Ssa1p has been identified as an important protein in prion maintenance. Ssa1p prevents the "curing" of [*PSI*$^+$] mediated by Hsp104p overexpression, overexpression of *SSA1* increases [*PSI*$^+$]-regulated nonsense suppression and mutations in the *SSA1* gene have an antagonistic effect on [*PSI*$^+$] (Newnam *et al.*, 1999, Jung *et al.*, 2000, Jones and Masison, 2003, Loovers *et al.*, 2007). In support of these results, Ssa proteins have been shown to induce *de novo* generation of [*PSI*$^+$] in [*psi*$^-$] cells, and this appears to be dependent on the peptide-binding domain (Allen *et al.*, 2005). Ssb proteins are not required for cell survival (Nelson *et al.*, 1992). Conversely to Ssa, there is evidence to suggest that Ssb proteins hinder [*PSI*$^+$] propagation. In Δ*ssb1* and Δ*ssb2* strains, there is a 10-fold increase in the appearance of [*PIN*$^+$]-dependent spontaneous [*PSI*$^+$]. Overexpressed Ssbp facilitates [*PSI*$^+$] curing by surplus Hsp104p (Chernoff *et al.*, 1999) and it has been demonstrated that in [*psi*$^-$] cells, diminished levels of Ssbp increases the level of nonsense suppression, albeit modestly (Jones *et al.*, 2003).

1.8.2.3 The Hsp70p ATPase binding cycle

Hsp70 proteins have two functional domains, an ATPase-binding domain (ABD) and a peptide-binding domain (PBD) (Flaherty *et al.*, 1990, Zhu *et al.*, 1996). As dictated by ATP hydrolysis, Hsp70p can exist in either a "closed" conformation, whereby the substrate is tightly bound to the PBD, or an "open" conformation, associated with rapid substrate exchange (Liberek *et al.*, 1991). ATP-binding results in a Hsp70p conformational change from a closed to an open state, allowing substrate dissociation. Alternatively, the ADP-bound form maintains tight affinity for substrates (Schmid *et al.*, 1994). The tight substrate-binding caused by ATP hydrolysis occurs through the closing of an α-helical lid domain that is displaced when ATP is bound (Zhu *et al.*, 1996). As substrates cycle between the Hsp70p-bound form and the free form, the functional activity of Hsp70p can be referred to as the Hsp70p ATPase binding cycle (Mayer and Bukau, 2005). This cycle is illustrated in figure 1.8.

Hsp70 proteins require the cooperation of co-chaperones to function successfully. One Hsp70p co-chaperone is Sti1p, a linker protein that forms a scaffold between Ssa1p and another chaperone protein Hsp90, which has shown to be a potent activator of Ssa1p ATPase activity (Wegele *et al.*, 2003). Like Sti1p, Cns1p acts as a co-chaperone for both Hsp70p and Hsp90p. This protein also activates Ssa1p ATPase activity through accelerating ATP hydrolysis (Hainzl *et al.*, 2004). Genetic evidence has been provided to suggest that another Hsp90p co-chaperone Cpr7p stimulates Hsp70p ATPase (Jones and Tuite, 2005). Sis1p, Ydj1p and Apj1p are members of the Hsp40p chaperone family and act as cofactors in facilitating Hsp70p activity (Caplan *et al.*, 1992, Ohba, 1997, Kryndushkin *et al.*, 2002). However, the above named co-chaperones are not alone in regulating the Hsp70p ATPase binding cycle.

Nucleotide exchange factors (NEFs) are also involved in the regulation of Hsp70p activity. These proteins, such as Fes1p and Sse1p (which is also a member of

the Hsp110 family) stimulate an increase in the ADP dissociation time, thus catalysing ATP replacement of ADP (Kabani *et al.*, 2002, Raviol *et al.*, 2006, Kabani, 2009).

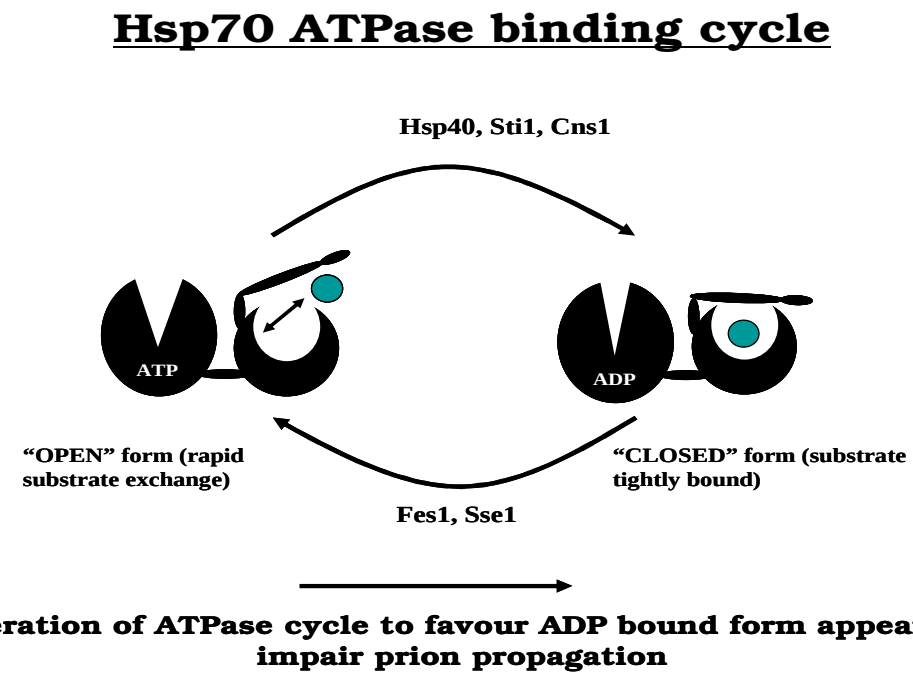

Figure 1.8 Proposed model illustrating the importance of Hsp70, co-chaperones and NEFs in prion propagation and maintenance within the cell. When ATP is bound to the ABD, the PBD exhibits an open conformation and rapid substrate exchange occurs. When ADP is bound, the PBD lid closes and substrate is tightly affixed. Co-chaperones and NEFs are required for regulation of this cycle. Evidence has been provided to suggest that disruption of this cycle leads to impairment of prion propagation.

It has been suggested that disruption of this cycle impairs prion propagation (Jones and Tuite, 2005). Jung *et al.* (2000) isolated a yeast mutant, containing a single amino acid change within the *SSA1* gene, designated *SSA1-21*. This mutation was found in the PBD and significantly weakened [PSI^+] stability, through reducing the number of prion seeds produced. Subsequent research demonstrated that Sup35p aggregates are larger in *SSA1-21* cells, probably because they contain more polymers (Song *et al.*, 2005). This supports previous work in that the loss of Sup35p polymer seeds in *SSA1-21* mutants is due to their employment in the formation of oversized aggregates and highlights a role for Ssa1p in prion propagation through prion seed production.

It has been considered that the *SSA1-21* mutation may negatively affect communication between the two functional domains of Hsp70p, thus disrupting the ATPase cycle (Jones and Tuite, 2005). Mutations were also identified in the Hsp70p ABD that impair [*PSI*$^+$] propagation (Jones and Masison, 2003). This group hypothesised that these mutations were modifying ATPase activity that resulted in a disruption of the open/closed conformational regulation. Needham and Masison (2008) have since generated mutations in the Ssa1p ABD and PBD that disrupt communication between that two domains and alter regulation of the cycle, e.g. through hypersensitive ATPase activity.

Interestingly, it appears that alteration of the ATPase-binding cycle to favour the ADP-bound form impairs prion propagation. Fes1p deletion has been shown to weaken [*PSI*$^+$] stability, as Fes1p absence decreases the rate of ATP-binding (Jones *et al.*, 2004). Loss of [*PSI*$^+$] has also been found to be a result of Sti1p overexpression, while Sti1p and Cpr7p deletion enhances [*PSI*$^+$] maintenance (Kryndushkin *et al.*, 2002, Jones *et al.*, 2004). The results described above strongly suggest that Hsp70p and its cooperative chaperone machinery assist in the highly sensitive regulation of prion propagation (figure 1.9).

1.9 Anti-prion drugs

Due to the detrimental effects caused to mammals by prion diseases, the requirement for efficient prion-curing agents remains urgent. A number of drugs possessing mammalian prion-curing ability have been identified and were reviewed by Trevitt and Collinge (2006). Yeast models are commonly employed in the search for therapeutic drugs, as molecular systems, such as Hsp70p are highly conserved from yeast to mammals (Jones and Tuite, 2005).

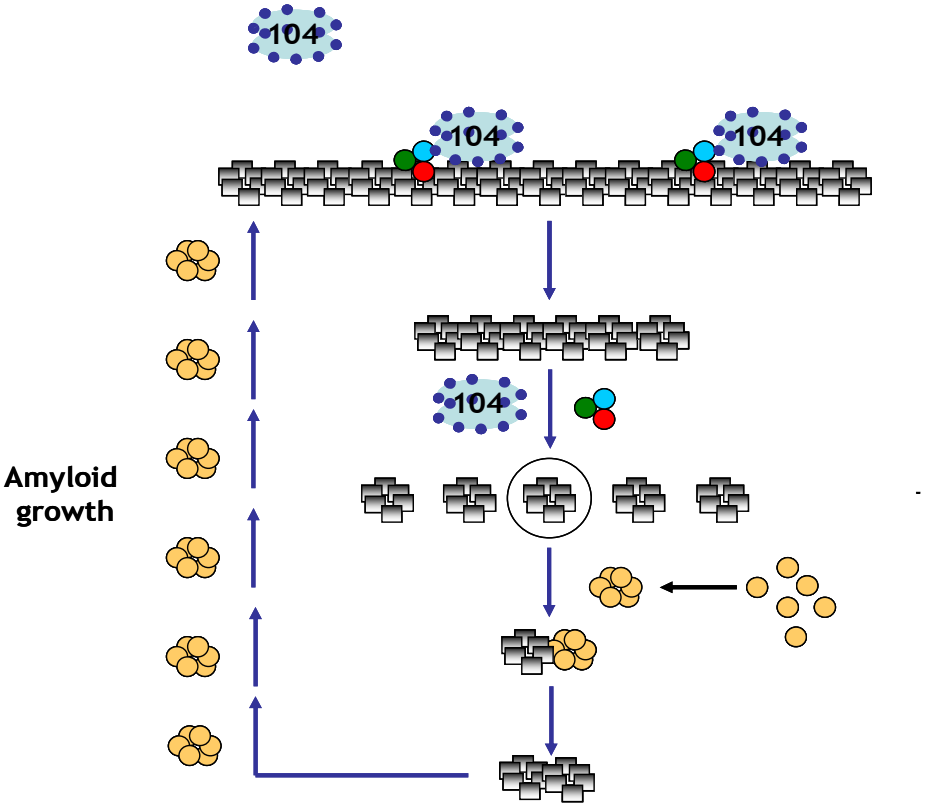

Figure 1.9 Representation of the importance of chaperone activity cooperation in prion propagation. Red, green and blue clustered circles represent Hsp40p, Hsp70p and other Hsp70p co-chaperones. Gold circles represent soluble Sup35p. Black squares represent [*PSI*$^{+}$] aggregates.

1.9.1 Guanidine Hydrochloride

Guanidine Hydrochloride (GdnHCl), a powerful denaturing agent (Levine *et al.*, 1963) was identified by Tuite *et al.* (1981) as a [*PSI*$^{+}$]-curing compound. GdnHCl efficiently cures yeast prions by abrogating prion propagation, leaving the remaining prions to be diluted out over time, and eventual [*psi*$^{-}$] appearance (Eaglestone *et al.*, 2000). In agreement with this model and in contrast to earlier work (Wu *et al.*, 2005), Byrne *et al.* (2007) reported that cell division is a certain requirement for GdnHCl-mediated [*PSI*$^{+}$] eradication. [*PSI*$^{+}$] elimination occurs through direct inhibition of Hsp104p ATPase activity by GdnHCl, although the intracellular level of the chaperone protein is not affected (Ferreira *et al.*, 2001, Jung and Masison, 2001, Jung *et al.*, 2002).

Although GdnHCl arrests the cleavage of new prion seeds by Hsp104p in [*PSI*$^+$] cells, it does induce the decomposition of preexisting Sup35p aggregates (Ness *et al.*, 2002).

1.9.2 6-aminophenanthridine

6-aminophenanthridine is a phenanthridine derivative, that has a modified amino group at position 11 that differentiates the two (Bach *et al.*, 2003). Its structure is depicted in figure 1.10.

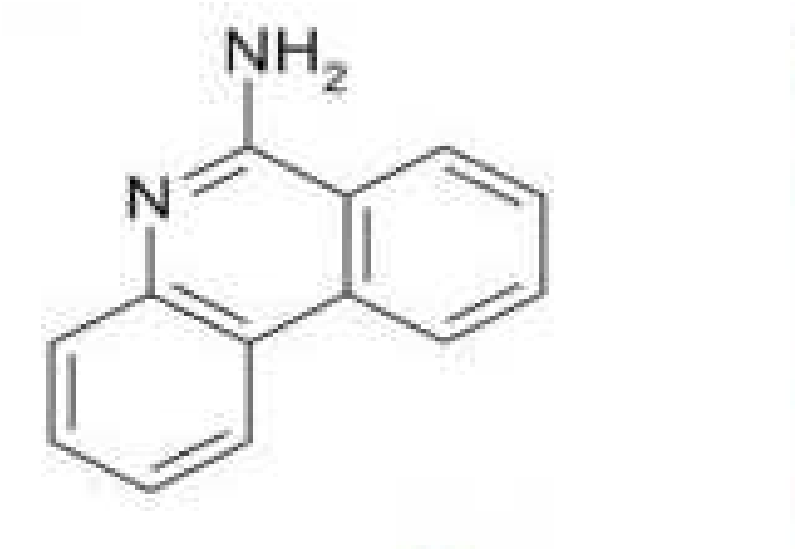

Figure 1.10 Structure of 6AP. Image from Tribouillard-Tanvier *et al.* (2008b).

Bach *et al.* (2003) identified 6-aminophenanthridine (6AP) as an anti-prion agent, using a yeast-based screening assay. They discovered that this drug alone inefficiently cures [*PSI*$^+$], but in combination with relatively low concentrations of GdnHCl, 6AP cures [*PSI*$^+$] very efficiently (figure 1.11).

Importantly, 6AP has also been shown to be active against the mammalian prion (Bach *et al.*, 2003), as illustrated by figure 1.12. 6AP interacts with the ribosome through an RNA-dependent process and hinders the rRNA-mediated protein folding

activity of the organelle, without affecting protein synthesis (Tribouillard-Tanvier *et al.*, 2008b).

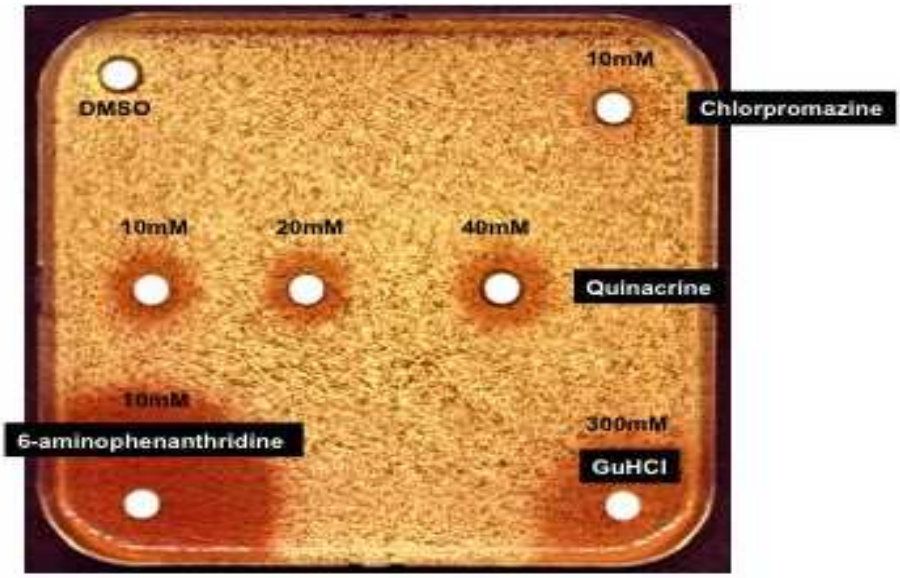

Figure 1.11 Plate assay showing the effects of different compounds on [*PSI*$^{+}$] cells. The agar contains 500 µM GdnHCl and other drugs were spotted onto filter paper. The red zones represent cured [*psi*$^{-}$] cells. Image from Bach *et al.* (2003).

6AP inhibits ribosomal-mediated protein folding by competing with unfolded proteins for ribosome binding (Reis *et al.*, 2011). However, this agent does not directly interact with prion proteins (Tribouillard-Tanvier *et al.*, 2008b).

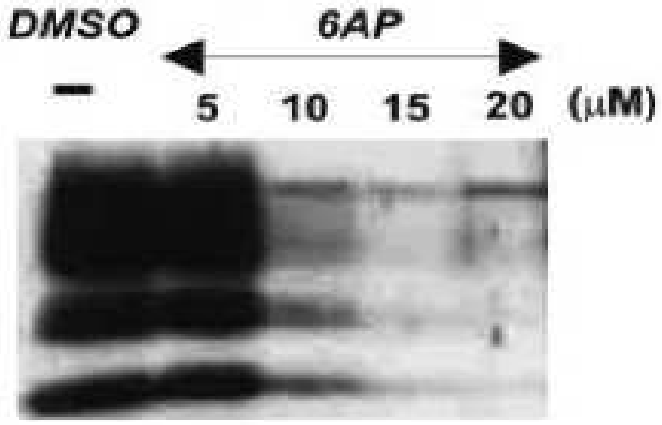

Figure 1.12 Representation of 6AP anti-prion activity. The banding patterns depict protease K resistant PrP^{Sc} from sheep. It can be seen that with increasing concentrations of 6AP, the sheep protein becomes sensitive to protease K digestion as the level of soluble PrP^{C} returns. Image from Tribouillard-Tanvier *et al.* (2008b).

1.9.3 Guanabenz

Guanabenz (GA) is a drug that has been used for decades to treat hypertension (McMahon *et al.*, 1974). GA was found to display anti-prion activity in both yeast and mammalian systems (Tribouillard-Tanvier *et al.*, 2008a). Although structurally unrelated to 6AP, like 6AP, GA does not directly interact with prion proteins, but specifically interacts with ribosomal components in an RNA-dependent manner (Tribouillard-Tanvier *et al.*, 2008b). As for 6AP, GA does not affect protein synthesis, but inhibits rRNA-regulated ribosomal protein folding activity (Tribouillard-Tanvier *et al.*, 2008b). Furthermore, both drugs utilise the same binding sites on ribosomal components and both impede the action of ribosomal folding modulators (RFMs), ribosomal components active in protein folding (Tribouillard-Tanvier *et al.*, 2008b, Reis *et al.*, 2011). The structure of GA is depicted in figure 1.13.

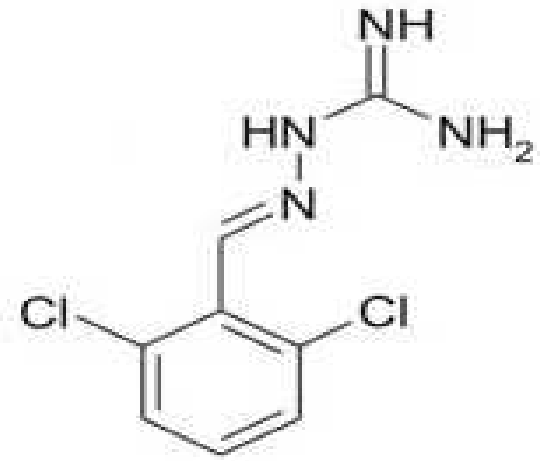

Figure 1.13 Structure of GA. Image from Tribouillard-Tanvier *et al.* (2008b).

1.9.4 Tacrine

Tacrine (1,2,3,4-tetrahydro-9-aminoacridine/THA/TA) is a compound that was identified as a prion-curing agent in a yeast-based assay. Although shown to be active against yeast prions, TA exhibited no potency against mammalian prions (Tribouillard-

Tanvier *et al.*, 2008a). It may be the case that TA, the structure of which is shown in figure 1.14, targets a yeast pathway too far diverged in mammalian systems. However, the fact that prion curing activity in yeast has been demonstrated means TA remains an interesting drug for prion researchers.

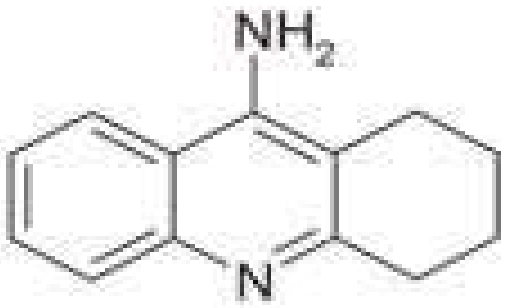

Figure 1.14 Structure of TA. Image from Tribouillard-Tanvier *et al.* (2008a).

1.9.4.1 Tacrine as a human drug

TA is a drug which has been prescribed to Alzheimer's patients, based on findings that this compound induces an improvement in memory and relieves symptoms of Alzheimer's dementia (Summers *et al.*, 1981, Summers *et al.*, 1986, Davis *et al.*, 1992). Although opinion has been divided over the effectiveness of TA and whether or not effects of the drug are significantly beneficial (Chatellier and Lacomblez, 1990, Molloy *et al.*, 1991, Wilcock *et al.*, 1994), reviewers have concluded that on cognitive function, TA has beneficial effects, albeit modest (Byrne and Arie, 1994, Qizilbash *et al.*, 1998).

Since the advent of TA administration, there has been mixed sentiment. Concerns were raised regarding TA toxicity when only two months into a clinical trial, liver damage was found in one fifth of patients (Marx, 1988). Further to this, many groups have demonstrated that hepatotoxicity can result from TA dosage (Forsyth *et al.*, 1989, Molloy *et al.*, 1991, Lagadic-Gossmann *et al.*, 1998) and that clinical hepatitis can subsequently occur (Molloy *et al.*, 1991, O'Brien *et al.*, 1991). However, lack of TA

mammalian toxicity has also been documented (Fitten *et al.*, 1987). Accordingly, many believe that under careful monitoring and regular enzyme level testing, Alzheimer's sufferers can profit from administration of this drug and to support this belief, in 1993 TA became "the first FDA-approved treatment for Alzheimer's disease" (Watkins *et al.*, 1994, Summers, 2006).

1.9.4.2 Tacrine mode of action

In 1951, Dr. Adrien Albert published data referencing TA, "aminacrine", an aminoacridine compound as a powerful antiseptic and antibacterial agent. He reported on the chemical and biological properties of the aminoacridines, in addition to their medicinal functions (Browning and Crawford, 1951).

TA is an acetylcholinesterase inhibitor and acts through arresting the breakdown of acetylcholine (ACh). This in turn prevents decline in cholinergic neurotransmission, which is symptomatic of Alzheimer's disease, and due to it's high solubility level, TA has easy access to the brain (Weinstock, 1995). More recent work has shown that in addition to the above, TA, although not an ACh receptor (AChR) agonist, competitively binds to agonist AChR sites "stabilising a non-conducting open channel receptor form" (Cheffer and Ulrich, 2011). Independent of its acetylcholinesterase inhibitory activity, TA can also inhibit the neuronal entry of calcium and can block potassium and sodium channels (Davis and Powchik, 1995, Dolezal *et al.*, 1997).

One of the main characteristics of Alzheimer's disease is the accumulation of amyloid plaques within the brain. These plaques consist of amyloid beta-proteins which are derivatives of the secreted beta amyloid precursor proteins (beta APP) (Haass and Selkoe, 1993). TA treatment results in a striking inhibition of beta APP secretion and also in slightly decreased levels of intracellular beta APP (Lahiri, 1994, Lahiri and Farlow, 1996).

1.9.4.3 Tacrine and prion proteins

Recently published data has demonstrated that the mammalian cellular prion protein functions as a receptor for amyloid beta-proteins, thus playing a role in synaptic dysfunction. In fact, PrP is not required to be in the infectious PrP^{Sc} isoform for this intercommunication to occur (Laurén *et al.*, 2009). Significantly, it also appears that for mammals to show cognitive deficiencies resulting from amyloid beta-protein accumulation, PrP^{C} expression is imperative (Gimbel *et al.*, 2010). From this, the link between Alzheimer's disease dysfunction and prions has been strengthened and for treatment, TA may be a useful common factor.

1.10 Ribosomal activity as a potential target for prion curing

Evidence has been provided to suggest that the ribosome may play a role in protein folding. Specifically, the domain V of the 23S large ribosomal subunit appears to be involved in protein re-and denaturation (Das *et al.*, 2008). As descibed above, protein folding is significantly implicated in prion propagation and interestingly, it is this domain V that undergoes specific interaction with the prion curing drugs 6AP and GA (Tribouillard-Tanvier *et al.*, 2008b). It has been proposed that ribosome-borne protein folding activity (RPFA) lies in the preparation of a pre-folded nascent peptide that downstream chaperones will alter further (Fåhraeus and Blondel, 2008). Taken together, it may be the case that RPFA contributes in some way to priongenesis and preservation of the [PSI^{+}] phenotype, and may thus be a potential target for prion curing drugs.

1.11 *YAR1, LTV1, RPL8A* and *RPL8B*

YAR1, LTV1, RPL8A and *RPL8B* are four ribosome-related genes identified as potentially important in prion research. Δ*yar1*, Δ*ltv1*, Δ*rpl8a* and Δ*rpl8b* all contain an

imbalance in the relevant ribosomal subunit and can only display weak [*PSI*$^{+}$]. Interestingly, when these strains are exposed to 6AP or GA, the prion is stabilised (M. Blondel, personal communication). *YAR1* is not an essential gene but growth of strains deleted for this gene is significantly retarded, especially at low temperatures (Lycan *et al.*, 1996). In addition to its role in regulating the rate of cellular proliferation, *YAR1* transcription is considerably repressed by heatshock (Lycan *et al.*, 1996). Physical interaction between Yar1p and another protein Ltv1p has been documented (Loar *et al.*, 2004). Evidence suggests that the latter protein may be an assembly factor, involved in the processing of pre-ribosomes (Schäfer *et al.*, 2003, Campbell and Karbstein, 2011). Overall, it is thought that both Yar1p and Ltv1p distinctly function in 40S subunit production (Loar *et al.*, 2004).

RPL8A (*MAK7*) and *RPL8B* (*KRB1*) encode the yeast ribosomal protein L4 of the of the large 60S subunit (Arevalo and Warner, 1990, Yon *et al.*, 1991, Ohtake and Wickner, 1995). The nearly identical *RPL8A* and *RPL8B* genes are orthologous to the mammalian *RPL7A* ribosomal protein gene (Yon *et al.*, 1991). The fact that mutants deleted for these four genes exhibit a weakened [*PSI*$^{+}$] may provide an important link between ribosomal function and prion propagation.

1.12 Main aims of this study

The principal objectives of this study were to assess the yeast prion-curing capacites of TA, and to investigate its mode of action. It was anticipated that RNA sequencing technology and proteomics would provide insight into the mode of action of TA, through analysis of the global *S. cerevisiae* response to the drug. As TA appears to mediate its effects through a different process to 6AP and GA, these drugs were selected for employment in a comparative study. It was hypothesised that TA might enhance the uptake of GdnHCl and we endeavoured to assess the validity of this supposition.

Chapter 2 Materials and methods

Yeast Handling Techniques

2.1 Yeast and bacterial strains used in this study

2.1.1 *Saccharomyces cerevisiae* strains

Listed below in table 2.1 are *Saccharomyces cerevisiae* strains which were used in this study, in addition to genotype description and where strains were sourced.

Table 2.1 *S. cerevisiae* strains used in this study.

Strain name	Genotype	Source
G600	*MAT***a**/*MATα** ade2.1 SUQ5 kar1-1 his3 leu2 trp1 ura3*	Jones *et al.* (2004)
G600 pRS315	*MAT***a** *ade2.1 SUQ5 kar1-1 his3 leu2 trp1 ura3* pRS315	This study
G600 pRS316	*MAT***a** *ade2.1 SUQ5 kar1-1 his3 leu2 trp1 ura3* pRS315	This study
BY4741	*MAT***a** *his3 leu2 met15 ura3*	Euroscarf
BY4741 Δ*cys3*	*MAT***a** *his3 leu2 met15 ura3 cys3::kanMX4*	Euroscarf
BY4741 Δ*trr2*	*MAT***a** *his3 leu2 met15 ura3 trr2::kanMX4*	Euroscarf
BY4741 *GliT*-pC210	*MAT***a** *his3 leu2 met15 ura3 GliT*-pC210	This study
BY4741 pRS315	*MAT***a** *his3 leu2 met15 ura3* pRS315	This study
BY4741 Δ*cys3* pRS315	*MAT***a** *his3 leu2 met15 ura3 cys3::kanMX4* pRS315	This study
BY4741 Δ*cys3* GliT-pC210	*MAT***a** *his3 leu2 met15 ura3 cys3::kanMX4 GliT*-pC210	This study
BY4741 pRS316	*MAT***a** *his3 leu2 met15 ura3* pRS316	This study
BY4741 *GliT*-pYES2	*MAT***a** *his3 leu2 met15 ura3 GliT*-pYES2	This study
G600 *GliT*-pYES2	*MAT***a** *ade2.1 SUQ5 kar1-1 his3 leu2 trp1 ura3 GliT*-pC210	This study
BY4741 Δ*yap1*	*MAT***a** *his3 leu2 met15 ura3 yap1::kanMX4*	Euroscarf

BY4741 Δ*sod1*	*MAT***a** *his3 leu2 met15 ura3 sod1::kanMX4*	Euroscarf
BY4741 Δ*gsh1*	*MAT***a** *his3 leu2 met15 ura3 gsh1::kanMX4*	Euroscarf
BY4741 Δ*gsh1* pRS315	*MAT***a** *his3 leu2 met15 ura3 gsh1::kanMX4* pRS315	This study
BY4741 Δ*gsh1* *GSH1*-pRS315	*MAT***a** *his3 leu2 met15 ura3 gsh1::kanMX4* *GSH1*-pRS315	This study
BY4741 Δ*cys4*	*MAT***a** *his3 leu2 met15 ura3 cys4::kanMX4*	Euroscarf
BY4741 Δ*gpx2*	*MAT***a** *his3 leu2 met15 ura3 gpx2::kanMX4*	Euroscarf
BY4741 Δ*frm2*	*MAT***a** *his3 leu2 met15 ura3 frm2::kanMX4*	Euroscarf
BY4741 Δ*hxt2*	*MAT***a** *his3 leu2 met15 ura3 hxt2::kanMX4*	Euroscarf
BY4741 Δ*met6*	*MAT***a** *his3 leu2 met15 ura3 met6::kanMX4*	Euroscarf
BY4741 Δ*met17*	*MAT***a** *his3 leu2 met15 ura3 met17::kanMX4*	Euroscarf
BY4741 Δ*met32*	*MAT***a** *his3 leu2 met15 ura3 met32::kanMX4*	Euroscarf
BY4741 Δ*ald6*	*MAT***a** *his3 leu2 met15 ura3 ald6::kanMX4*	Euroscarf
BY4741 Δ*sam1*	*MAT***a** *his3 leu2 met15 ura3 sam1::kanMX4*	Euroscarf
BY4741 Δ*hbn1*	*MAT***a** *his3 leu2 met15 ura3 hbn1::HIS5*	This study
BY4741 Δ*frm2*Δ*hbn1*	*MAT***a** *his3 leu2 met15 ura3 frm2::kanMX4* *hbn1::HIS5*	This study
G600 Δ*sse1*	*MAT***a** *ade2.1 SUQ5 kar1-1 his3 leu2 trp1* *ura3 sse1::kanMX4*	H. Loovers
G600 Δ*ssa1*	*MAT***a** *ade2.1 SUQ5 kar1-1 his3 leu2 trp1* *ura3 ssa1::kanMX4*	Jones *et al*. (2004)
G600 Δ*ssa2*	*MAT***a** *ade2.1 SUQ5 kar1-1 his3 leu2 trp1* *ura3 ssa2::HIS3*	Jones *et al*. (2004)
G600 Δ*ssa1*Δ*ssa2*	*MAT***a** *ade2.1 SUQ5 kar1-1 his3 leu2 trp1* *ura3 ssa1::kanMX4 ssa2::HIS3*	Jones *et al*. (2004)
G600 Δ*sti1*	*MAT***a** *ade2.1 SUQ5 kar1-1 his3 leu2 trp1* *ura3 sti1::kanMX4*	Jones *et al*. (2004)
G600 Δ*cpr7*	*MAT***a** *ade2.1 SUQ5 kar1-1 his3 leu2 trp1* *ura3 cpr7::HIS3*	Jones *et al*. (2004)

G600 Δ*sti1*Δ*cpr7*	*MAT***a** *ade2.1 SUQ5 kar1-1 his3 leu2 trp1 ura3 sti1::kanMX4 cpr7::HIS3*	Jones *et al.* (2004)
G600 Δ*fes1*	*MAT***a** *ade2.1 SUQ5 kar1-1 his3 leu2 trp1 ura3 fes1::kanMX4*	Jones *et al.* (2004)
74D	*MAT***a** *ade1.14 trp1 his3 ura3 leu2*	Marc Blondel
74D Δ*yar1*	*MAT***a** *ade1.14 trp1 his3 ura3 leu2 yar1::HIS5*	Marc Blondel
74D Δ*ltv1*	*MAT***a** *ade1.14 trp1 his3 ura3 leu2 ltv1::kanMX4*	Marc Blondel
74D Δ*rpl8a*	*MAT***a** *ade1.14 trp1 his3 ura3 leu2 rpl8a::kanMX4*	Marc Blondel
74D Δ*rpl8b*	*MAT***a** *ade1.14 trp1 his3 ura3 leu2 rpl8b::kanMX4*	Marc Blondel
G600 Δ*hsp104*	*MAT***a** *ade2.1 SUQ5 kar1-1 his3 leu2 trp1 ura3 hsp104::kanMX4*	Yeast Genetics
74D Δ*hsp104*	*MAT***a** *ade1.14 trp1 his3 ura3 leu2 hsp104::HIS5*	Marc Blondel
74D Δ*ltv1*Δ*hsp104*	*MAT***a** *ade1.14 trp1 his3 ura3 leu2 ltv1::kanMX4 hsp104::HIS5*	Marc Blondel
74D Δ*yar1*Δ*hsp104*	*MAT***a** *ade1.14 trp1 his3 ura3 leu2 yar1::HIS5 hsp104::kanMX4*	Marc Blondel
74D pDCM90	*MAT***a** *ade1.14 trp1 his3 ura3 leu2* pDCM90	This study
74D Δ*hsp104* pDCM90	*MAT***a** *ade1.14 trp1 his3 ura3 leu2 hsp104::HIS5* pDCM90	This study
74D Δ*yar1* pDCM90	*MAT***a** *ade1.14 trp1 his3 ura3 leu2 yar1::HIS5* pDCM90	This study
74D Δ*ltv1* pDCM90	*MAT***a** *ade1.14 trp1 his3 ura3 leu2 ltv1::kanMX4* pDCM90	This study
74D Δ*yar1*Δ*hsp104* pDCM90	*MAT***a** *ade1.14 trp1 his3 ura3 leu2 yar1::HIS5 hsp104::kanMX4* pDCM90	This study
74D Δ*ltv1*Δ*hsp104* pDCM90	*MAT***a** *ade1.14 trp1 his3 ura3 leu2 ltv1::kanMX4 hsp104::HIS5* pDCM90	This study

Working stocks of regularly used yeast strains were maintained at 4ºC on agar plates containing suitable growth media. Approximately every two weeks, these strains were sub-cultured onto fresh agar plates. Long-term stocks of all strains were prepared by adding a large number of cells to a solution containing 15% glycerol (v/v), 85% liquid YPD (v/v). These stocks were stored at -70ºC.

2.1.2 Bacterial strain

DH5α was the only *Escherichia coli* strain used in this study. Stocks of *E. coli* strain DH5α were stored at -70^{o}C in dH_2O or in 20% (v/v) glycerol to 80% (v/v) liquid LB.

2.2 Plasmid vectors used in this study

Listed in table 2.2 are plasmid vectors which were used in this study in addition to plasmid description and where plasmids were sourced.

Table 2.2 Plasmid vectors used in this study.

Plasmid Name	Description	Source
pRS315	Centromeric *Saccharomyces cerevisiae* shuttle vector *LEU2* marker	Sikorshi and Hieter (1989)
pRS316	Centromeric *Saccharomyces cerevisiae* shuttle vector *URA3* marker	Sikorski and Hieter (1989)
pC210	Vector containing *SSA1* under control of *SSA2* promoter *LEU2* marker	Schwimmer and Masison (2002)
pUG27	Vector containing *Schizosaccharomyces pombe HIS5* gene	Euroscarf
pYES2	*URA3*-based plasmid containing inducible *GAL1* promoter	Invitrogen
GliT-pYES2	*GliT* under control of *GAL1* promoter in pYES2 vector	This study
GliT-pC210	*GliT* replacing *SSA1* in pC210, under constitutive *SSA2* promoter control	This study
YEp13	High-copy plasmid containing gene bank of wild-type *S. cerevisiae* DNA *LEU2* marker	ATCC
pDCM90	*URA3*-based single-copy plasmid containing a gene for yeast expression of a thermolabile bacterial luciferase	Daniel C. Masison

2.3 Chemicals and reagents used in this study

All chemicals, reagents and metabolites were purchased from Sigma-Aldrich Chemical Co. Ltd. U.K., unless otherwise stated.

2.4 Drug and metabolite stocks used in this study

Tacrine, Guanabenz and 6-aminophenanthridine were provided by Marc Blondel, University of Brest, France.

Guanidine Hydrochloride (GdnHCl)

100 mM GdnHCl stock was made by adding 0.478 g to 50 ml sterile dH_2O. This was then separated into 1 ml aliquots and stored at -20ºC.

Tacrine (TA)

100 mM TA stocks were prepared by adding 26 mg TA in powder form to 1106.38 µl DMSO. From this, 10 mM working stocks were aliquoted and stored at -20ºC.

Guanabenz (GA)

100 mM GA stocks were prepared by adding 18.4 mg GA in powder form to 632.3 µl DMSO. From this, 10 mM working stocks were aliquoted and stored at -20ºC.

6-aminophenanthridine (6AP)

100 mM 6AP stocks were prepared by adding 15.6 mg 6AP in powder form to 804.12 µl DMSO. From this, 10 mM working stocks were aliquoted and stored at -20ºC.

Gliotoxin (GT)

1 mg/ml gliotoxin stocks were prepared by adding 25 mg of gliotoxin to 25 ml of methanol. This was dissolved, aliquoted and stored at -20ºC.

Cystathionine

1 mM cystathionine working stocks were made by adding 4.5 mg to 20 ml of sterile dH_2O. This was stored at -20ºC.

Ampicillin

To prepare ampicillin antibiotic stock solutions, 5 g of ampicillin was added to 100 ml of sterile dH_2O to give a concentration of 50 mg/ml. This was dissolved, filter sterilized, aliquoted and stored at -20ºC until usage was required.

2.5 Yeast and bacterial growth media

Bacteriological (bacto-) yeast extract, bacteriological (bacto-) peptone, bacteriological (bacto-) agar and yeast nitrogen base (YNB) without amino acids were all sourced from Becton, Dickinson and Company, Le Point de Claix, France (BD). Petri dishes were sourced from Greiner Bio-One.

2.5.1 Media for culturing yeast

|Yeast Peptone Dextrose (YPD)

10 g of bacto-yeast extract, 20 g of bacto-peptone and 20 g of D-glucose were added to 1 l of dH_2O. This complete media solution was autoclaved and stored at room temperature (RT). If solidification was required, 20 g bacto-agar was added to the other components described above, solution was autoclaved and allowed to cool. Agar was

then poured into sterile petri dishes under sterile conditions and allowed to set. Agar plates were stored at 4ºC.

Yeast Peptone Galactose (YPGAL)

10 g of bacto-yeast extract, 20 g of bacto-peptone and 20 g of galactose were added to 1 l of dH_2O. The solution was autoclaved stored at RT. If solidification was required, 20 g bacto-agar was added to the other components described above, solution was autoclaved and allowed to cool. Agar was poured into sterile petri dishes, under sterile conditions. Plates were allowed to set and were stored at 4ºC.

YPD-guanidine hydrochloride (GdnHCl)

YPD was made as described above. After autoclaving, media was allowed to cool to approximately 60ºC. GdnHCl stock was added to obtain the required concentration (table 2.3).

Table 2.3 Volume of 100 mM GdnHCl stock added to 1 l of YPD to obtain concentrations used.

Molarity Required	Volume of 100 mM stock added (ml)
3 mM	30
200 µM	2
500 µM	5

If agar had been added, the solution was poured into sterile petri dishes, under sterile conditions. Plates were allowed to set and were stored at 4ºC.

YPD-Tacrine/Guanabenz/6-aminophenanthridine

YPD was made as described in section above. After autoclaving, the YPD was allowed to cool to approximately 60ºC. Tacrine (TA), Guanabenz (GA) or 6-Amino phenanthridine (6AP) stock was added to obtain the required concentration (table 2.4).

Table 2.4 Volume of 10 mM TA/GA/6AP stock added to 1 l of YPD to obtain concentrations used.

Molarity Required	Volume of 10 mM stock added (ml)
5 µM	0.5
10 µM	1
15 µM	1.5
20 µM	2
25 µM	2.5
100 µM	10

If agar had been added, the solution was poured into sterile petri dishes, under sterile conditions. Plates were allowed to set and were stored at 4ºC.

YPD-GdnHCl-TA/GA/6AP

When a combination of both GdnHCl and TA/GA/6AP was required, appropriate volumes of both compounds, described above were added simultanaeously to YPD. E.g. to make 200 µM GdnHCl-20 µM 6AP media, 2 ml of 100 mM GdnHCl stock and 2 ml 10 mM 6AP stock were added to 1 l of YPD.

Synthetic Complete (SC)

6.7 g of YNB without amino acids, 20 g of glucose and 2 g of dropout mixture (table 2.5) were added to 1 l of dH_2O, This solution was then supplemented, depending on growth requirements of the strain, with required amino acids (table 2.6), autoclaved and stored at RT. If solidification was required, 20 g of bacto-agar was added to the other components described above, solution was autoclaved and allowed to cool. The agar was poured into sterile petri dishes, under sterile conditions. Plates were allowed to set and were stored at 4ºC.

Table 2.5 Composition of dropout mixture. The components below were added together, ground using a pestle and mortar and stored at RT.

Component	Quantity (g)
Alanine	2
Arginine	2
Asparagine	2
Aspartic Acid	2
Cysteine	2
Glutamic Acid	2
Glutamine	2
Glycine	2
Isoleucine	2
Lysine	2
Methionine	2
Phenylalanine	2
Proline	2
Serine	2
Threonine	2
Tyrosine	2
Valine	2
Para-aminobenzoic Acid	2
Inositol	2

Table 2.6 Amino acid stock concentrations and final concentration of amino acids supplemented into SC media.

Amino acid	Amino acid quantity added to 100 ml dH_2O to make stock solutions (g)	Volume of stock added to 1 l SC media (ml)	Final amino acid concentration in 1 l SC media (µg/ml)
Leucine	1	10	100
Adenine	0.2	10	20
Histidine	1	2	20
Tryptophan	1	2	20
Uracil	0.2	10	20

SC Galactose (SCGal)

6.7 g of YNB without amino acids, 20 g of galactose and 2 g of dropout mixture (table 2.5) were added to 1 l of dH_2O, This solution was then supplemented, depending on growth requirements of the strain, with required amino acids (table 2.6), autoclaved and stored at RT. If solidification was required, 20 g of bacto-agar was added to the other components described above, solution was autoclaved and allowed to cool. The

agar was poured into sterile petri dishes, under sterile conditions. Plates were allowed to set and were stored at 4ºC.

YPD/SC-Gliotoxin

YPD or SC was made as described above. After autoclaving, the media was allowed to cool to approximately 60ºC. Gliotoxin stock was added to obtain the required concentration (table 2.7)

Table 2.7 Volume of 1 mg/ml gliotoxin stock added to 30 ml SC. This made enough for one agar plate.

Concentration required (µg/ml)	Volume of 1 mg/ml stock added (µl)
2	60
4	120
8	240
12	360
16	480
32	960
64	1920

If agar had been added, the solution was poured into sterile petri dishes, under sterile conditions. Plates were allowed to set and were stored at 4ºC.

SC-cystathionine

SC was made as described above. After autoclaving, the media was allowed to cool to approximately 60ºC. Cystathionine stock was added to obtain the required concentration (table 2.8). If agar had been added, the solution was poured into sterile petri dishes, under sterile conditions. Plates were allowed to set and were stored at 4ºC.

Table 2.8 Volume of 1 mM cystathionine stock added to 30 ml SC. This made enough for one agar plate.

Concentration required (µM)	Volume of 1 mM stock added (ml)
100	3
250	7.5
350	10.5

SC-cystathionine-gliotoxin

When a combination of both gliotoxin and cystathionine was required, appropriate volumes of both compounds, described above were added simultanaeously to SC. E.g. to make 16 µg/ml GT-100 µM cystathionine media, 480 µl of 1 mg/ml gliotoxin stock and 3 ml of 1 mM cystathionine stock were added to 30 ml SC.

SC-H_2O_2

SC was made as described above. After autoclaving, the media was allowed to cool to approximately 60ºC. H_2O_2 (30 % (w/w) in H_2O) was added at the required concentration (table 2.9).

Table 2.9 Volume of 30 % H_2O_2 added to 250 ml SC.

Concentration Required (mM)	Volume of 1 mM stock added (µl)
1	21
2	42
3	63
4	84
5	105

2.5.2 Media for culturing *E. coli*

Luria Broth (LB)

20 g of Luria bertani broth was added to 1 l of dH_2O, autoclaved and stored at RT. If solidification was required, 20 g of bacto-agar was added to the luria broth, the

solution was autoclaved and allowed to cool. The agar was poured into sterile petri dishes, under sterile conditions. Plates were allowed to set and were stored at 4ºC.

LB-ampicillin

LB was made as described above and after cooling media, the antibiotic ampicillin was added. In LB-ampicillin, only bacterial strains containing an ampicillin resistance marker can survive. This enables selection of *E. coli* cells into which an ampicillin-resistance conferring plasmid has integrated. 1 ml of 50 mg/ml ampicillin stock was added to 999 ml of LB, resulting in LB with an ampicillin concentration of 50 µg/ml.

2.6 Sterilisation techniques

Sterilisation of growth media and materials required for aseptic techniques was achieved by autoclaving at 121^{o}C for 15 min. Any solutions that were susceptible to decomposition during autoclaving were filter sterilised using 0.22 µm Millipore membrane filters. All worktops and benches were washed with 70% (v/v) ethanol prior to carrying out experiments.

2.7 Yeast and bacterial culture conditions

2.7.1 Conditions for yeast liquid culture

Yeast strains required for an experiment were freshly cultured on suitable agar plates and grown at 30ºC (BD series Binder incubator, Mason Technology) for 48 hr. From these plates, liquid cultures were inoculated in 5 ml suitable media (in 14 ml round bottom falcon tubes, BD) unless otherwise stated. Cultures were incubated overnight at 30ºC, 200 rpm (Innova 4000 Orbital Shaker, New Brunswick Scientific, UK).

2.7.2 Conditions for *E. coli* liquid culture

E. coli required was freshly cultured on LB-ampicillin agar plates and grown at 37ºC for 24 hr., prior to inoculation of liquid culture. Liquid LB-ampicillin was inoculated with a single *E. coli* colony to obtain a 5 ml culture, unless otherwise stated. These cultures were incubated overnight at 37ºC, 200 rpm (Innova 44 Orbital Shaker, New Brunswick Scientific, UK).

2.7.3 Harvesting yeast and *E. coli* from liquid cultures

Yeast and *E. coli* were harvested from liquid cultures by centrifugation for five min. at 1258 x g and 3220 x g respectively (Centrifuge 5810R, Eppendorf).

2.8 Determination of yeast cell density

Yeast overnight cultures were diluted 1/100 with sterile dH_2O and counted using a haemocytometer (Bright Line, Hausser Scientific). The cells were counted using a light microscope (INGENIUS, Bio imaging Syngene) at a magnification of X 100. Other experiments required O.D. values of yeast growth over a certain time period. In this case cell concentration was determined using a spectrophotometer (Eppendorf) at OD_{600nm}.

2.9 Yeast comparative growth analysis

Yeast were cultured overnight at 30^{o}C (200 rpm) in 5 ml selective media. The following morning the cultures were diluted back to OD_{600nm}= 0.1 in 5 ml of fresh media and incubated at 30^{o}C shaking until the cells reached a concentration of $3x10^6$ cells/ml. The cells were harvested by centrifugation and resuspended in selective media to a final concentration of $5x10^6$ cells/ml. 200 µl of cultures were placed in wells in column 1 in a 96 well plate (Starstedt) and 160 µl of media was added to wells in

columns 2-6. A 1/5 serial dilution was performed on the cells using a multichannel pipette e.g. by removing and adding 20 µl of culture from well A1 through to A6. Using a 96 well metal replicator (Sigma), cells were transferred as spots onto appropriate agar plates and left to dry on the bench. The plates were incubated at 30^{o}C and in the case of temperature-sensitive tests plates were also incubated at 37^{o}C and 39^{o}C. The plates were incubated for 48 hr. and growth was monitored over that time.

2.10 Yeast transformation

In provision for this technique,

a) 1 M Lithium acetate was prepared by dissolving 10.2 g of Lithium acetate in 100 ml of dH_2O, followed by autoclaving the mixture. 100 mM Lithium acetate was prepared by mixing 1 ml of 1 M Lithium acetate with 9 ml of sterile dH_2O. Stocks were stored at RT.

b) 50% (w/v) polyethylene glycol (PEG) stock solutions were prepared by mixing 50 g PEG with 50 ml of dH_2O and adjusting it to a final volume of 100 ml with dH_2O, followed by autoclaving. PEG Stocks were stored at RT.

c) Carrier DNA was prepared by adding 200 mg of single stranded DNA into 100 ml of 10 mM Tris/1 mM EDTA solution. This gave a final carrier DNA concentration of 2 mg/ml. The 100 ml stocks were separated into 1 ml volumes in fresh 1.5 ml microfuge tubes (Eppendorf) and boiled at 100^{o}C for 5 min. on an Accublock Digital Dry Bath (Labnet International.Inc). The tubes were subsequently cooled on ice and stored at -20^{o}C.

d) DNA mix was prepared, for transformation into the competent yeast cells. For plasmid DNA transformations, 5 µl plasmid was added to 45 µl molecular H_2O. For cloning an insert into a vector, various volumes of both insert and vector DNA were added together for transformation.

e) 10 mM Tris/1 mM EDTA solutions in which the carrier cDNA was dissolved were prepared by making a 100X stock concentration. 12.14 g Tris and 2.92 g EDTA were added together and adjusted to 100 ml with dH_2O. The pH was adjusted to 7.5. The solution was autoclaved and 1 ml was removed and added to 99 ml sterile dH_2O to give a final concentration of 10 mMTris/1 mM EDTA.

2.10.1 Preparation of competent yeast

Yeast strains were inoculated as previously described in section 2.7.1. The following morning, the 5 ml overnight cultures were added to 50 ml fresh suitable liquid media. Yeast cultures were incubated at 30^oC shaking for a further 3-5 hr. until cell concentrations reached 1-2 x 10^7cells/ml. The cells were harvested by centrifugation at 1258 x g, washed in 25 ml of sterile dH_2O and centrifuged again. The supernatants were disposed of and pellets were resuspended in 1 ml of 100 mM Lithium acetate. The cells were transferred to microfuge tubes and pelleted in a table top centrifuge (Centrifuge 5415D, Eppendorf AG, Hamburg) at 15700 x g for 5 sec. and resuspended in 500 µl of 100 mM Lithium acetate. These cells could be stored at 4^oC for 1-2 weeks or used immediately for transformation.

2.10.2 Transformation of competent yeast with DNA

50 µl aliquots of competent yeast cell suspensions were added to fresh microfuge tubes and pelleted for 5 sec. Residual lithium acetate was removed. The following components were added to each microfuge tube in the order listed:

240 µl 50% (w/v) PEG

36 µl 1 M Lithium acetate

25 µl single stranded carrier DNA (taken from 2 mg/ml stock)

50 µl mix of molecular H_2O and desired DNA

The cell suspensions were mixed and incubated at 30°C for 30 min. The mixtures were then heat-shocked at 42°C in an Accublock Digital Dry Bath (Labnet International.Inc) for 20-25 min. The microfuge tubes were centrifuged at 15700 x g for 15 sec. and the pellets were resuspended in 200 µl of dH_2O and plated onto selective agar plates. These plates were incubated at 30°C for 2-3 days.

2.11 *E. coli* transformation

2.11.1 Preparation of competent *E. coli*

E. coli DH5α were inoculated in 10 ml of LB media and incubated overnight at 37ºC 200 rpm. The following day, the 10 ml culture was added to 1 l of LB media and incubated for 2 hr. at 37°C (200 rpm). This culture was split into 4 x 250 ml centrifugation tubes and chilled on ice for 10 min. The cells were centrifuged at 5000 rpm for 10 min. at 4ºC, in a GSA rotor. The pellets were resuspended in 10 ml RF1 Buffer (table 2.10) and kept on ice for 30 min. The cells were then centrifuged at 3220 x g for 10 min. at 4ºC and each pellet was resuspended in 3.2 ml RF2 Buffer (table 2.11). The tubes were kept on ice for 15 min. 100 µl aliquots were transferred into pre-cooled 1.5 ml microfuge tubes and the cells were stored at -70°C.

Table 2.10 Components of buffer RF1 used in the preparation of competent *E. coli*.

Component	Amount added	Final concentration/volume
K-Acetate	1.47 g	30 mM
$CaCl_2.2H_2O$ (dihydrate)	5 ml 1 M	10 mM
Glycerol	7.5 ml	15%
dH_2O		Adjusted to 450 ml*
RbCl	6 g	100 mM
$MnCl_2.4H_2O$ (tetrahydrate)	4.95 g	50 mM
dH_2O		Adjusted to 500 ml

* At this point, solution was adjusted to pH 5.92 with 0.2 M acetic acid (0.2 M = 3 g in 250 ml dH_2O).

Table 2.11 Components of buffer RF2 used in the preparation of competent *E. coli*.

Component	Amount added	Final concentration/volume
RbCl	5 ml 1 M	10 mM
$CaCl_2.2H_2O$	5.5. g	75 mM
dH_2O		Adjusted to 500 ml

All chemicals and solutions were added in consecutive order from top to bottom, as illustrated in the table. Both RF1 and RF2 buffers were filter sterilised and stored at 4ºC prior to use.

2.11.2 *E. coli* transformation (long method)

1-20 µl (approximately 1 µg) of plasmid DNA was added to 100 µl competent *E. coli* and incubated on ice for 30 min. The cells were subjected to 42ºC for 1 min. on a digital dry bath followed by immediate recovery by adding 1 ml of liquid LB to each 1.5 microfuge tube. The tubes were incubated at 37^{o}C shaking for 1 hr. and then plated onto LB-amp agar. These plates were incubated overnight at 37^{o}C.

2.11.3 *E. coli* transformation (5 min. method)

To ensure optimum conditions for efficient transformation, LB-amp plates were incubated at 37ºC for approximately 1 hr. prior to transformation. 50 µl of competent *E. coli* were thawed on ice and 1-5 µl plasmid DNA was added. These mixes were maintained on ice for 5 min., then plated onto warm LB-amp plates and incubated at 37ºC overnight.

2.12 Yeast genomic DNA isolation

In provision for this technique,

a) 1 M sorbitol/100 mM EDTA solutions were prepared by dissolving 18.2 g of sorbitol in 20 ml warm dH_2O and adding 2.92 g of EDTA. The solutions were adjusted to 100 ml with dH_2O, autoclaved and stored at RT.

b) Zymolase stocks were prepared by adding 500 mg of zymolase (Sigma) to 100 ml of dH_2O and filter sterilising. The stocks were aliquoted into 1 ml volumes and stored at -20^oC.

c) 1 M Tris/100 mM EDTA solutions were prepared by dissolving 2.92 g of EDTA and 12.1 g of Tris in 20 ml of dH_2O and adjusting the final volume to 100 ml with dH_2O. The solutions were autoclaved and stored at RT.

d) 10% (w/v) Sodium dodecyl sulfate (SDS) solutions were prepared by dissolving 10 g of SDS in 20 ml of dH_2O and adjusting the final volume to 100 ml with dH_2O. The solutions were autoclaved and stored at RT.

e) 5 M potassium acetate (KAc) solutions were prepared by dissolving 49 g of KAc in 20 ml of dH_2O and adjusting the final volume to 100 ml with dH_2O. The solutions were autoclaved and stored at RT.

To isolate genomic DNA from a desired strain, yeast were inoculated in 2 ml YPD and incubated overnight shaking at 30°C. The cells were pelleted at 1258 x g for 5 min. and pellets were resuspended in 150 µl of 1 M sorbitol/100 mM EDTA and transferred to 1.5 ml microfuge tubes. 12 µl of 5 mg/ml zymolase was added to each set of cells and the tubes were incubated for 1 hour at 37°C. The mixtures were centrifuged at 15700 x g for 5 sec. and resupended in 150 µl of 1 M Tris/100 mM EDTA. 15 µl of 10% (w/v) SDS was mixed with the cell suspensions and solutions were incubated at 65°C for 30 min. 60 µl of 5 M KAc was added to each tube and tubes were chilled on ice for 1 hr. The resulting mixtures were centrifuged at 15700 x g for 5 min. and the supernatants were retained. 195 µl of Isopropanol was added to each supernatant and

tubes were maintained for 5 min. at RT, to allow precipitation of DNA. The tubes were then centrifuged at 15700 x g for 10 sec., supernatants were removed and pellets were allowed to air dry. The DNA pellets were resuspended in 45 µl dH_2O and stored at -20°C.

2.13 Isolation of plasmid DNA from yeast

To isolate plasmid DNA from yeast, cells were inoculated overnight in 5 ml selective media at 30ºC, 200 rpm. The cells were harvested by centrifugation at 1258 x g for 5 min. All buffers used in this procedure were purchased in a plasmid miniprep kit from QIAGEN. The cell pellets were resuspended in 250 µl Resuspension Buffer in 1.5 ml microfuge tubes and approximately 200 µl of 0.5 mm soda lime glass beads (Biospec products Inc.) were added to the cell suspensions. The cells were vortexed (Vortex-2 Gene, Scientific Industries) for 5 min. at maximum speed. At this stage the glass beads were at the bottom of the microfuge tubes and the liquid cell mixtures were carefully removed. 250 µl of Lysis Buffer followed by 350 µl of Neutralising Buffer were added to the cells, mixed well and centrifuged for 10 min. at 15700 x g. The supernatants were then removed and transferred to DNA binding columns (QIAGEN) where they were centrifuged for 1 min. at 15700 x g. Flow-through into the catchment tubes were discarded and 750 µl of Wash Buffer was added to each column, this was followed by centrifugation for 1 min. at 15700 x g. Flow-through was discarded and columns were centrifuged for an additional min. to remove any residual buffer from the binding column. DNA was eluted by adding 50 µl of Elution Buffer directly into the binding columns and allowing them to sit for 1-2 min. The binding columns were transferred to fresh 1.5 ml microfuge tubes and plasmid DNA was isolated by a final 1 min. centrifugation at 15700 x g.

To ensure plasmid DNA was at an ideal concentration for further experimentation (ideal amount is 100-500 ng/µl), 17 µl of each DNA elution was transformed into *E. coli* by the 'long' method of transformation (section 2.11.2). Plasmid DNA was finally isolated by additional steps that will be discussed in section 2.14.

2.14 Isolation of plasmid DNA from *E. coli*

Following transformation of plasmid DNA into *E. coli*, individual bacterial colonies were isolated from the LB-amp plates. To isolate this DNA, a single colony was inoculated in 5 ml of LB-amp liquid and grown overnight at 37°C 200 rpm. The next day, cells were harvested by centrifugation for 5 min. at 3220 x g. All buffers used in this procedure were purchased in a plasmid miniprep kit from QIAGEN. The cell pellets were resuspended in 250 µl Resuspension Buffer. 250 µl of Lysis Buffer followed by 350 µl of Neutralising Buffer were added to the cells, mixed well and centrifuged for 10 min. at 15700 x g. The supernatants were then removed and transferred to DNA binding columns where they were centrifuged for 1 min. at 15700 x g. Flow-through in catchment tubes was discarded and 750 µl of Wash Buffer was added to each column, this was followed by centrifugation for 1 min. at 15700 x g. Flow-through was discarded again and columns were centrifuged for an additional 1 min. to remove any residual buffer from the binding column. DNA was eluted by adding 50 µl of Elution Buffer directly into the binding columns and allowing it sit for 1-2 min. The binding columns were transferred to fresh 1.5 ml microfuge tubes and plasmid DNA was isolated by a centrifugation at 15700 x g. Plasmid DNA was stored at -20°C.

2.15 Monitoring the presence of the prion [*PSI*$^+$] in *S. cerevisiae*

The presence or absence of the [*PSI*$^+$] prion can be monitored in yeast strains by a simple colour assay (figure 2.1).

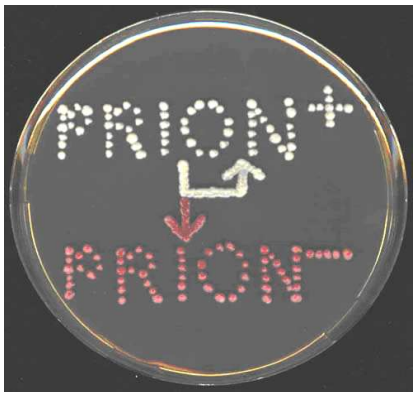

Figure 2.1 Monitoring the presence/absence of [*PSI*$^+$] using a simple colour assay. [*PSI*$^+$] cells grow as white colonies on media containing limited adenine, while [*psi*$^-$] cells grow as red colonies.

It can thus be determined whether or not the cells contain the prion ([*PSI*$^+$] cells) or do not ([*psi*$^-$] cells). The strains that we use to carry out experiments involving the monitoring of [*PSI*$^+$] contain an ochre mutation (*ade2.1*) in a gene responsible for adenine biosynthesis. Sup35p is a *S. cerevisiae* protein involved in translation termination and when in its fully functional state, halts translation at this premature stop codon, leading to the build-up of a red pigment in the cells. These cells are clearly seen as red when grown with limiting amounts of adenine. When Sup35p aggregates into a non-functional form it is called [*PSI*$^+$], and there is subsequently reduced translation termination of the *ade2* gene and cells appear white on limiting adenine media (figure 2.2).

A second way of monitoring the presence of [*PSI*$^+$] is by growth of yeast cells on medium lacking adenine. [*PSI*$^+$] cells grow on medium lacking adenine whereas [*psi*$^-$] cells do not. This is because [*PSI*$^+$] cells produce functional Ade2p which is involved in

the adenine biosynthesis pathway. In [*psi*$^-$] cells the adenine biosynthesis pathway is disrupted and cells require supplemented adenine for normal growth.

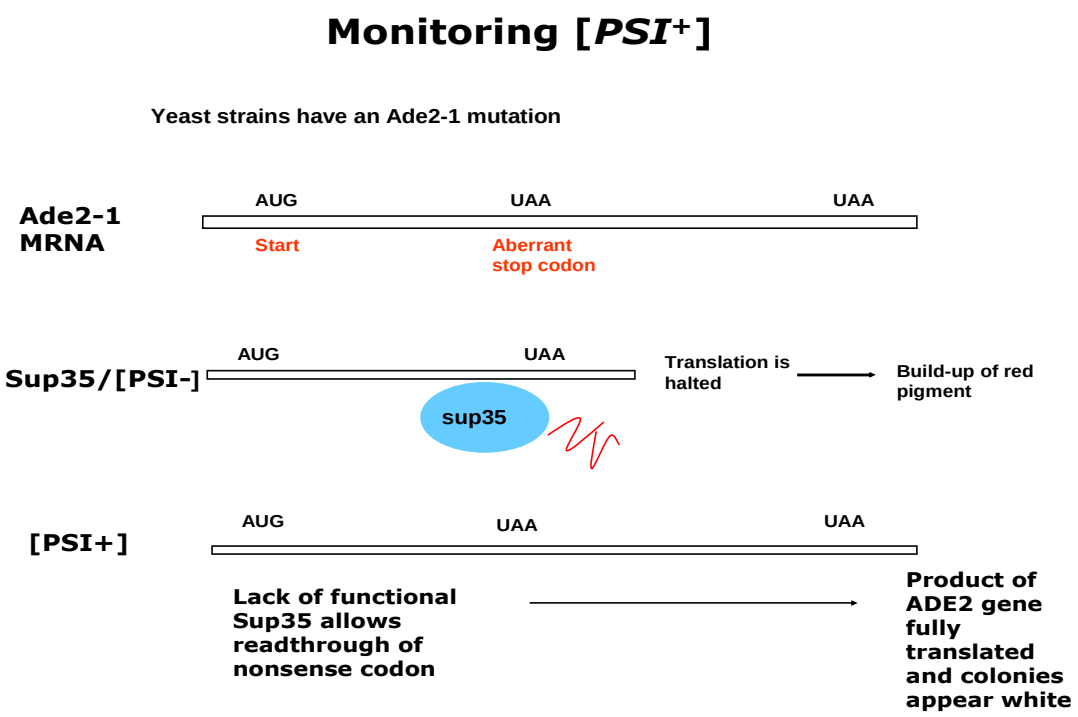

Figure 2.2 Consequences of [*PSI*$^+$]. Non-functional, aggregated Sup35p [*PSI*$^+$] allows readthrough of the *ade2-1* mutation.

2.16 Thermotolerance Assay

Yeast strains were prepared for comparative growth analysis as described in section 2.9. On the second day, after cultures were grown and resuspended to a final concentration of 5x10^6 cells/ml in 14 ml round-bottom tubes, cells were exposed to a temperature of 39ºC (200 rpm) for 1 hr. This temperature exposure can result in the induction of Hsp104p, which is important in conferring cellular thermotolerance, preventing denaturation of proteins when cells are undergoing heat stress. Subsequent to this, cell aliquots were maintained at 52ºC (200 rpm) for 0, 10, 20, 30 and 40 min., or 0, 2, 4, 6, 8, and 10 min., with cells undergoing heat-shock. Cells were immediately transferred to ice when removed from incubation. Comparative growth analyses were then carried out by making a 1/5 serial dilution as described in section 2.9. Cells were

plated on various plates dicatated by the nature of the experiment and incubated for 48 hr. at 30^{o}C.

2.17 Luciferase Assay

Prior to carrying out the luciferase assay, strains to be tested were transformed with the pDCM90 plasmid, following the method described in section 2.10. 1 mg/ml cycloheximide stocks were prepared by adding 5 mg of cycloheximide to 5 ml of sterile dH_2O. These were aliquoted and stored at -20^{o}C.

To perform the luciferase assay, yeast strains were cultured overnight in 5 ml of SC –uracil media to select for cells containing the plasmid. The following morning, cultures were diluted back to OD_{600} 0.2 and incubated for 1 hr. at 37^{o}C, 200 rpm, to induce expression of heat-shock proteins. Cellular luciferase activity of each strain was then measured in triplicate, by adding 10 µl of decanal to 200 µl of culture in 5 ml rohren tubes (Sarstedt). An FB 12 Luminometer (Berthold Detection Systems) was used to obtain the luciferase activity readings, which were taken as 100% activity readings. Cells were then incubated at 45ºC (200 rpm) for 50 min., after which cycloheximide was added at a concentration of 10 µg/ml to prevent protein synthesis activity and *de novo* synthesis of heatshock proteins. Cultures were then incubated at 45ºC for a further 10 min. After this 1 hr. heatshock, cellular luciferase activity of each strain was measured as before, in triplicate. If heatshock worked successfully, readings were at most 10% of those recorded as 100% activity levels.

Cultures were then shifted to 25ºC to let the cells recover from heatshock. After 30 min. at 25ºC, luciferase activity readings were taken again, as before, followed by readings after 60, 90, 120 and 150 min. at 25ºC.

When testing the effects of drugs on luciferase activity and recovery, cells were pre-exposed to the drug(s) at an appropriate concentration for 1 hr. at 30ºC (200 rpm), prior to the 1 hr. 37ºC incubation.

2.18 Carbon-14 [^{14}C]-GdnHCl uptake assay

All work requiring the use of [^{14}C] was carried out in a certified radiation suite. In preparation for [^{14}C] work, the workstation was decontaminated using 2% (v/v) Decon. A portable Geiger counter (Mini Instruments, Series 900 EP15 contamination meter, Perspective Instruments) was placed beside the workstation to record any airborne radiation. A personal Geiger counter (Perspective Instruments) was also worn to record personal radiation exposure.

Yeast strains were cultured overnight in 10 ml YPD. The following morning, cultures were diluted to OD_{600} 0.2 in 40 ml fresh YPD. 1 mM GdnHCl was added to the cultures (50 µl of 100 mM GdnHCl stock) and cultures were transferred to sterile flasks. To these flasks, [^{14}C]-labelled GdnHCl (American Radiolabeled Chemicals, Inc.) was added at a concentration of 0.05 µCi/ml from a 0.1 mCi/ml stock. At this point (T=0), in duplicate, 5 ml samples were removed from flasks and and transferred to 14 ml round-bottom tubes. Samples were centrifuged for 5 min. (1258 x g) and 1 ml of supernatants were removed to 1.5 ml microfuge tubes. The remaining supernatants were discarded and pellets were washed and resuspended in 1 ml sterile dH_2O. Both pellets and supernatants were stored at 4ºC until readings were taken. The flasks were incubated at 30ºC in a hybaid oven contained within in a fume hood. 5 ml samples were taken in duplicate after 2 and 4 hr. and prepared in the same way as before. Prior to sampling, OD_{600} was measured using a spectrophotometer. When all samples were prepared, [^{14}C]-labelled GdnHCl readings were made of all pellets and supernatants using a Beckman Scintillation Counter.

Molecular Techniques

2.19 Polymerase Chain Reaction (PCR) analysis

2.19.1 PCR amplification

All primers were purchased from Sigma in the de-salted powder from. The primers were dissolved in molecular-grade H_2O to give a final 100 µM concentration. The volume of water to be added was indicated on the specific primer sticker, as provided by Sigma. From these, 10 µM working stocks were made up by adding 10 µl of 100 µM stock to 90 µl molecular-grade H_2O (1/10 dilution). All primer stocks were stored at -20ºC. Two enzymes were used, depending on the experiment being carried out, taq polymerase or Platinum/High-Fidelity taq. PCR cycle conditions were thus adjusted accordingly. PCRs were carried out using a Peltier Thermal cycler (MJ Research) in sterile PCR tubes (Starstedt). Table 2.12 lists the specific PCR reaction mixtures and cycle conditions for the appropriate product. Tables 2.13-2.17 list primers used for PCR.

Table 2.12 PCR reaction mixtures and PCR cycles.

PCR	PCR mixture component	Volume added (µl)	PCR cycle conditions
PCR for diagnostic tests	*Taq* Buffer (New England Biolabs, NEB)	2	94°C 4 min. 94°C 1 min. 55°C 1 min.
	dNTP mix (Sigma)	1	72°C 1 min. per kb
	Forward primer	1	Cycle to step 2 x 30
	Reverse primer	1	times
	$MgCl_2$ (NEB)	1	72°C 6 min.
	Template DNA	2	4°C overnight
	Taq Polymerase (NEB)	0.5	
	Molecular-grade water	11.5	
PCR of template DNA for cloning/genomic knockout	Platinum/High Fidelity *Taq* Buffer (Invitrogen)	5	94°C 2 min. 94°C 30 sec. 55°C 30 sec.
	dNTP mix	2	68°C 1 min. per kb
	Forward primer	2	Cycle to step 2 x 30

Reverse primer	2	times
$MgSO_4$ (Invitrogen)	2	72°C 6 min.
Template DNA	2	4°C overnight
HF *Taq* Polymerase (Invitrogen)	0.5	
Molecular-grade water	34.5	

Table 2.13 Primers for *GliT* cloning.

Primer	Oligonucletide sequence
Cloning *GliT* into pC210 F	AGATTTTATACAGAAATATTTAT ACATATGATGTCGATCGGCAAAC TACTCTCCAAC
Cloning *GliT* into pC210 R	TTCCTGATTAAACAGGAAGACAA AGCATGCCTATAGCTCCTGATCG AGACGAAAC
Cloning *GliT* into pYES2 F	CTGTAATACGACTCACTATAGGG AATATTAATGTCGATCGGCAAAC TACT
Cloning *GliT* into pYES2 R	CATGATGCGGCCCTCTAGATGCA TGCTCGACTATAGCTCCTGATCG AGAC

Table 2.14 Primers for qPCR. Primers anneal within gene sequence.

Gene name	Oligonucleotide sequence
ERG9 F	GACTTATTTGGCCGGTATCCA
ERG9 R	GCGACACAGCCACGCAAAGTCC
VMA6 F	GGGGATTTTTGGAGACTGGT
VMA6 R	GTGCGATACATTCTGCAATCCAGG
MET7 F	CTAAGTGGGAAGGCAGATGTCAAG
MET7 R	TCTGGCGAAACAGATGAGTACAGG
SAM1 F	TGCCTTCTCCGGTAAGGACTACTCT
SAM1 R	AGACTTGGTCGCAGTACCATAGGTG
MET6 F	ATTCAACAAGGGCACCATCTCTG
MET6 R	TGGTCTGGACAAGTCACCAACAA
MET16 F	CAATTGGACGTTCGAGCAGGTTA
MET16 R	CCCTTCCATCTTCCTGCTCTCTC
MET17 F	TCAACTACACGCCGGCCAAGAGA
MET17 R	AAACAGCCAAAGCAGCAGCACCA
MET2 F	ATTGAATCTCCCGAAGGCCACGA
MET2 R	TTCGGCCTCACCAAAGACAGACG
MET14 F	TGGTGACAACATTCGTTTTGGATTGA
MET14 R	GGGTCCCTTTGCTCAGCGACTTC
MET22 F	GGCAACGTTATTGTCCATGAAGC

MET22 R	CGCATGATGTAGACACCACCAAG
HBN1 F	CTAGTTTCGCGGACCATACCTC
HBN1 R	GGTCCAAGACTCAGGGATTTTG
JEN1 F	GTGTCTTTGGTGTCTGGGGTATC
JEN1 R	AGAGCACCAGAGGCATCTCTTT
SIP18 F	CATGGACATGGGTATGGGTCAT
SIP18 R	ATCGTTCGCAATTCCTCTGC
BDH2 F	CATGTGCTACACACACCACGAT
BDH2 R	CTCCGTGATTGTTTGGAGTCAG
SDH2 F	AAGGATGGAACGGAAGTGCTAC
SDH2 R	TGTTCTTGGTTCCACCAGTACG
MLS1 F	GTTGCAGTACATGGAAGCTTGG
MLS1 R	GGACTTGCCTTAGACAGTCTTTCC

Table 2.15 Primers for cloning *GSH1*.

Primer	**Oligonucleotide sequence**
Cloning *GSH1* into pRS315 F	GGTGGCGGCCGCTCTAGAACTAGTGG ATCCGCTCTTGAATGGCGACAGCC
Cloning *GSH1* into pRS315 R	CCCCTCGAGGTCGACGGTATCGATAA GCTTTTAACATTTGCTTTCTATTG

Table 2.16 Primers for *HBN1* knockout *HBN1*::*HIS5*.

Primer	**Oligonucleotide sequence**
HBN1 knockout in wildtype F	AGACTGAAGTATCCTATATCAACA TATATACAAAAAAACAATCCAATA TCATGCAGCTGAAGCTTCG
HBN1 knockout in wildtype R	GACGTTCGCATTTAATCTATACCTA TAATTCTGTACTTATATACTGTTCC TTAGCATAGGCCACTAGTGGATCT G
HBN1 knockout in Δ*frm2* F	CCGCTCCTTCTCCTAACATCAA
HBN1 knockout in Δ*frm2* R	TACGAGCCTAGATTGACAGACG
Diagnostic *HBN1* knockout F	CTAGGGTCTTGGCATTTGCAC
Diagnostic *HBN1* knockout R	CGATGGATGGTGTCTGGTAGAA
HIS5 internal F	GGGTAGGAGGGCTTTTGTAGAA
HIS5 internal R	GCGCTTTCAGCACGATGATGGT

Table 2.17 Primers for sequencing YEp13.

Primer	**Oligonucleotide sequence**
Sequencing primer F	GCCAGTCACTATGGCGTGCTGC
Sequencing primer R	CGCCGAAACAAGCGCTCATGAG

2.19.2 Agarose gel electrophoresis

PCR products were resolved on 0.8% (w/v) agarose gel at 90 V for 45 min. in a Biorad electrophoresis power-pack. 0.8% (w/v) agarose was dissolved in 50 ml of 1X TAE Buffer (Millipore), boiled and allowed to cool. Once cooled, 1 µl of a 10 mg/ml ethidium bromide solution was added to make a final concentration of 0.2 µg/ml. Care was taken when handling the carcinogen ethidium bromide. All materials that were in contact with the agent were disposed of in a separate ethidium bromide waste container. The molten agarose was poured into a casting rig and allowed to set. PCR products (3 µl) were mixed with 1 µl of 6X Blue Loading Dye (NEB) and 2 µl of dH_2O. When set, the gel was submerged in 1X TAE Buffer and the PCR products were added to the wells alongside a 1 kb molecular grade marker (NEB), which had been as prepared in the same way as the PCR products.

2.20 DNA sequence analysis

Yeast genomic or plasmid DNA was prepared as described in sections 2.12 and 2.13. DNA concentrations were measured using a Nanodrop Spectrophotometer (Nanodrop 1000, Thermo Scientific). It was ensured that the DNA concentrations were not less than 200 ng/ml. For each piece of DNA to undergo sequence analysis, 3 µl of DNA and 4 µl forward primer were added to 3 µl molecular H_2O in a microfuge tube, giving a final volume of 10 µl. This was then repeated using the reverse primer. Microfuge tubes were tagged with a prepaid barcode and samples were sent to Agowa Sequencing Services Berlin, Germany. DNA was sequenced by dye-terminator sequencing and results were available on the Agowa website. Sequencing results were analysed using the BLAST function on NCBI.

2.21 Cloning DNA into plasmid vector by homologous recombination

To clone genes into plasmids, yeast were employed to do so by homologous recombination/gap repair. In this study, three plasmid clones were created, *GliT*-pC210, *GliT*-pYES2 and *GSH1*-pRS315.

2.21.1 Creating DNA fragment for cloning

Firstly, primers were designed to PCR amplify the region of interest to be cloned into a plasmid e.g. PCR reaction was set up to amplify *GliT* from the topovector plasmid. Primers were designed to create the product with overhangs both up- and downstream which were homologous to regions of the plasmid, into which the gene would be cloned. These primers annealed to approximately 30 bp of the gene of interest coding regions and incorporated approximately 30-40 bp of DNA sequence from the plasmid vector as overhangs. The PCR cycle used is described in table 2.12 and primers are listed in tables 2.13 and 2.15. HF *Taq* has better proof-reading than *Taq* and so was used for cloning. The PCR product sizes were confirmed by gel electrophoresis.

2.21.2 Restriction digest of plasmid DNA

Prior to digestion, plasmid DNA was prepared as described in section 2.14. When a high concentration of plasmid DNA was obtained (ideally over 200 ng/µl), restriction digests of the plasmids were set up.

pC210 vector DNA was digested with enzymes *Nde*I and *Sph*I (both NEB) in order to linearise the DNA and remove the *SSA1* gene. 4 µg plasmid was digested using 2 µl of each enzyme. 5 µl of NEB buffer 4 was added to this reaction and the volume was brought to 50 µl total with molecular-grade H_2O. pRS315 was digested with *BamH*I and *Hind*III (both NEB) to linearise the plasmid. 4 µg plasmid DNA was digested using 2 µl of each enzyme, 5 µl of NEB buffer 2 was added and the reaction

volume was adjusted to 50 µl with molecular-grade H_2O. pYES2 was digested with *Xho*I and *Hind*III to linearise the plasmid. 4 µg of plasmid DNA was digested using 2 µl of each enzyme, 5 µl of NEB buffer 2 was added and the reaction volume was adjusted to 50 µl with molecular-grade H_2O. For digestion to occur, reaction mixes were incubated in 1.5 ml microfuge tubes at 37ºC for approximately 3 hr.

2.21.3 Gel extraction and purification of digested plasmid DNA

After plasmids were digested, loading dye was added to the whole digestion reaction and run on an agarose gel (as described in section 2.19.2). The gel was then viewed under ultra-violet light to determine whether or not the digestion had been successful. After pC210 digestion with *NdeI* and *SphI*, the products visible under UV light were of approximately 2.2 kb and 6.7 kb. This demonstrated that *SSA1* had been removed from the rest of the plasmid, with a linear product remaining. The remaining plasmid fragments were removed for cloning. When pRS315 was digested successfully with *Bamh*I and *Hind*III, bands of approximately 6 kb was seen under UV light. These bands were excised from the gel. When pYES2 was digested using *Xho*I and *Hind*III, products of approximately 5.9 kb were seen and gel extracted.

Fragments were excised from the gel under UV light using a clean scalpel. The pieces of gel were added to 1.5 ml microfuge tubes and weighed on a fine balance. If the agarose gel weighed more than 400 mg then it was split into two microfuge tubes. Using a QIAGEN gel extraction kit, 3 volumes of Buffer QG was added to 1 volume of gel. The gels were then dissolved in the QG Buffer at 50^{o}C for 10 min. The dissolved samples were applied to QIAquick spin columns and centrifuged for 1 min. at 15700 x g. The flow-through was discarded and 750 µl Buffer PE was added to each column. The columns were centrifuged for 1 min., flow-through discarded and centrifuged for an additional min. 50 µl of Buffer EB was added to the columns and left to stand for 1 min.

DNA was eluted by centrifugation for 1 min. 3 µl of sample was analysed by agarose gel electrophoresis to confirm the presence of DNA.

2.21.4 Homologous recombination of vector and DNA fragment

Prior to cloning, yeast cells were prepared for transformation as described in section 2.10.1. The cells acted as vehicles for the cloning to occur. Figure 2.3 illustrates the methodology behind cloning by homologous recombination. Four DNA samples were prepared as follows: (a) 15 µl digested vector/35 µl insert, (b) 5 µl digested vector/20 µl insert (c) 10 µl digested vector/20 µl insert and (d)5 µl digested vector/20 µl molecular-grade H_2O. Each DNA mix was transformed into separate yeast cell aliquots as described in section 2.10.2. The cells were selected on SC-leucine (pRS315, pC210) and -uracil (pYES2). Any colonies that grew on these plates should have had an intact plasmid being expressed, as the wildtype cells used in this study cannot grow in the absence of these amino acids. When cloning worked successfully, there were colonies on plates a, b and c and there were no colonies on plated, as it had no intact vector.

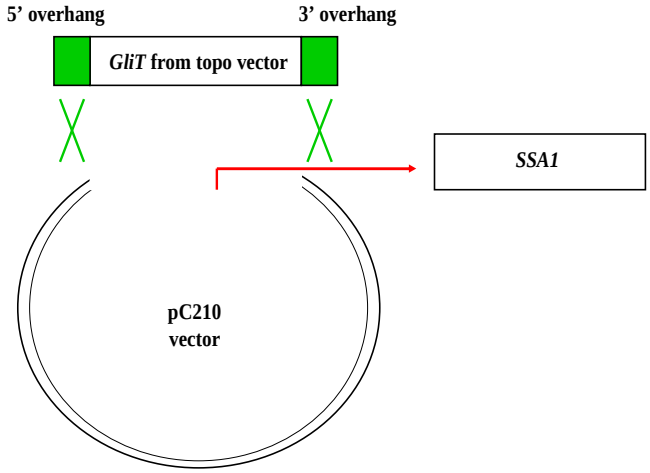

Figure 2.3 Cloning *GliT* into pC210. The *SSA1* gene which is found in the plasmid between the *Nde*I and *Sph*I restriction sites was first digested and removed from the plasmid. Then the *GliT* gene with 5' and 3' overhangs was cloned into the plasmid by homologous recombination.

Colonies from cloning plates a, b and/or c were replated onto fresh selective plates. After 48 hr., plasmids were extracted as described in section 2.13. These were then transformed into *E. coli* and isolated as described in sections 2.11 and 2.14. Each plasmid was enzyme digested as described in section 2.21.2 and examined by agarose gel electrophoresis. Potential clones should have at least two DNA bands, one corresponding to the linearised vector and the other the size of the gene cloned. This depends on where and how often the enzyme cuts.

The plasmids were sent to Agowa for sequencing to confirm the presence of the gene of interest. Figure 2.3 illustrates the methodology behind cloning by homologous recombination.

2.22 Knockout of genomic DNA by homologous recombination

Certain yeast knockout strains used in this study were purchased from EUROSCARF. All other strains were made in the laboratory. Yeast knockout strains were made by homologous recombination. This involves creating a gene disruption cassette that encodes a selectable marker. Located at either side of the selectable marker are segments of DNA homologous to the gene being knocked out. The knockout cassette incorporates itself into the genome at the corresponding chromosomal locus by homologous recombination. Genomic *HBN1* was knocked out in the wildtype BY4741 and Δ*frm2* backgrounds using the selectable marker *HIS5*. To replace *HBN1* with *HIS5* in the wild-type background, the *HIS5* gene, in addition to its promoter and terminator regions, was isolated from the pUG27 plasmid by PCR. These PCR products were created with overhangs homolgous to flanking regions of the gene to be knocked out, in this case *HBN1*. Conditions, reagents and primers are documented in tables 2.12 and 2.16. These products (50 µl) were then transformed into competent BY4741 cells, which were plated on synthetic complete plates lacking histidine (SC –histidine) to

select for mutants that can survive in the absence of exogenous histidine, i.e. cells in which *HBN1* was replaced by *HIS5*. Molecular-grade H_2O was also transformed into BY4741 as a negative control. Figure 2.4 represents this method.

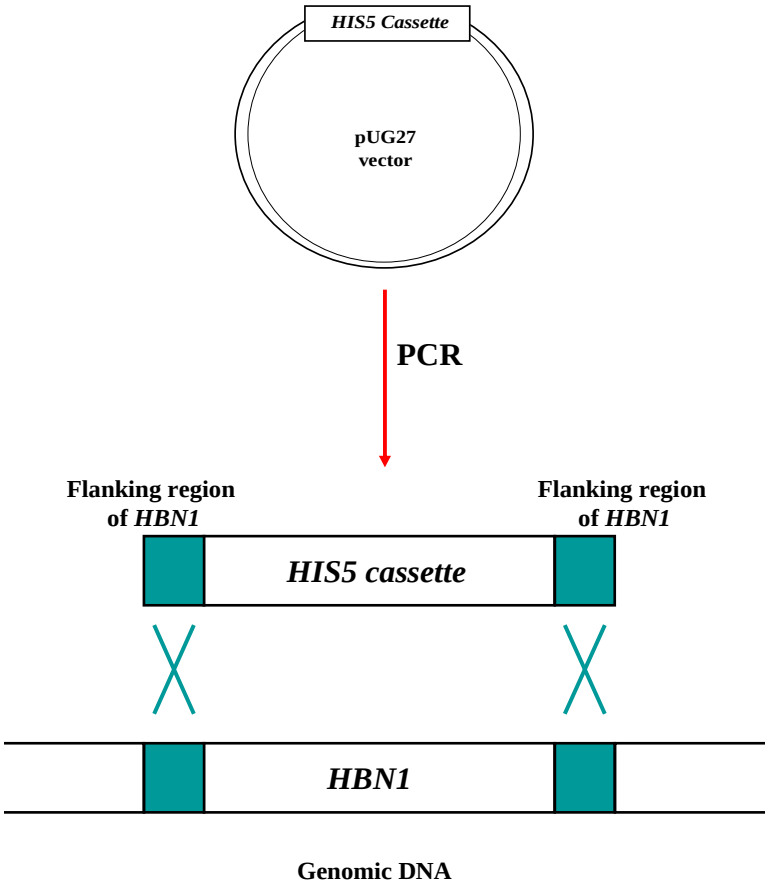

Figure 2.4 Method used to knock out genomic *HBN1* in BY4741 with *HIS5*. It was then possible to select for knockouts on –histidine plates.

To knock out *HBN1* in the BY4741 Δ*frm2* background, a similar method was employed. This time, the *HIS5* cassette was isolated from the BY4741 Δ*hbn1* strain by PCR. Primers were designed that annealed 343 and 264 bp up- and downstream of the *HIS5* region respectively (table 2.16). These products (50 µl) were transformed into competent BY4741 Δ*frm2* cells along with a molecular-grade H_2O negative control and selected on –histidine plates. Figure 2.5 illustates this method.

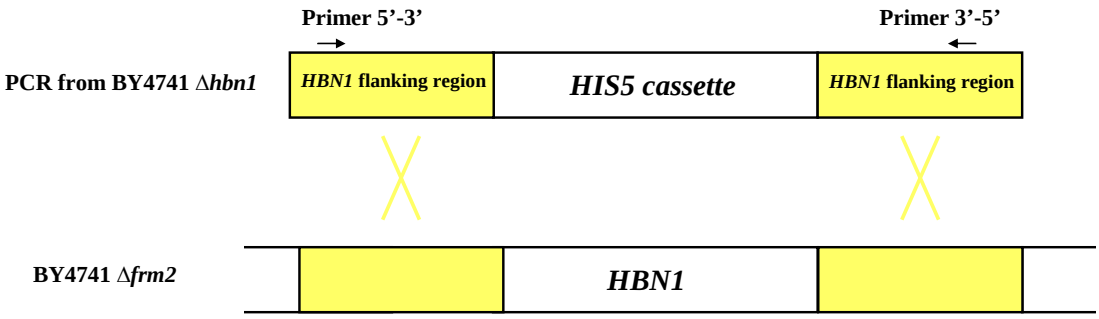

Figure 2.5 Method used to knock out genomic *HBN1* in BY4741 Δ*frm2* with *HIS5*. Knockouts were selected for on –histidine plates.

2.23 Real-time/quantitative PCR

Prior to RNA extraction, G600 cells were cultured overnight in 5 ml YPD. 1.5 ml of overnight cultures was added to 500 µl fresh YPD and gliotoxin was added at concentrations of 16 µg/ml and 64 µg/ml (32 µl and 128 µl of 1 mg/ml gliotoxin stock respectively). Cultures were exposed to gliotoxin for 1 hr. at 30°C, 200 rpm.

2.23.1 RNA extraction

Following 1 hr. gliotoxin exposure, RNA was extracted using the Qiagen RNeasy kit. Cells were harvested by centrifugation at 4°C (1258 x g, 5 min.). Cell pellets were resuspended in 600 µl Buffer RLT and transferred to 1.5 ml microfuge tubes. 0.5 mm soda lime glass beads were added at the same volume and the microfuge tubes were vortexed for 30 sec. and left on ice for 30 sec. This was repeated 5 times. Samples were then centrifuged at 4°C (700 x g, 3 min.) and supernatants were transferred to new 1.5 ml microfuge tubes. One volume of 70% (v/v) molecular ethanol (Merck) was added to lysates, mixed, transferred to spin columns and centrifuged at 4°C (9300 x g, 15 sec). 700 µl Buffer RW1 was added to columns and samples were centrifuged again at 4°C (9300 x g, 15 sec). 500 µl Buffer RPE was added to columns and centrifuged as above. Further 500 µl Buffer RPE was added to columns and

centrifuged at 4°C (9300 x g, 2 min.). RNA was eluted from columns in molecular H_2O through centrifugation (9300 x g, 1 min.).

2.23.2 RNA quantification

RNA concentrations were measured using NanoDrop 1000 Spectrophotometer (Mason Technologies).

2.23.3 DNAse treatment

DNA was removed using DNase I kit (Sigma). 1 µl 10X buffer and 1 µl DNase I were added to 1 µg RNA and volumes were brought to 10 µl with molecular H_2O. Solutions were incubated at RT for 15 min. Reactions were stopped by adding 1 µl EDTA solution and heated at 70ºC for 10 min.

2.23.4 RT-cDNA synthesis

cDNA was synthesized using Superscript III First-Strand Synthesis System (Invitrogen). To 8 µl DNase-treated RNA (from above reaction), 1 µl 50 µM oligo dT and 1 µl 10 mM dNTP were added. Solutions were incubated at 65ºC for 5 min., then chilled on ice. 10 µl reaction mix (2 µl RT buffer, 4 µl 25 mM $MgCl_2$, 2 µl 0.1M DTT, 1 µl RNase out, µl SSIII) was added and solutions were incubated at 50ºC for 50 min. Reactions were stopped by incubation at 85ºC for 5 min. Solutions were then chilled on ice. 1 µl RNase H was added to solutions, followed by incubation at 37ºC for 20 min. cDNA was then stored at -20ºC.

2.23.5 qPCR reaction

For each gene, both references and targets, a standard curve was first constructed. Five-sample serial dilutions (1:4) of the control cDNA (from non-treated cells) were

made and these were used as reaction template. Reaction mixes were prepared by combining 1 µl template cDNA, 1 µl forward primer, 1 µl reverse primer, 1 µl molecular H_2O (Roche) and 5 µl SYBR Green I Master reaction mix (Roche). These reactions were prepared in triplicate and loaded onto 96-well plates (Roche). For these standard samples, concentrations were assigned (table 2.18) and absolute quantification analysis using Lightcycler 480 (Roche) was performed, where only the fluorescence values measured in the exponentially growing phase of the PCR were taken into account during analysis. This analysis was then used to create a standard curve where the efficiency of the amplification reaction was calculated. When this data was generated, relative quantification analysis was carried out using experimental cDNA from cells exposed to 0, 16 and 64 µg/ml gliotoxin, in order to compare the level of expression of the gene in question. For this analysis, reaction efficiency was considered which had been calculated from the standard curve, as this maintains accuracy of the experiment. Before preparing reaction mixes using experimental cDNA, all cDNA was first diluted 1:1 to ensure that values would fall within standard values. Reaction samples were then prepared as before for standards, in triplicate and loaded onto 96-well plate. Absolute quantification and relative quantification analyses were carried out according to manufacturer's specifications. PCR conditions used are illustrated in table 2.19. Figure 2.6 depicts a typical example of how a 96-well plate may be laid out.

Table 2.18 Concentrations assigned to standards.

Standard number	Concentration
1	1000
2	250
3	62.5
4	15.625
5	3.90

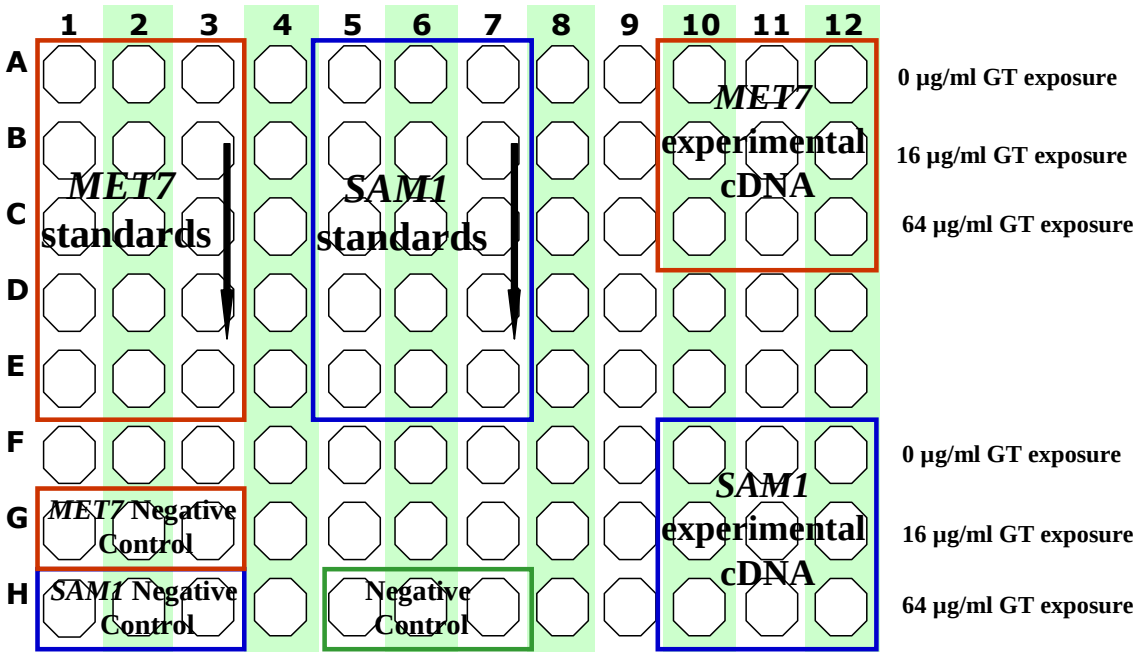

Figure 2.6 Example of how qPCR 96-well plate may be laid out.

Table 2.19 qPCR conditions. Conditions below are those used for *MET7*, *SAM1*, *MET22*, *MET6*, *MET16*, *MET17*, *MET2* and *MET14*. Annealing temperature 55ºC was changed to 56ºC for *JEN1*, *SIP18* and *BDH1*. Annealing temperature 55ºC was changed to 57ºC for *SDH2*, *MLS1* and *HBN1*.

Programme	No. Cycles	Temperature	Time
Pre-incubation	1	95ºC	10 min.
Amplification	55	95ºC 55ºC 72ºC	10 sec. 20 sec. 10 sec.
Melting Curve	1	95ºC 65ºC	5 sec. 1 min.
Cooling	1	37ºC	1 sec.

Proteomic Techniques

2.24 Western blot analysis

2.24.1 Preparation of cell lysates

Yeast strains were cultured overnight in 5 ml YPD or selective media The following morning, cells were diluted in 25 ml fresh YPD to an OD_{600} 0.1-0.2 and incubated as before, until an OD_{600} 0.6-0.8 was reached. Cells were harvested by centrifugation at 4ºC (5 min., 1258 x g) and pellets were immediately placed on ice. Pellets were resuspended in 750 µl cell lysis reagent and transferred to chilled 2 ml capped microcentrifuge tubes (Sarstedt) containing 0.5 mm soda lime glass beads. Tubes were inverted to remove air and additional lysis reagent was added if space remained. Cells were then bead-beated using a mini-beater (Biospec products) for 20 sec. and chilled on ice. This was repeated three times and tubes were then centrifuged (10 min., 4300 x g). Supernatants were transferred to pre-chilled 1.5 ml microfuge tubes and stored at -20ºC.

2.24.2 Protein quantification

5 µl thawed lysates and 5 µl cell lysis reagent (to provide blank) were added to 500 µl Bradford reagent (Quickstart Bradford dry reagent 1X, Biorad) and incubated at RT for approximately 20 min. Protein concentrations were determined using a Nanodrop spectrophotometer, Bradford Assay, following manufacturer's recommendations.

2.24.3 Preparation of Sodium Dodecyl Sulphate-Poly acrylamide (SDS-PAGE) gels

12.5% SDS-PAGE gels were prepared by mixing components listed in tables 2.20 and 2.21. Running gels were prepared first and allowed to set between two clean

glass plates (approximately 70% capacity of plates). 100% (v/v) isopropanol was added after running gel to ensure gel solidified with a level surface. Stacking gels were subsequently prepared and allowed to set between plates, above running gels, after isopropanol was discarded. Combs were placed between plates directly after stacking gel was added to create wells into which protein samples were placed.

Table 2.20 Composition of polyacrylamide running gel. All components of running gel stored at RT with the exception of 10% (w/v) APS (4ºC).

Reagents and quantities for 1 gel	Reagents and quantities for 2 gels
2.5 ml 4X Running Buffer (34.75 g Tris base and 4 g SDS dissolved in 500 ml dH_2O and adjusted to pH8)	3.75 ml 4X Running Buffer (34.75 g Tris base and 4 g SDS dissolved in 500 ml distilled H_2O and adjusted to pH8)
3.3 ml dH_2O	4.95 ml dH_2O
4.15 ml Protogel	6.225 ml Protogel
100 µl 10% Ammonium persulfate	150 µl 10% Ammonium persulfate
10 µl TeMed	15 µl TeMed

Table 2.21 Composition of polyacrylamide stacking gel. All components of stacking gel stored at RT with the exception of 10% (w/v) APS (4ºC).

Reagents and quantities for 1 gel	Reagents and quantities for 2 gels
1.25 ml 2X Stacking buffer (15 g Tris Base and 0.2 g SDS dissolved in 500 ml dH_20 and adjust to pH 6.8)	2.5 ml 2X Stacking buffer (15 g Tris Base and 0.2 g SDS dissolved in 500 ml dH_20 and adjust to pH 6.8)
0.825 ml dH_20	1.65 ml dH_20
400 µl Protogel	800 µl Protogel
25 µl 10% Ammonium persulfate	50 µl 10% Ammonium persulfate
2.5 µl TeMed	5 µl TeMed

2.24.4 SDS-PAGE

4X protein sample buffer (PSB) was made by mixing 625 µl of 10 mM Tris (pH 6.8), 500 µl of 200 mM EDTA, 15 ml of 20% (w/v) SDS, 10 ml of 100% (w/v) glycerol and a pinch of bromophenol blue. This was adjusted to 50 ml dH_20. 10X protein gel buffer was made by combining 15 g of Tris, 72 g of Glycine, 5 g of SDS and adjusting to 500 ml with dH_20.

PSB was added to required concentration of protein and boiled at 100ºC for 5 min. in a digital dry bath. The prepared protein gels were placed in an electrophoresis tank (Biorad) which was filled to appropriate level with 1X protein gel buffer made from 10X protein gel buffer. Combs were gently removed from gels and 10 µg of protein samples were loaded onto gel along with protein ladder (Page ruler plus prestained protein ladder 10-250 kDa, Fermentas, Life Sciences). Electric current (100 V, 50 mA/gel) was applied to gels (Biorad Powerpac Basic).

2.24.5 Protein transfer to PVDF membrane

Transfer Buffer was prepared by adding 3.03 g of Tris, 14.4 g of glycine and 200 ml of methanol, and adjusting to 1 l with dH_20. This was stored at -20ºC for approximately 1 hr.

For each protein gel, a PVDF membrane and four sheets of Whatman paper were cut to a similar size of the protein gel. PVDF membranes were soaked in 100% (v/v) methanol for a few seconds and then in dH_20 for 1 min. Membrane, Whatman paper and transfer sponges were all soaked in ice-cold transfer buffer for approximately 5 min. For each transfer, sponges were placed on each side of transfer case, followed by two sheets of Whatman paper on each side. The membrane was then placed on the clear side of the transfer case and the gel was placed on top of the membrane. The transfer case was closed, ensuring that no air bubbles were present and placed in the transfer tank (Biorad), with the clear side of the transfer case to the red side of the tank. The tank was filled with ice-cold transfer buffer, followed by addition of an ice block and a magnetic stirrer bar. An electric current was applied (100 V/ 350 mA/gel) for precisely 1 hr. while the buffer was stirred (Stuart Scientific magnetic Stirrer).

2.24.6 Protein detection using antibodies

10X TBS was formulated from 100 mM Tris pH 7.5, 1 M NaCl. From this, TBS-t was prepared by adding 50 ml of 10X TBS, 450 ml of sterile dH_2O and 500 µl of Tween. Both 10X TBS and TBS-t were stored at RT. Blocking solution consisted of 5% (w/v) Marvel milk powder in TBS-t.

The membranes were washed twice, at 5 min. intervals in 20 ml TBS-t and then blocked by incubation for 1-2 hr. at RT in 40 ml blocking solution. Following this, the membranes were incubated overnight, rocking (Rocker 35A, Labnet), with the primary antibody, diluted in 10 ml TBS-t according to manufacturer's recommendations (table 2.22). The membranes were subsequently washed three times, as before and then incubated with alkaline phosphatase-labelled secondary antibodies which were diluted in 10 ml of TBS-t according to manufacturer's recommendations (table 2.23). The membranes were probed with the secondary antibody for approximately 1-2 hr., rocking at RT. Following this, the membranes were washed three times, as before.

Table 2.22 Primary antibodies used in this study.

Name of Antibody	Animal of Origin	Source	Dilution
Hsp70 SPA-822	Mouse	Stressgen (Victoria, BC, Canada)	1/2,000
Hsp104	Rabbit	John Glover (University of Toronto)	1/150,000

Table 2.23 Secondary antibodies used in this study.

Name of Antibody	Animal of Origin	Source	Dilution
Anti-Mouse IgG (Fab specific) – Alkaline Phosphatase antibody	Goat	Sigma-Aldrich Chemical Co. Ltd. U.K.	1/2,000
Anti-Rabbit IgG (whole molecule) – Alkaline Phosphatase antibody	Goat	Sigma-Aldrich Chemical Co. Ltd. U.K.	1/2,000

2.24.7 Chemiluminescence and developing

The membranes were covered in 5 ml of Chemiluminescence substrate CDP-star (PerkinElmer) and rocked for 5 min. at RT. The membranes were then placed between two acetate sheets and in darkness, placed in an autoradiography cassette (FBAC 810 FisherBiotech). Kodak film (PerkinElmer) was placed on top of the membranes and the cassette was shut for varying times. The film was immediately transferred to developer (25 ml Kodak developer and 100 ml of dH_2O) for approximately 10 sec., or until image began to appear. The film was then washed in dH_2O and transferred to fixer (25 ml Kodak fixing solution and 100 ml of dH_2O) for approximately 30 sec. The film was washed in dH_2O and allowed to dry.

2.24.8 Stripping membrane

In order to probe a membrane with a second primary antibody, it was necessary to 'strip' the membrane to remove traces of the first antibodies used. The membranes were firstly washed twice for 5 min. with 5 ml of dH_2O, followed by 5 ml of TBS-t. This was followed by membrane incubation with 0.2 M sodium hydroxide for 5 min., rocking at RT. Sodium hydroxide was removed by washing with 5 ml of dH_2O for 5 min.

2.24.9 Coomassie staining of protein gels

Following electrophoresis, polyacrylamide gels were transferred to coomassie brilliant blue stain shaking, overnight at RT. The gels were washed with dH_2O and then incubated with destain solution (10% (v/v) Ethanol, 10% (v/v) Acetic acid and 80% (v/v) dH_2O) for 2 hr., or until enough stain was removed resulting in a clear band pattern.

2.24.10 Amido black staining of membrane

PVDF membranes were stained in 10 ml of amido black stain (0.1% (w/v) Naphthol blue black dissolved in 2% (v/v) acetic acid and 45% (v/v) MeOH) for 1 min. The membrane were then washed in dH_2O and incubated with destain (2% (v/v) acetic acid and 45% (v/v) Methanol) until a clear banding pattern appeared.

2.25 Two-dimensional gel electrophoresis (2D-GE)

2.25.1 Buffer preparation

In preparation for 2D-GE, buffers were prepared as below (tables 2.24-2.27)

Table 2.24 IEF Buffer constituents. The following were added together and IEF buffer was stored at -20ºC.

Component	Concentration	Quantity in 50 ml
Urea	8 M	24.024 g
Thiourea	2 M	7.612 g
CHAPS	4%	2 g
Triton X-100	1%	500 µl
Tris Base	10 mM	0.0606 g

Table 2.25 Rehydration Buffer (RB) constituents. The following were added together and rehydration buffer was stored at -20ºC.

Component	Concentration	Quantity in 50 ml
Urea	8 M	24.024 g
CHAPS	0.5%	0.25 g
Dithiothreitol (DTT)	0.2%	0.1 g
Ampholytes (GE Healthcare)	0.2%	100 µl

Table 2.26 IPG Equilibration Buffer constituents. The following were added together and IPG equilibration buffer was adjusted to pH 6.8 and stored at -20ºC.

Component	Concentration	Quantity in 500 ml
Glycerol	30%	150 ml
SDS	2%	10 g
Urea	6 M	180 g
Tris	50 mM	3.03 g

Table 2.27 10X SDS Buffer constituents. The following were added together and 10X SDS buffer was stored at RT.

Component	Concentration	Quantity in 2 l
Tris	25 mM	60.57 g
Glycine	192 mM	288.82 g
SDS	0.1%	20 g

2.25.2 Trichloroacetic acid (TCA) protein precipitation

Lysates were extracted as described in section 2.24.1. One volume of TCA was added to four volumes of thawed lysate in 1.5 ml microfuge tubes and incubated at 4°C for 10 min. Samples were then centrifuged at 15700 x g, for 7 min. and supernatants were removed. Protein pellets were washed in ice-cold acetone by resuspending in 200 µ acetone, followed by centrifugation for 7 min. at 15700 x g and removal of acetone. This wash step was repeated 3 times. Pellets were then dried by placing in a digital dry bath at 95ºC for 5-10 min., driving off acetone. Appropriate volumes of IEF buffer were thawed and DTT and ampholytes were added at concentrations of 65 mM and 0.8% (v/v) respectively. This was then used to resuspend pellets.

Precipitated proteins were quantified (section 2.24.2) and 10 µg of proteins were run under SDS-PAGE, followed by coomassie staining (2.24.9) to check for equal loading. It was ensured that the proteins had been quantified accurately and that equal loading was obtained before proceeding.

2.25.3 IPG strip rehydration

400-800 µg of precipitated proteins were added to thawed RB to give a total of 450 µl, e.g. if protein concentration was 4880 µg/ml, 122.95 µl (600 µg) wasadded to 327.05 µl RB to give a total of volume 450 µl. It was ensured that the exact same protein concentration, e.g. 600 µg was added for each sample to be run. A pinch of bromophenol blue was added to these protein samples, which were then pipetted into

lanes in an IPG strip rehydration tray (GE Healthcare). The plastic backing was removed from IPG strips (Immobiline Drystrip, pH3-10, 24 cm, GE Healthcare) which were then placed, gel-side down into the lanes containing protein samples. The strip codes were recorded to later identify protein samples. Cover fluid (GE Healthcare) was added to the lanes in the tray until the the strips were covered fully, to prevent strip dessication and the lid was closed tightly on the tray. The tray was incubated at RT for approximately 20 hr. Following this incubation, the strips immediately underwent isoelectric focusing.

2.25.4 Isoelectric focusing (IEF), first dimension

IEF was carried out on protein samples using Ettan IPGphor 3 IEF system (GE Healthcare), in which up to 12 strips could be run simultaneously. 108 ml of mineral oil (GE Healthcare) was added to the IEF tray in the IEF machine. The rehydrated strips were placed into the lanes of the IEF tray with gel sides facing up, ensuring that the strips were between lane notches and the positive strip ends were at the top of the tray. Electrode wicks (GE Healthcare) were soaked in MilliQ H_2O and placed touching both strip ends in between lane notches. Electrodes were fixed onto the tray, in contact with wicks and the machine lid was closed. The IEF instrument was closed and programme was run under conditions in table 2.28.

Table 2.28 IEF conditions.

Volts (V)	Time (hr.)
100	2
500	1.5
1000	1
2000	1
4000	1
6000	2
8000	3
500	4
8000	4

2.25.5 Preparation of 12% gels

12% gels were prepared by adding 280 ml of Protogel (National Diagnostics), 182 ml of Resolving Buffer (National Diagnostics), 230.3 ml of sterile dH_2O and 2.8 ml of 10% (w/v) APS. Glass plates (27 x 21 cm, GE Healthcare) were cleaned with 70% (v/v) ethanol, paired and placed into a gel casting system (GE Healthcare) with plastic spacers between plate pairs and filling casting cassette. The casting system was sealed tightly and clamped to prevent leakage. Immediately before casting, 280 µl of Temed was added to 12% gel solution and mixed gently. The gel was poured slowly into the caster and 0.1% 10X SDS buffer was sprayed on top to prevent bubble formation. The casting cassette was sealed with clingfilm and left overnight to allow gel solidification.

2.25.6 Gel electrophoresis, second dimension

In preparation for second dimension protein separation by electrophoresis, the IPG strips were equilibrated. Appropriate volumes of IPG equilibration buffer were thawed and Equilibration Buffer A was made by adding 2% (w/v) DTT while Equilibration Buffer B was prepared by adding 2.5% (w/v) Idoacetamide. A small amount of bromophenol blue was added to both buffers to act as a tracking dye. The strips were incubated in equilibration buffer A for 15 min., rocking, followed by equilibration buffer B for 15 min., rocking. Agarose sealing solution was then prepared, by combining 1.5 g of Trizma Base, 7.2 g of glycine, 0.5 g of SDS, 80 ml of dH_2O, 0.5 g of agarose (Electran), adjusting to 100 ml with dH_2O and adding a pinch of bromophenol blue. Each equilibrated strip was placed horizontally on top of a solidified 12% gel, gel-side facing backwards and positive side to the left. The agarose sealing solution was boiled and pipetted on to cover the strip completely, sealing it to the gel.

The Ettan DALTtwelve Separation unit (GE Healthcare) was used for second dimension protein separation by electrophoresis. The DALT was set to system circular

and 7.5 l of 1X SDS (made from the 10X stock) was added. When all gels and strips were prepared in the above described way, the gels were arranged in the DALT and spaces were filled using plastic spacers. 2.5 l of 2X SDS (made from the 10X stock) was poured into the filled DALT and the machine was closed tightly. The gels were run at 0.5 watt per gel for the first hour and 5 watt per gel for rest of programme, until the blue line from the tracking dye was no longer visible.

2.25.7 Coomassie staining (colloidal method)

A colloidal coomassie method was employed to stain the gels after electrophoresis. Immediately after the gels were removed from the electrophoresis tank, they were placed in coomassie staining solution made from 80 ml of stock A (table 2.29), 2 ml of stock B (table 2.30) and 20 ml of methanol.

Table 2.29 Constituents of coomassie stock A. Stock A was stored at RT following preparation.

Component	Concentration %	Amount added before adjusting to 1 l with dH_2O
Ammonium sulfate	10	100 g
Phosphoric Acid	2	20 ml

Table 2.30 Constituents of coomassie stock B. Stock B was stored at RT following preparation.

Component	Concentration %	Amount added before adjusting to 100 ml with dH_2O
Coomassie (Brilliant Blue G250, Serva)	5	5 g

The gels were incubated in the staining solution overnight, rocking at RT. The following day, the gels were removed from the staining solution and transferred to neutralisation buffer (table 2.31) for 1-3 min. and then washed in 25% (v/v) methanol for less than 1 min.

Table 2.31 Preparation of neutralisation buffer. Buffer was adjusted to pH 6.5 with phosphoric acid prior to use and stored at RT.

Component	Concentration	Amount added before adjusting to 1 l with dH_2O
Tris base	0.1 M	12.114 g

After the methanol wash, the gels were incubated in fixation solution (table 2.32) overnight, rocking at RT.

Table 2.32 Preparation of fixation solution. Solution was stored at RT following preparation.

Component	Concentration	Amount added before adjusting to 1 l with dH_2O
Ammonium sulfate	20%	200 g

This proceedure was repeated 3 times, after which the gels were placed between two sheets of acetate and scanned to record images.

2.26 Progenesis

Separated proteins were analysed using Progenesis™ same spot software. Protein spots were identified that showed differential expression resulting from different treatments.

2.27 Mass spectrometry (LC-MS)

2.27.1 Gel plug extraction

Gels of interest were placed on a clean, illuminated lightbox (A3 Lightbox, Hancock) and spots to be analysed were exised from the gels using a clean sharp scalpel. These gel plugs were placed in clean 1.5 ml microfuge tubes that were pre-cleaned using acetonitrile (ACN).

2.27.2 Gel destain

395 mg of ammonium bicoarbonate (AB) was added to 50 ml of HPLC-grade H_2O to prepare 100 mM ammonium bicarbonate solution. 5 ml was added to 5 ml ACN (1:1) and each gel plug was incubated in 100 µl of this with occasional vortexing at RT for approximately 30 min., until the stain was removed.

2.27.3 Tryptic digestion

20 µg of Trypsin (Promega) was reconstituted in 100 µl of reconstitution buffer (Promega). Aliquots were made and stored at -20ºC.

For trypsin digestion, 50 mM AB was prepared by adding 40 mg AB to 10 ml HPLC-grade H_2O. 500 µl was combined with 10 µl of reconstituted trypsin and this was added to each destained gel plug in the 1.5 ml microfuge tube. The plugs were then incubated at 4ºC for 30 min., after which additional AB was added, ensuring the plugs were covered. The plugs were then incubated for a further 90 min. at 4ºC, allowing diffusion of trypsin into the gel pieces. To ensure efficient tryptic digestion, the gel pieces were incubated at 37ºC overnight.

2.27.4 Peptide recovery

Microfuge tubes were centrifuged for 10 min. (9300 x g) and supernatants were transferred to new 1.5 ml tubes. Extraction buffer was prepared by adding one volume of 5% (v/v) formic acid to 2 volumes of ACN and (1:2). 100 µl of extraction buffer was added to each gel piece and the plugs were incubated at 37ºC for 15 min. (90 rpm approx.) Following this, the gel samples were centrifuged for 10 min. (9300 x g) and supernatants were added to supernatants isolated at the initial peptide recovery step. The extracts were dried overnight in a vacuum centrifuge (Eppendorf) and subsequently stored at -20ºC.

2.27.5 LC-MS preparation

Immediately prior to Mass Spectrometry analysis, the dried peptides were resuspended in 20 µl of 0.1% (v/v) formic acid and placed in a sonication bath for 5 min. The resuspended peptides were added to 0.22 µm centrifuge tube filters (Costar) and centrifuged for 15 min. (9300 x g) at 4°C to remove impurities. 20 µl of purified peptides were placed in mass spectrometry vials (Agilent) for analysis, which was achieved using an Agilent 6340 Ion Trap Liquid Chromatography Mass Spectrometer.

2.28 Enzymatic assay of gliotoxin reductase activity

2.28.1 Buffer preparation

Prior to performing this assay, buffers were prepared, filter sterilised and stored at 4°C, unless otherwise stated. 500 mM potassium phosphate buffer was prepared by adding 8.71 g and adjusting the volume to 100 ml dH_2O. The pH was adjusted to 7.5. 100 mM EDTA was made by combining 0.372 g with 10 ml dH_2O. 7 mM β-nicotinamide adenine dinucleotide phosphate (reduced form of β-NADPH) was prepared by adding 8 mg to 1 ml dH_2O. This was protected from light and stored at -20ºC. 0.5% (w/v) bovine serum albumin (BSA) was made by combining 25 mg and 5 ml dH_2O. 0.5 mg/ml gliotoxin was prepared in methanol by adding 5 ml methanol to 5 mg gliotoxin. The principal reaction buffer was made as described in table 2.33.

Table 2.33 Principal buffer constituents. This buffer was filter sterilised before use and stored at 4°C.

Component	Volume added (ml)
500 mM potassium phosphate	14
100 mM EDTA	7
0.5% BSA	2
dH_2O	26.5

Lysis buffer was prepared as described in table 2.34.

Table 2.34 Lysis buffer constituents. Lysis buffer was stored at -20°C following preparation.

Component	Stock Concentration	Amount added to make lysis buffer (µl)
Tris HCl	1 M (1.21 g in 10 ml dH_2O) pH 7.5	250
Potassim chloride	1 M (0.74 g in 10 ml dH_2O)	125
Magnesium chloride	1 M (2.03 g in 10 ml dH_2O)	50
RNase A	10 g/ml (10 g in 1 ml dH_2O)	100
Phenylmethylsulfonyl fluoride (PMSF)	200 mM (0.35 g in 10 ml ethanol)	50
Protease inhibitor cocktail	-	10

2.28.2 Assay procedure

Yeast strains were cultured overnight and lysates were extracted as described in section 2.24.1, using pre-prepared ice-cold lysis buffer (table 2.34) in the place of Sigma cell lysis reagent. Proteins were quantified as described in section 2.24.2 and appropriate dilutions were made to bring all samples to the same protein concentration. Per assay, into a glass cuvette 624 µl of the principal buffer was added, followed by 6 µl of gliotoxin and 50 µl of lysate. This was mixed by inversion and measured at 340 nm using a spectrophotometer. The reading was monitored until stable and recorded. 20 µl of β-NADPH was added, mixed by inversion and the decrease in absorbance at 340 nm was recorded over 3 min. This decrease represented GliTp activity through measuring the oxidation of β-NADPH to β-NADP(+).

Chapter 3 Using *Saccharomyces cerevisiae* as a model organism to investigate the eukaryotic response to the toxic fungal metabolite gliotoxin

3.1 Introduction

Gliotoxin is an epipolythiodioxopiperazine (ETP) that was first isolated in 1936 by Weindling and Emerson, who recorded its potent antimicrobial activity. Gliotoxin was soon shown to be toxic in higher mammals and *Aspergillus fumigatus* was identified as one of the strains responsible for its production. Of the three metabolites known to be produced by this fungal species by the 1940s, gliotoxin was documented as being the most active compound, the most toxic to animals and effective against the widest range of bacteria (Dutcher, 1941, Menzel *et al.*, 1944, Waksman and Geiger, 1944). Structurally characterised by Bell in 1958, gliotoxin and other ETPs have been well studied to date (Gardiner *et al.*, 2005). Characteristic of its toxin class, gliotoxin has an internal disulfide bridge that plays a critical role in many deleterious effects imposed by gliotoxin. An example of this is inhibition of NADPH oxidase activation, leading to suppression of superoxide production by neutrophils (Yoshida *et al.*, 2000, Tsunawaki *et al.*, 2004). Superoxide plays an important role in the eradication of microorganisms, thus abrogation of this response can result in a struggle by the host to efficiently deal with *A. fumigatus* (Miyasaki *et al.*, 1986, Clark, 1990). The disulfide linkage can also conjugate with free thiols on proteins forming mixed disulfides which can in turn result in protein inactivation and depletion (Hurne *et al.*, 2000, Bernardo *et al.*, 2001).

Gliotoxin has been shown to elicit immunomodulation in mammalian tissue, contributing significantly to *A. fumigatus* pathogenicity (Müllbacher and Eichner, 1984). Gliotoxin disrupts the antigen-presenting process by detecting and eradicating antigen-presenting cells such as dendritic cells and monocytes (Stanzani *et al.*, 2005) and in B and T cell lines, gliotoxin specifically suppresses NF-κB activation (Pahl *et al.*, 1996). This inhibitory effect on NF-κB is also seen *in vivo*, along with that imposed on IL-1α, resulting in disruption of the natural inflammatory response (Herfarth *et al.*, 2000).

Gliotoxin can cause damage to eukaryotic macrophage DNA through seemingly random fragmentation, but which is in fact symbolic of apoptosis-associated cleavage and independent of protein synthesis (Eichner *et al.*, 1988, Waring *et al.*, 1988, Waring, 1990).

The internal disulfide bond is also key in the ability of gliotoxin to undergo redox cycling, in doing so producing reactive oxygen species (ROS) (Munday, 1982, Waring *et al.*, 1995). Natural gliotoxin in the disulfide form can undergo reduction giving rise to the dithiol form, which can then in turn reoxidise with the reappearance of the disulfide bridge. Characteristic of this redox cycle is the production of hydrogen peroxide and superoxide (Eichner *et al.*, 1988, Waring and Beaver, 1996). As accumulation of ROS through this process can induce cellular oxidative stress (OS) (Freeman and Crapo, 1982, Nakano, 1992, Sies and de Groot, 1992), the stimulants which facilitate this cycle are vitally important.

Glutathione (GSH/L-γ-glutamyl-L-cysteinylglycine) has long been known to be important in protection against OS and in detoxification (Spielberg *et al.*, 1979, Kaplowitz, 1981, Schulz *et al.*, 2000). Glutathione can exist in the cell in the reduced form, GSH, or the oxidised form, GSSG, which is generated when GSH sulfhydral groups interact with oxidants in an attempt to destroy free radicals. Glutathione reductase is then responsible for regeneration of GSH and maintenance of the appropriate GSH:GSSG ratio (Stephen and Jamieson, 1996, Penninckx, 2000). The synthesis of this tripeptide, as illustrated in figure 3.1, requires glutamate and cysteine which combine to form L-γ-glutamylcysteine, a process mediated in *S. cerevisiae* by γ-glutamylcysteine synthetase (Gsh1p) followed by the addition of glycine. Glutathione synthetase (Gsh2p) subsequently catalyses glutathione formation from glycine and L-γ-glutamylcysteine (Penninckx, 2002).

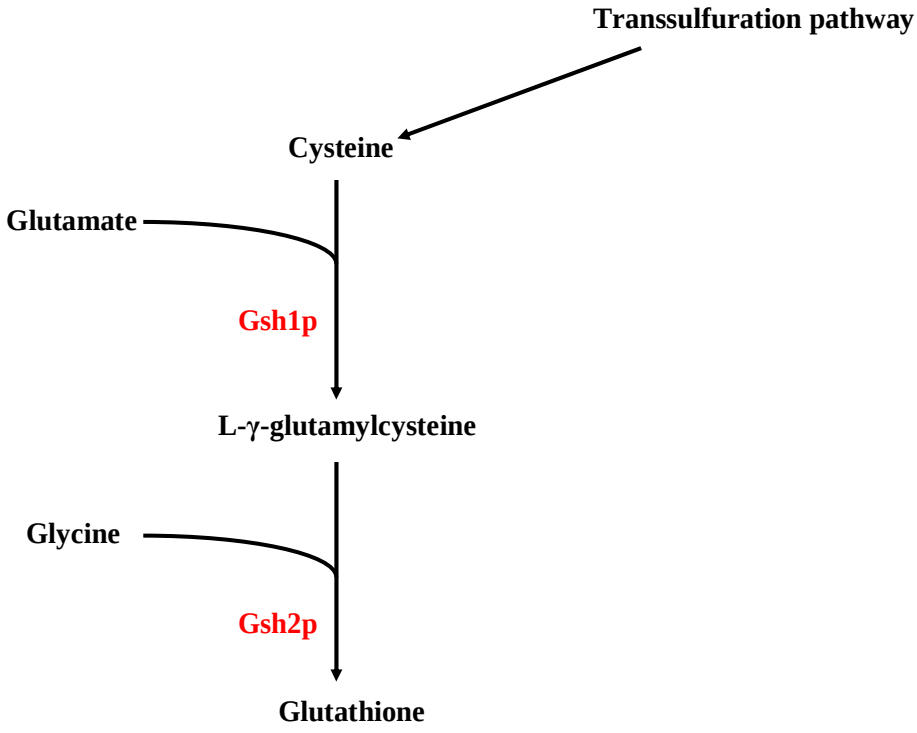

Figure 3.1 Glutathione biosynthesis pathway in yeast. Reproduced from Penninckx (2002).

Bernardo *et al.* (2001, 2003) reported that for uptake of gliotoxin by macrophage cells to occur, there must be glutathione present and only the disulfide form of the toxin can pass through the cell membrane. Inside the cell, the disulfide form is actively converted through reduction to the dithiol form by glutathione, and as a consequence of gliotoxin uptake, GSH levels are reduced and ROS are produced (Eichner *et al.*, 1988, Waring and Beaver, 1996).

Thioredoxins are oxidoreductases that function in redox regulation and protection against OS (Laurent *et al.*, 1964, Arnér and Holmgren, 2000). Interestingly, the sulfur amino acid biosynthesis pathway which gives rise to cysteine biosynthesis is linked to thioredoxin function. Thioredoxin has been found to activate APS kinase, a function carried out by the yeast Met14p which is necessary for sulfate assimilation so

that sulfur amino acids can be synthesised (Schriek and Schwenn, 1986, Thomas and Surdin-Kerjan, 1997).

There are many ways in which yeast respond to OS. The way in which yeast respond to other oxidative stressors such as hydrogen peroxide and copper has been well documented to date. The transcription factor Yap1p (yeast AP-1) plays a role in the regulation of genes that encode proteins involved in the OS response, such as *TRX2* which encodes thioredoxin, *GSH1*, which was discussed above and *GLR1*, a gene encoding glutathione reductase that is involved in maintaining intracellular supplies of reduced glutathione (Moye-Rowley *et al.*, 1989, Kuge and Jones, 1994, Wu and Moye-Rowley, 1994, Grant *et al.*, 1996). Yap1p also mediates the transcription of *HSP31*, which encodes a heat-shock protein that may function in scavenging ROS, and cooperates with the Skn7p transcription factor to regulate induction of *TRR1* which encodes a thioredoxin reductase (Morgan *et al.*, 1997, Skoneczna *et al.*, 2007). In response to OS, yeast also increase expression of superoxide dismutase, encoded by *SOD* genes, which disproportionates superoxide to H_2O_2 and dioxygen (Ravindranath and Fridovich, 1975, Fridovich, 1978, Bermingham-McDonogh *et al.*, 1988).

The generation of cysteine which is required for glutathione biosynthesis is dependent on the sulfur amino acid biosynthesis pathway. Transsulfuration plays a major part in this process, whereby proteins such as Cys3p, Cys4p, Str2p and Str3p regulate the interconversion of cysteine and homocysteine with cystathionine intermediate formation (Cherest *et al.*, 1993, Thomas and Surdin-Kerjan, 1997). Genes such as *MET1*, *MET4*, *MET8*, *MET18*, *MET19* and *MET22* encode products that are involved in the regulation of the sulfur amino acid biosynthesis pathway (Masselot and De Robichon-Szulmajster, 1975, Thomas *et al.*, 1992a).

To prevent damage by endogenous gliotoxin, the *A. fumigatus* genome encodes a protein, GliTp, which confers resistance to the organism. Research has demonstrated

that the absence of the *GliT* gene not only renders the fungus susceptible to the destructive capacities of the toxin, but also prevents gliotoxin production, highlighting the two-fold function of GliTp, protection and biosynthesis (Scharf *et al.*, 2010, Schrettl *et al.*, 2010).

Other fungal metabolites also appear to induce conditions of OS in groups of cells. Citrinin is a fungal mycotoxin produced by a variety of *Aspergillus* and *Penicillium* species (Bennett and Klich, 2003). Utilisation of DNA microarray and subsequent analysis revealed citrinin to induce OS-mediated toxicity in yeast, and activate methionine and glutathione biosynthetic pathways to counteract these effects (Iwahashi *et al.*, 2007). Similarly to citrinin, patulin is a fungal food contaminant that has been found to induce an increase in expression of sulfur amino acid biosynthesis genes by DNA microarray analysis (Sweeney and Dobson, 1998, Iwahashi *et al.*, 2006). However, patulin was also noted to stimulate proteolytic activity and other antioxidant defence systems (Iwahashi *et al.*, 2006). Yu *et al.* (2010) used a similar method to assess the yeast response induced by allicin, a biologically active compound isolated from garlic to which many anti-microbial characteristics have been attributed (Raghunandana Rao *et al.*, 1946, Ankri and Mirelman, 1999). It has been reported that allicin can interact with thiol containing proteins an interaction which in itself generates a product that exhibits clear antioxidant properties (Rabinkov *et al.*, 1998, Rabinkov *et al.*, 2000). Yu *et al.* (2010) discovered that yeast sulfur amino acid biosynthesis pathway genes undergo elevated transcription in response to allicin treatment, in addition to many other transcriptional changes that suggest allicin may exhibit some level of toxicity. In 1948, Dunlop reported that under acidic conditions, degradation of xylose can produce furfural (Palmqvist *et al.*, 1999). Furfural was shown using microarray to stimulate an upregulation of genes involved in the OS response, although not those that play a role in sulfur amino acid biosynthesis. In the same study, the toxin

was found to impede the metabolism of a number of chemicals essential in viable cells (Li and Yuan, 2010).

The main aim of the work described in this chapter was to gain insight into the mode of action of gliotoxin, using *Saccharomyces cerevisiae* as a tool. To address the question of how yeast respond to gliotoxin, advanced genetics, transcriptomics and proteomics were applied. Previous work has suggested that gliotoxin imposes OS in various cell lines, thus we endeavoured to determine if such conditions were induced in our yeast strains.

Section 1: Genetic and biochemical analysis of gliotoxin using *S. cerevisiae* as a model organism

3.2 Assessing the ability of gliotoxin to inhibit wild-type yeast growth

3.2.1 The effect of gliotoxin on wild-type yeast cell growth on solid medium

The first experiments performed in this study involved assessing the growth of wild-type *S. cerevisiae* in the presence of gliotoxin. As a model organism, *S. cerevisiae* is commonly employed to study many aspects of the biology of eukaryotes (Botstein *et al.*, 1997). The genome is fully sequenced and data, along with resources and tools are readily available on *Saccharomyces* Genome Database (www.yeastgenome.org). For these assays, yeast were grown on different types of media containing gliotoxin, to assess the ability of gliotoxin to inhibit yeast growth. Additionally, two different wild-type strains were tested to determine the most useful for future assays (figure 3.2).

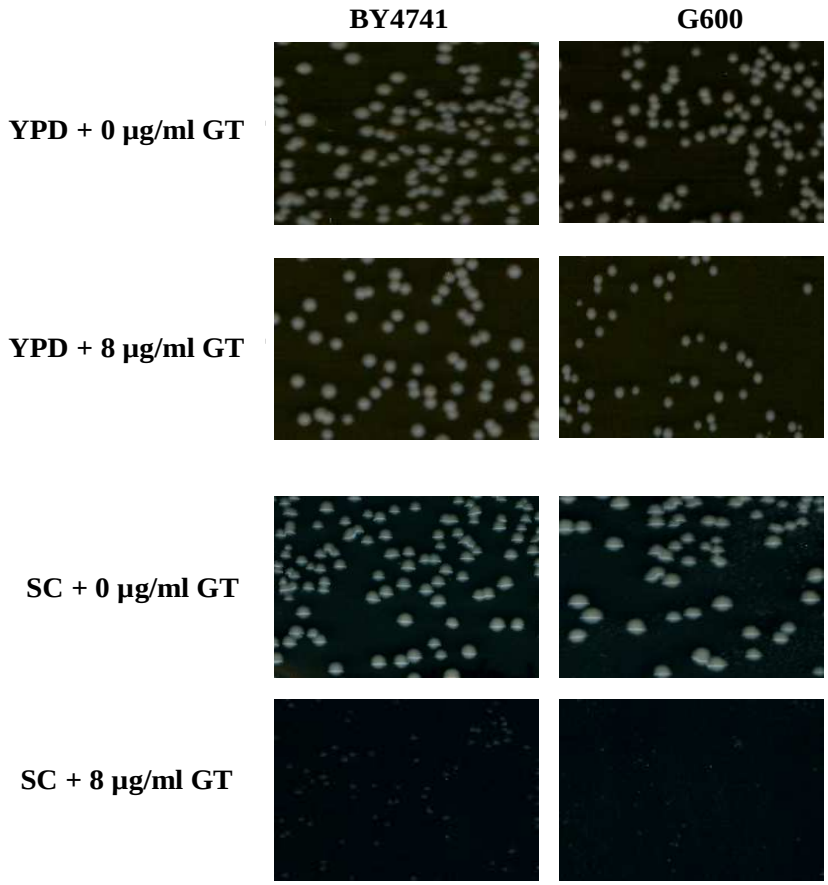

Figure 3.2. Gliotoxin inhibits the growth of *S. cerevisiae*. Cells were grown in culture to OD_{600} 0.2 and 200 µl of each culture was plated on YPD and SC plates containing 0 and 8 µg/ml gliotoxin. The images above are sections of these plates after 48 hr. at 30ºC.

Results from single colony assays depicted in figure 3.2 show that gliotoxin can exhibit an inhibitory affect on yeast growth at a concentration of 8 µg/ml, and *S. cerevisiae* growth is considerably retarded under exposure to gliotoxin.

The G600 background strain generally did not grow as well as the BY4741 strain and appeared to be more easily inhibited by gliotoxin. From these results, it was decided that for the majority of future gliotoxin plate assays, BY4741 and mutants in this background would be employed. YPD is a nutrient-rich broth, while synthetic complete (SC) has minimal nutrients and amino acids required for growth. It soon became clear that SC would be the medium of choice for gliotoxin assays, as inhibition of both wild-type strains was seen to a greater degree on SC medium than YPD, thus lower concentrations of gliotoxin would be needed to yield results (figure 3.2).

Comparative growth analysis was performed (figure 3.3) in addition to the single colony assays. Growth of *S. cerevisiae* was inhibited by gliotoxin, again illustrating the detrimental effects the toxic metabolite gliotoxin has on yeast cell growth.

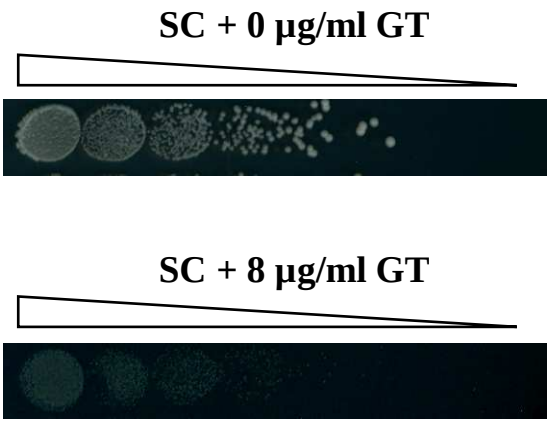

Figure 3.3 Gliotoxin suppresses yeast growth. Comparative growth analysis assays were carried out using the wild-type BY4741 strain. The cells were plated on 0 and 8 µg/ml gliotoxin SC plates to compare growth. The above images represent cellular growth after 48 hr. at 30ºC.

3.2.2 The effect of gliotoxin on wild-type yeast cell growth in liquid culture

The question of whether gliotoxin has a similar affect on yeast growth in liquid culture was also addressed. Gliotoxin was added to BY4741 and G600 cultures at concentrations of 0, 16 and 64 µg/ml. These concentrations were used due to their significant inhibitory effects documented in previous plate assays, results as shown in figure 3.4.

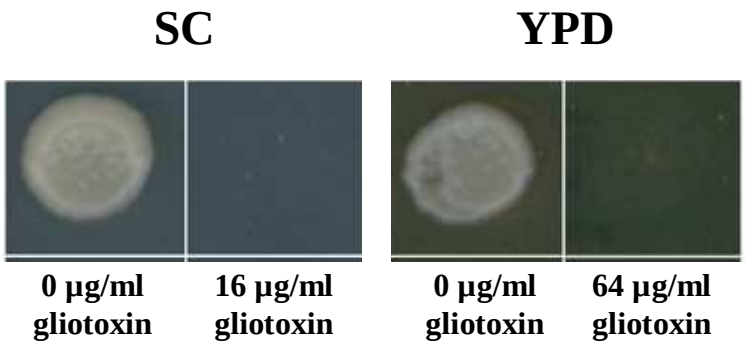

Figure 3.4 Inhibitory effect of 16 and 64 µg/ml gliotoxin on BY4741 growth. Results indicated that on SC medium, 16 µg/ml gliotoxin is sufficient to inhibit yeast growth and on YPD medium 64 µg/ml gliotoxin yields the same result. The above images represent cellular growth after 48 hr. at 30ºC.

The cultures were incubated at 30ºC and samples were taken and OD_{600} determined every 30 min. over a total 180 min. Figure 3.5 shows that BY4741 consistently grows more efficiently than G600 in liquid culture, in both the absence and presence of gliotoxin. At an exposure level of 64 µg/ml, neither strain undergoes growth to any significant extent over a period of 3 hr. After 3 hr. exposure to 16 µg/ml gliotoxin, BY4741 has almost doubled, while G600 has grown at a considerably slower rate.

The toxicity of gliotoxin can clearly be seen in figure 3.5 from 60 min. onwards. There is an extensive difference between the growth in the control cultures and that in the gliotoxin cultures.

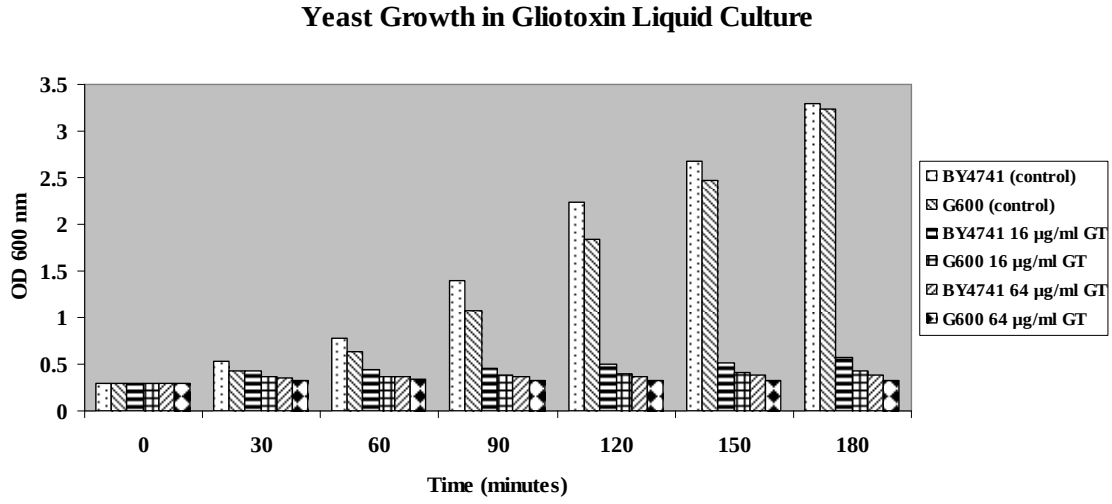

Figure 3.5 Growth of wild-type strains in liquid culture containing gliotoxin. Throughout the experiment, BY4741 grew better than G600. There is an severe inhibition of growth in general by gliotoxin and this is more acute at a concentration of 64µg/ml than 16µg/ml.

The experiment illustrated in figure 3.6 depicts the rapid cell death induced by gliotoxin. Cells incubated with 16 and 64 µg/ml gliotoxin for 1 hr. give rise to a much smaller number of colonies than untreated cells.

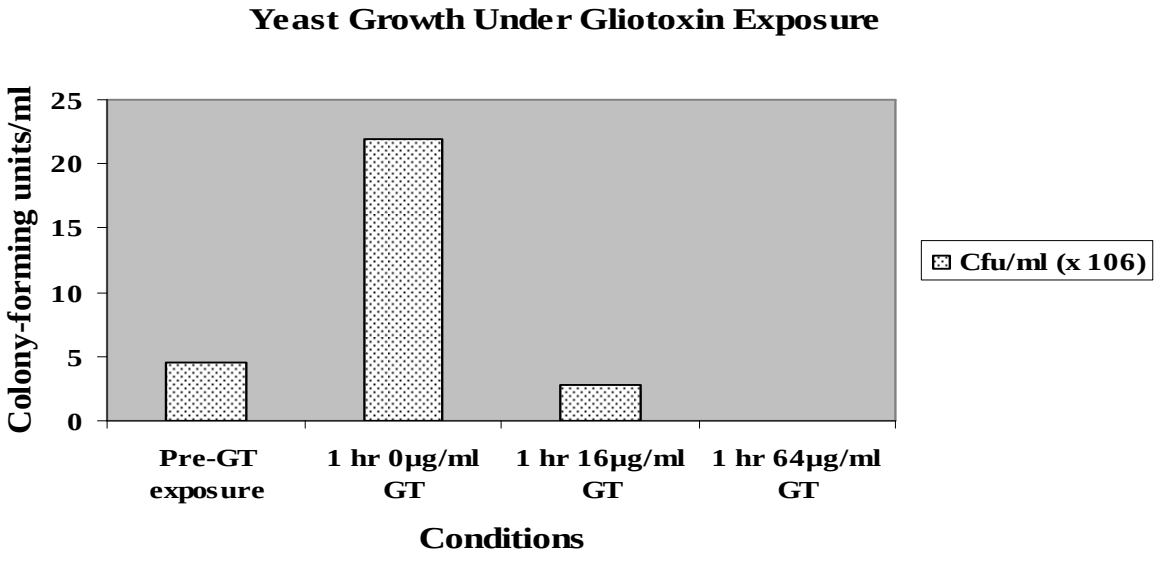

Figure 3.6 The ability of BY4741 to grow after gliotoxin exposure in liquid culture. BY4741 was cultured in liquid YPD containing 0, 16 and 64 µg/ml gliotoxin. After a 1 hr. incubation at 30ºC, 200 µl of cells were plated on YPD, along with 200 µl of the pre-exposed culture. It should be noted that the 0 µg/ml sample gave rise to an unusually high number of colonies after 1 hr. incubation, which may indicate an inaccuracy in the assay results.

3.3 Investigation into the importance of oxidative stress response genes in yeast growth under gliotoxin exposure

3.3.1 Comparative growth analysis of BY4741, Δ*cys3*, Δ*yap1* and Δ*sod1*

Previous studies have reported that gliotoxin causes OS through the generation of ROS (Eichner *et al.*, 1988, Waring *et al.*, 1988, Zhou *et al.*, 2000, Orr *et al.*, 2004). Chamilos *et al.* (2008) carried out a genome-wide screen in an attempt to pinpoint yeast genes involved in conferring increased sensitivity or increased resistance to gliotoxin. One of the genes they found to be important in protection against gliotoxin was *CYS3*, when this gene was disrupted the resultant phenotype showed increased sensitivity to the metabolite. The *CYS3* gene encodes the cystathionine γ-lyase enzyme which plays a role in the transsulfuration pathway that is characterised by an interconversion of cysteine and homocysteine (Ono *et al.*, 1984, Ono *et al.*, 1992). Cysteine plays an essential role in the biosynthesis of glutathione, along with the other amino acids glycine and glutamate. As glutathione plays a critical part in maintaining an appropriate redox state and preventing oxidative damage, it can be said that the *CYS3* gene has a valuable part to play in protection against OS, through its production of cysteine (Ono *et al.*, 1992, Penninckx, 2002).

In agreement with Chamilos *et al.* (2008) it was determined from comparative growth analysis (figure 3.7) of BY4741 and the isogenic Δ*cys3* strain, that Δ*cys3* is indeed more sensitive to gliotioxin exposure than wild-type. This illustrates the importance of Cys3p in protection against gliotoxin exposure and suggests that the toxin may be eliciting effects through OS.

Both Yap1p and Sod1p play key roles in modulating yeast resistance to OS.

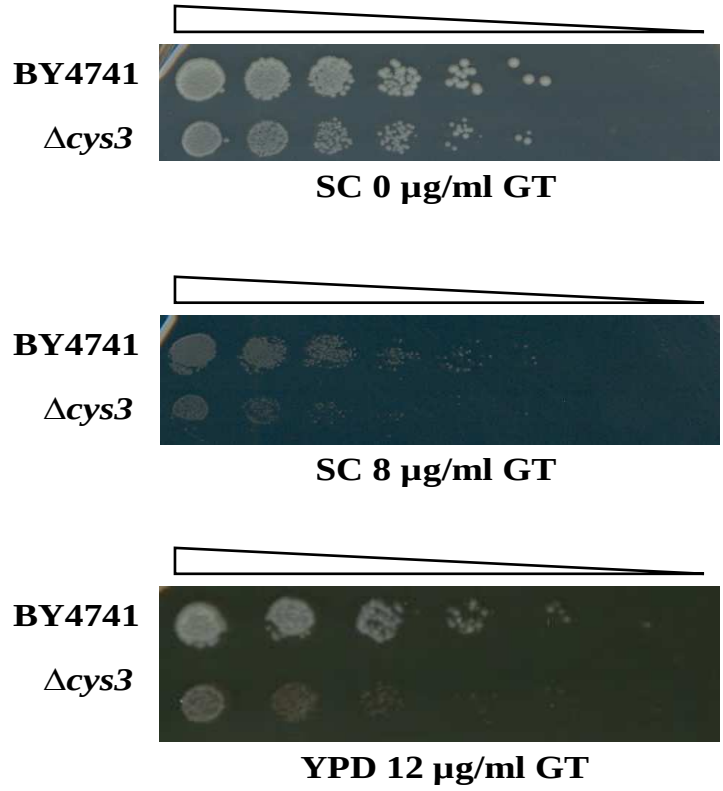

Figure 3.7 Comparative growth analysis of BY4741 and Δ*cys3*. Δ*cys3* is more sensitive to gliotoxin than wild-type. The above images represent cellular growth after 48 hr. at 30ºC.

Yap1p is a transcription factor which upon activation, undergoes relocation from the cytoplasm to the nucleus and regulates the expression of a number of genes that contribute to stress tolerance, including *GSH1* (Wu and Moye-Rowley, 1994, Kuge *et al.*, 1997). The *SOD1* product is a copper, zinc-superoxide dismutase, involved in the conversion of superoxide radicals to oxygen and hydrogen peroxide which in turn can be rendered harmless to the cell (Fridovich, 1978, Bermingham-McDonogh *et al.*, 1988, Gralla and Kosman, 1992). Given that gliotoxin has been reported to induce cellular OS, the sensitivity of *YAP1* and *SOD1* deletion strains to gliotoxin was tested. In figure 3.8 it can be seen that both Δ*sod1* and Δ*yap1* show increased sensitivity to gliotoxin, in comparison to wild-type.

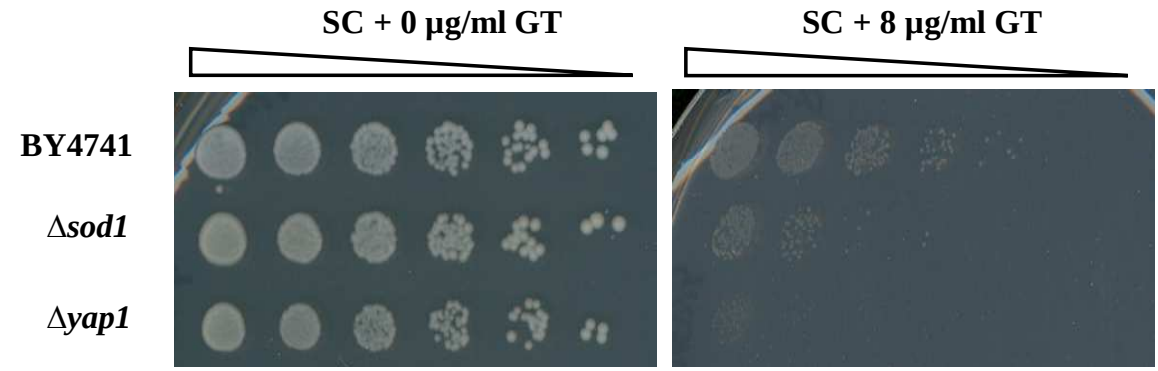

Figure 3.8 Comparative growth analysis of BY4741, Δ*yap1* and Δ*sod1*. At 8 µg/ml gliotoxin exposure, both mutants are more sensitive to gliotoxin than wild-type. Δ*yap1* is the most sensitive strain. The above images represent cellular growth after 72 hr. at 30ºC.

3.3.2 Analysis of Δ*gsh1* sensitivity to gliotoxin

3.3.2.1 Comparative growth analysis of BY4741 and Δ*gsh1*

As previously discussed, *CYS3* is involved in the superpathway of sulfur amino acid biosynthesis, that can lead to the production of glutathione. As suggested by Williamson *et al.* (1982), the principal contributing factor to Δ*cys3* sensitivity may be absence of glutathione, through disruption of the said pathway. This group illustrated that increased cysteine results in a higher level of toxin protection through boosting glutathione concentration. Thus, we decided to assess the growth in the presence of gliotoxin of a yeast strain unable to produce glutathione, Δ*gsh1*. The *GSH1* gene is vital for glutathione synthesis, as the first functional enzyme in the biosynthesis pathway (Grant, 2001). Surprisingly, comparative growth analysis showed the BY4741 Δ*gsh1* strain to be more resistant to gliotoxin than wild-type, it grew better at 16 µg/ml gliotoxin than BY4741.

3.3.2.2 Complementation study

To confirm that this result was real we performed a complementation study that demonstrated how the re-introduction of *GSH1* into BY4741 Δ*gsh1* restored the wild-type phenotype (figure 3.9). The 2,036 bp *GSH1* region, plus 500 bp upstream

containing the promoter sequence, was amplifed from BY4741 via PCR. The 2.5 kb *GSH1* amplicon, depicted in figure 3.9, contained at both 5' and 3' ends overhangs homologous to regions within pRS315.

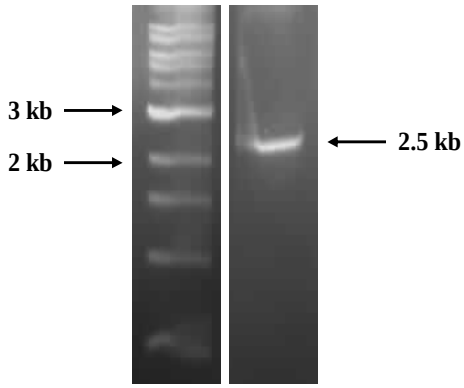

Figure 3.9 PCR amplified *GSH1*. *GSH1* was amplified from BY4741 by PCR for cloning into pRS315.

The *GSH1* gene sequence and promoter region were cloned by homologous recombination into the pRS315 vector, which contains the *LEU2* gene marker. To achieve this, pRS315 was digested using the *BamH*I and *Hind*III restriction enzymes, giving a linear product of approximately 6 kb. The regions immediately up- and downstream of the cleavage sites were homologous to the sequence at the ends of the *GSH1* amplicon. Therefore, when both digested vector and insert were transformed into BY4741 simultanaeously, homologous recombination occurred, giving rise to colonies containing the new *GSH1*-pRS315 plasmid. The new construct was extracted and a diagnostic PCR was carried out to ensure that *GSH1* had been cloned into the said plasmid effectively. PCR amplified a fragment of approximately 2.5 kb (as seen for that in figure 3.9) from the vector, a region which in normal pRS315 is occupied by 24 bp, demonstrating that *GSH1* had been cloned efficiently. Figure 3.10 illustrates the plasmid maps for pRS315 and *GSH1*-pRS315.

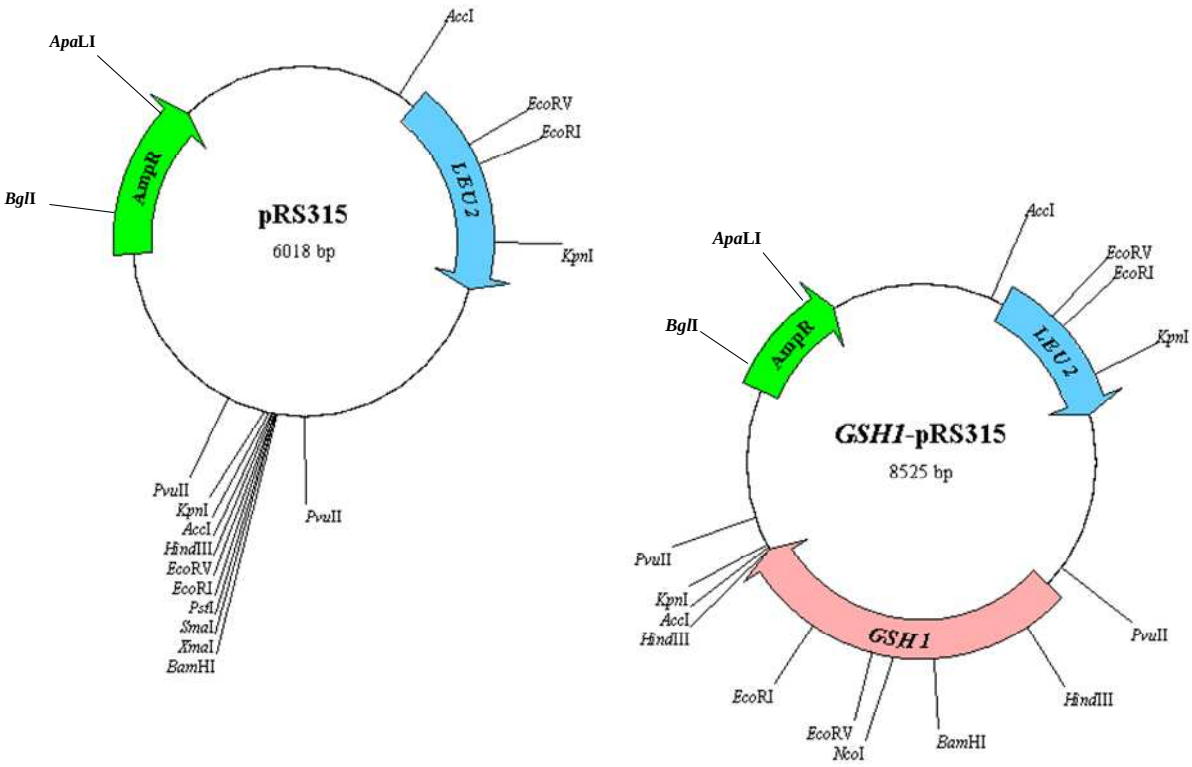

Figure 3.10 Plasmid maps constructed for pRS315 and *GSH1*-pRS315. pRS315 was digested using *Bam*HI and *Hind*III. 30 bp were removed and the *GSH1* coding sequence and promoter were cloned into the plasmid by homologous recombination. Both plasmids contain leucine and ampicillin resistance marker genes and a number of restriction sites as depicted above.

Comparative growth analysis confirmed that the absence of *GSH1* confers increased yeast resistance to gliotoxin and revealed that Δ*gsh1* complementation restores wild-type phenotype (figure 3.11)

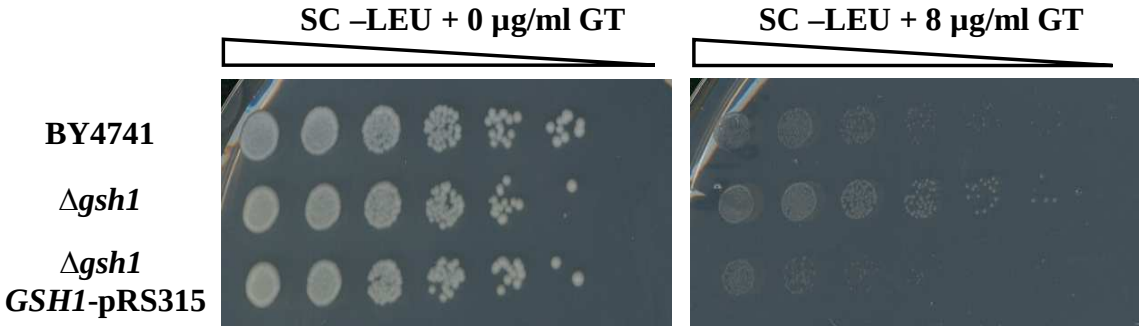

Figure 3.11 Comparative growth analysis of BY4741, Δ*gsh1* and Δ*gsh1* *GSH1*-pRS315. BY4741 and Δ*gsh1* harbour the pRS315 vector. Δ***gsh1*** *GSH1*-pRS315 is the mutant complemented with *GSH1* within the pRS315 vector. The absence of *GSH1* confers increased resistance to BY4741. When this gene is re-introduced on a plasmid to the deletion strain, wild-type phenotype is restored. The above images represent cellular growth after 72 hr. at 30ºC.

3.3.3 Summary of mutant phenotypic response to gliotoxin exposure

Previous proteomic studies in Prof. S. Doyle's laboratory, NUIM (Carberry, 2008) using *A. fumigatus* resulted in the identification of a number of proteins that are differentially expressed in the presence of gliotoxin. In the absence of exogenous application of the toxin, Sod1p was undetectable. Conversely, when gliotoxin was added to cultures, there was a significant increase in production of this protein as Sod1p was expressed at a detectable level. This data supports our results, highlighting the importance of *SOD1* in gliotoxin resisitance.

Similar trends were seen for Tef (translation elongation factor) proteins in *A. fumigatus*. *TEF3* and *TEF4* are *S. cerevisiae* genes with homology to those encoding Tef proteins in *A. fumigatus* and so we tested the sensitivity to gliotoxin of single mutants lacking these genes. The yeast *TEF3* and *TEF4* genes encode a translation elongation factor eEF1Bγ, although Tef3p and Tef4p do not function in the same manner suggesting that they encode different isoforms with different specialised capacities (Kinzy *et al.*, 1994, Jeppesen *et al.*, 2003). eEF1B has been shown to be involved in the OS response and it appears that downregulation of *TEF3* and *TEF4* is important in the OS response (Godon *et al.*, 1998, Olarewaju *et al.*, 2004, Carberry *et al.*, 2006). However, our Δ*tef3* and Δ*tef4* strains exhibited a wildtype phenotype (data not shown).

Work in Prof. Doyles' laboratory also documented the decrease in *A. fumigatus* mycelial catalase I in the presence of gliotoxin (Carberry, 2008). The yeast *CTT1* gene is the equivalent homologue and encodes a cytosolic catalase T which functions in the detoxification of H_2O_2 (Hartig and Ruis, 1986, Grant *et al.*, 1998). From the data obtained from *A. fumigatus* work, it was hypothesised that without Ctt1p, there would be less gliotoxin reduction leading to free radical production and therefore a phenotype displaying increased resistance to the toxin. Despite this, when the *S. cerevisiae* mutant

Δ*ctt1* was grown in the presence of gliotoxin, it grew in a similar manner to wild-type (figure 3.12).

Growth of the yeast strain Δ*trx2* was also assessed in the presence of gliotoxin. Thioredoxin encoded by *TRX2* functions in the stress response through repairing proteins which have been damaged by OS and regulating sulfur metabolism (Kuge and Jones, 1994, Grant, 2001) *TRR1*, a thioredoxin reductase which plays an essential role in facilitating thioredoxin function, is induced by Yap1p under OS (Morgan *et al.*, 1997, Pedrajas *et al.*, 1999). Although *TRX2* appears considerably influential in the OS response, the deletion strain grew as wild-type under gliotoxin exposure, suggesting Trx2p is not essential in survival in the presence of this toxin.

Ace2p was an additional protein identified in Prof. Doyles' laboratory as being key in *A. fumigatus* response to exogenous gliotoxin. This protein is involved in delaying daughter cells in G_1 prior to entering S phase of the cell cycle (Laabs *et al.*, 2003), and in its absence, yeast cells displayed no change in sensitivity to gliotoxin. Other strains that underwent phenotypic analysis were those deleted for glutathione synthetase *GSH2* and the glutathione reductase *GLR1*, which function in the final step of glutathione synthesis and maintaining a high level of intracellular reduced GSH respectively (Grant *et al.*, 1996, Grant *et al.*, 1997, Inoue *et al.*, 1998, Grant, 2001). In this study both Δ*gsh2* and Δ*glr1* were found to exhibit a wild-type phenotype under gliotoxin exposure.

In figure 3.12 the Δ*ctt1*, Δ*ace2*, Δ*gsh2*, Δ*glr1* and Δ*trx2* phenotypic responses to gliotoxin can be seen. The variety of deletions strains tested for sensitivity to gliotoxin and their respective phenotypes are depicted in table 3.1.

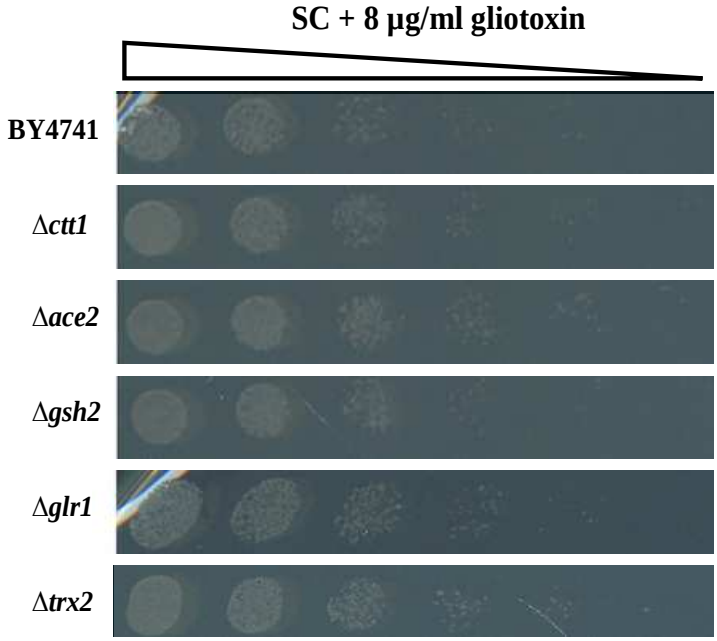

Figure 3.12 Comparative growth analysis of BY4741, Δ*ctt1*, Δ*ace2*, Δ*gsh2*, Δ*glr1* and Δ*trx2* under gliotoxin exposure. The above images represent cellular growth after 72 hr. at 30ºC.

Table 3.1 Summary of strains tested through comparative growth analysis for altered phenotype under gliotoxin exposure. IR indicates increased resistance. IS indicates increased sensitivity.

Strain	Phenotype
Δ*gsh1*	IR
Δ*sod1*	IS
Δ*yap1*	IS
Δ*gsh2*	WT
Δ*ace2*	WT
Δ*ctt1*	WT
Δ*glr1*	WT
Δ*trx2*	WT
Δ*tef3*	WT
Δ*tef4*	WT

3.3.4 Comparison of mutant response to gliotoxin and hydrogen peroxide

As a comparison, the mutants which showed a divergent phenotype to that of wild-type on gliotoxin plates were assessed under the exposure of another common

oxidative stressor. Growth of BY4741, Δ*gsh1*, Δ*yap1* and Δ*sod1* was assessed in the presence of 0, 1, and 3 mM H_2O_2 (figure 3.13). Under 1 mM H_2O_2 exposure there was a clear difference in growth capacities of the strains. While wild-type is virtually unaffected by this concentration, Δ*yap1* cannot grow at all and the growth ability of Δ*gsh1* is clearly impaired. However, Δ*sod1* does not appear to be greatly inhibited by 1 mM H_2O_2. 3 mM H_2O_2 considerably inhibits wild-type growth, Δ*gsh1* and Δ*yap1* cannot grow in the presence of this concentration and Δ*sod1* grows to a small degree.

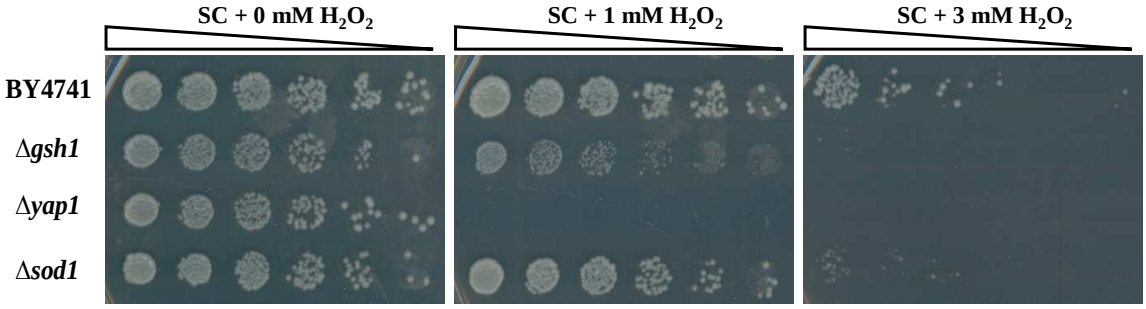

Figure 3.13 Comparative growth analsysis of BY4741, Δ*gsh1*, Δ*yap1* and Δ*sod1* in response to various concentrations of H_2O_2. The above images represent cellular growth after 72. hr at 30ºC.

3.4 Conferring *S. cerevisiae* resistance to gliotoxin by expressing the *Aspergillus fumigatus GliT* gene

3.4.1 Cloning of *GliT* into pC210

GliT is a gene found in *Aspergillus fumigatus*. It is part of a biosynthetic 12-gene cluster that was identified due to its high level of sequence conservation with that of the *Leptosphaeria maculans* biosynthetic gene cluster (Gardiner *et al.*, 2004, Gardiner and Howlett, 2005, Gardiner *et al.*, 2005). Using the CADRE resource described by Mabey *et al.* (2004) http://www.cadre.man.ac.uk, the *GliT* gene has been annotated as 1005 bp in length (figure 3.14) and the 334 amino acid GliTp is 36 kDA in weight. This gene has been shown to be paramount in enabling *A. fumigatus* to protect itself from exogenous gliotoxin (Schrettl *et al.*, 2010).

ATGTCGATCGGCAAACTACTCTCCAACGGAGCCCTGCTCGTCGACGTGCTCATCATCGG
CGCCGGTCCCGCTGGTCTCTCGACAGCCACCGGCCTGGCCCGTCAACTGCACACGGCAG
TCGTCTTCGACTCTGGCGTCTACCGCAATGCAAAGACCCAGCACATGCACAACGTCCTC
GGATGGGACCACCGCAACCCGGCCGAGCTGCGCGCCGCGGGTCGCGCCGACCTGACCAC
CCGCTACTCCACCATCCAGTTCCAGAACAGCACGATCGAGGCGATCCGCCAGGTCGAGA
CCAACCAGCTGTTCGAGGCGCGCGACAACGAGGGCCACAGCTGGTACGGTCGCAAGGTC
GTGCTGGCGACCGGCGTCCGCGACATCCCCCTCGACATCGAGGGATACTCGGAGTGCTG
GGCGAACGGCATCTACCACTGTCTCTTCTGCGACGGCTACGAGGAACGTGGCCAGGAGA
CCGTGGGTGTCCTGGCTCTGGGGCCCATCGCGAACCCTGCGCGCGCTCTGCATTTGGCT
CGCATGGCCCTCCGGCTTTCCGAGTCCGTCACCATCTACACGAATGGCAATGAGCAGCT
GGCCAAGGAGATCCAGCAGGCCGCCGAGGAATCCCCTGTCGGTGCCTCGGGACTGAAAT
TCGAGGCTCGACCCATCCGGCGATTCGAAAAGGGCGATGTCGCCAAGACCGTCATTGTT
CATCTTGGGGAGTCGGAGTCGAAAACGGAGGGCTTTTTGGTACGTTGTCCAGTTTACTC
GACAGAGATATCCTTGCTAACCGCGGCAAACCGCTCAGGTGTACAACCCCCAAACGGAG
GTCAATGGACCGTTTGCCAAGCAGCTCGCCTTGAATATGACAGAAGGAGGGGATATCCT
GACCACGCCGCCCTTCTATGAGACCAGTGTGCCCGGAGTATTTGCCGTGGGGGATTGTG
CCACGCCGTTAAAGGCCGTCACGCCCGCGGTGTCGATGGGATCTTTGGCCGCTGGCGGT
CTCGTGGCTCAGCTGCAGGCTCAGGCATTGCCGGAGTTTCGTCTCGATCAGGAGCTATA
G

Figure 3.14 Genomic sequence of *GliT*. This gene is made up of two exons, separated by a 58 bp intron. Blue depicts coding region. Red depicts intron.

GliT was cloned by homologous recombination into pC210 yeast vector. pC210 is a plasmid 8,928 bp in size containing a leucine marker, the *LEU2* gene. It contains the yeast *SSA1* gene, under the control of the constitutive *SSA2* promoter. Prior to cloning, the plasmid was digested at sites surrounding *SSA1*, using *NdeI* and *SphI*. The digested plasmid was run on an agarose gel and the remaining vector, lacking the 2,210 bp *SSA1* gene plus terminator region, was gel extracted and purified. *GliT* cDNA within TOPOvector® was obtained from Dr. Markus Schrettl and was amplified by PCR, with overhangs homologous to regions within pC210 up- and downstream of where the plasmid had been cut. Subsequent transformation of both *GliT* and digested pC210 simultanaeously led to recombination and the formation of a new vector, containing constitutively expressed *GliT*. Cells containing the new construct were selected on SC plates lacking leucine and plasmids from the selected clonies were isolated to confirm presence of *GliT*-pC210. Figure 3.15 illustrates the plasmid maps for pC210 and *GliT*-pC210.

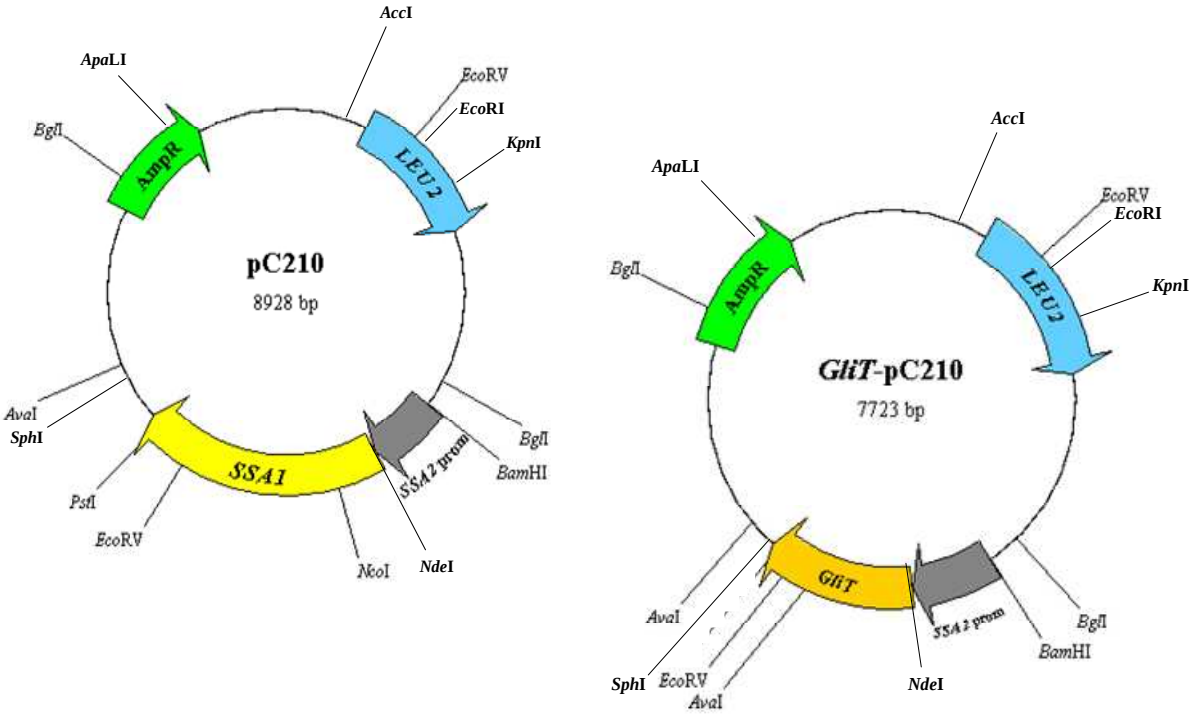

Figure 3.15 Plasmid maps constructed for pC210 and *GliT*-pC210. pC210 was digested using *Nde*I and *Sph*I. The *SSA1* region including terminator sequence was digested from pC210 and replaced with *GliT*. Both plasmids contain leucine and ampicillin marker genes and a number of restriction sites as depicted above.

To confirm that *GliT* had been cloned into pC210, the plasmid was digested using *NdeI* and *SphI* resulting in fragments of approximately 6.7 kb and 1 kb, pC210 and *GliT* respectively. This provided evidence that *GliT* had been successfully cloned.

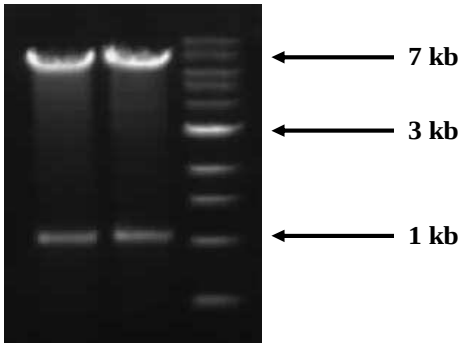

Figure 3.16 Agarose gel illustrating *GliT* cloned into pC210 vector. The new construct was digested yielding products of approximately 7 kb and 1 kb, pC210 and *GliT* respectively.

To obtain further proof that *GliT* was cloned and also to check for mutations within the *GliT* sequence, the plasmid was sequenced (figure 3.17).

CCATTTCCTACGCATCGAGGTTTTGACGACATTTCATTCTTAAGCACTATGGGAAGGTG
TGGACGAATTGTTATATATAAGCCGCAATTGGGCTGGGTTTTCTCCAAAAAATGTTGAA
AATATAATACTCTCTTATTTAAGTTACTTCTATTCTTCAATTGATTAATTCCAACAGAT
CAAGCAGATTTTTATACAGAAATATTTATACATATGATGTCGATCGGCAAACTACTCTC
CAACGGAGCCCTGCTCGTCGACGTGCTCATCATCGGCGCCGGTCCCGCTGGTCTCTCGA
CAGCCACCGGCCTGGCCCGTCAACTGCACACGGCAGTCGTCTTCGACTCTGGCGTCTAC
CGCAATGCAAAGACCCAGCACATGCACAACGTCCTCGGATGGGACCACCGCAACCCGGC
CGAGCTGCGCGCCGCGGGTCGCGCCGACCTGACCACCCGCTACTCCACCATCCAGTTCC
AGAACAGCACGATCGAGGCGATCCGCCAGGTCGAGACCAACCAGCTGTTCGAGGCGCGC
GACAACGAGGGCCACAGCTGGTACGGTCGCAAGGTCGTGCTGGCGACCGGCGTCCGCGA
CATCCCCCTCGACATCGAGGGATACTCGGAGTGCTGGGCGAACGGCATCTACCACTGTC
TCTTCTGCGACGGCTACGAGGAACGTGGCCAGGAGACCGTGGGTGTCCTGGCTCTGGGG
CCCATCGCGAACCCTGCGCGCGCTCTGCATTTGGCTCGCATGGCCCTCCGGCTTTCCGA
GTCCGTCACCATCTACACGAATGGCAATGAGCAGCTGGCTAAGGAGATCCAGCAGGCCG
CCGAGGAATCCCCTGTCGGTGCCTCGGGACTGAAATTCGAGGCTCGACCCATCCGGCGA
TTCGAAAAGGGCGATGTCGCCAAGACCGTCATTGTTCATCTTGGGGAGTCGGAGTCGAA
AACGGAGGGCTTTTTGGTGTACAACCCCCAAACGGAGGTCAATGGACCGTTTGCCAAGC
AGCTCGCCTTGAATATGACAGAAGGAGGGGATATCCTGACCACGCCGCCCTTCTATGAG
ACCAGTGTGCCCGGAGTATTTGCCGTGGGGGATTGTGCCACGCCGTTAAAGGCCGTCAC
GCCCGCGGTGTCGATGGGATCTTTGGCCGCTGGCGGTCTCGTGGCTCAGCTGCAGGCTC
AGGCATTGCCGGAGTTTCGTCTCGATCAGGAGCTATAGGCATGCTTTGTCTTCCTGTTT
AATCAGGAAGTCGCCCAAAGCGAGAATCATACCACTAGACCACACGCCCGTACTAATTG
ATGTCTTCCTTTTCGGATAGATGTATATATATACAAATTGGTCAGATTGCTTTTGGCTC
CCTTTCGTACGTAACTCATTTAGACTACGAAGCTTATCGATACCGTCGACCTCGAGGGA
CTTTGACCCA

Figure 3.17 Agowa sequencing result. The start and stop codons are highlighted in purple. The result revealed one mutation, C→T at position 594, highlighted in yellow. When translated, this mutation was shown not to alter the GliTp amino acid sequence and was therefore suitable to use in experimentation.

3.4.2 The effects of constitutive *GliT* expression on yeast growth

To assess the effects of constitutive *GliT* expression on the growth of both wild-type and mutant yeast strains, the newly created construct described above containing the *GliT* gene was transformed into BY4741 and Δ*cys3* and comparative growth analysis was carried out on these strains in the presence of gliotoxin. As controls, the pRS315 plasmid containing the *LEU2* gene was transformed into the two strains to enable an accurate growth comparison to be made on SC –LEU gliotoxin plates. At a concentration of 16 µg/ml, gliotoxin completely inhibited the growth of both wild-type and Δ*cys3*. However, when these strains expressed GliTp, a significant increase in

resistance to the toxin was observed (figure 3.18). It was thus concluded that constitutive expression of the *GliT* gene confers resistance to gliotoxin in *S. cerevisiae*.

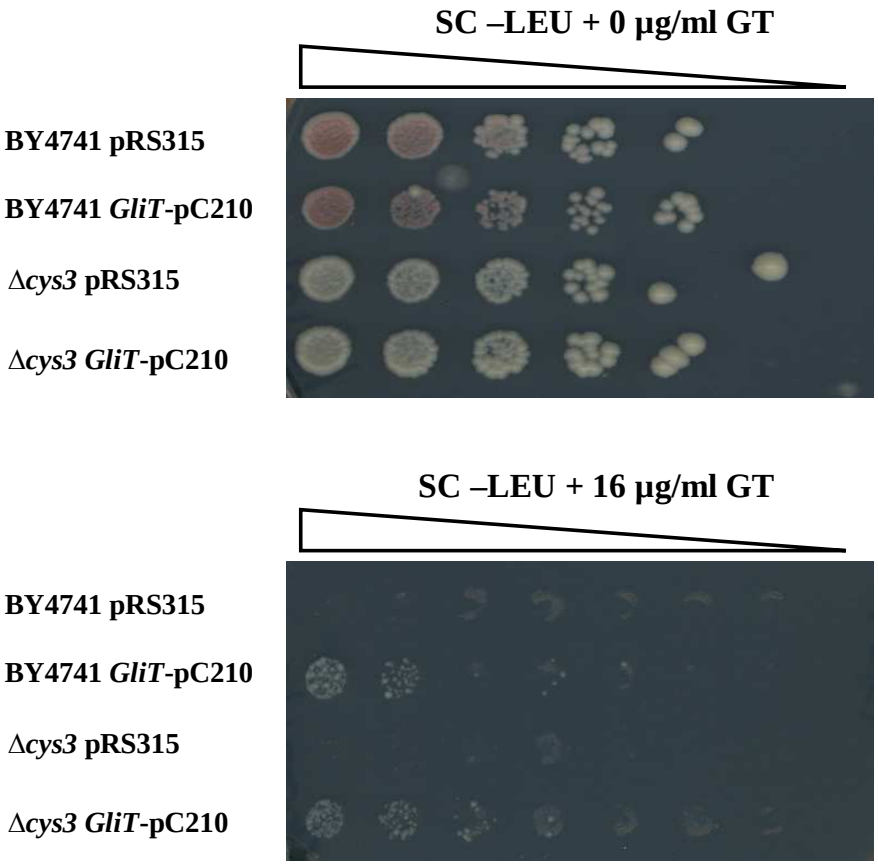

Figure 3.18 Comparative growth analysis of BY4741 and Δ*cys3* under gliotoxin exposure. The presence of *GliT* conferred resistance in both strains. SC plates lacking leucine were used to select for cells containing the pC210 plasmid and thus those expressing *GliT*. The above images represent cellular growth after 36 hr. at 30ºC.

This result was further verified by assessing single colony growth under exposure to gliotoxin. Figure 3.19 illustrates this gliotoxin resistance afforded by *GliT* expression and shows the considerable increase in cellular survival when cells express GliTp.

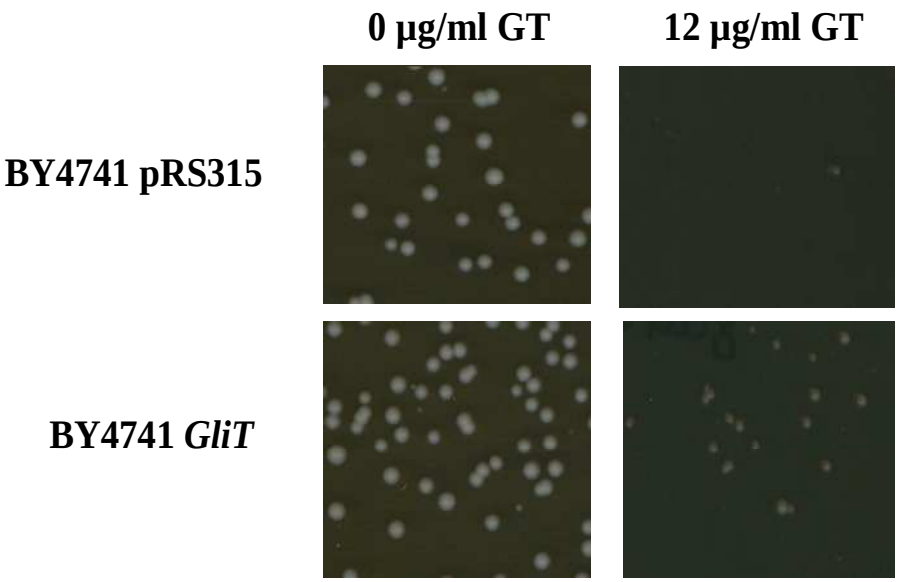

Figure 3.19 Single colony growth assay of BY4741 under gliotoxin exposure. There is increased survival under gliotoxin exposure of cells expressing GliTp. The above images represent cellular growth on SC –Leu media after 48 hr. at 30ºC.

3.4.3 Detecting GliTp when constitutively expressed

Due to the fact that the presence of *GliT* under a constitutive promoter conferred gliotoxin resistance to *S. cerevisiae*, an attempt was made to detect GliTp production in yeast cells.

3.4.3.1 Coomassie stain of SDS-PAGE gel (*GliT*-pC210)

Lysates were extracted from BY4741 *GliT*-pC210, BY4741 pRS315, G600 *GliT*-pC210, G600 pRS315, BY4741 Δ*cys3 GliT*-pC210 and BY4741 Δ*cys3* pRS315. 10 µg of each lysate sample was run on a SDS-PAGE gel and coomassie stained in an attempt to observe possible GliTp bands in the protein samples from strains containing the *GliT* gene (figure 3.20).

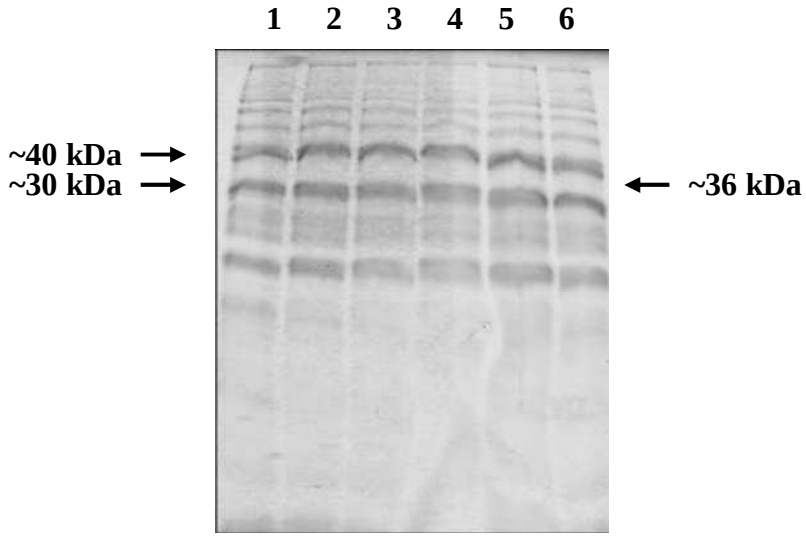

Figure 3.20 Coomassie stain of SDS-PAGE gel with protein from strains containing *GliT*-pC210. 1 = BY4741 *GliT*-pC210; 2 = BY4741 pRS315; 3 = G600 *GliT*-pC210; 4 = G600 pRS315; 5 = BY4741 Δ*cys3 GliT*-pC210; 6 = BY4741 Δ*cys3* pRS315. No discrepancy in band intensity at 36 kDA.

GliTp has a molecular mass of 36 kDa, however no bands representative of this protein were visible. Coomassie-stained 1-dimensional gels do not reveal differences between proteins from yeast strains without *GliT* and *GliT* transformant strains.

3.4.3.2 Enzymatic assay of gliotoxin reductase activity (*GliT*-pC210)

Gliotoxin can cause an inhibition of NADPH oxidase activity (Yoshida *et al.*, 2000, Tsunawaki *et al.*, 2004). Schrettl *et al.* (2010) demonstrated the ability of GliTp to cleave the gliotoxin disulfide bridge (gliotoxin reductase activity), which has been shown to play a key role in the deleterious activity exhibited by the toxin (Trown and Bilello, 1972, Müllbacher *et al.*, 1986). Thus, NADPH oxidase activity can be used as an indirect measure of gliotoxin activity. This NADPH assay was carried out in an attempt to observe a difference in NADPH oxidase activity inhibition by gliotoxin, in the absence and presence of GliTp. The assay was carried out as described in section 2.28 and comparisons were made between BY4741 and BY4741 *GliT*, and G600 and G600 *GliT*. Figure 3.21 represents a typical graph observed from the data obtained.

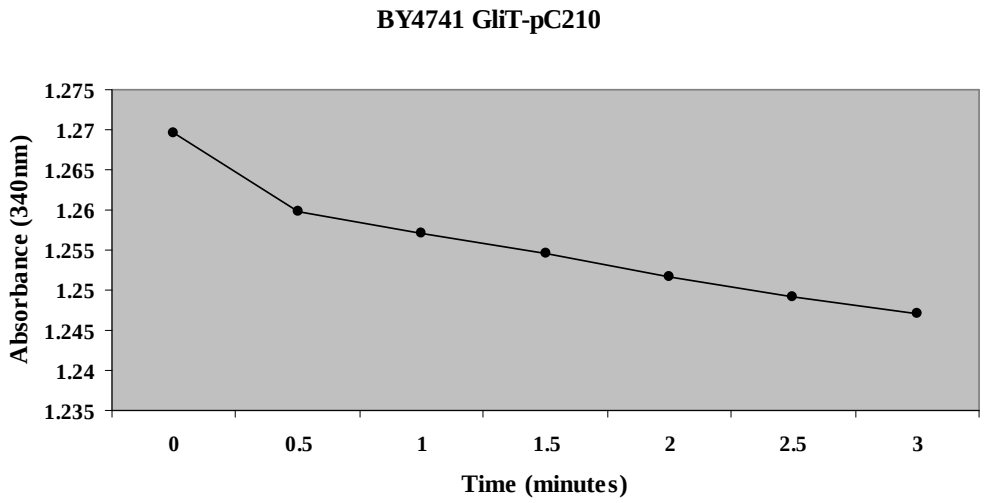

Figure 3.21 NADPH oxidase activity in BY4741 when *GliT* is present. This graph is representative of the typical trend seen over time.

To enable more accurate comparisons to be made, the absorbance figures obtained during the 3 min. following NADPH addition were converted to percentages of the initial reading. This allowed us to examine the oxidase activity in each sample relative to the others (figure 3.22).

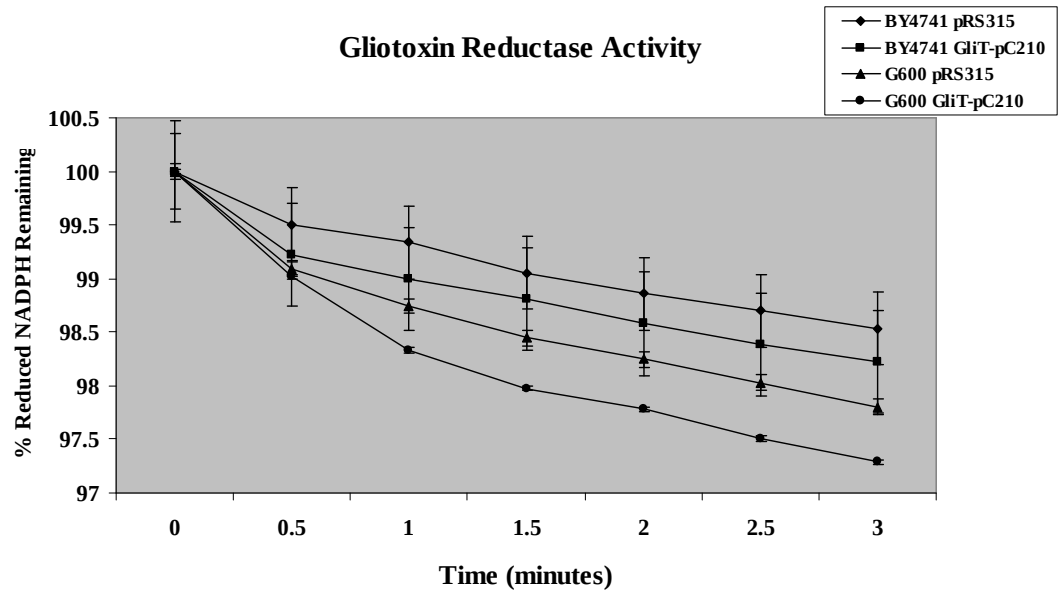

Figure 3.22 NADPH oxidase activity in BY4741 and G600 (*GliT*-pC210)

The results from this assay show that expression of GliTp impairs the ability of gliotoxin to inhibit NADPH oxidase activity. In both BY4741 and G600, when *GliT* is

present along with gliotoxin, there is more rapid oxidation of NADPH. It appears based on the observations in figure 3.22 that the GliTp is inactivating gliotoxin to some extent, probably by exhibiting gliotoxin reductase activity, thus alleviating the toxin's inhibition of NADPH oxidase activity. This suggests that there is GliTp production within *GliT* transformant cells, albeit a low level.

Further to this, we wanted to quantify the amount of GliTp in the cell lysates. From here, gliotoxin reductase activity, and subsequent inability of the toxin to inhibit NADPH oxidase activity, was taken to represent GliTp. We used the formula below and figures recorded in this assay to calculate the units of NADPH oxidase per mg of protein.

Units/ml enzyme = $(\Delta A_{340\ nm}$ Sample – $\Delta A_{340\ nm}$ Blank)(0.7)/(6.22)(0.05)

0.7 = volume of assay (ml)
6.22 = extinction coefficient of β-NADPH
0.05 = volume of enzyme added (ml)

Units/mg = Units per ml enzyme/mg protein per ml enzyme

For each sample, the assay was performed in triplicate. Units of NADPH oxidase per µg of protein were calculated using the equation above and the average value of the three was taken. These values are shown in table 3.2.

Table 3.2 Calculated units of NADPH oxidase representing the estimated amount of gliotoxin reductase/GliTp, per µg of protein for BY4741 and G600 samples.

Sample	Units NADPH oxidase/µg of protein
BY4741 pRS315	3.08
BY4741 *GliT*-pC210	6.74
G600 pRS315	10.59
G600 *GliT*-pC210	19.63

Table 3.2 shows that in *GliT* transformants there is a higher level of NADPH oxidase and thus gliotoxin reductase activity. BY4741 and G600 constitutively expressing *GliT* exhibit approximately double the gliotoxin reductase than wild-type.

3.5 Assessing *GliT* expression in yeast under an inducible promoter

3.5.1 Cloning *GliT* into pYES2

After the discovery that constitutive expression of the *A. fumigatus GliT* gene confers increased resistance to gliotoxin in yeast, we wanted to increase the level of GliTp *in vivo* by galactose induction. To this end, we cloned the *GliT* gene by homologous recombination into the pYES2 vector which contains a *GAL1* promoter and the *URA3* gene marker. pYES2 was digested using the *Xho*I and *Hind*III restriction enzymes, gel electrophoresed and extracted. *GliT* was amplified, as before, from topovector with overhangs homologous to regions approaching the cleavage sites of pYES2. Simultaneous transformation of linear pYES2 and *GliT* followed by selection on SC plates lacking uracil resulted in colonies containing *GliT*-pYES2. Figure 3.23 represents the plasmid maps constructed for pYES2 and *GliT*-pYES2.

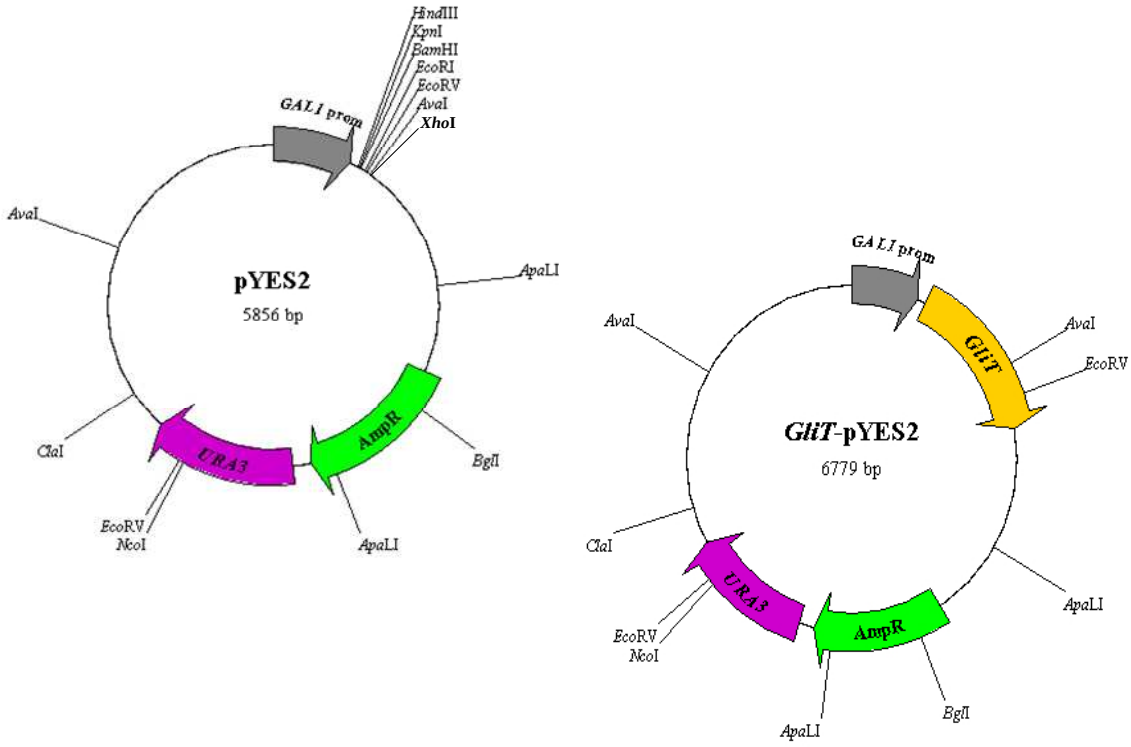

Figure 3.23 Plasmid maps constructed for pYES2 and *GliT*-pYES2. pYES2 was digested using *Hind*III and *Xho*I. 82 bp was removed and *GliT* was cloned into the plasmid by homologous recombination. Both plasmids contain uracil markers and a number of restriction sites as depicted above.

To confirm that cloning had been achieved, PCR was performed on the plasmid, the results are shown in figure 3.24. The primers used bound to pYES2 30 bp up- and downstream of *GliT*, resulting in a product of 1,065 bp (lane 1). No product was observed for the negative control, in which digested pYES2 was used as template DNA. As the primers contained sequence homologous to *GliT*, *GliT* was amplified from *GliT*-pC210 as a positive control giving a product of 1 kb (lane 3).

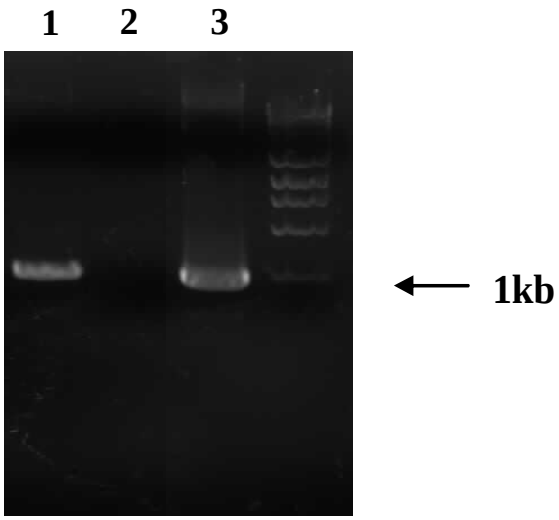

Figure 3.24 Diagnostic PCR depicting the cloning of *GliT* into pYES2. 1 = *GliT*-pYES2; 2 = pYES2; 3 = *GliT*-pC210

The PCR product amplified from the new construct was sent to Agowa for sequencing to check for mutations. The sequencing data retrieved depicted the *GliT* sequence containing the same mutation as was seen for *GliT*-pC210 (section 3.4.1). No other mutations were found.

3.5.2 Examining the effects of galactose-induced *GliT* expression on yeast growth

To assess the effects of galactose-induced GliTp on the growth of *S. cerevisiae*, we transformed the new construct of *GliT* under the control of the inducible *GAL1* promoter in pYES2 into BY4741 and G600. We selected for cells containing the plasmid on SC plates lacking uracil and used both glucose and galactose for metabolism.

Gliotoxin was added to these plates enabling us to compare and contrast a) the cellular growth when different carbohydrate sources were used and b) the protective abilities of *GliT* in response to gliotoxin when induced by galactose metabolism. As a control, an empty pYES2 vector was used to allow comparative growth. Figure 3.25 reveals how BY4741 utilises galactose much more efficiently than G600.

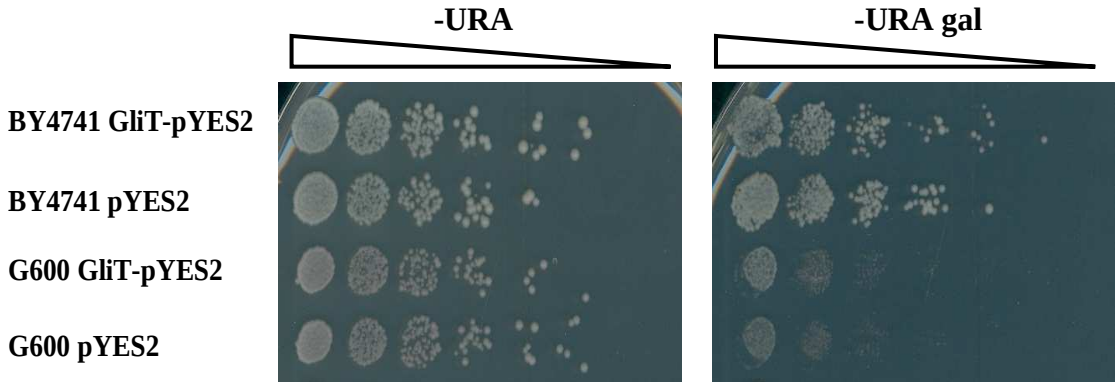

Figure 3.25 Comparative growth analysis of wild-type strains during metabolism of glucose and galactose (48 hr. 30ºC). G600 cannot metabolise galactose as efficiently as glucose.

In figure 3.26 it can be seen that at 8 µg/ml gliotoxin exposure, BY4741 grew notably better than G600. When glucose was metabolised and cells were exposed to 8 µg/ml gliotoxin, *GliT*-pYES2 transformants grew as wild-type, as *GliT* expression was not induced. Under 8 µg/ml gliotoxin exposure when galactose was used as a carbohydrate source, overall growth was largely diminished and *GliT* expression, rather than exhibiting protective effects actually appeared to confer an increase in sensitivity to gliotoxin in yeast. The cells containing the empty pYES2 vector grew more efficiently than those expressing galactose inducible *GliT*.

These plates were incubated at room temperature for a further 48 hours after which a clearer difference in growth of BY4741 *GliT*-pYES2 and pYES2 was observed (figure 3.27). The strain containing the empty vector grew better than the *GliT*

transformant, suggesting galactose induction of *GliT* increasingly sensitises yeast to gliotoxin.

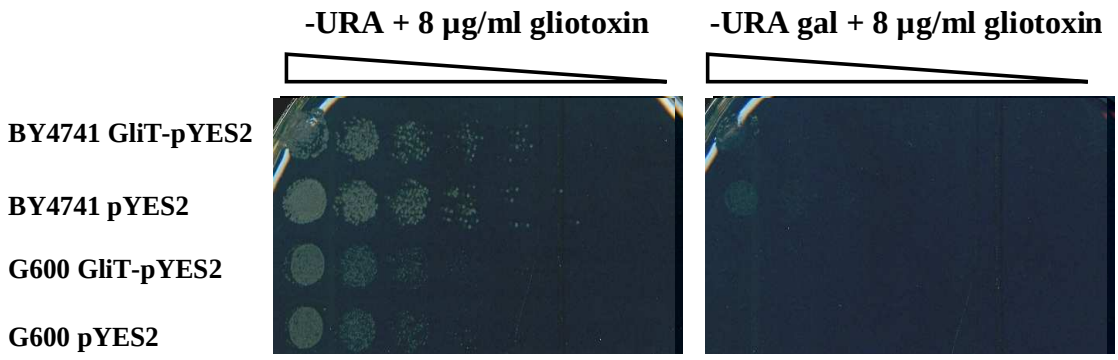

Figure 3.26 Comparative growth analysis of wild-type strains during metabolism of glucose and galactose with 8 µg/ml gliotoxin addition (48 hr. 30ºC). 8 µg/ml gliotoxin caused a strong inhibition of G600 when glucose was metabolised. On 8 µg/ml gliotoxin galactose plates, G600 does not grow.

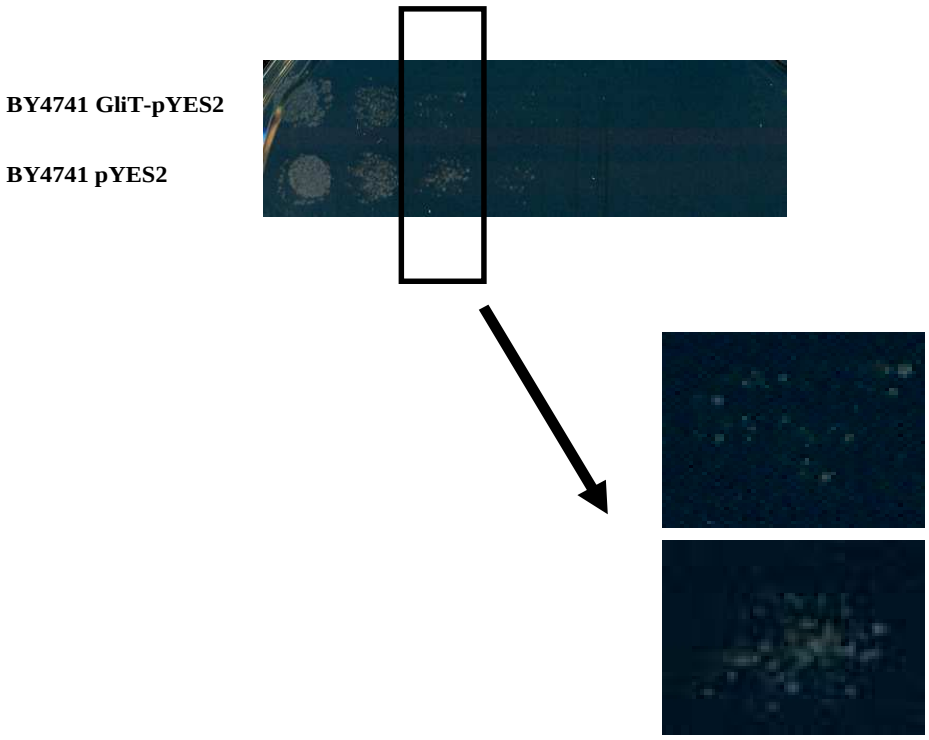

Figure 3.27 Comparative growth analysis of BY4741 during galactose metabolism with 8 µg/ml gliotoxin addition (48 hr. 30ºC + 48 hr. RT). Galactose induction of *GliT* appeared to further sensitise yeast to gliotoxin.

3.5.3 Detecting GliTp under galactose induction

Following the findings described above, we attempted to detect GliTp levels in cell lysates. Our results demonstrated that the *GliT* gene displays different effects in yeast, depending on regulation of its expression, thus we wanted to assess levels of GliTp that could be detected when induced by galactose.

3.5.3.1 Coomassie stain of SDS-PAGE gel (*GliT*-pYES2)

To investigate if controlled induction time is relevant to GliTp production, the levels of detectable GliTp was assessed after chronic and acute galactose exposure. SDS-PAGE and coomassie staining was performed as described in section 3.4.3.1. For chronically galactose-exposed lysates, cells were cultured in SC –URA gal liquid media overnight and grown in the same liquid media on the day of lysate extraction. For acutely exposed lysates, cells were cultured in SC –URA overnight and SC –URA gal on the day of lysate extraction. This allowed us to compare how chronic and acute metabolism of galactose (and thus induction of *GliT* expression) impact on the ability to detect GliTp (figure 3.28).

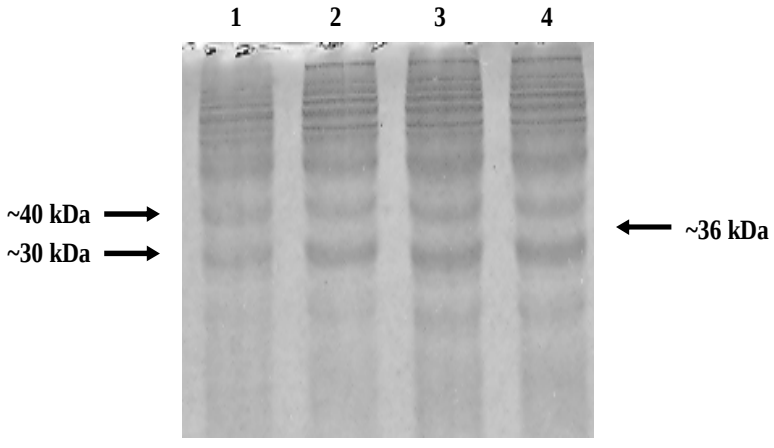

Figure 3.28 Coomassie stain of SDS-PAGE gel with protein from BY4741 containing *GliT*-pYES2 and pYES2 (chronic and acute galactose metabolism) 1 = *GliT*-pYES2 (acute); 2 = pYES2 (acute); 3 = *GliT*-pYES2 (chronic); 4 = pYES2 (chronic).

10 µg of each lysate sample was run on a SDS-PAGE gel and coomassie stained in an attempt to observe possible GliTp bands in the protein samples from strains containing the *GliT* gene. Figure 3.28 showns that there was no protein expression at 36 kDa, therefore GliTp detection in yeast appears to be difficult. Regardless of chronic or acute galactose metabolism and controlled induction of *GliT* expression, GliTp could not be identified.

3.5.3.2 Enzymatic assay of gliotoxin reductase activity (*GliT*-pYES2)

Again we wanted to compare GliTp detection after chronic and acute galactose metabolism. The enzymatic gliotoxin reductase assay was performed as described in section 3.4.3.2. For chronically galactose-exposed lysates, cells were cultured in SC – URA gal liquid media overnight and grown in the same liquid media on the day of lysate extraction. For acutely exposed lysates, cells were cultured in SC –URA overnight and SC –URA gal on the day of lysate extraction. This allowed us to compare how chronic and acute metabolism of galactose (and thus induction of *GliT* expression) impact on GliTp detection (figure 3.29).

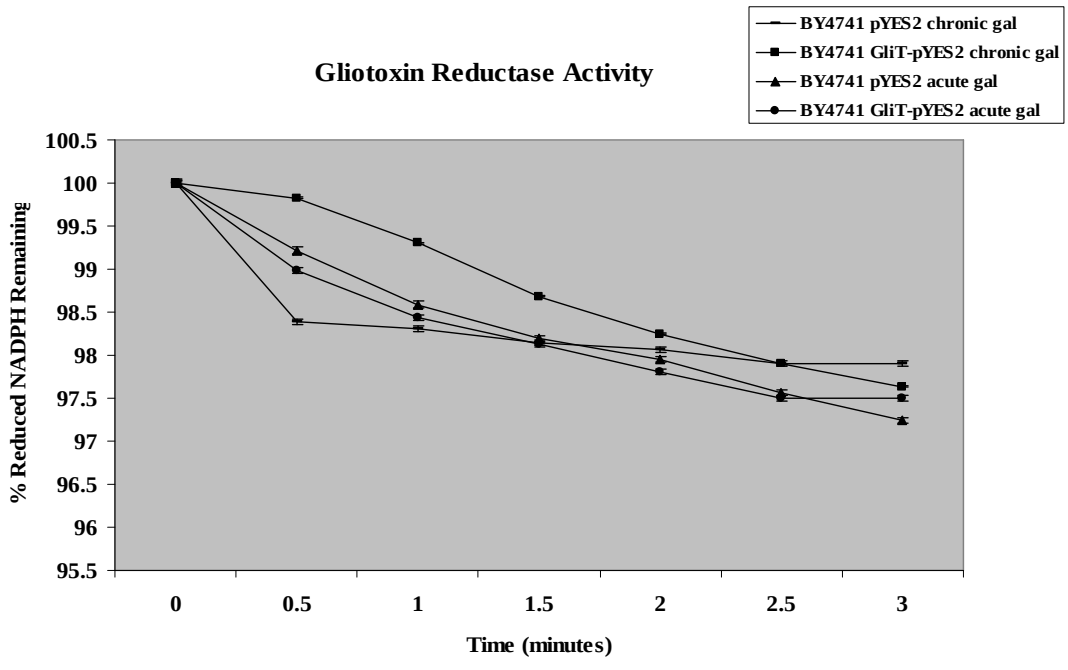

Figure 3.29 NADPH oxidase activity in BY4741 (*GliT*-pYES2).

There is no clear trend seen in figure 3.29. After three minutes, the highest level of NADPH oxidase activity is seen for the pYES2 acute galactose metabolism sample. The *GliT*-pYES2 acute galactose metabolism sample showed the second highest level of activity and both the chronic galactose metabolism samples showed lower levels of NADPH oxidase activity. However, these results were not consistent at all time points during the three minutes. Thus, due to the lack of consistency within this graph, no accurate conclusions can be made about the detectable level of GliTp.

We calculated the units of NADPH oxidase as before and these values are presented in table 3.3. It is again clear from this table that there is no specific trend, *GliT* under controlled galactose induction does not produce a detectable level of GliTp. The same was apparent for both chronic and acute galactose-induced expression.

Table 3.3 Calculated units of NADPH oxidase representing the estimated amount of GliTp, per µg of protein from BY4741 samples.

Sample	Units of NADPH oxidase/µg of protein
pYES2 chronic gal	13.96
GliT-pYES2 chronic gal	21.27
pYES2 acute gal	30.39
GliT-pYES2 acute gal	17.78

Section 2: Investigation into the global response to gliotoxin exhibited by *S. cerevisiae*

3.6 Investigation into the global response of *S. cerevisiae* to gliotoxin

To gain further insight into the deleterious effects caused by gliotoxin, we investigated the global yeast response to the toxin. To do this, we applied transcriptomic and proteomic techniques, RNA sequencing analysis and two-dimensional gel electrophoresis respectively.

3.6.1 Using transcriptomics to explore the mechanism of action of gliotoxin

G600 wild-type yeast were exposed to gliotoxin at concentrations of 0, 16 and 64 µg/ml for 1 hr., RNA was extracted from the cells and residual DNA was removed. Approximately 8 mg of total RNA from each sample underwent sequenced using Illumina® technology, whereby the total RNA was converted into a library of template molecules which were quantified to give figures representative of expression levels of genes. Thus, for each treatment, data was obtained listing any gene that was transcribed and its expression level detected.

On retrieval of transcriptome data for each treatment, comparisons were made between the data from samples that were exposed to a) 0 and 16 µg/ml gliotoxin, and b) 0 and 64 µg/ml gliotoxin. The genes from lists returned were first grouped into those upregulated and downregulated, and then sub-grouped depending on their fold change. The groups that underwent further analysis were those that had more than 2-fold increase or decrease in expression.

3.6.1.1 Analysis of the effect of 16 µg/ml gliotoxin exposure on global transcription in yeast cells

In response to 16 µg/ml gliotoxin exposure, 172 genes showed increased expression of more than 3-fold and 423 2-3-fold. From this, analysis was performed on the 595 genes that underwent more than 2-fold upregulation in response to 16 µg/ml

gliotoxin exposure. In contrast, 318 and 335 genes underwent more than 3-fold and 2-3-fold downregulation repectively, thus 653 genes which exhibited more than 2-fold downregulation were analysed.

Each of these genes that showed a noteworthy change in the level of transcription was assigned GO Identities reflective of the gene function. Most genes were designated more than one GO Identity due to multiple functions. There are three GO Identity categories which were used, Molecular Function, Biological Process and Cellular Component, see table 3.4.

Table 3.4 GO Identity terms used to characterise genes and proteins (taken from *Saccharomyces* Genome Database).

Biological Process Terms	Molecular Function Terms	Cellular Component Terms
None	None	None
Biological process unknown	Molecular function unknown	Cellular component unknown
DNA metabolic processes	DNA binding	Golgi apparatus
RNA metabolic processes	RNA binding	Cell cortex
Cell budding	Enzyme regulator activity	Cell wall
Cell cycle	Helicase activity	Cellular bud
Cellular amino acid metabolic processes	Hydrolase activity	Chromosome
Cellular aromatic compound metabolic processes	Isomerase activity	Cytoplasm
Cellular carbohydrate metabolic processes	Ligase activity	Cytoplasmid membrane-bounded vesicle
Cellular component morphogenesis	Lipid binding	Cytoskeleton
Cellular homeostasis	Lyase activity	Endomembrane system
Cellular lipid metabolic process	Motor activity	Endoplasmic reticulum
Cellular membrane organization	Neucleotidyltransferase activity	Extracellular region membrane
Cellular protein catabolic process	Oxidoreductase activity	Membrane fraction
Cellular respiration	Peptidase activity	Microtubule organising centre
Chromosome organization	Phosphoprotein phosphatase activity	Mitochondrial envelope
Chromosome segregation	Protein binding	Mitochondrion
Cofactor metabolic process	Protein kinase activity	Nucleolus
Conjugation	Signal transducer activity	Nucleus
Cytokinesis	Structural molecule activity	Peroxisome
Cytoskeleton organization	Transcription regulator activity	Plasma membrane
Cell wall organization	Transferase activity	Ribosome
Generation of precursor metabolites and energy	Translation regulator activity	Site of polarized growth
Heterocycle metabolic process	Transporter activity	Vacuole
Meiosis	Triplet codon-amino acid adaptor activity	
Mitochondrion organization		
Nucleus organization		
Peroxisome organization		
Protein complex biogenesis		
Protein folding		
Protein modification process		
Pseudohyphal growth		
Response to chemical stimulus		

Response to stress
Ribosome biogenesis
Signaling
Sporulation
Transcription
Translation
Transport
Transposition
Vacuole organization
Vesicle organization
Vesicle-mediated transport
Vitamin metabolic process

Thus, each gene was categorised respective to its biological and molecular functions, in addition to the cellular component affected by the expression of the gene. For both up- and downregulated genes, the number of genes in each category was then expressed as a percentage of the total transcriptional changes. For example, genes that underwent a more than 2-fold increase in transcription were classified based on their molecular function. Four genes were found to have helicase activity, ergo these genes occupy 0.7% of the total molecular function activity carried out by the said genes.

It must be noted however that there are limitations in analysing gene percentages in each of the three categories. For example, the proportion of cytoplasm- and vacuole-associated genes that exist may not be the same across the genome. Thus, the percentage change outcomes are likely to be skewed to reflect the proportions of genes in the entire genome that are associated with a particular component/function/process.

Summary of the overall effects of gene upregulation on cells

Figures 3.30-3.32 illustrate the overall effects on cells induced by genes upregulated more than 2-fold in response to 16 µg/ml gliotoxin exposure.

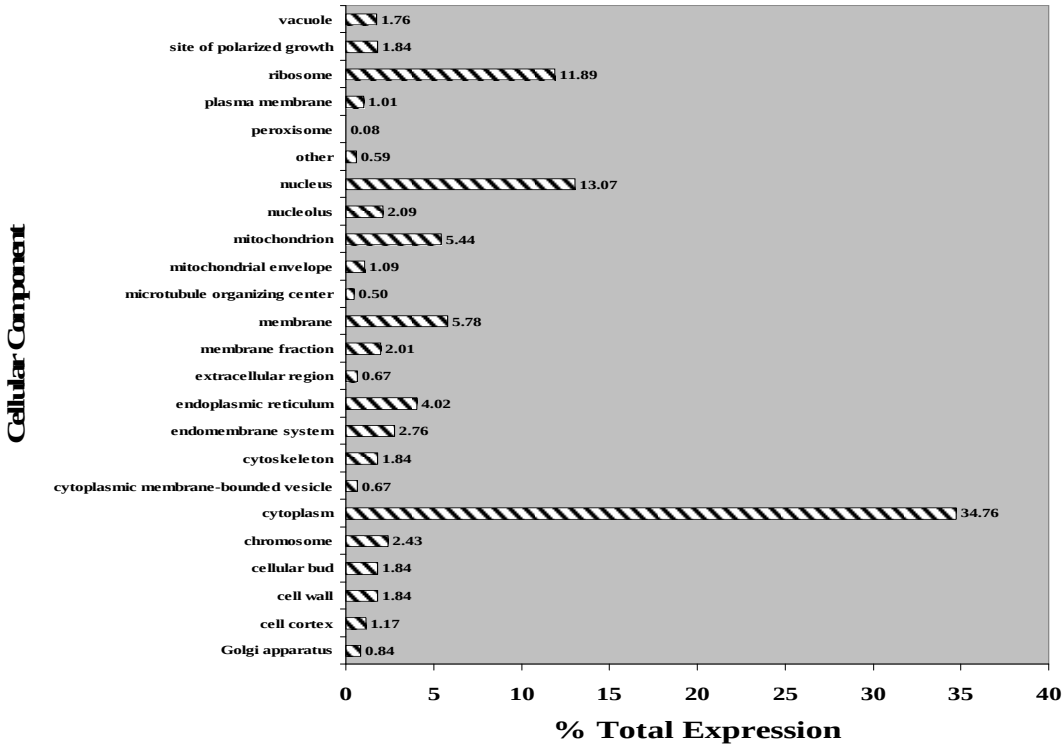

Figure 3.30 The percentage of each cellular component category (16 µg/ml upregulated genes). Genes upregulated more than two-fold were assigned cellular component categories. The number of genes in each category was expressed as a percentage of the number of total genes.

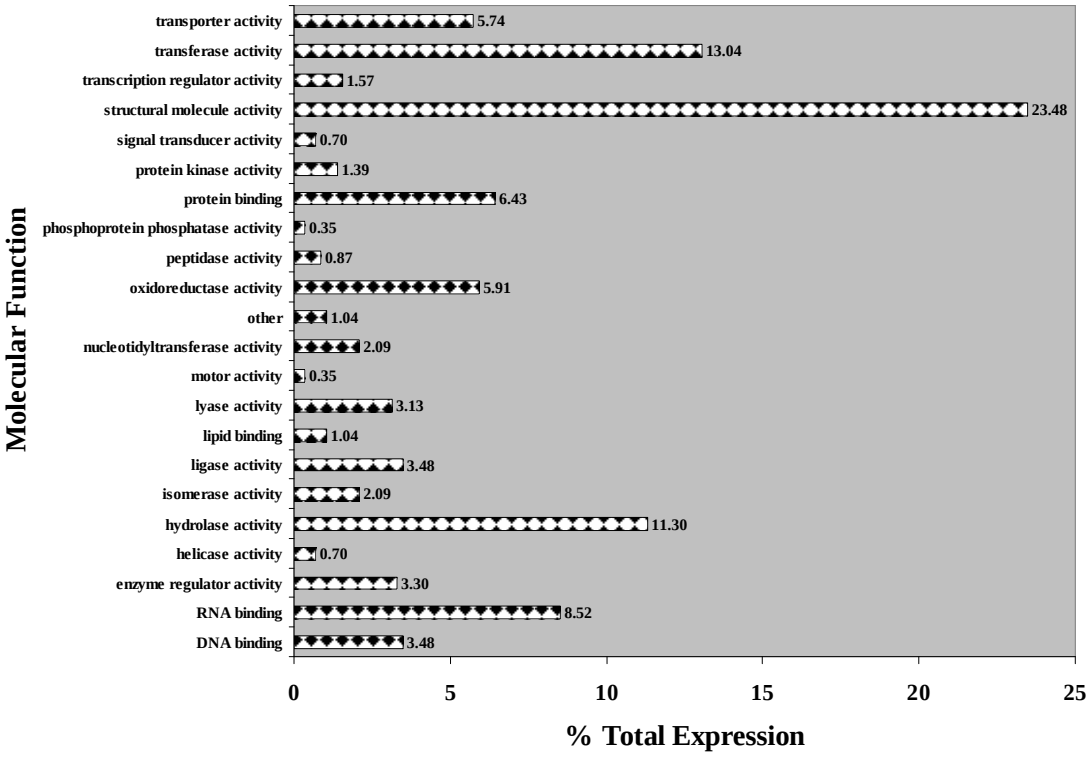

Figure 3.31 The percentage of each molecular function category (16 µg/ml upregulated genes). Genes upregulated more than two-fold were assigned molecular function categories. The number of genes in each category was expressed as a percentage of the number of total genes.

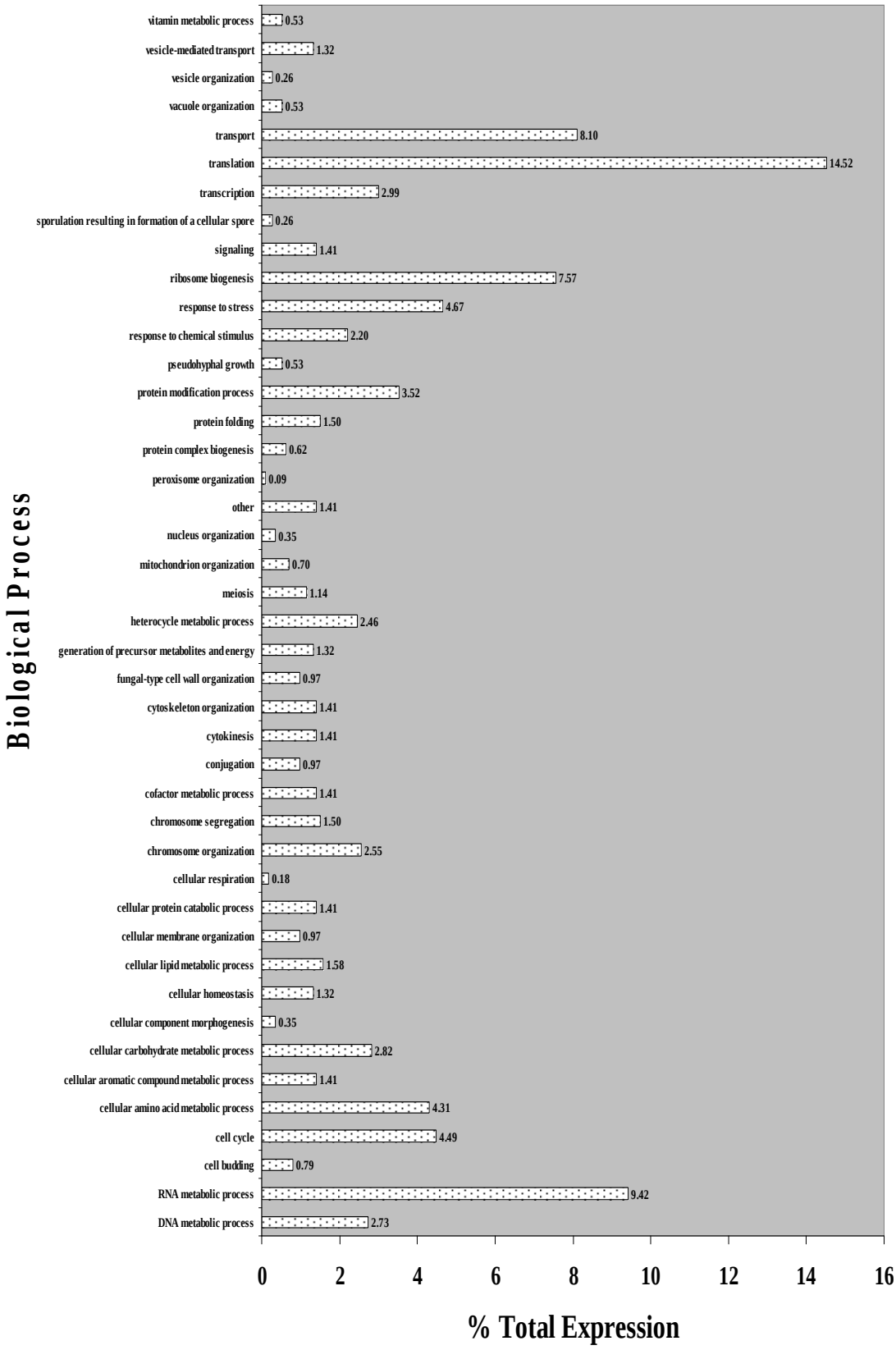

Figure 3.32 The percentage of each biological process category (16 µg/ml upregulated genes). Genes upregulated more than two-fold were assigned biological process categories. The number of genes in each category was expressed as a percentage of the number of total genes.

In order to further analyse the cellular response to gliotoxin, the five most highly upregulated biological processes, molecular functions and associated cellular components were further examined. These are illustrated in figures 3.33-3-35.

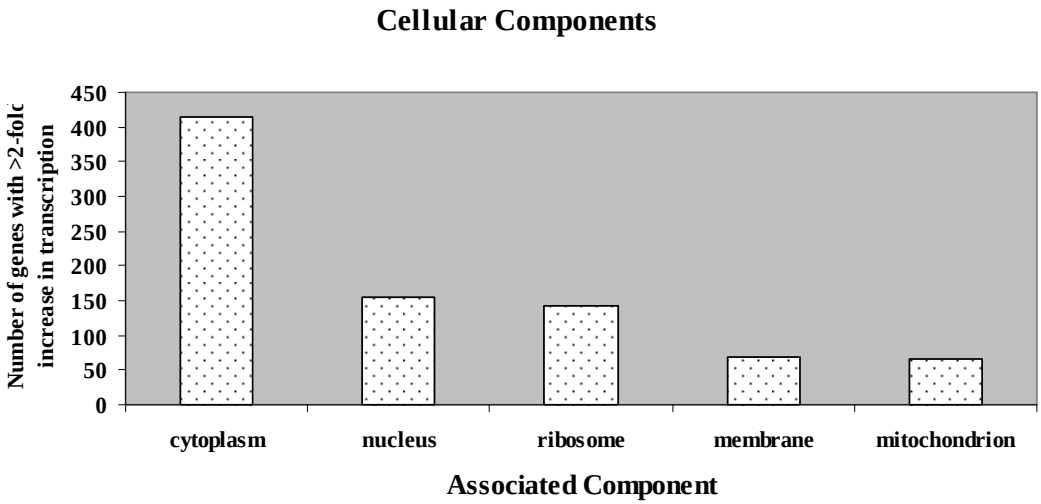

Figure 3.33 The five associated cellular components most highly upregulated by exposure to 16 µg/ml gliotoxin.

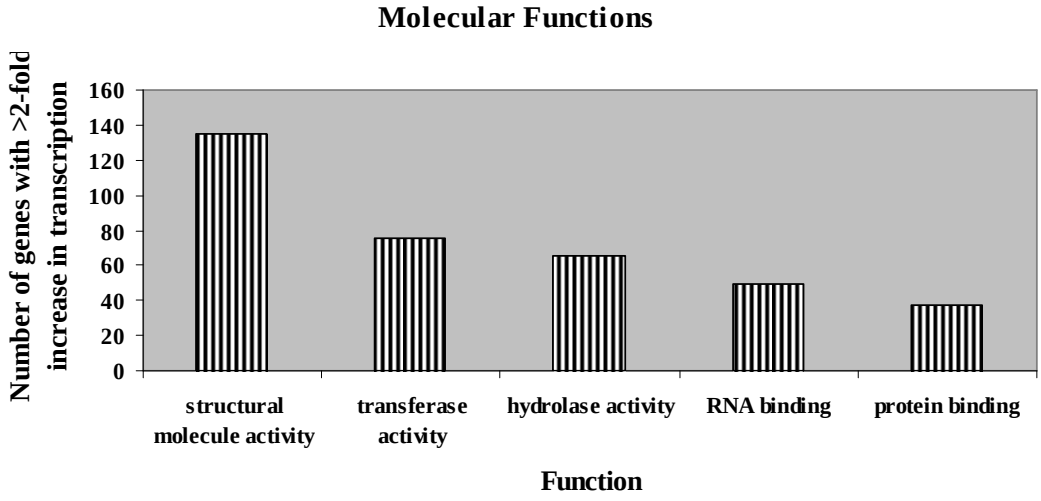

Figure 3.34 The five molecular functions most highly upregulated by exposure to 16 µg/ml gliotoxin.

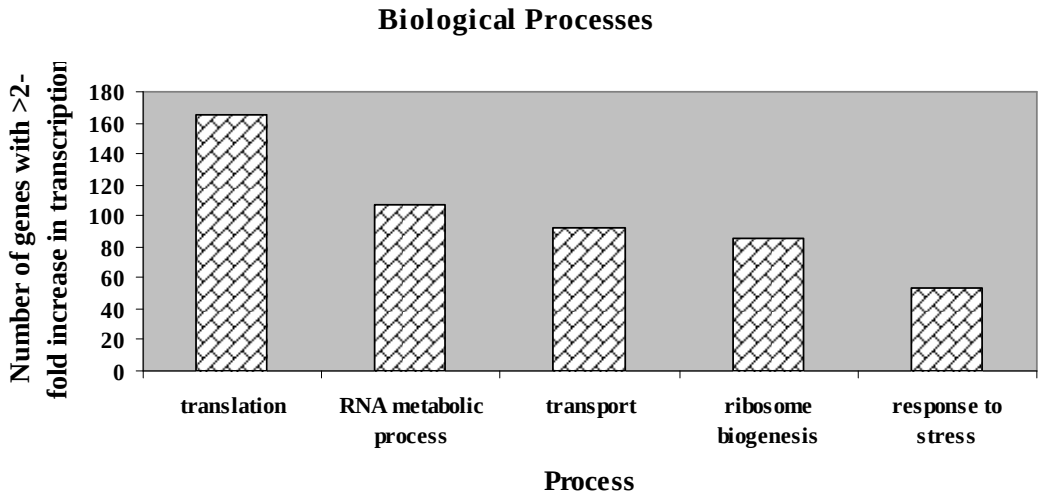

Figure 3.35 The five biological processes most highly upregulated by exposure to 16 µg/ml gliotoxin.

Table 3.5 lists the fifty genes, and their respective functions, that underwent the highest increase in transcription in response to 16 µg/ml gliotoxin.

Table 3.5 The fifty genes most highly upregulated in response to 16 µg/ml gliotoxin exposure. Gene functions were obtained from www.yeastgenome.org (SGD).

Gene	Fold Change	Gene Function
MET3	11.70	ATP sulfurylase, catalyzes the primary step of intracellular sulfate activation, essential for assimilatory reduction of sulfate to sulfide, involved in methionine metabolism
RPS29B	9.36	Protein component of the small (40S) ribosomal subunit; nearly identical to Rps29Ap and has similarity to rat S29 and E. coli S14 ribosomal proteins
BTN2	9.13	v-SNARE binding protein that facilitates specific protein retrieval from a late endosome to the Golgi; modulates arginine uptake, possible role in mediating pH homeostasis between the vacuole and plasma membrane H(+)-ATPase
MET14	7.44	Adenylylsulfate kinase, required for sulfate assimilation and involved in methionine metabolism
RPL28	6.64	Ribosomal protein of the large (60S) ribosomal subunit, has similarity to E. coli L15 and rat L27a ribosomal proteins; may have peptidyl transferase activity; can mutate to cycloheximide resistance
RPS9B	5.98	Protein component of the small (40S) ribosomal subunit; nearly identical to Rps9Ap and has similarity to E. coli S4 and rat S9 ribosomal proteins
RNR1	5.86	One of two large regulatory subunits of ribonucleotide-diphosphate reductase; the RNR complex catalyzes rate-limiting step in dNTP synthesis, regulated by DNA replication and DNA damage checkpoint pathways via localization of small subunits
RPL2B	5.67	Protein component of the large (60S) ribosomal subunit, identical to Rpl2Ap and has similarity to E. coli L2 and rat L8 ribosomal proteins; expression is upregulated at low temperatures
RPL31A	5.61	Protein component of the large (60S) ribosomal subunit, nearly

		identical to Rpl31Bp and has similarity to rat L31 ribosomal protein; associates with the karyopherin Sxm1p; loss of both Rpl31p and Rpl39p confers lethality
RPP1B	5.55	Ribosomal protein P1 beta, component of the ribosomal stalk, which is involved in interaction of translational elongation factors with ribosome; accumulation is regulated by phosphorylation and interaction with the P2 stalk component
MET17	5.54	Methionine and cysteine synthase (O-acetyl homoserine-O-acetyl serine sulfhydrylase), required for sulfur amino acid synthesis
YFR032C	5.42	Putative protein of unknown function; non-essential gene identified in a screen for mutants with increased levels of rDNA transcription; expressed at high levels during sporulation
RPS26B	5.17	Protein component of the small (40S) ribosomal subunit; nearly identical to Rps26Ap and has similarity to rat S26 ribosomal protein
RPL8A	4.99	Ribosomal protein L4 of the large (60S) ribosomal subunit, nearly identical to Rpl8Bp and has similarity to rat L7a ribosomal protein; mutation results in decreased amounts of free 60S subunits
RPL34B	4.98	Protein component of the large (60S) ribosomal subunit, nearly identical to Rpl34Ap and has similarity to rat L34 ribosomal protein
RPS30B	4.94	Protein component of the small (40S) ribosomal subunit; nearly identical to Rps30Ap and has similarity to rat S30 ribosomal protein
PAU18	4.91	Protein of unknown function, member of the seripauperin multigene family encoded mainly in subtelomeric regions; identical to Pau6p
PAU6	4.91	Member of the seripauperin multigene family encoded mainly in subtelomeric regions, active during alcoholic fermentation, regulated by anaerobiosis, negatively regulated by oxygen, repressed by heme; identical to Pau18p
SPH1	4.87	Protein involved in shmoo formation and bipolar bud site selection; homologous to Spa2p, localizes to sites of polarized growth in a cell cycle dependent- and Spa2p-dependent manner, interacts with MAPKKs Mkk1p, Mkk2p, and Ste7p
RPL6B	4.80	Protein component of the large (60S) ribosomal subunit, has similarity to Rpl6Ap and to rat L6 ribosomal protein; binds to 5.8S rRNA
RPS24B	4.77	Protein component of the small (40S) ribosomal subunit; identical to Rps24Ap and has similarity to rat S24 ribosomal protein
RPL17A	4.70	Protein component of the large (60S) ribosomal subunit, nearly identical to Rpl17Bp and has similarity to E. coli L22 and rat L17 ribosomal proteins; copurifies with the Dam1 complex (aka DASH complex)
TOS3	4.67	Protein kinase, related to and functionally redundant with Elm1p and Sak1p for the phosphorylation and activation of Snf1p; functionally orthologous to LKB1, a mammalian kinase associated with Peutz-Jeghers cancer-susceptibility syndrome
RPL2A	4.67	Protein component of the large (60S) ribosomal subunit, identical to Rpl2Bp and has similarity to E. coli L2 and rat L8 ribosomal proteins
RPL26B	4.66	Protein component of the large (60S) ribosomal subunit, nearly identical to Rpl26Ap and has similarity to E. coli L24 and rat L26 ribosomal proteins; binds to 5.8S rRNA
MET16	4.63	3'-phosphoadenylsulfate reductase, reduces 3'-phosphoadenylyl sulfate to adenosine-3',5'-bisphosphate and free sulfite using reduced thioredoxin as cosubstrate, involved in sulfate assimilation and methionine metabolism
RPS24A	4.62	Protein component of the small (40S) ribosomal subunit; identical to Rps24Bp and has similarity to rat S24 ribosomal

		protein
ZPS1	4.61	Putative GPI-anchored protein; transcription is induced under low-zinc conditions, as mediated by the Zap1p transcription factor, and at alkaline pH
RPS10A	4.60	Protein component of the small (40S) ribosomal subunit; nearly identical to Rps10Bp and has similarity to rat ribosomal protein
RPL26A	4.58	Protein component of the large (60S) ribosomal subunit, nearly identical to Rpl26Bp and has similarity to E. coli L24 and rat L26 ribosomal proteins; binds to 5.8S rRNA
RPS28B	4.56	Protein component of the small (40S) ribosomal subunit; nearly identical to Rps28Ap and has similarity to rat S28 ribosomal protein
MCD4	4.52	Protein involved in glycosylphosphatidylinositol (GPI) anchor synthesis; multimembrane-spanning protein that localizes to the endoplasmic reticulum; highly conserved among eukaryotes
RPP2A	4.39	Ribosomal protein P2 alpha, a component of the ribosomal stalk, which is involved in the interaction between translational elongation factors and the ribosome; regulates the accumulation of P1 (Rpp1Ap and Rpp1Bp) in the cytoplasm
RPL34A	4.38	Protein component of the large (60S) ribosomal subunit, nearly identical to Rpl34Bp and has similarity to rat L34 ribosomal protein
RPL8B	4.37	Ribosomal protein L4 of the large (60S) ribosomal subunit, nearly identical to Rpl8Ap and has similarity to rat L7a ribosomal protein; mutation results in decreased amounts of free 60S subunits
RPS0B	4.33	Protein component of the small (40S) ribosomal subunit, nearly identical to Rps0Ap; required for maturation of 18S rRNA along with Rps0Ap; deletion of either RPS0 gene reduces growth rate, deletion of both genes is lethal
BNA3	4.33	Kynurenine aminotransferase, catalyzes formation of kynurenic acid from kynurenine; potential Cdc28p substrate
RPS0A	4.32	Protein component of the small (40S) ribosomal subunit, nearly identical to Rps0Bp; required for maturation of 18S rRNA along with Rps0Bp; deletion of either RPS0 gene reduces growth rate, deletion of both genes is lethal
VEL1	4.32	Protein of unknown function; highly induced in zinc-depleted conditions and has increased expression in NAP1 deletion mutants
MET10	4.30	Subunit alpha of assimilatory sulfite reductase, which converts sulfite into sulfide
RPS29A	4.30	Protein component of the small (40S) ribosomal subunit; nearly identical to Rps29Bp and has similarity to rat S29 and E. coli S14 ribosomal proteins
RPS7B	4.27	Protein component of the small (40S) ribosomal subunit, nearly identical to Rps7Ap; interacts with Kti11p; deletion causes hypersensitivity to zymocin; has similarity to rat S7 and Xenopus S8 ribosomal proteins
RPL16A	4.26	N-terminally acetylated protein component of the large (60S) ribosomal subunit, binds to 5.8 S rRNA; has similarity to Rpl16Bp, E. coli L13 and rat L13a ribosomal proteins; transcriptionally regulated by Rap1p
RPL7B	4.21	Protein component of the large (60S) ribosomal subunit, nearly identical to Rpl7Ap and has similarity to E. coli L30 and rat L7 ribosomal proteins; contains a conserved C-terminal Nucleic acid Binding Domain (NDB2)
GAT4	4.21	Protein containing GATA family zinc finger motifs
RPL37A	4.19	Protein component of the large (60S) ribosomal subunit, has similarity to Rpl37Bp and to rat L37 ribosomal protein
RPL15A	4.18	Protein component of the large (60S) ribosomal subunit, nearly identical to Rpl15Bp and has similarity to rat L15 ribosomal protein; binds to 5.8 S rRNA

RPS9A	4.17	Protein component of the small (40S) ribosomal subunit; nearly identical to Rps9Bp and has similarity to E. coli S4 and rat S9 ribosomal proteins
RPL13B	4.17	Protein component of the large (60S) ribosomal subunit, nearly identical to Rpl13Ap; not essential for viability; has similarity to rat L13 ribosomal protein
RPS5	4.16	Protein component of the small (40S) ribosomal subunit, the least basic of the non-acidic ribosomal proteins; phosphorylated in vivo; essential for viability; has similarity to E. coli S7 and rat S5 ribosomal proteins

One of the first significant observations made was that out of 172 genes that underwent a more than 3-fold increase in transcription, 107 were noted to encode components of either the small or large subunit of the ribosome. It was also discovered that many genes involved in sulfur amino acid and glutathione biosynthesis were upregulated in response to gliotoxin, in addition to a number of genes involved in glucose fermentation. These will be discussed in detail later.

Summary of the overall effects of gene downregulation on cells

Genes which were transcriptionally repressed under 16 µg/ml gliotoxin exposure were subsequently assessed. Figures 3.36-3.38 illustrate the overall effects on cells induced by genes downregulated more than 2-fold in response to 16 µg/ml gliotoxin exposure.

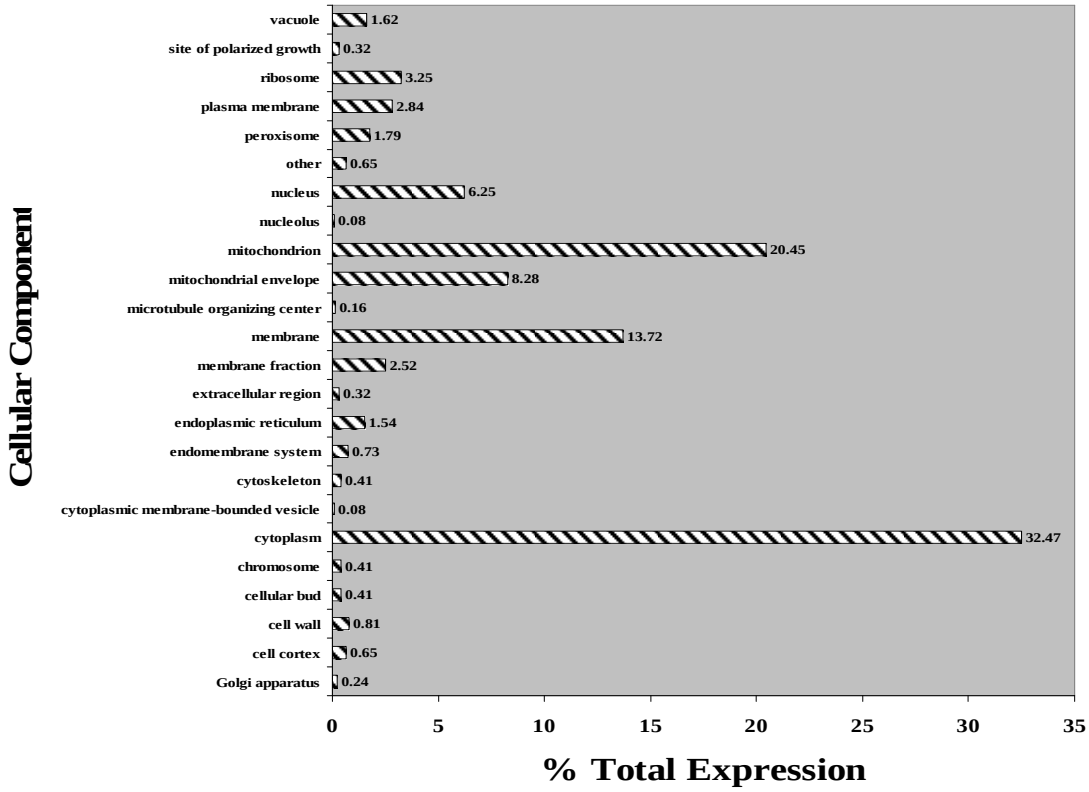

Figure 3.36 The percentage of each cellular component category (16 µg/ml downregulated genes). Genes downregulated more than two-fold were assigned cellular component categories. The number of genes in each category was expressed as a percentage of the number of total genes.

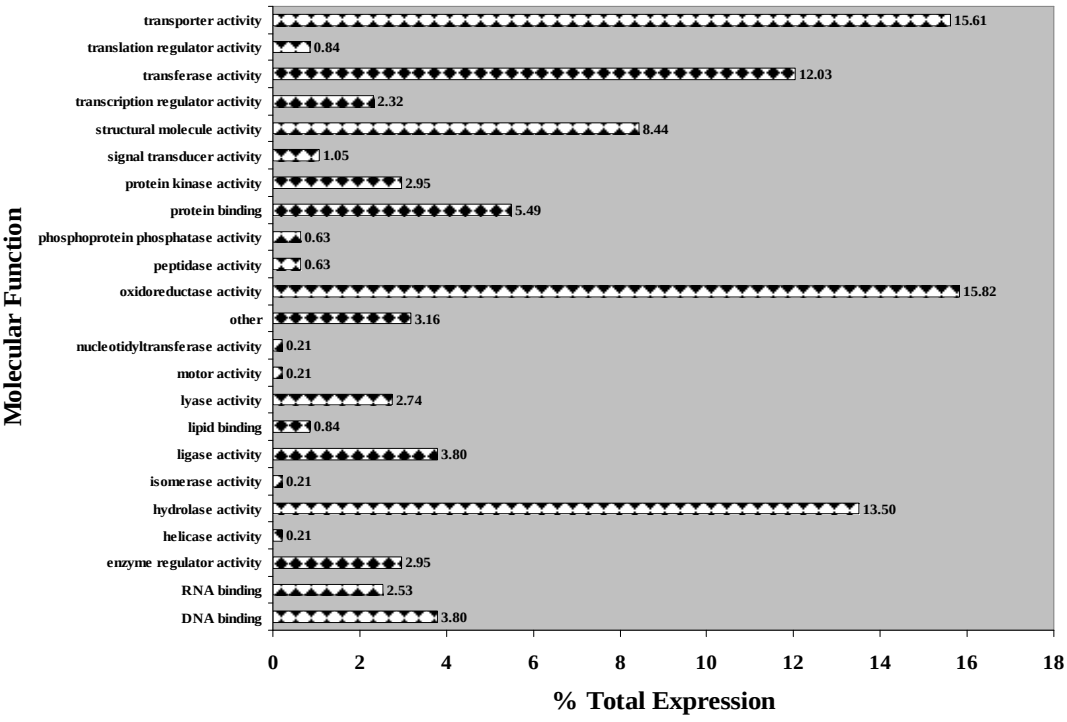

Figure 3.37 The percentage of each molecular function category (16 µg/ml downregulated genes). Genes downregulated more than two-fold were assigned molecular function categories. The number of genes in each category was expressed as a percentage of the number of total genes.

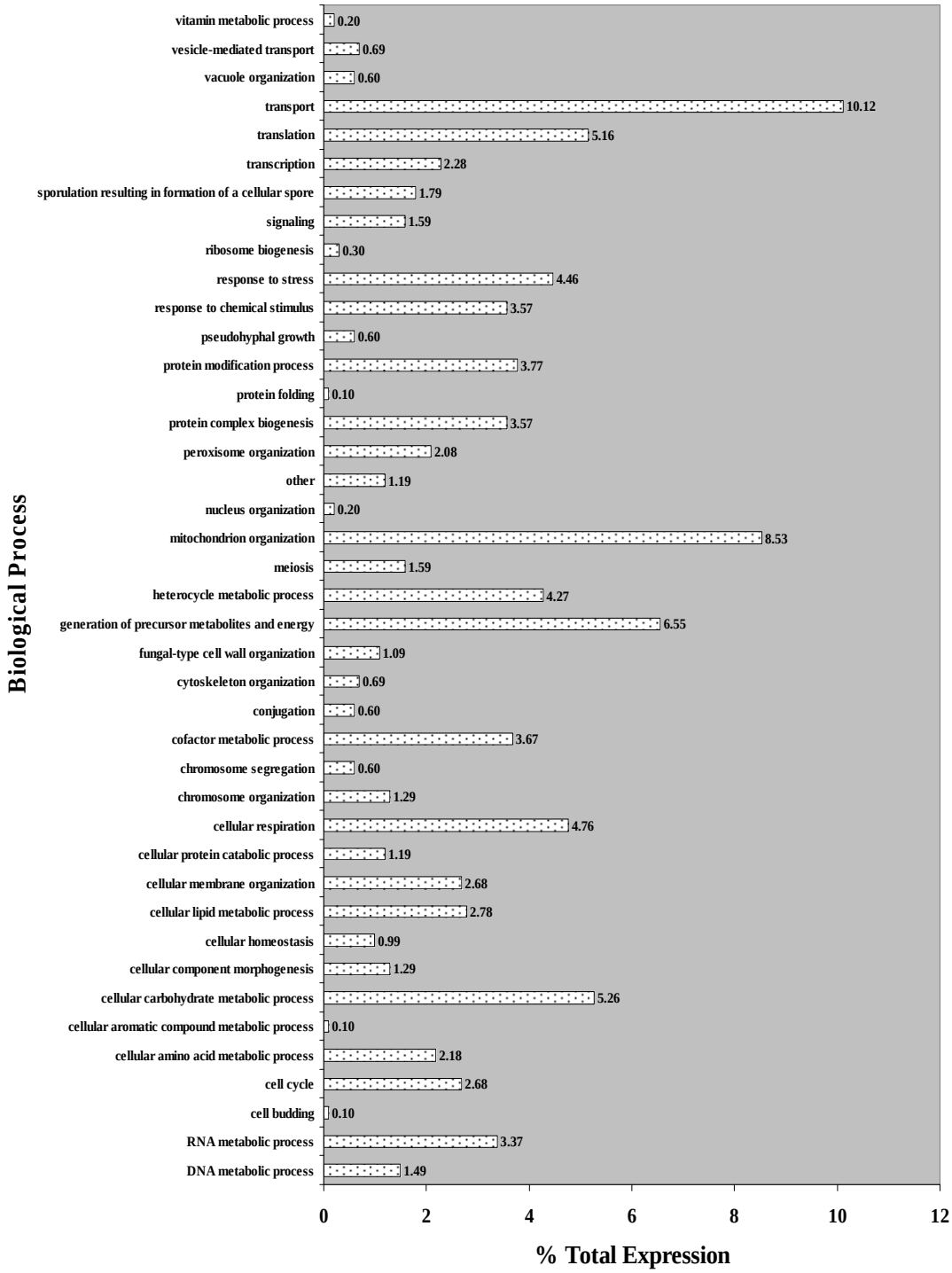

Figure 3.38 The percentage of each biological process category (16 µg/ml downregulated genes). Genes downregulated more than two-fold were assigned biological process categories. The number of genes in each category was expressed as a percentage of the number of total genes.

As for the transcriptionally upregulated genes, the the five most transcriptionally repressed biological processes, molecular functions and associated cellular components were investigated. These results can be observed in figures 3.39-3.41.

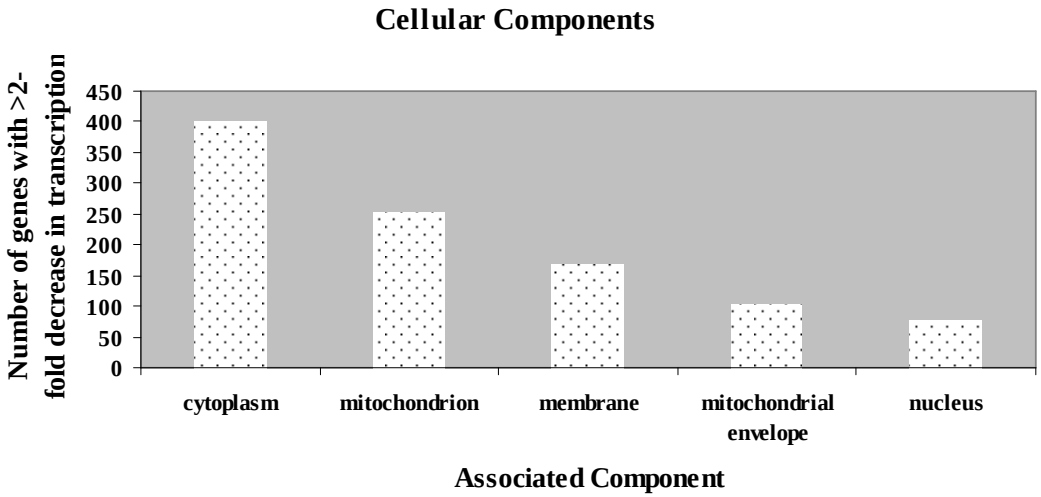

Figure 3.39 The five associated cellular components most highly downregulated by exposure to 16 µg/ml gliotoxin.

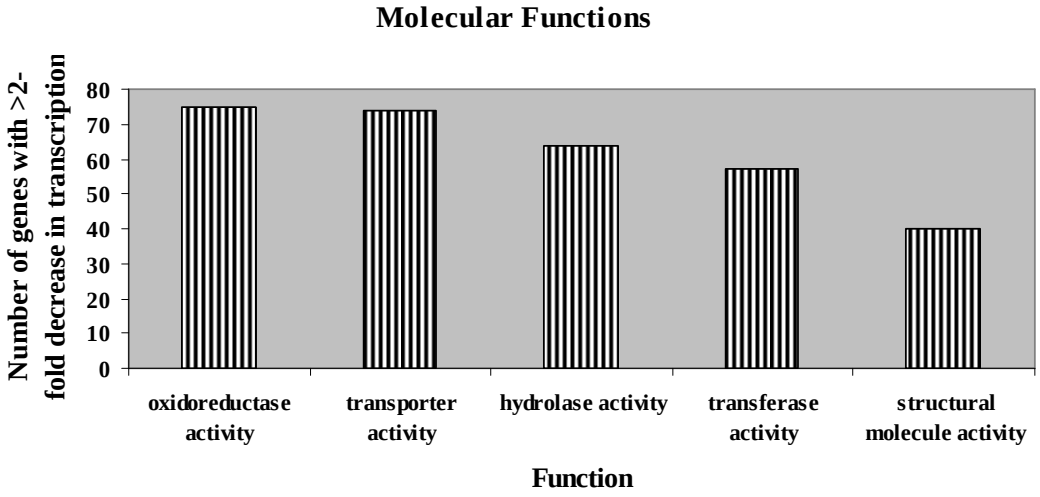

Figure 3.40 The five molecular functions most highly downregulated by exposure to 16 µg/ml gliotoxin.

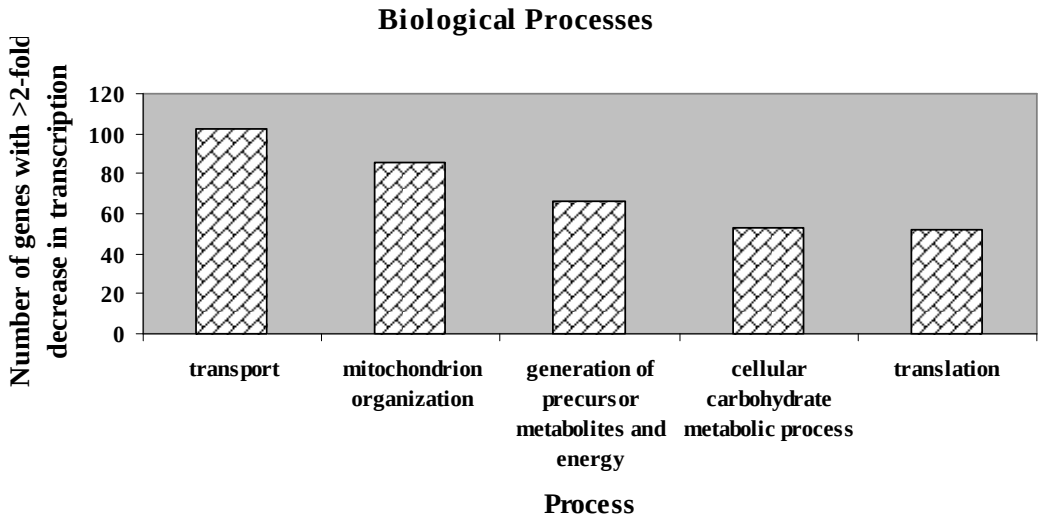

Figure 3.41 The five biological processes most highly downregulated by exposure to 16 µg/ml gliotoxin.

Table 3.6 lists the fifty genes, and their respective functions, that underwent the highest decrease in transcription in response to 16 µg/ml gliotoxin.

Table 3.6 The fifty genes most highly downregulated in response to 16 µg/ml gliotoxin exposure. Gene functions were obtained from www.yeastgenome.org (SGD).

Gene	Fold Change	Gene Function
YIL057C	-204.79	Protein of unknown function involved in energy metabolism under respiratory conditions; expression induced under carbon limitation and repressed under high glucose
YDR119W-A	-186.53	Putative protein of unknown function; may interact with respiratory chain complexes III (ubiquinol-cytochrome c reductase) or IV (cytochrome c oxidase)
SPG1	-136.45	Protein required for survival at high temperature during stationary phase; not required for growth on nonfermentable carbon sources; the authentic, non-tagged protein is detected in highly purified mitochondria in high-throughput studies
YIG1	-106.67	Protein that interacts with glycerol 3-phosphatase and plays a role in anaerobic glycerol production; localizes to the nucleus and cytosol
SFC1	-67.46	Mitochondrial succinate-fumarate transporter, transports succinate into and fumarate out of the mitochondrion; required for ethanol and acetate utilization
SIP18	-62.65	Phospholipid-binding protein; expression is induced by osmotic stress
SPG4	-50.52	Protein required for survival at high temperature during stationary phase; not required for growth on nonfermentable carbon sources
YGR067C	-36.99	Putative protein of unknown function; contains a zinc finger motif similar to that of Adr1p
MLS1	-34.38	Malate synthase, enzyme of the glyoxylate cycle, involved in utilization of non-fermentable carbon sources; expression is subject to carbon catabolite repression; localizes in peroxisomes during growth in oleic acid medium

ACH1	-33.96	Protein with CoA transferase activity, particularly for CoASH transfer from succinyl-CoA to acetate; has minor acetyl-CoA-hydrolase activity; phosphorylated; required for acetate utilization and for diploid pseudohyphal growth
JEN1	-33.65	Lactate transporter, required for uptake of lactate and pyruvate; phosphorylated; expression is derepressed by transcriptional activator Cat8p during respiratory growth, and repressed in the presence of glucose, fructose, and mannose
SDH2	-33.01	Iron-sulfur protein subunit of succinate dehydrogenase (Sdh1p, Sdh2p, Sdh3p, Sdh4p), which couples the oxidation of succinate to the transfer of electrons to ubiquinone as part of the TCA cycle and the mitochondrial respiratory chain
YMR175W-A	-31.16	Putative protein of unknown function
ADY2	-30.94	Acetate transporter required for normal sporulation; phosphorylated in mitochondria
HXT5	-26.87	Hexose transporter with moderate affinity for glucose, induced in the presence of non-fermentable carbon sources, induced by a decrease in growth rate, contains an extended N-terminal domain relative to other HXTs
SDH1	-23.57	Flavoprotein subunit of succinate dehydrogenase (Sdh1p, Sdh2p, Sdh3p, Sdh4p), which couples the oxidation of succinate to the transfer of electrons to ubiquinone as part of the TCA cycle and the mitochondrial respiratory chain
POT1	-21.95	3-ketoacyl-CoA thiolase with broad chain length specificity, cleaves 3-ketoacyl-CoA into acyl-CoA and acetyl-CoA during beta-oxidation of fatty acids
GRE1	-20.69	Hydrophilin of unknown function; stress induced (osmotic, ionic, oxidative, heat shock and heavy metals); regulated by the HOG pathway
CSM4	-19.85	Protein required for accurate chromosome segregation during meiosis; involved in meiotic telomere clustering (bouquet formation) and telomere-led rapid prophase movements
YNL195C	-17.62	Putative protein of unknown function; shares a promoter with YNL194C; the authentic, non-tagged protein is detected in highly purified mitochondria in high-throughput studies
CAT2	-17.44	Carnitine acetyl-CoA transferase present in both mitochondria and peroxisomes, transfers activated acetyl groups to carnitine to form acetylcarnitine which can be shuttled across membranes
FMP43	-17.03	Putative protein of unknown function; expression regulated by osmotic and alkaline stresses; the authentic, non-tagged protein is detected in highly purified mitochondria in high-throughput studies
IDP2	-16.68	Cytosolic NADP-specific isocitrate dehydrogenase, catalyzes oxidation of isocitrate to alpha-ketoglutarate; levels are elevated during growth on non-fermentable carbon sources and reduced during growth on glucose
YAT1	-16.51	Outer mitochondrial carnitine acetyltransferase, minor ethanol-inducible enzyme involved in transport of activated acyl groups from the cytoplasm into the mitochondrial matrix; phosphorylated
ACS1	-15.69	Acetyl-coA synthetase isoform which, along with Acs2p, is the nuclear source of acetyl-coA for histone acetlyation; expressed during growth on nonfermentable carbon sources and under aerobic conditions
NDE2	-15.18	Mitochondrial external NADH dehydrogenase, catalyzes the oxidation of cytosolic NADH; Nde1p and Nde2p are involved in providing the cytosolic NADH to the mitochondrial respiratory chain
FBP1	-14.95	Fructose-1,6-bisphosphatase, key regulatory enzyme in the gluconeogenesis pathway, required for glucose metabolism; undergoes either proteasome-mediated or autophagy-mediated degradation depending on growth conditions; interacts with

		Vid30p
YGL188C	-14.63	Putative protein of unknown function; YMR206W is not an essential gene
RIP1	-13.42	Ubiquinol-cytochrome-c reductase, a Rieske iron-sulfur protein of the mitochondrial cytochrome bc1 complex; transfers electrons from ubiquinol to cytochrome c1 during respiration
YNL194C	-13.09	Integral membrane protein required for sporulation and plasma membrane sphingolipid content; has sequence similarity to SUR7 and FMP45; GFP-fusion protein is induced in response to the DNA-damaging agent MMS
YML087C	-12.53	Putative protein of unknown function, highly conserved across species and orthologous to human CYB5R4; null mutant displays reduced frequency of mitochondrial genome loss
SDH4	-12.15	Membrane anchor subunit of succinate dehydrogenase (Sdh1p, Sdh2p, Sdh3p, Sdh4p), which couples the oxidation of succinate to the transfer of electrons to ubiquinone as part of the TCA cycle and the mitochondrial respiratory chain
CRC1	-12.10	Mitochondrial inner membrane carnitine transporter, required for carnitine-dependent transport of acetyl-CoA from peroxisomes to mitochondria during fatty acid beta-oxidation
COX5A	-11.78	Subunit Va of cytochrome c oxidase, which is the terminal member of the mitochondrial inner membrane electron transport chain; predominantly expressed during aerobic growth while its isoform Vb (Cox5Bp) is expressed during anaerobic growth
YAT2	-11.07	Carnitine acetyltransferase; has similarity to Yat1p, which is a carnitine acetyltransferase associated with the mitochondrial outer membrane
NDI1	-10.41	NADH:ubiquinone oxidoreductase, transfers electrons from NADH to ubiquinone in the respiratory chain but does not pump protons, in contrast to the higher eukaryotic multisubunit respiratory complex I; phosphorylated; homolog of human AMID
ODC1	-10.27	Mitochondrial inner membrane transporter, exports 2-oxoadipate and 2-oxoglutarate from the mitochondrial matrix to the cytosol for lysine and glutamate biosynthesis and lysine catabolism; suppresses, in multicopy, an fmc1 null mutation
CBP4	-10.14	Mitochondrial protein required for assembly of ubiquinol cytochrome-c reductase complex (cytochrome bc1 complex); interacts with Cbp3p and function is partially redundant with that of Cbp3p
SDH3	-9.77	Cytochrome b subunit of succinate dehydrogenase (Sdh1p, Sdh2p, Sdh3p, Sdh4p), which couples the oxidation of succinate to the transfer of electrons to ubiquinone as part of the TCA cycle and the mitochondrial respiratory chain
FOX2	-9.72	Multifunctional enzyme of the peroxisomal fatty acid beta-oxidation pathway; has 3-hydroxyacyl-CoA dehydrogenase and enoyl-CoA hydratase activities
GLG2	-9.63	Self-glucosylating initiator of glycogen synthesis, also glucosylates n-dodecyl-beta-D-maltoside; similar to mammalian glycogenin
CAT8	-9.51	Zinc cluster transcriptional activator necessary for derepression of a variety of genes under non-fermentative growth conditions, active after diauxic shift, binds carbon source responsive elements
OM45	-9.06	Protein of unknown function, major constituent of the mitochondrial outer membrane; located on the outer (cytosolic) face of the outer membrane
CYT1	-9.02	Cytochrome c1, component of the mitochondrial respiratory chain; expression is regulated by the heme-activated, glucose-repressed Hap2p/3p/4p/5p CCAAT-binding complex
HXT6	-8.94	High-affinity glucose transporter of the major facilitator superfamily, nearly identical to Hxt7p, expressed at high basal

		levels relative to other HXTs, repression of expression by high glucose requires SNF3
HXT7	-8.88	High-affinity glucose transporter of the major facilitator superfamily, nearly identical to Hxt6p, expressed at high basal levels relative to other HXTs, expression repressed by high glucose levels
RPM2	-8.63	Protein subunit of mitochondrial RNase P, has roles in nuclear transcription, cytoplasmic and mitochondrial RNA processing, and mitochondrial translation; distributed to mitochondria, cytoplasmic processing bodies, and the nucleus
HAP4	-8.62	Subunit of the heme-activated, glucose-repressed Hap2p/3p/4p/5p CCAAT-binding complex, a transcriptional activator and global regulator of respiratory gene expression; provides the principal activation function of the complex
YKL187C	-8.61	Putative protein of unknown function; the authentic, non-tagged protein is detected in a phosphorylated state in highly purified mitochondria in high-throughput studies
COX4	-8.53	Subunit IV of cytochrome c oxidase, the terminal member of the mitochondrial inner membrane electron transport chain; precursor N-terminal 25 residues are cleaved during mitochondrial import; phosphorylated; spermidine enhances translation

3.6.1.2 Analysis of the effect of 64 µg/ml gliotoxin exposure on global transcription in yeast cells

In response to 64 µg/ml gliotoxin exposure, 246 and 493 genes underwent more than 3-fold and 2-3-fold upregulation respectively. Thus, analysis was performed on the 739 genes that underwent more than 2-fold upregulation in response to 64 µg/ml gliotoxin exposure. In contrast, 475 and 530 genes underwent more than 3-fold and 2-3-fold downregulation repectively, and these 1,005 genes which exhibited more than 2-fold downregulation were analysed. The same procedure was carried out on these genes, as for the previous set. These genes were allocated GO Identities and categorised under the headings of Molecular Function, Biological Process and Cellular Component, see table 3.4. Gene number in each category was subsequently expressed as a percentage of the total transcriptional changes, as before.

Summary of the overall effects of gene upregulation on cells

Figures 3.42-3.44 illustrate the overall effects on cells induced by genes upregulated more than 2-fold in response to 64 µg/ml gliotoxin exposure.

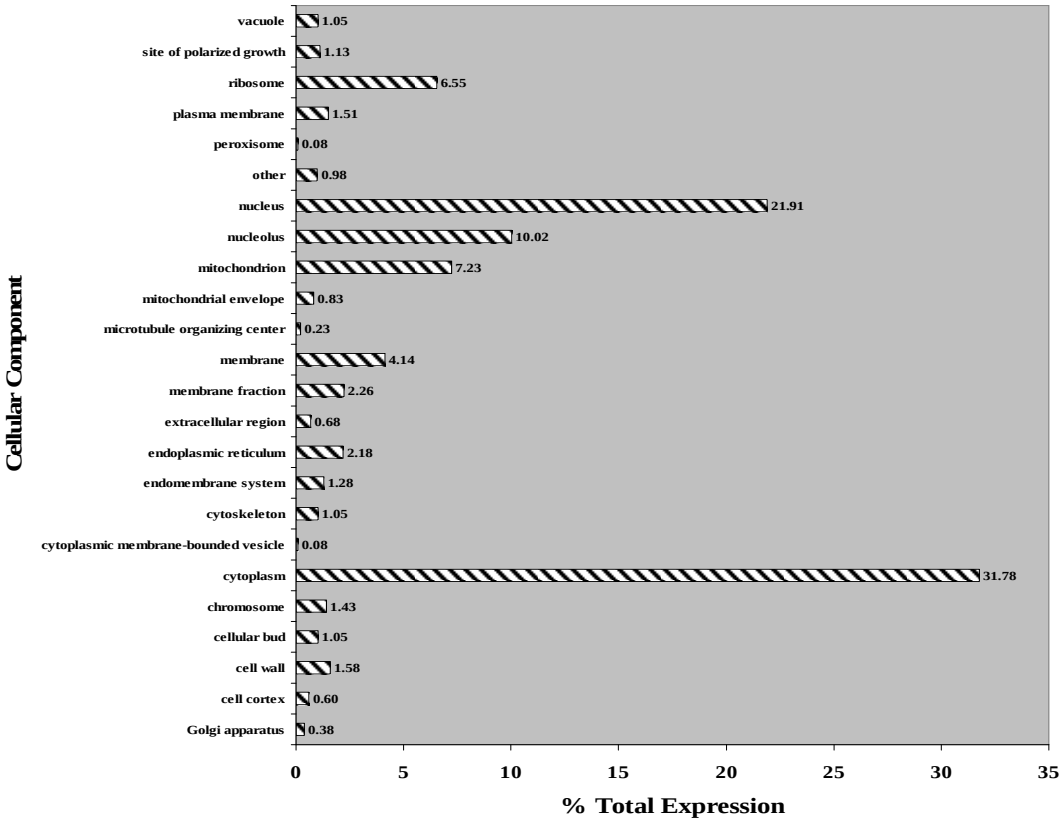

Figure 3.42 The percentage of each cellular component category (64 µg/ml upregulated genes). Genes upregulated more than two-fold were assigned cellular component categories. The number of genes in each category was expressed as a percentage of the number of total genes.

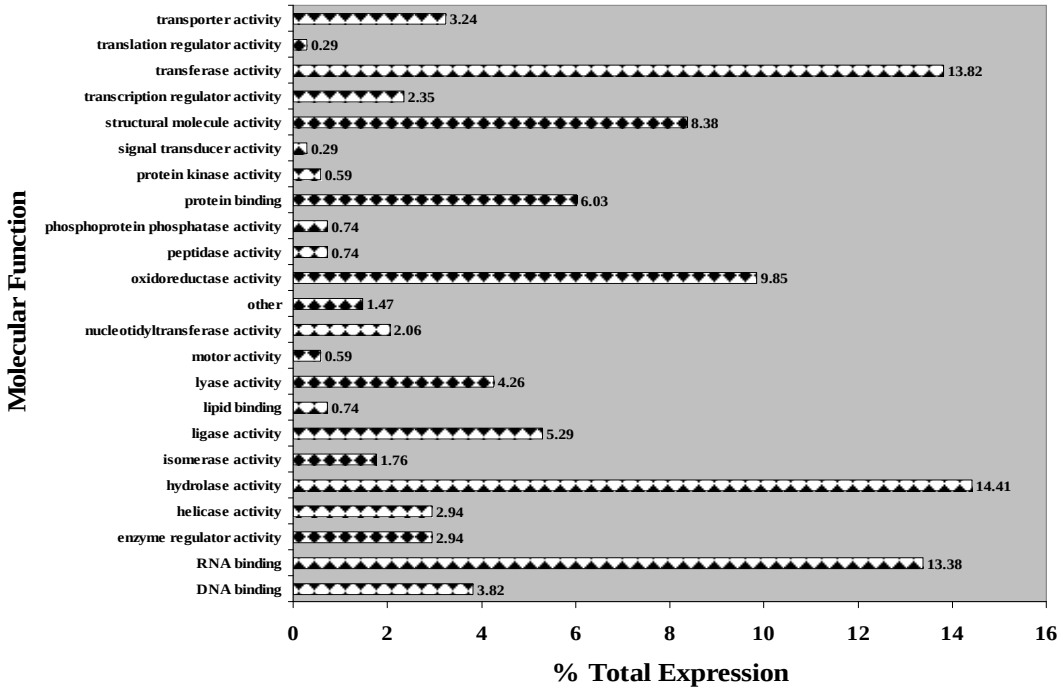

Figure 3.43 The percentage of each molecular function category (64 µg/ml upregulated genes). Genes upregulated more than two-fold were assigned molecular function categories. The number of genes in each category was expressed as a percentage of the number of total genes.

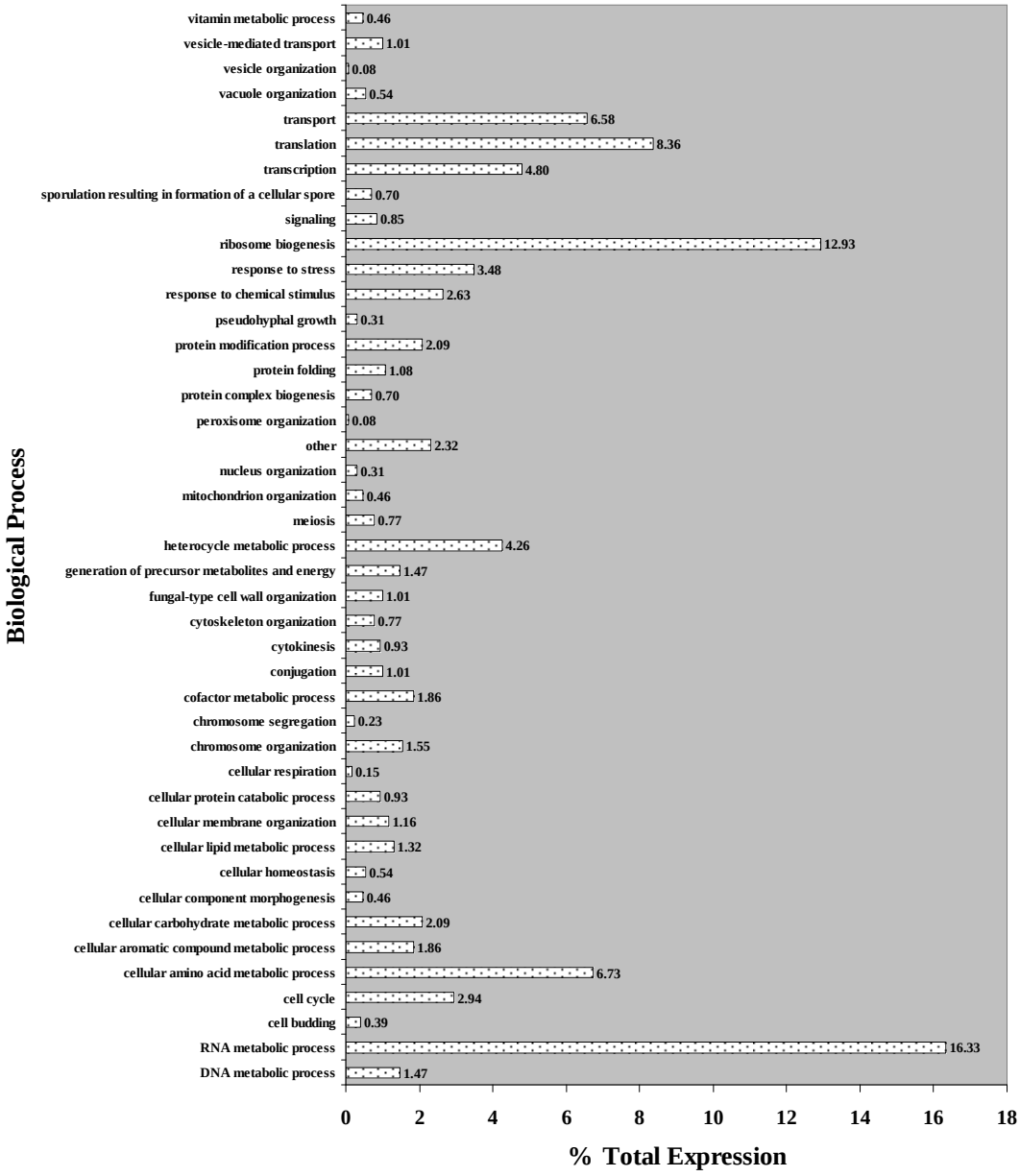

Figure 3.44 The percentage of each biological process category (64 µg/ml upregulated genes). Genes upregulated more than two-fold were assigned biological process categories. The number of genes in each category was expressed as a percentage of the number of total genes.

To further analyse the cellular response to the toxin in question, the five most highly upregulated biological processes, molecular functions and associated cellular components were examined. These are illustrated in figures 3.45-3.47.

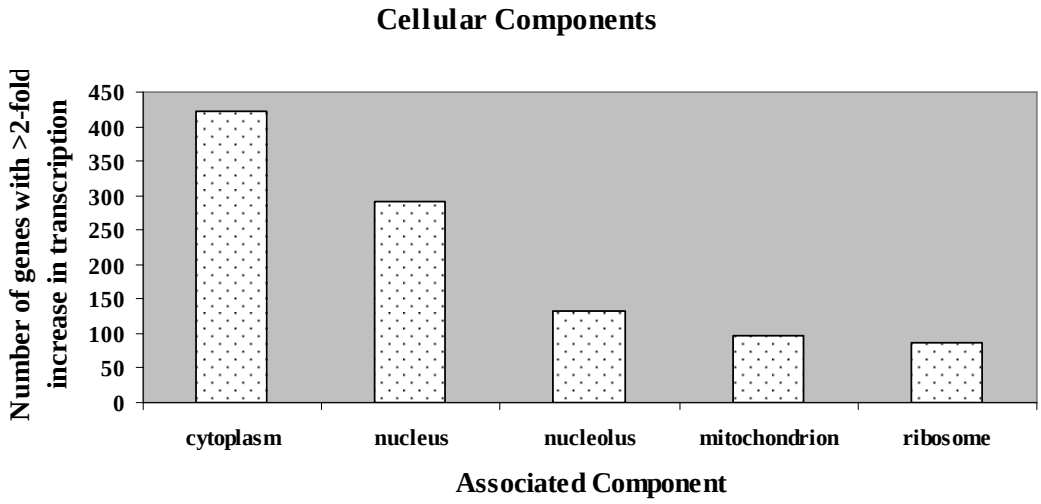

Figure 3.45 The five associated cellular components most highly upregulated by exposure to 64 µg/ml gliotoxin.

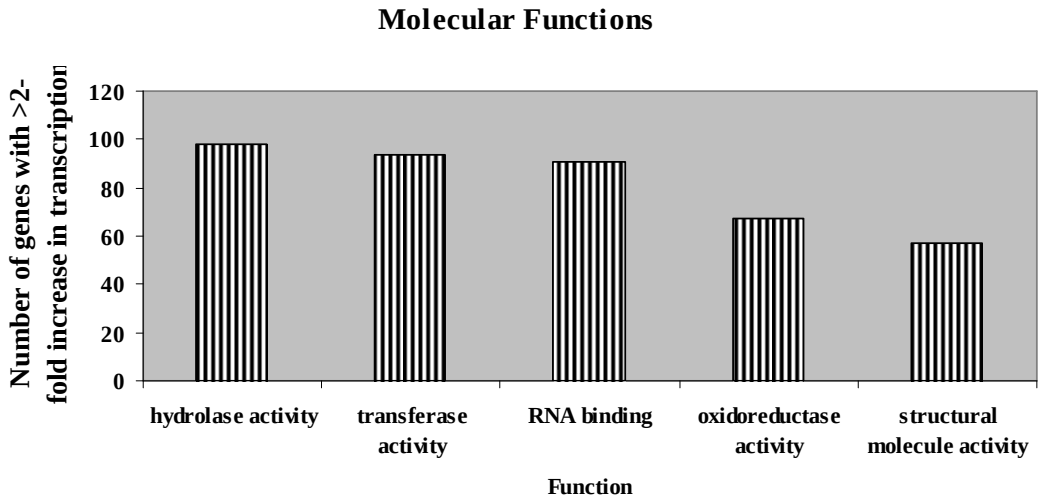

Figure 3.46 The five molecular functions most highly upregulated by exposure to 64 µg/ml gliotoxin.

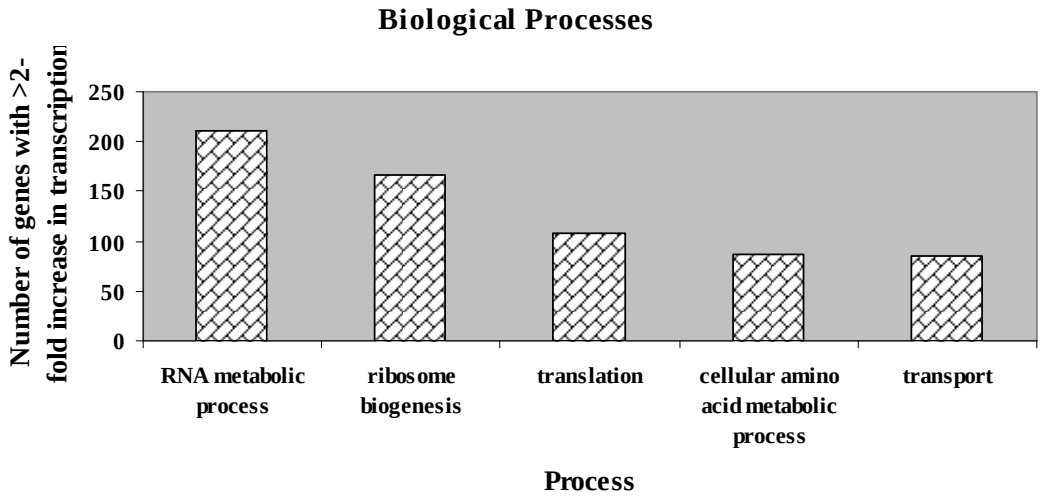

Figure 3.47 The five biological processes most highly upregulated by exposure to 64 µg/ml gliotoxin.

Table 3.7 lists the fifty genes, and their respective functions, that underwent the highest increase in transcription in response to 64 µg/ml gliotoxin.

Table 3.7 The fifty genes most highly upregulated in response to 64 µg/ml gliotoxin exposure. Gene functions were obtained from www.yeastgenome.org (SGD).

Gene	Fold Change	Gene Function
CUP1-2	171.19	Metallothionein, binds copper and mediates resistance to high concentrations of copper and cadmium; locus is variably amplified in different strains, with two copies, CUP1-1 and CUP1-2, in the genomic sequence reference strain S288C
CUP1-1	171.19	Metallothionein, binds copper and mediates resistance to high concentrations of copper and cadmium; locus is variably amplified in different strains, with two copies, CUP1-1 and CUP1-2, in the genomic sequence reference strain S288C
YFR032C	18.63	Putative protein of unknown function; non-essential gene identified in a screen for mutants with increased levels of rDNA transcription; expressed at high levels during sporulation
FRM2	15.75	Protein of unknown function, involved in the integration of lipid signaling pathways with cellular homeostasis; expression induced in cells treated with the mycotoxin patulin; has similarity to bacterial nitroreductases
MET16	13.57	3'-phosphoadenylsulfate reductase, reduces 3'-phosphoadenylyl sulfate to adenosine-3',5'-bisphosphate and free sulfite using reduced thioredoxin as cosubstrate, involved in sulfate assimilation and methionine metabolism
MET14	13.56	Adenylylsulfate kinase, required for sulfate assimilation and involved in methionine metabolism
MET3	13.15	ATP sulfurylase, catalyzes the primary step of intracellular sulphate activation, essential for assimilatory reduction of sulfate to sulfide, involved in methionine metabolism
HBN1	11.00	Putative protein of unknown function; similar to bacterial nitroreductases; green fluorescent protein (GFP)-fusion protein localizes to the cytoplasm and nucleus; protein becomes insoluble upon intracellular iron depletion

YMR001C-A	9.94	Putative protein of unknown function
IMD2	9.88	Inosine monophosphate dehydrogenase, catalyzes the rate-limiting step in GTP biosynthesis, expression is induced by mycophenolic acid resulting in resistance to the drug, expression is repressed by nutrient limitatio
NRG2	9.71	Transcriptional repressor that mediates glucose repression and negatively regulates filamentous growth; has similarity to Nrg1p
SAM1	9.48	S-adenosylmethionine synthetase, catalyzes transfer of the adenosyl group of ATP to the sulfur atom of methionine; one of two differentially regulated isozymes (Sam1p and Sam2p)
HXT2	8.80	High-affinity glucose transporter of the major facilitator superfamily, expression is induced by low levels of glucose and repressed by high levels of glucose
YPR160C-A	8.78	Identified by gene-trapping, microarray-based expression analysis, and genome-wide homology searching
MET6	8.75	Cobalamin-independent methionine synthase, involved in methionine biosynthesis and regeneration; requires a minimum of two glutamates on the methyltetrahydrofolate substrate, similar to bacterial metE homologs
STR3	8.67	Cystathionine beta-lyase, converts cystathionine into homocysteine
ICY2	8.54	Protein of unknown function; mobilized into polysomes upon a shift from a fermentable to nonfermentable carbon source; potential Cdc28p substrate
YKL071W	8.52	Putative protein of unknown function; expression induced in cells treated with the mycotoxin patulin, and also the quinone methide triterpene celastrol; green fluorescent protein (GFP)-fusion protein localizes to the cytoplasm
NRD1	8.51	RNA-binding protein that interacts with the C-terminal domain of the RNA polymerase II large subunit (Rpo21p), preferentially at phosphorylated Ser5; required for transcription termination and 3' end maturation of nonpolyadenylated RNAs
MET17	8.49	Methionine and cysteine synthase (O-acetyl homoserine-O-acetyl serine sulfhydrylase), required for sulfur amino acid synthesis
CYS3	8.03	Cystathionine gamma-lyase, catalyzes one of the two reactions involved in the transsulfuration pathway that yields cysteine from homocysteine with the intermediary formation of cystathionine
SER33	7.77	3-phosphoglycerate dehydrogenase, catalyzes the first step in serine and glycine biosynthesis; isozyme of Ser3p
RPS29B	6.72	Protein component of the small (40S) ribosomal subunit; nearly identical to Rps29Ap and has similarity to rat S29 and E. coli S14 ribosomal proteins
YDR524W-C	6.57	Putative protein of unknown function; small ORF identified by SAGE; deletion strains are moderately sensitive to the radiomimetic drug bleomycin
BIO2	6.47	Biotin synthase, catalyzes the conversion of dethiobiotin to biotin, which is the last step of the biotin biosynthesis pathway; complements E. coli bioB mutant
GPX2	6.43	Phospholipid hydroperoxide glutathione peroxidase induced by glucose starvation that protects cells from phospholipid hydroperoxides and nonphospholipid peroxides during oxidative stress
ALD5	5.87	Mitochondrial aldehyde dehydrogenase, involved in regulation or biosynthesis of electron transport chain components and acetate formation; activated by K+; utilizes NADP+ as the preferred coenzyme; constitutively expressed
MUP3	5.83	Low affinity methionine permease, similar to Mup1p
HOF1	5.78	Bud neck-localized, SH3 domain-containing protein required for cytokinesis; regulates actomyosin ring dynamics and septin

		localization; interacts with the formins, Bni1p and Bnr1p, and with Cyk3p, Vrp1p, and Bni5p
ADH6	5.73	NADPH-dependent medium chain alcohol dehydrogenase with broad substrate specificity; member of the cinnamyl family of alcohol dehydrogenases; may be involved in fusel alcohol synthesis or in aldehyde tolerance
OYE2	5.56	Conserved NADPH oxidoreductase containing flavin mononucleotide (FMN), homologous to Oye3p with different ligand binding and catalytic properties; may be involved in sterol metabolism, oxidative stress response, and programmed cell death
SAM2	5.55	S-adenosylmethionine synthetase, catalyzes transfer of the adenosyl group of ATP to the sulfur atom of methionine; one of two differentially regulated isozymes (Sam1p and Sam2p)
TRR1	5.50	Cytoplasmic thioredoxin reductase, key regulatory enzyme that determines the redox state of the thioredoxin system, which acts as a disulfide reductase system and protects cells against both oxidative and reductive stress
MET8	5.48	Bifunctional dehydrogenase and ferrochelatase, involved in the biosynthesis of siroheme, a prosthetic group used by sulfite reductase; required for sulfate assimilation and methionine biosynthesis
YLR460C	5.46	Member of the quinone oxidoreductase family, up-regulated in response to the fungicide mancozeb; possibly up-regulated by iodine
MMT1	5.42	Putative metal transporter involved in mitochondrial iron accumulation; closely related to Mmt2p
DBP2	5.41	Essential ATP-dependent RNA helicase of the DEAD-box protein family, involved in nonsense-mediated mRNA decay and rRNA processing
YKL070W	5.38	Putative protein of unknown function; expression induced in cells treated with mycotoxins patulin or citrinin; the authentic, non-tagged protein is detected in highly purified mitochondria in high-throughput studies
RPL29	5.25	Protein component of the large (60S) ribosomal subunit, has similarity to rat L29 ribosomal protein; not essential for translation, but required for proper joining of the large and small ribosomal subunits and for normal translation rate
ADE5	5.21	Bifunctional enzyme of the 'de novo' purine nucleotide biosynthetic pathway, contains aminoimidazole ribotide synthetase and glycinamide ribotide synthetase activities
YGR271C-A	5.15	Essential protein required for maturation of 18S rRNA; null mutant is sensitive to hydroxyurea and is delayed in recovering from alpha-factor arrest; green fluorescent protein (GFP)-fusion protein localizes to the nucleolus
PHO89	5.04	Na+/Pi cotransporter, active in early growth phase; similar to phosphate transporters of Neurospora crassa; transcription regulated by inorganic phosphate concentrations and Pho4p
ILV3	5.03	Dihydroxyacid dehydratase, catalyzes third step in the common pathway leading to biosynthesis of branched-chain amino acids
SAH1	4.99	S-adenosyl-L-homocysteine hydrolase, catabolizes S-adenosyl-L-homocysteine which is formed after donation of the activated methyl group of S-adenosyl-L-methionine (AdoMet) to an acceptor
ECM17	4.96	Sulfite reductase beta subunit, involved in amino acid biosynthesis, transcription repressed by methionine
YAP7	4.94	Putative basic leucine zipper (bZIP) transcription factor
MFA1	4.91	Mating pheromone a-factor, made by a cells; interacts with alpha cells to induce cell cycle arrest and other responses leading to mating; biogenesis involves C-terminal modification, N-terminal proteolysis, and export; also encoded by MFA2
YLR146W-	4.87	Putative protein of unknown function

A PHO12	4.78	One of three repressible acid phosphatases, a glycoprotein that is transported to the cell surface by the secretory pathway; nearly identical to Pho11p; upregulated by phosphate starvation
MET22	4.73	Bisphosphate-3'-nucleotidase, involved in salt tolerance and methionine biogenesis; dephosphorylates 3'-phosphoadenosine-5'-phosphate and 3'-phosphoadenosine-5'-phosphosulfate, intermediates of the sulfate assimilation pathway

Summary of the overall effects of gene downregulation on cells

Genes which underwent more than 2-fold transcriptional repression as a result of exposure to 64 µg/ml gliotoxin were also assessed. Figures 3.48-3.50 illustrate the overall effects on cells induced by genes downregulated more than 2-fold in response to 64 µg/ml gliotoxin exposure.

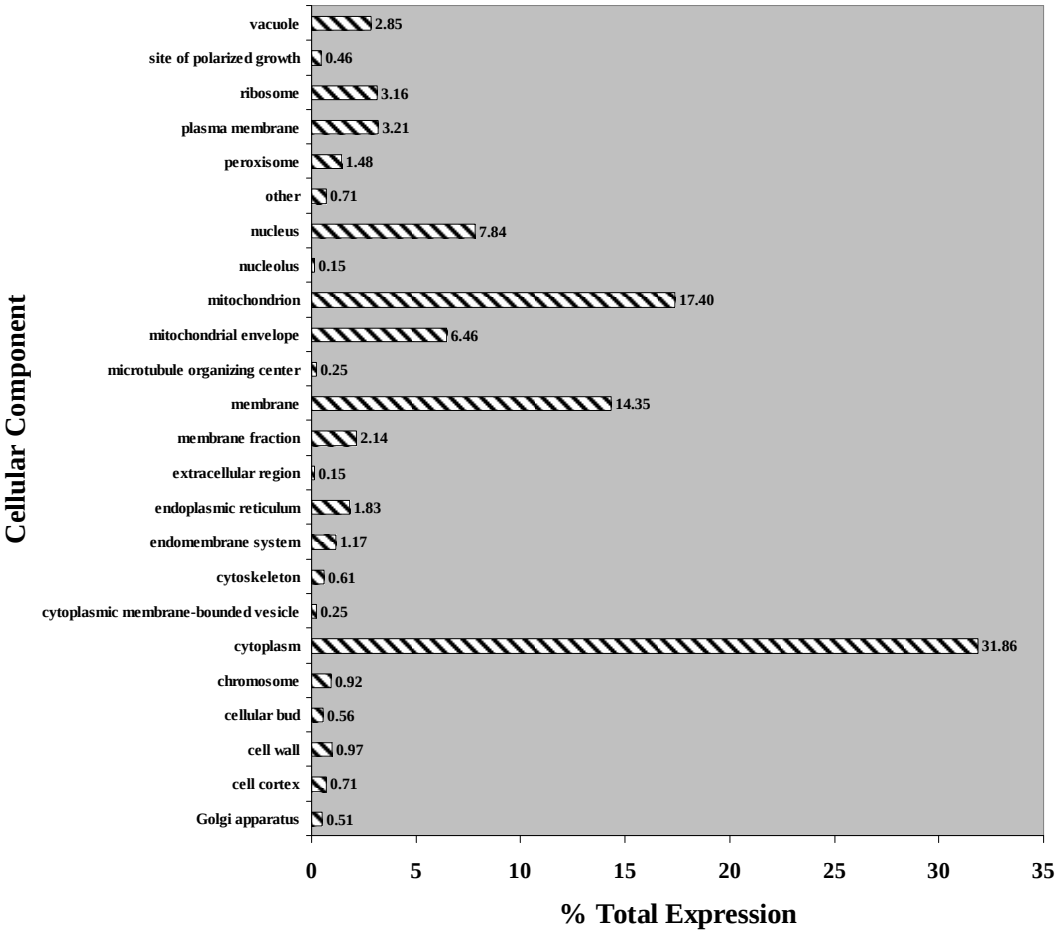

Figure 3.48 The percentage of each cellular component category (64 µg/ml downregulated genes). Genes downregulated more than two-fold were assigned cellular component categories. The number of genes in each category was expressed as a percentage of the number of total genes.

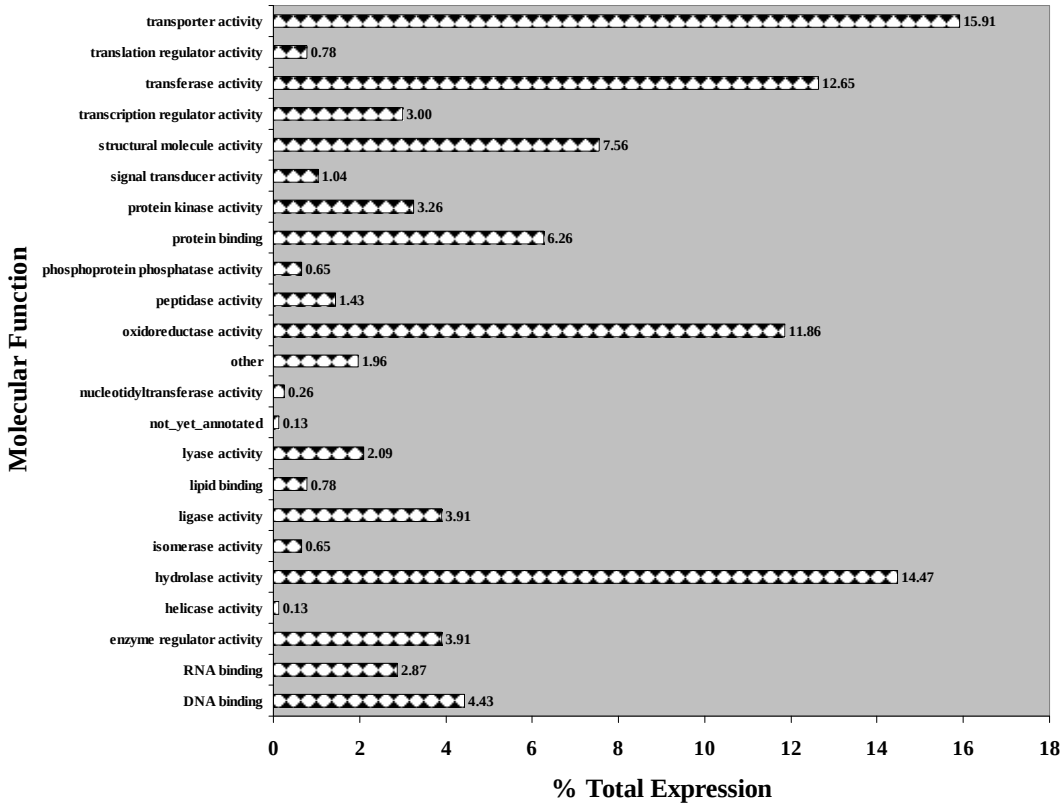

Figure 3.49 The percentage of each molecular function category (64 µg/ml downregulated genes). Genes downregulated more than two-fold were assigned molecular function categories. The number of genes in each category was expressed as a percentage of the number of total genes.

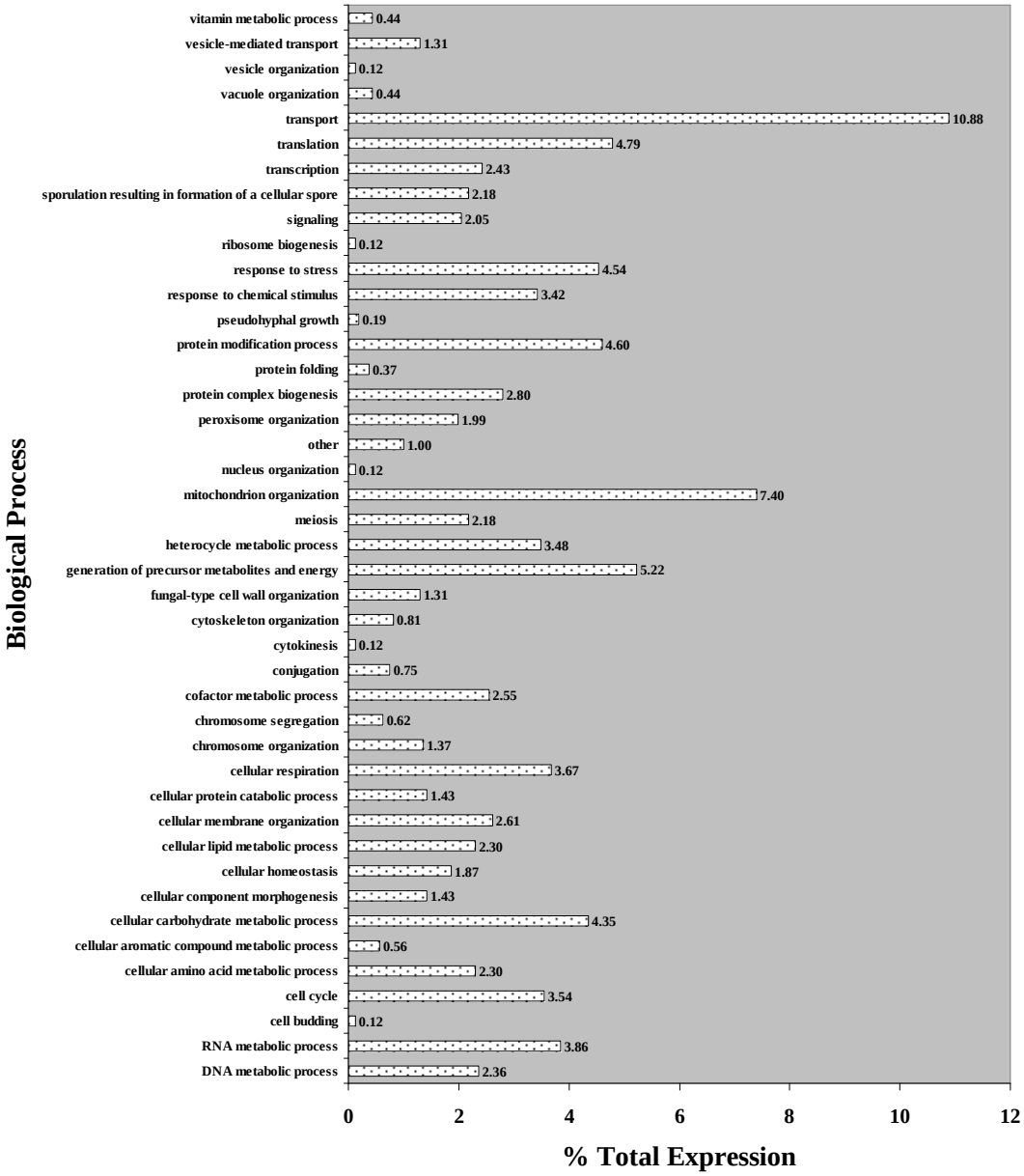

Figure 3.50 The percentage of each biological process category (64 µg/ml downregulated genes). Genes downregulated more than two-fold were assigned biological process categories. The number of genes in each category was expressed as a percentage of the number of total genes.

The five most common functions in each GO Identity category of these genes downregulated at a high degree were assessed (figures 3.51-3.53).

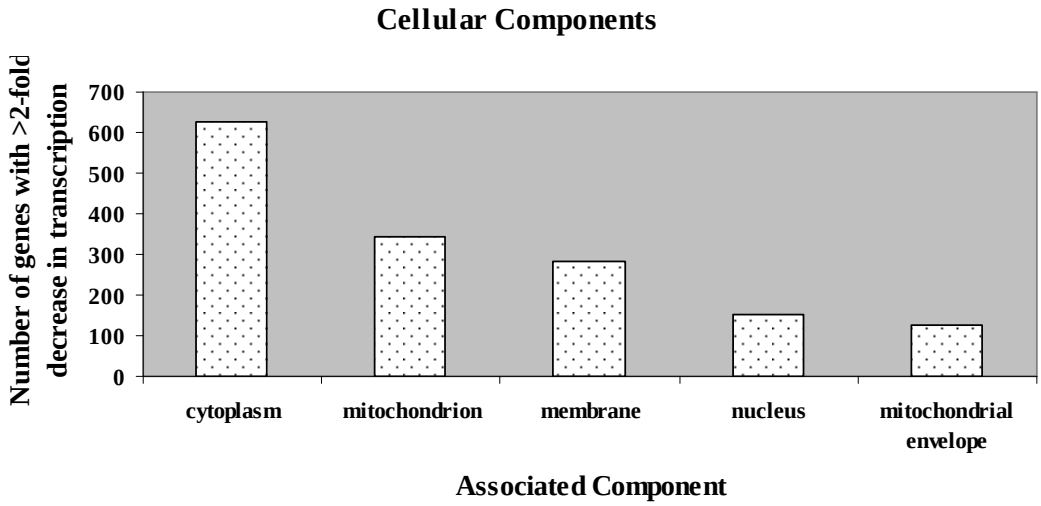

Figure 3.51 The five associated cellular components most highly downregulated by exposure to 64 µg/ml gliotoxin.

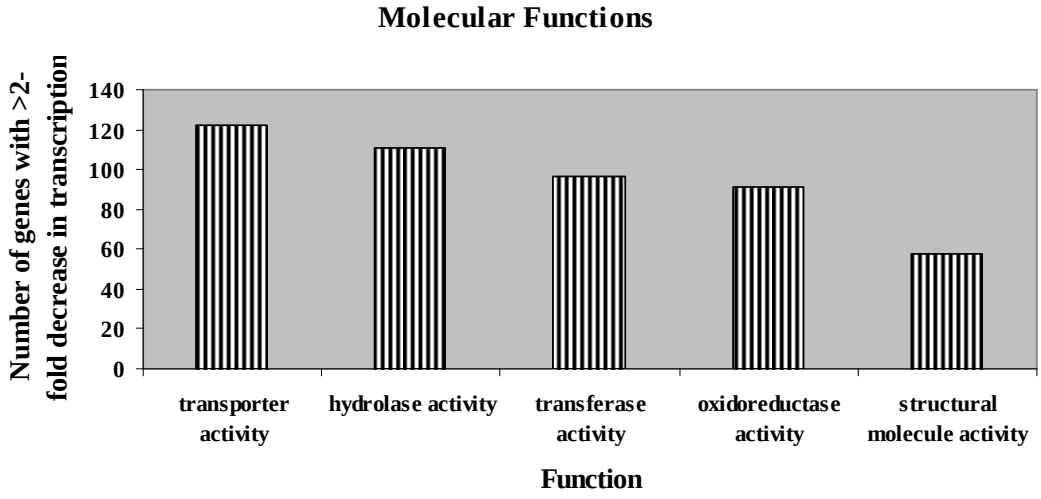

Figure 3.52 The five molecular functions most highly downregulated by exposure to 64 µg/ml gliotoxin.

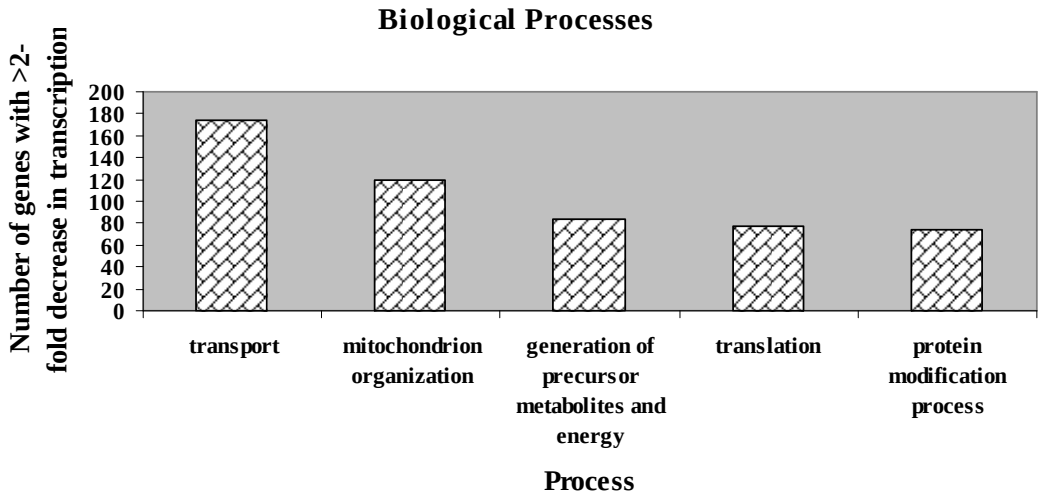

Figure 3.53 The five biological processes most highly downregulated by exposure to 64 µg/ml gliotoxin.

The fifty genes that underwent the highest level of downregulation are illustrated in table 3.8

Table 3.8 The fifty genes most highly downregulated in response to 64 µg/ml gliotoxin exposure. Gene functions were obtained from www.yeastgenome.org (SGD).

Gene	Fold Change	Gene Function
SIP18	-131.20	Phospholipid-binding protein; expression is induced by osmotic stress
SPG1	-124.46	Protein required for survival at high temperature during stationary phase; not required for growth on nonfermentable carbon sources; the authentic, non-tagged protein is detected in highly purified mitochondria in high-throughput studies
YIL057C	-92.27	Protein of unknown function involved in energy metabolism under respiratory conditions; expression induced under carbon limitation and repressed under high glucose
SPG4	-70.25	Protein required for survival at high temperature during stationary phase; not required for growth on nonfermentable carbon sources
GRE1	-50.50	Hydrophilin of unknown function; stress induced (osmotic, ionic, oxidative, heat shock and heavy metals); regulated by the HOG pathway
YMR175W-A	-49.45	Putative protein of unknown function
SFC1	-44.99	Mitochondrial succinate-fumarate transporter, transports succinate into and fumarate out of the mitochondrion; required for ethanol and acetate utilization
YGR067C	-44.01	Putative protein of unknown function; contains a zinc finger motif similar to that of Adr1p
NDE2	-43.64	Mitochondrial external NADH dehydrogenase, catalyzes the oxidation of cytosolic NADH; Nde1p and Nde2p are involved in providing the cytosolic NADH to the mitochondrial respiratory chain
YDR119W-A	-43.47	Putative protein of unknown function; may interact with respiratory chain complexes III (ubiquinol-cytochrome c

		reductase) or IV (cytochrome c oxidase)
FMP45	-43.06	Integral membrane protein localized to mitochondria (untagged protein); required for sporulation and maintaining sphingolipid content; has sequence similarity to SUR7 and YNL194C
HXT5	-41.98	Hexose transporter with moderate affinity for glucose, induced in the presence of non-fermentable carbon sources, induced by a decrease in growth rate, contains an extended N-terminal domain relative to other HXTs
YIG1	-41.75	Protein that interacts with glycerol 3-phosphatase and plays a role in anaerobic glycerol production; localizes to the nucleus and cytosol
POT1	-39.33	3-ketoacyl-CoA thiolase with broad chain length specificity, cleaves 3-ketoacyl-CoA into acyl-CoA and acetyl-CoA during beta-oxidation of fatty acids
ECM13	-33.03	Non-essential protein of unknown function; induced by treatment with 8-methoxypsoralen and UVA irradiation
JEN1	-32.82	Lactate transporter, required for uptake of lactate and pyruvate; phosphorylated; expression is derepressed by transcriptional activator Cat8p during respiratory growth, and repressed in the presence of glucose, fructose, and mannose
PCK1	-32.46	Phosphoenolpyruvate carboxykinase, key enzyme in gluconeogenesis, catalyzes early reaction in carbohydrate biosynthesis, glucose represses transcription and accelerates mRNA degradation, regulated by Mcm1p and Cat8p, located in the cytosol
ADY2	-30.61	Acetate transporter required for normal sporulation; phosphorylated in mitochondria
HSP12	-29.47	Plasma membrane localized protein that protects membranes from desiccation; induced by heat shock, oxidative stress, osmostress, stationary phase entry, glucose depletion, oleate and alcohol; regulated by the HOG and Ras-Pka pathways
YNL195C	-27.34	Putative protein of unknown function; shares a promoter with YNL194C; the authentic, non-tagged protein is detected in highly purified mitochondria in high-throughput studies
ACH1	-26.62	Protein with CoA transferase activity, particularly for CoASH transfer from succinyl-CoA to acetate; has minor acetyl-CoA-hydrolase activity; phosphorylated; required for acetate utilization and for diploid pseudohyphal growth
YAL018C	-26.38	Putative protein of unknown function
CRC1	-24.63	Mitochondrial inner membrane carnitine transporter, required for carnitine-dependent transport of acetyl-CoA from peroxisomes to mitochondria during fatty acid beta-oxidation
YER053C-A	-24.00	Putative protein of unknown function; green fluorescent protein (GFP)-fusion protein localizes to the endoplasmic reticulum
YAT1	-22.93	Outer mitochondrial carnitine acetyltransferase, minor ethanol-inducible enzyme involved in transport of activated acyl groups from the cytoplasm into the mitochondrial matrix; phosphorylated
YRO2	-22.66	Putative protein of unknown function; the authentic, non-tagged protein is detected in a phosphorylated state in highly purified mitochondria in high-throughput studies; transcriptionally regulated by Haa1p
CAT2	-21.61	Carnitine acetyl-CoA transferase present in both mitochondria and peroxisomes, transfers activated acetyl groups to carnitine to form acetylcarnitine which can be shuttled across membranes
NQM1	-21.32	Transaldolase of unknown function; transcription is repressed by Mot1p and induced by alpha-factor and during diauxic shift
ACS1	-19.01	Acetyl-coA synthetase isoform which, along with Acs2p, is -

		the nuclear source of acetyl-coA for histone acetlyation; expressed during growth on nonfermentable carbon sources and under aerobic conditions
YMR118C	-18.66	Protein of unknown function with similarity to succinate dehydrogenase cytochrome b subunit; YMR118C is not an essential gene
GLG2	-18.58	Self-glucosylating initiator of glycogen synthesis, also glucosylates n-dodecyl-beta-D-maltoside; similar to mammalian glycogenin
YNL194C	-18.55	Integral membrane protein required for sporulation and plasma membrane sphingolipid content; has sequence similarity to SUR7 and FMP45; GFP-fusion protein is induced in response to the DNA-damaging agent MMS
HSP30	-18.46	Hydrophobic plasma membrane localized, stress-responsive protein that negatively regulates the H(+)-ATPase Pma1p; induced by heat shock, ethanol treatment, weak organic acid, glucose limitation, and entry into stationary phase
POX1	-18.40	Fatty-acyl coenzyme A oxidase, involved in the fatty acid beta-oxidation pathway; localized to the peroxisomal matrix
FMP16	-18.28	Putative protein of unknown function; proposed to be involved in responding to conditions of stress; the authentic, non-tagged protein is detected in highly purified mitochondria in high-throughput studies
YMR206W	-18.27	Putative protein of unknown function; YMR206W is not an essential gene
SDH2	-18.19	Iron-sulfur protein subunit of succinate dehydrogenase (Sdh1p, Sdh2p, Sdh3p, Sdh4p), which couples the oxidation of succinate to the transfer of electrons to ubiquinone as part of the TCA cycle and the mitochondrial respiratory chain
MLS1	-17.93	Malate synthase, enzyme of the glyoxylate cycle, involved in utilization of non-fermentable carbon sources; expression is subject to carbon catabolite repression; localizes in peroxisomes during growth in oleic acid medium
HBT1	-17.74	Substrate of the Hub1p ubiquitin-like protein that localizes to the shmoo tip (mating projection); mutants are defective for mating projection formation, thereby implicating Hbt1p in polarized cell morphogenesis
YKL065W-A	-17.37	Putative protein of unknown function
RTN2	-16.36	Protein of unknown function; has similarity to mammalian reticulon proteins; member of the RTNLA (reticulon-like A) subfamily
GUT2	-16.17	Mitochondrial glycerol-3-phosphate dehydrogenase; expression is repressed by both glucose and cAMP and derepressed by non-fermentable carbon sources in a Snf1p, Rsf1p, Hap2/3/4/5 complex dependent manner
YDR018C	-14.94	Probable membrane protein with three predicted transmembrane domains; homologous to Ybr042cp, similar to C. elegans F55A11.5 and maize 1-acyl-glycerol-3-phosphate acyltransferase
RIP1	-14.94	Ubiquinol-cytochrome-c reductase, a Rieske iron-sulfur protein of the mitochondrial cytochrome bc1 complex; transfers electrons from ubiquinol to cytochrome c1 during respiration
IDP2	-14.87	Cytosolic NADP-specific isocitrate dehydrogenase, catalyzes oxidation of isocitrate to alpha-ketoglutarate; levels are elevated during growth on non-fermentable carbon sources and reduced during growth on glucose
NCE102	-14.78	Protein of unknown function; contains transmembrane domains; involved in secretion of proteins that lack classical secretory signal sequences; component of the detergent-insoluble glycolipid-enriched complexes (DIGs)

FMP43	-14.70	Putative protein of unknown function; expression regulated by osmotic and alkaline stresses; the authentic, non-tagged protein is detected in highly purified mitochondria in high-throughput studies
PHM7	-14.54	Protein of unknown function, expression is regulated by phosphate levels; green fluorescent protein (GFP)-fusion protein localizes to the cell periphery and vacuole
COX4	-14.46	Subunit IV of cytochrome c oxidase, the terminal member of the mitochondrial inner membrane electron transport chain; precursor N-terminal 25 residues are cleaved during mitochondrial import; phosphorylated; spermidine enhances translation
MSC1	-14.35	Protein of unknown function; mutant is defective in directing meiotic recombination events to homologous chromatids; the authentic, non-tagged protein is detected in highly purified mitochondria and is phosphorylated

3.6.1.3 Comparison of the yeast transcriptomic response to 16 and 64 µg/ml gliotoxin exposure

It would be reasonable to expect a similar yeast response to 16 and 64 µg/ml gliotoxin exposure, to some degree. If these reactions are real, there should be overlap in the data when comparing the response to 16 and 64 µg/ml gliotoxin. To investigate if this is the case, correlation was searched for by comparing and contrasting the five most highly up- and downregulated molecular functions, biological processes and associated cellular components. Figures 3.54-3.59 illustrate these comparisons.

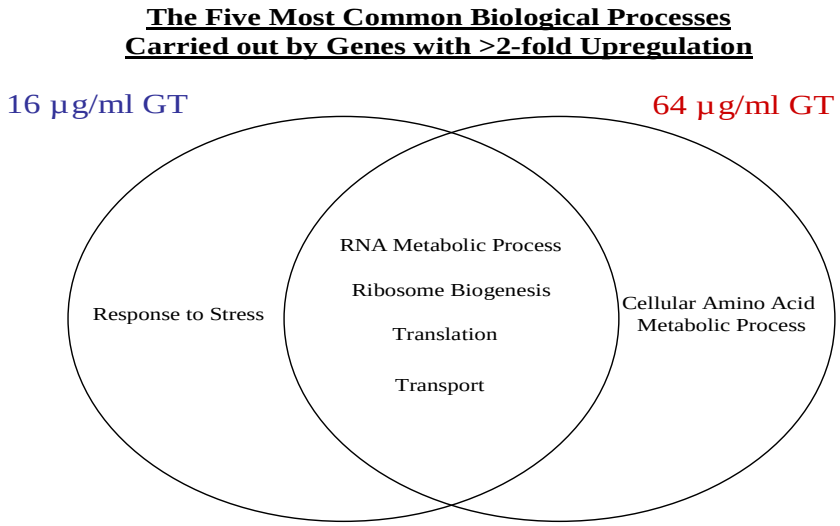

Figure 3.54 Comparison of the five most common biological processes performed by genes with >2-fold upregulation.

From the above figure it can be seen that four out of the top five most common upregulated biological processes characteristic of response to gliotoxin are induced by the two concentrations, these are RNA metabolic process, ribosome biogenesis, translation and transport. However, the response to stress is one of the most common processes performed by cells under 16 µg/ml gliotoxin exposure, but not 64 µg/ml. At the same time, cellular amino acid metabolic process is highly stimulated by the latter concentration but not the former.

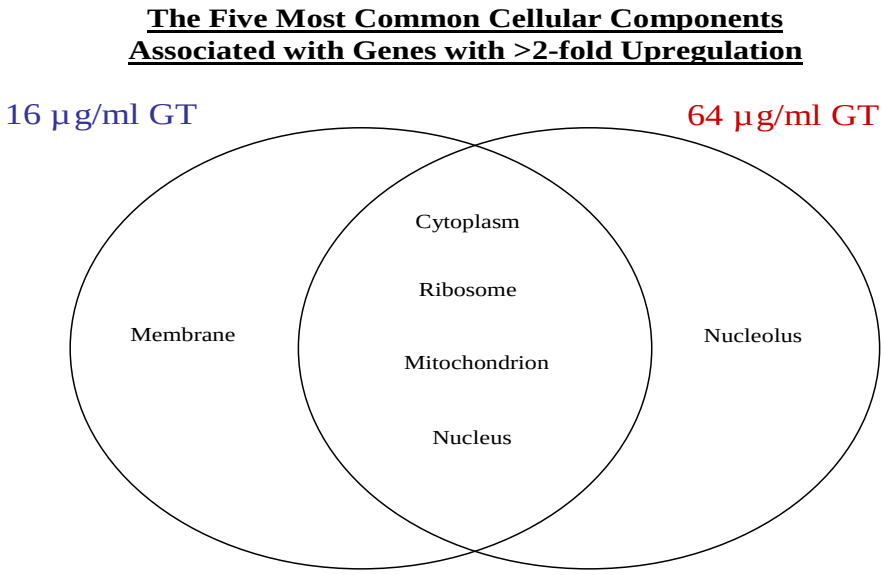

Figure 3.55 Comparison of the five most common associated cellular components of genes with >2-fold upregulation.

Under exposure to both concentrations of gliotoxin, genes associated with the cytoplasm, ribosome, mitochondrion and nucleus are all highly upregulated (figure 3.55). Membrane-associated genes fall into the most commonly upregulated category only under exposure to 16 µg/ml gliotoxin, not under 64 µg/ml. On the other hand, genes associated with the nucleolus were upregulated to a high degree when cell were treated with 64 µg/ml gliotoxin, but not with the lower concentration.

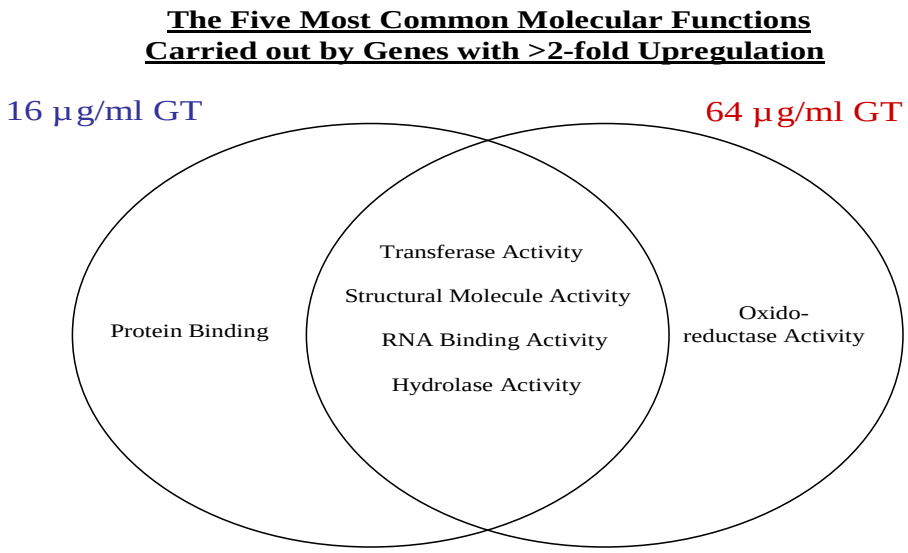

Figure 3.56 Comparison of the five most common molecular functions performed by genes with >2-fold upregulation.

In relation to molecular function, protein binding was one of the highest functions to be stimulated by the lower concentration of gliotoxin, but not by the higher. In contrast, oxidoreductase activity was very highly stimulated by 64 µg/ml gliotoxin exposure, but not by 16 µg/ml. Transferase activity, structural molecule activity, RNA binding activity and hydrolase activity were all stimulated to the highest degree under exposure to the toxin at both concentations (figure 3.56).

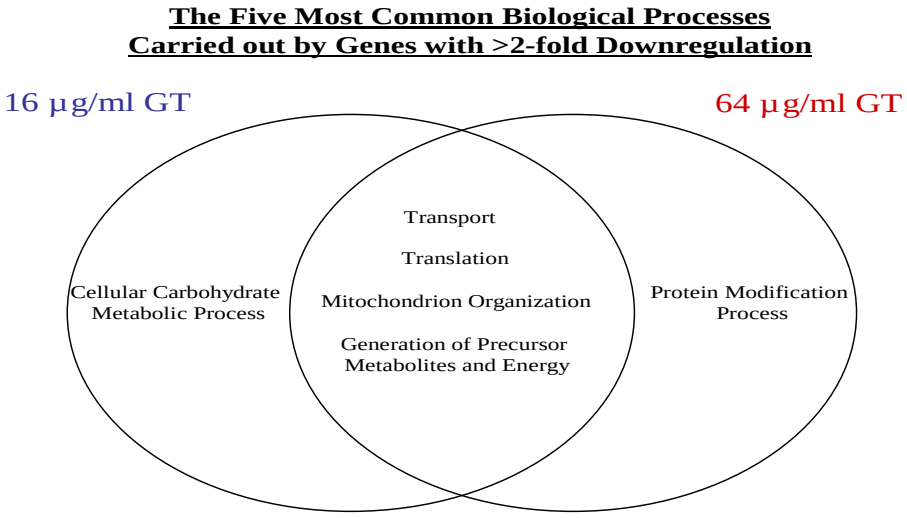

Figure 3.57 Comparison of the five most common biological processes performed by genes with >2-fold downregulation.

Downregulated gene GO identities were also compared and contrasted. Of all the biological processes inhibited by exposure to 16 µg/ml gliotoxin, only one, the cellular carbohydrate metabolic process was unique to this concentration, the rest were shared with the response to 64 µg/ml exposure; transport, translation, mitochondrion organisation, generation of precursor metabolites and energy. Protein modification process genes were strongly repressed by exposure to the higher concentration of gliotoxin, but not to the lower (figure 3.57).

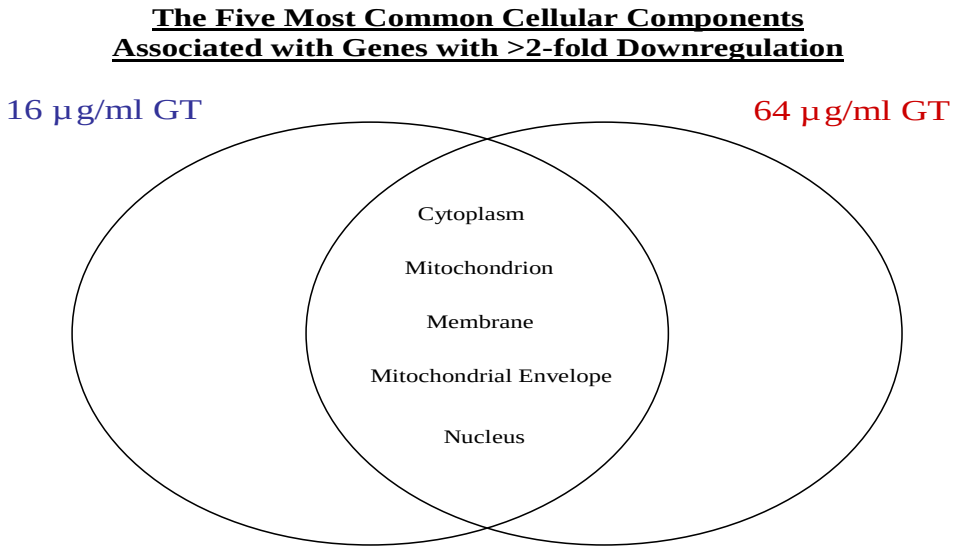

Figure 3.58 Comparison of the five most common associated cellular components of genes with >2-fold downregulation.

Figure 3.58 outlines how the five most common cellular components associated with >2-fold downregulated genes are highly transcriptionally repressed under exposure to both gliotoxin concentrations. The cellular components inhibited by the toxin are the cytoplasm, mitochondrion, membrane, mitochondrial envelope and nucleus.

Regarding molecular function, the five most common transcriptionally inhibited categories were identical when considering gliotoxin exposure levels of 16 and 64 µg/ml. Structural molecule activity, oxidoreductase activity, transporter activity, transferase activity and hydrolase activity were all extremely repressed.

Overall, good correlation of GO identities indicating the yeast response to two different gliotoxin exposure concentrations was observed.

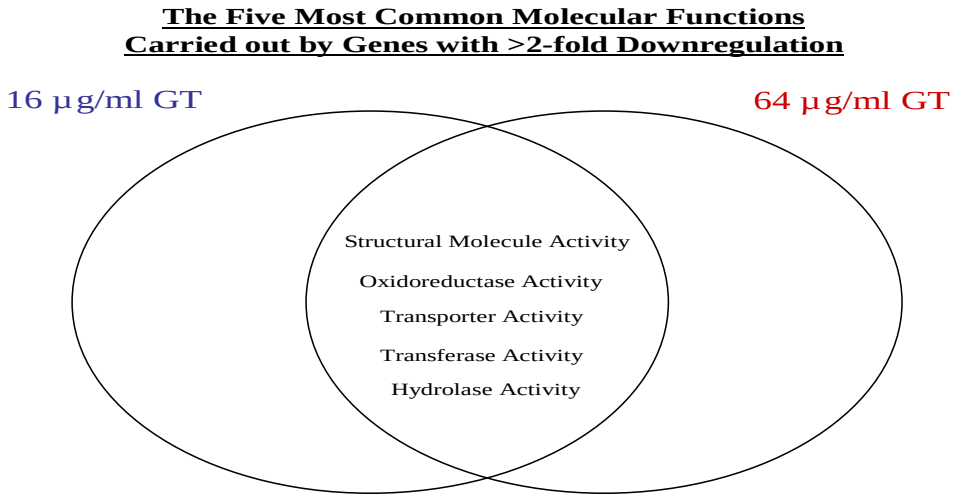

Figure 3.59 Comparison of the five most common molecular functions performed by genes with >2-fold downregulation.

3.6.1.4 Exploration for pathways transcriptionally altered by gliotoxin exposure

Organisation and categorisation of data allowed us to examine the overall effects that gliotoxin imposes on *S. cerevisiae*. Further to this I was able to compare and constrast the cellular transcriptional responses to different concentrations of the toxin. In addition, the data was examined in an attempt to pinpoint pathways directly induced or repressed by gliotoxin. One such pathway identified was the superpathway of sulfur amino acid biosynthesis. All but one gene in this pathway was found to be transcribed at an elevated level in response to gliotoxin. As depicted by figure 3.60, the superpathway of sulfur amino acid biosynthesis begins with a sulphate ion. Following the formation of four intermediates, the resultant hydrogen sulfide combines with O-Acetyl-L-homoserine to form homocysteine (Thauer *et al.*, 1977, Setya *et al.*, 1996, Berndt *et al.*, 2004). Homocysteine goes on to play a role in methionine biosynthesis but can also enter the transsulfuration pathway. This involves the interconversion of cysteine and

homocysteine with cystathionine acting as an intermediate (Thomas and Surdin-Kerjan, 1997, Finkelstein, 1998).

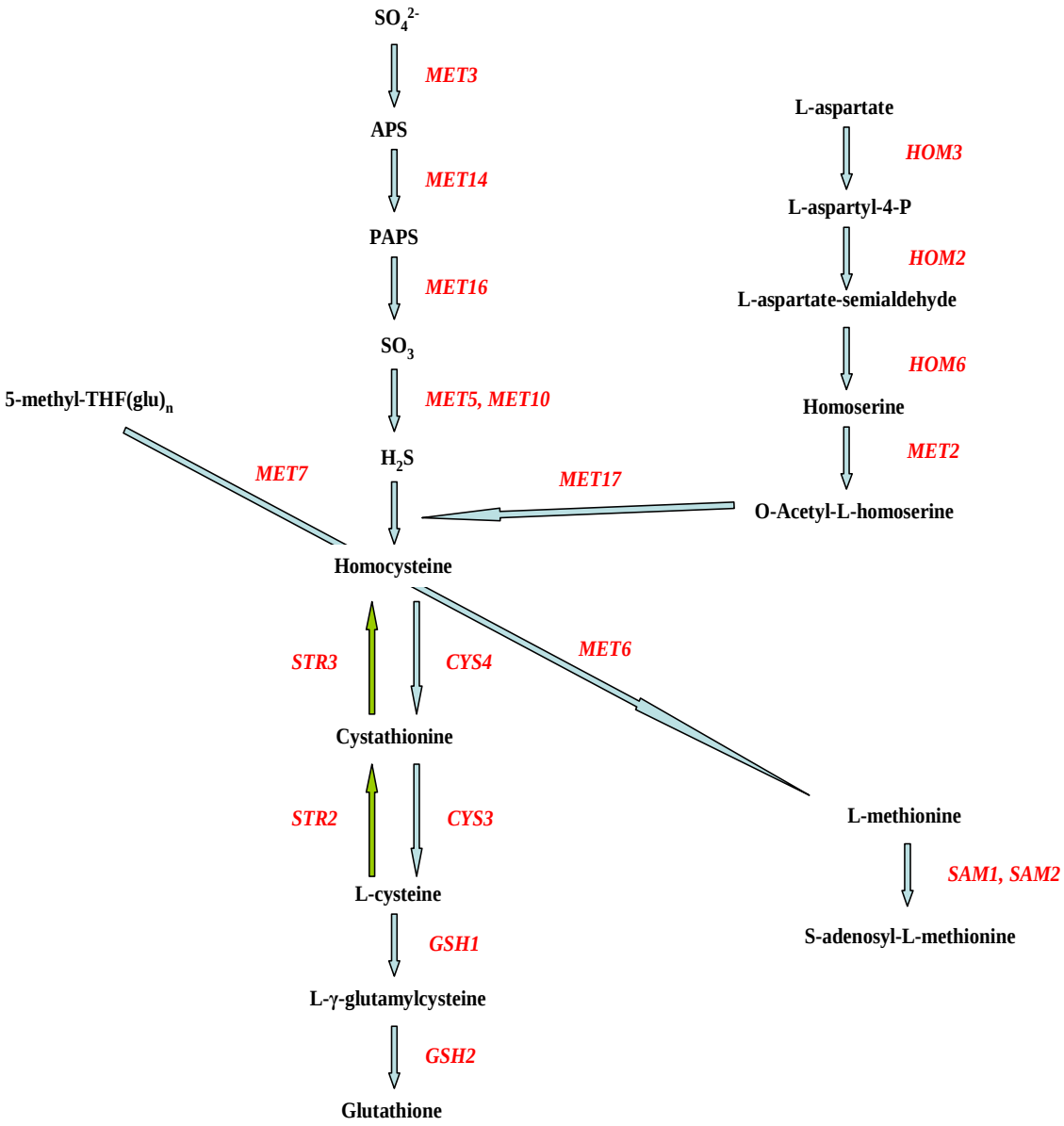

Figure 3.60 The superpathway of sulfur amino acid and glutathione biosynthesis (reproduced from SGD). Gene names are depicted in red. These represent the enzymes involved in conversion of one intermediate to another.

L-cysteine produced from the transsulfuration pathway is then utilised, along with L-glycine and L-glutamate, in glutathione biosynthesis. This makes cysteine a potential rate-limiting amino acid in the OS response (Arrick *et al.*, 1982, Williamson *et al.*, 1982, Anderson, 1998, Dickinson and Forman, 2002). Furthermore, it has been demonstrated

that the sulfur amino acid biosynthesis structural system must be functional before *GSH1* can be expressed under OS (Dormer *et al.*, 2000).

Every gene illustrated above, with the exception of *STR2*, undergoes an increase in transcription level when yeast cells are exposed to gliotoxin. The fold change in level of transcription is outlined in table 3.9.

Table 3.9 Fold change in level of transcription of genes involved in sulfur amino acid and glutathione biosynthesis in response to two concentrations of gliotoxin. Ø depicts no increase in transcription level.

Gene Name	Fold increase in level of transcription under 16 µg/ml gliotoxin exposure	Fold increase in level of transcription under 64 µg/ml gliotoxin exposure
MET7	1.5	1.5
MET3	11.7	13.2
MET14	7.4	13.6
MET16	4.6	13.6
MET5 (ECM17)	3.9	4.9
MET10	4.3	3.5
MET17	5.5	8.5
HOM3	2.4	4.1
HOM2	1.7	2.3
HOM6	1.9	1.5
MET2	2.9	4.2
STR3	4	8.7
STR2	Ø	Ø
CYS3	4.1	8
CYS4	1.6	3.8
MET6	2.9	8.7
SAM2	3.8	5.6
SAM1	1.8	9.5
GSH1	Ø	2.2
GSH2	1.2	1.8

This demonstrates that under the stress imposed on cells by the gliotoxin, *S. cerevisiae* cells rapidly upregulate the transcription of genes involved in sulfur amino acid and glutathione biosynthesis. Other genes exist that encode proteins that play a role in mediation of the sulfur amino acid biosynthesis pathway. The *MET1*, *MET4*, *MET8*, *MET18*, *MET19* and *MET22* , *MET28*, *MET30*, *MET31*, *MET32* gene products are involved in this regulation (Masselot and De Robichon-Szulmajster, 1975, Thomas *et*

al., 1992a). *MET1* and *MET8* and *MET18* encode proteins that have been shown to exhibit sulfite reductase activity, in the same manner as *MET5* and *MET10*, depicted in figure 3.60 (Masselot and De Robichon-Szulmajster, 1975, Thomas *et al.*, 1992a). Met4p modulates transcriptional activation of the pathway (Thomas *et al.*, 1992b). Met19p is required for functional sulfur amino acid biosynthesis as the null mutant depends on organic sulfur supplementation for survival and *MET19* deletion has led to increased sensitivity to OS (Thomas *et al.*, 1991, Krems *et al.*, 1995). The *MET22* gene product is also required for sulfate assimilation in addition to playing a role in salt tolerance (Gläser *et al.*, 1993, Murguía *et al.*, 1995). *MET22* deletion gives rise to methionine auxotrophs (Masselot and De Robichon-Szulmajster, 1975). Met31p and Met32p are additional transcription factors involved in the regulation of said pathway and the transcription of *MET3* and *MET14* is dependent on the presence of at least one of these proteins (Blaiseau *et al.*, 1997). In contrast, Met30p negatively regulates the sulfur amino acid biosynthesis pathway, through repressing Met19p and the transcriptional activities of Met4p in the presence of high S-adenosyl-L-methionine (SAM/AdoMet) levels, a product of the said pathway (Thomas *et al.*, 1995). Expression of the above mentioned genes in response to two concentrations of gliotoxin is illustrated in table 3.10. *MET4*, *MET19* and *MET30* are not upregulated in response to gliotoxin exposure, unlike *MET1*, *MET8*, *MET18*, *MET22*, *MET31* and *MET32*. Upregulation of these genes has been observed in response to two concentrations of gliotoxin, demonstrating overlap and supporting results and conclusions that can subsequently be made.

Genes involved in glucose fermentation were also seen to be upregulated in the presence of gliotoxin. Depending on the availability of oxygen, yeast metabolise glucose by fermentation or respiration. From the RNA sequencing data, it became

apparent that gliotoxin exposure induces increased transcription of most genes involved in the glucose fermentation pathway.

Fermentation, illustrated in figure 3.61, involves the formation of pyruvate, which is then converted to acetaldehyde under the control of pyruvate decarboxylase (Pdc) (Zhang *et al.*, 1995, Bongers *et al.*, 2005).

Table 3.10 Fold change in level of transcription of genes involved in regulation of the sulfur amino acid biosynthesis pathway in response to two concentrations of gliotoxin. Ø depicts no increase in transcription level. N/A depicts no test result

Gene Name	Fold increase in level of transcription under 16 µg/ml gliotoxin exposure	Fold increase in level of transcription under 64 µg/ml gliotoxin exposure
MET1	2.5	3.8
MET4	Ø	Ø
MET8	3.1	5.5
MET18	1.3	1.5
MET19	Ø	Ø
MET22	2.9	4.7
MET28	N/A	N/A
MET30	Ø	Ø
MET31	1.7	2.0
MET32	1.6	2.9

Although not all genes involved in the glucose fermentation pathway were upregulated under gliotoxin exposure, the majority did undergo an increase in transcription. Five genes, *HXK1*, *GLK1*, *PYK2*, *PDC6* and *ALD4* were downregulated to some degree by the presence of gliotoxin.

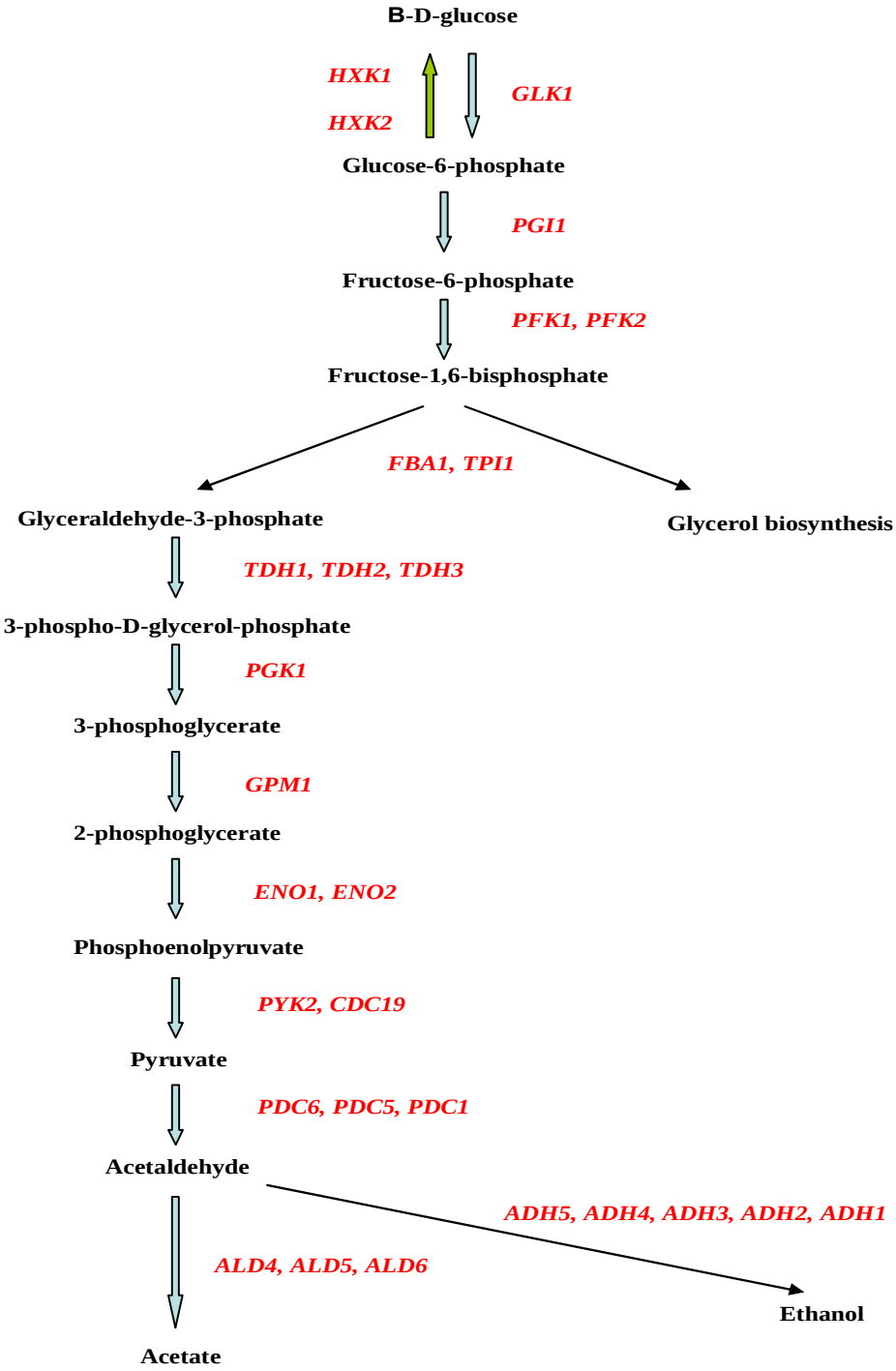

Figure 3.61 Glucose fermentation pathway (reproduced from SGD). Gene names are depicted in red. These represent the enzymes involved in conversion of one intermediate to another.

Table 3.11 Fold change in level of transcription of genes involved in glucose fermentation in response to two concentrations of gliotoxin. Ø depicts no increase in transcription level.

Gene Name	Fold increase in level of transcription under 16 µg/ml gliotoxin exposure	Fold increase in level of transcription under 64 µg/ml gliotoxin exposure
HXK1	Ø	Ø
HXK2	2.3	2.5
GLK1	Ø	Ø
PGI1	1.9	2.1
PFK1	1.9	1.9
PFK2	1.9	1.9
FBA1	1.7	2.8
TPI1	2.5	2.7
TDH1	1.9	1.9
TDH2	2.9	3.4
TDH3	2.7	2.2
PGK1	2.5	2.2
GPM1	2.3	2.8
ENO1	1.9	2.2
ENO2	2.6	3.4
PYK2	Ø	Ø
CDC19	2.6	3.3
PDC6	Ø	Ø
PDC5	3.0	2.3
PDC1	3.2	1.9
ADH5	Ø	1.7
ADH4	1.4	Ø
ADH3	Ø	1.1
ADH2	1.5	2.8
ADH1	1.7	3.0
ALD4	Ø	Ø
ALD5	1.8	5.9
ALD6	1.1	3.8

Gluconeogenesis, the synthesis of glucose is fundamentally the opposite of glycolysis, an intricate part of the fermentation process and genes involved in this process are listed in table 3.12

Table 3.12 Fold change in level of transcription of genes involved in gluconeogenesis in response to two concentrations of gliotoxin. Ø depicts no decrease in transcription level.

Gene Name	Fold decrease in level of transcription under 16 µg/ml gliotoxin exposure	Fold decrease in level of transcription under 64 µg/ml gliotoxin exposure
MAE1	1.2	Ø
MDH2	4.7	10.5
PYC1	6.9	5.9
PYC2	1.7	1.1
PCK1	80.1	32.5
ENO1	Ø	Ø
ENO2	Ø	Ø
GPM1	Ø	Ø
PGK1	Ø	Ø
TDH1	Ø	Ø
TDH2	Ø	Ø
TDH3	Ø	Ø
FBA1	Ø	Ø
FBP1	14.9	13.2
PGI1	Ø	Ø

Many of the genes involved in gluconeogenesis also play a role in glucose fermentation and these are transcribed at a higher level in the presence of gliotoxin as this toxin appears to "switch on" the latter pathway. Interestingly, the other genes involved in gluconeogenesis are all transcriptionally downregulated. Our data suggests these two antithetical processes are both affected by cellular exposure to gliotoxin in that the glucose fermentation pathway is "switched on" and gluconeogenesis is "switched off".

3.6.1.5 Comparative evaluation of the effects of gliotoxin and other mycotoxins

Previous studies have utilised *S. cerevisiae* to investigate the global expressional response to other toxins, including mycotoxins. Transcriptomic data, representing the global response to gliotoxin was compared and contrasted with that for citrinin, patulin, allicin and furfural obtained from Iwahashi *et al.* (2007), Iwahashi *et al.* (2006), Yu *et al.* (2010) and Li & Yuan (2010) respectively. Genes which undergo an increase or

decrease in transcription in response to the mycotoxins were compared and similarities were investigated. Table 3.13 illustrates the upregulated genes of interest.

Table 3.14 lists the downregulated genes of interest. Tables 3.13 and 3.14 demonstrate significant overlap in genes that undergo up- and downregulation in response to the different toxins listed above. Analysis of results using other mycotoxins may help us build a bigger picture of the yeast response to gliotoxin. Discrepancies in genes up- and downregulated were also investigated and are listed in table 3.15. This contrast could provide insight into differences in mycotoxin targets etc. For example, *ARO9* is upregulated in response to gliotoxin, furfural and allicin exposure. Conversely, it is downregulated when cells are exposed to citrinin. Thus, the former three toxins may exert a particular type of stress on the cell that requires Aro9p response to resist the toxin, the same stress may not be elicited by citrinin.

3.6.1.6 Utilisation of quantitative PCR to confirm transcriptome data

To assess the efficacy of our RNA sequencing expression data, quantitative PCR (qPCR) was performed. Total RNA was extracted from yeast cultures exposed to 0, 16 and 64 µg/ml gliotoxin. cDNA was synthesised as described in section 2.23.4 and was used as reaction template for qPCR. The expression level of fourteen genes in response to gliotoxin exposure was analysed. Genes were chosen based on their importance in pathways identified and also due to pronounced up- or downregulation recorded in transcriptomic data.

VMA6 and *ERG9* were selected as reference genes based on the fact that the RNA sequencing data did not record a significant change in their transcription levels in response to gliotoxin exposure.

Table 3.13 Comparison of genes that are upregulated in the presence of the respective compound. X denotes upregulation. Gene function data was recorded from SGD. Genes listed show an upregulation in response to one or more toxins.

Gene	Citrinin	Patulin	Allicin	Furfural	Gliotoxin	Gene Function
FRM2	X	X			X	Protein of unknown function, involved in the integration of lipid signaling pathways with cellular homeostasis; expression induced in cells treated with the mycotoxin patulin; has similarity to bacterial nitroreductases
AAD16	X	X	X			Putative aryl-alcohol dehydrogenase with similarity to P. chrysosporium aryl-alcohol dehydrogenase; mutational analysis has not yet revealed a physiological role
AAD6	X	X	X			Putative aryl-alcohol dehydrogenase with similarity to P. chrysosporium aryl-alcohol dehydrogenase, involved in the oxidative stress response; expression induced in cells treated with the mycotoxin patulin
AAD4	X	X				Putative aryl-alcohol dehydrogenase with similarity to P. chrysosporium aryl-alcohol dehydrogenase, involved in the oxidative stress response; expression induced in cells treated with the mycotoxin patulin
FLR1	X	X	X			Plasma membrane multidrug transporter of the major facilitator superfamily, involved in efflux of fluconazole, diazaborine, benomyl, methotrexate, and other drugs; expression induced in cells treated with the mycotoxin patulin
OYE3	X	X	X			Conserved NADPH oxidoreductase containing flavin mononucleotide (FMN), homologous to Oye2p with different ligand binding and catalytic properties; has potential roles in oxidative stress response and programmed cell death
AAD15	X	X				Putative aryl-alcohol dehydrogenase with similarity to P. chrysosporium aryl-alcohol dehydrogenase; mutational analysis has not yet revealed a physiological role
AAD10	X	X				Putative aryl-alcohol dehydrogenase with similarity to P. chrysosporium aryl-alcohol dehydrogenase; mutational analysis has not yet revealed a physiological role
AAD14	X	X	X			Putative aryl-alcohol dehydrogenase with similarity to P. chrysosporium aryl-alcohol dehydrogenase; mutational analysis has not yet revealed a physiological role
GRE2	X	X	X			3-methylbutanal reductase and NADPH-dependent methylglyoxal reductase (D-lactaldehyde dehydrogenase); stress induced (osmotic, ionic, oxidative, heat shock and heavy metals); regulated by the HOG pathway
AAD3	X	X				Putative aryl-alcohol dehydrogenase with similarity to P. chrysosporium aryl-alcohol dehydrogenase; mutational analysis has not yet revealed a physiological role
YLL056C	X	X				Putative protein of unknown function, transcription is activated by paralogous transcription factors Yrm1p and Yrr1p and genes involved in pleiotropic drug resistance (PDR); expression is induced in cells treated with the mycotoxin patulin
GTT2	X	X				Glutathione S-transferase capable of homodimerization; functional overlap with Gtt2p, Grx1p, and Grx2p
ECM4	X	X				Omega class glutathione transferase; not essential; similar to Ygr154cp; green fluorescent protein (GFP)-fusion protein localizes to the cytoplasm

YKL070W	X	X			Putative protein of unknown function; expression induced in cells treated with mycotoxins patulin or citrinin; the authentic, non-tagged protein is detected in highly purified mitochondria in high-throughput studies
MET1	X	X	X	X	S-adenosyl-L-methionine uroporphyrinogen III transmethylase, involved in the biosynthesis of siroheme, a prosthetic group used by sulfite reductase; required for sulfate assimilation and methionine biosynthesis
MET10	X	X	X	X	Subunit alpha of assimilatory sulfite reductase, which converts sulfite into sulphide
MET14	X	X	X	X	Adenylylsulfate kinase, required for sulphate assimilation and involved in methionine metabolism
MET16	X	X	X	X	3'-phosphoadenylsulfate reductase, reduces 3'-phosphoadenylyl sulfate to adenosine-3',5'-bisphosphate and free sulfite using reduced thioredoxin as cosubstrate, involved in sulfate assimilation and methionine metabolism
MET17	X	X	X	X	Methionine and cysteine synthase (O-acetyl homoserine-O-acetyl serine sulfhydrylase), required for sulfur amino acid synthesis
MET2	X	X	X		L-homoserine-O-acetyltransferase, catalyzes the conversion of homoserine to O-acetyl homoserine which is the first step of the methionine biosynthetic pathway
MET22	X	X	X	X	Bisphosphate-3'-nucleotidase, involved in salt tolerance and methionine biogenesis; dephosphorylates 3'-phosphoadenosine-5'-phosphate and 3'-phosphoadenosine-5'-phosphosulfate, intermediates of the sulfate assimilation pathway
MET3	X	X	X	X	ATP sulfurylase, catalyzes the primary step of intracellular sulfate activation, essential for assimilatory reduction of sulfate to sulfide, involved in methionine metabolism
MET30	X	X			F-box protein containing five copies of the WD40 motif, controls cell cycle function, sulfur metabolism, and methionine biosynthesis as part of the ubiquitin ligase complex; interacts with and regulates Met4p, localizes within the nucleus
MET32	X	X			Zinc-finger DNA-binding protein, involved in transcriptional regulation of the methionine biosynthetic genes, similar to Met31p
MET8	X	X		X	Bifunctional dehydrogenase and ferrochelatase, involved in the biosynthesis of siroheme, a prosthetic group used by sulfite reductase; required for sulfate assimilation and methionine biosynthesis
CYS3	X	X		X	Cystathionine gamma-lyase, catalyzes one of the two reactions involved in the transsulfuration pathway that yields cysteine from formation of cystathionine
CYS4	X	X		X	Cystathionine beta-synthase, catalyzes synthesis of cystathionine from serine and homocysteine, the first committed step in cysteine biosynthesis; responsible for hydrogen sulfide generation; mutations in human ortholog cause homocystinuria
SNQ2	X	X			Plasma membrane ATP-binding cassette (ABC) transporter, multidrug transporter involved in multidrug resistance and resistance to singlet oxygen species
ARN1	X		X	X	Transporter, member of the ARN family of transporters that specifically recognize siderophore-iron chelates; responsible for uptake of iron bound to ferrirubin, ferrirhodin, and related siderophores
TRX2	X	X			Cytoplasmic thioredoxin isoenzyme of the thioredoxin system which protects cells against oxidative and reductive stress, forms LMA1 complex with Pbi2p, acts as a cofactor for Tsa1p, required for ER-Golgi transport and vacuole inheritance

MXR1	X	X			Methionine-S-sulfoxide reductase, involved in the response to oxidative stress; protects iron-sulfur clusters from oxidative inactivation along with MXR2; involved in the regulation of lifespan
PST2	X	X			Protein with similarity to members of a family of flavodoxin-like proteins; induced by oxidative stress in a Yap1p dependent manner; the authentic, non-tagged protein is detected in highly purified mitochondria in high-throughput studies
RAD59	X	X	X	X	Protein involved in the repair of double-strand breaks in DNA during vegetative growth via recombination and single-strand annealing; anneals complementary single-stranded DNA; homologous to Rad52p
UBC13	X	X			Ubiquitin-conjugating enzyme involved in the error-free DNA postreplication repair pathway; interacts with Mms2p to assemble ubiquitin chains at the Ub Lys-63 residue; DNA damage triggers redistribution from the cytoplasm to the nucleus
MAG1	X	X	X		3-methyl-adenine DNA glycosylase involved in protecting DNA against alkylating agents; initiates base excision repair by removing damaged bases to create abasic sites that are subsequently repaired
HPA2	X	X			Tetrameric histone acetyltransferase with similarity to Gcn5p, Hat1p, Elp3p, and Hpa3p; acetylates histones H3 and H4 in vitro and exhibits autoacetylation activity
RPT1	X	X			One of six ATPases of the 19S regulatory particle of the 26S proteasome involved in the degradation of ubiquitinated substrates; required for optimal CDC20 transcription; interacts with Rpn12p and Ubr1p; mutant has aneuploidy tolerance
DDR48	X	X		X	DNA damage-responsive protein, expression is increased in response to heat-shock stress or treatments that produce DNA lesions; contains multiple repeats of the amino acid sequence NNNDSYGS
RFA1	X	X	X		Subunit of heterotrimeric Replication Protein A (RPA), which is a highly conserved single-stranded DNA binding protein involved in DNA replication, repair, and recombination
DDC1	X	X			DNA damage checkpoint protein, part of a PCNA-like complex required for DNA damage response, required for pachytene checkpoint to inhibit cell cycle in response to unrepaired recombination intermediates; potential Cdc28p substrate
TRX1	X	X		X	Cytoplasmic thioredoxin isoenzyme of the thioredoxin system which protects cells against oxidative and reductive stress, forms LMA1 complex with Pbi2p, acts as a cofactor for Tsa1p, required for ER-Golgi transport and vacuole inheritance
RAD23	X	X			Protein with ubiquitin-like N terminus, subunit of Nuclear Excision Repair Factor 2 (NEF2) with Rad4p that recognizes and binds damaged DNA; enhances protein deglycosylation activity of Png1p; homolog of human HR23A and HR23B
RFA2	X	X			Subunit of heterotrimeric Replication Protein A (RPA), which is a highly conserved single-stranded DNA binding protein involved in DNA replication, repair, and recombination
SSL2	X	X			Component of the holoenzyme form of RNA polymerase transcription factor TFIIH, has DNA-dependent ATPase/helicase activity and is required, with Rad3p, for unwinding promoter DNA; involved in DNA repair; homolog of human ERCC3
RAD7	X	X			Protein that recognizes and binds damaged DNA in an ATP-dependent manner (with Rad16p) during nucleotide excision repair; subunit of Nucleotide Excision Repair Factor 4 (NEF4) and the Elongin-Cullin-Socs (ECS) ligase complex
RAD52	X	X			Protein that stimulates strand exchange by facilitating Rad51p binding to single-stranded DNA; anneals complementary single-stranded DNA; involved in the repair of double-strand breaks in DNA during vegetative growth and meiosis

MND2	X	X			Subunit of the anaphase-promoting complex (APC); necessary for maintaining sister chromatid cohesion in prophase I of meiosis by inhibiting premature ubiquitination and subsequent degradation of substrates by the APC(Ama1) ubiquitin ligase
RAD50	X	X	X		Subunit of MRX complex, with Mre11p and Xrs2p, involved in processing double-strand DNA breaks in vegetative cells, initiation of meiotic DSBs, telomere maintenance, and nonhomologous end joining
CSM1	X	X			Nucleolar protein that forms a complex with Lrs4p and then Mam1p at kinetochores during meiosis I to mediate accurate homolog segregation; required for condensin recruitment to the replication fork barrier site and rDNA repeat segregation
NCA3		X	X		Protein that functions with Nca2p to regulate mitochondrial expression of subunits 6 (Atp6p) and 8 (Atp8p) of the Fo-F1 ATP synthase; member of the SUN family; expression induced in cells treated with the mycotoxin patulin
RPT2		X	X		One of six ATPases of the 19S regulatory particle of the 26S proteasome involved in the degradation of ubiquitinated substrates; required for normal peptide hydrolysis by the core 20S particle
RPN6		X	X		Essential, non-ATPase regulatory subunit of the 26S proteasome lid required for the assembly and activity of the 26S proteasome; the human homolog (S9 protein) partially rescues Rpn6p depletion
MGT1		X	X		DNA repair methyltransferase (6-O-methylguanine-DNA methylase) involved in protection against DNA alkylation damage
SAM2	X			X	S-adenosylmethionine synthetase, catalyzes transfer of the adenosyl group of ATP to the sulfur atom of methionine; one of two differentially regulated isozymes (Sam1p and Sam2p)
STR3	X			X	Cystathionine beta-lyase, converts cystathionine into homocysteine
PDR16	X			X	Phosphatidylinositol transfer protein (PITP) controlled by the multiple drug resistance regulator Pdr1p, localizes to lipid particles and microsomes, controls levels of various lipids, may regulate lipid synthesis, homologous to Pdr17p
AHP1		X		X	Thiol-specific peroxiredoxin, reduces hydroperoxides to protect against oxidative damage; function in vivo requires covalent conjugation to Urm1p
TSA1		X		X	Thioredoxin peroxidase, acts as both a ribosome-associated and free cytoplasmic antioxidant; self-associates to form a high-molecular weight chaperone complex under oxidative stress; deletion results in mutator phenotype
LAP4		X		X	Vacuolar aminopeptidase yscI; zinc metalloproteinase that belongs to the peptidase family M18; often used as a marker protein in studies of autophagy and cytosol to vacuole targeting (CVT) pathway
PRE6		X		X	Alpha 4 subunit of the 20S proteasome; may replace alpha 3 subunit (Pre9p) under stress conditions to create a more active proteasomal isoform; GFP-fusion protein relocates from cytosol to the mitochondrial surface upon oxidative stress
TRP3			X	X	Bifunctional enzyme exhibiting both indole-3-glycerol-phosphate synthase and anthranilate synthase activities, forms multifunctional hetero-oligomeric anthranilate synthase:indole-3-glycerol phosphate synthase enzyme complex with Trp2p
TRP5			X	X	Tryptophan synthase, catalyzes the last step of tryptophan biosynthesis; regulated by the general control system of amino acid biosynthesis
ILS1			X	X	Cytoplasmic isoleucine-tRNA synthetase, target of the G1-specific inhibitor reveromycin A
ARO8			X	X	Aromatic aminotransferase I, expression is regulated by general control of amino acid biosynthesis

SER33		X		X	3-phosphoglycerate dehydrogenase, catalyzes the first step in serine and glycine biosynthesis; isozyme of Ser3p
HOM3		X		X	Aspartate kinase (L-aspartate 4-P-transferase); cytoplasmic enzyme that catalyzes the first step in the common pathway for methionine and threonine biosynthesis; expression regulated by Gcn4p and the general control of amino acid synthesis
THR4		X		X	Threonine synthase, conserved protein that catalyzes formation of threonine from O-phosphohomoserine; expression is regulated by the GCN4-mediated general amino acid control pathway
FTR1		X		X	High affinity iron permease involved in the transport of iron across the plasma membrane; forms complex with Fet3p; expression is regulated by iron
FET3		X		X	Ferro-O2-oxidoreductase required for high-affinity iron uptake and involved in mediating resistance to copper ion toxicity, belongs to class of integral membrane multicopper oxidases
TIS11		X		X	mRNA-binding protein expressed during iron starvation; binds to a sequence element in the 3'-untranslated regions of specific mRNAs to mediate their degradation; involved in iron homeostasis
PRE2		X		X	Beta 5 subunit of the 20S proteasome, responsible for the chymotryptic activity of the proteasome
EPT1			X	X	sn-1,2-diacylglycerol ethanolamine- and cholinephosphotranferase; not essential for viability
YBR096W			X	X	Putative protein of unknown function; green fluorescent protein (GFP)-fusion protein localizes to the ER

Table 3.14 Comparison of genes that are downregulated in the presence of the respective compound. X denotes upregulation. Gene function data was recorded from SGD. Genes listed show a downregulation in response to one or more toxins.

Gene	Citrinin	Patulin	Allicin	Furfural	Gliotoxin	Gene Function
ATP4			X	X	X	Subunit b of the stator stalk of mitochondrial F1F0 ATP synthase, which is a large, evolutionarily conserved enzyme complex required for ATP synthesis; phosphorylated
ADE17	X				X	Enzyme of 'de novo' purine biosynthesis containing both 5-aminoimidazole-4-carboxamide ribonucleotide transformylase and inosine monophosphate cyclohydrolase activities, isozyme of Ade16p; ade16 ade17 mutants require adenine and histidine
SSU1	X				X	Plasma membrane sulfite pump involved in sulfite metabolism and required for efficient sulfite efflux; major facilitator superfamily protein
LEU1			X		X	Isopropylmalate □uinine□e, catalyzes the second step in the leucine biosynthesis pathway
GLT1			X		X	NAD(+)-dependent glutamate synthase (GOGAT), synthesizes glutamate from glutamine and alpha-ketoglutarate; with Gln1p, forms the secondary pathway for glutamate biosynthesis from ammonia; expression regulated by nitrogen source
AGX1			X		X	Alanine:glyoxylate aminotransferase (AGT), catalyzes the synthesis of glycine from glyoxylate, which is one of three pathways for glycine biosynthesis in yeast; has similarity to mammalian and plant alanine:glyoxylate aminotransferases

LPD1	X	X	Dihydrolipoamide dehydrogenase, the lipoamide dehydrogenase component (E3) of the pyruvate dehydrogenase and 2-oxoglutarate dehydrogenase multi-enzyme complexes
NDE1	X	X	Mitochondrial external NADH dehydrogenase, a type II NAD(P)H:□uinine oxidoreductase that catalyzes the oxidation of cytosolic NADH; Nde1p and Nde2p provide cytosolic NADH to the mitochondrial respiratory chain
NDI1	X	X	NADH:ubiquinone oxidoreductase, transfers electrons from NADH to ubiquinone in the respiratory chain but does not pump protons, in contrast to the higher eukaryotic multisubunit respiratory complex I; phosphorylated; homolog of human AMID
SDH1	X	X	Flavoprotein subunit of succinate dehydrogenase (Sdh1p, Sdh2p, Sdh3p, Sdh4p), which couples the oxidation of succinate to the transfer of electrons to ubiquinone as part of the TCA cycle and the mitochondrial respiratory chain
SDH2	X	X	Iron-sulfur protein subunit of succinate dehydrogenase (Sdh1p, Sdh2p, Sdh3p, Sdh4p), which couples the oxidation of succinate to the transfer of electrons to ubiquinone as part of the TCA cycle and the mitochondrial respiratory chain
SDH3	X	X	Cytochrome b subunit of succinate dehydrogenase (Sdh1p, Sdh2p, Sdh3p, Sdh4p), which couples the oxidation of succinate to the transfer of electrons to ubiquinone as part of the TCA cycle and the mitochondrial respiratory chain
SDH4	X	X	Membrane anchor subunit of succinate dehydrogenase (Sdh1p, Sdh2p, Sdh3p, Sdh4p), which couples the oxidation of succinate to the transfer of electrons to ubiquinone as part of the TCA cycle and the mitochondrial respiratory chain
COR1	X	X	Core subunit of the ubiquinol-cytochrome c reductase complex (bc1 complex), which is a component of the mitochondrial inner membrane electron transport chain
CYT1	X	X	Cytochrome c1, component of the mitochondrial respiratory chain; expression is regulated by the heme-activated, glucose-repressed Hap2p/3p/4p/5p CCAAT-binding complex
QCR2	X	X	Subunit 2 of the ubiquinol cytochrome-c reductase complex, which is a component of the mitochondrial inner membrane electron transport chain; phosphorylated; transcription is regulated by Hap1p, Hap2p/Hap3p, and heme
QCR6	X	X	Subunit 6 of the ubiquinol cytochrome-c reductase complex, which is a component of the mitochondrial inner membrane electron transport chain; highly acidic protein; required for maturation of cytochrome c1
QCR7	X	X	Subunit 7 of the ubiquinol cytochrome-c reductase complex, which is a component of the mitochondrial inner membrane electron transport chain; oriented facing the mitochondrial matrix; N-terminus appears to play a role in complex assembly
QCR8	X	X	Subunit 8 of ubiquinol cytochrome-c reductase complex, which is a component of the mitochondrial inner membrane electron transport chain; oriented facing the intermembrane space; expression is regulated by Abf1p and Cpf1p
QCR9	X	X	Subunit 9 of the ubiquinol cytochrome-c reductase complex, which is a component of the mitochondrial inner membrane electron transport chain; required for electron transfer at the ubiquinol oxidase site of the complex
RIP1	X	X	Ubiquinol-cytochrome-c reductase, a Rieske iron-sulfur protein of the mitochondrial cytochrome bc1 complex; transfers electrons from ubiquinol to cytochrome c1 during respiration
CYC1	X	X	Cytochrome c, isoform 1; electron carrier of the mitochondrial intermembrane space that transfers electrons from ubiquinone-cytochrome c oxidoreductase to cytochrome c oxidase during cellular respiration

COX4	X		X	Subunit IV of cytochrome c oxidase, the terminal member of the mitochondrial inner membrane electron transport chain; precursor N-terminal 25 residues are cleaved during mitochondrial import; phosphorylated; spermidine enhances translation
COX5A	X		X	Subunit Va of cytochrome c oxidase, which is the terminal member of the mitochondrial inner membrane electron transport chain; predominantly expressed during aerobic growth while its isoform Vb (Cox5Bp) is expressed during anaerobic growth
COX6	X		X	Subunit VI of cytochrome c oxidase, which is the terminal member of the mitochondrial inner membrane electron transport chain; expression is regulated by oxygen levels
COX7	X		X	Subunit VII of cytochrome c oxidase, which is the terminal member of the mitochondrial inner membrane electron transport chain
COX8	X		X	Subunit VIII of cytochrome c oxidase, which is the terminal member of the mitochondrial inner membrane electron transport chain
COX9	X		X	Subunit VIIa of cytochrome c oxidase, which is the terminal member of the mitochondrial inner membrane electron transport chain
COX12	X		X	Subunit Vib of cytochrome c oxidase, which is the terminal member of the mitochondrial inner membrane electron transport chain; required for assembly of cytochrome c oxidase but not required for activity after assembly; phosphorylated
COX13	X		X	Subunit Via of cytochrome c oxidase, which is the terminal member of the mitochondrial inner membrane electron transport chain; not essential for cytochrome c oxidase activity but may modulate activity in response to ATP
ATP3	X		X	Gamma subunit of the F1 sector of mitochondrial F1F0 ATP synthase, which is a large, evolutionarily conserved enzyme complex required for ATP synthesis
ATP5	X		X	Subunit 5 of the stator stalk of mitochondrial F1F0 ATP synthase, which is an evolutionarily conserved enzyme complex required for ATP synthesis; homologous to bovine subunit OSCP (oligomycin sensitivity-conferring protein); phosphorylated
ATP7	X		X	Subunit d of the stator stalk of mitochondrial F1F0 ATP synthase, which is a large, evolutionarily conserved enzyme complex required for ATP synthesis
ATP14	X		X	Subunit h of the F0 sector of mitochondrial F1F0 ATP synthase, which is a large, evolutionarily conserved enzyme complex required for ATP synthesis
ATP16	X		X	Delta subunit of the central stalk of mitochondrial F1F0 ATP synthase, which is a large, evolutionarily conserved enzyme complex required for ATP synthesis; phosphorylated
ATP17	X		X	Subunit f of the F0 sector of mitochondrial F1F0 ATP synthase, which is a large, evolutionarily conserved enzyme complex required for ATP synthesis
ATP20	X		X	Subunit g of the mitochondrial F1F0 ATP synthase; reversibly phosphorylated on two residues; unphosphorylated form is required for dimerization of the ATP synthase complex
FRE2	X		X	Ferric reductase and cupric reductase, reduces siderophore-bound iron and oxidized copper prior to uptake by transporters; expression induced by low iron levels but not by low copper levels
MEF2	X		X	Mitochondrial elongation factor involved in translational elongation
TEC1		X	X	Transcription factor required for full Ty1 expression, Ty1-mediated gene activation, and haploid invasive and diploid pseudohyphal growth; TEA/ATTS DNA-binding domain family member
MIH1		X	X	Protein tyrosine phosphatase involved in cell cycle control; regulates the phosphorylation state of Cdc28p; homolog of S. pombe cdc25
YBR225W		X	X	Putative protein of unknown function; non-essential gene identified in a screen for mutants affected in mannosylphophorylation of cell wall components

T**able 3.15 Discrepancies in transcription trends in response to the different compounds.** Gene function data was recorded from SGD. Genes listed show differences in expression trends in response to one or more toxins.U indicates the upregulation and D the downregulation of the gene in response to exposure of the respective toxin.

Gene	Citrinin	Patulin	Allicin	Furfural	Gliotoxin	Gene Function
PDR5	U		D			Plasma membrane ATP-binding cassette (ABC) transporter, multidrug transporter actively regulated by Pdr1p; also involved in steroid transport, cation resistance, and cellular detoxification during exponential growth
ARO10	D			U		Phenylpyruvate decarboxylase, catalyzes decarboxylation of phenylpyruvate to phenylacetaldehyde, which is the first specific step in the Ehrlich pathway
ARO9	D		U	U	U	Aromatic aminotransferase II, catalyzes the first step of tryptophan, phenylalanine, and tyrosine catabolism
BNA4	D			U		Kynurenine 3-mono oxygenase, required for the de novo biosynthesis of NAD from tryptophan via kynurenine; expression regulated by Hst1p; putative therapeutic target for Huntington disease
MET28	U	U	D			Basic leucine zipper (bZIP) transcriptional activator in the Cbf1p-Met4p-Met28p complex, participates in the regulation of sulfur metabolism
MET31		D				Zinc-finger DNA-binding protein, involved in transcriptional regulation of the methionine biosynthetic genes, similar to Met32p
MET4		U				Leucine-zipper transcriptional activator, responsible for the regulation of the sulfur amino acid pathway, requires different combinations of the auxiliary factors Cbf1p, Met28p, Met31p and Met32p
MET6	U	D			U	Cobalamin-independent methionine synthase, involved in methionine biosynthesis and regeneration; requires a minimum of two glutamates on the methyltetrahydrofolate substrate, similar to bacterial metE homologs
RAD54		U				DNA-dependent ATPase, stimulates strand exchange by modifying the topology of double-stranded DNA; involved in the recombinational repair of double-strand breaks in DNA during vegetative growth and meiosis; member of the SWI/SNF family
AHC1		U			D	Subunit of the Ada histone acetyltransferase complex, required for structural integrity of the complex
MCM6		U				Protein involved in DNA replication; component of the Mcm2-7 hexameric complex that binds chromatin as a part of the pre-replicative complex
PHB2		U				Subunit of the prohibitin complex (Phb1p-Phb2p), a 1.2 MDa ring-shaped inner mitochondrial membrane chaperone that stabilizes newly synthesized proteins; determinant of replicative life span; involved in mitochondrial segregation
HSP12	D	U			D	Plasma membrane localized protein that protects membranes from desiccation; induced by heat shock, oxidative stress, osmostress, stationary phase entry, glucose depletion, oleate and alcohol; regulated by the HOG and Ras-Pka pathways
PRP12	D	U				Integral inner mitochondrial membrane protein with a role in maintaining mitochondrial nucleoid structure and number; mutants exhibit an increased rate of mitochondrial DNA escape; shows some sequence similarity to exonucleases
RAD14	D	U				Protein that recognizes and binds damaged DNA during nucleotide excision repair; subunit of Nucleotide Excision Repair Factor 1 (NEF1); contains zinc finger motif; homolog of human XPA protein
HST1	D	U				NAD(+)-dependent histone deacetylase; essential subunit of the Sum1p/Rfm1p/Hst1p complex required for ORC-dependent silencing and mitotic repression; non-essential subunit of the Set3C deacetylase complex; involved in telomere maintenance

MAG2		U				Cytoplasmic protein of unknown function; induced in response to mycotoxin patulin; ubiquitinated protein similar to the human ring finger motif protein RNF10; predicted to be involved in repair of alkylated DNA due to interaction with MAG1
RDH54		U			U	DNA-dependent ATPase, stimulates strand exchange by modifying the topology of double-stranded DNA; involved in recombinational repair of DNA double-strand breaks during mitosis and meiosis; proposed to be involved in crossover interference
SHP1			U	D		UBX (ubiquitin regulatory X) domain-containing protein that regulates Glc7p phosphatase activity and interacts with Cdc48p; interacts with ubiquitylated proteins in vivo and is required for degradation of a ubiquitylated model substrate
YLR346C	U				D	Putative protein of unknown function found in mitochondria; expression is regulated by transcription factors involved in pleiotropic drug resistance, Pdr1p and Yrr1p; YLR346C is not an essential gene
HO	D				U	Site-specific endonuclease required for gene conversion at the MAT locus (homothallic switching) through the generation of a ds DNA break; expression restricted to mother cells in late G1 as controlled by Swi4p-Swi6p, Swi5p and Ash1p
SAM4	D				U	S-adenosylmethionine-homocysteine methyltransferase, functions along with Mht1p in the conversion of S-adenosylmethionine (AdoMet) to methionine to control the methionine/AdoMet ratio
YHK8	U				D	Presumed antiporter of the DHA1 family of multidrug resistance transporters; contains 12 predicted transmembrane spans; expression of gene is up-regulated in cells exhibiting reduced susceptibility to azoles
PRX1	U	U			D	Mitochondrial peroxiredoxin (1-Cys Prx) with thioredoxin peroxidase activity, has a role in reduction of hydroperoxides; reactivation requires Trr2p and glutathione; induced during respiratory growth and oxidative stress; phosphorylated
PUG1	U				D	Plasma membrane protein with roles in the uptake of protoprophyrin IX and the efflux of heme; expression is induced under both low-heme and low-oxygen conditions; member of the fungal lipid-translocating exporter (LTE) family of proteins
RIM4	U	U			D	Putative RNA-binding protein required for the expression of early and middle sporulation genes
EAF3	U	U			D	Esa1p-associated factor, nonessential component of the NuA4 acetyltransferase complex, homologous to Drosophila dosage compensation protein MSL3; plays a role in regulating Ty1 transposition
SPS100		U			D	Protein required for spore wall maturation; expressed during sporulation; may be a component of the spore wall; expression also induced in cells treated with the mycotoxin patulin
YJL045W		U			D	Minor succinate dehydrogenase isozyme; homologous to Sdh1p, the major isozyme reponsible for the oxidation of succinate and transfer of electrons to ubiquinone; induced during the diauxic shift in a Cat8p-dependent manner
SRX1		U		U	D	Sulfiredoxin, contributes to oxidative stress resistance by reducing cysteine-sulfinic acid groups in the peroxiredoxin Tsa1p, which is formed upon exposure to oxidants; conserved in higher eukaryotes
GRE1		U			D	Hydrophilin of unknown function; stress induced (osmotic, ionic, oxidative, heat shock and heavy metals); regulated by the HOG pathway
SOD2		U			D	Mitochondrial superoxide dismutase, protects cells against oxygen toxicity; phosphorylated
OXR1		U			D	Protein of unknown function required for normal levels of resistance to oxidative damage, null mutants are sensitive to hydrogen

					peroxide; member of a conserved family of proteins found in eukaryotes
ATG8	U		U	D	Component of autophagosomes and Cvt vesicles; undergoes conjugation to phosphatidylethanolamine (PE); Atg8p-PE is anchored to membranes, is involved in phagophore expansion, and may mediate membrane fusion during autophagosome formation
PAI3	U			D	Cytoplasmic proteinase A (Pep4p) inhibitor, dependent on Pbs2p and Hog1p protein kinases for osmotic induction; intrinsically unstructured, N-terminal half becomes ordered in the active site of proteinase A upon contact
ATG1	U			D	Protein ser/thr kinase required for vesicle formation in autophagy and the cytoplasm-to-vacuole targeting (Cvt) pathway; structurally required for phagophore assembly site formation; during autophagy forms a complex with Atg13p and Atg17p
YHR138C	U			D	Putative protein of unknown function; has similarity to Pbi2p; double null mutant lacking Pbi2p and Yhr138p exhibits highly fragmented vacuoles
ECM29	U	U		D	Major component of the proteasome; tethers the proteasome core particle to the regulatory particle, and enhances the stability of the proteasome
SER3		U		D	3-phosphoglycerate dehydrogenase, catalyzes the first step in serine and glycine biosynthesis; isozyme of Ser33p
MDM34		U		D	Mitochondrial component of the ERMES complex that links the ER to mitochondria and may promote inter-organellar calcium and phospholipid exchange as well as coordinating mitochondrial DNA replication and growth
ISU1		U		D	Conserved protein of the mitochondrial matrix, performs a scaffolding function during assembly of iron-sulfur clusters, interacts physically and functionally with yeast frataxin (Yfh1p); isu1 isu2 double mutant is inviable
PYC1		U		D	Pyruvate carboxylase isoform, cytoplasmic enzyme that converts pyruvate to oxaloacetate; highly similar to isoform Pyc2p but differentially regulated; mutations in the human homolog are associated with lactic acidosis
MIS1			D	U	Mitochondrial C1-tetrahydrofolate synthase, involved in interconversion between different oxidation states of tetrahydrofolate (THF); provides activities of formyl-THF synthetase, methenyl-THF cyclohydrolase, and methylene-THF dehydrogenase
RHR2			D	U	Constitutively expressed isoform of DL-glycerol-3-phosphatase; involved in glycerol biosynthesis, induced in response to both anaerobic and, along with the Hor2p/Gpp2p isoform, osmotic stress
CTA1			U	D	Catalase A, breaks down hydrogen peroxide in the peroxisomal matrix formed by acyl-CoA oxidase (Pox1p) during fatty acid beta-oxidation
GRX5			U	D	Hydroperoxide and superoxide-radical responsive glutathione-dependent oxidoreductase; mitochondrial matrix protein involved in the synthesis/assembly of iron-sulfur centers; monothiol glutaredoxin subfamily member along with Grx3p and Grx4p
CYC7			U	D	Cytochrome c isoform 2, expressed under hypoxic conditions; electron carrier of the mitochondrial intermembrane space that transfers electrons from ubiquinone-cytochrome c oxidoreductase to cytochrome c oxidase during cellular respiration
EMG1			D	U	Member of the alpha/beta knot fold methyltransferase superfamily; required for maturation of 18S rRNA and for 40S ribosome production; interacts with RNA and with S-adenosylmethionine; associates with spindle/microtubules; forms homodimers

GAR1	D	U	Protein component of the H/ACA snoRNP pseudouridylase complex, involved in the modification and cleavage of the 18S pre-rRNA
ZUO1	D	U	Ribosome-associated chaperone, functions in ribosome biogenesis and, in partnership with Ssz1p and SSb1/2, as a chaperone for nascent polypeptide chains; contains a DnaJ domain and functions as a J-protein partner for Ssb1p and Ssb2p
YNL305C	U	D	Putative protein of unknown function; green fluorescent protein (GFP)-fusion protein localizes to the vacuole; YNL305C is not an essential gene
MPM1	U	D	Mitochondrial membrane protein of unknown function, contains no hydrophobic stretches
YKL091C	U	D	Putative homolog of Sec14p, which is a phosphatidylinositol/phosphatidylcholine transfer protein involved in lipid metabolism; localizes to the nucleus
CRC1	U	D	Mitochondrial inner membrane carnitine transporter, required for carnitine-dependent transport of acetyl-CoA from peroxisomes to mitochondria during fatty acid beta-oxidation
UBX6	U	D	UBX (ubiquitin regulatory X) domain-containing protein that interacts with Cdc48p, transcription is repressed when cells are grown in media containing inositol and choline
YPL189C-A			Cytochrome oxidase assembly factor; null mutation results in respiratory deficiency with specific loss of cytochrome oxidase activity; functions downstream of assembly factors Mss51p and Coa1p and interacts with assembly factor Shy1p
YER053C-A			Putative protein of unknown function; green fluorescent protein (GFP)-fusion protein localizes to the endoplasmic reticulum

The RNA sequencing data values obtained for these genes are depicted in table 3.16.

Table 3.16 Transcript levels of reference genes used for qPCR obtained from RNA sequencing data.

Gene	Trancription level value under 0 µg/ml gliotoxin exposure	Trancription level value under 16 µg/ml gliotoxin exposure	Trancription level value under 64 µg/ml gliotoxin exposure
VMA6	273.08	292.57	258.41
ERG9	234.67	222.58	262.58

As the transcript levels of *VMA6* and *ERG9* remain relatively stable when yeast cells are exposed to the two concentrations of gliotoxin, these genes were ideal for use as references. Before proceeding with qPCR for the fourteen genes chosen (listed in table 3.17), standard curves were constructed for these two reference genes. Standard curves were subsequently constructed for the fourteen genes of interest. The production of standard curves allowed the PCR reaction efficiency to be considered in the generation of results, as the multiplication factor is not always two after each PCR cycle. The fourteen genes of interest and their fold change according to the RNA sequencing data are listed in table 3.17.

qPCR was carried out using primers for these genes and methodology described in sections 2.19.1 and 2.23.5. To make the analyses more accurate, advanced relative quantification was performed to compare transcript levels of a specific gene when cells are exposed to the concentrations of the toxin described above. This involved importation of reference gene transcript levels and standard curves, which were used in generation of results.

Table 3.17 Fold change recorded in RNA sequencing data of fourteen genes used for qPCR. + indicates upregulation and – indicates downregulation.

Gene Name	Fold change when exposed to 16 µg/ml gliotoxin	Fold change when exposed to 64 µg/ml gliotoxin
MET7	+1.5	+1.5
SAM1	+1.8	+9.5
MET6	+2.9	+8.7
MET16	+4.6	+13.6
MET17	+5.5	+8.5
MET2	+2.9	+4.2
MET14	+7.4	+13.6
MET22	+2.98	+4.8
HBN1	+3.9	+11.0
JEN1	-33.7	-32.8
SIP18	-62.7	-131.2
BDH2	-6.3	-10.2
SDH2	-33.0	-18.2
MLS1	-34.4	-17.9

Figures 3.62-3.68 illustrate the comparison of transcript levels of genes involved in the sulfur amino acid biosynthesis pathway (figure 3.60), identified from transcriptomic data as a process upregulated by gliotoxin exposure.

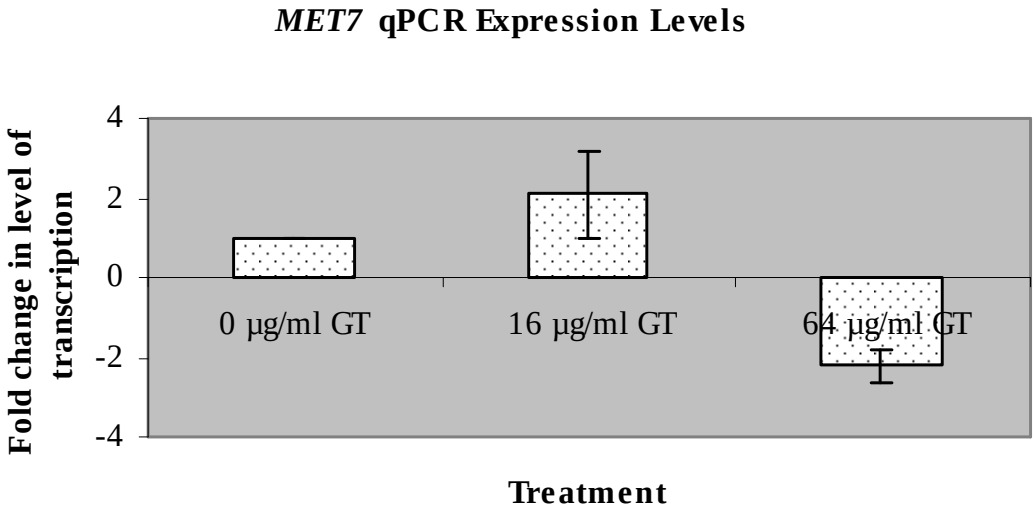

Figure 3.62 Fold changes in the level of transcription of *MET7* in response to 16 and 64 µg/ml gliotoxin exposure.

In figure 3.62 it can be observed that when cells are exposed to 16 µg/ml gliotoxin, there is a 2.095-fold increase in the level of transcription of *MET7*. However under exposure to 64 µg/ml gliotoxin, the cellular *MET7* RNA level decreases to 0.4524 of the level seen without gliotoxin exposure. This is equivalent to a 2.2-fold decrease in the level of transcription.

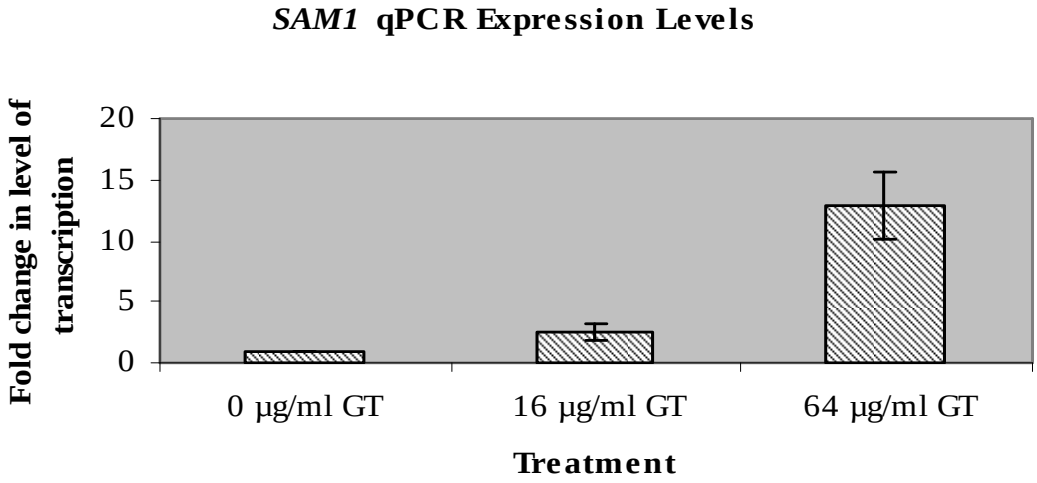

Figure 3.63 Fold changes in the level of transcription of *SAM1* in response to 16 and 64 µg/ml gliotoxin exposure.

It can be seen in the figure above that under 16 µg/ml gliotoxin exposure, the transcription level of *SAM1* increases 2.595-fold. Under an exposure concentration of 64 µg/ml, there is an increase to 12.94-fold observed in wild-type.

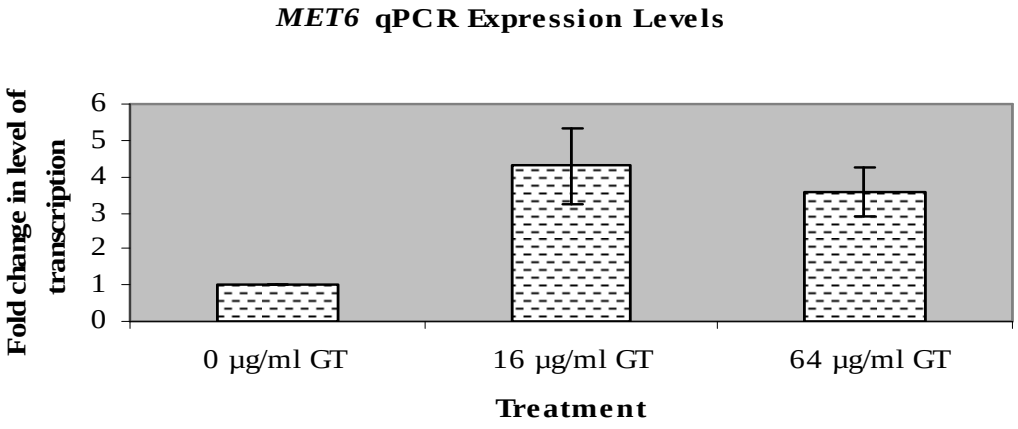

Figure 3.64 Fold changes in the level of transcription of *MET6* in response to 16 and 64 µg/ml gliotoxin exposure.

The transcription level of *MET6* increases significantly in the presence of both concentrations of the metabolite under investigation. There is a 4.284-fold increase at the lower concentration of gliotoxin and a 3.587-fold increase at the higher concentration, as illustrated by figure 3.64.

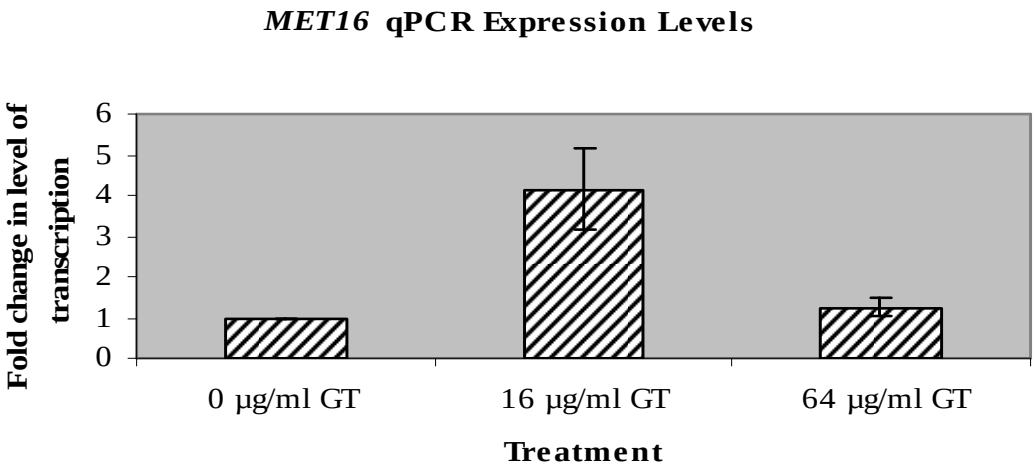

Figure 3.65 Fold changes in the level of transcription of *MET16* in response to 16 and 64 µg/ml gliotoxin exposure.

Figure 3.65 presents the upregulation of *MET16* when cells are treated with gliotoxin. In the presence of 16 µg/ml and 64 µg/ml gliotoxin, the transcription level of *MET16* increases 4.158-fold and 1.238-fold respectively.

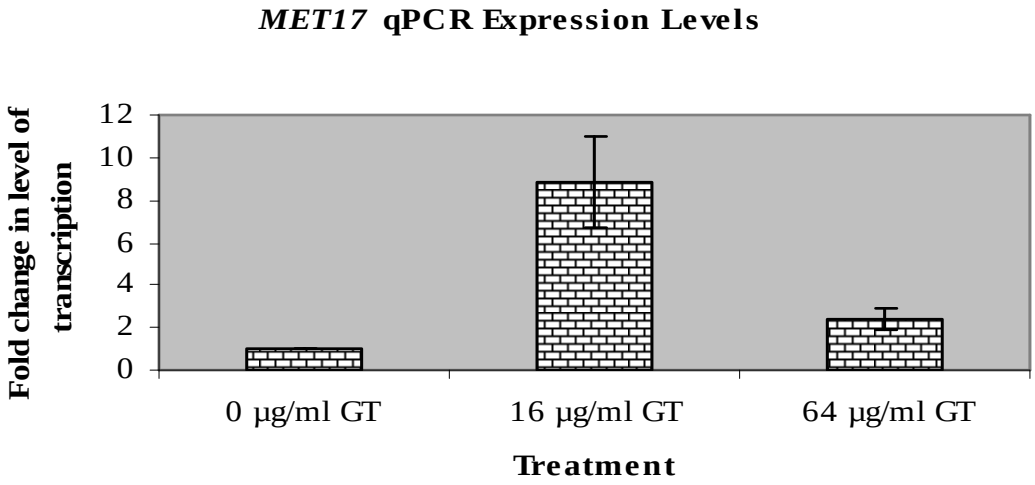

Figure 3.66 Fold changes in the level of transcription of *MET17* in response to 16 and 64 µg/ml gliotoxin exposure.

It can be seen above that there is an 8.808-fold increase in *MET17* transcription under the lower gliotoxin concentration and an increase of 2.387-fold under the higher concentration.

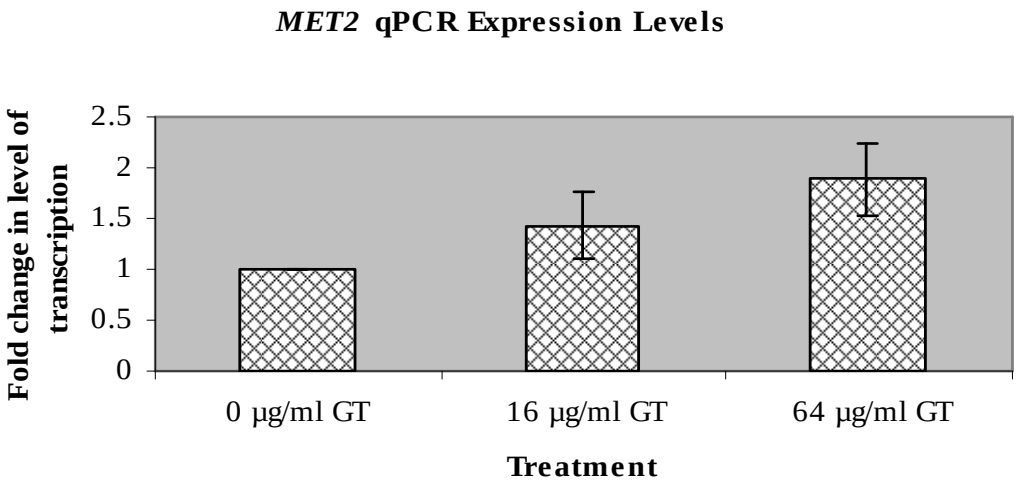

Figure 3.67 Fold changes in the level of transcription of *MET2* in response to 16 and 64 µg/ml gliotoxin exposure.

When cells are exposed to 16 µg/ml gliotoxin, the level of *MET2* transcription increases 1.434-fold and under 64 µg/ml exposure, 1.886-fold. This data is presented in the above figure.

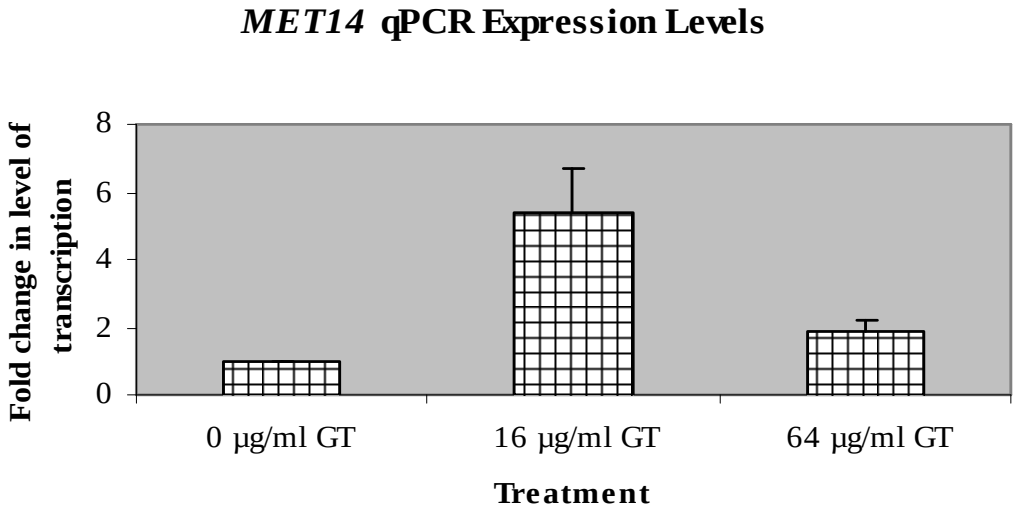

Figure 3.68 Fold changes in the level of transcription of *MET14* in response to 16 and 64 µg/ml gliotoxin exposure.

Figure 3.68 depicts that under 16 and 64 µg/ml gliotoxin, *MET14* is transcribed at levels 5.398- and 1.886-fold higher than normal respectively.

These results, presented in figures 3.62-3.68 demonstrate that gliotoxin does indeed induce a general increase in transcription of many genes involved in the sulfur amino acid biosynthesis pathway. A comparison of RNA sequencing data and qPCR data is depicted in figure 3.69. All changes are documented as fold-change.

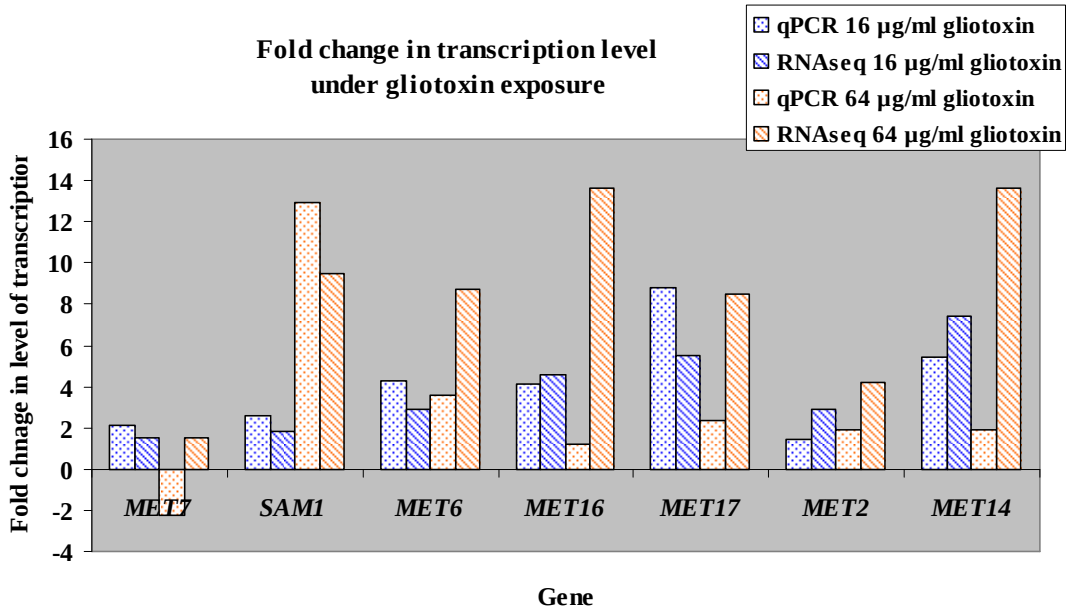

Figure 3.69 Fold change in transcription of sulfur amino acid biosynthesis genes under gliotoxin exposure documented from RNA sequencing and qPCR. Blue pattern represents 16 µg/ml and orange represents 64 µg/ml.

The above figure shows that both the RNA sequencing data and qPCR data support one another. The two methods of analysis demonstrate the upregulation of genes involved in sulfur amino acid biosynthesis. Discrepancy in the degree of upregulation is likely to be due to complications linked to a high level of cell death, particularly in the presence of 64 µg/ml gliotoxin.

In addition to the sulfur amino acid biosynthesis genes, advanced relative quantification PCR was also carried out on some genes found to be highly up- and downregulated transcriptionally under gliotoxin exposure. Figures 3.70-3.71 illustrate

the comparison of transcription of genes identified from transcriptomic data as being upregulated by gliotoxin exposure.

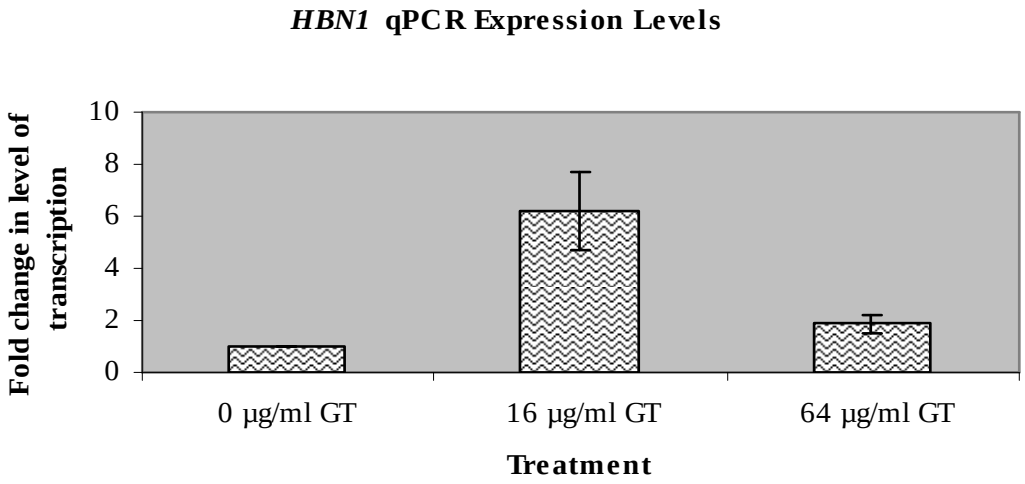

Figure 3.70 Fold changes in the level of transcription of *HBN1* in response to 16 and 64 µg/ml gliotoxin exposure.

HBN1 was selected for qPCR as it was identified from RNA sequencing data as a gene that is highly upregulated in response to gliotoxin exposure. qPCR illustrated this gene to be upregulated 6.212-fold in the presence of the lower toxin concentration and 1.886-fold in the presence of the higher.

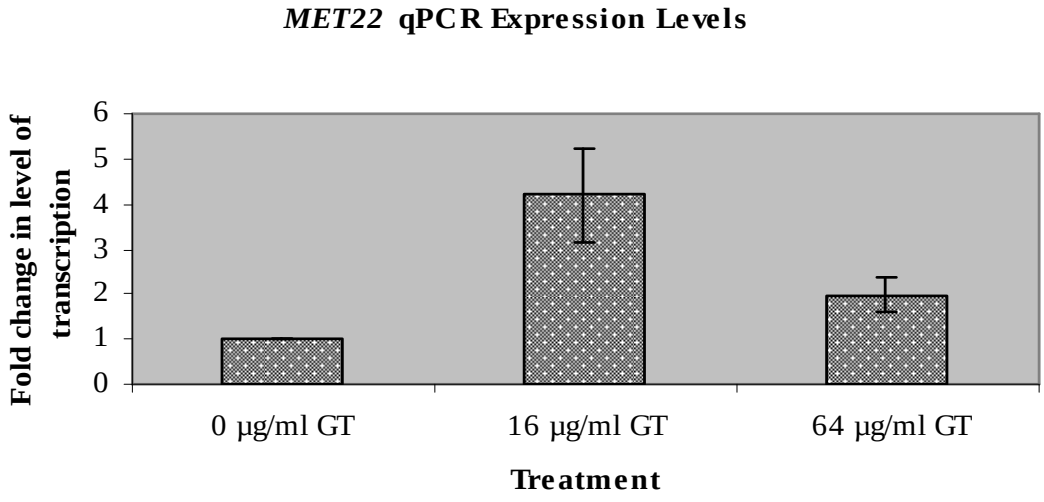

Figure 3.71 Fold changes in the level of transcription of *MET22* in response to 16 and 64 µg/ml gliotoxin exposure.

Relative analysis was carried out on *MET22* due to its involvement in sulfur amino acid biosynthesis regulation. qPCR results showed that it undergoes a 4.213- and 1.986-fold increase in transcription under exposure to 16 and 64 µg/ml gliotoxin respectively, this is shown in the above figure.

Again, we graphically presented qPCR and RNA sequencing data together in order to make an accurate comparison. This is depicted in figure 3.72, and good correlation is seen again.

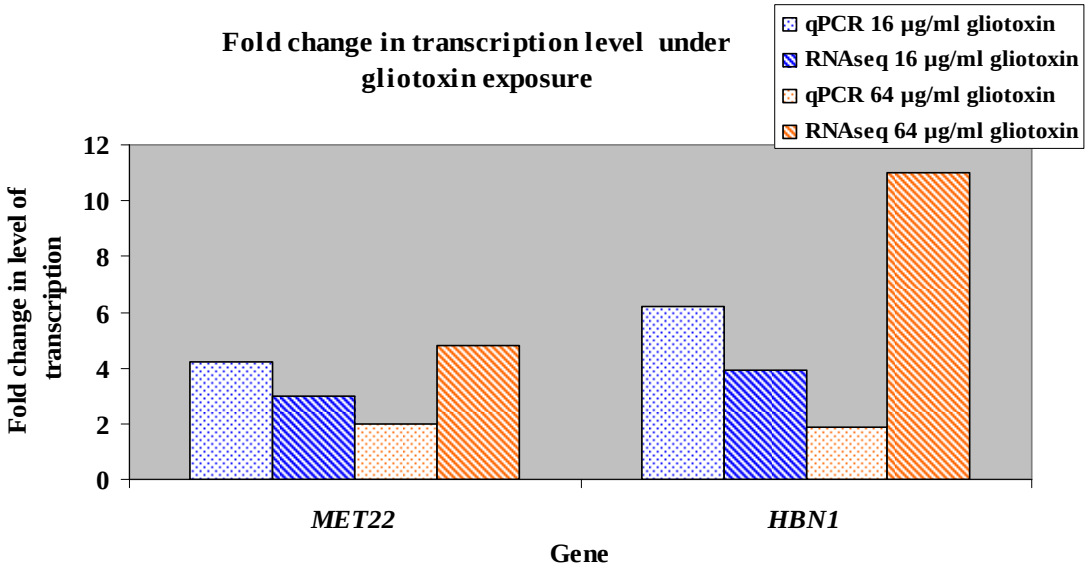

Figure 3.72 Fold change in transcription of *MET22* and *HBN1* under gliotoxin exposure documented from RNA sequencing and qPCR. Blue pattern represents 16 µg/ml and orange represents 64 µg/ml.

Figures 3.73-3.77 illustrate the comparison of transcription of genes identified from transcriptomic data as being downregulated by gliotoxin exposure.

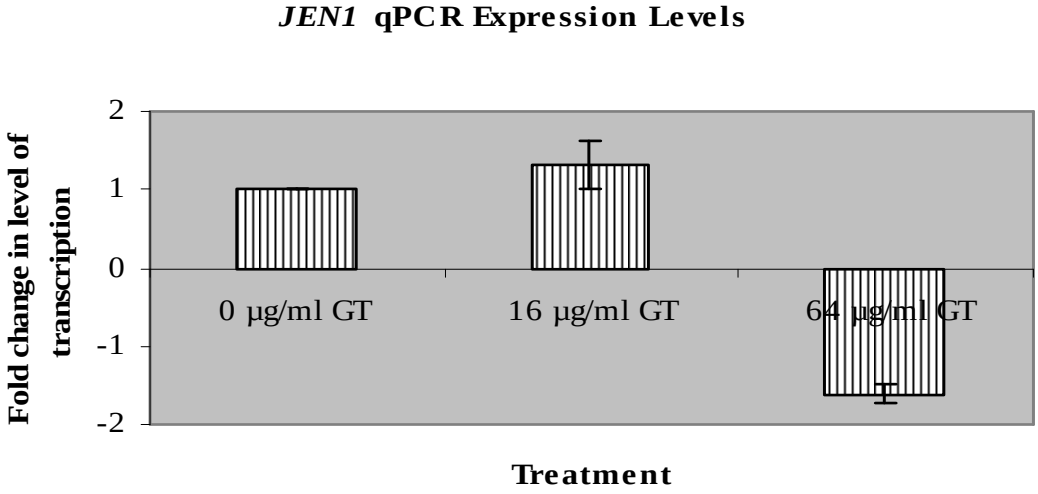

Figure 3.73 Fold changes in the level of transcription of *JEN1* in response to 16 and 64 µg/ml gliotoxin exposure.

The qPCR data reflected an 1.302-fold increase in the transcription of *JEN1* in response to 16 µg/ml gliotoxin and a 1.609-fold decrease in response to 64 µg/ml gliotoxin exposure.

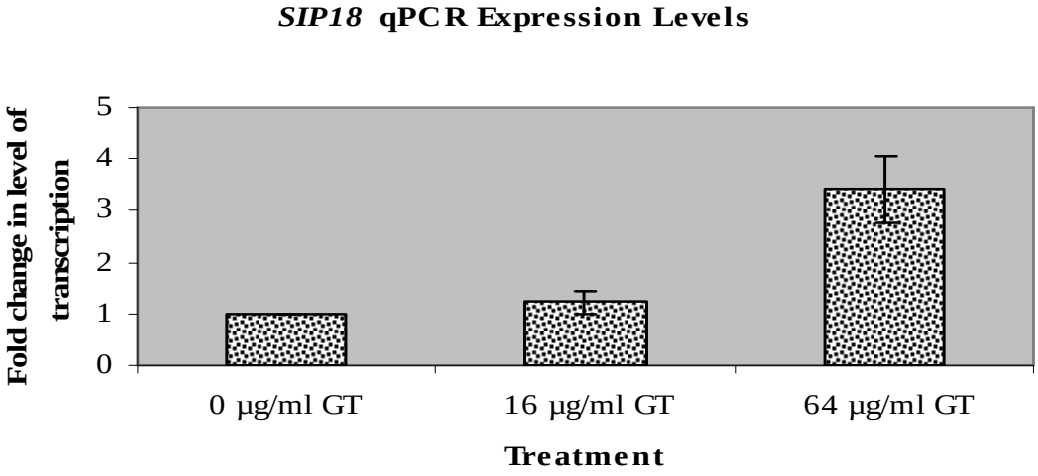

Figure 3.74 Fold changes in the level of transcription of *SIP18* in response to 16 and 64 µg/ml gliotoxin exposure.

In the above figure, it can be seen that the *SIP18* transcription level documented from qPCR does not correlate with that of the RNA sequencing analysis. qPCR depicted 1.219- and 3.437-fold increases in *SIP18* transcription in response to 16 and 64 µg/ml gliotoxin respectively.

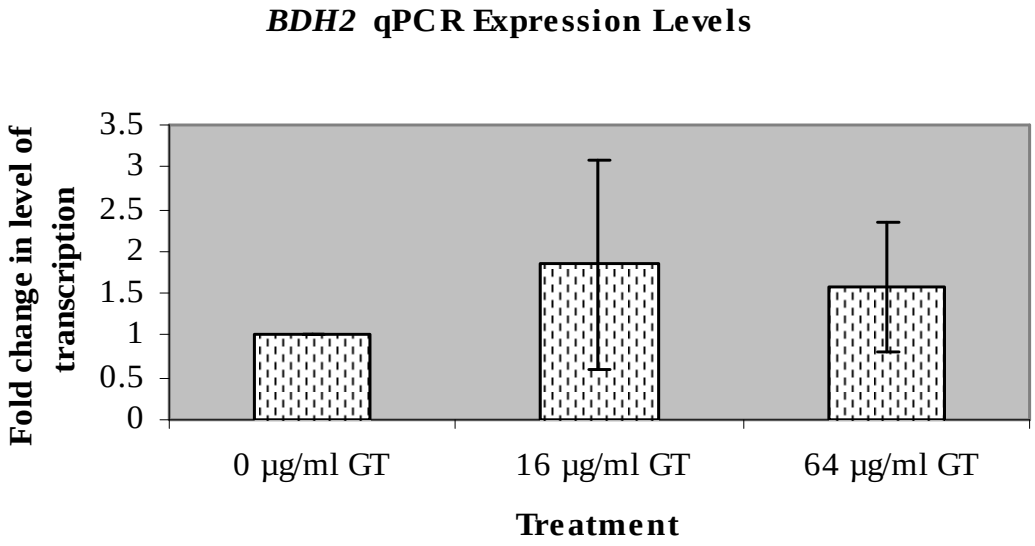

Figure 3.75 Fold changes in the level of transcription of *BDH2* in response to 16 and 64 µg/ml gliotoxin exposure.

The *BDH2* qPCR data from also contradicted transcriptome data as increases in transcription of 1.851- and 1.574-fold were seen in the presence of lower and higher gliotoxin levels respectively.

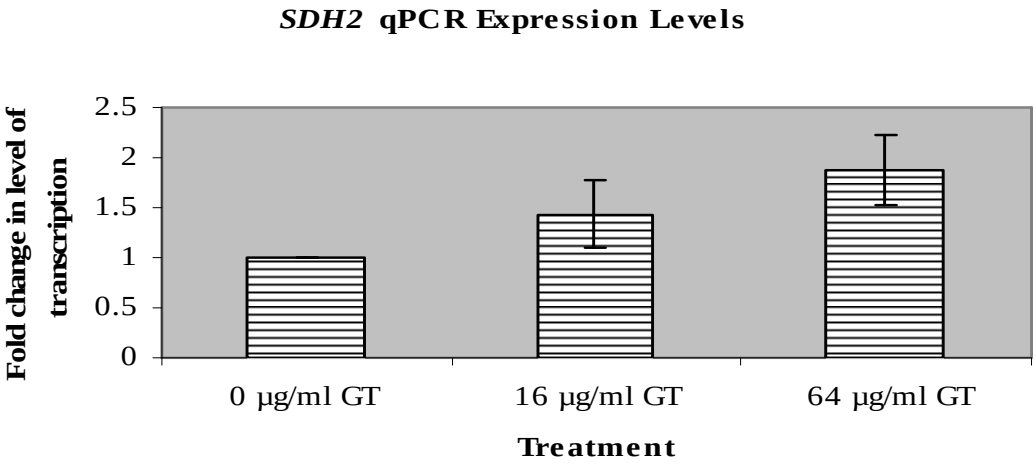

Figure 3.76 Fold changes in the level of transcription of *SDH2* in response to 16 and 64 µg/ml gliotoxin exposure.

Similar discrepancies in results from the two methods of analysis were observed for *SDH2*. *SDH2* qPCR demonstrated a 1.428-fold increase in transcription in the presence of 16 µg/ml gliotoxin and 1.886-fold in the under 64 µg/ml exposure.

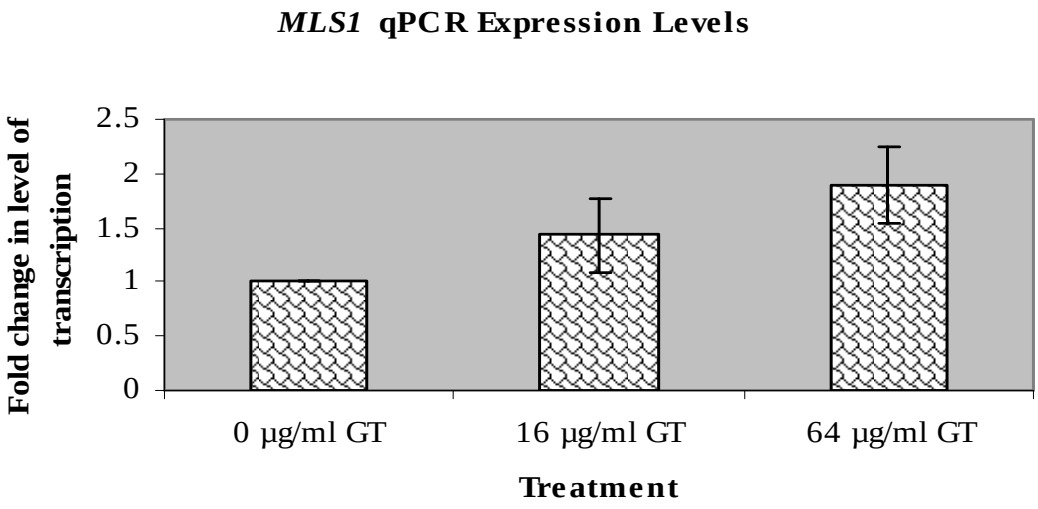

Figure 3.77 Fold changes in the level of transcription of *MLS1* in response to 16 and 64 µg/ml gliotoxin exposure.

As was seen for the other genes in this category, *MLS1* qPCR illustrated an unexpected increase in transcription of 1.428- and 1.886-fold under 16 and 64 µg/ml gliotoxin exposure respectively.

Figure 3.78 shows the comparison of the two modes of analysis and their respective results. These genes were analysed based on the fact that RNA sequencing data determined them to be downregulated in response to gliotoxin exposure. However, *JEN1*, *SIP18*, *BDH2*, *SDH2* and *MLS1* were shown to be upregulated under gliotoxin exposure by qPCR, thus a lack of correlation was seen in the assessment of these genes.

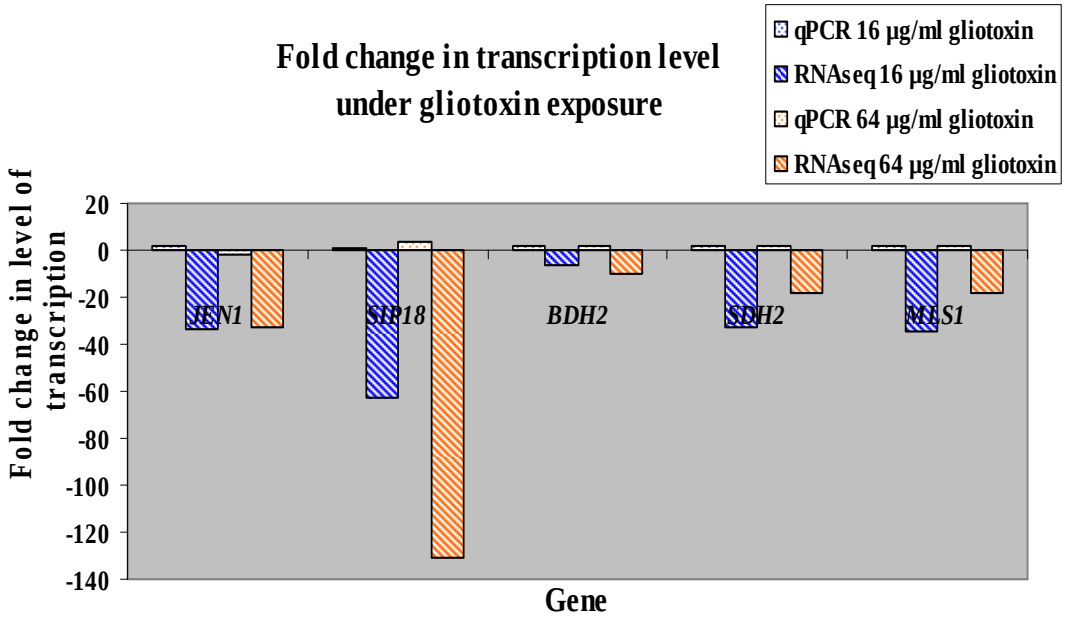

Figure 3.78 Comparison of expression levels of *JEN1*, *SIP18*, *BDH2*, *SDH2* and *MLS1* in response to gliotoxin exposure using data from RNA sequencing and qPCR. Blue pattern represents 16 µg/ml and orange represents 64 µg/ml.

3.6.2 Using proteomics to explore the mechanism of action of gliotoxin

We employed two-dimensional gel electrophoresis to explore the global proteomic yeast response to gliotoxin. Wild-type G600 yeast were cultured and exposed to gliotoxin at concentrations of 0, 16 and 64 µg/ml (as for transcriptome analysis) for 1 hr. before lysates were extracted. Proteins were precipitated using trichloroacetic acid (TCA), quantified and were isoelectrically focused on 24 cm, pH 3-10 IPG strips. After focusing, protein was separated based on weight by gel electrophoresis, followed by colloidal coomassie staining and Progenesis^{TM} same spot software analysis. This programme identified protein spots showing alterations in expression levels under different gliotoxin treatments. Protein from cells exposed to 0 and 16 µg/ml gliotoxin were compared and those exposed to 0 and 64 µg/ml. Subsequent to this, protein spots of interest were excised and Liquid Chromatography Mass Spectrometry (LC-MS) was used to identify proteins extracted. This process allowed us to examine the overall response to gliotoxin initiated by yeast via the production of specific proteins.

3.6.2.1 Analysis of the effect of 16 µg/ml gliotoxin exposure on global protein expression in yeast cells

Separated proteins isolated from cells that were exposed to 16 µg/ml gliotoxin were compared to wild-type proteins using Progenesis^{TM} same spot software. 500 µg of protein was analysed for each sample in duplicate. 29 protein spots were identified based on their differential expression level induced by exposure to 16 µg/ml gliotoxin. Figure 3.79 illustrates the pattern of peptide spots typically seen on one of the gels containing two-dimensionally separated proteins. Circled spots are proteins identified as differentially expressed, either up- or downregulated in response to 16 µg/ml gliotoxin exposure.

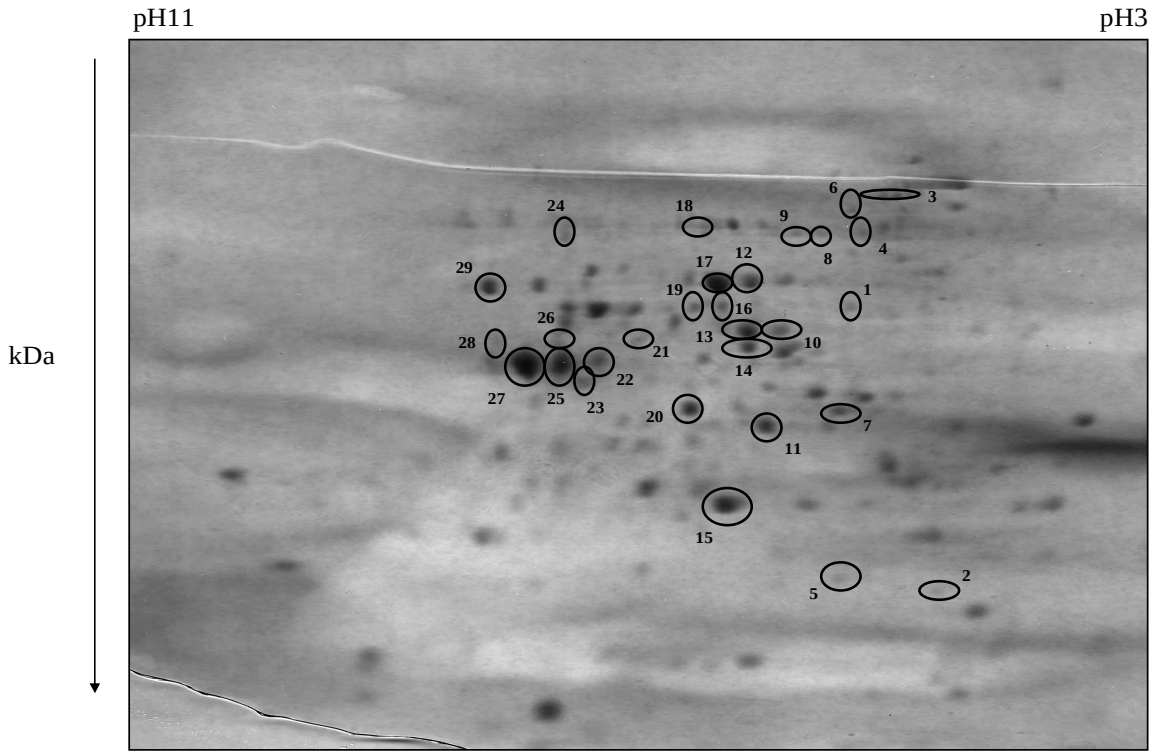

Figure 3.79 2-D gel electrophoresis separated proteins from G600 cells. Spots circled represent proteins that undergo an increase or decrease in level of expression in response to 16 µg/ml gliotoxin exposure.

The protein spots circled were then excised from the above gel, prepared as described in section 2.27, and sequenced using LC-MS. Mascot search engine was subsequently used to identify these yeast proteins, percentage coverage was calculated and identity

scores were assigned. Table 3.18 outlines details relating to the expression of the proteins of interest and compares results to transcriptome data analysed previously.

From table 3.18 it can be seen that yeast global proteomic responses generally correlate well with data obtained from transcriptome analysis. Of significant note, Cys3p and Cys4p were expressed more than 2-fold higher than normal when cells were treated with 16 µg/ml gliotoxin. Under the same treatment, the genes *CYS3* and *CYS4* that encode these proteins were found to be upregulated 4.1- and 1.6-fold. Not only were the sulfur amino acid and closely linked glutathione biosynthesis pathways discovered to be upregulated at both the RNA and protein level, the same was ascertained for the glucose fermentation pathway. In response to the lower level of gliotoxin used, Fba1p was increased 2.7-fold and transcriptionally 1.7-fold. Tdh1p was upregulated at the protein and RNA level 3-fold and 1.9-fold respectively. Mascot identified three upregulated proteins as Tdh3p isoforms. Taking the average value representing an increase in Tdh3p expression, it can be said that this protein is upregulated 2.5-fold under exposure to 16 µg/ml gliotoxin and 2.7-fold from transcriptomic reports. Additionally, three different upregulated proteins were identified as Pgk1p isoforms. For this protein, the average increase was seen to be 2.2-fold and this correlated with the RNA sequencing result which showed a 2.5-fold increase. Eight proteins were identified by Mascot as being Eno2p protein, of which seven were upregulated. Of these seven the average fold increase was 3. In support of this result, the *ENO2* gene was transcriptionally upregulated 2.6-fold in response to the lower concentration of gliotoxin used.

Table 3.18 Yeast proteins identified as undergoing an increase or decrease in expression under 16 µg/ml gliotoxin exposure.

Spot No.	Protein Name	Fold Change	Change	PI Value	Molecular Mass (Da)	Peptides Matched	Mascot Score	Coverage (%)	Protein Function	RNA seq Results
1	Ssb2	1.6	Up-	5.37	66668	11 (2)	558	24	Cytoplasmic ATPase that is a ribosome-associated molecular chaperone, functions with J-protein partner Zuo1p; may be involved in the folding of newly-synthesized polypeptide chains; member of the HSP70 family; homolog of SSB1	Upregulated
2	Eno2	3	Down-	5.67	46942	6 (0)	273	7	Enolase II, a phosphopyruvate hydratase that catalyzes the conversion of 2-phosphoglycerate to phosphoenolpyruvate during glycolysis and the reverse reaction during gluconeogenesis; expression is induced in response to glucose	Upregulated
3	Ssb1	3.6	Up-	5.32	66732	19 (5)	983	44	Cytoplasmic ATPase that is a ribosome-associated molecular chaperone, functions with J-protein partner Zuo1p; may be involved in folding of newly-made polypeptide chains; member of the HSP70 family; interacts with phosphatase subunit Reg1p	Upregulated
4	Ssa2	2	Up-	4.95	69599	12 (2)	436	16	ATP binding protein involved in protein folding and vacuolar import of proteins; member of heat shock protein 70 (HSP70) family; associated with the chaperonin-containing T-complex; present in the cytoplasm, vacuolar membrane and cell wall	Upregulated
5	Ssb1	1.7	Down-	5.32	66561	2 (0)	112	4	Cytoplasmic ATPase that is a ribosome-associated molecular chaperone, functions with J-protein partner Zuo1p; may be involved in folding of newly-made polypeptide chains; member of the HSP70 family; interacts with phosphatase subunit Reg1p	Upregulated

6	Ald6	4.2	Up-	5.31	54779	6 (1)	297	14	Cytosolic aldehyde dehydrogenase, activated by Mg2+ and utilizes NADP+ as the preferred coenzyme; required for conversion of acetaldehyde to acetate; constitutively expressed; locates to the mitochondrial outer surface upon oxidative stress	Upregulated
7	Rhr2	2.8	Up-	5.35	28100	5 (1)	247	22	Constitutively expressed isoform of DL-glycerol-3-phosphatase; involved in glycerol biosynthesis, induced in response to both anaerobic and, along with the Hor2p/Gpp2p isoform, osmotic stress	Upregulated
8	Pdc1	2.4	Up-	5.8	61689	5(1)	279	15	Major of three pyruvate decarboxylase isozymes, key enzyme in alcoholic fermentation, decarboxylates pyruvate to acetaldehyde; subject to glucose-, ethanol-, and autoregulation; involved in amino acid catabolism	Upregulated
9	Pdc1	2.9	Up-	5.74	46909	4 (2)	234	9	Major of three pyruvate decarboxylase isozymes, key enzyme in alcoholic fermentation, decarboxylates pyruvate to acetaldehyde; subject to glucose-, ethanol-, and autoregulation; involved in amino acid catabolism	Upregulated
10	Fba1	2.7	Up-	5.51	39881	4 (0)	199	9	Fructose 1,6-bisphosphate aldolase, required for glycolysis and gluconeogenesis; catalyzes conversion of fructose 1,6 bisphosphate to glyceraldehyde-3-P and dihydroxyacetone-P; locates to mitochondrial outer surface upon oxidative stress	Upregulated
11	Asc1	2.6	Up-	5.8	34898	5 (1)	268	16	G-protein beta subunit and guanine nucleotide dissociation inhibitor for Gpa2p; ortholog of RACK1 that inhibits translation; core component of the small (40S) ribosomal subunit; represses Gcn4p in the absence of amino acid starvation	Upregulated

12	Eno2	2.8	Up-	5.67	46942	13 (3)	697	26	Enolase II, a phosphopyruvate hydratase that catalyzes the conversion of 2-phosphoglycerate to phosphoenolpyruvate during glycolysis and the reverse reaction during gluconeogenesis; expression is induced in response to glucose	Upregulated
13	Eno2	3.3	Up-	5.67	46942	4(2)	224	7	Enolase II, a phosphopyruvate hydratase that catalyzes the conversion of 2-phosphoglycerate to phosphoenolpyruvate during glycolysis and the reverse reaction during gluconeogenesis; expression is induced in response to glucose	Upregulated
14	Eno2	3.2	Up-	5.67	46942	4(2)	224	7	Enolase II, a phosphopyruvate hydratase that catalyzes the conversion of 2-phosphoglycerate to phosphoenolpyruvate during glycolysis and the reverse reaction during gluconeogenesis; expression is induced in response to glucose	Upregulated
15	Eno2	2.3	Up-	5.67	40942	8 (0)	384	13	Enolase II, a phosphopyruvate hydratase that catalyzes the conversion of 2-phosphoglycerate to phosphoenolpyruvate during glycolysis and the reverse reaction during gluconeogenesis; expression is induced in response to glucose	Upregulated
16	Rps3	2.2	Up-	9.42	26543	2 (1)	120	16	Protein component of the small (40S) ribosomal subunit, has apurinic/apyrimidinic (AP) endonuclease activity; essential for viability; has similarity to E. coli S3 and rat S3 ribosomal proteins	Upregulated
17	Eno2	3.7	Up-	5.67	46942	47 (10)	1145	46	Enolase II, a phosphopyruvate hydratase that catalyzes the conversion of 2-phosphoglycerate to phosphoenolpyruvate during glycolysis and the reverse reaction during gluconeogenesis; expression is induced in response to glucose	Upregulated

18	Eno2	3	Up-	5.67	46942	11(4)	356	20	Enolase II, a phosphopyruvate hydratase that catalyzes the conversion of 2-phosphoglycerate to phosphoenolpyruvate during glycolysis and the reverse reaction during gluconeogenesis; expression is induced in response to glucose	Upregulated
19	Eno2	3	Up-	5.67	46942	12 (2)	396	16	Enolase II, a phosphopyruvate hydratase that catalyzes the conversion of 2-phosphoglycerate to phosphoenolpyruvate during glycolysis and the reverse reaction during gluconeogenesis; expression is induced in response to glucose	Upregulated
20	Tdh3	2	Up-	6.46	35838	6 (0)	205	17	Glyceraldehyde-3-phosphate dehydrogenase, isozyme 3, involved in glycolysis and gluconeogenesis; tetramer that catalyzes the reaction of glyceraldehyde-3-phosphate to 1,3 bis-phosphoglycerate; detected in the cytoplasm and cell wall	Upregulated
21	Cys3	2.4	Up-	6.06	42516	2 (0)	95	5	Cystathionine gamma-lyase, catalyzes one of the two reactions involved in the transsulfuration pathway that yields cysteine from homocysteine with the intermediary formation of cystathionine	Upregulated
22	Tdh3	2.6	Up-	6.46	35838	3 (0)	78	5	Glyceraldehyde-3-phosphate dehydrogenase, isozyme 3, involved in glycolysis and gluconeogenesis; tetramer that catalyzes the reaction of glyceraldehyde-3-phosphate to 1,3 bis-phosphoglycerate; detected in the cytoplasm and cell wall	Upregulated
23	Pgk1	2.2	Up-	7.11	44768	4 (0)	203	9	3-phosphoglycerate kinase, catalyzes transfer of high-energy phosphoryl groups from the acyl phosphate of 1,3-bisphosphoglycerate to ADP to produce ATP; key enzyme in glycolysis and gluconeogenesis	Upregulated

24	Cys4	2.6	Up-	6.25	56074	6 (1)	271	10	Cystathionine beta-synthase, catalyzes synthesis of cystathionine from serine and homocysteine, the first committed step in cysteine biosynthesis; responsible for hydrogen sulfide generation; mutations in human ortholog cause homocystinuria	Upregulated
25	Tdh1	3	Up-	6.25	35825	4 (0)	131	11	Involved in superpathway of glucose fermentation	Upregulated
26	Ilv5	2.2	Up-	9.06	44585	1 (1)	75	2	Bifunctional acetohydroxyacid reductoisomerase and mtDNA binding protein; involved in branched-chain amino acid biosynthesis and maintenance of wild-type mitochondrial DNA; found in mitochondrial nucleoids	Upregulated
27	Tdh3	2.9	Up-	6.46	35838	17(0)	496	26	Glyceraldehyde-3-phosphate dehydrogenase, isozyme 3, involved in glycolysis and gluconeogenesis; tetramer that catalyzes the reaction of glyceraldehyde-3-phosphate to 1,3 bis-phosphoglycerate; detected in the cytoplasm and cell wall	Upregulated
28	Pgk1	1.5	Up-	8	44595	9(0)	314	22	3-phosphoglycerate kinase, catalyzes transfer of high-energy phosphoryl groups from the acyl phosphate of 1,3-bisphosphoglycerate to ADP to produce ATP; key enzyme in glycolysis and gluconeogenesis	Upregulated
29	Pgk1	3	Up-	7.11	44768	15 (0)	530	25	3-phosphoglycerate kinase, catalyzes transfer of high-energy phosphoryl groups from the acyl phosphate of 1,3-bisphosphoglycerate to ADP to produce ATP; key enzyme in glycolysis and gluconeogenesis	Upregulated

Two proteins were found to be isoforms of Pdc1p, for which the average increase was 2.7-fold. The gene encoding this protein underwent a 3.2-fold increase in transcription. Finally, *ALD6* was transcriptionally increased 1.1-fold in response to 16 µg/ml gliotoxin while the Ald6p it encodes was upregulated 4.2-fold.

Only two of the twenty-nine proteins of interest underwent a decrease in expression in response to the lower concentration of gliotoxin, these were identified to be Eno2p and Ssb1p. The Eno2p downregulatory result is probably due to a flaw in identification or inaccuracy in the technique, as Eno2p was largely recorded as being upregulated (described above). Ssb1p is one member of a class of cytosolic heat-shock proteins, Ssb proteins, that associate with ribosome-bound nascent polypeptides and appear to be involved in correct folding of the protein upon emergence from the ribosome (Craig *et al.*, 1993, Gautschi *et al.*, 2002, Kim and Craig, 2005). Our finding outlining the downregulation of this protein could be indicative of an increase in yeast cell death under gliotoxin exposure. It may be the case that cells cannot carry out normal functions to the full extent and protein folding may be one of the processes negatively effected. However, another protein was also identified as an Ssb1p isoform, and this was shown to undergo 3.6-fold upregulation. This second Ssb1p result is more in line with RNA sequencing data which reports *SSB1* to be upregulated 2.9-fold under 16 µg/ml gliotoxin exposure. Two-dimensional gel analysis exposed a change in the level of another Ssb protein, Ssb2p in the presence of the lower concentration of gliotoxin. Ssb2p is 99% identical to Ssb1p (Craig and Jacobsen, 1985, Craig *et al.*, 1993) and was found to undergo a 1.6-fold increase in expression in response to the toxin. This correlates with the RNA sequencing data which shows the *SSB2* gene encoding this protein to be upregulated 2.7-fold. Ssa and Ssb proteins are part of the Hsp70p family, a 70 kDA cytosolic protein family which is one of the major molecular chaperone groups (Ingolia *et al.*, 1982, Werner-Washburne *et al.*, 1987, Craig *et al.*,

1993). We found that Ssa2p, one of the four Ssa subfamily members, was increased 2-fold in response to 16 µg/ml gliotoxin treatment and was transcriptomically elevated 2.5-fold. Although Ssa and Ssb proteins are part of the Hsp70 protein family, they are functionally divergent in many repects, one paramount example being the absolute requirement for at least one Ssa protein for cell viability (Werner-Washburne *et al.*, 1987, Nelson *et al.*, 1992, Chernoff *et al.*, 1999). It may be the case that the lower concentration of gliotoxin used enhances both Hsp70 RNA and protein production. Another protein found undergo a change in level of expression here was Rhr2p, also known as Gpp1p, which is involved in glycerol biosynthesis (Norbeck *et al.*, 1996). Absence of *RHR2* has previously been shown to result in increased sensitivity to OS (Pahl *et al.*, 1996, Pahlman *et al.*, 2001, Wei *et al.*, 2009). We found that in response to 16 µg/ml gliotoxin, Rhr2p is expressed 2.8-fold more and is transcriptionally upregulated 2.7-fold. Upregulation of *RHR2* and Rhr2p could be indicative of gliotoxin causing cellular OS. As shown in section 3.6.1.1 and clearly depicted in table 3.5, from the RNA sequencing data the upregulation of many genes encoding ribosomal subunits was observed. The proteomic analysis data here demonstrates the 2.6- and 2.2-fold increases in expression of Asc1p and Rps3p respectively. These are both protein components of the small ribosomal subunit (Planta and Mager, 1998, Baum *et al.*, 2004) and we found that the *ASC1* and *RPS3* genes encoding these proteins undergo increases in transcription of 3.6- and 3.2-fold respectively. This supports the observations made from the transcriptomic data, whereby it appears the cells attempt to develop more ribosomes when treated with 16 µg/ml gliotoxin. Interstingly, Asc1p is also known to be involved in the glucose signalling pathway (Zeller *et al.*, 2007), which may in turn be a key intermediate in the upregulation of the glucose fermentation pathway aforementioned. The final protein which was found to have altered expression in response to this concentration of gliotoxin was Ilv5p. This highly-expressed protein is

involved in isoleucine and valine biosynthesis and also plays an important role in maintaining mitochondrial genome stability (Petersen and Holmberg, 1986, Zelenaya-Troitskaya *et al.*, 1995). We found that Ilv5p and *ILV5* were upregulated 2.2-fold and 1.7-fold respectively. Gliotoxin is known to cause DNA damage (Eichner *et al.*, 1988), perhaps the increase in production of this protein combats the effects of gliotoxin as cells attempt to maintain internal stability.

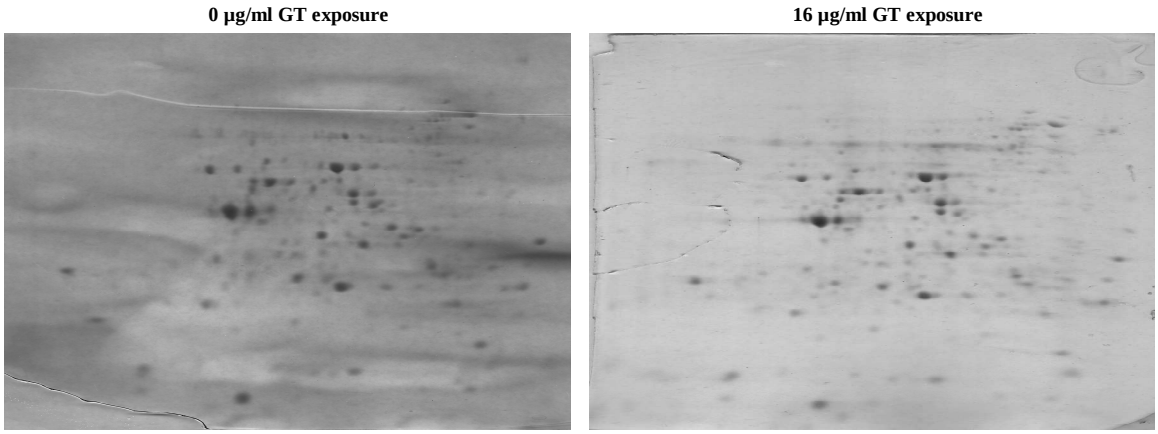

Figure 3.80 Comparison of gels containing separated proteins from cells exposed to 0 and 16 µg/ml gliotoxin.

The gels above contain two-dimensionally separated proteins from cells exposed to 0 and 16 µg/ml gliotoxin. Differential protein expression represents the yeast global proteomic response to this gliotoxin concentration.

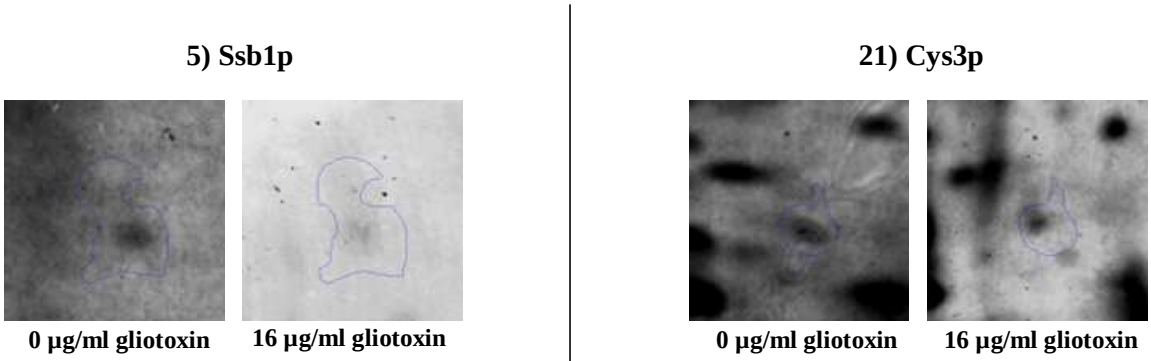

Figure 3.81 Representation of one protein that underwent a decrease in expression, Ssb1p (l) and one that underwent an increase in expression, Cys3p (r), in the presence of 16 µg/ml gliotoxin.

Figure 3.81 shows an example of one down- and one upregulated protein. It is clear that for Ssb1p, the protein spot on the left is more intense than that on the right, illustrating

downregulation of the protein in the presence of 16 µg/ml gliotoxin. Cys3p is visibly more intense in the protein spot in the right as it undergoes an increase in expression under the same gliotoxin exposure concentration.

3.6.2.2 Analysis of the effect of 64 µg/ml gliotoxin exposure on global protein expression in yeast cells

Separated proteins from cells that were treated with 64 µg/ml gliotoxin were compared to wild-type expressed proteins using Progenesis^{TM} same spot software. 350 µg of protein was analysed for each sample in triplicate. 22 protein spots were identified based on their different levels of expression when cells were exposed to 64 µg/ml gliotoxin. Figure 3.82 illustrates the typical pattern of protein spots on one of the gels containing two-dimensionally separated proteins. As before, the circled proteins are those which were found to have alterations in intensity level when comparing proteins from the two treatment cultures. This demonstrated that these proteins underwent a change in levels of expression when cells were exposed to 64 µ/ml gliotoxin.

The circled protein spots were excised from the gel. Peptides were retrieved, trypsin digested and underwent LC-MS and Mascot analysis, leading to identification of the yeast proteins of interest. Of these 22 differentially expressed proteins, 15 were upregulated and 7 were downregulated. These proteins, along with their descriptions are listed in table table 3.19. Included in this table is comparison of proteomic alterations with that documented by transcriptomics.

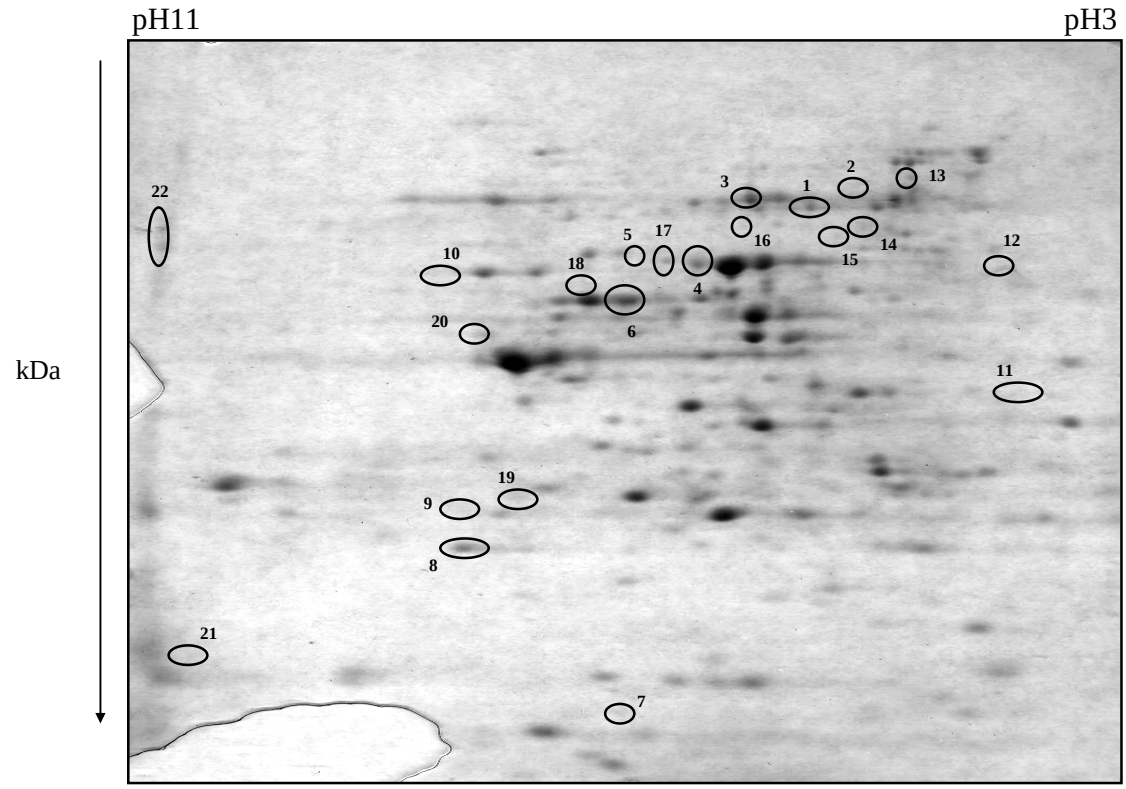

Figure 3.82 Separated proteins from G600 cells. Spots circled represent proteins that undergo an increase or decrease in level of expression in response to 64 µg/ml gliotoxin exposure.

The data outlined in the table below also concurs to some degree with the RNA sequencing analysis. With reference to the sulfur amino acid and glutathione biosynthesis pathways, the upregulation in response to 64 µg/ml gliotoxin of both Cys4p and Met17p was detected at the RNA and protein level. *CYS3* underwent a 3.8-fold increase in transcription and a 1.5-fold increase in protein expression. *MET17* was upregulated 8.5-fold and the protein it encodes 1.8-fold.

As was found with proteomic and RNA sequencing data for cells exposed to 16 µg/ml gliotoxin, some genes and proteins involved in the glucose fermentation pathway also underwent an increase in expression in response to 64 µg/ml gliotoxin exposure. Three proteins were identified as upregulated Pdc1p and the average fold increase for these was 1.6. The gene *PDC1* encoding this protein was documented in transcriptome data as being upregulated 1.9-fold.

Table 3.19 Yeast proteins identified as undergoing an increase or decrease in expression under 64 µg/ml gliotoxin exposure.

Spot No.	Protein Name	Fold Change	Change	PI Value	Molecular Mass (Da)	Peptides Matched	Mascot Score	Coverage (%)	Protein Function	RNA seq Results
1	Pdc1	1.6	Up-	5.8	61689	14(2)	602	28	Major of three pyruvate decarboxylase isozymes, key enzyme in alcoholic fermentation, decarboxylates pyruvate to acetaldehyde; subject to glucose-, ethanol-, and autoregulation; involved in amino acid catabolism	Upregulated
2	Ecm10	1.6	Up-	5.9	70042	4(1)	69	8	Heat shock protein of the Hsp70 family, localized in mitochondrial nucleoids, plays a role in protein translocation, interacts with Mge1p in an ATP-dependent manner; overexpression induces extensive mitochondrial DNA aggregations	Downregulated
3	Pdc1	1.5	Up-	5.8	61689	17(3)	771	34	Major of three pyruvate decarboxylase isozymes, key enzyme in alcoholic fermentation, decarboxylates pyruvate to acetaldehyde; subject to glucose-, ethanol-, and autoregulation; involved in amino acid catabolism	Upregulated
4	Eno2	1.5	Up-	5.67	46943	5(3)	297	13	Enolase II, a phosphopyruvate hydratase that catalyzes the conversion of 2-phosphoglycerate to phosphoenolpyruvate during glycolysis and the reverse reaction during gluconeogenesis; expression is induced in response to glucose	Upregulated
5	Rph1	4.3	Up-	9.1	71516	4(0)	32	4	JmjC domain-containing histone demethylase which can specifically demethylate H3K36 tri- and dimethyl modification states; transcriptional repressor of PHR1; Rph1p phosphorylation during DNA damage is under control of the MEC1-RAD53 pathway	Downregulated
6	Adh1	1.3	Down-	6.21	37290	3(0)	108	6	Alcohol dehydrogenase, fermentative isozyme active as homo- or heterotetramers; required for the reduction of acetaldehyde to ethanol, the last step in the glycolytic pathway	Upregulated
7	Pgk1	1.3	Down-	7.8	23238	2(0)	99	10	3-phosphoglycerate kinase, catalyzes transfer of high-energy phosphoryl groups from the acyl phosphate of 1,3-bisphosphoglycerate to ADP to produce ATP; key enzyme in glycolysis and gluconeogenesis	Upregulated
8	Tdh3	2.1	Down-	6.46	35840	4(0)	168	8	Glyceraldehyde-3-phosphate dehydrogenase, isozyme 3, involved in glycolysis and gluconeogenesis; tetramer that catalyzes the reaction of glyceraldehyde-3-phosphate to 1,3 bis-phosphoglycerate; detected in the cytoplasm and cell wall	Upregulated

9	Ilv5	1.9	Down-	9.1	44515	2(0)	122	5	Bifunctional acetohydroxyacid reductoisomerase and mtDNA binding protein; involved in branched-chain amino acid biosynthesis and maintenance of wild-type mitochondrial DNA; found in mitochondrial nucleoids	Upregulated
10	Pgk1	1.6	Up-	7.1	44769	9(2)	62	13	3-phosphoglycerate kinase, catalyzes transfer of high-energy phosphoryl groups from the acyl phosphate of 1,3-bisphosphoglycerate to ADP to produce ATP; key enzyme in glycolysis and gluconeogenesis	Upregulated
11	Rps0ap	1.7	Up-	4.65	28065	2(0)	77	5	Protein component of the small (40S) ribosomal subunit, nearly identical to Rps0Bp; required for maturation of 18S rRNA along with Rps0Bp; deletion of either RPS0 gene reduces growth rate, deletion of both genes is lethal	Upregulated
12	SceI	1.9	Up-	5.41	70757	3(0)	140	7	I-SceI DNA endonuclease, encoded by the mitochondrial group I intron of the 21S_rRNA gene; mediates gene conversion that propagates the intron into intron-less copies of the 21S_rRNA gene	N/A
13	Wtm1	1.9	Up-	5.18	48469	4(1)	214	17	Transcriptional modulator involved in regulation of meiosis, silencing, and expression of RNR genes; required for nuclear localization of the ribonucleotide reductase small subunit Rnr2p and Rnr4p; contains WD repeats	Downregulated
14	Ssa1	1.6	Up-	5.5	42014	4(1)	78	11	ATPase involved in protein folding and nuclear localization signal (NLS)-directed nuclear transport; member of heat shock protein 70 (HSP70) family; forms a chaperone complex with Ydj1p; localized to the nucleus, cytoplasm, and cell wall	Upregulated
15	Pdc1	1.6	Up-	5.8	60384	4(1)	268	13	Enzyme in alcoholic fermentation, decarboxylates pyruvate to acetaldehyde, regulation is glucose- and ethanol-dependent	Upregulated
16	Cys4	1.5	Up-	6.25	56045	2(1)	138	6	Cystathionine beta-synthase, catalyzes synthesis of cystathionine from serine and homocysteine, the first committed step in cysteine biosynthesis; responsible for hydrogen sulfide generation; mutations in human ortholog cause homocystinuria	Upregulated
17	Eno2	2	Up-	5.67	46943	3(2)	220	12	Enolase II, a phosphopyruvate hydratase that catalyzes the conversion of 2-phosphoglycerate to phosphoenolpyruvate during glycolysis and the reverse reaction during gluconeogenesis; expression is induced in response to glucose	Upregulated
18	Met17	1.8	Up-	5.97	48700	1(1)	81	3	Methionine and cysteine synthase (O-acetyl homoserine-O-acetyl serine sulfhydrylase), required for sulfur amino acid synthesis	Upregulated

19	Rhr2	1.7	Down-	5.24	28103	2(0)	97	9	Constitutively expressed isoform of DL-glycerol-3-phosphatase; involved in glycerol biosynthesis, induced in response to both anaerobic and, along with the Hor2p/Gpp2p isoform, osmotic stress	Upregulated
20	Pgk1	1.3	Down-	7.11	44769	13(4)	93	22	3-phosphoglycerate kinase, catalyzes transfer of high-energy phosphoryl groups from the acyl phosphate of 1,3-bisphosphoglycerate to ADP to produce ATP; key enzyme in glycolysis and gluconeogenesis	Upregulated
21	Eno2	1.7	Up-	5.67	46943	1(1)	83	4	Enolase II, a phosphopyruvate hydratase that catalyzes the conversion of 2-phosphoglycerate to phosphoenolpyruvate during glycolysis and the reverse reaction during gluconeogenesis; expression is induced in response to glucose	Upregulated
22	Tef2	1.4	Down-	9.1	50407	5(2)	90	8	Translational elongation factor EF-1 alpha; also encoded by TEF1; functions in the binding reaction of aminoacyl-tRNA (AA-tRNA) to ribosomes; may also have a role in tRNA re-export from the nucleus	Upregulated

Eno2p identity was assigned to three proteins, all of which were upregulated. The average fold increase was calculated to be 1.7, which corresponded with the 3.4-fold transcriptional increase reported for *ENO2* gene.

In contrast, the Tdh3 proteomic and transcriptomic responses contradicted one another. Tdh3p was found to be 2.1-fold downregulated under 64 µg/ml gliotoxin exposure, while the *TDH3* gene was upregulated 2.2-fold more than normal. A similar scenario was noted for Pgk1p. Three proteins were determined to be Pgk1p. Two of these were observed as downregulated and one as upregulated. If the majority result was taken, it could be said that this protein undergoes an average 1.3-fold decrease in expression in response to the higher toxin concentration. However, this would then dispute the transcriptome data which recorded a 2.2-fold increase in the *PGK1* gene. There were also conflicting results for the alcohol dehydrogenase Adh1p. The protein was reported by Progenesis™ as being 1.3-fold downregulated while the gene *ADH1* gene encoding the protein was found in the RNA sequencing data to be transcriptionally upregulated 3-fold. These last three results are indicative of the fact that there is an added complication with analysis of effects of the higher concentration of gliotoxin, due to the high level of cell death that occurs. Rhr2p was discovered to be downregulated in response to the higher level of gliotoxin, while previously it was upregulated under exposure to the lower gliotoxin concentration. Transcriptionally, the *RHR2* gene was upregulated 3.2-fold in response to 64 µg/ml gliotoxin exposure. In section 3.6.2.1, the increase in Hsp70 genes and proteins was discussed. When cells were exposed to the toxin at 64 µg/ml, two Hsp70 proteins underwent an increase in expression, Ecm10p and Ssa1p. The former, unlike the cytosolic Ssa1p, is a mitochondrial Hsp70 protein (Baumann *et al.*, 2000) and was increased 1.6-fold proteomically. RNA sequencing analysis did record an accurate expression value for *ECM1*. In cells exposed to the higher gliotoxin concentration, Ssa1p was upregulated 1.6-fold and the *SSA1*

transcription level remained relatively stable. Thus when cells are cultured in the presence of 64 µg/ml, Hsp70 proteins are not induced to the extent as seen under 16 µg/ml exposure. Rph1p was identified as the protein which underwent the highest fold change here, it was upregulated 4.3-fold. However, it was transcriptionally downregulated 1.1-fold. Rph1p is involved in the regulation of the stress response (Jang *et al.*, 1999), so perhaps transcriptional downregulation is again indicative of cell death, while the increase in production of Rph1p is part of the response to the damaging effects of gliotoxin. Alternatively, the downregulation of *RPH1* could be a mode of negative feedback due to the already hightened levels of the protein encoded by the gene. In the comparative analysis of these gels, Ilv5p was, like before, discovered to undergo a change in expression, although this time it was seen to be downregulated 1.9-fold. Trancriptionally, *ILV5* only underwent a 1.2-fold upregulation under the higher concentration of gliotoxin. Only one ribosomal protein was expressed to a higher degree in the presence of 64 µg/ml gliotioxin, Rps0ap was elevated 1.7-fold and *RPS0A* was upregulated 1.8-fold. Another protein with enhanced expression found in this study was SceIp. Although no transcriptome data was obtained for the *SCEI* gene, the protein it encodes, an endonuclease that facilitates intron propagation (Dujon, 1989, Perrin *et al.*, 1993) was proteomically upregulated 1.9-fold. Like SceIp, Wtm1p was found at a level 1.9-fold higher than in unexposed cells, however, it was transcriptionally downregulated 1.1-fold. This protein is involved in transcriptional repression, particularly of a meiosis-specific gene and it also induces amplification of a gene important in the DNA damage response (Bowdish and Mitchell, 1993, Pemberton and Blobel, 1997, Tringe *et al.*, 2006). Thus, the elevated expression of this protein may be in response to genotoxic stress caused by gliotoxin. In the presence of 64 µg/ml gliotoxin, Tef2p, translation elongation factor EF-1α (Schirmaier and Philippsen, 1984) was one of the seven

proteins found to be produced at a reduced rate. It was downregulated 1.4-fold, although contrastingly, the transcription of *TEF2* was increased 1.9-fold.

Figure 3.83 exemplifies gels containing separated proteins from cells that were not exposed to gliotoxin and cells that were exposed to 64 µg/ml gliotoxin.

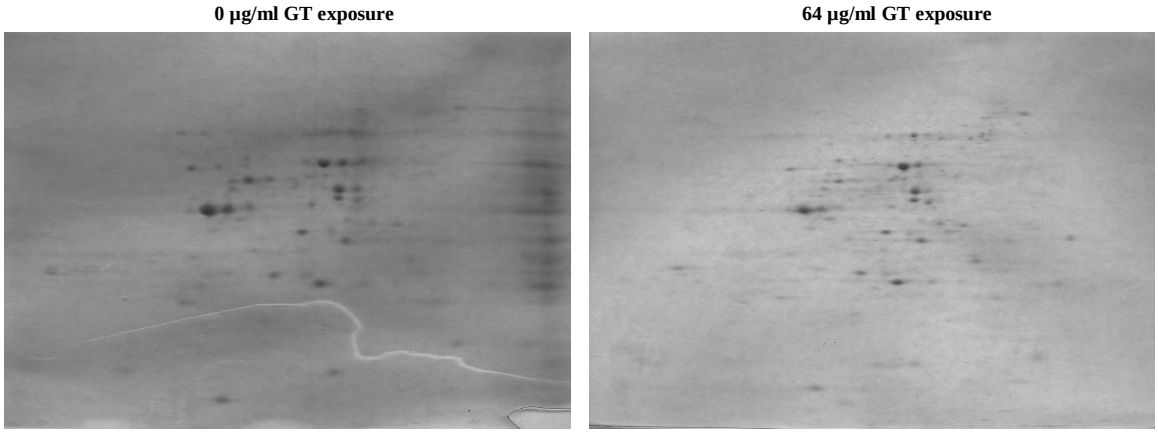

Figure 3.83 Comparison of gels containing separated proteins from cells exposed to 0 and 64 µg/ml gliotoxin.

In figure 3.84, one protein that underwent an increase in expression and one which was upregulated are shown. On the left of the figure there is a sharp decrease in intensity of Tdh3p under 64 µg/ml gliotoxin exposure, in comparison the control.
In contrast, the Pgk1p is visibly more intense in the presence of the higher concentration of gliotoxin.

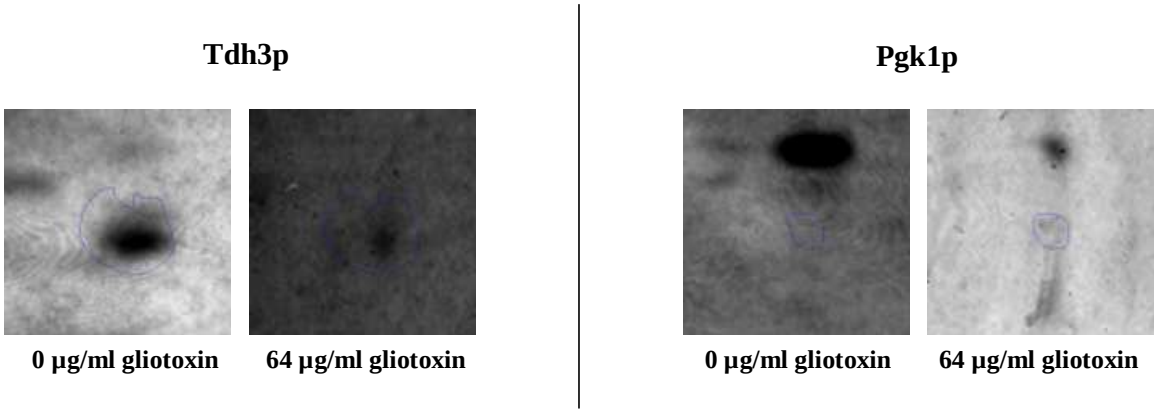

Figure 3.84 Representation of one protein that underwent a decrease in expression, Tdh3p (l) and one that underwent an increase in expression, Pgk1p (r), in the presence of 64 µg/ml gliotoxin.

3.7 Genetic analysis of genes identified as differentially expressed in response to gliotoxin

A number of genes and proteins were found to be differentially expressed in response to gliotoxin exposure, as described above. Further to this, we applied functional genetics and phenotypic analyses to assess our findings. Based on data obtained from global response analyses, it appears that the induction of sulfur amino acid and glutathione biosynthesis pathways is elevated when cells are exposed to gliotoxin. This suggests that these pathways are key processes employed by yeast to protect against the gliotoxin.

3.7.1 Assessment of growth response to gliotoxin of yeast cells deleted for genes involved in sulfur amino acid biosynthesis

We hypothesised that the importance of the sulfur amino acid biosynthesis pathway in resistance to gliotoxin would be reflected in the growth ability of sulfur mutants. Comparative growth analysis was carried out using wild-type BY4741 in combination with the isogenic Δ*met6*, Δ*met17*, Δ*cys4* and Δ*sam1* mutants, lacking genes involved in the said pathway. These strains were phenotypically compared under 0 and 8 µg/ml gliotoxin exposure, depicted in figure 3.85.

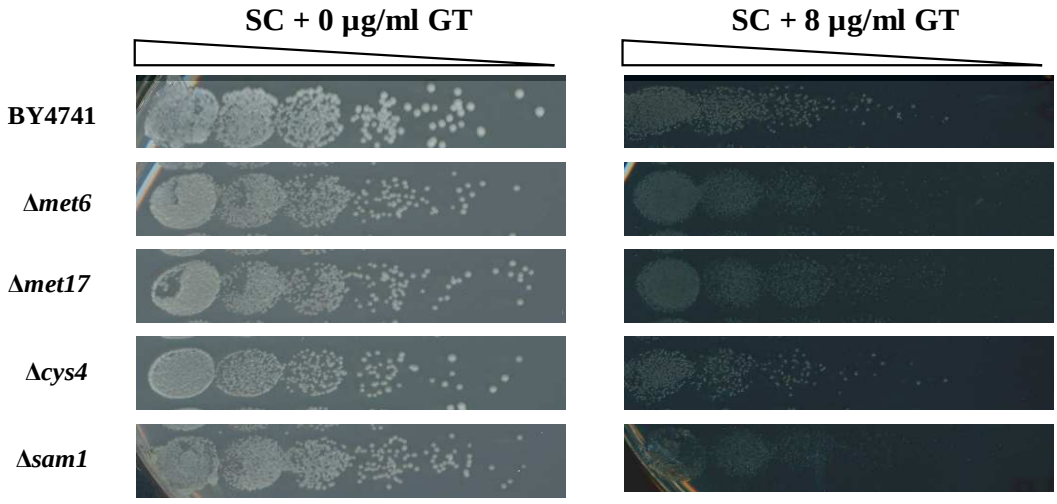

Figure 3.85 Comparative growth analysis of BY4741, Δ*met6*, Δ*met17*, Δ*cys4*, and Δ*sam1* in the presence of 0 and 8 µg/ml gliotoxin. The above image represents cellular growth after 72 hr. incubation at 30ºC.

Repeated performance of this assay revealed no significant change in the level of growth in the absence of the above mentioned genes. This demonstrates that cells maintain the ability to survive like wild-type when single genes involved in the sulfur amino acid biosynthesis pathway are disrupted.

3.7.2 Investigating the role of the transsulfuration pathway in mediating gliotoxin effects in yeast

Results described in previous sections indicate the importance of the sulfur amino acid biosynthesis pathway, that contributes to glutathione biosynthesis, in response to effects incurred by gliotoxin. Figure 3.86 illustrates the role of transsulfuration in glutathione biosynthesis.

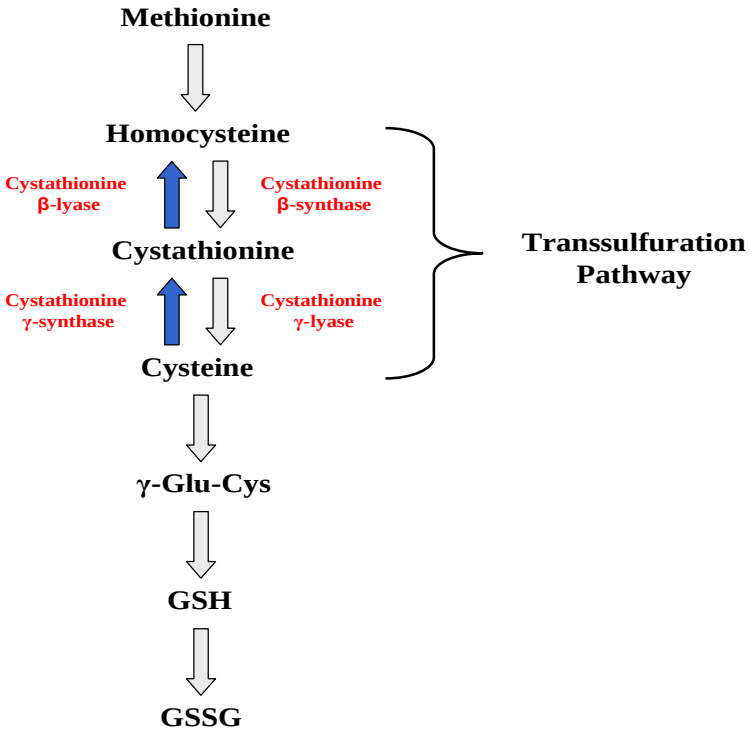

Figure 3.86 Representation of the importance of transsulfuration in glutathione biosynthesis.

Cystathionine β-synthase- and cystathionine γ-lyase-mediated conversion of homocysteine to cystathionine and subsequently to cysteine encompasses the

transsulfuration pathway (Ono *et al.*, 1984, Cherest *et al.*, 1993). As glutamate, glycine and cysteine form glutathione, homocysteine reserve pools and the emanating transsulfuration pathway are key in ensuing glutathione production (Finkelstein, 1998, Mosharov *et al.*, 2000). In fact, increasing cysteine levels has been shown to give rise to enhanced glutathione production, with the addition of ATP resulting in further elevated levels. (Alfafara *et al.*, 1992, Liang *et al.*, 2008, Nisamedtinov *et al.*, 2010). In response to gliotoxin, we have shown that *CYS3* and *CYS4* encoding cystathionine γ-lyase and cystathionine β-synthase respectively are upregulated at the RNA and protein levels.

We surmised that if the sulfur amino acid and resultant glutathione biosynthesis pathways play a pivotal role in protection against gliotoxin, primarily through the transsulfuration process, exogenous chemical modification of the pathway would affect resistance to the toxin. We also took into consideration the results described in section 3.3.2 where the Δ*gsh1* mutant displayed increased resistance to gliotoxin. In contrast, these results suggested that in the absence of γ-glutamylcysteine synthetase (*GSH1*) and consequential glutathione production, cells exhibit increased resistance to gliotoxin. Either way, we wanted to investigate the effects of exogenous chemical modification of the transsulfuration pathway. Cysteine could not be used in this assay due to the ability of gliotoxin to bind to this protein via its sulfhydral group (Pahl *et al.*, 1996, Bertling *et al.*, 2010) so alternatively, another intemermediate in glutathione biosynthesis was employed, cystathionine. Comparative growth analysis was carried out with strains grown under exposure to 12 µg/ml gliotoxin, alone and in combination with 50, 100, 250 and 350 µM cystathionine. For this assay, wild-type BY4741 and Δ*cys3* were utilised, and both containing the *GliT* gene under a constitutive promoter. Figure 3.87 illustrates the results from this analysis. It can be seen above that as before, *GliT* transformation confers an increase in gliotoxin resistance. The figure clearly

demonstrates that as the concentration of cystathionine increases, the ability of both BY4741 and Δ*cys3* to grow under gliotoxin exposure intensifies.

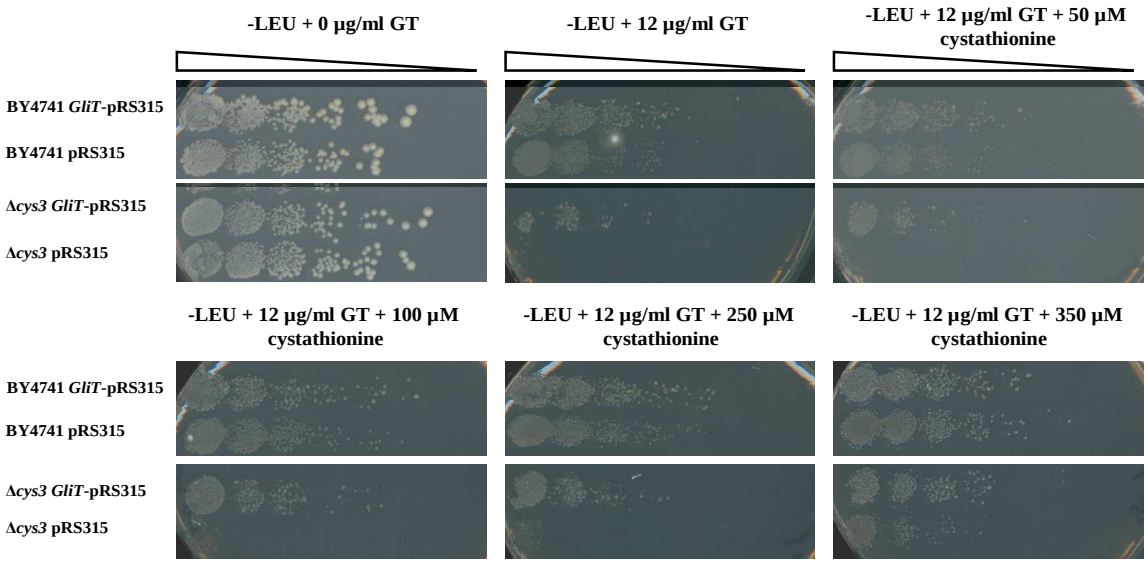

Figure 3.87 Comparative growth analysis of BY4741 and Δ*cys3*, with and without *GliT*, in the presence of gliotoxin and cystathionine. Plates were incubated at 30ºC for 72 hr.

In the presence of gliotoxin and 350 µM exogenous cystathionine, wild-type grows at the same rate as that constitutively expressing *GliT*. Under 12 µg/ml gliotoxin exposure, Δ*cys3* was completely inhibited, but was able to grow when constitutively expressing *GliT*. With the addition of 350 µM exogenous cystathionine, both strains grew considerably better. In general, an acceleration in the rate of growth correlates with the addition of exogenous cystathionine. These results demonstrate that through increased stimulation of the transsulfuration pathway, cells appear to be protected against the detrimental toxic effects of gliotoxin.

3.7.3 Assessment of the utility of *GPX2*, *HXT2*, *MET32* and *ALD6* in yeast survival in the presence of gliotoxin

Following global expression analysis, four genes were chosen for further evaluation, based on their biological roles and expression levels. To determine the importance of these genes in yeast resistance to gliotoxin, comparative growth analysis

was carried out on mutants deleted for these genes, under cellular exposure to the toxin at concentrations of 0 and 8 µg/ml. Expression of the glutathione peroxidase *GPX2* is Yap1p-controlled and is induced by OS. Its activity catalyses glutathione oxidation and reduction of hydroperoxides, such as H_2O_2, thus playing a role in cellular detoxification (Mills, 1957, Galiazzo *et al.*, 1987, Inoue *et al.*, 1999, Avery and Avery, 2001). Due to the strong functional link of *GPX2* with glutathione, a protein known to play a role in protection against OS, and its more than 6-fold increase in expression in response to 64 µg/ml gliotoxin, the Δ*gpx2* phenotype was examined. Additionally, Δ*hxt2* was phenotypically assessed. *HXT2* encodes a yeast hexose transporter induced by low glucose concentrations (Ozcan and Johnston, 1999) and the mutant lacking this gene was chosen due to the elevated level of *HXT2* transcription observed under cellular exposure to the higher level of gliotoxin used. *MET32* encodes a transcription factor involved in regulation of the sulfur amino acid biosynthesis pathway described previously (Blaiseau *et al.*, 1997) and BY4741 lacking the gene was thus selected for analysis. The importance *ALD6*, a gene which plays a role in glucose fermentation, described in section 3.6.1.4, was also explored via phenotypic analysis of the Δ*ald6* mutant.

Table 3.20 Fold increase in response to gliotoxin exposure of *GPX2*, *HXT2*, *MET32* and *ALD6*

Gene	Fold increase under exposure to 16 µg/ml gliotoxin	Fold increase under exposure to 64 µg/ml gliotoxin
GPX2	1.6	6.4
HXT2	1.7	8.8
MET32	1.6	2.9
ALD6	1.1	3.8

None of the four mutants described above showed a considerable differential growth rate when exposed to 8 µg/ml gliotoxin. However, it should be noted that there may be a possible reproducible growth defect seen for Δ*ald6*.

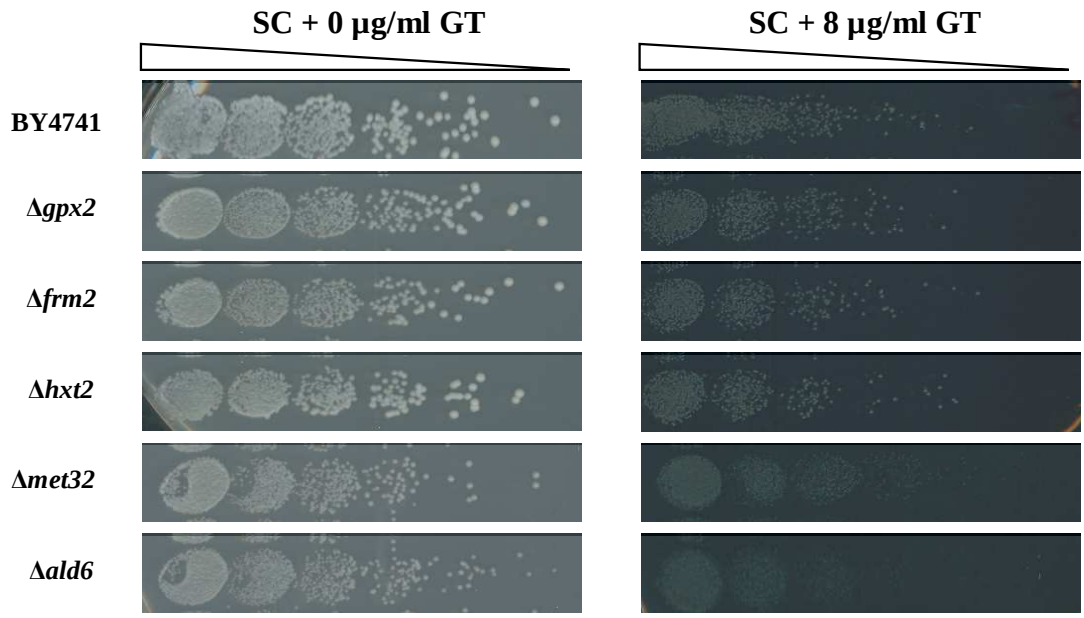

Figure 3.88 Comparative growth analysis of BY4741, Δ*gpx2*, Δ*hxt2*, Δ*met32* and Δ*ald6* in the presence of 0 and 8 µg/ml gliotoxin. The above image represents cellular growth after 72 hr. incubation at 30ºC.

3.7.4 Phenotypic analysis of Δ*hbn1*, Δ*frm2* and Δ*hbn1*Δ*frm2*

Two genes upregulated at the mRNA level on exposure to both 16 and 64 µg/ml gliotoxin were *HBN1* and *FRM2*. In response to 16 µg/ml gliotoxin exposure, *HBN1* and *FRM2* undergo 3.9- and 1.9-fold upregulation respectively. In the presence of 64 µg/ml gliotoxin, *HBN1* is upregulated 11-fold and *FRM2* 15.8-fold.

These two genes are known to genetically interact (de Oliveira *et al.*, 2010). De Oliveira *et al.* (2010) reported that Hbn1p and Frm2p, both putative nitroreductases, are involved in yeast cellular protection against OS and the absence of either or both *HBN1* and *FRM2* leads to altered levels of glutathione, superoxide dismutase, catalase and glutathione peroxidase. We therefore decided to carry out phenotypic analysis of Δ*hbn1*, Δ*frm2* and Δ*hbn1*Δ*frm2* in the presence of gliotoxin.

3.7.4.1 Creation of Δ*hbn1*mutant

The Δ*hbn1* strain was not available for purchase from Euroscarf and so was created in this study by homologous recombination. *HIS5*, plus its promoter and

terminator sequence was amplified from the pUG27 plasmid by PCR. Primers for this reaction were designed so that the amplicon contained regions at both 5' and 3' ends that were homologous to genomic *HBN1* flanking regions, as illustrated in figure 3.89.

AGACTGAAGTATCCTATATCAACATATATACAAAAAAACAATCCAATATC**A**
TGCAGCTGAAGCTTCG

TCTGCTGTTGCAACTTATTTGAAAACTTTAACTGCTCGTCGTACTATTTAC
GCTTTGAAACCGGAGTTACCTGGTGAAATTACTATCAACGACATCCAATC
CGTCGTCCAAACCATCATTAAAGAAACACCCACCGCTTTCAACTCCCAGC
CAAATCGCGCTGTTATCTTGACTGGTGAAACTCACAAAAAAGTTTGGGAC
GAAGTGACTAAGGCTATAGAAAGCCCTGCCGGTCAAAAGAGGCCTGCTT
CAGCAAGGGATGAGGCCTTTGGTTCTGTAATCTTCTTCACCGACGACAA
GGTAACTGAAAAGCTAAAGGCTGACTTCCCAGCGTACGCAGCTGCATTC
CCTAGTTTCGCGGACCATACCTCTGGTGCCGCTCAAATCAACTCGTGGG
TTGCCTTGGAGGCAATGGGCCTGGGTGGTCACCTACAACACTACAATGG
TTACATAAAAGCTGCTTTGCCAAGCAAAATCCCTGAGTCTTGGACCGTAC
AAGCTCAATTAGTCTTCGGTACCCCAGCCGCACCTCCAGGTGAAAAGAC
CTACATCAAAAACGATGTTGAAATCTTCAAT

CAGATCCACTAGTGGCCTATGC**TAA**GGAACAGTATATAAGTACAGAATT
ATAGGTATAGATTAAATGCGAACGTC

Figure 3.89 Primers used to obtain amplicon for *HBN1* replacement with *HIS5* by homologous recombination. Forward primer is underlined at the top of the figure. Reverse complement of reverse primer is underlined at the bottom of the figure. Black text represents *HBN1* and flanking sequence. Green text depicts regions of pUG27 up- and downstream of *HIS5*. Bold texts indicates start and stop codons of *HBN1* gene.

Transformation of the PCR product into BY4741 and selection on SC plates lacking histidine led to a number of colonies which potentially contained *HIS5* replacing *HBN1*. Genomic DNA was then extracted from a number of colonies and a diagnostic PCR was performed to determine whether *HBN1* had been deleted by homologous recombination replacement. Four different PCRs were set up for both the potential knockout under examination and a wild-type BY4741 control, as described in figure 3.90.

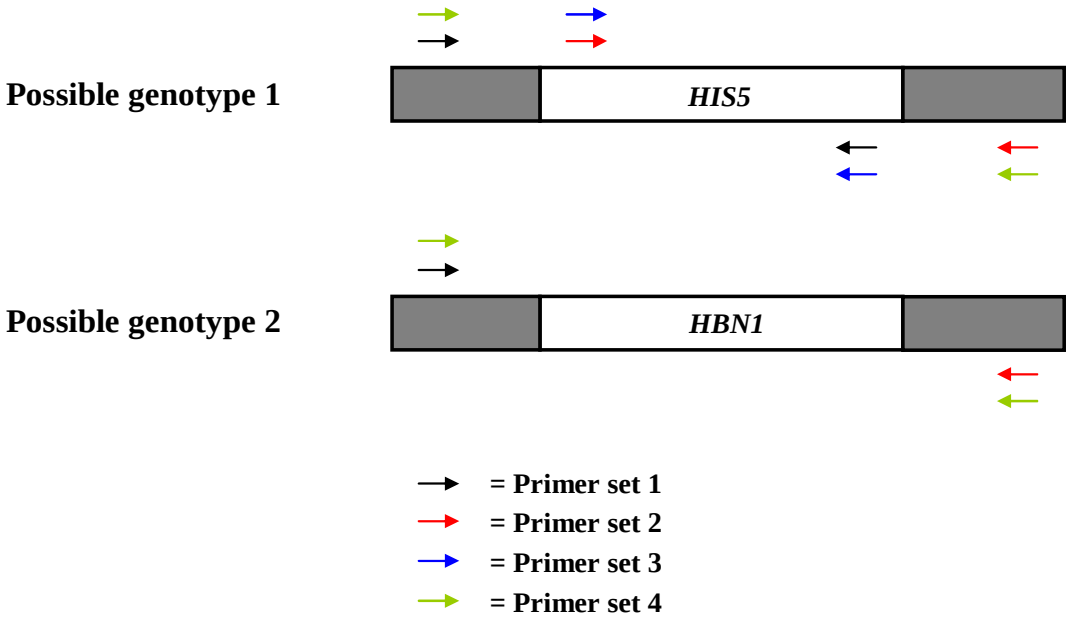

Figure 3.90 Four different primer sets used for diagnostic PCR and possible genotypes. The external forward primer binds 141 bp upstream of the wild-type *HBN1* start codon. The *HIS5* internal reverse primer binds 1,041 bp downstream of the beginning of the pUG27 region replacing *HBN1*. Use of these primers in combination (primer set 1) in PCR gives rise to a product of 1,182 bp. The external reverse primer binds 193 bp downstream of the natural *HBN1* stop codon. The *HIS5* internal forward binds 980 bp upstream from the end of the pUG27 region replacing *HBN1*. Use of these primers in combination (primer set 2) in PCR gives rise to a product of 1,173 bp.

For both the potential knockout and wild-type BY4741, PCRs were performed using the sets of primers illustrated above. The results of these reactions are depicted in figure 3.91. Lanes 1, 3, 5 and 7 represent PCRs using potential Δ*hbn1* genomic DNA and lanes 2, 4, 6 and 8 show PCRs using wild-type control DNA. In lane one, there is a product of 1,182 bp, resultant from use of primer set one. In the second lane, there is no product visible as only the external forward primer bound, there was no *HIS5* sequence for the reverse primer to anneal. Lane three presents the 1,182 bp product formed from PCR using primer set two. There is no product in the fourth lane as only the external reverse primer annealed to the DNA in the absence of *HIS5*. In lane five there can be seen a 567 bp product, produced by PCR using both the internal *HIS5* primers, primer set three. No product resulted from the PCR illustrated in lane six as there was no *HIS5* sequence to which either primer could bind. The *HBN1* open reading frame is 582 bp and the external forward and reverse primers anneal 141 and 193 bp up- and

downstream of this region respectively. Thus, a PCR using these primers, primer set four, gives rise to a 916 bp product, as is visible in lane eight. However, the *HIS5* region used is 1,454 bp, and *HBN1* replacement by this sequence gives rise to a 1,788 bp amplicon that can be observed in lane seven. Figure 3.91 confirms successful replacement of the *HBN1* gene with *HIS5*.

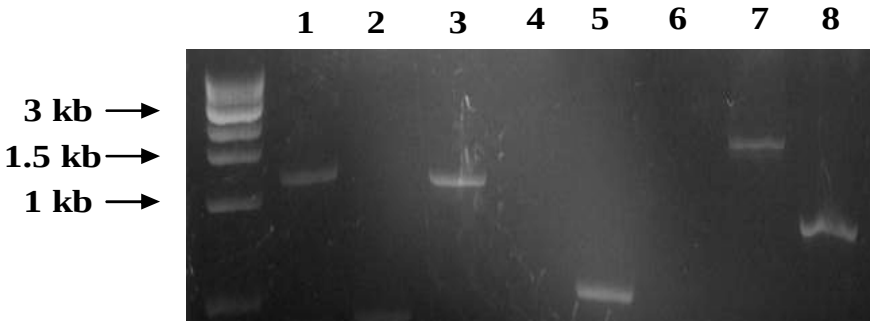

Figure 3.91 Diagnostic PCR products that underwent gel electrophoresis, illustrating *HBN1* knockout in BY4741 background. 1 = Δ*hbn1* primer set 1; 2 = WT primer set 1; 3 = Δ*hbn1* primer set 2; 4 = WT primer set 2; 5 = Δ*hbn1* primer set 3; 6 = WT primer set 3; 7 = Δ*hbn1* primer set 4; 8 = WT primer set 4.

3.7.4.2 Generation of Δ*hbn1*Δ*frm2* double knockout

BY4741 Δ*frm2* was purchased from Euroscarf. The double knockout Δ*hbn1*Δ*frm2* was created by amplification of the novel *HIS5* region in BY4741 Δ*hbn1* and transformation into competent BY4741 Δ*frm2* followed by selection on SC –his plates. This process gave rise to a number of colonies which were tested to determine whether or not *HBN1* had been deleted. Diagnostic PCRs were performed as before, using primer combinations described in figure 3.90 and the amplicons underwent gel electrophoresis, as shown in figure 3.92. The diagnostic PCRs demonstrated that *HBN1* had been replaced by *HIS5*. This was seen firstly by the fact that there are products in lanes 1, 3 and 5, of the anticipated sizes and there are no products yielded from the control reactions, in lanes 2, 4 and 6, due to the absence of *HIS5*. Additionally, between lanes seven and eight there is an 872 bp dicrepancy in sequence size amplified between

external primers. This represents the difference in the size of the *HBN1* open reading frame and the *HIS5* sequence replacing it in the confirmed knockout.

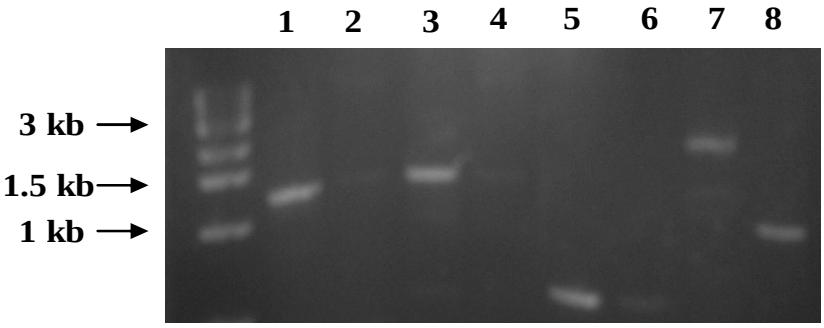

Figure 3.92 Diagnostic PCR products that underwent gel electrophoresis, illustrating *HBN1* knockout in BY4741 Δ*frm2* background. 1 = Δ*hbn1*Δ*frm2* primer set 1; 2 = WT primer set 1; 3 = Δ*hbn1*Δ*frm2* primer set 2; 4 = WT primer set 2; 5 = Δ*hbn1*Δ*frm2* primer set 3; 6 = WT primer set 3; 7 = Δ*hbn1*Δ*frm2* primer set 4; 8 = WT primer set 4.

3.7.4.3 Comparative growth analysis of BY4741, Δ*hbn1*, Δ*frm2* and Δ*hbn1*Δ*frm2*

The growth of BY4741, Δ*hbn1*, Δ*frm2* and Δ*hbn1*Δ*frm2* in the presence of 0 and 8 µg/ml gliotoxin was subsequently compared, as shown in figure 3.93. Unfortunately, no difference in level of resistance or sensitivity was seen for any of the three mutants. All grew at the same rate as wild-type and growth of these strains appeared to be inhibited to the same extent as wild-type.

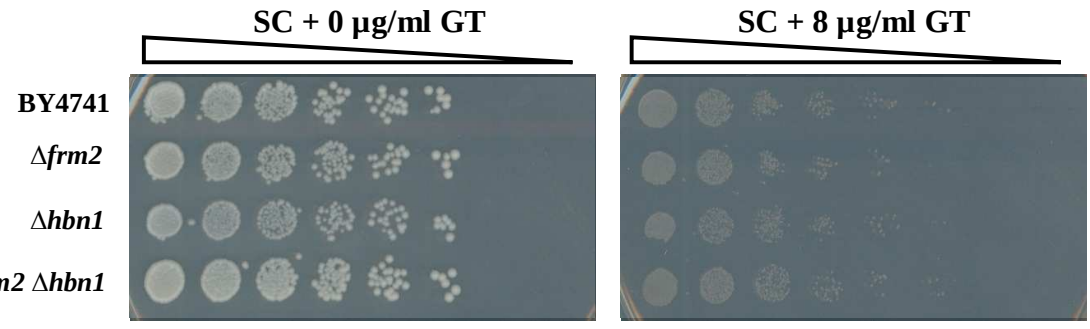

Figure 3.93 Comparative growth analysis of BY4741, Δ*hbn1*, Δ*frm2* and Δ*hbn1*Δ*frm2* in the presence of 0 and 8 µg/ml gliotoxin. The above image represents cellular growth after 72 hr incubation at 30ºC.

To evaluate the similarities in the cellular stress incited by gliotoxin and other common oxidative stressors, comparative growth analysis of these strains was then

carried out in the presence of H_2O_2. BY4741, Δ*hbn1*, Δ*frm2* and Δ*hbn1*Δ*frm2* were grown under exposure to 0, 1, 2, 3, 4 and 5 mM H_2O_2, depicted in figure 3.94. Unlike gliotoxin, H_2O_2 severely inhibits the growth of Δ*hbn1* and this was observed at concentrations of 3 mM and above. Both Δ*frm2* and Δ*hbn1*Δ*frm2* exhibit a wild-type phenotype in the presence of H_2O_2. The finding that yeast cells devoid of Hbn1p exhibit increased sensitivity to H_2O_2 but not gliotoxin indicates that there must be a tangible difference in the ways in which H_2O_2 and gliotoxin mediate their deleterious effects.

Figure 3.94 suggests that in the absence of Hbn1p, Frm2p mediates H_2O_2 toxicity possibly through facilitating the production of a toxic by-product. Hbn1p when present may abolish this product or directly inhibit Frm2p activity.

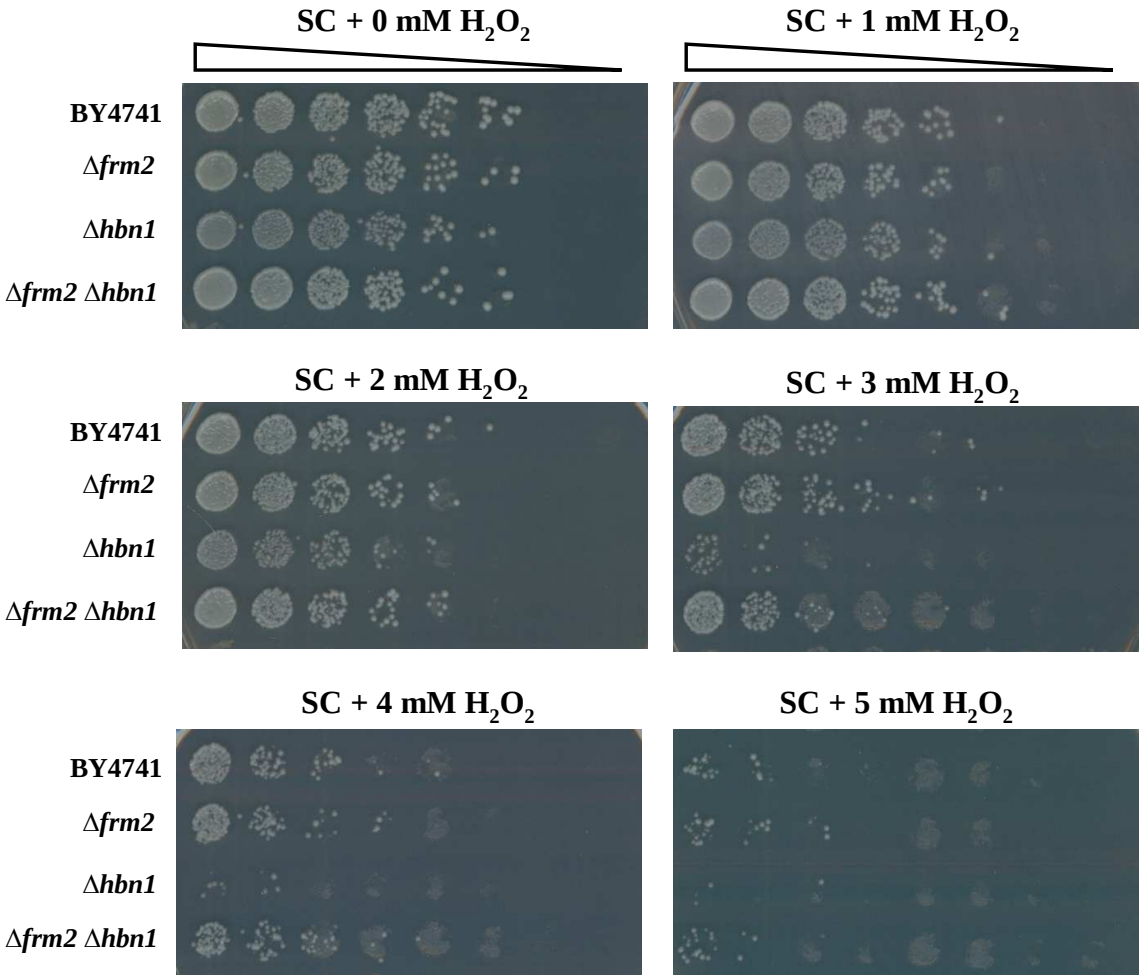

Figure 3.94 Comparative growth analysis of BY4741, Δ*hbn1*, Δ*frm2* and Δ*hbn1*Δ*frm2* in the presence of 0, 1, 2, 3, 4 and 5 mM H_2O_2. The above image represents cellular growth after 72 hr incubation at 30ºC.

3.8 Discussion

The inhibitory effects of gliotoxin on *S. cerevisiae* at the macrobiological level have been assessed, through the use of different toxin concentrations and media, and the employment of a variety of yeast strains. Undoubtedly, gliotoxin causes deleterious effects within the cell resulting in inhibition of growth and increased cell death, in both liquid culture and solid media. This has been a paramount observation throughout this study. Further to this, it has been ascertained that the *A. fumigatus GliT* gene, a member of a twelve-gene gliotoxin biosynthetic cluster, has the capacity to confer resistance to gliotoxin when constitutively expressed in yeast. The protective ability of *GliT* in *S. cerevisiae* mimics that observed in *A. fumigatus* (Scharf *et al.*, 2010, Schrettl *et al.*, 2010). The disulfide bridge present in gliotoxin, to which its toxicity has been attributed through redox cycling and conjugation to host thiols, has been identified as a target of GliTp (Waring *et al.*, 1995, Hurne *et al.*, 2000, Schrettl *et al.*, 2010). We observed that constitutive expression of the *GliT* gene afforded protection against gliotoxin to strains such as wild-type and Δ*cys3*, deficient in ability to deal with OS. However, it appears that carbohydrate source may be a factor in GliTp-induced resistance. Under control of the *GAL1* promoter, galactose metabolism-induced expression of *GliT* did not give rise to a phenotype exhibiting an increase in resistance to the metabolite. In fact, these strains actually demonstrated a slight increase in sensitivity to gliotoxin. This suggests that galactose metabolism may undermine the ability of GliTp to elicit protective effects. Under constitutive expression, I was able to detect a low level of GliTp using an enzymatic assay to indirectly detect gliotoxin reductase activity. It appears that in the presence of *GliT*-pC210, gliotoxin activity is inhibited, thus NADPH oxidase activity was not suppressed. In contrast, this was not observed for *GliT*-pYES2 transformants.

In this study, the question of whether cellular OS is the predominant detrimental consequence of gliotoxin exposure was addressed. Reports have provided evidence that

the toxin appears to have the capacity to induce stress of this classification in different cell lines (Waring *et al.*, 1995, Zhou *et al.*, 2000, Orr *et al.*, 2004). The results shown here have demonstrated that yeast cells do elicit an OS response to gliotoxin and transcriptomic, proteomic and functional genetic analyses have illustrated this fact. We have shown that some genes involved in the first line of cellular defence against OS are critical for optimal survival in the presence of gliotoxin, such as *SOD1* and *YAP1*. Without these genes, there is diminished conversion of superoxide to less harmful products oxygen and hydrogen peroxide and curtailed regulation of the general OS response respectively (McCord and Fridovich, 1969a, Bermingham-McDonogh *et al.*, 1988, Herrero *et al.*, 2008). Mutant strains lacking these genes display sensitivity to gliotoxin, in its presence there is a considerable difference in the growth capacities of Δ*sod1* and Δ*yap1*, in comparison to wild-type. Of the two, the latter exhibits the highest degree of gliotoxin-induced growth inhibition, a phenotype that coheres with *YAP1* function. As a transcription factor involved in the regulation of OS-response genes such as *TRX2* encoding a thioredoxin isoenzyme and *GSH1*, which encodes glutathione synthetase (Kuge and Jones, 1994, Wu and Moye-Rowley, 1994), Yap1p has substantial control over this type of cellular reaction. Although *SOD1* is also significantly implicated in the OS response, its control is not as extensive as that of *YAP1*. These results were corroborated by further growth analysis of these strains under exposure to a common oxidative stressor, H_2O_2. In the presence of H_2O_2, a similar result was seen, with both Δ*yap1* and Δ*sod1* showing increased sensitivity in comparison to wild-type. Again, the most sensitive strain was Δ*yap1*, growth of Δ*sod1* was less inhibited by H_2O_2. In comparing the suppression imposed on these strains by gliotoxin and H_2O_2, it was noticed that Δ*yap1* appears to be more repressed by H_2O_2 than gliotoxin. Under H_2O_2 exposure at a concentration that results in no significant impairment of wild-type

growth, Δ*yap1* cannot grow. However, when wild-type growth is clearly hindered by gliotoxin, growth of Δ*yap1* still occurs, albeit at a minimal level.

Phenotypic analysis of another strain Δ*cys3* led to a similar observation. We discovered that *CYS3*, involved in transsulfuration and subsequent glutathione biosynthesis (Ono *et al.*, 1984, Ono *et al.*, 1992, Mosharov *et al.*, 2000), is vital for a fully functional response to gliotoxin exposure. This supports previous work carried out by Chamilos *et al.* (2008), who also identified *CYS3* as a gene that plays a key role in resistance to the toxin and have reported that disruption of *CYS3* results in cells that exhibit an increase in sensitivity.

Comparative growth analyses of Δ*yap1*, Δ*sod1* and Δ*cys3*, described above, support previous evidence that gliotoxin can induce conditions characteristic of OS. Conversely, Δ*gsh1* phenotypic analysis initially appeared to suggest otherwise. This mutant is lacking the glutathione synthetase gene that allows cells to synthesise glutathione, an important antioxidant that also acts as a reductant facilitating glutaredoxin oxidoreductase activity (Grant, 2001). Due to the fact that this gene encodes a protein that is key in the OS response, we hypothesised that Δ*gsh1* would exhibit increased sensitivity to gliotoxin, however the opposite was seen. Phenotypic analysis of Δ*gsh1* showed that this strain grows considerably more efficiently in the presence of gliotoxin than wild-type. Although this appears to directly contrast with results for other OS response-deficient mutants this phenotype may be attributed to other factors. Bernardo *et al.* (2001, 2003) reported that the ability of gliotoxin to enter into murine cells is limited to the oxidised form. They found that inside the cell, gliotoxin is concentrated by reduction to the cell membrane-impermeable form almost certainly by glutathione. Subsequent glutathione depletion, associated with gliotoxin-induced apoptosis and cell death, diminishes the reduction of gliotoxin and the toxin effluxes from the cell. The same group also revealed that gliotoxin uptake by cells is

negated by the absence of glutathione. Furthermore, research has demonstrated that in another cell line, neuroblastoma cells, glutathione stimulates cytotoxicity induced by gliotoxin. When intracellular glutathione levels in these cells are depressed, gliotoxin cytotoxicity is significantly mitigated (Axelsson *et al.*, 2006). With relevance to our results, this provides an explanation for the Δ*gsh1* phenotypic description recorded. It is quite possible that the absence of *GSH1*, and thus glutathione, benefits yeast cells when exposed to gliotoxin in that the toxin is prevented from becoming concentrated intracellularly which would result in additional damage to the cell. Upon efflux, gliotoxin can enter neighbouring cells but again cannot be retained within the cell and it escapes. Further to this, it may be the case that deletion of *CYS3* decreases the cellular GSH concentration, sufficient to arrest its protective effects, yet leaving enough GSH to retain gliotoxin within the cell leading to increased cell death. Δ*gsh1*, in the same manner as Δ*yap1* and Δ*sod1*, showed increased sensitivity to H_2O_2, in comparison to wild-type, as was expected. It grew somewhat less successfully than Δ*sod1*, but much better than Δ*yap1*.

Further investigation into the *S. cerevisiae* cellular response induced by gliotoxin exposure led us to gather additional evidence in support of gliotoxin being an OS-causing agent. Through investigation into the global response of *S. cerevisiae* to gliotoxin, two metabolic pathways were identified as being upregulated in response to the toxin, at two different concentrations. Firstly, through RNA sequencing analysis and proteomic studies, the sulfur amino acid biosynthesis pathway was identified as one which is switched on in response to cellular exposure to gliotoxin. There are eighteen genes implicated in this process, which yields cysteine, methionine and S-adenosylmethionine (SAM/AdoMet). One sub-section of this process is the transsulfuration pathway, mentioned above, that involves *CYS3* and results in the yield of cysteine from homocysteine with cystathionine as an intermediate (Thomas and

Surdin-Kerjan, 1997). Due to the fact that cysteine is thus a rate-limiting factor in glutathione biosynthesis (Williamson *et al.*, 1982, Penninckx, 2002), the stimulation of this pathway indicates that gliotoxin is causing conditions of OS, to which the cells are responding. To validate these results, quantitative PCR was performed to assess the level of transcription of seven of the eighteen genes under exposure to 16 and 64 µg/ml gliotoxin. All seven were confirmed as upregulated in the presence of the lower toxin concentration. Under the higher concentration six of the seven were found to undergo an increase in transcription, although not all to the same degree as RNA sequencing had shown. Generally, the qPCR results correlated well with those from the transcriptome analysis, despite some discrepancies in the level of transcriptional change documented. Similar results were previously recorded depicting the upregulation of sulfur amino acid biosynthesis genes in the *S. cerevisiae* response to cadmium stresses (Momose and Iwahashi, 2001). To further emphasise the importance of the sulfur amino acid biosynthesis pathway in yeast response to gliotoxin, the differential expression was recorded of a number of genes involved in the mediation of this pathway, under exposure to gliotoxin. Similarly to *MET10* and *MET5*, the *MET1, MET8* and *MET18* genes all possess sulfite reductase activity, an essential step in sulfur amino acid biosynthesis whereby sulfite, which has been formed from the reduction of activated sulfate, is reduced to sulfide (Masselot and De Robichon-Szulmajster, 1975, Thomas *et al.*, 1992a, Thomas and Surdin-Kerjan, 1997). These three genes are stimulated by two different concentrations of gliotoxin, demonstrating the fact that yeast cells, when treated with gliotoxin, raise the level of sulfide available for use in sulfur amino acid biosynthesis. *MET22*, encoding a product also involved in sulfate assimilation (Masselot and De Robichon-Szulmajster, 1975, Gläser *et al.*, 1993, Murguía *et al.*, 1995) is upregulated in response to gliotoxin, as are genes required for transcriptional activation of the pathway, *MET4*, *MET31* and *MET32* (Thomas *et al.*, 1992b, Blaiseau

et al., 1997). The fact that the above cited genes are all upregulated at the transcription level indicates that in response to the toxin, the cells are stimulating the sulfur amino acid pathway, which can then increase glutathione biosynthesis and protect against OS. Conversely, some of the regulatory genes were downregulated when cells were exposed to gliotoxin. High cellular levels of SAM, generated from the sulfur amino acid biosynthesis pathway, induce *MET30* inhibition of sulfate assimilation and thus amino acid biosynthesis. This negative feedback occurs through Met4p and Met19p inhibition by Met30p (Krems *et al.*, 1995, Thomas *et al.*, 1995). *MET19* encodes glucose-6-phosphate dehydrogenase whose importance in OS resistance has been documented (Thomas *et al.*, 1991, Izawa *et al.*, 1998). *MET30*, *MET4* and *MET19* were all found to be downregulated in response to gliotoxin. Further to previous results described above, it was expected that *MET30* would be repressed, to prevent inhibition of sulfur assimilation in the presence of gliotoxin. It was anticipated that due to *MET30* downregulation, expression of both *MET4* and *MET19* would not be hindered, however, this was not the case. As thioredoxin is reportedly involved in activation of APS kinase, encoded by *MET14* (Schriek and Schwenn, 1986, Thomas and Surdin-Kerjan, 1997), it was of notable interest that genes involved in thioredoxin generation *TRX1*, *TRX2* and *TRR1* were all considerably upregulated in response to both concentrations of gliotoxin. Analysis of the yeast global proteomic response to gliotoxin reinforced some of the findings described above. Cys3p, Cys4p and Met17p (also known as Met25p) were established as proteins that undergo an increase in production in response to gliotoxin. Met17p is critical in the formation of homocysteine, the cornerstone in the sulfur amino acid biosynthesis pathway and has when overexpressed been shown to induce higher levels of cysteine and glutathione production (Matityahu *et al.*, 2006). The increased level of Met17p, in addition to Cys3p and Cys4p, both essential for transsulfuration,

signals that on the proteomic response level, the cells are initiating the same reaction to gliotoxin exposure as on the transcription level.

When cells were exposed to 64 µg/ml gliotoxin, the two genes that underwent the highest level of upregulation were *CUP1-1* and *CUP1-2*. Although they were transcriptionally stimulated in the presence of 16 µg/ml gliotoxin, they were not to the extent observed at the higher concentration. *CUP1-1* and *CUP1-2* are two copies of yeast metallothionein which complements the lack of Sod1p function and when overexpressed, enhances resistance to cadmium and copper, thus linking them to the OS response (Winge *et al.*, 1985, Jeyaprakash *et al.*, 1991, Tamai *et al.*, 1993). These genes are clearly of major importance in cellular reaction to high levels of gliotoxin exposure, and the stress induced by this. The fact that *CUP1* appears to play a role in the OS response only strengthens the supposition that gliotoxin is imposing a stress of this kind on our cells.

This study has also resulted in the identification of another yeast cellular pathway that is induced when cells are exposed to gliotoxin, the glucose fermentation pathway. As documented by the RNA sequencing data, only 5 of the 28 genes involved in this process are downregulated in response to the toxin, the remaining 23 are upregulated. In fact, genes that play a role in gluconeogenesis, fundamentally the opposite of fermentation, but not fermentation, are downregulated in response to gliotoxin exposure, demonstrating the cell is heavily commissioning fermentation and glucose utilisation over gluconeogenesis and glucose production in response to gliotoxin. Proteomic analysis yielded results consistent with those from RNA sequencing analysis. 25 of the 42 proteins found to be augmented in response to gliotoxin, at two different concentrations, play a role in the glucose fermentation pathway. Interestingly, this course of action concurs with the induction of the sulfur amino acid biosynthesis pathway. Cysteine and glutathione have been found to suppress

the level of O_2 uptake in the presence of glucose and increase the rate of CO_2 production through fermentation, thereby controlling the rate of respiration and fermentation within the cell (Quastel and Wheatley, 1932). This presents to us the fact that when yeast cells are treated with gliotoxin, they react in a way which is typical of an OS response, subsequently giving rise to an increase in the level of glucose fermentation. NADPH is a product of the glucose fermentation pathway. The fact that NADPH is required for fully functional thioredoxin and glutaredoxin systems, which play an important role in protection against OS (Holmgren, 1989) provides a possible link for the glucose fermentation pathway and the OS response. An intermediate of the glucose fermentation pathway is pyruvate, which has been shown to have the ability to protect against peroxides such as H_2O_2 in mammalian cells (Nath *et al.*, 1995, Desagher *et al.*, 1997). Stimulation of said pathway may be further indication that gliotoxin induces OS.

It must also be acknowledged that of the 172 genes that were found to be upregulated more than three-fold under 16 µg/ml gliotoxin exposure, 107 were annotated as encoding components of either the small or large ribosomal subunits. As Loar *et al.* (2004) pointed out, from transcription profiling, not all changes in gene expression are thought to occur specifically to protect the cells against the stress under which the cells have been imposed. Changes may be a result of a cellular effort to adjust metabolism under poor growth conditions and this could be what is represented by the alteration in the transcription level of ribosomal genes.

Gliotoxin was used at concentrations of 16 and 64 µg/ml to explore the global response it instigates in *S. cerevisiae*. The five most common biological processes stimulated at the transcription level by the two concentrations were compared. RNA metabolic process, ribosome biogenesis, translation and transport were enhanced in the presence of both concentrations, however the response to stress was unique to the lower concentration and cellular amino acid metabolic process was unique to the higher

concentration. Orr *et al.* (2004) demonstrated using fluorescence dye that gliotoxin can cause cellular OS in hepatic cells. In this study a maximum of 50 µM gliotoxin was used, which equates to approximately 16 µg/ml, and this 'high' concentration was deemed to induce ROS, reduce the level of cellular GSH and bring about OS. The fact that the same concentration activated a response to stress in our cells falls in line with observations by the above mentioned group. Stress imposed on cells by unfolded proteins in the endoplasmic reticulum gives rise to ROS and OS conditions, and has been shown to activate amino acid metabolism genes (Barbosa-Tessmann *et al.*, 1999, Harding *et al.*, 2003, Haynes *et al.*, 2004). Thus, acute stimulation of the cellular amino acid metabolic process in our cells under exposure to 64 µg/ml gliotoxin could be another result of OS induced by the toxin. Moreover we found *GCN4*, involved in amino acid starvation response (Hinnebusch, 1984, Natarajan *et al.*, 2001), to be downregulated under both concentrations of gliotoxin exposure. Additionally, Asc1p which functions in repressing Gcn4p, (Hoffmann *et al.*, 1999) was noted to be upregulated almost 3-fold in the presence of 16 µg/ml gliotoxin.

Four of the five most common cellular components associated with genes that underwent a considerable degree of upregulation were the cytoplasm, ribosome, mitochondrion and nucleus and these were found to be stimulated by the two concentrations of gliotoxin. Uniquely, under the lower and higher concentrations, membrane- and nucleolus-associated genes were some of the most highly induced respectively. Landolfo *et al.* (2008, 2010) demonstrated that ROS actually target the cellular plasma membrane and through lipid nutrient supplementation, oxidative damage was alleviated. They suggested that this was due to additional nutrients aiding in the maintenance of membrane integrity, in turn allowing cells to adapt to stressful conditions. Perhaps there is a similar situation occurring in yeast cells under exposure to

gliotoxin and at the lower concentration they are making an attempt to increase membrane-associated proteins in order to abate OS induced by the metabolite.

The fact that exposure to the higher gliotoxin concentration induces the upregulation of many genes associated with the nucleolus could also be indicative of ROS generation. In mammals, OS gives rise to nucleolar stress which in turn initiates apoptosis, outlining the stress-sensing function for the nucleolus. The transcription factor TIF-IA is essential for this process and functions in ceasing rRNA synthesis (Mayer and Grummt, 2005). The TIF-IA yeast homologue Rnr3p has been shown to be important in OS signalling and regulation and the crucial role of the nucleolus in sensing OS has been demonstrated (Lewinska *et al.*, 2010). Wtm1p which we determined to be upregulated in the presence of 64 µg/ml gliotoxin actually plays a role in triggering *RNR3* stimulation (Tringe *et al.*, 2006), supporting the hypothesis that stress of an oxidative manner imposed by gliotoxin is sensed by the nucleolus and appropriate responses are initiated.

When the most common molecular functions stimulated by the two gliotoxin concentrations were compared, transferase activity, structural molecule activity, RNA binding activity and hydrolase activity were found to be common to both. In contrast, protein binding was uniquely one of the functions most highly stimulated by the lower concentration and the same applied to oxidoreductase activity by the higher. Many functions associated with protein-binding are implicated in the OS response. *RAD59* is a gene that encodes a protein involved in protein-binding that was upregulated in response to the lower toxin concentration and is key in DNA damage repair (Petukhova *et al.*, 1999, Pannunzio *et al.*, 2008). Upregulation of genes such as this one may be yeast cells responding to DNA damage caused by gliotoxin, which has been reported before (Eichner *et al.*, 1988). Glutaredoxins are just some of the proteins produced that exhibit oxidoreductase activity which protect against ROS (Ruoppolo *et al.*, 1997,

Luikenhuis *et al.*, 1998) and the fact that oxidoreductase activity is one of the most highly stimulated molecular functions in the presence of 64 µg/ml gliotoxin is likely to represent the OS response being instigated by the cells.

Taken together, the results described above illustrate the manner in which *S. cerevisiae* attempts to react to gliotoxin exposure. Yeast produce a strong OS response in the presence of the toxin in many respects, demonstrating that gliotoxin does indeed induce stress of this kind as a means to bring about inhibition and ultimately cell death. *A. fumigatus* employs this toxin to effectuate this process in order to colonise its host (Gardiner *et al.*, 2005). However, some results did not entirely comply with this model. Although it was initially anticipated that Δ*gsh1* would display increased sensitivity to gliotoxin, we have provided reasons as to why the opposite was observed. *TRX2* encoding a thioredoxin, strongly implicated in the OS response (Kalinina *et al.*, 2008), did not appear to be of any considerable importance in protecting cells against the effects of gliotoxin. Comparative growth analysis of Δ*trx2* and wild-type depicted that these two strains do not exhibit differential growth patterns in the presence of gliotoxin. The fact that Δ*yap1* exhibits increased sensitivity to this mycotoxin, while Δ*trx2* does not requires consideration, as *TRX2* is under the control of the Yap1p transcription factor (Kuge and Jones, 1994, Grant *et al.*, 1996). This indicates that it is other genes controlled by Yap1p, not thioredoxin-related, that are essential for resistance to gliotoxin in yeast. Through comparative growth analysis, *GLR1* and *GSH2*, which are required through different functions for maintaining an appropriate level of GSH within the cell (Grant *et al.*, 1996, Grant *et al.*, 1997, Inoue *et al.*, 1998, Grant, 2001), also failed to demonstrate their prominence in resistance to the toxin, as strains lacking these genes grew at a similar rate to wild-type. Δ*ctt1* did not show an increase in sensitivity or resistance to gliotoxin either, illustrating the lack of importance of catalase T, which normally functions in catalysing the conversion of H_2O_2 to water (Hartig and Ruis, 1986,

Jamieson, 1998). However Δ*ctt1* has been reported not to be more sensitive to H_2O_2 than wild-type strains, but GSH-deficient strains also lacking *CTT1* have displayed an intensified sensitivity (Grant *et al.*, 1998). *TEF3* and *TEF4* encode the translation elongation factor eEF1Bγ and their deletion has caused increased resistance to OS, in a similar manner to Yap1p overexpression (Kinzy *et al.*, 1994, Olarewaju *et al.*, 2004). Thus, we expected that Δ*tef3* and Δ*tef4* would exhibit increased resistance to gliotoxin, which was not observed. The evidence presented here suggests that if indeed gliotoxin is imposing conditions characteristic of OS on yeast cells, the toxin may either induce stress somewhat different to other common oxidative stressors, or, mediate the transcriptomic or proteomic reaction instigated in response.

But what additional modes of action does gliotoxin utilise and how does this prompt cells to respond? We endeavoured to compare the *S. cerevisiae* genes that are up-and downregulated under gliotoxin exposure with those that are stimulated and repressed by other toxins to learn more about the metabolite. Comparison and contrast was made between gliotoxin and allicin (Yu *et al.*, 2010), citrinin (Iwahashi *et al.*, 2007), patulin (Iwahashi *et al.*, 2006) and furfural (Li and Yuan, 2010). Gliotoxin, citrinin, patulin and allicin all induced stimulation of the sulfur amino acid biosynthesis pathway in yeast, the latter to the least extent. Taking all results together, gliotoxin is probably most similar to allicin in the response prompted, many of the same genes are transcriptionally altered when cells are exposed to these toxins.

Allicin, a garlic derivative, is active against a range of bacteria and fungi, including both animal and plant pathogens (Cañizares *et al.*, 2004, Cutler and Wilson, 2004, Khodavandi *et al.*, 2010). Like gliotoxin, allicin modifies thiol residues on proteins (Rabinkov *et al.*, 1998, Hurne *et al.*, 2000) and allicin has been shown to induce apoptosis in yeast (Gruhlke *et al.*, 2010). It is possible that gliotoxin acts in a similar manner (particularly as it has been shown to induce apoptosis in immune cells

(Waring *et al.*, 1988, Zhou *et al.*, 2000, Stanzani *et al.*, 2005)) and much of the differential gene expression may result from yeast apoptosis under gliotoxin exposure.

To conclude, it appears that gliotoxin does to some extent cause OS in yeast cell cultures and many lines of enquiry have presented evidence for this, as described above. When the OS response is initiated in cells, it may be the case that normal housekeeping functions are negatively affected by this as all cellular effort is going into the stress response. For example Ssb1p, which is involved in the correct folding of proteins (Craig *et al.*, 1993, Gautschi *et al.*, 2002, Kim and Craig, 2005), is produced to a lesser extent when cells are exposed to 16 µg/ml gliotoxin. Through screening the Euroscarf library, Chamilos *et al.* (2008) failed to identify *GSH1* as a gene that when deleted alters yeast sensitivity to gliotoxin. We assigned importance to this gene using a targeted gene approach and through this we have discovered that yeast resistance to gliotoxin is extremely sensitive to changes in GSH levels.

Chapter 4 Investigation into the mode of action of the prion-curing drug Tacrine

4.1 Introduction

The spongiform encephalopathies Creutzfeldt-Jakob disease (CJD), bovine spongiform encephalopathy (BSE) and scrapie are just some of the fatal mammalian diseases characterised by the aggregation of misfolded proteins called prions (Prusiner, 1982). Accumulation of misfolded protein is also representative of neurodegenerative disorders such as Parkinson's and Huntington's Diseases (Gregersen, 2006).

Mammalian prion diseases are caused by a conversion of the prion protein (PrP^{C}) from a soluble functional form to a non-functional protease-resistant form (PrP^{Sc}) (Prusiner, 1982, McKinley *et al.*, 1983). The appearance of the infectious pathogenic PrP^{Sc} can occur spontanaeously, through infectious transmission, or as a result of mutation in the *PRNP* prion gene (Prusiner, 1998). PrP^{C}-PrP^{Sc} conversion is characterised by the refolding of α-helical segments into β-sheets and the assembly of PrP^{Sc} amyloid plaques in the brain (Roberts *et al.*, 1988, Pan *et al.*, 1993). Amyloid plaques are also a distinguishing feature of Alzheimer's Disease, however these plaques are composed of amyloid beta proteins (Roberts *et al.*, 1988).

As analogues to the causative agents of mammalian spongiform encephalopathies, the study of yeast prions is of great importance (Wickner, 1994). [PSI^{+}] was the first yeast prion discovered and is one of the most widely studied today (Cox, 1965). [PSI^{+}] is the prion form of Sup35p, which is a component of the translation termination complex (Wickner, 1994, Zhouravleva *et al.*, 1995). In the presence of *SUQ5*, encoding a serine-inserting tRNA, [PSI^{+}] can suppress nonsense ochre mutations (Cox, 1965, Liebman *et al.*, 1975, Cox *et al.*, 1988). In this study, this phenomenon is utilised in that [PSI^{+}] facilitates the readthrough of the synthetic *ade2-1* mutation resulting in the growth of white cells if present and red cells if absent.

Due to fact that proteomic conformational changes are key in prion formation, many investigations have been carried out to assess the importance of chaperone protein

function in prion propagation. It has been determined that the chaperone Hsp104p is crucial for yeast cells to propagate [*PSI*$^{+}$] and that a delicate balance of Hsp104p must be maintained as overexpression and depletion of this protein results in loss of the prion (Chernoff *et al.*, 1995). Hsp104p when expressed at wild-type levels, functions in disaggregating prion amyloids and cleaving prion seeds which can be passed to daughter cells, facilitating prion maintenance (Paushkin *et al.*, 1996). The [*PSI*$^{+}$]-curing agent GdnHCl functions in preventing the production of new propagons by Hsp104p, rendering the cells unable to propagate the prion (Tuite *et al.*, 1981, Eaglestone *et al.*, 2000).

Hsp104p functions in rescuing and refolding aggregated proteins through close cooperation with other Hsp104p machinery components Hsp70p and Hsp40p (Glover and Lindquist, 1998). In terms of priongenesis, Hsp70p and Hsp40p are thus likely to also be involved on this basis (Masison *et al.*, 2009).

The *S. cerevisiae* Hsp70p family consists of the cytosolic proteins Ssa1p-4p, Ssb1p, Ssb2p, Sse1p, Sse2p and Ssz1p, the mitochondrial proteins Ssc1p, Ssq1p and Ecm10p and the endoplasmic reticulum-associated proteins Kar2p and Lhs1p (Craig *et al.*, 1993, Mukai *et al.*, 1993, Craven *et al.*, 1996, Schilke *et al.*, 1996, Hallstrom *et al.*, 1998, Baumann *et al.*, 2000). Hsp70p binds and releases proteins in a functional cycle termed the ATPase binding cycle. Hsp70p has a well characterised peptide-binding domain (PBD) and an ATPase-binding domain (ABD). Whether the PBD adopts an open or closed conformation, depends entirely on the ABD. When ATP is bound to the ABD, rapid substrate exchange occurs in the adjacent domain. However, when ATP is hydrolysed to ADP, the PBD maintains tight adherence to its substrate. Rebinding of ATP may then occur, with the reappearance of the PBD open conformation (Masison *et al.*, 2009). As the Hsp70p ATP hydrolysis and ADP release is intrinsically slow, the cycle is heavily regulated by co-chaperone proteins (Masison *et al.*, 2009). In fact the

rate-limiting step, the hydrolysis of ATP, is prompted by associated Hsp40 proteins (Mayer *et al.*, 2000, Wittung-Stafshede *et al.*, 2003). *S. cerevisiae* Hsp40p family members include Ydj1p and Sis1p, both of which interact with Hsp70p and regulate the ATPase binding cycle (Cyr *et al.*, 1992, Lu and Cyr, 1998). Apj1p is a protein which contains a well conserved J-domain, characteristic of the Hsp40p chaperone family and when overexpressed disrupts [*PSI*$^+$] propagation (Kryndushkin *et al.*, 2002, Walsh *et al.*, 2004). Nucleotide exchange factors (NEFs) also play an important role in regulating the ATPase binding cycle, e.g Fes1p and Sse1p, which stimulate ATP binding and thus Hsp70p rapid substrate exchange (Kabani *et al.*, 2002, Raviol *et al.*, 2006). Furthermore, the Hsp90p co-chaperones Sti1p, Cns1p and Cpr7p function in regulation of this cycle (Wegele *et al.*, 2003). Cns1p stimulates the Hsp70p ATPase binding cycle through provoking ATP hydrolysis (Dolinski *et al.*, 1998). Cpr7p appears to intensify Hsp70p substrate binding (Mayr *et al.*, 2000, Jones *et al.*, 2004).

The chaperone protein Hsp70p and a number of co-chaperone proteins are thought to be involved in prion maintenance for a number of reasons. It has been demonstrated that *HSP70* mutations impair [*PSI*$^+$] propagation (Jung *et al.*, 2000, Jones and Masison, 2003). Overexpression of *SSA1* gives rise to an increase in the level of nonsense suppression mediated by [*PSI*$^+$] (Newnam *et al.*, 1999). It has been suggested that disruption of the Hsp70p ATPase binding cycle may hinder prion propagation (Jones and Tuite, 2005). When this cycle is disrupted through imbalance of Hsp70p co-chaperones, the ability of the cell to remain [*PSI*$^+$] becomes significantly impaired. For example, when Fes1p, a nucleotide exchange factor involved in Hsp70p ATPase binding cycle regulation is depleted, [*PSI*$^+$] is weakened (Jones *et al.*, 2004). While Sti1p overexpression weakens [*PSI*$^+$], *STI1* deletion favours the [*PSI*$^+$] phenotype (Kryndushkin *et al.*, 2002, Jones *et al.*, 2004). As a result, this cycle could be a potential target for anti-prion drugs.

Recently, the ability of the ribosome to carry out functional chaperone activity has come to light. As part of the large ribosomal subunit, the domain V of the large rRNA (25S in *S. cerevisiae*) has the ability to assist in the re-folding of denatured proteins (Das *et al.*, 2008, Fåhraeus and Blondel, 2008).

Yar1p and Ltv1p are two proteins that have be shown to interact and appear to function, distinctly from one another, in 40S ribosomal subunit production (Loar *et al.*, 2004). It has been demonstrated that deletion of *YAR1* and *LTV1* in *S. cerevisiae* causes prion instability in [*PSI*$^+$] strains (M. Blondel, personal communication). This suggests that ribosome imbalance induces [*PSI*$^+$] instability. Thus, the ribosome may somehow be linked to prion maintenance within the cell, perhaps through chaperone function. It may be the case that loss of *LTV1* or *YAR1*, leading to a decrease in 40S ribosomal subunit production (Loar *et al.*, 2004, Seiser *et al.*, 2006) leads to overall ribosome instability causing dysfunction and rRNA function disruption, including chaperone activity. *RPL8A* and *RPL8B* deletion was also found to give rise to prion instability (M. Blondel, personal communication). The protein products of these genes encode the ribosomal protein L4 of the 60S ribosomal subunit (Arevalo and Warner, 1990, Yon *et al.*, 1991, Ohtake and Wickner, 1995).

Tacrine (TA), 6-aminophenanthridine (6AP) and Guanabenz (GA) are three structurally unrelated anti-prion drugs that were identified through a yeast-based prion-curing screen. All three were show to be active against yeast prions, while only 6AP and GA possess prion-curing capacities in mammalian systems (Tribouillard-Tanvier *et al.*, 2008a, Tribouillard-Tanvier *et al.*, 2008b). The fact that 6AP, GA and other anti-prion drug such as Quinacrine (QC) and Chlorpromazine (CPZ) efficiently cure prions in both yeast and mammalian systems indicates that there is some degree of conservation in prion-controlling mechanisms between the two (Bach *et al.*, 2003, Tribouillard-Tanvier *et al.*, 2008b). 6AP and GA appear to exhibit similar effects, acting in *trans* by

disrupting processes involved in prion propagation, rather than directly targeting prions in *cis* (Reis *et al.*, 2011). Both drugs inhibit the ribosomal-mediated protein folding activity of the large subunit's large rRNA, specifically interacting with the domain V. Importantly, this does not have an affect on protein synthesis (Tribouillard-Tanvier *et al.*, 2008b). 6AP and GA compete with unfolded protein for sites on the ribosome thus causing a reduction in the production of refolded protein (Reis *et al.*, 2011).

Interestingly, exposure of Δ*ltv1* and Δ*yar1* to 6AP and GA appears to stabilise the prion in [*PSI*$^+$] cells (M. Blondel, personal communication). Taking the above described results together, the model depicted in figure 4.1 was constructed.

TA is a drug currently approved for prescription to treat Alzheimer's Disease (Summers, 2006). As in mammalian prion diseases, Alzheimer's Disease is characterised by the formation of amyloid plaques in the brain of the patient. These plaques are composed of amyloid β proteins which are derived from the break-down of secreted β amyloid precursor proteins (β APP) (Haass and Selkoe, 1993). TA treatment considerably inhibits the secretion of soluble β APP in a number of cell lines (Lahiri *et al.*, 1994).

Regarding prion curing, in contrast to 6AP and GA, little is known about the mode of action of TA. Due to the fact that it is not a mammalian prion-curing agent, it is thought that its yeast target is too far diverged in mammals (Tribouillard-Tanvier *et al.*, 2008a). Hsp104p, a key chaperone protein in prion propagation has no known mammalian homologue (Jones and Tuite, 2005). This led us to hypothesise that TA may target Hsp104p, increasing the rate of [*PSI*$^+$] curing, particularly as either overexpression or deletion of *HSP104* eliminates [*PSI*$^+$] (Chernoff *et al.*, 1995).

In this study, the principal aim was to gain insight into the prion-curing mode of action of TA, using functional genetic techniques, transcriptomics and proteomics. One of the initial aims of this project was to assess if TA uses a similar mode of action to

GdnHCl in relation to [*PSI*$^+$] curing. It was anticipated that the question of whether or not TA enhances the uptake of GdnHCl would be addressed. We also wanted to investigate the importance of various aspects of chaperone function in prion propagation. We endeavoured to use 6AP and GA in a number of provisional assays, to compare the effects of these drugs with that of TA.

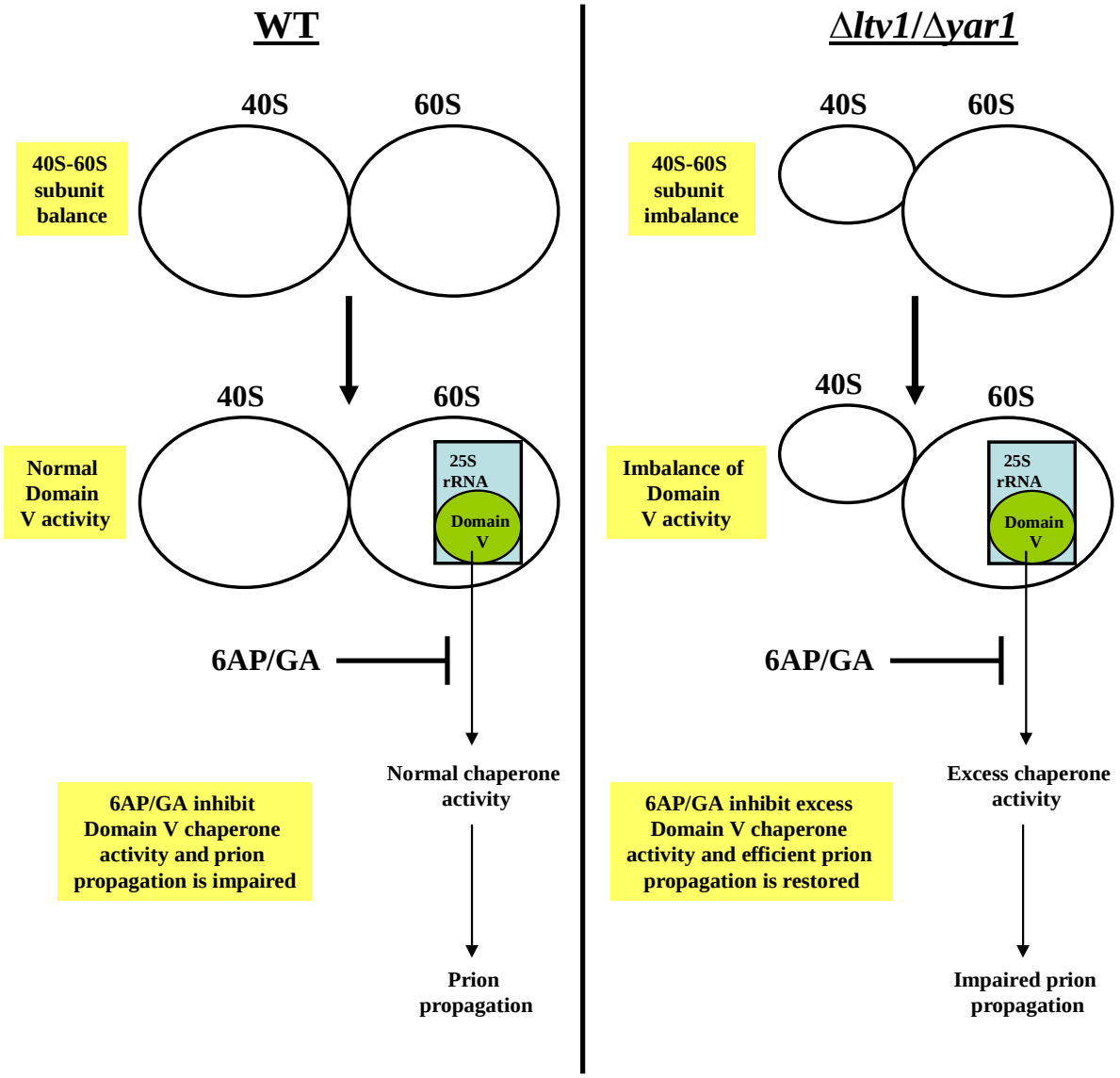

Figure 4.1 Possible model for [*PSI*$^+$] curing by 6AP and GA. Efficent prion propagation facilitated by 25S rRNA-mediated protein folding may depend on a crucial balance of chaperone activity, similarly to Hsp104p. In wild-type cells, 6AP and GA appear to cure [*PSI*$^+$] by inhibiting domain V activity of the 25S-rRNA, as shown on the left of the figure (Tribouillard-Tanvier et al., 2008b). It may be the case that the absence of *LTV1* or *YAR1*, resulting in ribosomal imbalance (Loar et al., 2004), disrupts the delicate balance of 25S rRNA chaperone activity giving rise to prion instability. 6AP or GA exposure may then restore the balance by reducing the said chaperone activity.

Section 1: Using functional genetics to analyse the prion-curing ability of Tacrine, 6-aminophenanthridine and Guanabenz and investigate the Tacrine mode of action

4.2 Assessing Tacrine, 6-aminophenanthridine and Guanabenz as prion-curing agents

Guanidine hydrochloride (GdnHCl) is commonly used to "cure" prions in yeast since its discovery as an anti-prion agent (Tuite *et al.*, 1981). It acts by inhibiting the action of Hsp104p, which is involved in cleaving new propagons or prion seeds from protein aggregates (Parsell *et al.*, 1994, Jung and Masison, 2001). Tacrine (TA), 6-aminophenanthridine (6AP) and Guanabenz (GA) do not cure [*PSI*$^+$] alone, but in combination with GdnHCl, can eradicate the prion.

4.2.1 Tacrine cures [*PSI*$^+$] at relatively low concentrations in combination with GdnHCl

In testing the ability of TA to cure [*PSI*$^+$], it was demonstrated that relatively low concentrations of TA (5 µM) are sufficient to successfully cure the prion in the presence of GdnHCl (figure 4.2).

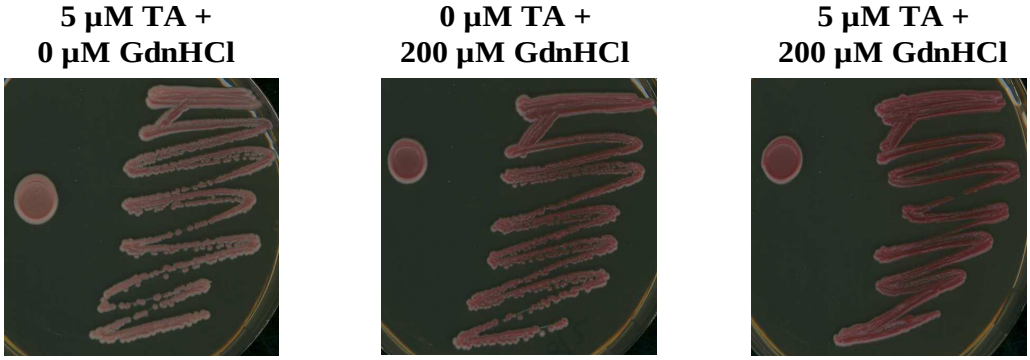

Figure 4.2 Plate streaks depicting TA curing of [*PSI*$^+$] in G600. Samples were taken from a G600 culture and streaked onto YPD containing 1) 5 µM TA + 0 µM GdnHCl, 2) 0 µM TA + 200 µM GdnHCl and 3) 5 µM TA + 200 µM GdnHCl. Plates were incubated at 30ºC for 72 hr. The greater production of red pigment suggests more efficient [*PSI*$^+$] curing. [*psi*$^-$] phenotypes were confirmed by mating and growth on –ade was absent.

To confirm the above result and ensure the curing of [*PSI*$^+$] was not due to GdnHCl alone, single colony plate assays were carried out. Approximately 250 cells were plated on YPD containing GdnHCl alone and GdnHCl supplemented with TA (figure 4.3). Assessment of single colonies provides a clearer representation of the level

of cellular [*PSI*$^+$] due to more even utilisation of adenine by the cells. There was a distinct difference in colony colour of cells exposed to GdnHCl alone and GdnHCl combined with TA. TA addition clearly confers a [*psi*$^-$] phenotype to GdnHCl-exposed [*PSI*$^+$] cells.

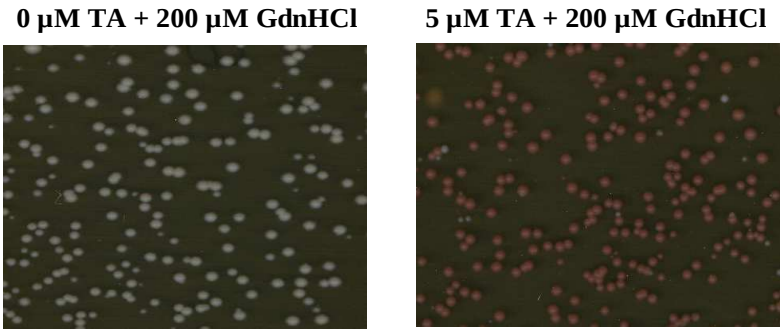

Figure 4.3 Single colony assay to assess the curing ability of TA. Approximately 250 cells were plated evenly on YPD containing 1) 0 µM TA + 200 µM GdnHCl and 2) 5 µM TA + 200 µM GdnHCl. Plates were incubated at 30ºC for 72 hr. [*psi*$^-$] phenotypes were confirmed by mating and growth on –ade was absent.

It was necessary to investigate whether or not the cells cured by TA were truly [*psi*$^-$]. From the plates illustrated in figure 4.3, single colonies were removed and restreaked onto fresh YPD plates. Cells from plates containing 5 µM TA and 200 µM GdnHCl maintain a [*psi*$^-$] state. Single colonies restreaked from plates containing only 5 µM TA or 200 µM GdnHCl alone remain predominantly [*PSI*$^+$] (figure 4.4).

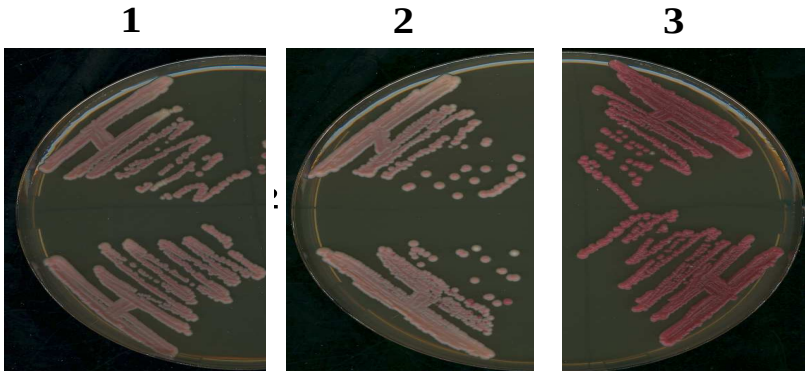

Figure 4.4 Examining if cells cured by TA remain [*psi*$^-$] when grown on YPD. Colonies on plate 1) were originally exposed to 200 µM GdnHCl alone, 2) were exposed to 5 µM TA alone and 3) were treated with a combination of 5 µM TA and 200 µM GdnHCl. [*psi*$^-$] phenotypes were confirmed by mating and growth on –ade was absent.

For all plate assays described above, higher concentrations of TA were also tested. 10 µM, 15 µM, 20 µM and 30 µM TA with 200 µM GdnHCl did not significantly cure [*PSI*$^{+}$] better than 5 µM TA (data not shown). Interestingly, it was noted when comparing the effects of 20 µM TA + 0 µM GdnHCl and 20 µM TA + 200 µM GdnHCl, the latter caused much smaller single colonies, suggesting a combination of GdnHCl and TA at these concentrations inhibits rapid cell growth.

4.2.2 6-aminophenanthridine cures [*PSI*$^{+}$] at relatively low concentrations in combination with GdnHCl

Provisional curing experiments were performed for 6AP as for TA and similar results were observed (figure 4.5).

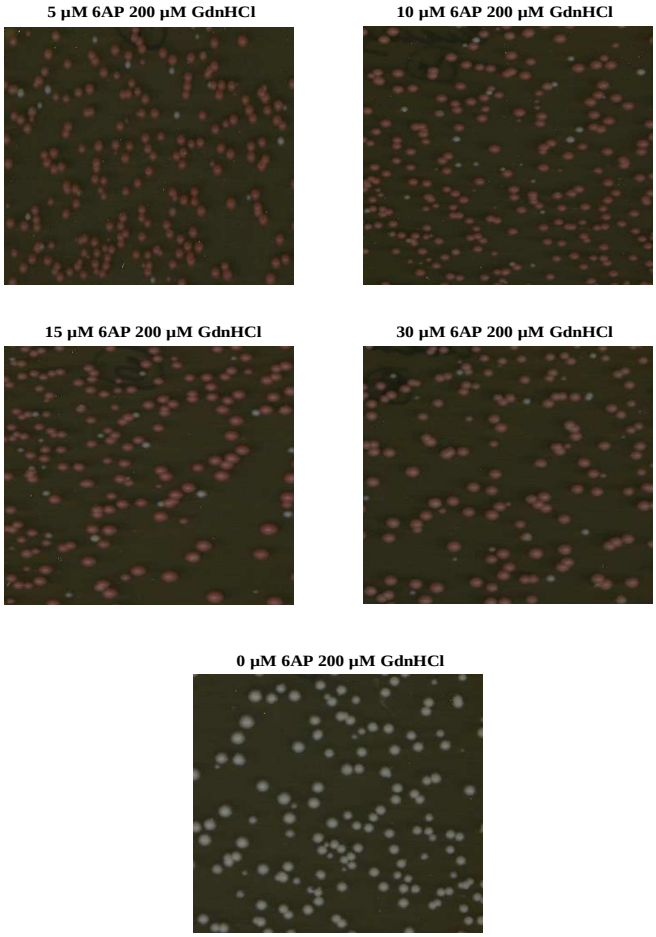

Figure 4.5 Single colony assay to assess the curing ability of 6AP. Plates were incubated at 30ºC for 72 hr. A range of 6AP concentrations were tested, in combination with 200 µM GdnHCl. [*psi*$^{-}$] phenotypes were confirmed by mating and growth on –ade was absent.

Figure 4.5 illustrates the fact that 5 µM 6AP in combination with 200 µM GdnHCl cures [*PSI*$^+$] as efficiently as 30 µM 6AP.

4.2.3 Guanabenz cures [*PSI*$^+$] at relatively low concentrations in combination with GdnHCl

As for TA and 6AP, the ability of GA to cure yeast [*PSI*$^+$] was assessed. Various concentrations were analysed and again, relatively low concentration were found to cure the prion as efficiently as higher concentrations. Figure 4.6 shows that 5 µM GA in combination with 200 µM GdnHCl cures [*PSI*$^+$] as efficiently as 30 µM GA.

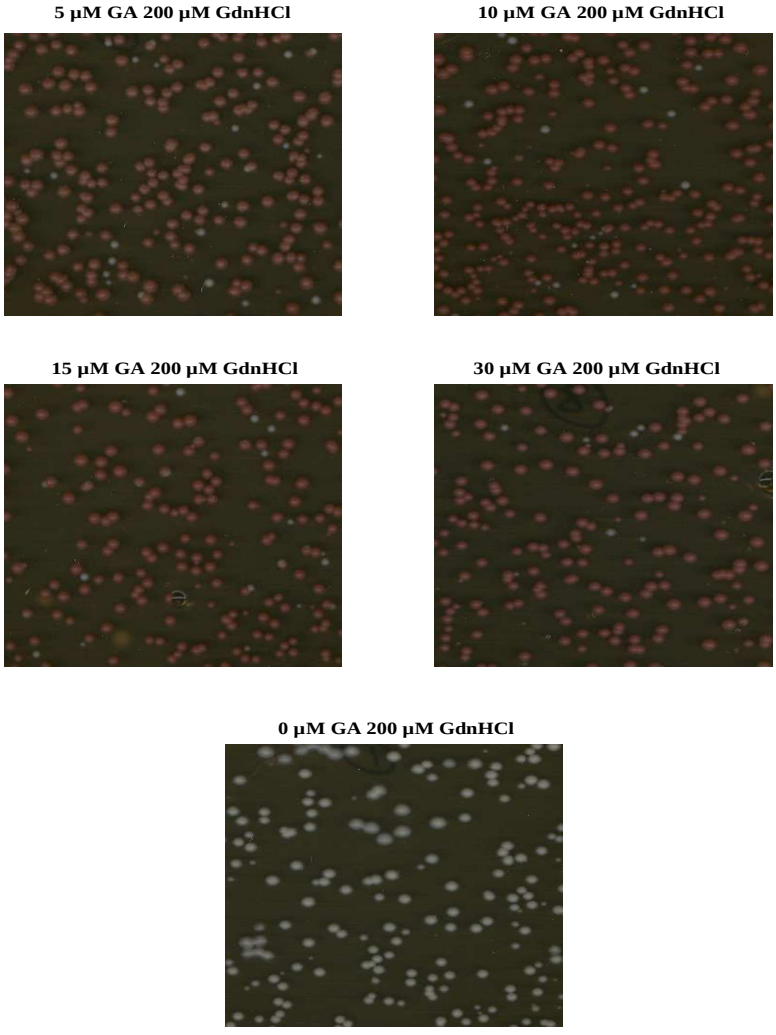

Figure 4.6 Single colony assay to assess the curing ability of GA. Plates were incubated at 30ºC for 72 hr. [*psi*$^-$] phenotypes were confirmed by mating and growth on –ade was absent.

4.3 Examining the ability of TA to cure prions in the absence of yeast growth

Regarding the mode of action of TA, one hypothesis was that TA may inhibit Hsp104p activity in a similar manner to GdnHCl. It has been demonstrated that active cell growth is required for GdnHCl to cure [*PSI*$^+$] (Byrne *et al.*, 2007). Thus, the requirement for cell division in TA curing of [*PSI*$^+$] was assessed, to investigate if TA is similar to GdnHCl in this respect. An experiment was designed to test the curing efficacy of TA in the absence of yeast growth (figure 4.7).

Three G600 cultures were set up, each containing fresh media, GdnHCl and TA. Cultures 1 and 2 were incubated at 30ºC overnight and went through nine generations, while culture 3 maintained at 4ºC overnight only doubled once. These cells were plated on YPD and colour was observed after 48 hr at 30ºC. Colonies grown from culture cells 1 and 2 were approximately 40% [*psi*$^-$], while those from culture 3 were 100% [*PSI*$^+$]. This demonstrated that growth is required for TA to cure [*PSI*$^+$], as although cultures had been exposed to the drugs for the same amount of time, only the cells that underwent a considerable amount of growth became [*psi*$^-$]. Media was replenished in culture 1 only and fresh drugs were added to all. Samples from each culture were then plated at three further time points. As culture 2 did not contain fresh media, efficient growth did not occur as for culture 1 and this resulted in a lower number of [*psi*$^-$] cells. Strikingly, the cells in culture 3 remained 100% [*PSI*$^+$] as during the experiment, cells only progressed through one generation. Taken together, this result provides evidence that similarly to GdnHCl, active growth is required for TA to exhibit curing effects.

4.4 Curing curve analysis

As already stated, GdnHCl acts by inhibiting Hsp104p-mediated prion propagation. In the absence of prion seed renewal, the propagons are diluted out over subsequent generations (Eaglestone *et al.*, 2000).

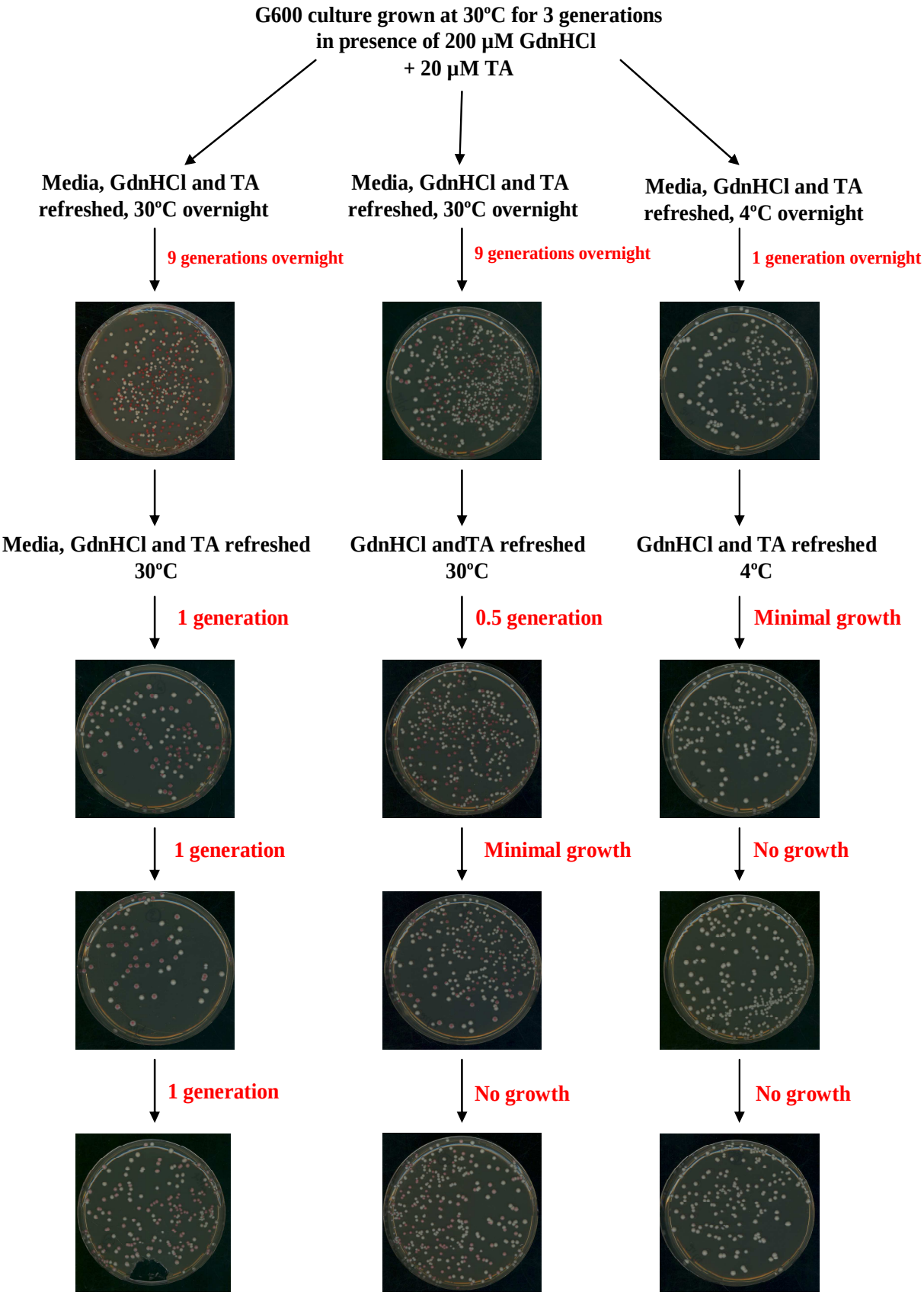

Figure 4.7 Growth of cells is required for TA to cure [*PSI*$^+$]. Plates were incubated at 30ºC for 72 hr. Experiment was performed as described in the above text.

To investigate whether TA functions in a similar manner, a curing curve technique was employed. Unpublished work by Jones *et al.* has demonstrated that 200 µM GdnHCl alone is not sufficient to merit a similar effect to that seen in figure 4.8 and that for similar data to be obtained, cells must be exposed to at least 3 mM GdnHCl alone.

Figure 4.8 illustrates that when cells are exposed to TA in combination with GdnHCl, after six generations the percentage of [*PSI*$^{+}$] cells begins to fall as cells begin to be cured of the prion. After 11 generations the population is virtually completely [*psi*$^{-}$]. This raises the possibility that TA may be preventing prion replication rather than abolishing prions, leaving the pre-existing prions to be diluted out over time, in a similar manner to GdnHCl. It must also be noted that there is no considerable difference in curing capacity between 20, 40 and 60 µM TA, as all give rise to a similar curing curve.

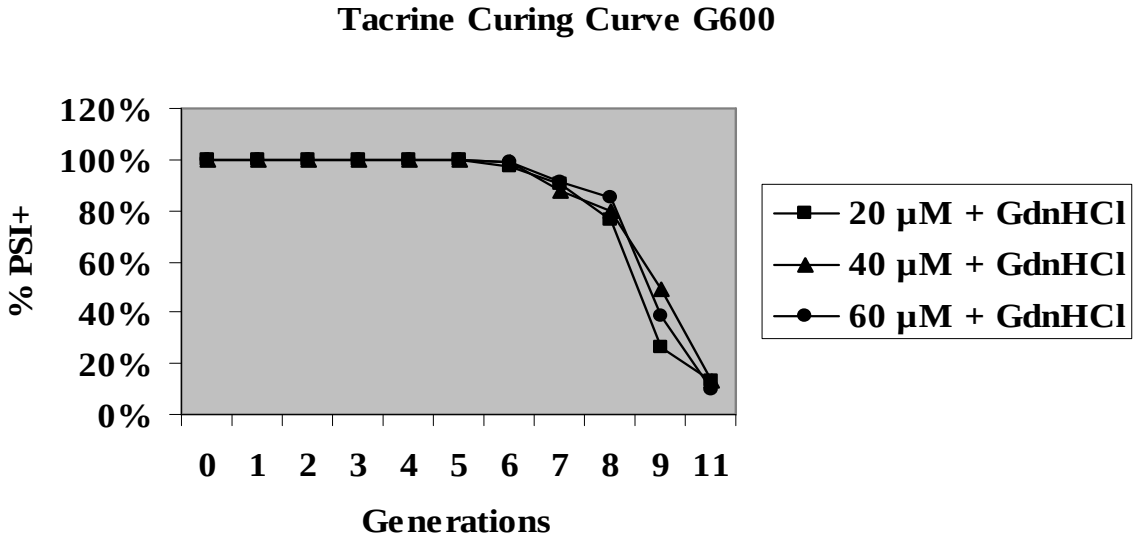

Figure 4.8 Curing curve depicting the percentage [*PSI*$^{+}$] remaining after TA exposure for 11 generations.

Although little is known about the mode of action utilised by TA to cure yeast prions, somewhat more is known about 6AP and GA. Unlike TA, both 6AP and GA exhibit anti-prion activity against mammalian prions, in addition to yeast prions (Tribouillard-Tanvier *et al.*, 2008a, Tribouillard-Tanvier *et al.*, 2008b). It has been

shown that 6AP and GA inhibit ribosomal-mediated protein folding (Tribouillard-Tanvier *et al.*, 2008b), thus prion maintenance in the cell could be facilitated by rRNA. If this is the case, 6AP- and GA-mediated prion curing may be equivalent to GdnHCl anti-prion activity in that both inhibit chaperone activity that is essential for prion propagation.

Curing curve analysis was performed to examine the trend associated with [*PSI*$^+$] curing by 6AP and GA. In figure 4.9 it can be seen that after five generations, all three concentrations of 6AP begin to exhibit curing effects on G600. By eleven generations, almost 80% of cells are [*psi*$^-$]. The 6AP curing curve is very different to that for TA as there is a more rapid decrease in the percentage of [*PSI*$^+$] cells remaining and the decline occurs earlier in the drug exposure.

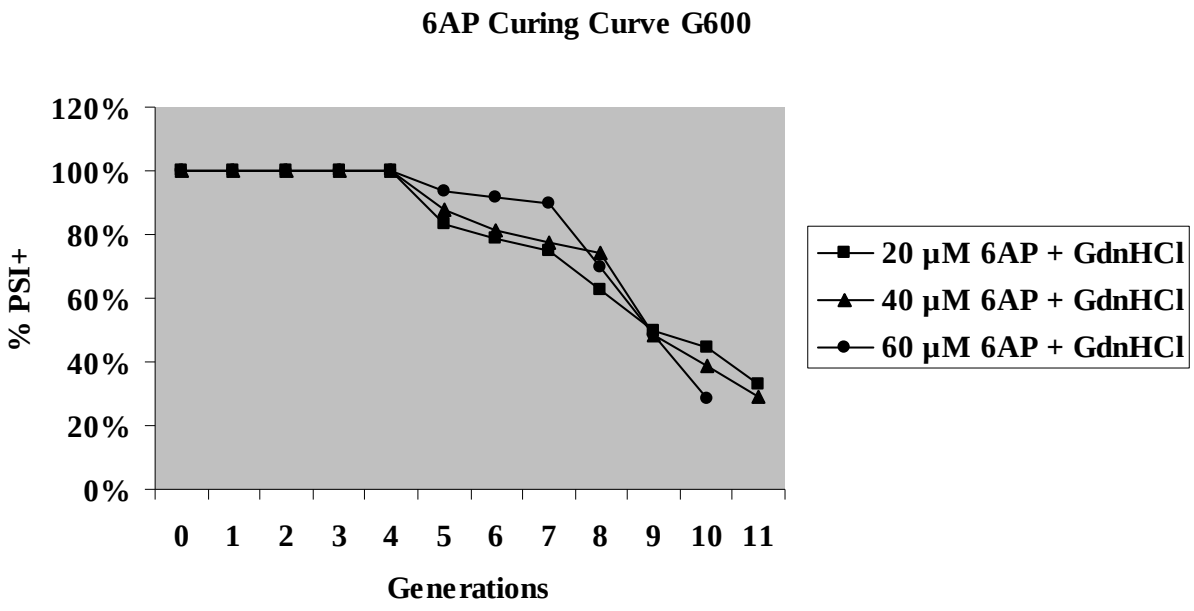

Figure 4.9 Curing curve depicting the percentage [*PSI*$^+$] remaining after 6AP exposure for 11 generations.

As for TA and 6AP, a curing curve was constructed to illustrate the potency and curing trend of GA. The GA curing curve is more similar to that for 6AP than TA, as depicted by figure 4.10. Signs of GA activity are observed after five generations and the

fall in percentage of [*PSI*$^{+}$] cells was rapid. At ten generations almost 80% of cells are [*psi*$^{-}$].

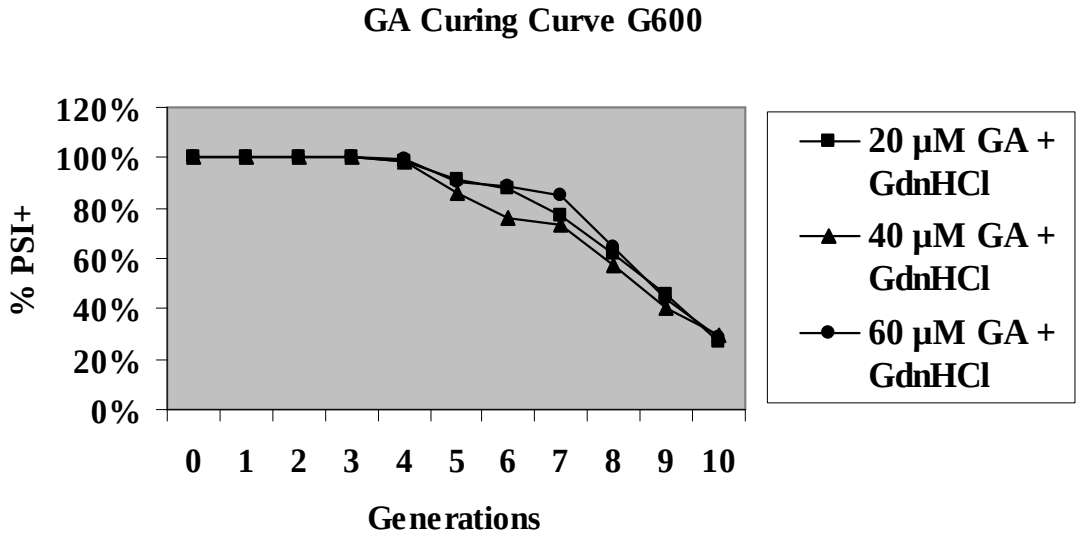

Figure 4.10 Curing curve depicting the percentage [*PSI*$^{+}$] remaining after GA exposure for 10 generations.

4.5 Employment of [^{14}C]-labelled GdnHCl to test the level of GdnHCl uptake by *S. cerevisiae*

Jones *et al.* (2003) showed that increased sensitivity to [*PSI*$^{+}$] curing by GdnHCl can be a result of enhanced cellular uptake of the compound. We utilised [^{14}C]-labelled GdnHCl with a view to analyse the effects of TA on its uptake. This followed the hypothesis that the ability of TA to enhance the effects of GdnHCl may be due to the drug inducing a higher level of GdnHCl uptake. It was anticipated that over time, the level of [^{14}C] measured for the supernatant would fall and that for the cell pellet would rise, representing GdnHCl uptake by the cells. In comparing the levels of [^{14}C]-labelled GdnHCl in the cell pellets and supernatants of wild-type strains 74D (discussed in more detail later) and G600, no real differences were observed between the two strains (figure 4.11). Over 75 min., the cellular concentration of [^{14}C]-labelled GdnHCl remained relatively constant, as did the concentration in both supernatants.

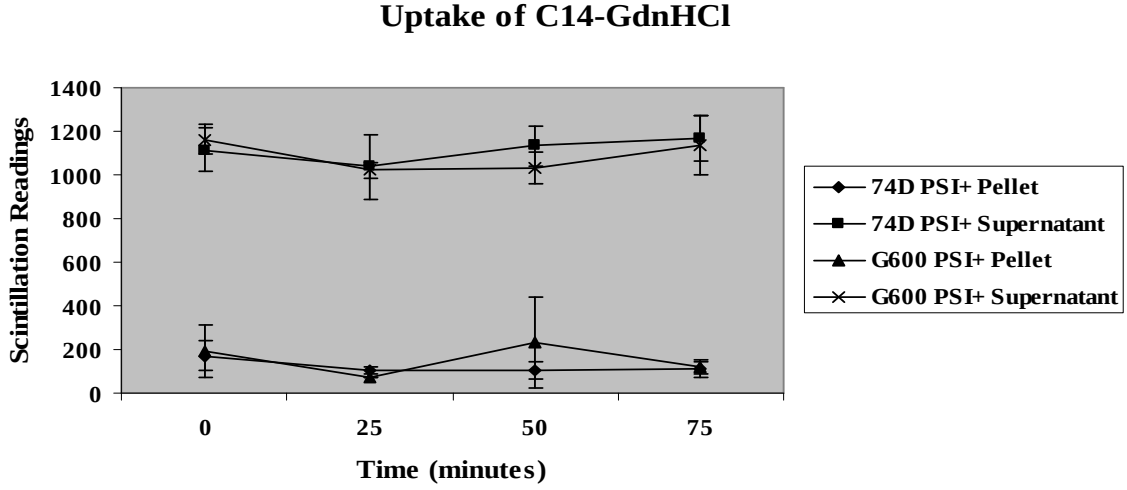

Figure 4.11 Determination of the level of [^{14}C]-labelled GdnHCl in 74D and G600 cultures. At the indicated intervals, samples were taken from cultures, cells were separated from supernatants and the levels of [^{14}C] in both were measured in triplicate.

The same procedure was carried out using mutant strains and various incubation times, including 24 hr. However, an increase in pellet readings representing uptake of GdnHCl was never observed.

4.6 Assessing if TA targets Hsp104p using a thermotolerance assay

Hsp104p plays an essential role in acquired thermotolerance (Sanchez and Lindquist, 1990). When yeast cells are exposed to high temperatures such as 52ºC, Hsp104p activity allows cells to survive by resolubilising heat-damaged proteins (Parsell *et al.*, 1994). We used a well established thermotolerance assay to assess the effects of drugs on Hsp104p, whereby cell survival represented functional Hsp104p activity. Figure 4.12 depicts the ability of wild-type G600 to withstand a temperature of 52ºC in the presence of a variety of drug concentrations. Increased cell death occurs with longer 52ºC exposure times (A), when 3 mM GdnHCl is applied to the agar, there is significant cellular growth inhibition as Hsp104p activity is inhibited (B), the presence of 200 µM GdnHCl does not exhibit a significant effect on cellular thermotolerance (C), nor does 20 µM TA alone (D). A combination of 20 µM TA and

200 µM GdnHCl considerably inhibits the ability of cells to withstand high temperatures, however not to the same extent as 3 mM GdnHCl (E).

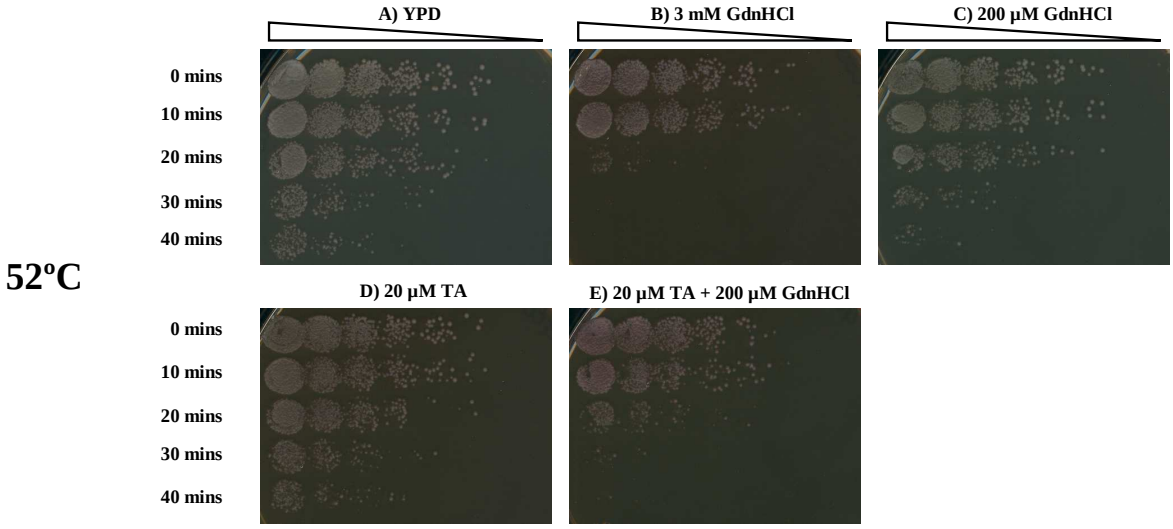

Figure 4.12 The effect of TA and GdnHCl on G600 thermotolerance. G600 cells were incubated at 39ºC to induce Hsp104p expression to protect against heatshock. Cells were then incubated at 52ºC for 0, 10, 20, 30 and 40 minutes and plated on YPD containing GdnHCl and TA, as indicated above for comparative growth analysis. Plates above were incubated at 30ºC for 48 hr.

The same experiment was carried out using G600 deleted for *HSP104*. Figure 4.13 represents the ability of G600 to grow at high temperatures when *HSP104* has been deleted.

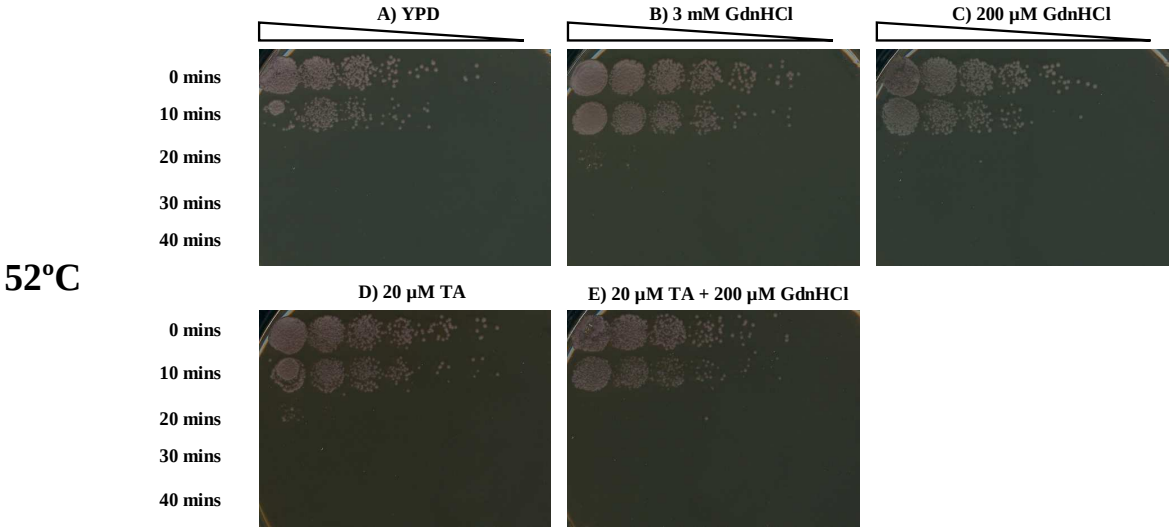

Figure 4.13 The effect of TA and GdnHCl on G600 Δ*hsp104* thermotolerance. G600 Δ*hsp104* cells were incubated at 39ºC and then at 52ºC for 0, 10, 20, 30 and 40 minutes and plated on YPD containing GdnHCl and TA, as indicated above for comparative growth analysis. Plates above were incubated at 30ºC for 48 hr.

Images A-E in figure 4.13 are all very similar. G600 Δ*hsp104* cells cannot survive at 52ºC for more than 10 min due to lack of ability to refold heat-damaged proteins. Heat-shocked cells plated on YPD (A) exhibit the same level of growth as wild-type treated with 3 mM GdnHCl, illustrated in the previous figure. No drug concentrations give rise to differential phenotypes, possibly because all abrogate Hsp104p activity, which in this case is absent.

Further to this, additional thermotolerance assays were performed to investigate if higher levels of TA induced more pronounced effects (figure 4.14).

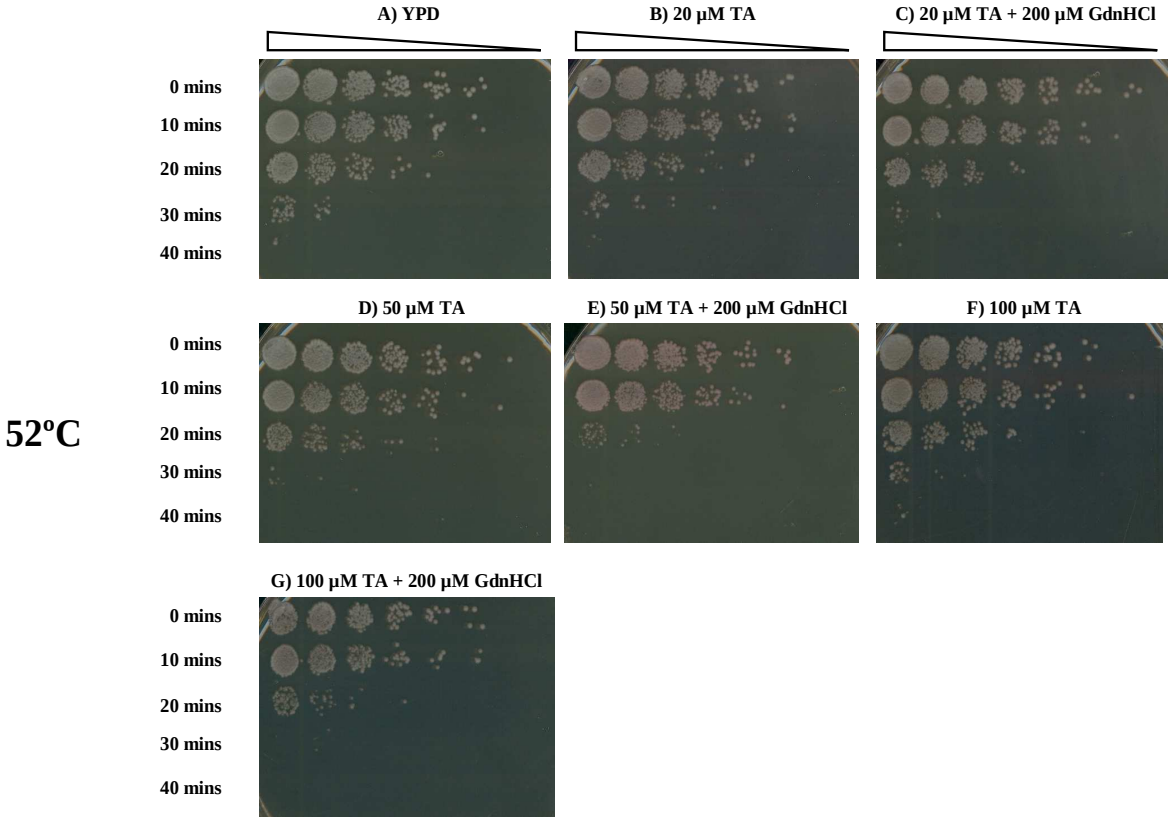

Figure 4.14 The effect of higher TA concentrations on G600 thermotolerance. G600 cells were incubated at 39ºC and then at 52ºC for 0, 10, 20, 30 and 40 minutes and plated on YPD containing GdnHCl and TA, as indicated above for comparative growth analysis. Plates above were incubated at 30ºC for 48 hr.

In comparing the effects of 20 µM, 50 µM and 100 µM TA alone (B, D, F), there are no considerable differences in wild-type yeast growth. It does appear however

that in the presence of GdnHCl, 50 µM and 100 µM TA inhibit thermotolerance somewhat more than 20 µM (C, E, G), but the difference is small.

The level of G600 Δ*hsp104* thermotolerance was also tested in the presence of higher concentrations of TA, alone and combined with GdnHCl (figure 4.15).

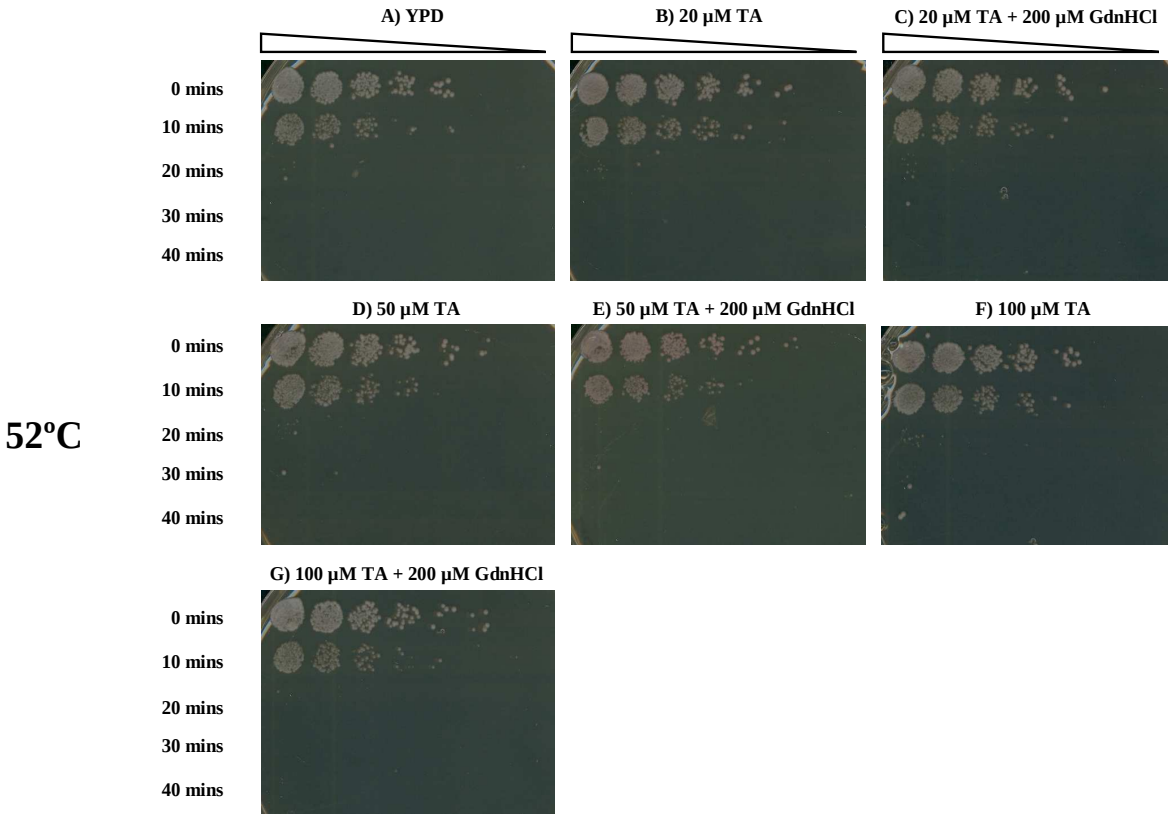

Figure 4.15 The effect of higher TA concentrations on G600 Δ*hsp104* thermotolerance. G600 Δ*hsp104* cells were incubated at 39ºC and then at 52ºC for 0, 10, 20, 30 and 40 minutes and plated on YPD containing GdnHCl and TA, as indicated above for comparative growth analysis. Plates above were incubated at 30ºC for 48 hr.

No differences in growth were observed between treatment with 20 µM, 50 µM or 100 µM TA. This again suggests that TA may be targeting Hsp104p, as in its absence no inhibition is induced.

4.7 Thermotolerance assay using 6AP

Thermotolerance assays using G600 and G600 Δ*hsp104* were performed and resultant cellular growth was assessed in the presence of 6AP. As depicted by figure

4.16, 20 µM 6AP alone does not affect G600 thermotolerance. Combined with 200 µM GdnHCl, there is still no significant inhibition of growth.

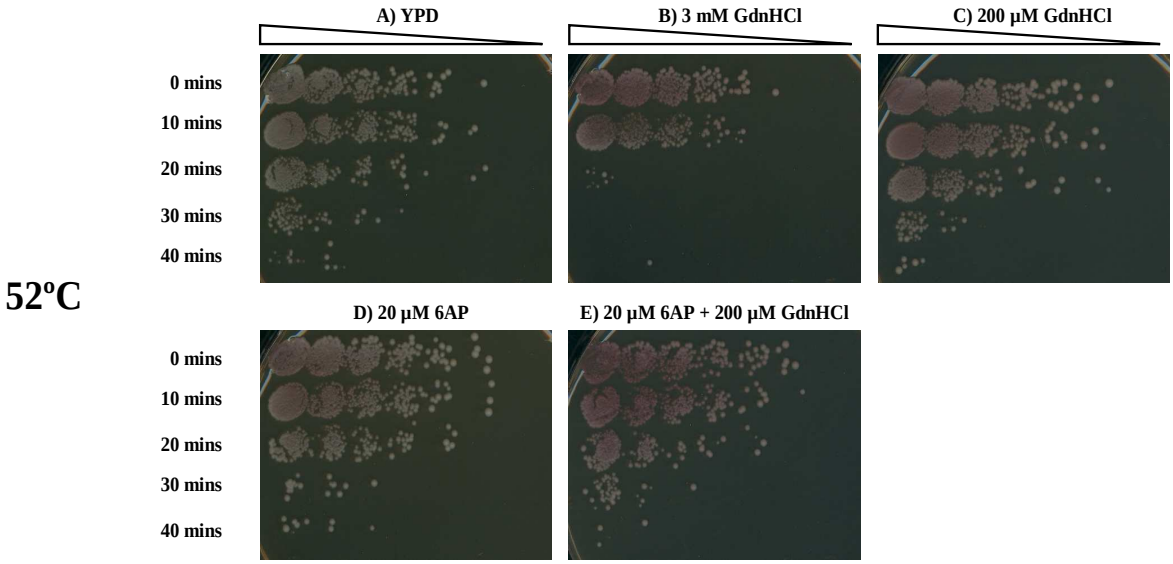

Figure 4.16 The effect of 6AP and GdnHCl on G600 thermotolerance. G600 cells were incubated at 39ºC and then at 52ºC for 0, 10, 20, 30 and 40 minutes and plated on YPD containing GdnHCl and 6AP, as indicated above for comparative growth analysis. Plates above were incubated at 30ºC for 48 hr.

Thermotolerance assays using G600 and G600 Δ*hsp104* were performed and resultant cellular growth was assessed in the presence of GA. A similar result was obtained for GA as for 6AP.

4.8 Assessing the effect of *HSP70*-related mutations on the prion-curing efficiency of TA, 6AP and GA

Disruption of the Hsp70p ATPase binding cycle, involving a number of co-chaperones and NEFs as previously discussed, appears to impair prion propagation (Jones and Tuite, 2005). The ability of TA, 6AP and GA to cure strains deleted for genes involved in the Hsp70p ATPase binding cycle was analysed. We hypothesised that if these drugs either directly or indirectly target this cycle, then treating *HSP70*-related mutants would exacerbate the prion-curing efficiency of the drugs.

Drug spotting assays were designed whereby cells were spread evenly onto YPD plates and drugs were spotted onto filter paper discs on plates. As contols, DMSO and 3 mM GdnHCl was also spotted onto plates. As GdnHCl presence is required for TA, 6AP and GA curing to be visualised, GdnHCl was added to the plates at concentrations of 0, 200 and 500 µM.

Figure 4.17 demonstrates that TA alone has no visible effect on wildtype. However, with increasing concentrations of GdnHCl within the growth media, TA curing can be seen. Conversely, TA alone has the ability to cure [*PSI*$^{+}$] cells deleted for *STI1*, *CPR7* and the double mutant, and this is enhanced by the presence of GdnHCl. It appears that the double mutant displays the most exacerbated curing effect. It is therefore possible that TA could be affecting the Hsp70p ATPase binding cycle. It could be the case that the deletion of Hsp70p co-chaperone genes in combination with cellular exposure to TA results in a greater impairment of the binding cycle, giving rise to an enhanced [*psi*$^{-}$] phenotype.

It is clear from figures 4.18 and 4.19 that deletion of genes involved in the Hsp70p ATPase binding cycle renders cells more susceptible to curing by all three drugs. All mutant strains tested, deficient in fully functional Hsp70p ATPase activity, were cured by the drugs in the absence of GdnHCl. This contrasted drastically from wild-type, which required the presence of GdnHCl to undergo [*PSI*$^{+}$] curing by any one of the agents.

Additionally, it appears that GA possesses considerably weaker curing capacity than TA or 6AP. For each strain tested, the zone of curing resulting from GA exposure is smaller than that induced by either TA or 6AP. It must be considered however that this may be specific to the G600 background strain.

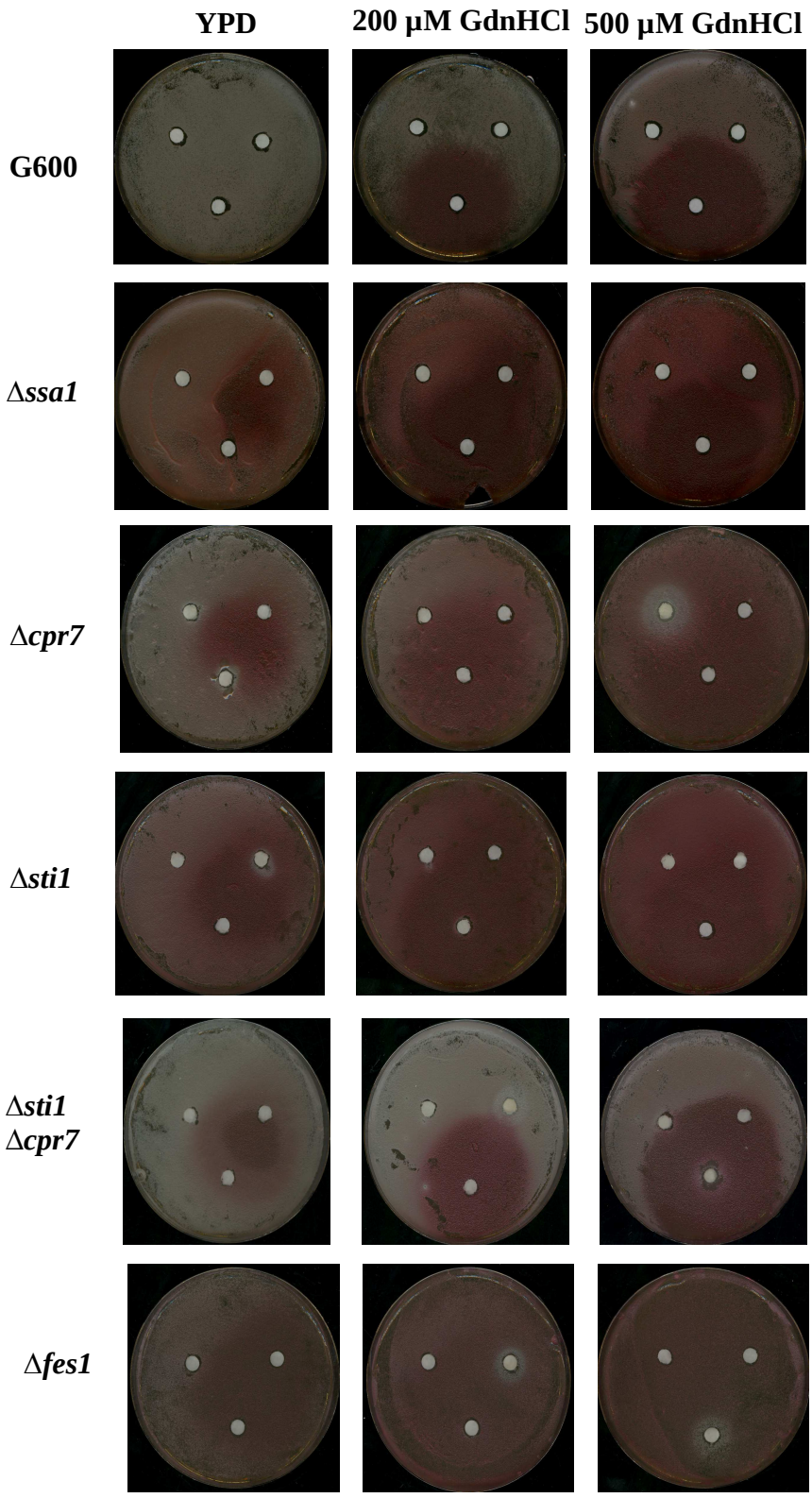

Figure 4.17 Disc assay for Hsp70p-related mutants assessing the curing activity of TA. The top left disc contains DMSO, the top right disc contains 3 mM GdnHCl and the bottom disc contains 10 mM TA. Plates above were incubated at 30ºC for 72 hr.

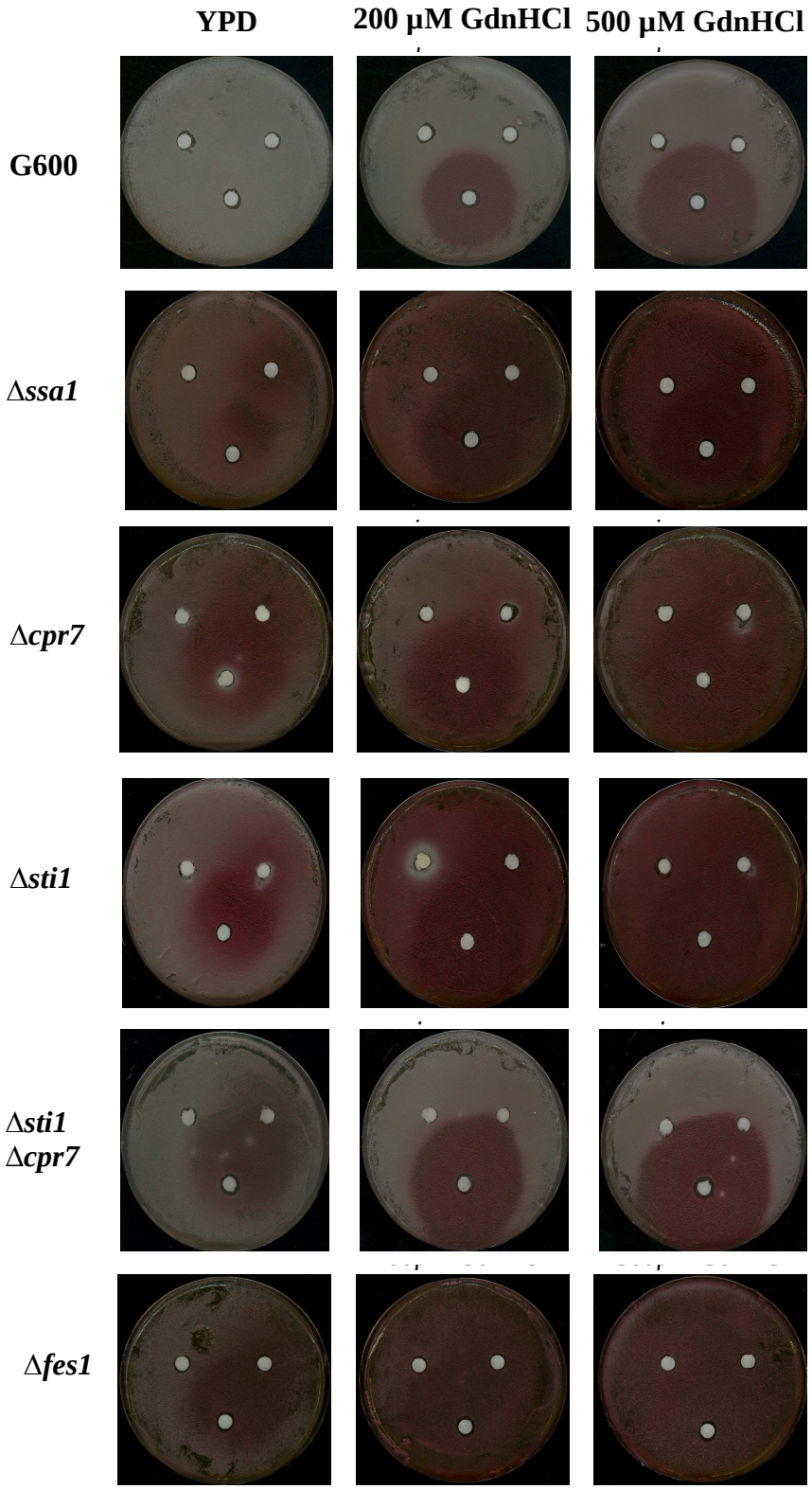

Figure 4.18 Disc assay for Hsp70p-related mutants assessing the curing activity of 6AP. The top left disc contains DMSO, the top right disc contains 3 mM GdnHCl and the bottom disc contains 10 mM 6AP. Plates above were incubated at 30ºC for 72 hr.

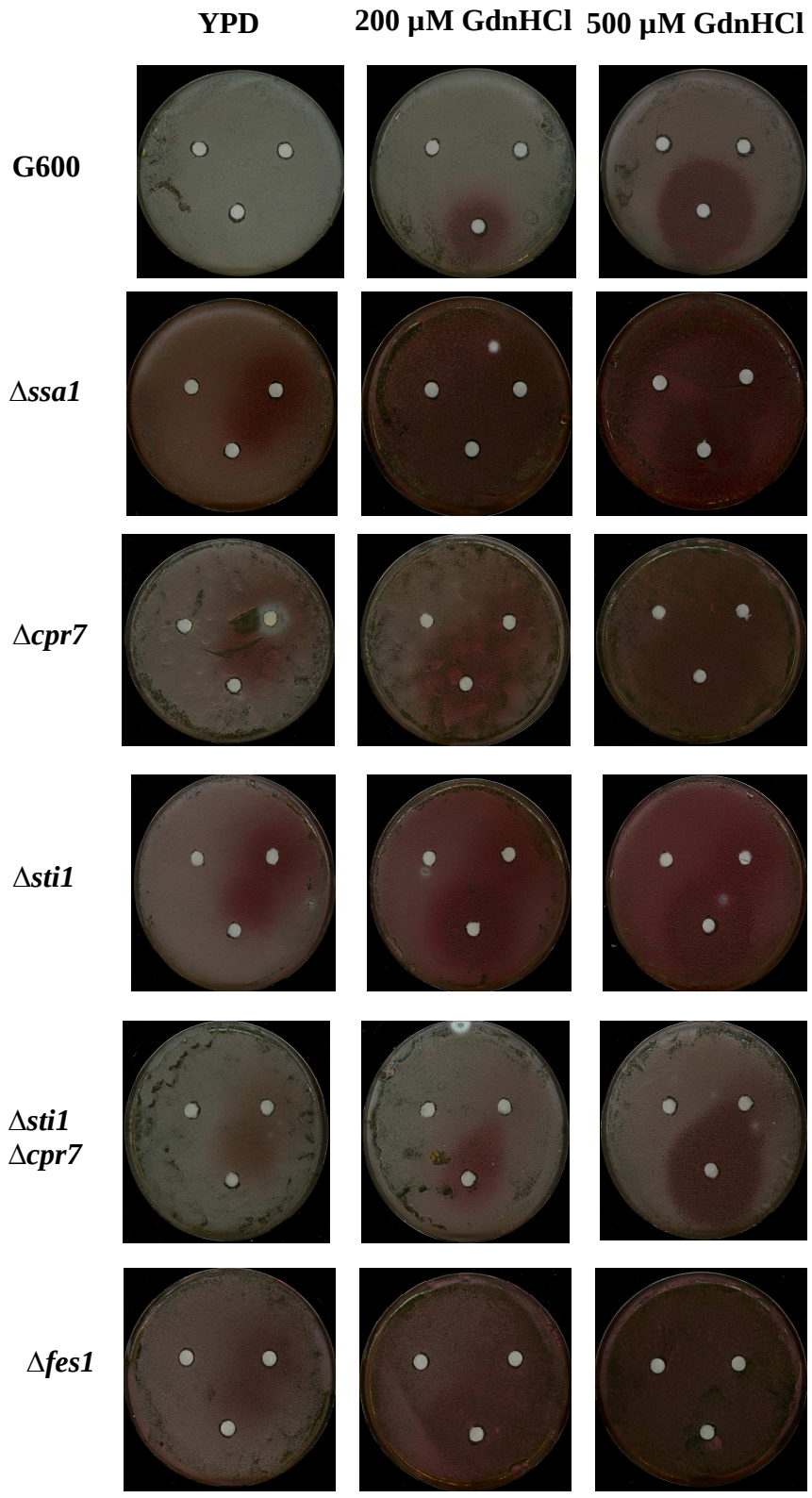

Figure 4.19 Disc assay for Hsp70p-related mutants assessing the curing activity of GA. The top left disc contains DMSO, the top right disc contains 3 mM GdnHCl and the bottom disc contains 10 mM GA. Plates above were incubated at 30ºC for 72 hr.

4.9 Analysis of the G600 Hsp70p and Hsp104p expression levels in response to TA, 6AP and GA exposure

Lahiri (1994) reported that TA does not induce a change in the level of Hsp70p in mammalian cell lines. Western blot analysis was performed to investigate if the same applies to yeast cells. The effects of TA, 6AP and GA on G600 expression of Hsp70p and Hsp104p was assessed.

Figure 4.20 demonstrates that no detectable differences in the levels of Hsp70p and Hsp104p expression are induced by TA, 6AP or GA. Untreated G600 expresses the same level of Hsp70p and Hsp104p as cells treated with GdnHCl alone and in combination with the said drugs.

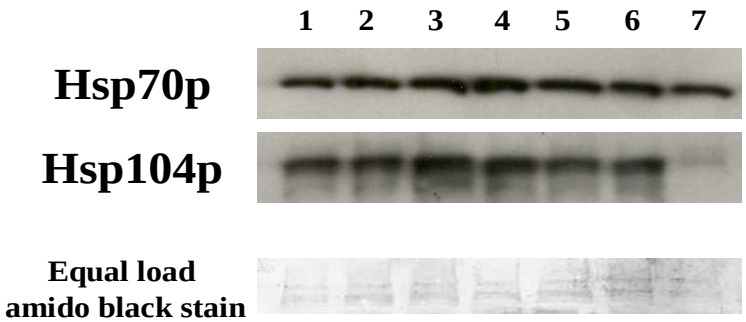

Figure 4.20 Western blot representing the expression of Hsp70p (Ssa1p) and Hsp104p in response to drug exposure. 1 = untreated G600, 2 = G600 200 µM GdnHCl exposure, 3 = G600 200 µM GdnHCl + 20 µM 6AP exposure, 4 = G600 200 µM GdnHCl + 20 µM GA exposure, 5 = G600 200 µM GdnHCl + 20 µM TA exposure, 6 = untreated G600, 7 = untreated G600 Δ*hsp104*.

4.10 Assessment of [*PSI*$^+$] instability in four mutant strains exhibiting ribosomal imbalance

Using the yeast [*PSI*$^+$] 74D-694 (74D) strain, it has been suggested that deletion of *YAR1*, *LTV1*, *RPL8A* and *RPL8B* confers yeast ribosomal imbalance and [*PSI*$^+$] instability (M. Blondel, personal communication). Wild-type 74D deleted for these genes were plated on YPD. Figure 4.21 depicts the spontanaeous appearance of [*psi*$^-$] colonies in the strains deleted for *YAR1* and *LTV1*, but not *RPL8A* or *RPL8B*.

1 **2**

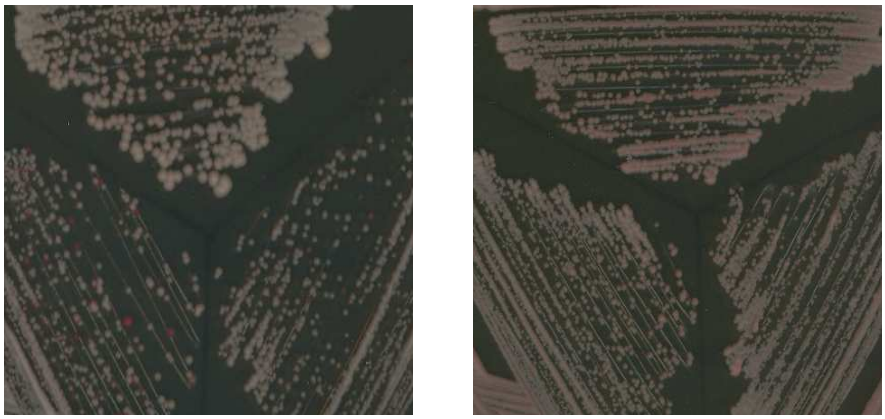

Figure 4.21 Plates depicting [*PSI*$^+$] instability in Δ*ltv1* and Δ*yar1* strains. 1) Top = 74D, left = Δ*yar1*, right = Δ*ltv1*. 2) Top = 74D, left = Δ*rpl8b*, right = Δ*rpl8a*. Plates were incubated at 30ºC for 48 hr.

4.11 Investigation into the importance of ribosomal subunit balance in [*PSI*$^+$] curing by TA, 6AP and GA

6AP and GA exposure has been reported to stabilise the weak prion in Δ*yar1*, Δ*ltv1*, Δ*rpl8a* and Δ*rpl8b* (M. Blondel, personal communication). The effects of TA, 6AP and GA on [*PSI*$^+$] in these mutant strains was assessed using disc assays.

In figures 4.22-4.24, the pinker colonies of the mutant strains will be due to the effects of the absence of *YAR1*/*LTV1*/*RPL8A*/*RPL8B* on [*PSI*$^+$]. Firstly, figure 4.22 confirms that TA possesses the capacity to cure [*PSI*$^+$] in this 74D strain. The mutant that cures most similarly to wild-type under TA exposure is Δ*yar1*. The curing patterns of Δ*rpl8a* and Δ*rpl8b* also resemble that of 74D. Δ*ltv1* however does not appear to undergo [*PSI*$^+$] curing to the same extent as the other strains. Rather than enhance the curing induced by TA, the higher GdnHCl concentration appears to repress the conversion of cells to a [*psi*$^-$] state.

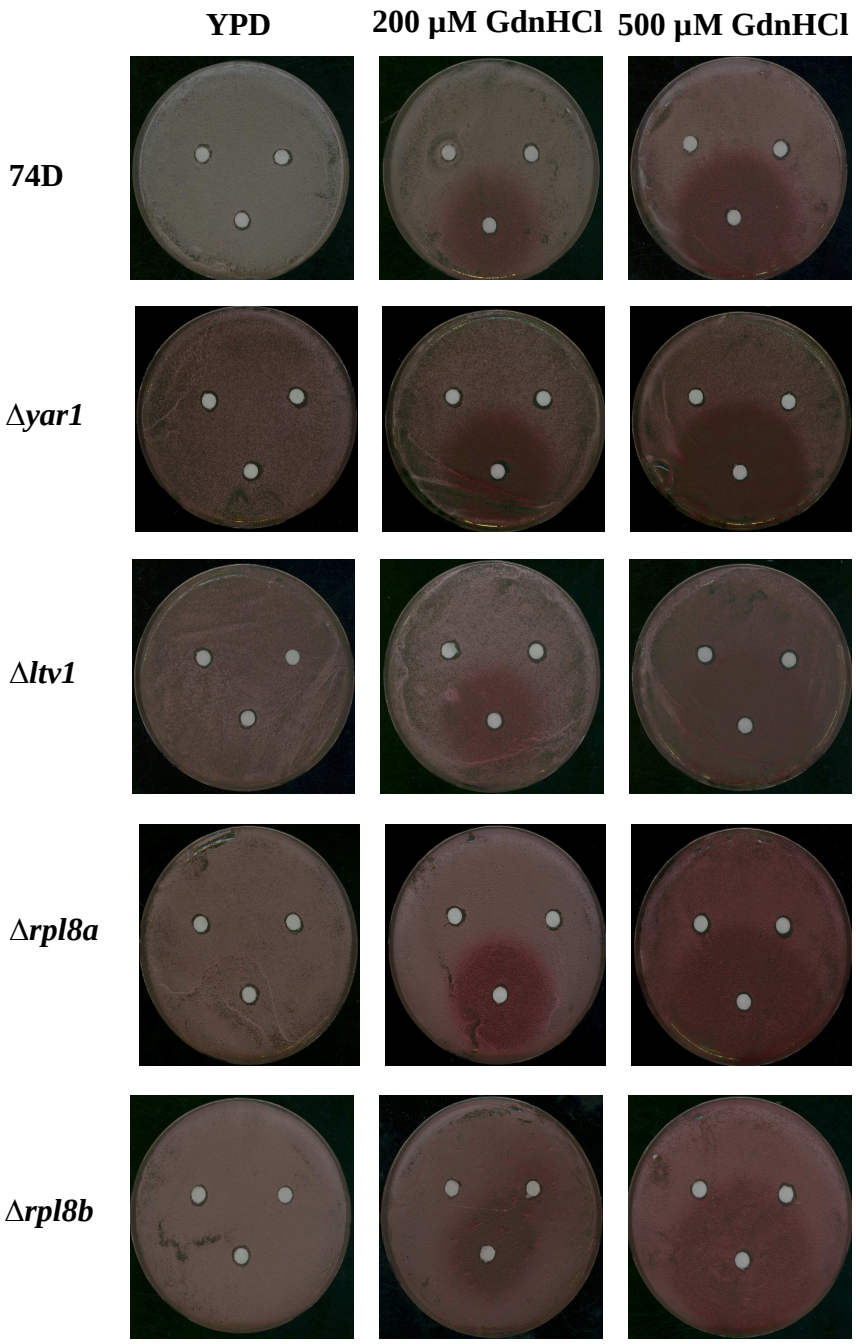

Figure 4.22 Disc assay for ribosome mutants assessing the curing activity of TA. The top left disc contains DMSO, the top right disc contains 3 mM GdnHCl and the bottom disc contains 10 mM TA. Plates were incubated at 30ºC for 72 hr.

Figures 4.23 and 4.24 demonstrate the ability of 6AP and GA to cure these mutants in the 74D background strain.

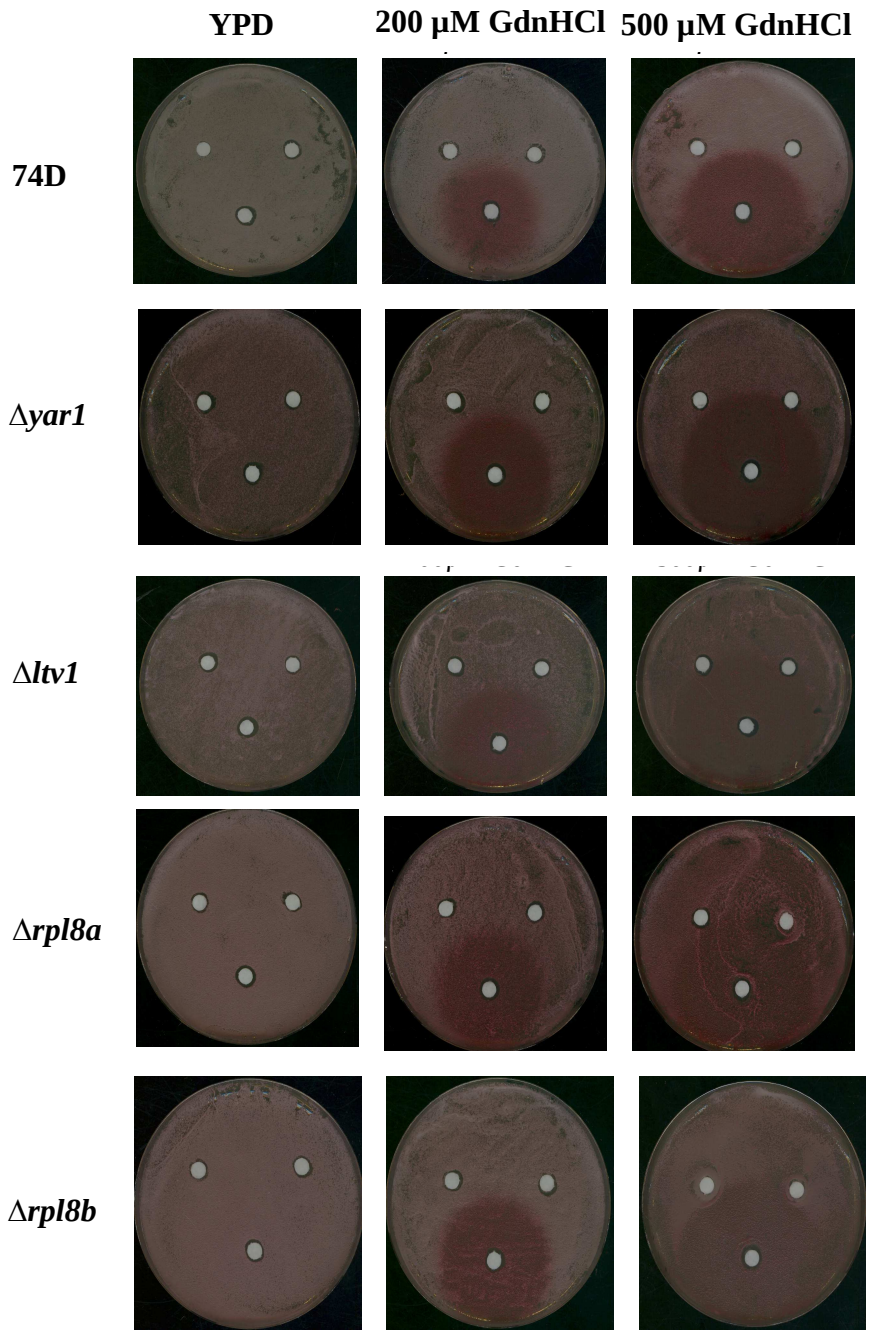

Figure 4.23 Disc assay for ribosome mutants assessing the curing activity of 6AP. The top left disc contains DMSO, the top right disc contains 3 mM GdnHCl and the bottom disc contains 10 mM 6AP. Plates were incubated at 30ºC for 72 hr.

Figure 4.23 demonstrates that 6AP also possesses the capacity to cure [*PSI*$^+$] in the 74D strain. As for TA, Δ*yar1*, Δ*rpl8a* and Δ*rpl8b* all display a similar curing pattern to wild-type under 6AP exposure, while that for Δ*ltv1* is quite different. It appears that 6AP has even less of a [*PSI*$^+$] curing effect on Δ*ltv1* than TA, as the curing zones are considerably smaller and less red.

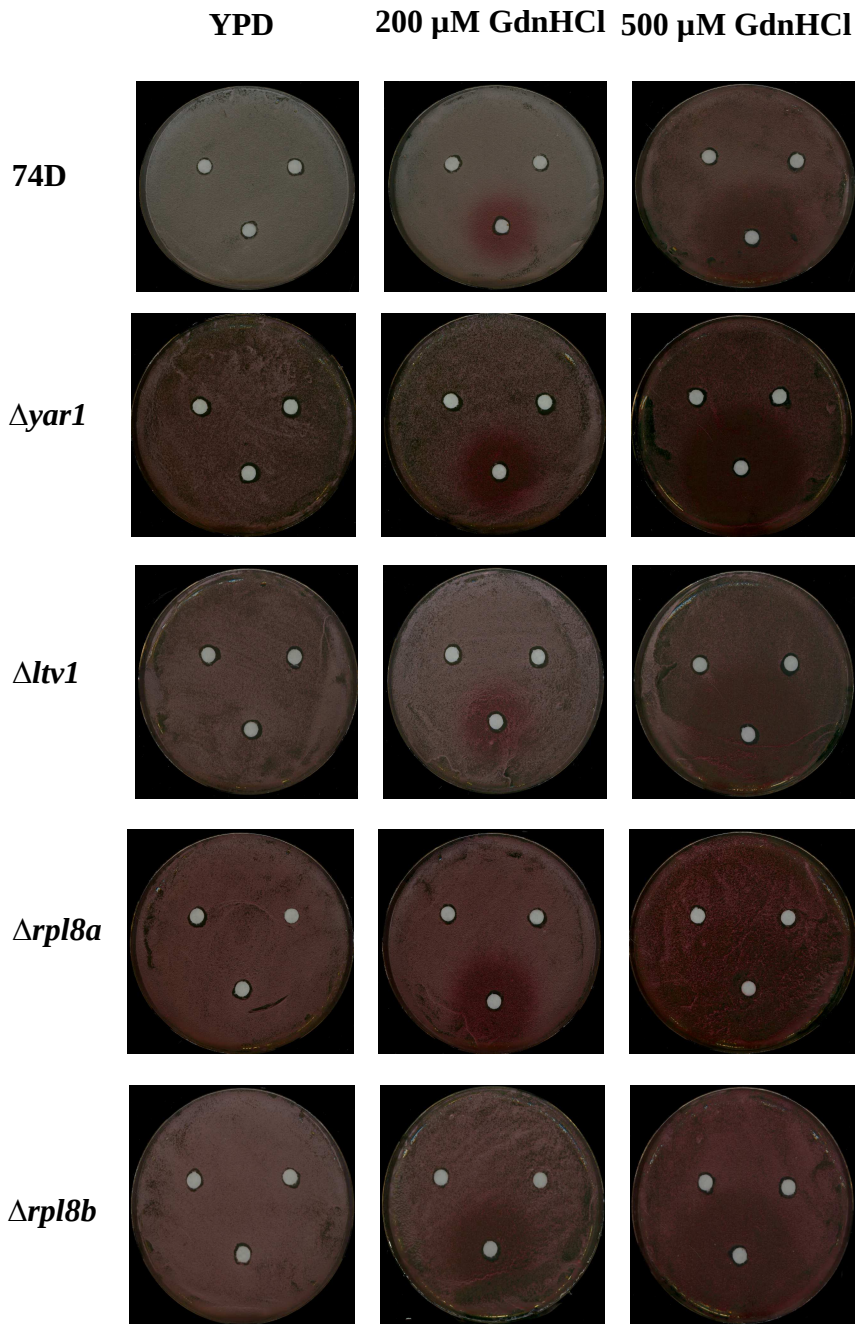

Figure 4.24 Disc assay for ribosome mutants assessing the curing activity of GA. The top left disc contains DMSO, the top right disc contains 3 mM GdnHCl and the bottom disc contains 10 mM GA. Plates were incubated at 30ºC for 72 hr.

Figure 4.24 suggests that GA overall does not possess the ability to cure [*PSI*$^{+}$] to the extent that TA or 6AP do, in the 74D background. All curing zones are significantly smaller. However, a similar conclusion can be drawn from the GA disc assay as for TA and 6AP. Yet again, all strains exhibit similar curing patterns, with the exception of Δ*ltv1*.

Taking all three disc assays into account, it appears that ribosomal imbalance does not exaggerate curing induced by these drugs, as was seen for the Hsp70p-related mutants. Also, these results support the previously described work that demonstrated the ability of prion-curing drugs to stabilise the prion in these mutant strains. In combination with increasing levels of GdnHCl, TA, 6AP and GA all appeared to display an agonistic effect on [*PSI*$^{+}$].

4.12 74D, Δ*yar1* and Δ*ltv1* thermotolerance assays

Inhibition of both Hsp104p and ribosomal-mediated protein folding are believed to cure [*PSI*$^{+}$] (Chernoff *et al.*, 1995, Eaglestone *et al.*, 2000, Tribouillard-Tanvier *et al.*, 2008b). Thus, chaperone activity displayed by Hsp104p and the ribosome appear to be involved in prion propagation and [*PSI*$^{+}$] maintenance. To address the question of whether Hsp104p and ribosomal chaperone activity overlap in relation to acquired thermotolerance, thermotolerance assays were performed using Δ*hsp104* the mutants exhibiting ribosomal imbalance. Figure 4.25 illustrates 74D thermotolerance in the presence of GdnHCl and TA.

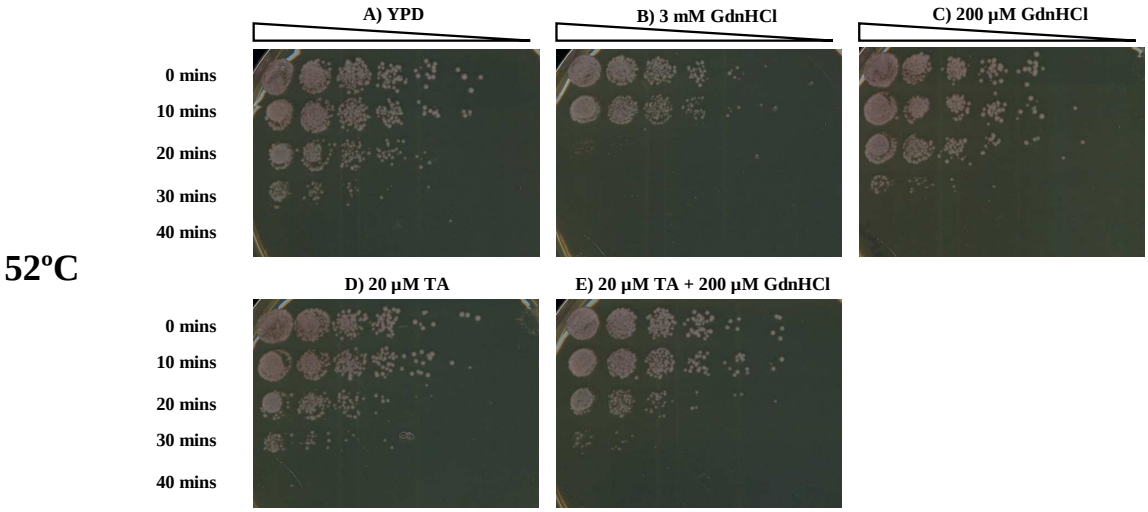

Figure 4.25 The effect of TA and GdnHCl on 74D thermotolerance. Cells were incubated at 39ºC to induce Hsp104p expression to protect against heatshock. Cells were then incubated at 52ºC for 0, 10, 20, 30 and 40 minutes and plated on YPD containing GdnHCl and TA, as indicated above for comparative growth analysis. Plates above were incubated at 30ºC for 48 hr.

74D is somewhat less tolerant to heatshock than G600, as there is no cellular survival after exposure to 52ºC for 40 min (A). Besides that, similar effects on thermolerance are induced by TA on 74D as seen for G600. 3 mM GdnHCl significantly inhibits thermotolerance (B), while 20 µM TA and 200 µM GdnHCl alone and do not obviously affect thermotolerance (C, D). However, exposure to a combination of the two results in a slight decrease in growth after heatshock, although this is not as pronounced as was observed for G600 (E).

As was observed for G600 Δ*hsp104*, 74D deleted for the *HSP104* gene (A) displayed a similar level of thermotolerance as wild-type exposed to 3 mM GdnHCl (figure 4.26).

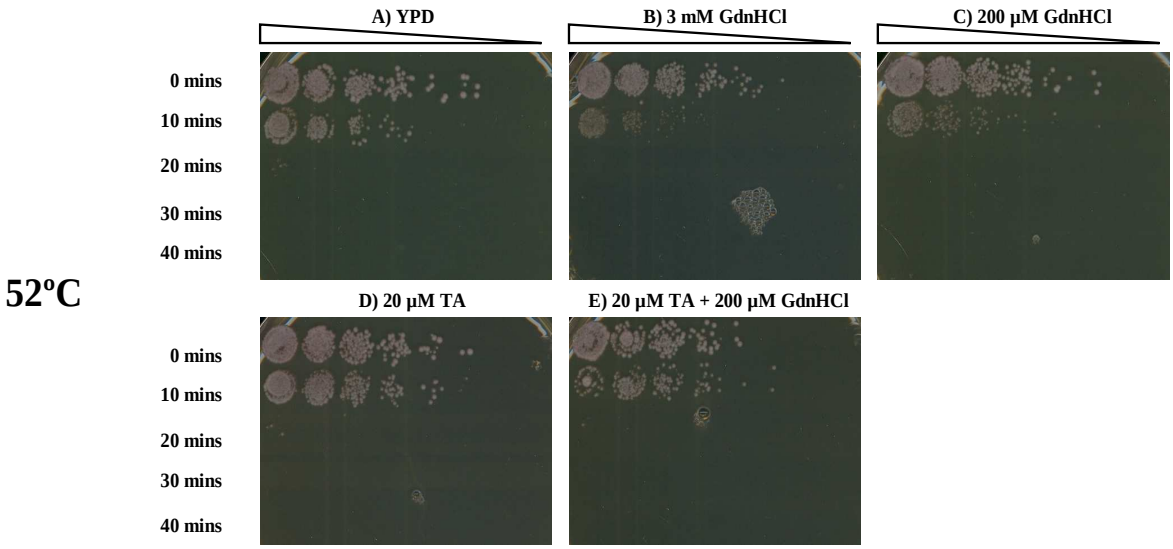

Figure 4.26 The effect of TA and GdnHCl on 74D Δ*hsp104* thermotolerance. Cells were incubated at 39ºC to induce Hsp104p expression to protect against heatshock. Cells were then incubated at 52ºC for 0, 10, 20, 30 and 40 minutes and plated on YPD containing GdnHCl and TA, as indicated above for comparative growth analysis. Plates above were incubated at 30ºC for 48 hr.

Further to this, no significant inhibition in thermotolerance was induced by drug treatment (B-E).

Moreover, we wanted to investigate the 74D Δ*hsp104* level of thermotolerance after 52ºC exposure during shorter intervals. Thus we plated cells heatshocked for 0, 2,

4, 6, 8 and 10 min. Additionally, the effect on thermotolerance of higher concentrations of TA were also assessed, as shown in figure 4.27.

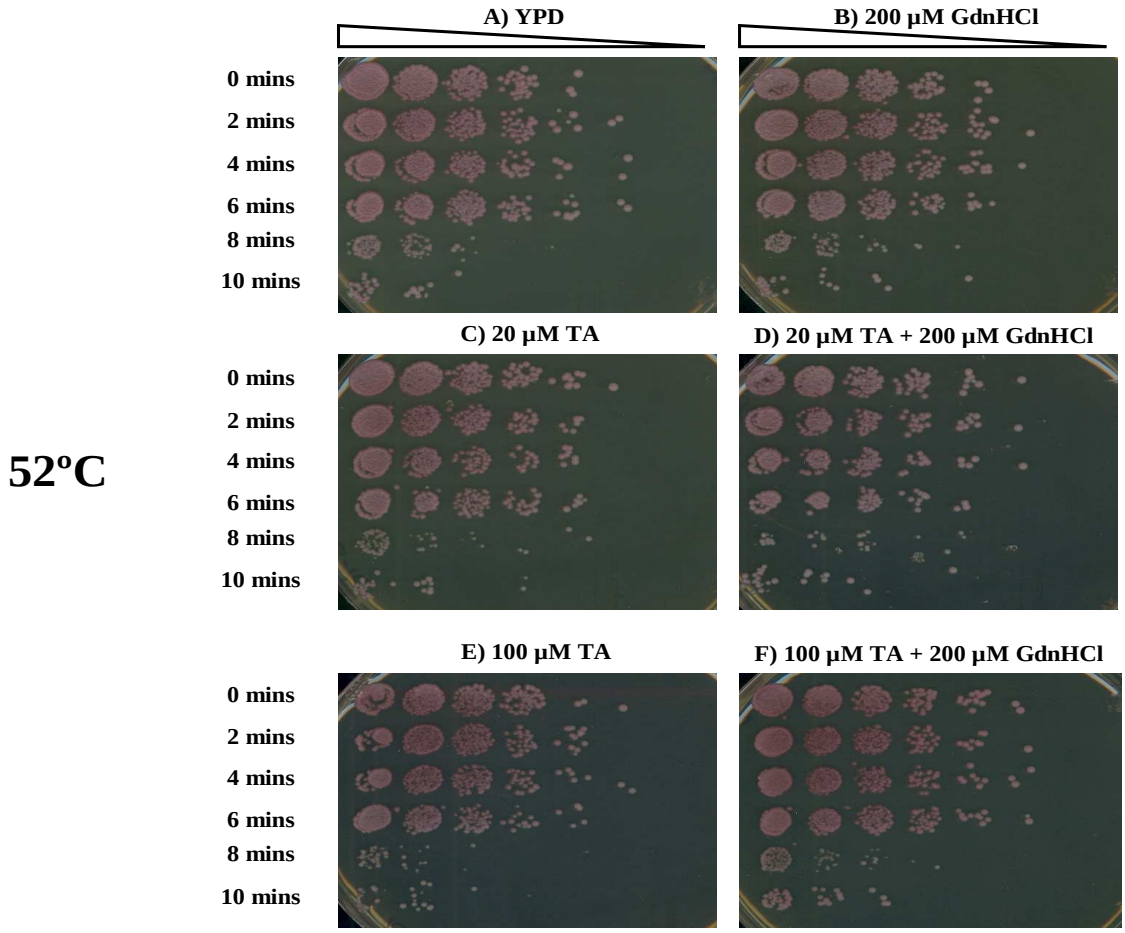

Figure 4.27 The effect of higher TA concentrations on 74D Δ*hsp104* thermotolerance. Cells were incubated at 39ºC to induce Hsp104p expression to protect against heatshock. Cells were then incubated at 52ºC for 0, 2, 4, 6, 8, 10 minutes and plated on YPD containing GdnHCl and TA, as indicated above for comparative growth analysis. Plates above were incubated at 30ºC for 72 hr.

As depicted in the figure above, 100 µM TA in combination with 200 µM GdnHCl (F) does not inhibit thermotolerance any more than 20 µM TA with GdnHCl does (D). The same figure illustrates that is it only after 8 min at 52ºC that cells begin to lose the ability to withstand the high temperature.

It can be seen in figure 4.28 that in the absence of *LTV1*, 74D does not exhibit as high a degree of thermotolerance as wild-type (A). 3 mM GdnHCl significantly inhibits the growth of this Δ*ltv1* (B), and in fact hinders the thermotolerance of this strain more than Δ*hsp104*. Interestingly, Δ*ltv1* displays a higher level of thermotolerance than

Δ*hsp104* when untreated, but thermotolerance inhibition by 3 mM GdnHCl is more acute in Δ*ltv1* than Δ*hsp104*.

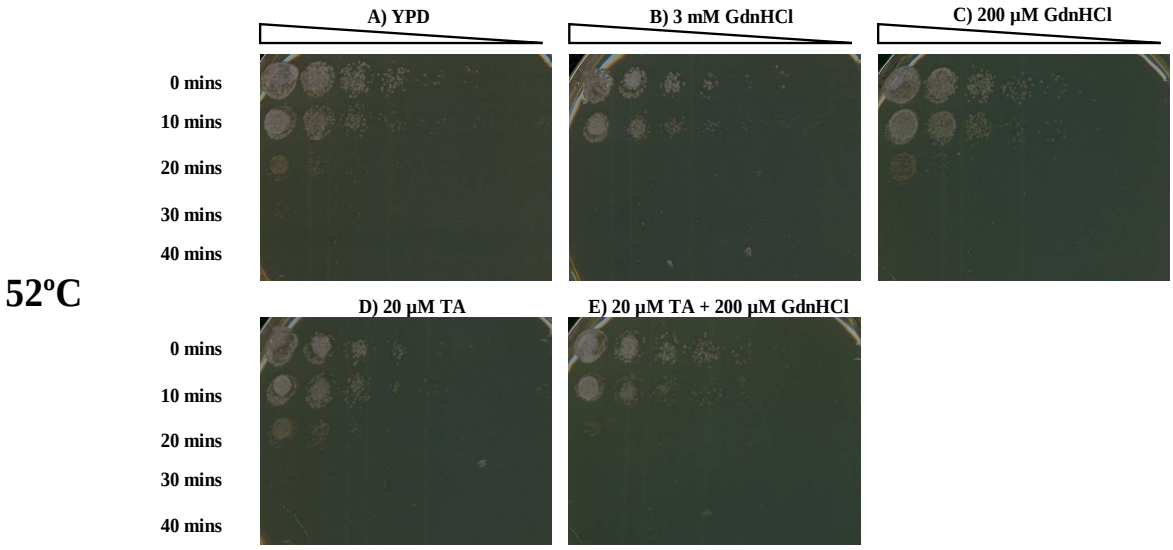

Figure 4.28 The effect of TA and GdnHCl on 74D Δ*ltv1* thermotolerance. Cells were incubated at 39ºC to induce Hsp104p expression to protect against heatshock. Cells were then incubated at 52ºC for 0, 10, 20, 30 and 40 minutes and plated on YPD containing GdnHCl and TA, as indicated above for comparative growth analysis. Plates above were incubated at 30ºC for 48 hr.

As illustrated in figure 4.29, the double mutant Δ*ltv1*Δ*hsp104* is unable to survive after 10 min 52ºC heatshock.

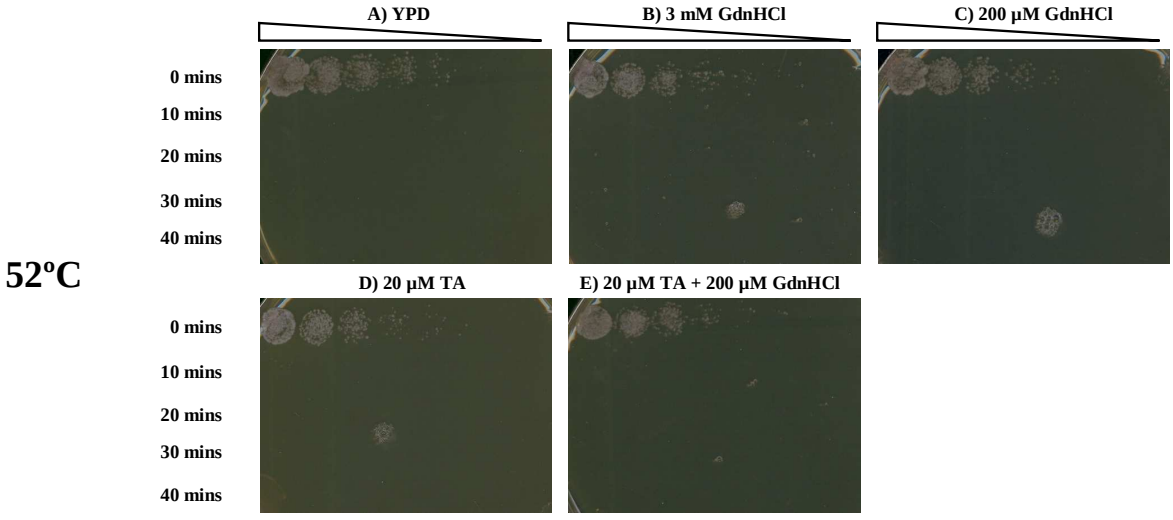

Figure 4.29 The effect of TA and GdnHCl on 74D Δ*ltv1*Δ*hsp104* thermotolerance. Cells were incubated at 39ºC to induce Hsp104p expression to protect against heatshock. Cells were then incubated at 52ºC for 0, 10, 20, 30 and 40 minutes and plated on YPD containing GdnHCl and TA, as indicated above for comparative growth analysis. Plates above were incubated at 30ºC for 48 hr.

In figure 4.30 it can be seen that Δ*yar1* appears to be hypersensitive to extreme temperatures (A), much moreso than Δ*ltv1*. With the exception of exposure to 3 mM GdnHCl (B), all other treatments seem to affect cell growth quite similarly (C-E). The naturally low level of Δ*yar1* thermotolerance is highly repressed by 3 mM GdnHCl.

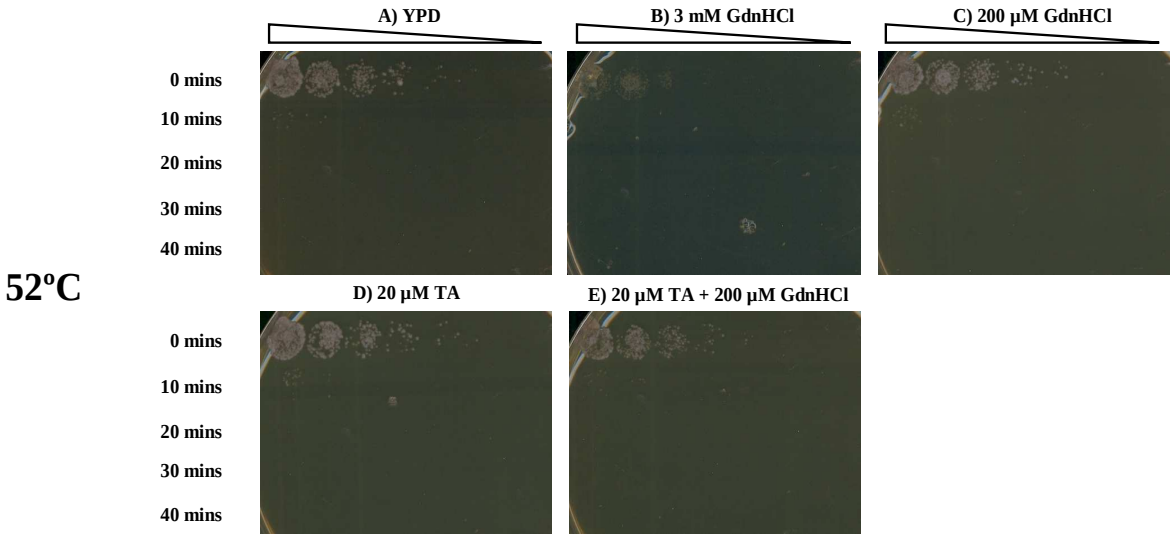

Figure 4.30 The effect of TA and GdnHCl on 74D Δ*yar1* thermotolerance. Cells were incubated at 39ºC to induce Hsp104p expression to protect against heatshock. Cells were then incubated at 52ºC for 0, 10, 20, 30 and 40 minutes and plated on YPD containing GdnHCl and TA, as indicated above for comparative growth analysis. Plates above were incubated at 30ºC for 48 hr.

Interestingly, it appears from figure 4.31, that in general, cells grow better when *HSP104* is deleted in the Δ*yar1* strain. While Δ*yar1* does not grow after 10 min. incubation at 52ºC, Δ*yar1*Δ*hsp104* does (A). Δ*yar1*Δ*hsp104* also grows better than Δ*yar1* under 3 mM GdnHCl exposure (B). A similar result was obtained for cells exposed to 20 µM TA and 200 µM GdnHCl after heatshock, as the double mutant consistently grew more strongly than Δ*yar1* (C-E). From this, there appears to be a positive genetic effect from the deletion of *HSP104* in Δ*yar1*.

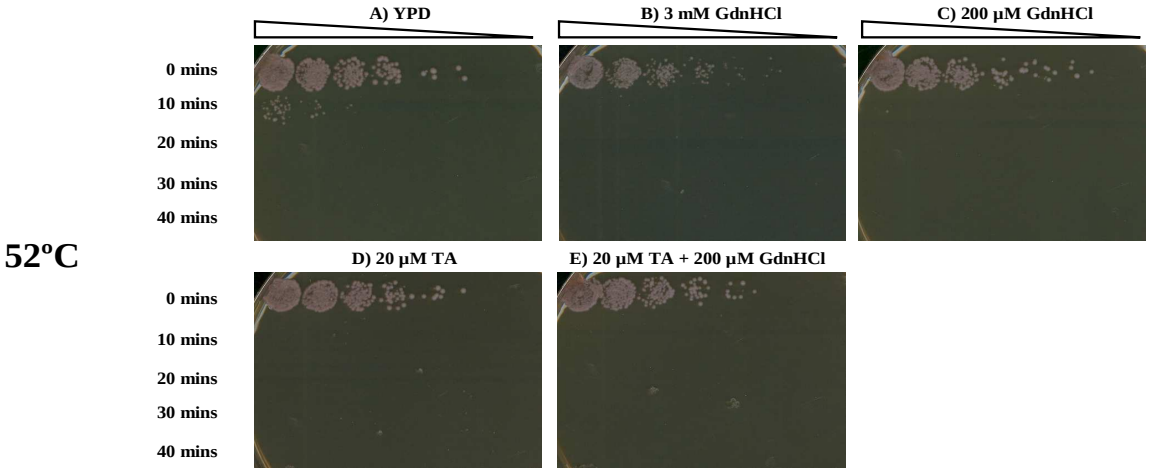

Figure 4.31 The effect of TA and GdnHCl on 74D Δ*yar1*Δ*hsp104* thermotolerance. Cells were incubated at 39ºC to induce Hsp104p expression to protect against heatshock. Cells were then incubated at 52ºC for 0, 10, 20, 30 and 40 minutes and plated on YPD containing GdnHCl and TA, as indicated above for comparative growth analysis. Plates above were incubated at 30ºC for 48 hr.

4.13 Assessing the effects of *YAR1* and *LTV1* deletion on heatshock recovery in yeast

Luciferase assays were performed to investigate how the absence of *LTV1* and *YAR1* effects yeast chaperone function. As chaperone activity, particularly that of Hsp104p, is essential in facilitating cellular recovery after heatshock, this particular aspect of chaperone function was examined.

pDCM90 is a *URA3*-based plasmid containing a gene for expression of a thermolabile bacterial luciferase and was used as a reporter vector allowing analysis of luciferase protein function after heatshock. Decanal is a substrate for bacterial luciferase and upon reaction light is emitted, which can can be measured using a luminometer. pDCM90 was transformed into strains used in this assay, which in culture were subsequently incubated at 37ºC to induce heatshock protein expression. Luciferase activity was measured at this point and taken to represent full protein activity. Cultures were then exposed to 45ºC to subject the cells to heatshock conditions, after which luciferase activity was measured again. Cells were incubated at 25ºC to allow recovery and luciferase activity measurements were taken at regular intervals.

Figure 4.32 shows the rate at which luciferase activity recovers over time after heatshock, reflecting the ability of chaperone proteins to refold luciferase into its functional state. In the absence of *LTV1*, luciferase activity recovers more rapidly, while recovery is fastest in the Δ*yar1* strain. This suggests that deletion of *LTV1* and *YAR1* has a positive effect on the chaperone protein activity and the ability of yeast cells to efficiently recover after thermostress. Cells deleted for *HSP104* are unable to recover luciferase function efficiently as Hsp104p plays an important role in yeast thermotolerance (Sanchez and Lindquist, 1990). As the absence of *LTV1* and *YAR1* have positive effects on luciferase activity recovery, it was anticipated that deletion of these genes in the Δ*hsp104* backgound would assist in compensating for the lack of Hsp104p, however this did not occur. Disruption of both *LTV1* and *YAR1* function appears to exacerbate the inability of Δ*hsp104* heatshock recovery. Although Δ*yar1* chaperone activity recovered most rapidly, that of Δ*yar1*Δ*hsp104* was the slowest to recover. Δ*ltv1* recovered second fastest and Δ*ltv1*Δ*hsp104* recovered second slowest.

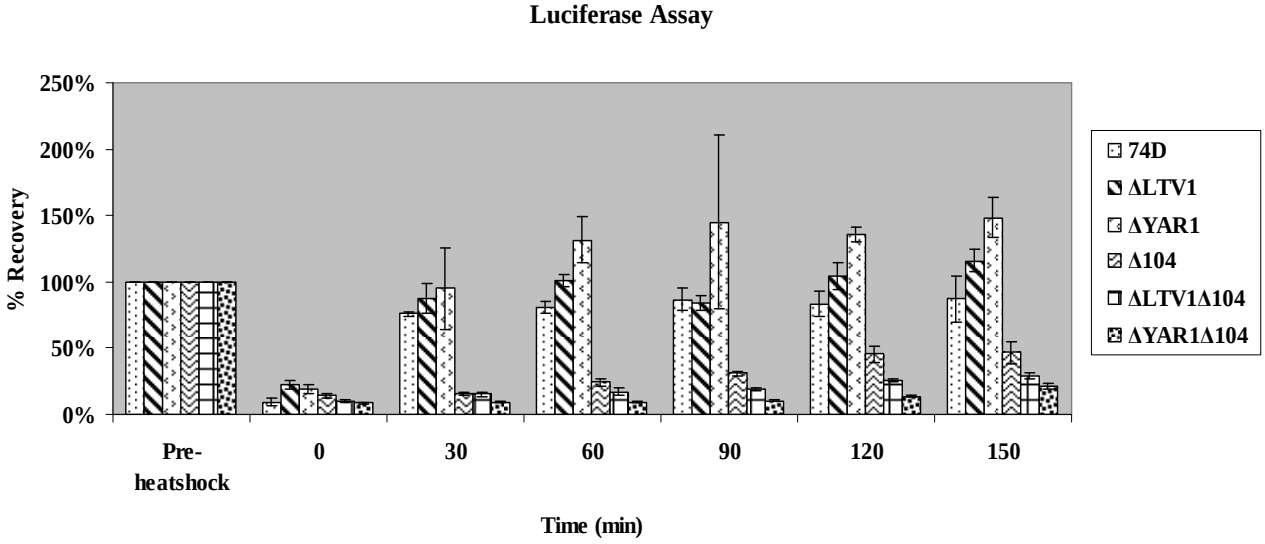

Figure 4.32 Luciferase assay for 74D and *HSP104*, *LTV1* and *YAR1* deletion strains. Student t-test determined that when comparing control and mutant strain recovery readings, $p<0.05$ for all but Δ*ltv1* at 30, 90 and 120 min., Δ*yar1* at 30 and 90 min. and Δ*ltv1*Δ*hsp104* at 0 min.

4.14 Analysis of 74D sensitivity to temperature change

Acquired thermotolerance assays performed suggested differences in G600 and 74D ability to grow at high temperatures. Comparative growth analyses were carried out and cells exposed to 30ºC, 37ºC and 39ºC were analysed (figure 4.33). This revealed that at 37ºC, 74D growth begins to falter. Although G600 grows well at 39ºC, it appears that 74D does not grow at all. It can thus be concluded that 74D is substantially more temperature sensitive (TS) than G600.

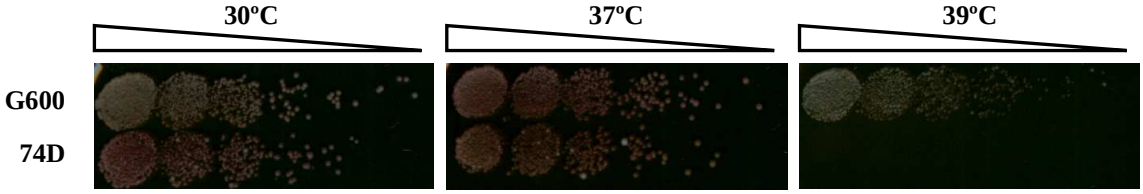

Figure 4.33 Comparative growth analysis of G600 and 74D on YPD at 30ºC, 37ºC and 39ºC. Plates above were incubated at the indicated temperature for 48 hr.

4.15 Identification of 74D single nucleotide polymorphisms (SNPs) and possible implications for temperature sensitivity

Next generation sequencing was performed to obtain data that might account for the high level of 74D temperature sensitivity. The genome sequence of 74D was retrieved and compared to the reference *S. cerevisiae* sequenced strain S288C (Fitzpatrick *et al.*, paper currently under review). Approximately 25,500 high quality SNPs were identified in strain 74D, equating to approximately 5,500 non-synonymous amino acid changes. A complete summary list of 74D SNPs, with corresponding amino acid changes, are shown in table 4.1.

Table 4.1 SNPs identified in 74D compared to reference strain S288C and corresponding amino acid changes. Gene information was obtained from www.yeastgenome.org (SGD).

Chromosome	Size (bp)	ORFs	Total number of SNPs	SNPs in ORFs	Non- synonymous amino acid changes
I	230,208	117	923	559	200
II	813,178	456	1443	955	309
III	316,616	183	614	306	122
IV	1,531,919	836	2243	1380	482
V	576,869	324	1156	590	193
VI	270,148	141	507	245	86
VII	1,090,947	583	2611	1588	627
VIII	562,643	321	1678	1080	386
IX	439,885	241	1907	1065	383
X	745,741	398	1284	808	310
XI	666,454	348	1925	1117	365
XII	1,078,175	578	1752	1118	342
XIII	924,429	505	1533	978	368
XIV	784,333	435	1846	1147	411
XV	1,091,289	598	2619	1659	566
XVI	948,062	510	1584	1007	361
mito	85,779	28	212	67	5
Totals	12,070,898	6,602	25,837	15,669	5,516

Many SNPs that led to non-synonymous changes were identified in chaperone and cochaperone proteins, as described in table 4.2. The extreme temperature sensitivity of 74D may be attributed to all or some of these mutations.

Table 4.2 Missense mutations in chaperone and cochaperones implicated in prion propagation. Gene functions were obtained from www.yeastgenome.org (SGD).

Gene name	Biological function[a]	Chromosomal SNP position(s)	Non-synonymous change(s)
SSA1	ATPase involved in protein folding and nuclear localization signal (NLS)-directed nuclear transport; member of heat shock protein 70 (Hsp70) family; forms a chaperone complex with Ydj1; localized to the nucleus, cytoplasm, and cell wall	141,186	A83G

HSF1	Trimeric heat shock transcription factor, activates multiple genes in response to stresses that include hyperthermia; recognizes variable heat shock elements (HSEs) consisting of inverted NGAAN repeats; posttranslationally regulated	369,170 369,356 369,366 369,603 369,669 369,884 370,320 370,350 370,644 370,650 370,740 371,247	D139N F201L T204M N283S S305I Q377K S522F P532L W630L N632S S662W A831V
CPR7	Peptidyl-prolyl cis-trans isomerase (cyclophilin), catalyzes the cis-trans isomerization of peptide bonds N-terminal to proline residues; binds to Hsp82 and contributes to chaperone activity	491,334 491,782	S87L L237F
YDJ1	Protein chaperone involved in regulation of the Hsp90 and Hsp70 functions; involved in protein translocation across membranes; member of the DnaJ family	507,059 506,921 506,907	P14S P60S D64E
APJ1	Putative chaperone of the HSP40 (DNAJ) family; overexpression interferes with propagation of the [*PSI*$^{+}$] prion	482,040 482,961	K217E D524N
STI1	Hsp90 cochaperone, interacts with the Ssa group of the cytosolic Hsp70 chaperones; activates the ATPase activity of Ssa1; homolog of mammalian Hop protein	381,777	K242R
SSE1	ATPase that is a component of the heat shock protein Hsp90 chaperone complex; binds unfolded proteins; member of the heat shock protein 70 (Hsp70) family; localized to the cytoplasm	350,651	G541A
HSP82	Hsp90 chaperone required for pheromone signaling and negative regulation of Hsf1; docks with Tom70 for mitochondrial preprotein delivery; promotes telomerase DNA binding and nucleotide addition	97,732	N298K

4.16 Exploration for genes that confer 74D thermotolerance

A high-copy plasmid screen was carried out in an attempt to identify genes that when overexpressed confer increased thermotolerance to 74D and overcome the extreme temperature sensitivity exhibited by the strain. High-copy yEP13 plasmids were transformed into 74D and cells were grown at 39ºC. Transformants were isolated that possessed the ability to grow at this temperature, as illustrated in figure 4.34.

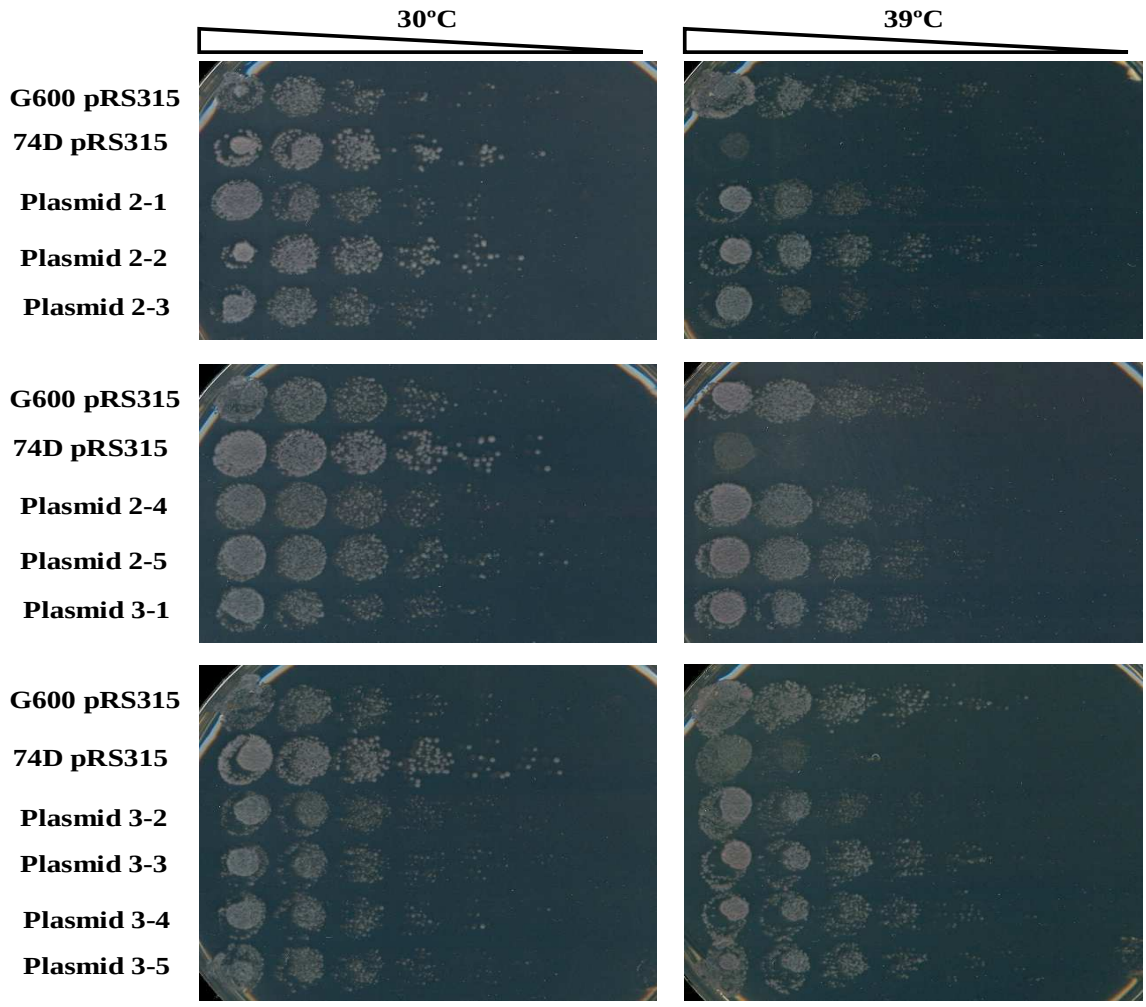

Figure 4.34 Comparative growth analysis representing strains that retain the capacity to survive at 39ºC as a result of high-copy plasmid. Plates were incubated at 30ºC for 48 hr. Ten strains transformed with high-copy plasmids demonstrate ability to grow at 39ºC, unlike 74D.

The transformants that grew well when containing the high-copy yEP13 plasmid were isolated and the plasmids were extracted. These plasmids were Agowa sequenced to determine what genes they contained. The plasmids were sequenced from the ends

inwards to obtain sequence data for the fragment of interest on the plasmid, results for which are illustrated in figure 4.35.

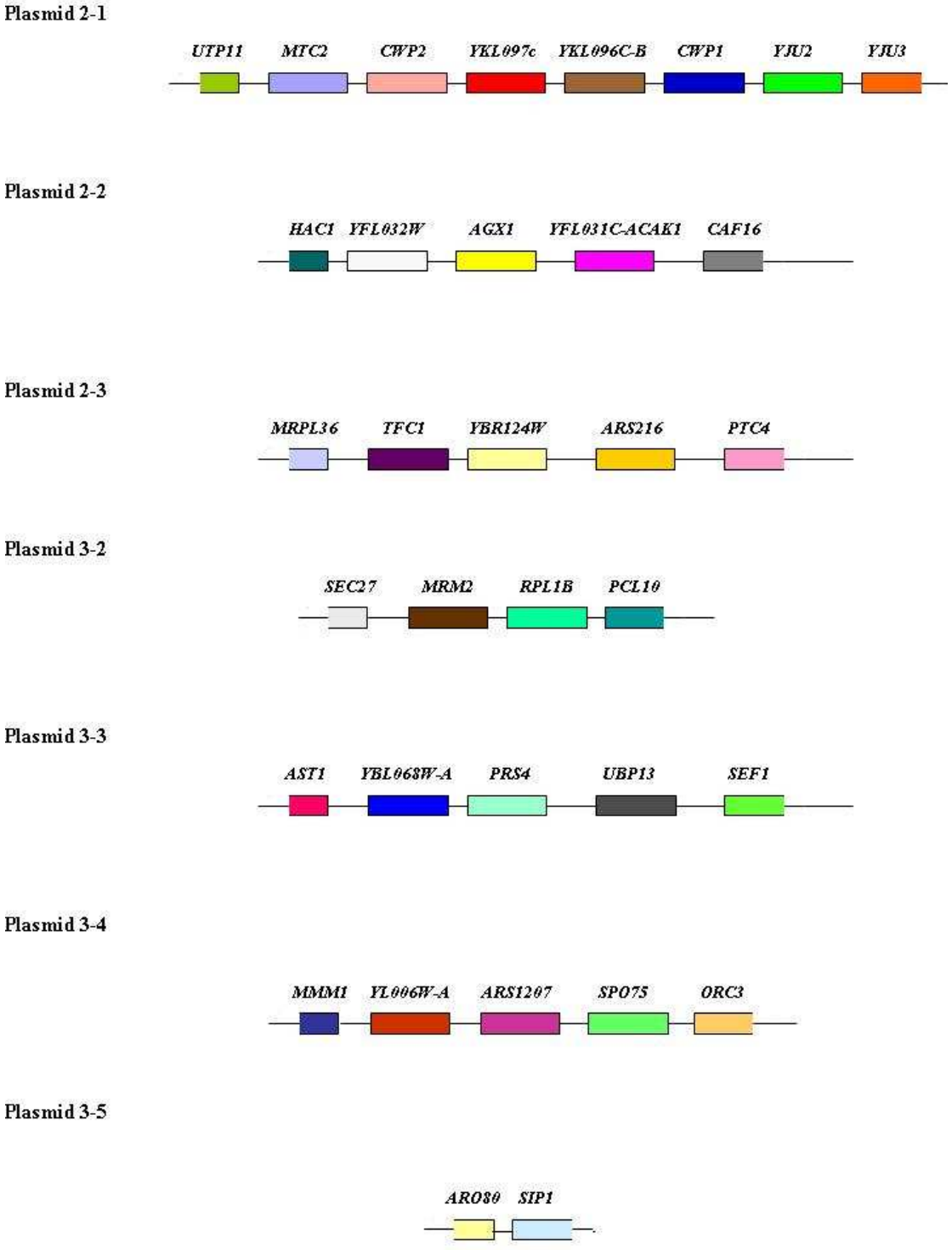

Figure 4.35 Genes encoded that when overexpressed may contribute to the abolition of 74D temperature sensitivity.

As illustrated in figure 4.35, there is no overlap of genes that appear to encode products that overcome temperature sensitivity. Each plasmid when sequenced was found to contain a different variety of genes. This suggests that the temperature sensitivity of 74D is complexely attributed to a range of factors. Due to the diversity of plasmid sequencing results, no further work could be carried out.

4.17 Comparative expression analysis of heat-shock proteins produced by G600 and 74D using Western Blot analysis

Western blot analysis was carried out to compare the levels of Hsp70p and Hsp104p expressed by G600 and 74D. The effects of 1 hr. 37ºC and 39ºC exposures on protein expression were also analysed (figure 4.36).

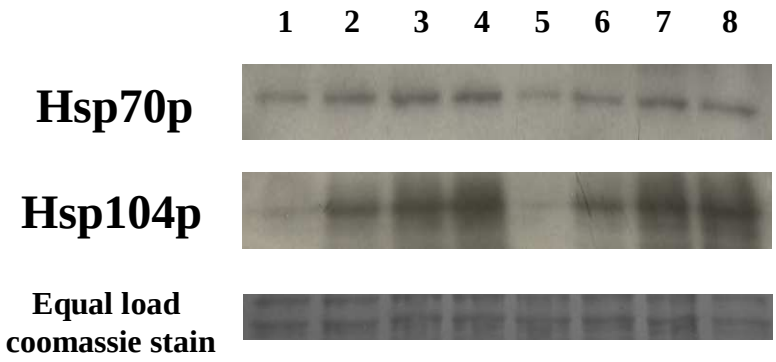

Figure 4.36 Western blot illustrating the expression of Hsp70p (Ssa1p) and Hsp104p in response to increased temperatures. 1 = G600 Δ*hsp104* 30ºC incubation, 2 = G600 30ºC incubation, 3 = G600 30ºC incubation 37ºC last 1 hr, 4 = G600 30ºC incubation 39ºC last 1 hr, 5 = 74D Δ*hsp104* 30ºC incubation, 6 = 74D 30ºC incubation, 7 = 74D 30ºC incubation 37ºC last 1 hr, 8 = 74D 30ºC incubation 39ºC last 1 hr.

Figure 4.36 demonstrates that 74D expresses a lower basal level of both Hsp70p and Hsp104p than G600. When heat-shock proteins are induced by elevated temperatures, both strains produce an augmented level of both Hsp70p and Hsp104p. It appears that under incubation at higher temperatures G600 expresses more Hsp70p than 74D, and a similar level of Hsp104p.

Section 2: Investigation into the yeast global expressional response to the prion-curing agent Tacrine

4.18 Investigation into the global expressional response of *S. cerevisiae* to TA exposure

In order to further understand the way in which yeast respond to the prion-curing drug TA, we assessed the global transcriptional and proteomic responses, employing RNA sequencing and two-dimensional gel electrophoresis techniques. Since we have shown that in wild-type cells, TA requires the presence of GdnHCl to induce an effect, the cellular response to GdnHCl alone and in combination with TA was explored.

4.18.1 Using transcriptomics to assess the *S. cerevisiae* response to TA

RNA sequencing analysis was carried out on G600 cells and data obtained was compared

1. From untreated samples
2. From samples treated with 200 µM GdnHCl for 14 generations
3. From samples treated with 200 µM GdnHCl + 20 µM Tacrine for 14 generations

and

4. From untreated samples
5. From samples treated with 200 µM GdnHCl + 20 µM Tacrine for 1 hr
6. From samples treated with 200 µM GdnHCl + 20 µM Tacrine for 3 hr

As for the gliotoxin response data, for each treatment, genes were first grouped into those upregulated and downregulated, and then sub-grouped depending on their fold change. Genes that displayed >2-fold increase or decrease in expression were further assessed. Genes were assigned gene ontology (GO) Identities reflective of the gene function and most were designated more than one GO Identity due to multiple functions. Go identities are listed in table 3.4.

Thus, each gene was categorised respective to its biological and molecular functions, in addition to the cellular component affected by the expression of the gene. Analysis was then carried out to determine the most common GO Identities for each category,

associated with genes that have >2-fold up- or downregulation in response to each treatment.

4.18.1.1 Analysis of the effect of 200 µM GdnHCl exposure for 14 generations on yeast cells

When yeast cells were treated for 14 generations with 200 µM GdnHCl, 134 genes were upregulated in excess of 2-fold, 23 of them more than 3-fold. 1175 genes were downregulated more than 2-fold, 542 of these over 3-fold. The figures below illustrate the cellular components, molecular functions and biological processes stimulated or repressed by GdnHCl exposure and the percentages of total changes they represent.

Summary of the overall effects of gene upregulation on cells

Figures 4.37-4.39 illustrate the overall effects on cells induced by genes upregulated more than 2-fold in response to 200 µM GdnHCl exposure.

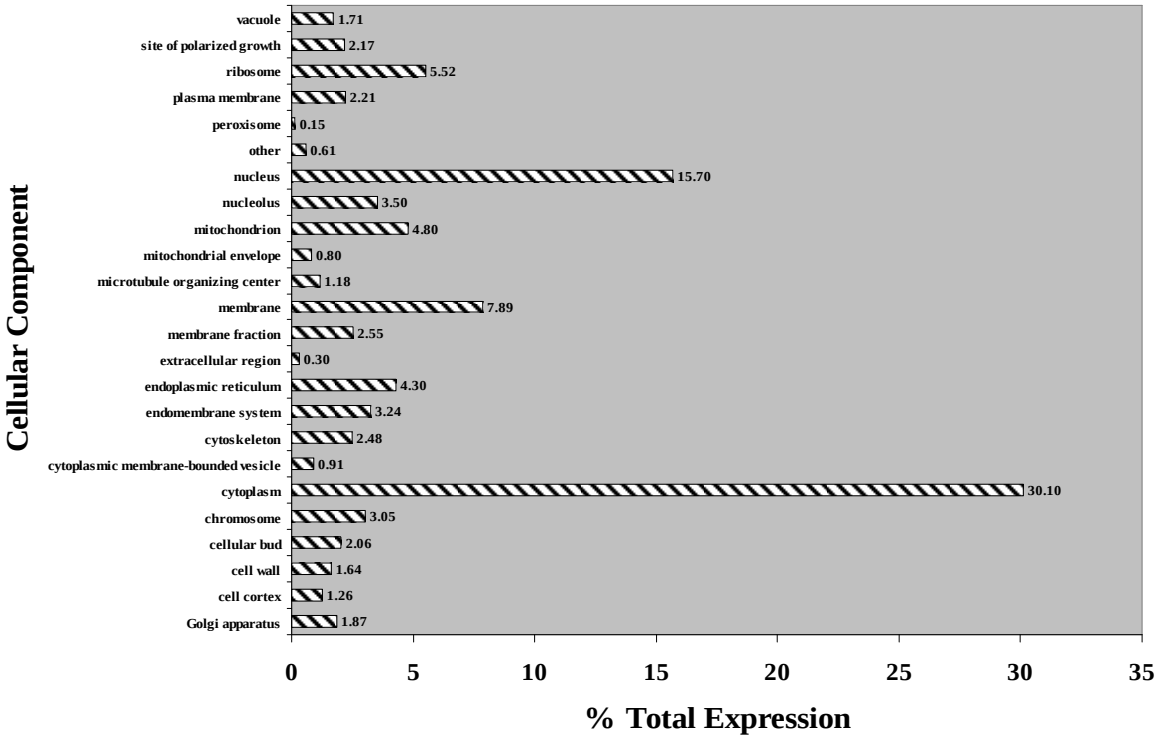

Figure 4.37 The percentage of each cellular component category (200 µM GdnHCl 14 generation upregulated genes). Genes upregulated more than two-fold were assigned cellular component categories. The number of genes in each category was expressed as a percentage of the number of total genes.

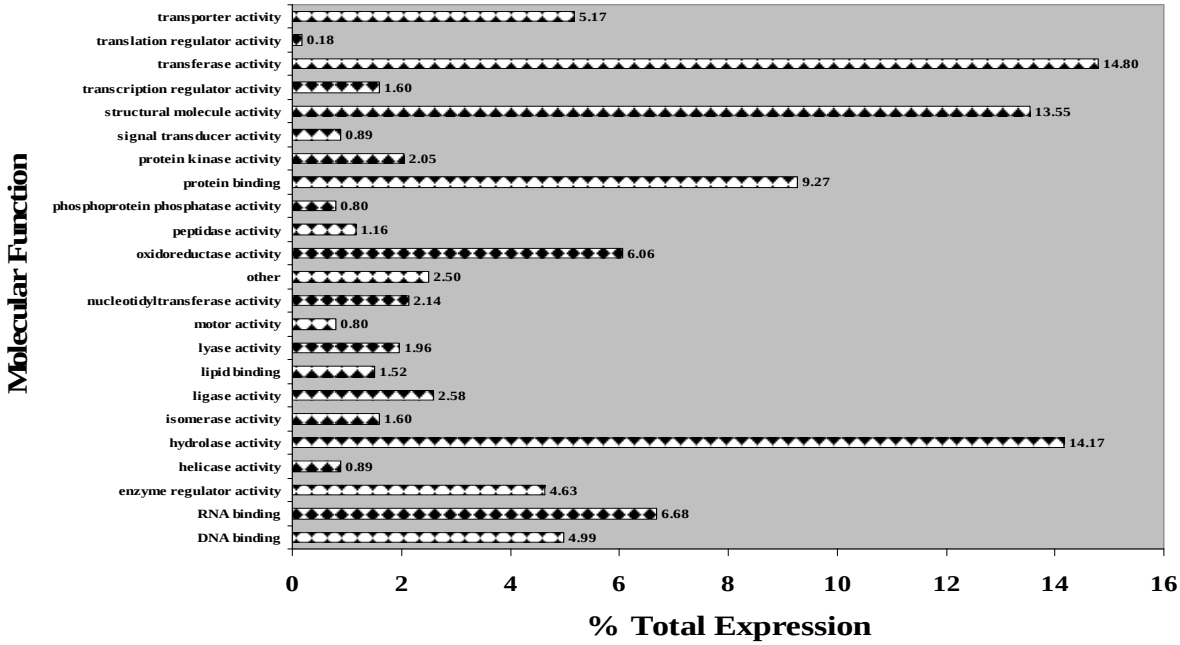

Figure 4.38 The percentage of each molecular function category (200 µM GdnHCl 14 generation upregulated genes). Genes upregulated more than two-fold were assigned molecular function categories. The number of genes in each category was expressed as a percentage of the number of total genes.

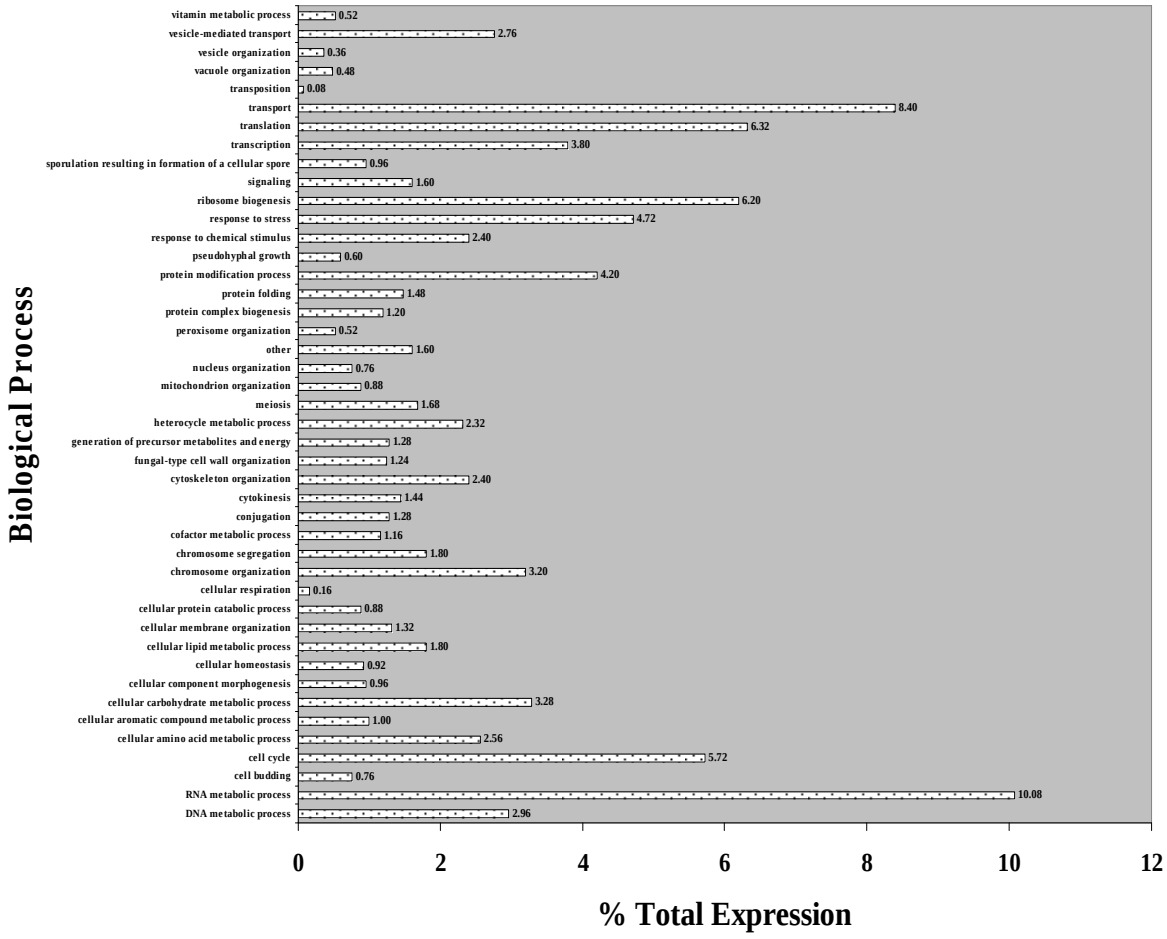

Figure 4.39 The percentage of each biological process category (200 µM GdnHCl 14 generation upregulated genes). Genes upregulated more than two-fold were assigned biological process categories. The number of genes in each category was expressed as a percentage of the number of total genes.

The five biological processes, molecular functions and associated cellular components most highly stimulated by 200 µM GdnHCl were further grouped. These are illustrated in figures 4.40-4.42.

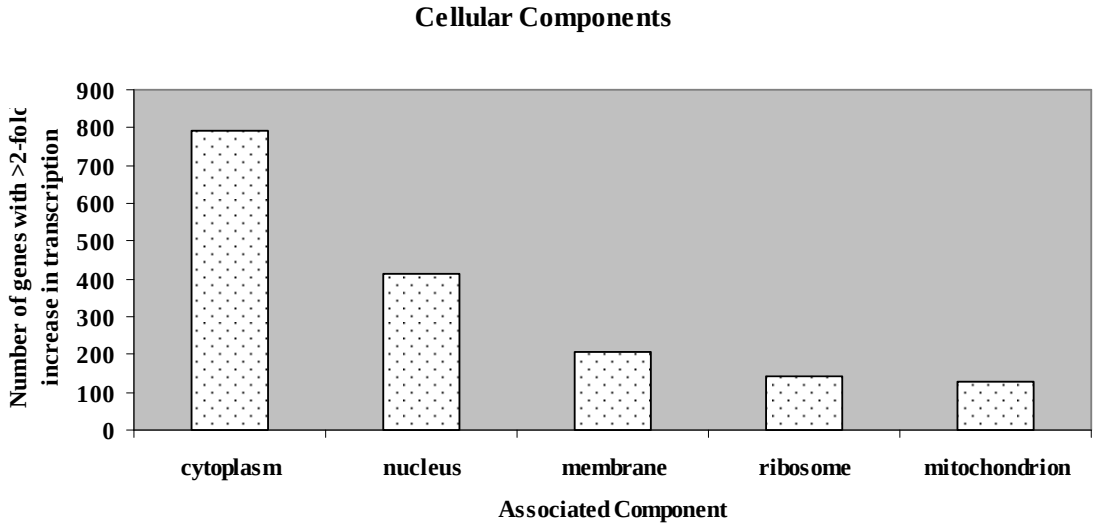

Figure 4.40 The five associated cellular components most highly upregulated by exposure to 200 µM GdnHCl for 14 generations.

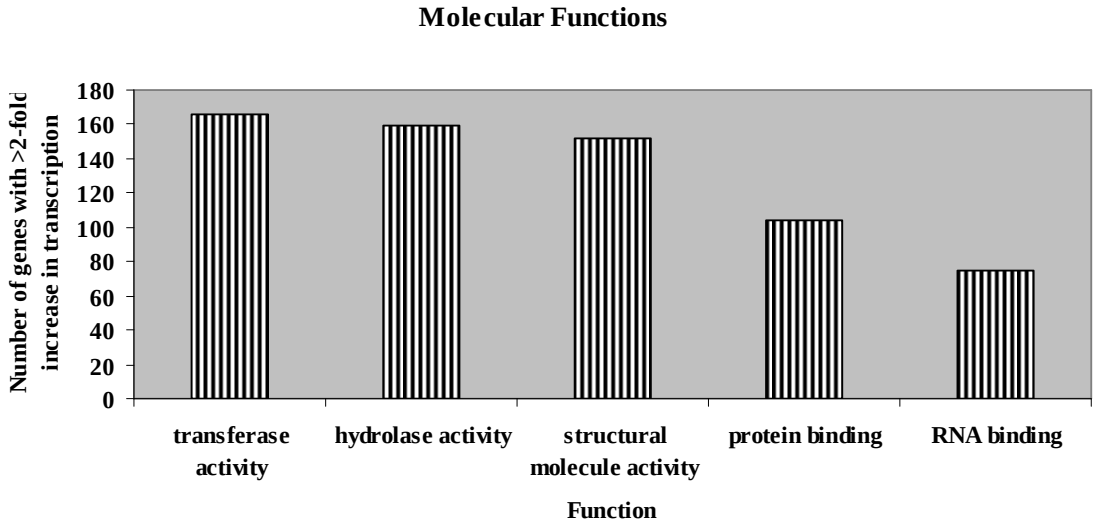

Figure 4.41 The five molecular functions most highly upregulated by exposure to 200 µM GdnHCl for 14 generations.

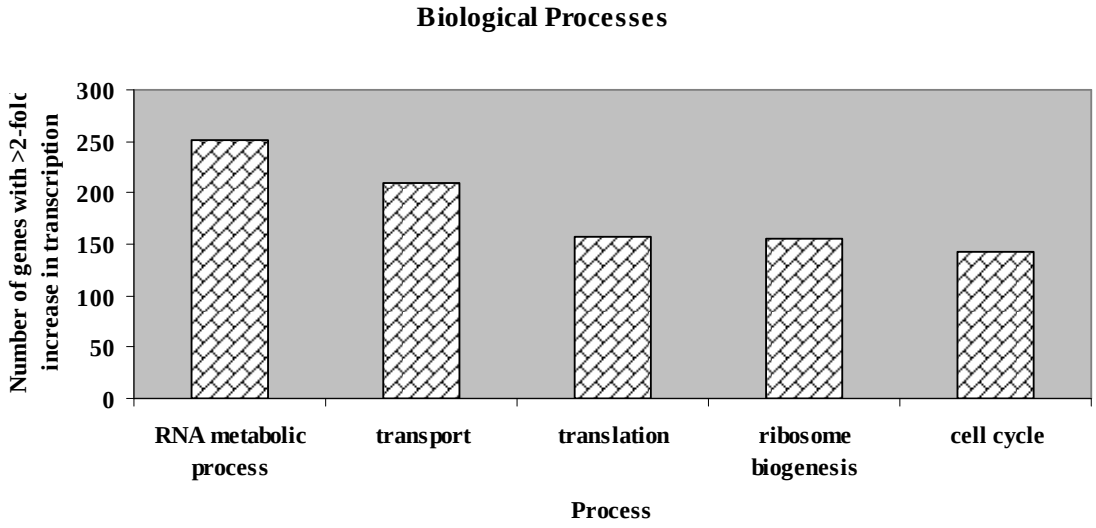

Figure 4.42 The five biological processes most highly upregulated by exposure to 200 µM GdnHCl for 14 generations.

Table 4.3 lists the fifty individual genes, and their respective functions, that underwent the highest increase in transcription in response to 200 µM GdnHCl.

Table 4.3 The fifty genes most highly upregulated in response to 200 µM GdnHCl exposure for 14 generations. Gene functions were obtained from www.yeastgenome.org (SGD).

Gene	Fold Change	Gene Function
OLE1	10.73	Delta(9) fatty acid desaturase, required for monounsaturated fatty acid synthesis and for normal distribution of mitochondria
MLS1	6.17	Malate synthase, enzyme of the glyoxylate cycle, involved in utilization of non-fermentable carbon sources; expression is subject to carbon catabolite repression; localizes in peroxisomes during growth in oleic acid medium
IZH4	6.17	Membrane protein involved in zinc ion homeostasis, member of the four-protein IZH family, expression induced by fatty acids and altered zinc levels; deletion reduces sensitivity to excess zinc; possible role in sterol metabolism
IZH1	5.90	Membrane protein involved in zinc ion homeostasis, member of the four-protein IZH family; transcription is regulated directly by Zap1p, expression induced by zinc deficiency and fatty acids; deletion increases sensitivity to elevated zinc
FBP1	5.09	Fructose-1,6-bisphosphatase, key regulatory enzyme in the gluconeogenesis pathway, required for glucose metabolism; undergoes either proteasome-mediated or autophagy-mediated degradation depending on growth conditions; interacts with Vid30p
PCK1	4.81	Phosphoenolpyruvate carboxykinase, key enzyme in gluconeogenesis, catalyzes early reaction in carbohydrate biosynthesis, glucose represses transcription and accelerates mRNA degradation, regulated by Mcm1p and Cat8p, located in the cytosol

CUP1-1	4.38	Metallothionein, binds copper and mediates resistance to high concentrations of copper and cadmium; locus is variably amplified in different strains, with two copies, CUP1-1 and CUP1-2, in the genomic sequence reference strain S288C
CUP1-2	4.38	Metallothionein, binds copper and mediates resistance to high concentrations of copper and cadmium; locus is variably amplified in different strains, with two copies, CUP1-1 and CUP1-2, in the genomic sequence reference strain S288C
FDH1	4.13	NAD(+)-dependent formate dehydrogenase, may protect cells from exogenous formate
SMF2	3.74	Divalent metal ion transporter involved in manganese homeostasis; has broad specificity for di-valent and tri-valent metals; post-translationally regulated by levels of metal ions; member of the Nramp family of metal transport proteins
SDS23	3.66	One of two S. cerevisiae homologs (Sds23p and Sds24p) of the S. pombe Sds23 protein, which is implicated in APC/cyclosome regulation; involved in cell separation during budding
PHO89	3.47	Na+/Pi cotransporter, active in early growth phase; similar to phosphate transporters of Neurospora crassa; transcription regulated by inorganic phosphate concentrations and Pho4p
ACC1	3.42	Acetyl-CoA carboxylase, biotin containing enzyme that catalyzes the carboxylation of acetyl-CoA to form malonyl-CoA; required for de novo biosynthesis of long-chain fatty acids
YAR035C-A	3.42	Putative protein of unknown function; identified by gene-trapping, microarray-based expression analysis, and genome-wide homology searching; predicted to have a role in cell budding based on computational "guilt by association" analysis
JEN1	3.27	Lactate transporter, required for uptake of lactate and pyruvate; phosphorylated; expression is derepressed by transcriptional activator Cat8p during respiratory growth, and repressed in the presence of glucose, fructose, and mannose
ATO2	3.25	Putative transmembrane protein involved in export of ammonia, a starvation signal that promotes cell death in aging colonies; phosphorylated in mitochondria; member of the TC 9.B.33 YaaH family; homolog of Ady2p and Y. lipolytica Gpr1p
YAT1	3.25	Outer mitochondrial carnitine acetyltransferase, minor ethanol-inducible enzyme involved in transport of activated acyl groups from the cytoplasm into the mitochondrial matrix; phosphorylated
MRPL38	3.17	Mitochondrial ribosomal protein of the large subunit; appears as two protein spots (YmL34 and YmL38) on two-dimensional SDS gels
YDL012C	3.13	Tail-anchored plasma membrane protein containing a conserved CYSTM module, possibly involved in response to stress; may contribute to non-homologous end-joining (NHEJ) based on ydl012c htz1 double null phenotype
CEM1	3.11	Mitochondrial beta-keto-acyl synthase with possible role in fatty acid synthesis; required for mitochondrial respiration
ACH1	3.06	Protein with CoA transferase activity, particularly for CoASH transfer from succinyl-CoA to acetate; has minor acetyl-CoA-hydrolase activity; phosphorylated; required for acetate utilization and for diploid pseudohyphal growth
GDH3	3.04	NADP(+)-dependent glutamate dehydrogenase, synthesizes glutamate from ammonia and alpha-ketoglutarate; rate of alpha-ketoglutarate utilization differs from Gdh1p; expression regulated by nitrogen and carbon sources
IDP2	3.04	Cytosolic NADP-specific isocitrate dehydrogenase, catalyzes oxidation of isocitrate to alpha-ketoglutarate; levels are elevated during growth on non-fermentable carbon sources

		and reduced during growth on glucose
ALT1	2.95	Alanine transaminase (glutamic pyruvic transaminase); involved in alanine biosynthetic and catabolic processes; the authentic, non-tagged protein is detected in highly purified mitochondria in high-throughput studies
MIR1	2.95	Mitochondrial phosphate carrier, imports inorganic phosphate into mitochondria; functionally redundant with Pic2p but more abundant than Pic2p under normal conditions; phosphorylated
NPL3	2.93	RNA-binding protein that promotes elongation, regulates termination, and carries poly(A) mRNA from nucleus to cytoplasm; required for pre-mRNA splicing; dissociation from mRNAs promoted by Mtr10p; phosphorylated by Sky1p in the cytoplasm
YOR084W	2.90	Oleic acid-inducible, peroxisomal matrix localized lipase; transcriptionally activated by Yrm1p along with genes involved in multidrug resistance; peroxisomal import is dependent on the PTS1 receptor, Pex5p and on self-interaction
ICL1	2.88	Isocitrate lyase, catalyzes the formation of succinate and glyoxylate from isocitrate, a key reaction of the glyoxylate cycle; expression of ICL1 is induced by growth on ethanol and repressed by growth on glucose
GLC3	2.88	Glycogen branching enzyme, involved in glycogen accumulation; green fluorescent protein (GFP)-fusion protein localizes to the cytoplasm in a punctate pattern
AGP1	2.86	Low-affinity amino acid permease with broad substrate range, involved in uptake of asparagine, glutamine, and other amino acids; expression is regulated by the SPS plasma membrane amino acid sensor system (Ssy1p-Ptr3p-Ssy5p)
IZH3	2.84	Membrane protein involved in zinc ion homeostasis, member of the four-protein IZH family, expression induced by zinc deficiency; deletion reduces sensitivity to elevated zinc and shortens lag phase, overexpression reduces Zap1p activity
ADR1	2.83	Carbon source-responsive zinc-finger transcription factor, required for transcription of the glucose-repressed gene ADH2, of peroxisomal protein genes, and of genes required for ethanol, glycerol, and fatty acid utilization
DLD1	2.83	D-lactate dehydrogenase, oxidizes D-lactate to pyruvate, transcription is heme-dependent, repressed by glucose, and derepressed in ethanol or lactate; located in the mitochondrial inner membrane
RPN4	2.77	Transcription factor that stimulates expression of proteasome genes; Rpn4p levels are in turn regulated by the 26S proteasome in a negative feedback control mechanism; RPN4 is transcriptionally regulated by various stress responses
REG2	2.76	Regulatory subunit of the Glc7p type-1 protein phosphatase; involved with Reg1p, Glc7p, and Snf1p in regulation of glucose-repressible genes, also involved in glucose-induced proteolysis of maltose permease
YER185W	2.70	Plasma membrane protein with roles in the uptake of protoprophyrin IX and the efflux of heme; expression is induced under both low-heme and low-oxygen conditions; member of the fungal lipid-translocating exporter (LTE) family of proteins
MSK1	2.68	Mitochondrial lysine-tRNA synthetase, required for import of both aminoacylated and deacylated forms of tRNA(Lys) into mitochondria and for aminoacylation of mitochondrially encoded tRNA(Lys)
FAA4	2.68	Long chain fatty acyl-CoA synthetase, activates imported fatty acids with a preference for C12:0-C16:0 chain lengths; functions in long chain fatty acid import; important for survival during stationary phase; localized to lipid particles

YLR162W	2.67	Putative protein of unknown function; overexpression confers resistance to the antimicrobial peptide MiAMP1
CRC1	2.65	Mitochondrial inner membrane carnitine transporter, required for carnitine-dependent transport of acetyl-CoA from peroxisomes to mitochondria during fatty acid beta-oxidation
IXR1	2.65	Protein that binds DNA containing intrastrand cross-links formed by cisplatin, contains two HMG (high mobility group box) domains, which confer the ability to bend cisplatin-modified DNA; mediates aerobic transcriptional repression of COX5b
HTA1	2.64	Histone H2A, core histone protein required for chromatin assembly and chromosome function; one of two nearly identical subtypes (see also HTA2); DNA damage-dependent phosphorylation by Mec1p facilitates DNA repair; acetylated by Nat4p
SFC1	2.64	Mitochondrial succinate-fumarate transporter, transports succinate into and fumarate out of the mitochondrion; required for ethanol and acetate utilization
GCV1	2.61	T subunit of the mitochondrial glycine decarboxylase complex, required for the catabolism of glycine to 5,10-methylene-THF; expression is regulated by levels of levels of 5,10-methylene-THF in the cytoplasm
RKI1	2.60	Ribose-5-phosphate ketol-isomerase, catalyzes the interconversion of ribose 5-phosphate and ribulose 5-phosphate in the pentose phosphate pathway; participates in pyridoxine biosynthesis
CYC1	2.60	Cytochrome c, isoform 1; electron carrier of the mitochondrial intermembrane space that transfers electrons from ubiquinone-cytochrome c oxidoreductase to cytochrome c oxidase during cellular respiration
COX7	2.58	Subunit VII of cytochrome c oxidase, which is the terminal member of the mitochondrial inner membrane electron transport chain
SCS7	2.57	Sphingolipid alpha-hydroxylase, functions in the alpha-hydroxylation of sphingolipid-associated very long chain fatty acids, has both cytochrome b5-like and hydroxylase/desaturase domains, not essential for growth
ODC1	2.56	Mitochondrial inner membrane transporter, exports 2-oxoadipate and 2-oxoglutarate from the mitochondrial matrix to the cytosol for lysine and glutamate biosynthesis and lysine catabolism; suppresses, in multicopy, an fmc1 null mutation
NAB2	2.56	Nuclear polyadenylated RNA-binding protein required for nuclear mRNA export and poly(A) tail length control; binds nuclear pore protein Mlp1p; autoregulates mRNA levels; related to human hnRNPs; nuclear localization sequence binds Kap104p

Summary of the overall effects of gene downregulation on cells

Figures 4.43-4.45 illustrate the overall effects on cells induced by genes downregulated more than 2-fold in response to 200 µM GdnHCl exposure.

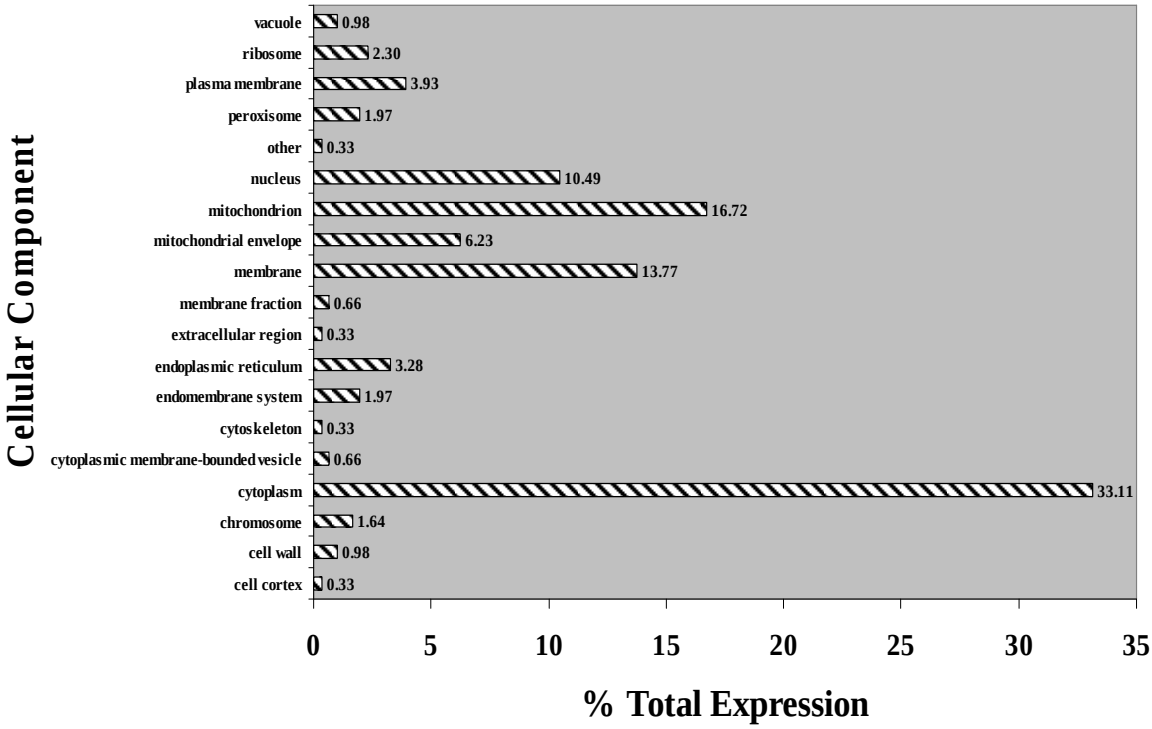

Figure 4.43 The percentage of each cellular component category (200 µM GdnHCl 14 generation downregulated genes). Genes downregulated more than two-fold were assigned cellular component categories. The number of genes in each category was expressed as a percentage of the number of total genes.

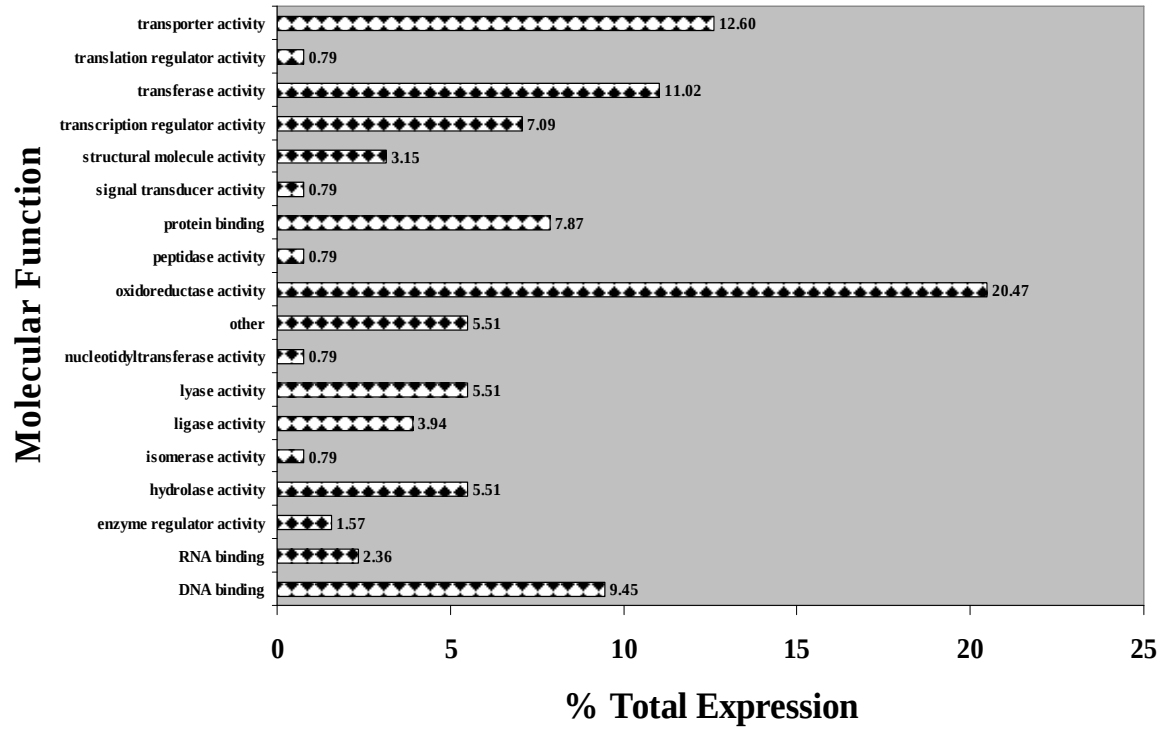

Figure 4.44 The percentage of each molecular function category (200 µM GdnHCl 14 generation downregulated genes). Genes downregulated more than two-fold were assigned molecular function categories. The number of genes in each category was expressed as a percentage of the number of total genes.

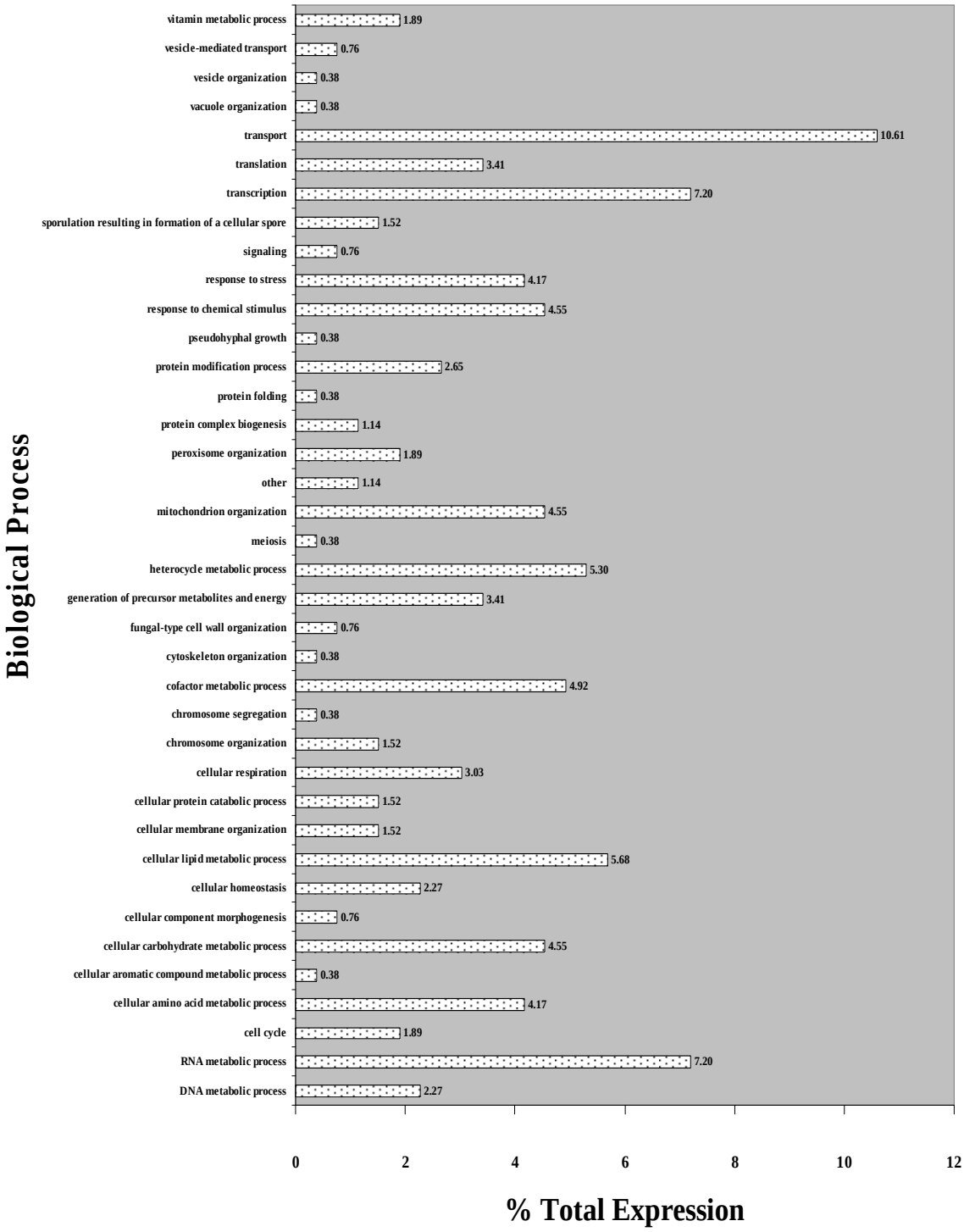

Figure 4.45 The percentage of each biological process category (200 µM GdnHCl 14 generation downregulated genes). Genes downregulated more than two-fold were assigned biological process categories. The number of genes in each category was expressed as a percentage of the number of total genes.

The five most transcriptionally repressed biological processes, molecular functions and associated cellular components are depicted in figures 4.46-4.48.

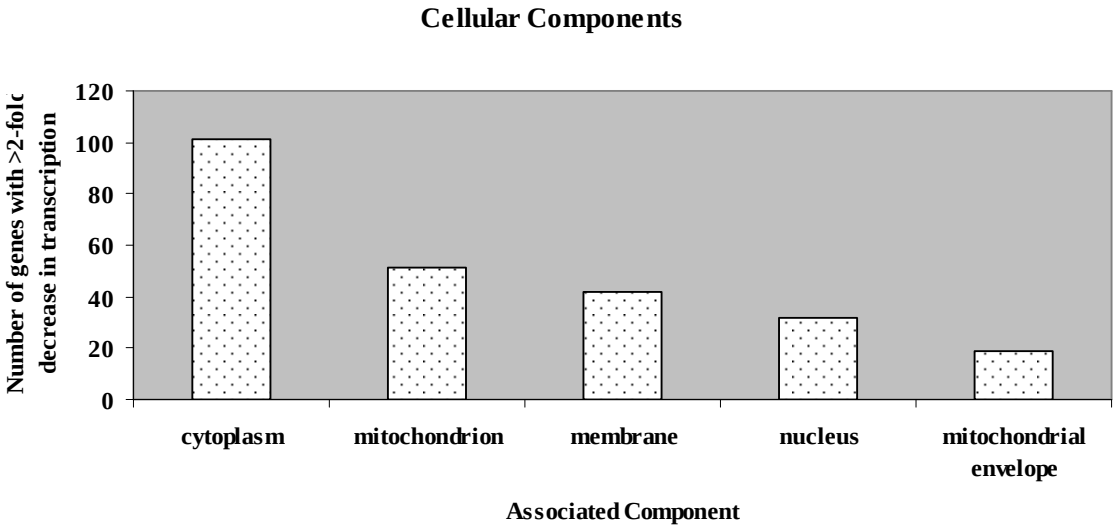

Figure 4.46 The five associated cellular components most highly downregulated by exposure to 200 µM GdnHCl for 14 generations.

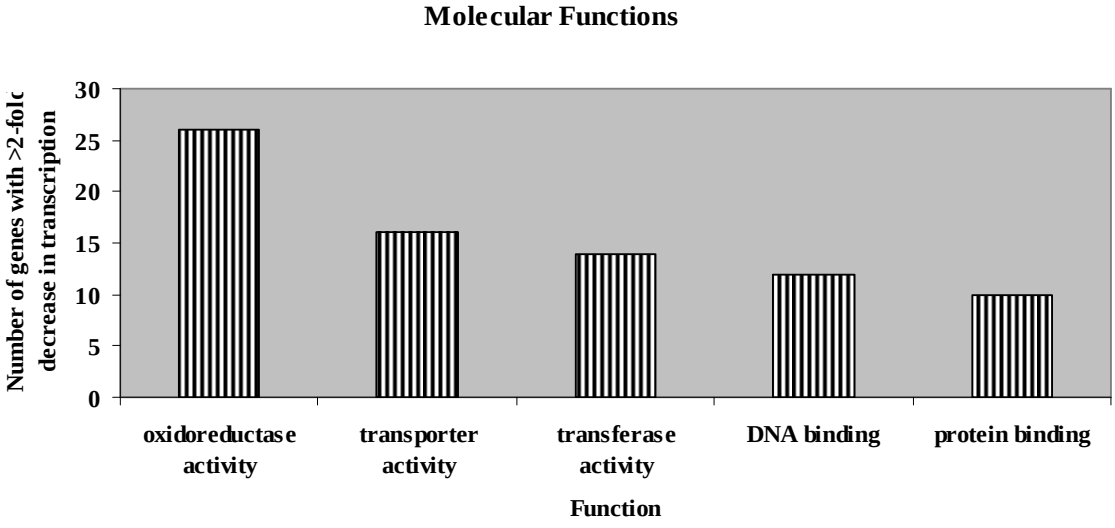

Figure 4.47 The five molecular functions most highly downregulated by exposure to 200 µM GdnHCl for 14 generations.

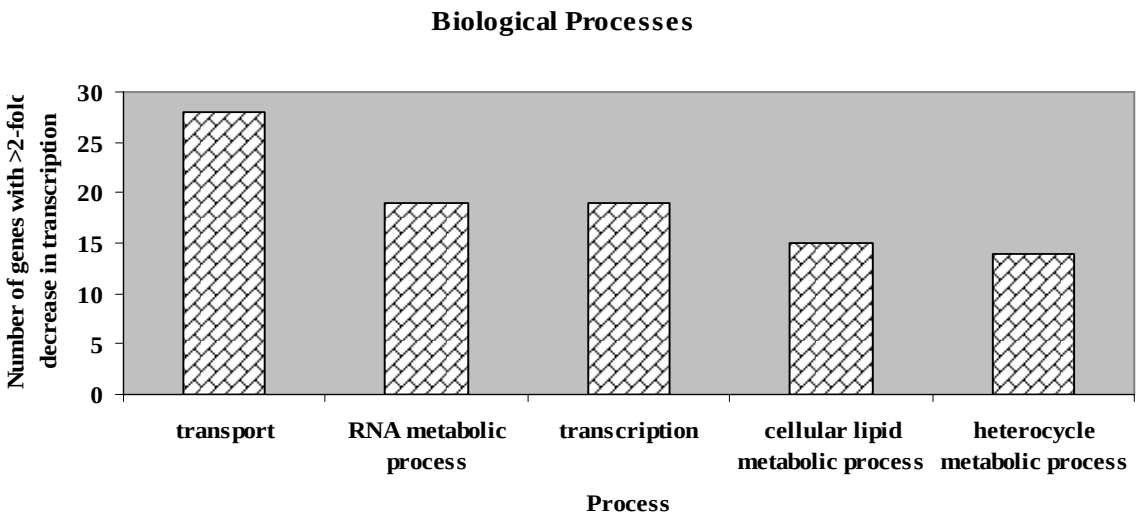

Figure 4.48 The five biological processes most highly downregulated by exposure to 200 µM GdnHCl for 14 generations.

Table 4.4 lists the fifty individual genes, and their respective functions, that underwent the most acute decrease in transcription in response to 14 generation 200 µM GdnHCl exposure.

Table 4.4 The fifty genes most highly downregulated in response to 200 µM GdnHCl exposure for 14 generations. Gene functions were obtained from www.yeastgenome.org (SGD).

Gene	Fold Change	Gene Function
PMA1	-58.90	Plasma membrane H+-ATPase, pumps protons out of the cell; major regulator of cytoplasmic pH and plasma membrane potential; part of the P2 subgroup of cation-transporting ATPases
HXT4	-27.44	High-affinity glucose transporter of the major facilitator superfamily, expression is induced by low levels of glucose and repressed by high levels of glucose
ENO2	-25.37	Enolase II, a phosphopyruvate hydratase that catalyzes the conversion of 2-phosphoglycerate to phosphoenolpyruvate during glycolysis and the reverse reaction during gluconeogenesis; expression is induced in response to glucose
PGK1	-24.49	3-phosphoglycerate kinase, catalyzes transfer of high-energy phosphoryl groups from the acyl phosphate of 1,3-bisphosphoglycerate to ADP to produce ATP; key enzyme in glycolysis and gluconeogenesis
RPS22A	-23.82	Protein component of the small (40S) ribosomal subunit; nearly identical to Rps22Bp and has similarity to E. coli S8 and rat S15a ribosomal proteins
TOS4	-23.17	Forkhead Associated domain containing protein and putative transcription factor found associated with chromatin; target of SBF transcription factor; expression is periodic and peaks in G1; similar to PLM2

BSC1	-21.17	Protein of unconfirmed function, similar to cell surface flocculin Muc1p; ORF exhibits genomic organization compatible with a translational readthrough-dependent mode of expression
YGR272C	-19.46	Essential protein required for maturation of 18S rRNA; null mutant is sensitive to hydroxyurea and is delayed in recovering from alpha-factor arrest; green fluorescent protein (GFP)-fusion protein localizes to the nucleolus
PCL1	-19.44	Cyclin, interacts with cyclin-dependent kinase Pho85p; member of the Pcl1,2-like subfamily, involved in the regulation of polarized growth and morphogenesis and progression through the cell cycle; localizes to sites of polarized cell growth
DCD1	-19.28	Deoxycytidine monophosphate (dCMP) deaminase required for dCTP and dTTP synthesis; expression is NOT cell cycle regulated
EXG1	-18.74	Major exo-1,3-beta-glucanase of the cell wall, involved in cell wall beta-glucan assembly; exists as three differentially glycosylated isoenzymes
GPM1	-17.48	Tetrameric phosphoglycerate mutase, mediates the conversion of 3-phosphoglycerate to 2-phosphoglycerate during glycolysis and the reverse reaction during gluconeogenesis
INM1	-16.58	Inositol monophosphatase, involved in biosynthesis of inositol and in phosphoinositide second messenger signaling; INM1 expression increases in the presence of inositol and decreases upon exposure to antibipolar drugs lithium and valproate
HXK2	-16.45	Hexokinase isoenzyme 2 that catalyzes phosphorylation of glucose in the cytosol; predominant hexokinase during growth on glucose; functions in the nucleus to repress expression of HXK1 and GLK1 and to induce expression of its own gene
AAC3	-16.07	Mitochondrial inner membrane ADP/ATP translocator, exchanges cytosolic ADP for mitochondrially synthesized ATP; expressed under anaerobic conditions; similar to Pet9p and Aac1p; has roles in maintenance of viability and in respiration
PDC1	-15.70	Major of three pyruvate decarboxylase isozymes, key enzyme in alcoholic fermentation, decarboxylates pyruvate to acetaldehyde; subject to glucose-, ethanol-, and autoregulation; involved in amino acid catabolism
ARO7	-15.43	Chorismate mutase, catalyzes the conversion of chorismate to prephenate to initiate the tyrosine/phenylalanine-specific branch of aromatic amino acid biosynthesis
CDC19	-15.11	Pyruvate kinase, functions as a homotetramer in glycolysis to convert phosphoenolpyruvate to pyruvate, the input for aerobic (TCA cycle) or anaerobic (glucose fermentation) respiration
RPL33B	-14.71	Ribosomal protein L37 of the large (60S) ribosomal subunit, nearly identical to Rpl33Ap and has similarity to rat L35a; rpl33b null mutant exhibits normal growth while rpl33a rpl33b double null mutant is inviable
FBA1	-14.56	Fructose 1,6-bisphosphate aldolase, required for glycolysis and gluconeogenesis; catalyzes conversion of fructose 1,6 bisphosphate to glyceraldehyde-3-P and dihydroxyacetone-P; locates to mitochondrial outer surface upon oxidative stress
FEN1	-14.09	Fatty acid elongase, involved in sphingolipid biosynthesis; acts on fatty acids of up to 24 carbons in length; mutations have regulatory effects on 1,3-beta-

		glucan synthase, vacuolar ATPase, and the secretory pathway
YPL033C	-13.93	Protein of unknown function; involved in regulation of dNTP production; null mutant suppresses the lethality of lcd1 and rad53 mutations; expression is induced by Kar4p
YOR051C	-13.69	Nuclear protein that inhibits replication of Brome mosaic virus in S. cerevisiae, which is a model system for studying replication of positive-strand RNA viruses in their natural hosts; deletion increases stop codon readthrough
TKL1	-13.23	Transketolase, similar to Tkl2p; catalyzes conversion of xylulose-5-phosphate and ribose-5-phosphate to sedoheptulose-7-phosphate and glyceraldehyde-3-phosphate in the pentose phosphate pathway; needed for synthesis of aromatic amino acids
TDH3	-13.01	Glyceraldehyde-3-phosphate dehydrogenase, isozyme 3, involved in glycolysis and gluconeogenesis; tetramer that catalyzes the reaction of glyceraldehyde-3-phosphate to 1,3 bis-phosphoglycerate; detected in the cytoplasm and cell wall
YBR238C	-12.56	Mitochondrial membrane protein with similarity to Rmd9p; not required for respiratory growth but causes a synthetic respiratory defect in combination with rmd9 mutations; transcriptionally up-regulated by TOR; deletion increases life span
URA7	-12.39	Major CTP synthase isozyme (see also URA8), catalyzes the ATP-dependent transfer of the amide nitrogen from glutamine to UTP, forming CTP, the final step in de novo biosynthesis of pyrimidines; involved in phospholipid biosynthesis
IMD4	-12.26	Inosine monophosphate dehydrogenase, catalyzes the first step of GMP biosynthesis, member of a four-gene family in S. cerevisiae, constitutively expressed
CLB2	-12.24	B-type cyclin involved in cell cycle progression; activates Cdc28p to promote the transition from G2 to M phase; accumulates during G2 and M, then targeted via a destruction box motif for ubiquitin-mediated degradation by the proteasome
RPS17B	-12.10	Ribosomal protein 51 (rp51) of the small (40s) subunit; nearly identical to Rps17Ap and has similarity to rat S17 ribosomal protein
PHM6	-12.07	Protein of unknown function, expression is regulated by phosphate levels
ALD5	-11.93	Mitochondrial aldehyde dehydrogenase, involved in regulation or biosynthesis of electron transport chain components and acetate formation; activated by K+; utilizes NADP+ as the preferred coenzyme; constitutively expressed
SUR4	-11.86	Elongase, involved in fatty acid and sphingolipid biosynthesis; synthesizes very long chain 20-26-carbon fatty acids from C18-CoA primers; involved in regulation of sphingolipid biosynthesis
ANB1	-11.78	Translation elongation factor eIF-5A, previously thought to function in translation initiation; similar to and functionally redundant with Hyp2p; undergoes an essential hypusination modification; expressed under anaerobic conditions
FRM2	-11.38	Protein of unknown function, involved in the integration of lipid signaling pathways with cellular homeostasis; expression induced in cells treated with the mycotoxin patulin; has similarity to bacterial nitroreductases

RAX2	-11.36	N-glycosylated protein involved in the maintenance of bud site selection during bipolar budding; localization requires Rax1p; RAX2 mRNA stability is regulated by Mpt5p
ALG12	-11.36	Alpha-1,6-mannosyltransferase localized to the ER; responsible for the addition of the alpha-1,6 mannose to dolichol-linked Man7GlcNAc2, acts in the dolichol pathway for N-glycosylation
RNR1	-11.15	Major isoform of the large subunit of ribonucleotide-diphosphate reductase; the RNR complex catalyzes rate-limiting step in dNTP synthesis, regulated by DNA replication and DNA damage checkpoint pathways via localization of small subunits
TPI1	-10.97	Triose phosphate isomerase, abundant glycolytic enzyme; mRNA half-life is regulated by iron availability; transcription is controlled by activators Reb1p, Gcr1p, and Rap1p through binding sites in the 5' non-coding region
ATX2	-10.71	Golgi membrane protein involved in manganese homeostasis; overproduction suppresses the sod1 (copper, zinc superoxide dismutase) null mutation
SPO19	-10.71	Meiosis-specific prospore protein; required to produce bending force necessary for proper assembly of the prospore membrane during sporulation; identified as a weak high-copy suppressor of the spo1-1 ts mutation
RHR2	-10.68	Constitutively expressed isoform of DL-glycerol-3-phosphatase; involved in glycerol biosynthesis, induced in response to both anaerobic and, along with the Hor2p/Gpp2p isoform, osmotic stress
DTD1	-10.56	D-Tyr-tRNA(Tyr) deacylase, functions in protein translation, may affect nonsense suppression via alteration of the protein synthesis machinery; ubiquitous among eukaryotes
YLR301W	-10.56	Protein of unknown function that interacts with Sec72p
TDH2	-10.51	Glyceraldehyde-3-phosphate dehydrogenase, isozyme 2, involved in glycolysis and gluconeogenesis; tetramer that catalyzes the reaction of glyceraldehyde-3-phosphate to 1,3 bis-phosphoglycerate; detected in the cytoplasm and cell wall
RAD53	-10.40	Protein kinase, required for cell-cycle arrest in response to DNA damage; activated by trans autophosphorylation when interacting with hyperphosphorylated Rad9p; also interacts with ARS1 and plays a role in initiation of DNA replication
HGH1	-10.40	Nonessential protein of unknown function; predicted to be involved in ribosome biogenesis; green fluorescent protein (GFP)-fusion protein localizes to the cytoplasm; similar to mammalian BRP16 (Brain protein 16)
NRK1	-10.13	Nicotinamide riboside kinase, catalyzes the phosphorylation of nicotinamide riboside and nicotinic acid riboside in salvage pathways for NAD+ biosynthesis
CYB5	-10.02	Cytochrome b5, involved in the sterol and lipid biosynthesis pathways; acts as an electron donor to support sterol C5-6 desaturation
ERG25	-9.92	C-4 methyl sterol oxidase, catalyzes the first of three steps required to remove two C-4 methyl groups from an intermediate in ergosterol biosynthesis; mutants accumulate the sterol intermediate 4,4-dimethylzymosterol

4.18.1.2 Analysis of the effect of 200 µM GdnHCl + 20 µM TA exposure for 14 generations on yeast cells

When yeast cells were treated for 14 generations with 200 µM GdnHCl in combination with 20 µM TA, 100 genes were upregulated more than 2-fold, and of these, 12 more than 3-fold. 1363 genes were downregulated over 2-fold, 696 of these in excess of 3-fold. The figures below illustrate the cellular components, molecular functions and biological processes stimulated or repressed by GdnHCl + TA exposure and the percentages of total changes they represent.

Summary of the overall effects of gene upregulation on cells

Figures 4.49-4.51 depict the overall effects on cells induced by genes upregulated more than 2-fold in response to 200 µM GdnHCl + 20 µM TA exposure.

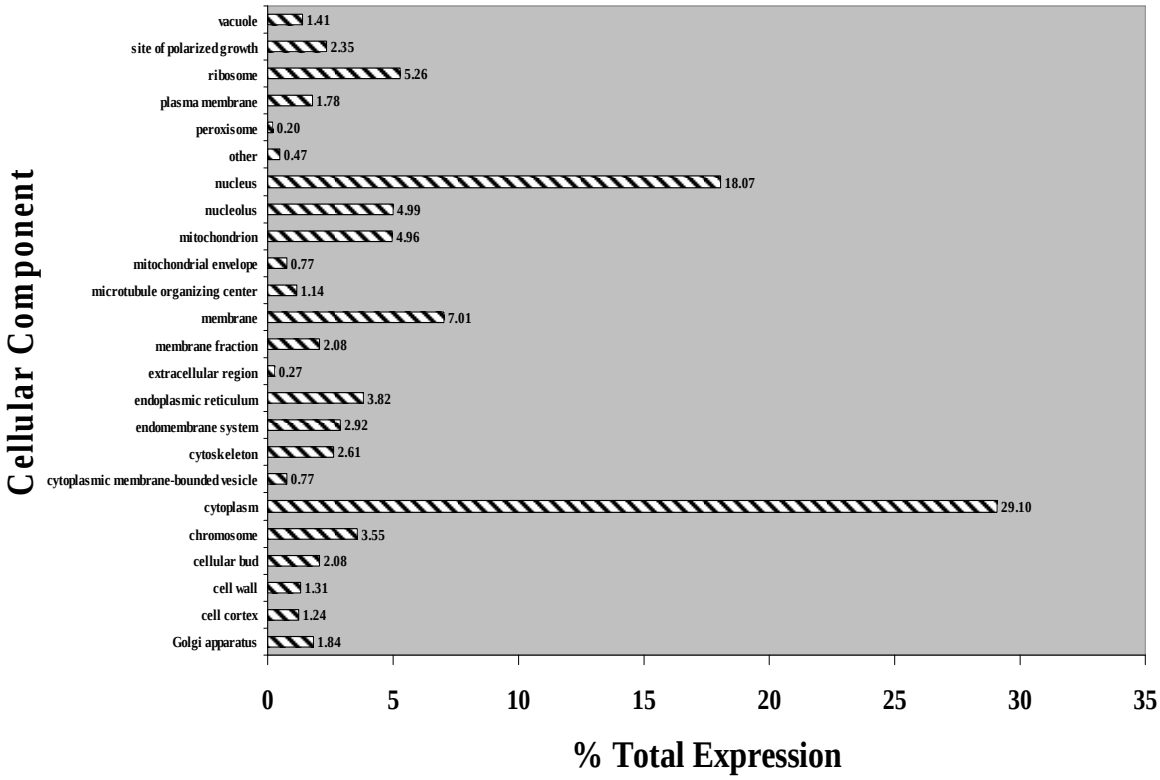

Figure 4.49 The percentage of each cellular component category (200 µM GdnHCl + 20 µM TA 14 generation upregulated genes). Genes upregulated more than two-fold were assigned cellular component categories. The number of genes in each category was expressed as a percentage of the number of total genes.

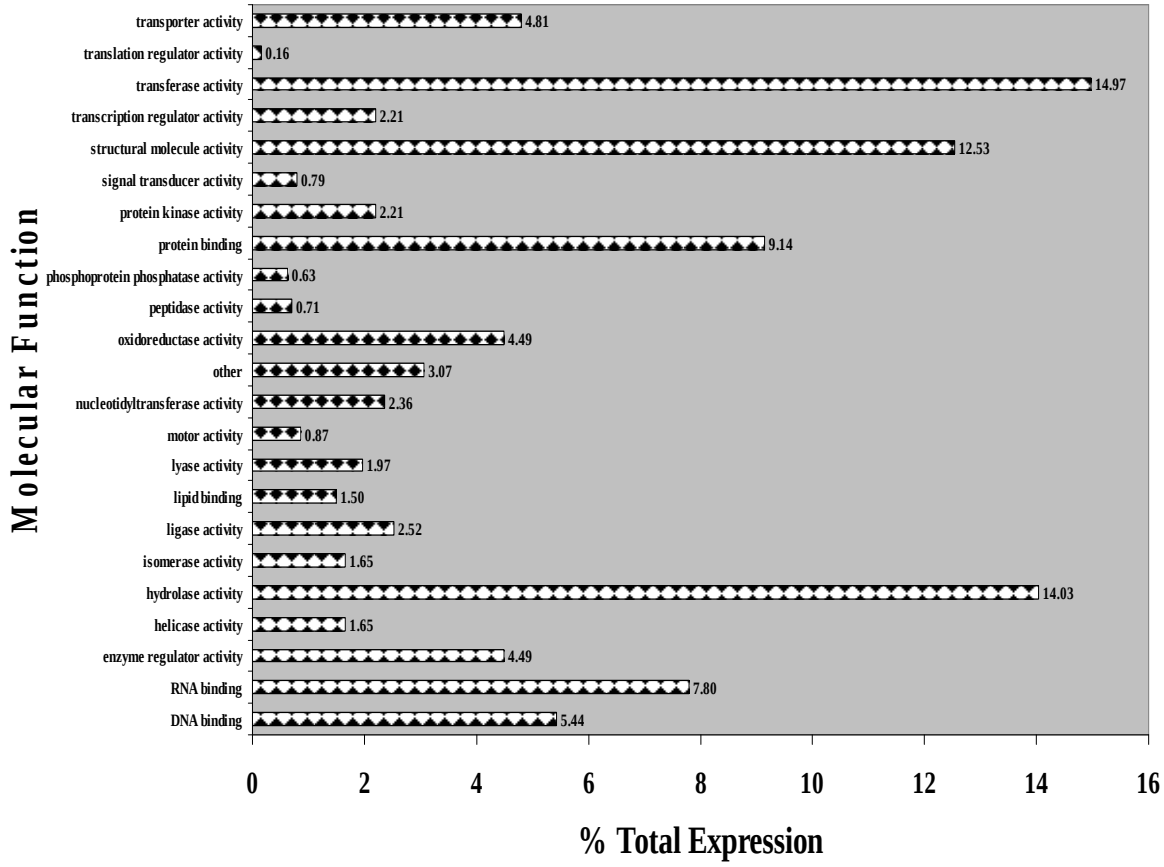

Figure 4.50 The percentage of each molecular function category (200 µM GdnHCl + 20 µM TA 14 generation upregulated genes). Genes upregulated more than two-fold were assigned molecular function categories. The number of genes in each category was expressed as a percentage of the number of total genes.

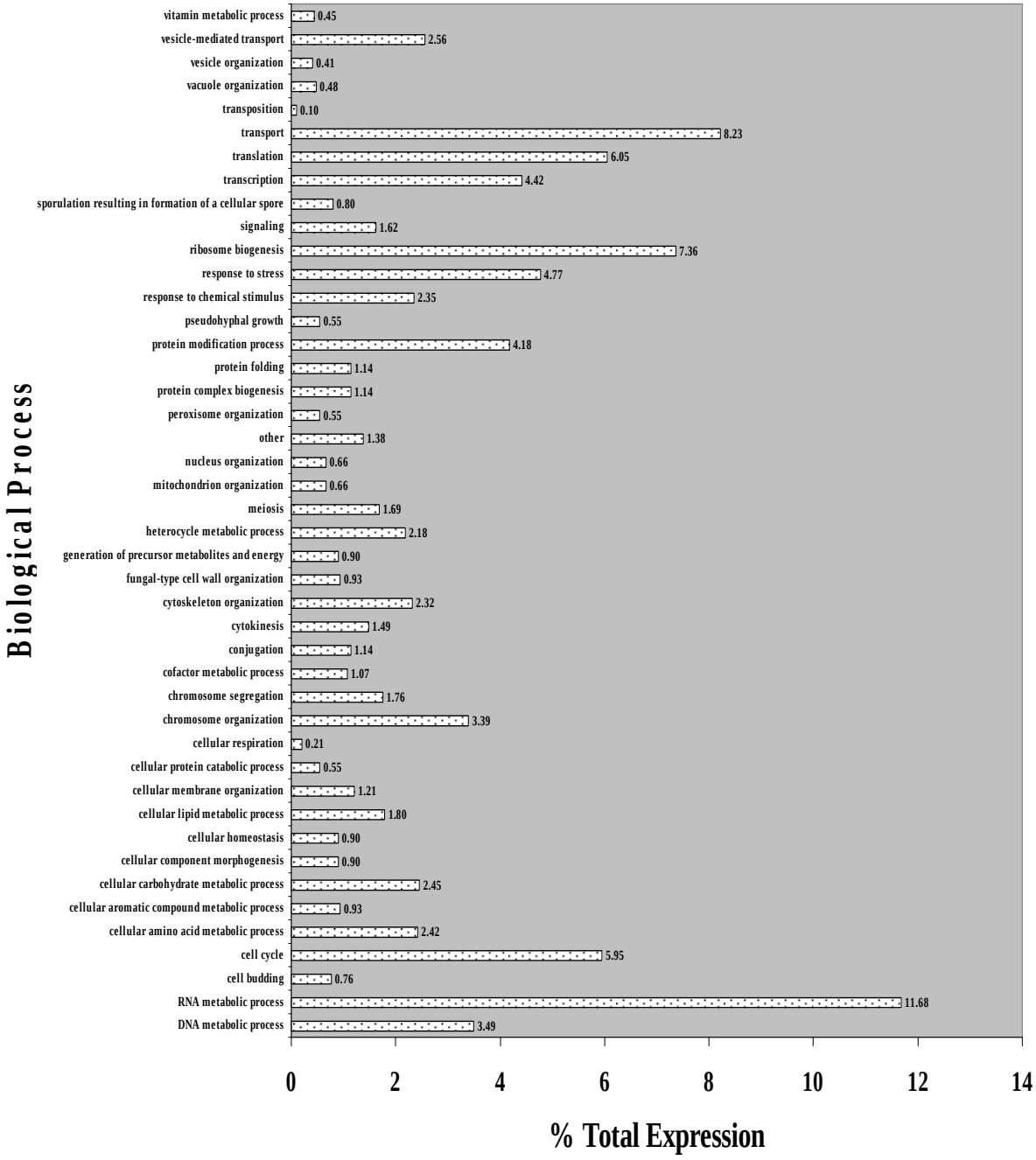

Figure 4.51 The percentage of each biological process category (200 µM GdnHCl + 20 µM TA 14 generation upregulated genes). Genes upregulated more than two-fold were assigned biological process categories. The number of genes in each category was expressed as a percentage of the number of total genes.

The five biological processes, molecular functions and associated cellular components most highly stimulated by a combination of 200 µM GdnHCl + 20 µM TA were investigated. These are illustrated in figures 4.52-4.54.

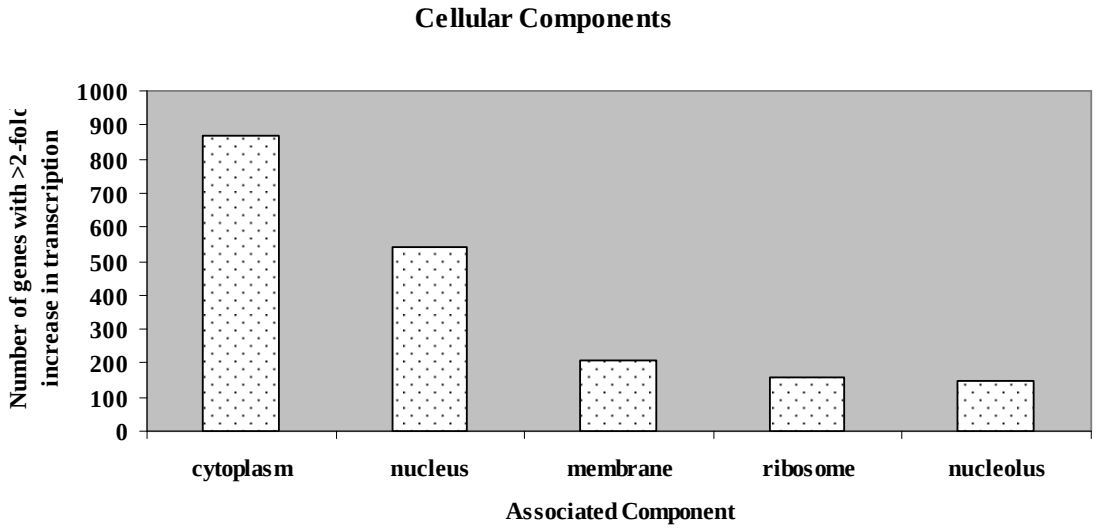

Figure 4.52 The five associated cellular components most highly upregulated by exposure to 200 µM GdnHCl + 20 µM TA for 14 generations.

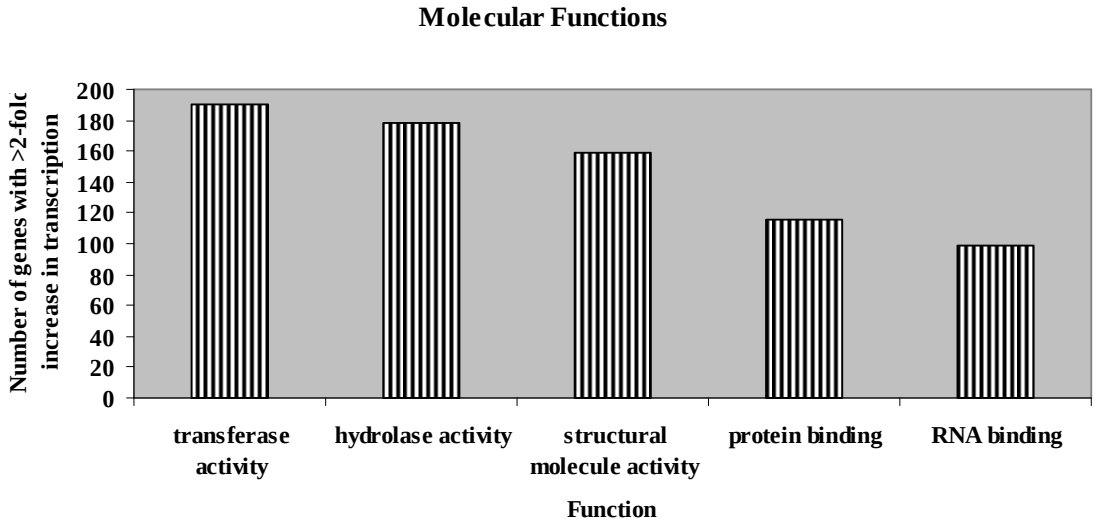

Figure 4.53 The five molecular functions most highly upregulated by exposure to 200 µM GdnHCl + 20 µM TA for 14 generations.

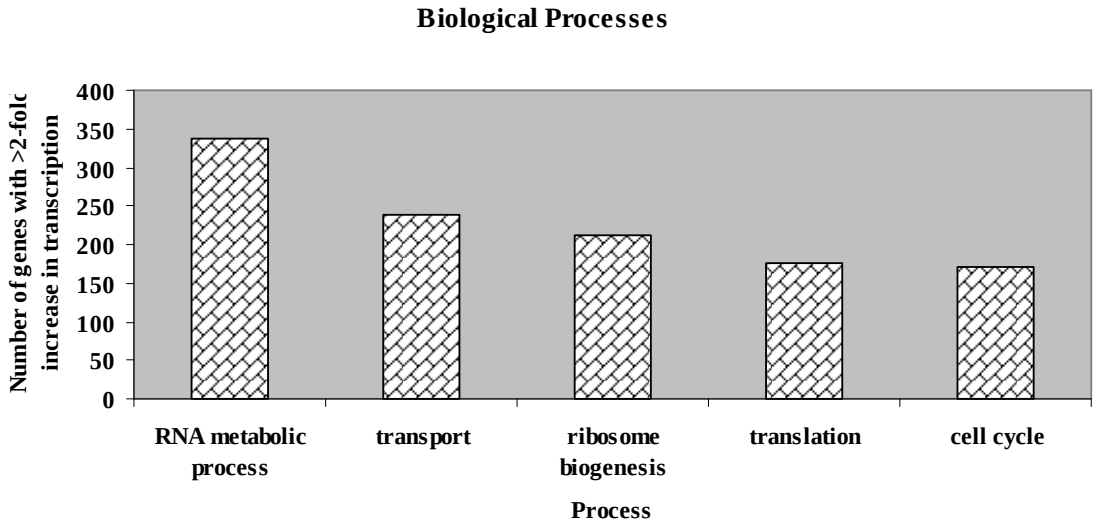

Figure 4.54 The five biological processes most highly upregulated by exposure to 200 µM GdnHCl + 20 µM TA for 14 generations.

Table 4.5 lists the fifty individual genes, and their respective functions, that underwent the highest increase in transcription in response to 200 µM GdnHCl + 20 µM TA exposure for 14 generations. A substantial level of overlap was seen for genes that are upregulated in response to GdnHCl alone for 14 generations, and GdnHCl combined with TA.

Table 4.5 The fifty genes most highly upregulated in response to 200 µM GdnHCl + 20 µM TA exposure for 14 generations. Gene functions were obtained from www.yeastgenome.org (SGD).

Gene	Fold Change	Gene Function
OLE1	9.25	Delta(9) fatty acid desaturase, required for monounsaturated fatty acid synthesis and for normal distribution of mitochondria
MRPL38	4.52	Mitochondrial ribosomal protein of the large subunit; appears as two protein spots (YmL34 and YmL38) on two-dimensional SDS gels
IZH1	4.35	Membrane protein involved in zinc ion homeostasis, member of the four-protein IZH family; transcription is regulated directly by Zap1p, expression induced by zinc deficiency and fatty acids; deletion increases sensitivity to elevated zinc
IZH4	4.15	Membrane protein involved in zinc ion homeostasis, member of the four-protein IZH family, expression induced by fatty acids and altered zinc levels; deletion reduces sensitivity to excess zinc; possible role in sterol metabolism
ALT1	4.08	Alanine transaminase (glutamic pyruvic transaminase); involved in alanine biosynthetic and catabolic processes; the authentic, non-tagged protein is detected in highly purified

		mitochondria in high-throughput studies
GLC3	3.92	Glycogen branching enzyme, involved in glycogen accumulation; green fluorescent protein (GFP)-fusion protein localizes to the cytoplasm in a punctate pattern
SDS23	3.64	One of two S. cerevisiae homologs (Sds23p and Sds24p) of the S. pombe Sds23 protein, which is implicated in APC/cyclosome regulation; involved in cell separation during budding
ATO2	3.45	Putative transmembrane protein involved in export of ammonia, a starvation signal that promotes cell death in aging colonies; phosphorylated in mitochondria; member of the TC 9.B.33 YaaH family; homolog of Ady2p and Y. lipolytica Gpr1p
CEM1	3.38	Mitochondrial beta-keto-acyl synthase with possible role in fatty acid synthesis; required for mitochondrial respiration
SMF2	3.28	Divalent metal ion transporter involved in manganese homeostasis; has broad specificity for di-valent and tri-valent metals; post-translationally regulated by levels of metal ions; member of the Nramp family of metal transport proteins
GCV1	3.13	T subunit of the mitochondrial glycine decarboxylase complex, required for the catabolism of glycine to 5,10-methylene-THF; expression is regulated by levels of levels of 5,10-methylene-THF in the cytoplasm
NPL3	3.05	RNA-binding protein that promotes elongation, regulates termination, and carries poly(A) mRNA from nucleus to cytoplasm; required for pre-mRNA splicing; dissociation from mRNAs promoted by Mtr10p; phosphorylated by Sky1p in the cytoplasm
PIR3	2.95	O-glycosylated covalently-bound cell wall protein required for cell wall stability; expression is cell cycle regulated, peaking in M/G1 and also subject to regulation by the cell integrity pathway
GDH3	2.92	NADP(+)-dependent glutamate dehydrogenase, synthesizes glutamate from ammonia and alpha-ketoglutarate; rate of alpha-ketoglutarate utilization differs from Gdh1p; expression regulated by nitrogen and carbon sources
MLS1	2.90	Malate synthase, enzyme of the glyoxylate cycle, involved in utilization of non-fermentable carbon sources; expression is subject to carbon catabolite repression; localizes in peroxisomes during growth in oleic acid medium
SPI1	2.89	GPI-anchored cell wall protein involved in weak acid resistance; basal expression requires Msn2p/Msn4p; expression is induced under conditions of stress and during the diauxic shift; similar to Sed1p
ADE13	2.84	Adenylosuccinate lyase, catalyzes two steps in the 'de novo' purine nucleotide biosynthetic pathway; expression is repressed by adenine and activated by Bas1p and Pho2p; mutations in human ortholog ADSL cause adenylosuccinase deficiency
YOR161W-B	2.77	Identified by gene-trapping, microarray-based expression analysis, and genome-wide homology searching
ACH1	2.75	Protein with CoA transferase activity, particularly for CoASH transfer from succinyl-CoA to acetate; has minor acetyl-CoA-hydrolase activity; phosphorylated; required for acetate utilization and for diploid pseudohyphal growth
YDL012C	2.72	Tail-anchored plasma membrane protein containing a conserved CYSTM module, possibly involved in response to stress; may contribute to non-homologous end-joining (NHEJ) based on ydl012c htz1 double null phenotype
MTD1	2.70	NAD-dependent 5,10-methylenetetrahydrafolate dehydrogenase, plays a catalytic role in oxidation of cytoplasmic one-carbon units; expression is regulated by Bas1p and Bas2p, repressed by adenine, and may be induced by inositol and choline

YPR013C	2.69	Putative zinc finger protein; YPR013C is not an essential gene
BDH2	2.65	Putative medium-chain alcohol dehydrogenase with similarity to BDH1; transcription induced by constitutively active PDR1 and PDR3
PCK1	2.63	Phosphoenolpyruvate carboxykinase, key enzyme in gluconeogenesis, catalyzes early reaction in carbohydrate biosynthesis, glucose represses transcription and accelerates mRNA degradation, regulated by Mcm1p and Cat8p, located in the cytosol
SNZ1	2.60	Protein involved in vitamin B6 biosynthesis; member of a stationary phase-induced gene family; coregulated with SNO1; interacts with Sno1p and with Yhr198p, perhaps as a multiprotein complex containing other Snz and Sno proteins
YAT1	2.59	Outer mitochondrial carnitine acetyltransferase, minor ethanol-inducible enzyme involved in transport of activated acyl groups from the cytoplasm into the mitochondrial matrix; phosphorylated
CAT5	2.59	Protein required for ubiquinone (Coenzyme Q) biosynthesis; localizes to the matrix face of the mitochondrial inner membrane in a large complex with ubiquinone biosynthetic enzymes; required for gluconeogenic gene activation
MET13	2.58	Major isozyme of methylenetetrahydrofolate reductase, catalyzes the reduction of 5,10-methylenetetrahydrofolate to 5-methyltetrahydrofolate in the methionine biosynthesis pathway
RPN4	2.55	Transcription factor that stimulates expression of proteasome genes; Rpn4p levels are in turn regulated by the 26S proteasome in a negative feedback control mechanism; RPN4 is transcriptionally regulated by various stress responses
MSK1	2.47	Mitochondrial lysine-tRNA synthetase, required for import of both aminoacylated and deacylated forms of tRNA(Lys) into mitochondria and for aminoacylation of mitochondrially encoded tRNA(Lys)
FMP46	2.46	Putative redox protein containing a thioredoxin fold; the authentic, non-tagged protein is detected in highly purified mitochondria in high-throughput studies
MIR1	2.42	Mitochondrial phosphate carrier, imports inorganic phosphate into mitochondria; functionally redundant with Pic2p but more abundant than Pic2p under normal conditions; phosphorylated
VHR1	2.42	Transcriptional activator, required for the vitamin H-responsive element (VHRE) mediated induction of VHT1 (Vitamin H transporter) and BIO5 (biotin biosynthesis intermediate transporter) in response to low biotin concentrations
SHR5	2.41	Subunit of a palmitoyltransferase, composed of Shr5p and Erf2p, that adds a palmitoyl lipid moiety to heterolipidated substrates such as Ras1p and Ras2p through a thioester linkage; palmitoylation is required for Ras2p membrane localization
IRC9,YAK1	2.37	Cytosolic serine hydroxymethyltransferase, converts serine to glycine plus 5,10 methylenetetrahydrofolate; major isoform involved in generating precursors for purine, pyrimidine, amino acid, and lipid biosynthesis
YOR329W-A	2.36	Peripheral membrane protein located at Vid (vacuole import and degradation) vesicles; regulates fructose-1,6-bisphosphatase (FBPase) targeting to the vacuole; promotes proteasome-dependent catabolite degradation of FBPase
VID24	2.36	Mitochondrial protein; may interact with ribosomes based on co-purification experiments; similar to E. coli and human mitochondrial S12 ribosomal proteins
YNR036C	2.36	Lactate transporter, required for uptake of lactate and pyruvate; phosphorylated; expression is derepressed by transcriptional activator Cat8p during respiratory growth, and repressed in the presence of glucose, fructose, and mannose
JEN1	2.35	Substrate of the Hub1p ubiquitin-like protein that localizes to the shmoo tip (mating projection); mutants are defective for

		mating projection formation, thereby implicating Hbt1p in polarized cell morphogenesis
HBT1	2.35	Protein that binds DNA containing intrastrand cross-links formed by cisplatin, contains two HMG (high mobility group box) domains, which confer the ability to bend cisplatin-modified DNA; mediates aerobic transcriptional repression of COX5b
IXR1	2.34	Mitochondrial ribosomal protein of the large subunit
MRPL4	2.32	Glucokinase, catalyzes the phosphorylation of glucose at C6 in the first irreversible step of glucose metabolism; one of three glucose phosphorylating enzymes; expression regulated by non-fermentable carbon sources
GLK1	2.32	Membrane protein involved in zinc ion homeostasis, member of the four-protein IZH family, expression induced by zinc deficiency; deletion reduces sensitivity to elevated zinc and shortens lag phase, overexpression reduces Zap1p activity
IZH3	2.31	Na+/Pi cotransporter, active in early growth phase; similar to phosphate transporters of Neurospora crassa; transcription regulated by inorganic phosphate concentrations and Pho4p
PHO89	2.31	Putative protein of unknown function; YMR206W is not an essential gene
YMR206W	2.31	Nucleotide exchange factor for the endoplasmic reticulum (ER) lumenal Hsp70 chaperone Kar2p, required for protein translocation into the ER; homolog of Yarrowia lipolytica SLS1; GrpE-like protein
SLS1	2.29	Mitochondrial membrane protein that coordinates expression of mitochondrially-encoded genes; may facilitate delivery of mRNA to membrane-bound translation machinery
NDI1	2.29	NADH:ubiquinone oxidoreductase, transfers electrons from NADH to ubiquinone in the respiratory chain but does not pump protons, in contrast to the higher eukaryotic multisubunit respiratory complex I; phosphorylated; homolog of human AMID
YGR035C	2.28	Putative protein of unknown function, potential Cdc28p substrate; transcription is activated by paralogous transcription factors Yrm1p and Yrr1p along with genes involved in multidrug resistance
FBP1	2.27	Fructose-1,6-bisphosphatase, key regulatory enzyme in the gluconeogenesis pathway, required for glucose metabolism; undergoes either proteasome-mediated or autophagy-mediated degradation depending on growth conditions; interacts with Vid30p

Summary of the overall effects of gene downregulation on cells

Genes which were transcriptionaly repressed under 200 µM GdnHCl + 20 µM TA exposure were also explored. Figures 4.55-4.57 depict the overall effects on cells induced by genes downregulated more than 2-fold in response to 200 µM GdnHCl + 20 µM TA exposure.

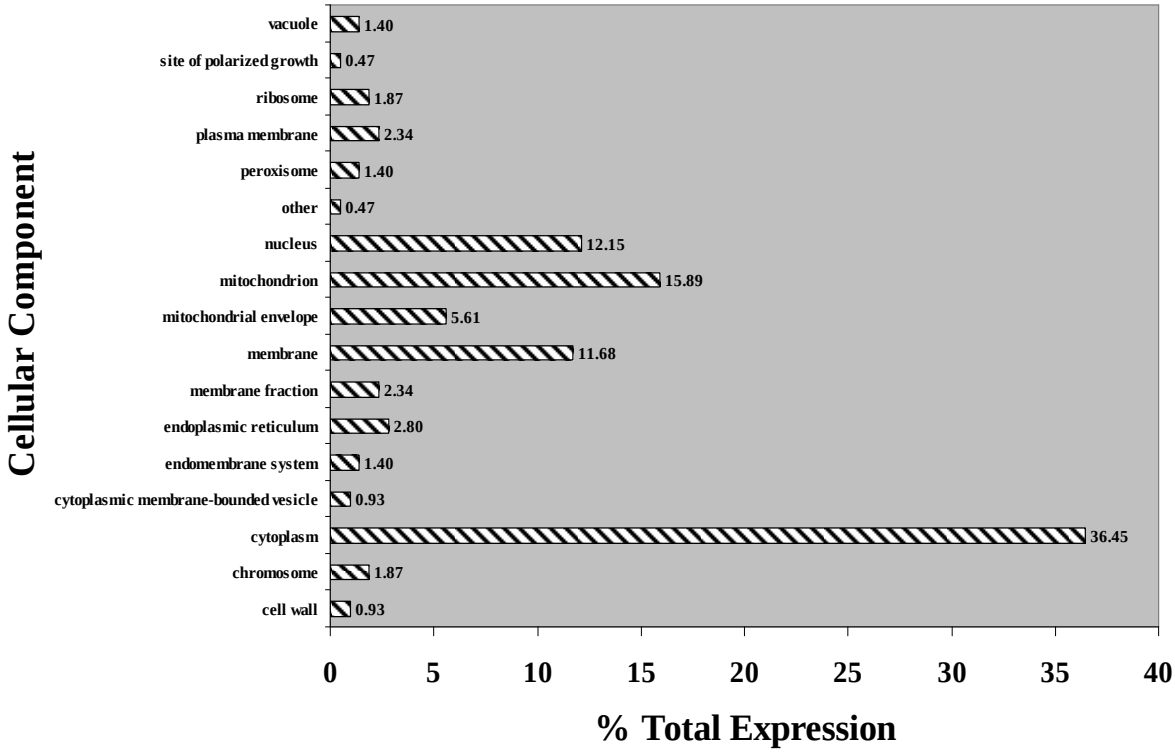

Figure 4.55 The percentage of each cellular component category (200 µM GdnHCl + 20 µM TA 14 generation downregulated genes). Genes downregulated more than two-fold were assigned cellular component categories. The number of genes in each category was expressed as a percentage of the number of total genes.

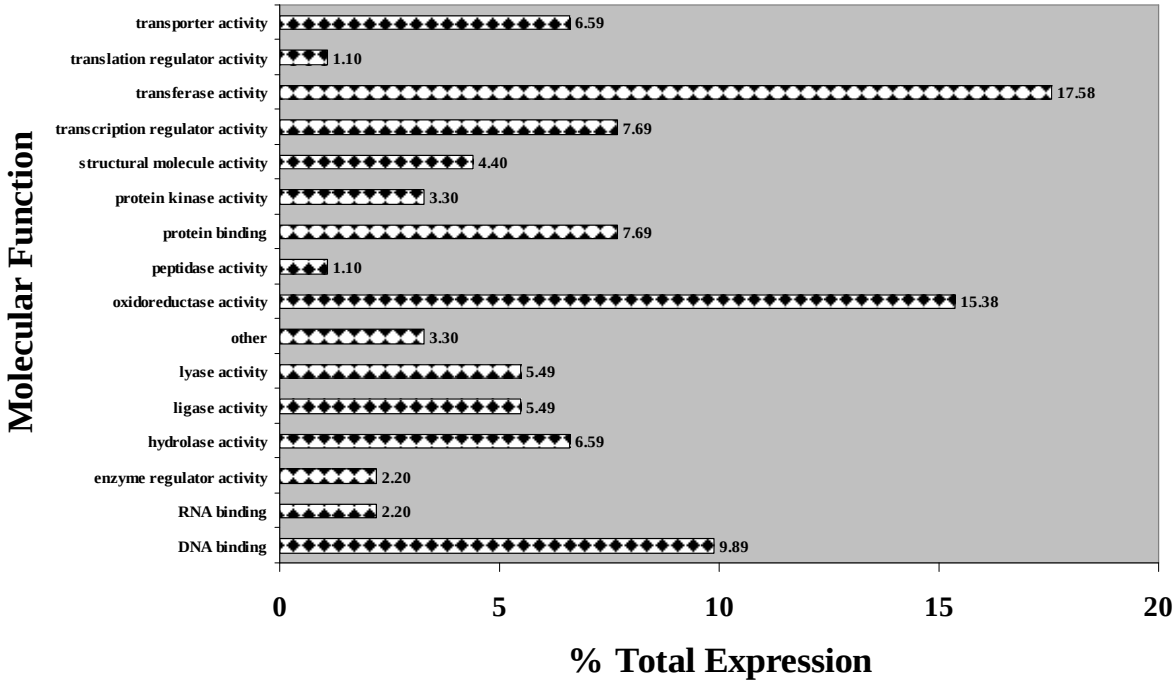

Figure 4.56 The percentage of each molecular function category (200 µM GdnHCl + 20 µM TA 14 generation downregulated genes). Genes downregulated more than two-fold were assigned molecular function categories. The number of genes in each category was expressed as a percentage of the number of total genes.

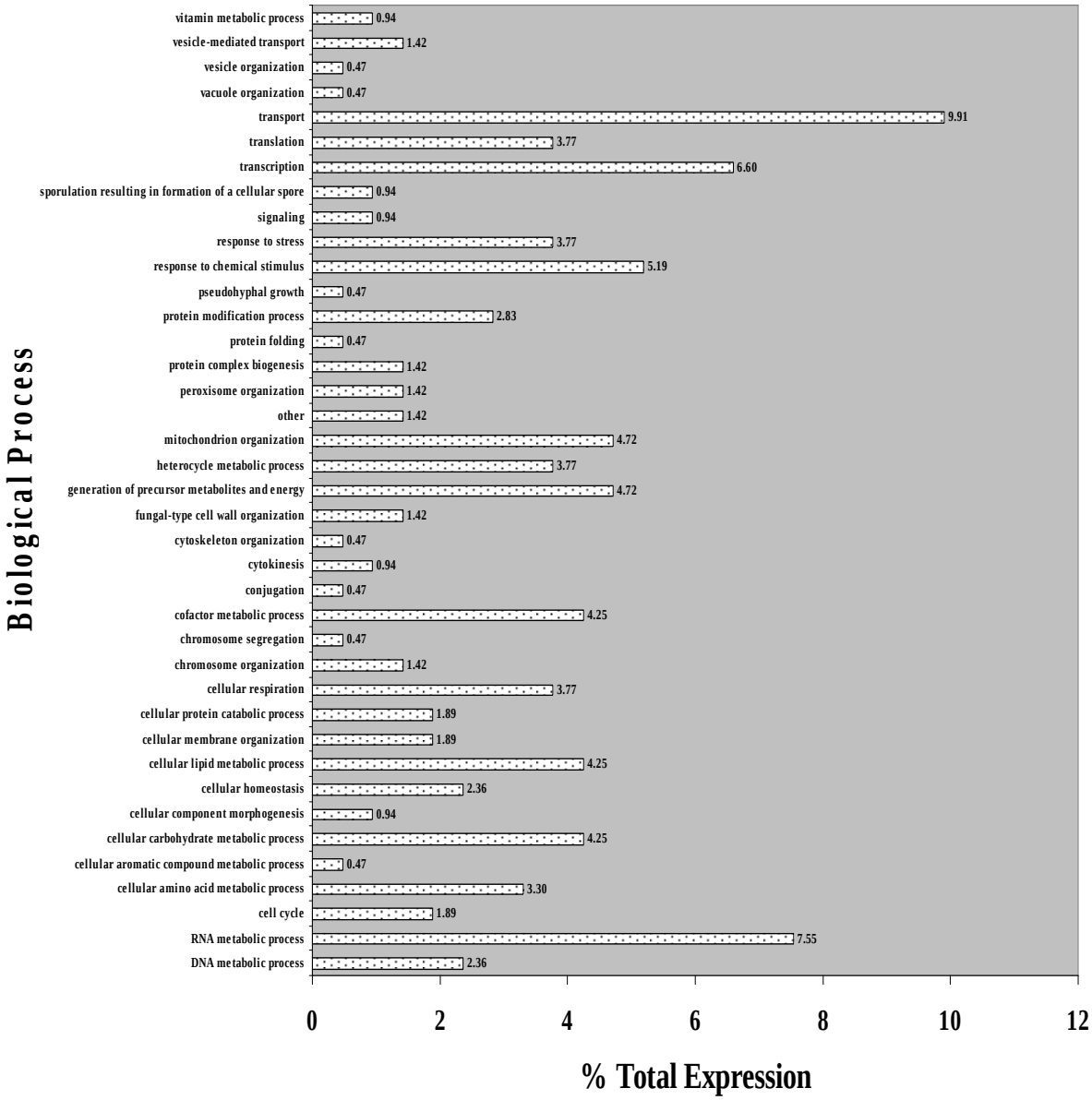

Figure 4.57 The percentage of each biological process category (200 µM GdnHCl + 20 µM TA 14 generation downregulated genes). Genes downregulated more than two-fold were assigned biological process categories. The number of genes in each category was expressed as a percentage of the number of total genes.

The five biological processes, molecular functions and associated cellular components most repressed by a combination of 200 µM GdnHCl + 20 µM TA were explored. These are illustrated in figures 4.58-4.60.

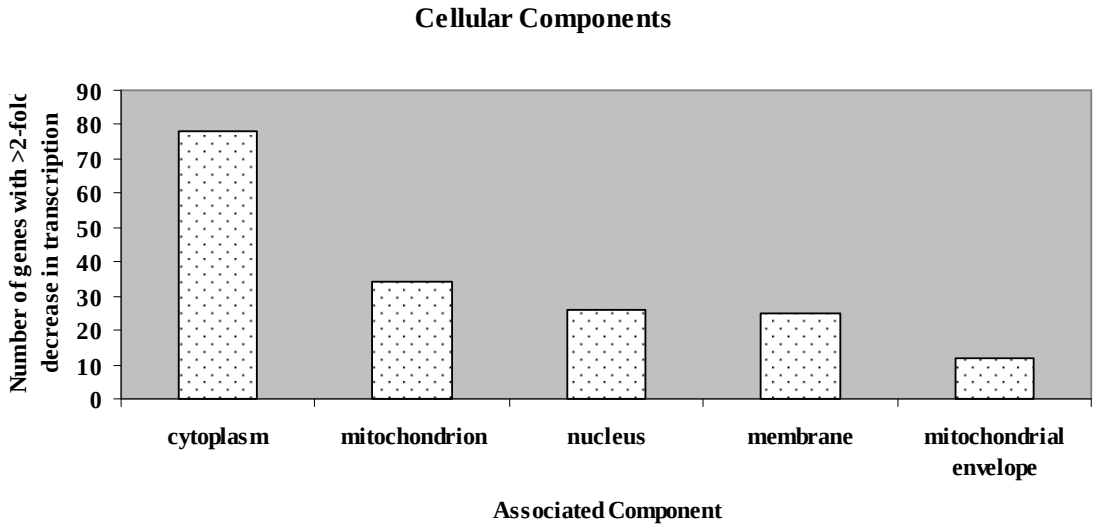

Figure 4.58 The five associated cellular components most highly downregulated by exposure to 200 µM GdnHCl + 20 µM TA for 14 generations.

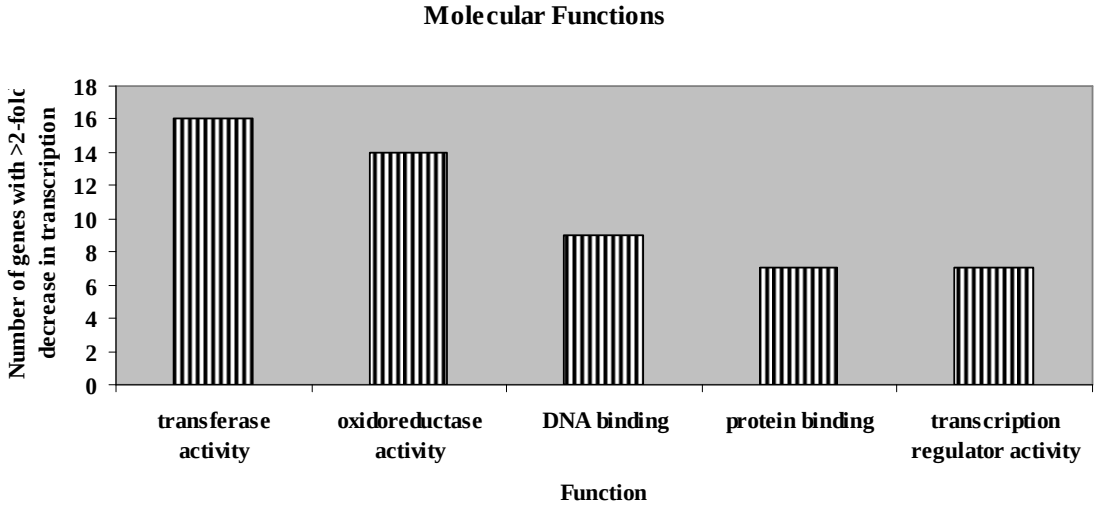

Figure 4.59 The five molecular functions most highly downregulated by exposure to 200 µM GdnHCl + 20 µM TA for 14 generations.

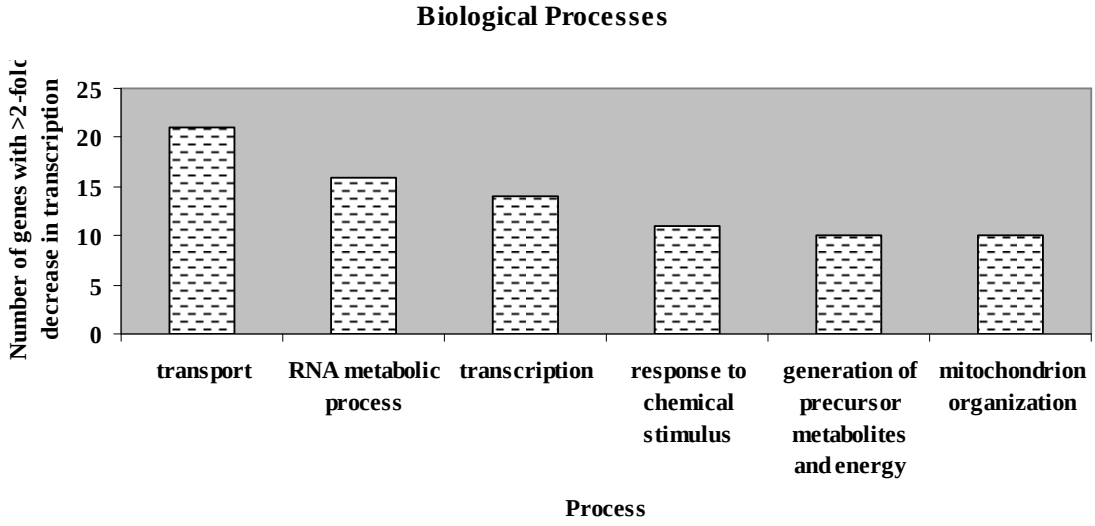

Figure 4.60 The *five biological processes most highly downregulated by exposure to 200 µM GdnHCl + 20 µM TA for 14 generations. * The 5th and 6th most repressed biological processes are represented by the same number of genes and are thus both included.

Table 4.6 lists the fifty individual genes, and their respective functions, that underwent the most acute decrease in transcription in response to 200 µM GdnHCl + 20 µM TA exposure for 14 generations.

Table 4.6 The fifty genes most highly downregulated in response to 200 µM GdnHCl + 20 µM TA exposure for 14 generations. Gene functions were obtained from www.yeastgenome.org (SGD).

Gene	Fold Change	Gene Function
PMA1	-61.79	Plasma membrane H+-ATPase, pumps protons out of the cell; major regulator of cytoplasmic pH and plasma membrane potential; part of the P2 subgroup of cation-transporting ATPases
CYB5	-50.91	Cytochrome b5, involved in the sterol and lipid biosynthesis pathways; acts as an electron donor to support sterol C5-6 desaturation
RPS22A	-35.29	Protein component of the small (40S) ribosomal subunit; nearly identical to Rps22Bp and has similarity to E. coli S8 and rat S15a ribosomal proteins
RPL33B	-34.027	Ribosomal protein L37 of the large (60S) ribosomal subunit, nearly identical to Rpl33Ap and has similarity to rat L35a; rpl33b null mutant exhibits normal growth while rpl33a rpl33b double null mutant is inviable
DTD1	-33.14	D-Tyr-tRNA(Tyr) deacylase, functions in protein translation, may affect nonsense suppression via alteration of the protein synthesis machinery; ubiquitous among eukaryotes
YGR272C	-26.17	Essential protein required for maturation of 18S rRNA; null mutant is sensitive to hydroxyurea and is delayed in recovering from alpha-factor arrest; green fluorescent protein (GFP)-fusion

		protein localizes to the nucleolus
TOS4	-23.74	Forkhead Associated domain containing protein and putative transcription factor found associated with chromatin; target of SBF transcription factor; expression is periodic and peaks in G1; similar to PLM2
YER053C-A	-21.85	Putative protein of unknown function; green fluorescent protein (GFP)-fusion protein localizes to the endoplasmic reticulum
HXT4	-20.90	High-affinity glucose transporter of the major facilitator superfamily, expression is induced by low levels of glucose and repressed by high levels of glucose
RPS17B	-20.41	Ribosomal protein 51 (rp51) of the small (40s) subunit; nearly identical to Rps17Ap and has similarity to rat S17 ribosomal protein
BRN1	-19.45	Subunit of the condensin complex; required for chromosome condensation and for clustering of tRNA genes at the nucleolus; may influence multiple aspects of chromosome transmission
EXG1	-17.48	Major exo-1,3-beta-glucanase of the cell wall, involved in cell wall beta-glucan assembly; exists as three differentially glycosylated isoenzymes
RNR1	-17.11	Major isoform of the large subunit of ribonucleotide-diphosphate reductase; the RNR complex catalyzes rate-limiting step in dNTP synthesis, regulated by DNA replication and DNA damage checkpoint pathways via localization of small subunits
CLB2	-17.07	B-type cyclin involved in cell cycle progression; activates Cdc28p to promote the transition from G2 to M phase; accumulates during G2 and M, then targeted via a destruction box motif for ubiquitin-mediated degradation by the proteasome
FEN1	-16.52	Fatty acid elongase, involved in sphingolipid biosynthesis; acts on fatty acids of up to 24 carbons in length; mutations have regulatory effects on 1,3-beta-glucan synthase, vacuolar ATPase, and the secretory pathway
INM1	-16.16	Inositol monophosphatase, involved in biosynthesis of inositol and in phosphoinositide second messenger signaling; INM1 expression increases in the presence of inositol and decreases upon exposure to antibipolar drugs lithium and valproate
JJJ3	-15.75	Protein of unknown function, contains a J-domain, which is a region with homology to the E. coli DnaJ protein
ENO2	-15.67	Enolase II, a phosphopyruvate hydratase that catalyzes the conversion of 2-phosphoglycerate to phosphoenolpyruvate during glycolysis and the reverse reaction during gluconeogenesis; expression is induced in response to glucose
RPL21A	-15.33	Protein component of the large (60S) ribosomal subunit, nearly identical to Rpl21Bp and has similarity to rat L21 ribosomal protein
MCM16	-14.89	Protein involved in kinetochore-microtubule mediated chromosome segregation; binds to centromere DNA
IMD4	-14.59	Inosine monophosphate dehydrogenase, catalyzes the first step of GMP biosynthesis, member of a four-gene family in S. cerevisiae, constitutively expressed
RPS1B	-14.51	Ribosomal protein 10 (rp10) of the small (40S) subunit; nearly identical to Rps1Ap and has similarity to rat S3a ribosomal protein
RPL6B	-14.45	Protein component of the large (60S) ribosomal subunit, has similarity to Rpl6Ap and to rat L6 ribosomal protein; binds to 5.8S rRNA
RPL42B	-14.42	Protein component of the large (60S) ribosomal subunit, identical to Rpl42Ap and has similarity to rat L44; required for propagation of the killer toxin-encoding M1 double-stranded RNA satellite of the L-A double-stranded RNA virus
YRO2	-14.40	Putative protein of unknown function; the authentic, non-tagged protein is detected in a phosphorylated state in highly purified mitochondria in high-throughput studies; transcriptionally regulated by Haa1p

ATX2	-14.40	Golgi membrane protein involved in manganese homeostasis; overproduction suppresses the sod1 (copper, zinc superoxide dismutase) null mutation
RPS28B	-14.08	Protein component of the small (40S) ribosomal subunit; nearly identical to Rps28Ap and has similarity to rat S28 ribosomal protein
RAX2	-14.04	N-glycosylated protein involved in the maintenance of bud site selection during bipolar budding; localization requires Rax1p; RAX2 mRNA stability is regulated by Mpt5p
ACM1	-13.92	Pseudosubstrate inhibitor of the anaphase-promoting complex/cyclosome (APC/C), that suppresses APC/C [Cdh1]-mediated proteolysis of mitotic cyclins; associates with Cdh1p, Bmh1p and Bmh2p; cell cycle regulated protein
YLR063W	-13.86	Putative S-adenosylmethionine-dependent methyltransferase; green fluorescent protein (GFP)-fusion protein localizes to the cytoplasm; YLR063W is not an essential gene
GPM3	-13.86	Homolog of Gpm1p phosphoglycerate mutase, which converts 3-phosphoglycerate to 2-phosphoglycerate in glycolysis; may be non-functional derivative of a gene duplication event
RPS9B	-13.78	Protein component of the small (40S) ribosomal subunit; nearly identical to Rps9Ap and has similarity to E. coli S4 and rat S9 ribosomal proteins
HXK2	-13.75	Hexokinase isoenzyme 2 that catalyzes phosphorylation of glucose in the cytosol; predominant hexokinase during growth on glucose; functions in the nucleus to repress expression of HXK1 and GLK1 and to induce expression of its own gene
PGK1	-13.53	3-phosphoglycerate kinase, catalyzes transfer of high-energy phosphoryl groups from the acyl phosphate of 1,3-bisphosphoglycerate to ADP to produce ATP; key enzyme in glycolysis and gluconeogenesis
URA7	-13.44	Major CTP synthase isozyme (see also URA8), catalyzes the ATP-dependent transfer of the amide nitrogen from glutamine to UTP, forming CTP, the final step in de novo biosynthesis of pyrimidines; involved in phospholipid biosynthesis
GPM1	-13.43	Tetrameric phosphoglycerate mutase, mediates the conversion of 3-phosphoglycerate to 2-phosphoglycerate during glycolysis and the reverse reaction during gluconeogenesis
RPC17	-13.34	RNA polymerase III subunit C17; physically interacts with C31, C11, and TFIIIB70; may be involved in the recruitment of pol III by the preinitiation complex
RPS12	-13.30	Protein component of the small (40S) ribosomal subunit; has similarity to rat ribosomal protein S12
RPL31A	-13.29	Protein component of the large (60S) ribosomal subunit, nearly identical to Rpl31Bp and has similarity to rat L31 ribosomal protein; associates with the karyopherin Sxm1p; loss of both Rpl31p and Rpl39p confers lethality
NCE103	-13.25	Carbonic anhydrase; poorly transcribed under aerobic conditions and at an undetectable level under anaerobic conditions; involved in non-classical protein export pathway
BSC1	-13.18	Protein of unconfirmed function, similar to cell surface flocculin Muc1p; ORF exhibits genomic organization compatible with a translational readthrough-dependent mode of expression
ARO7	-12.96	Chorismate mutase, catalyzes the conversion of chorismate to prephenate to initiate the tyrosine/phenylalanine-specific branch of aromatic amino acid biosynthesis
RPL34A	-12.61	Protein component of the large (60S) ribosomal subunit, nearly identical to Rpl34Bp and has similarity to rat L34 ribosomal protein
NRK1	-12.48	Nicotinamide riboside kinase, catalyzes the phosphorylation of nicotinamide riboside and nicotinic acid riboside in salvage pathways for NAD+ biosynthesis
HOM3	-12.43	Aspartate kinase (L-aspartate 4-P-transferase); cytoplasmic enzyme that catalyzes the first step in the common pathway for

		methionine and threonine biosynthesis; expression regulated by Gcn4p and the general control of amino acid synthesis
PCL1	-12.20	Cyclin, interacts with cyclin-dependent kinase Pho85p; member of the Pcl1,2-like subfamily, involved in the regulation of polarized growth and morphogenesis and progression through the cell cycle; localizes to sites of polarized cell growth
FRM2	12.17	Protein of unknown function, involved in the integration of lipid signaling pathways with cellular homeostasis; expression induced in cells treated with the mycotoxin patulin; has similarity to bacterial nitroreductases
RPL2B	11.88	Protein component of the large (60S) ribosomal subunit, identical to Rpl2Ap and has similarity to E. coli L2 and rat L8 ribosomal proteins; expression is upregulated at low temperatures
RPL27A	11.67	Protein component of the large (60S) ribosomal subunit, nearly identical to Rpl27Bp and has similarity to rat L27 ribosomal protein
MSH2	11.59	Protein that forms heterodimers with Msh3p and Msh6p that bind to DNA mismatches to initiate the mismatch repair process; contains a Walker ATP-binding motif required for repair activity; Msh2p-Msh6p binds to and hydrolyzes ATP

4.18.1.3 Comparison of the effect of 200 µM GdnHCl alone and in combination with 20 µM TA for 14 generations on yeast cells

Cells were exposed to these compounds for 14 generations due to the fact that TA, in the presence of GdnHCl at these concentrations fully cures [PSI^{+}]. Further to the results illustrated above, RNA sequencing data was compared. We attempted to search for yeast responses induced by a combination of GdnHCl and TA, but not by GdnHCl alone. It was anticipated that this would provide an indication of the type of impact caused by TA in yeast cultures, and perhaps offer insight into the mode of action of the drug. Figures 4.61-4.63 depict comparisons of the biological processes, cellular components and molecular functions stimulated by GdnHCl and TA.

As illustrated by figure 4.61, ribosome biogenesis, RNA metabolic process, transport, translation and cell cycle are the five biological processes most highly stimulated by GdnHCl alone, and in combination with TA.

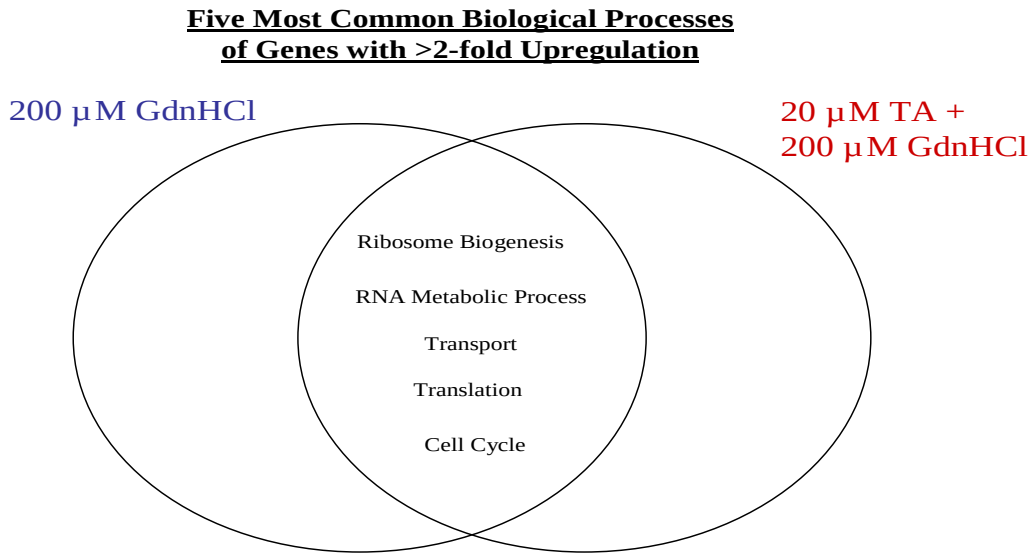

Figure 4.61 Comparison of the five most common biological processes of genes with >2-fold upregulation.

Figure 4.62 demonstrates that when cells are treated with GdnHCl alone, genes involved with the cytoplasm, nucleus, membrane, ribosome and mitochondrion are most highly upregulated. With the addition of TA, genes involved with the nucleolus are most highly upregulated, and not those associated with the mitochondrion.

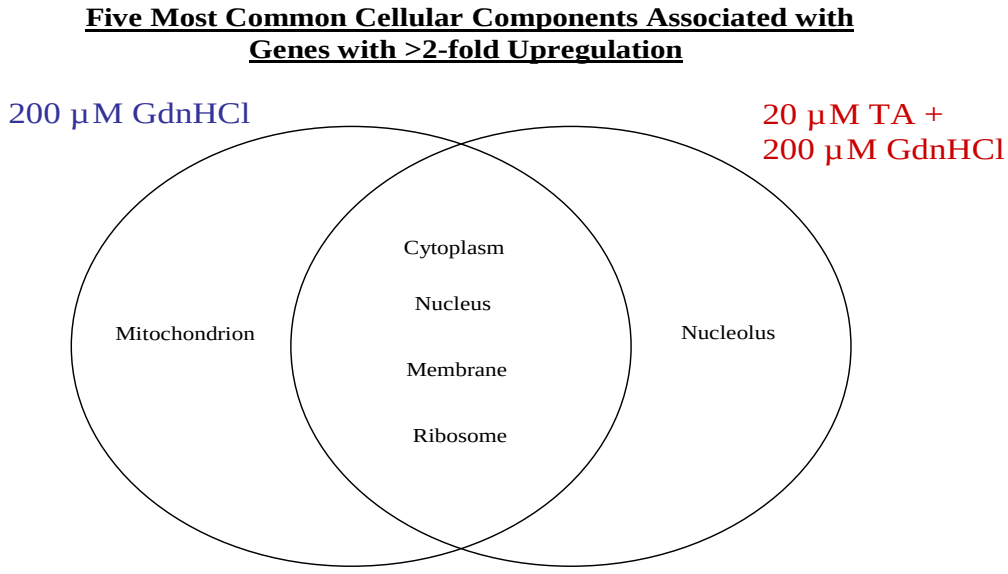

Figure 4.62 Comparison of the five most common associated cellular components of genes with >2-fold upregulation.

Cellular exposure to GdnHCl alone and in combination with TA results in induction of the same most common molecular functions. As shown in figure 4.63, these are transferase activity, hydrolase activity, structural molecule activity, RNA binding and protein binding.

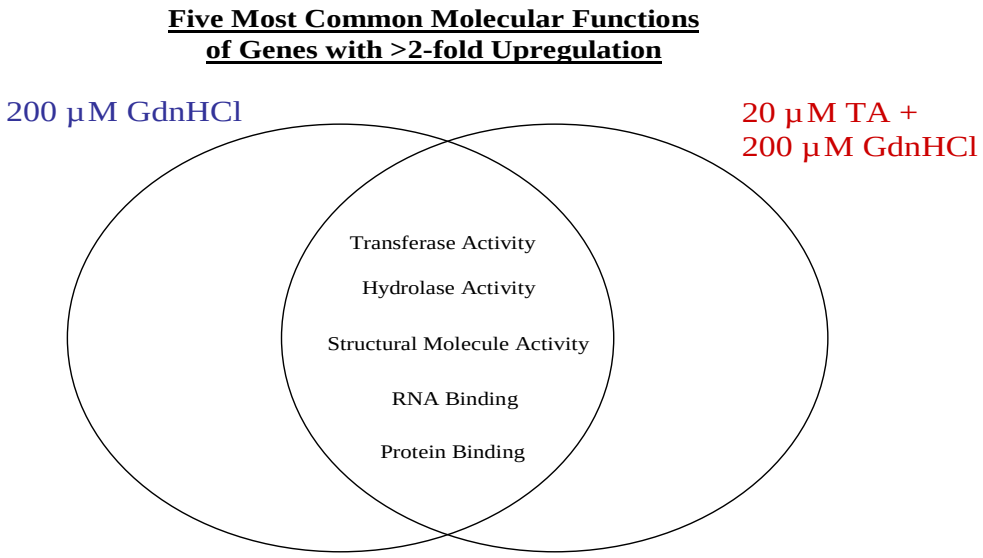

Figure 4.63 Comparison of the five most common molecular functions of genes with >2-fold upregulation.

Downregulated gene GO identities were also compared and contrasted, as illustrated in figures 4.64-4.66. In the case of genes downregulated in response to treatment with GdnHCl alone and in combination with TA, there are considerably more differences. Three of the five biological processes most repressed under exposure are common to both treatments and these are transport, RNA metabolic process and transcription. However, cellular lipid metabolic process and heterocycle metabolic process are two of the higest biological processes inhibited by GdnHCl alone, but not in combination with TA. In contrast, response to chemical stimulus, generation of precursor metabolites and energy and mitochondrion organisation are all highly repressed by GdnHCl + TA exposure, but not by GdnHCl alone.

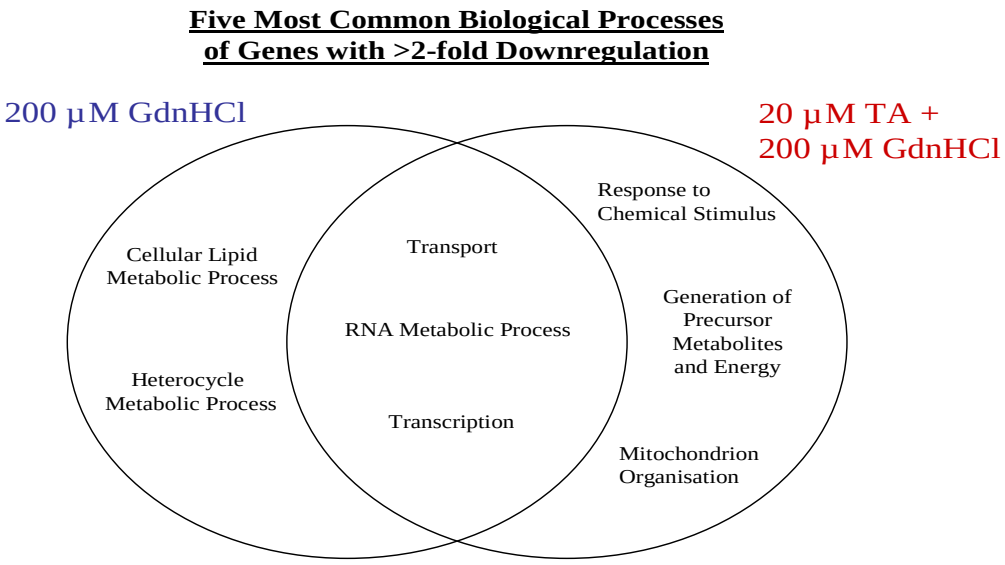

Figure 4.64 Comparison of the *five most common biological processes of genes with >2-fold downregualation. *In response to GdnHCl + TA exposure, the 5th and 6th most repressed biological processes are represented by the same number of genes and are thus both included.

Genes associated with the membrane, cytoplasm, mitochondrial envelope, mitochondrion and nucleus are those most highly downregulated by exposure to GdnHCl alone and combined with TA.

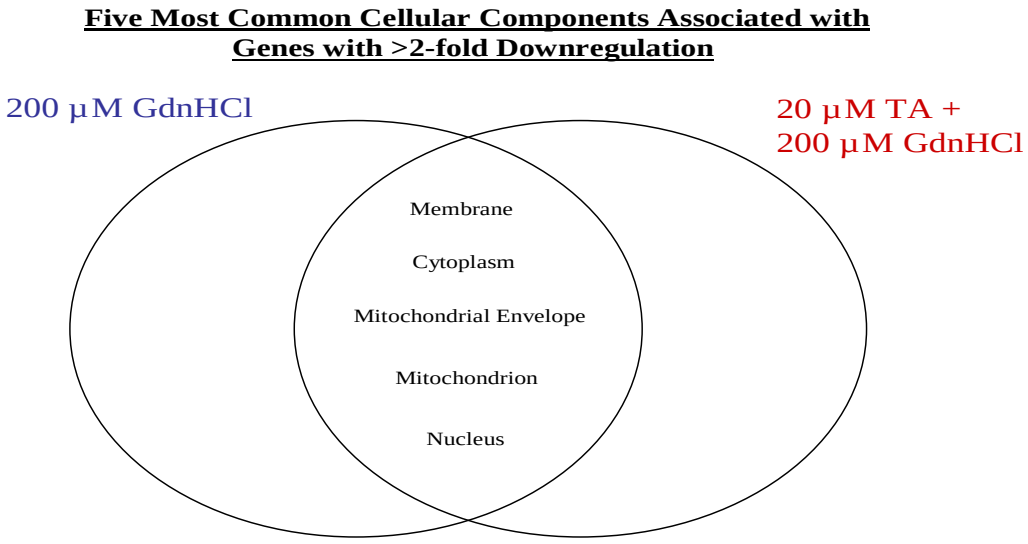

Figure 4.65 Comparison of the five most common associated cellular components of genes with >2-fold downregulation.

Figure 4.66 demonstrates that oxidoreductase activity, transferase activity, DNA binding and protein binding are all some of the most highly inhibited functions by both treatments. However, repression of transporter activity is specific to GdnHCl treatment alone, while downregulation of transcription regulator activity is specific to GdnHCl treatment in combination with TA.

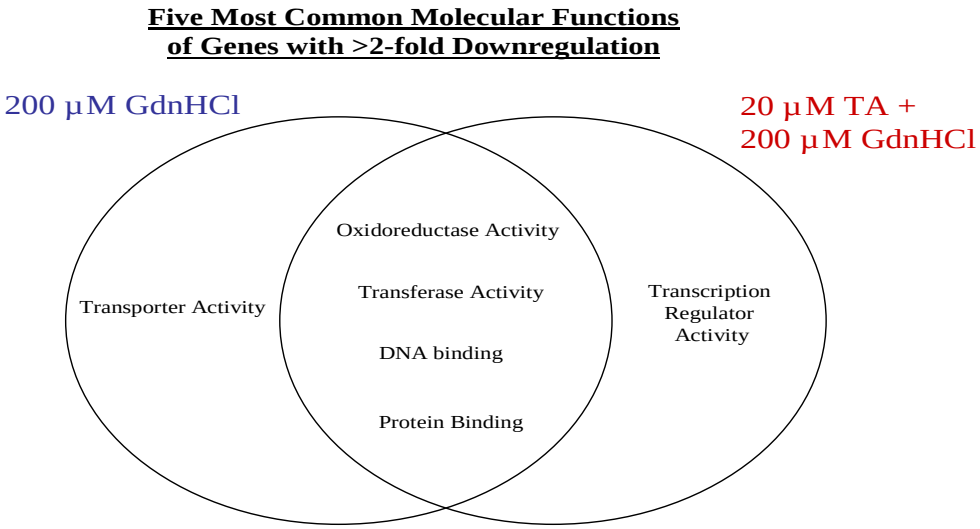

Figure 4.66 Comparison of the five most common molecular functions of genes with >2-fold downregulation.

Following this analysis, an attempt was made to identify genes that are upregulated upon GdnHCl exposure and further upregulated in the presence of GdnHCl and TA combined. It was anticipated that if a specific pathway was identified that was stimulated in the presence of GdnHCl alone and further so in the presence of both GdnHCl and TA, it might provide evidence that TA enhances the curing effects of GdnHCl, either directly or indirectly. A number of genes displaying this pattern of expression were identified and are described in table 4.7.

Few genes were identified that were that were downregulated under GdnHCl exposure and considerably moreso in the presence of a combination of GdnHCl and TA.

Table 4.7 Expression levels of a number of genes upregulated by GdnHCl alone and furthermore by GdnHCl and TA combined. Gene functions were obtained from www.yeastgenome.org (SGD).

Gene Name	Function	Basal expression level	Expression level under 200 µM GdnHCl exposure (14 generations)	Expression level under 200 µM GdnHCl + 20 µM TA exposure (14 generations)
MRPL38	Mitochondrial ribosomal protein of the large subunit;	69.43	215.48	314.14
ALT1	Alanine transaminase (glutamic pyruvic transaminase); involved in alanine biosynthetic and catabolic processes; the authentic, non-tagged protein is detected in highly purified mitochondria in high-throughput studies	84.27	249.43	344.00
PIR3	O-glycosylated covalently-bound cell wall protein required for cell wall stability; expression is cell cycle regulated, peaking in M/G1 and also subject to regulation by the cell integrity pathway	697.16	861.49	2063.50
SPI1	GPI-anchored cell wall protein involved in weak acid resistance; basal expression requires Msn2p/Msn4p; expression is induced under conditions of stress and during the diauxic shift; similar to Sed1p	2278.04	4990.85	6603.60
CAT5	Protein required for ubiquinone (Coenzyme Q) biosynthesis; localizes to the matrix face of the mitochondrial inner membrane in a large complex with ubiquinone biosynthetic enzymes; required for gluconeogenic gene activation	77.42	141.75	200.64

BDH2	Putative medium-chain alcohol dehydrogenase with similarity to BDH1; transcription induced by constitutively active PDR1 and PDR3	499.11	930.11	1326.29
HBT1	Substrate of the Hub1p ubiquitin-like protein that localizes to the shmoo tip (mating projection); mutants are defective for mating projection formation, thereby implicating Hbt1p in polarized cell morphogenesis	540.09	581.27	1269.92
GLK1	Glucokinase, catalyzes the phosphorylation of glucose at C6 in the first irreversible step of glucose metabolism; one of three glucose phosphorylating enzymes; expression regulated by non-fermentable carbon sources	2622.84	4872.50	6098.06
CMK1	Calmodulin-dependent protein kinase; may play a role in stress response, many CA++/calmodulan dependent phosphorylation substrates demonstrated in vitro, amino acid sequence similar to Cmk2p and mammalian Cam Kinase II	143.84	214.11	312.65
ADE1	N-succinyl-5-aminoimidazole-4-carboxamide ribotide (SAICAR) synthetase, required for 'de novo' purine nucleotide biosynthesis; red pigment accumulates in mutant cells deprived of adenine	285.98	478.53	610.86
ADE17	Enzyme of 'de novo' purine biosynthesis containing both 5-aminoimidazole-4-carboxamide ribonucleotide transformylase and inosine monophosphate cyclohydrolase activities, isozyme of Ade16p; ade16 ade17 mutants require adenine and histidine	291.74	370.34	547.34

4.18.1.4 Analysis of the effect of 1 hr 200 µM GdnHCl + 20 µM TA exposure on yeast cells

S. cerevisiae cultures were treated with 200 µM GdnHCl + 20 µM TA for 1 hr, after which the genes differentially expressed were investigated. In response to this treatment, 164 genes were upregulated more than 2-fold, 45 of these more than 3-fold. 421 genes were downregulated more than 2-fold, 157 of these in excess of 3-fold.

Summary of the overall effects of gene upregulation on cells

Figures 4.67-4.69 depict the overall effects on cells induced by genes upregulated more than 2-fold in response to 200 µM GdnHCl + 20 µM TA exposure for 1 hr.

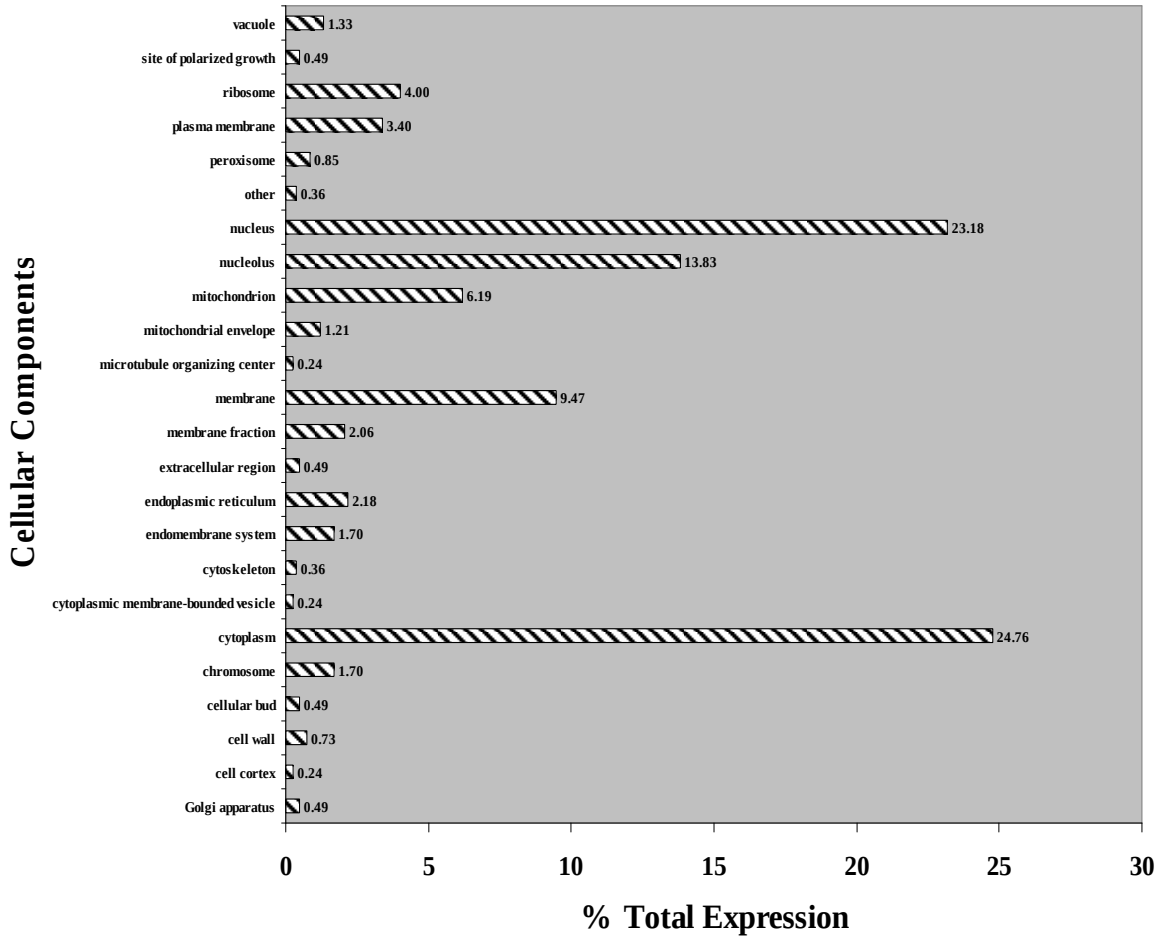

Figure 4.67 The percentage of each cellular component category (200 µM GdnHCl + 20 µM TA 1 hr upregulated genes). Genes upregulated more than two-fold were assigned cellular component categories. The number of genes in each category was expressed as a percentage of the number of total genes.

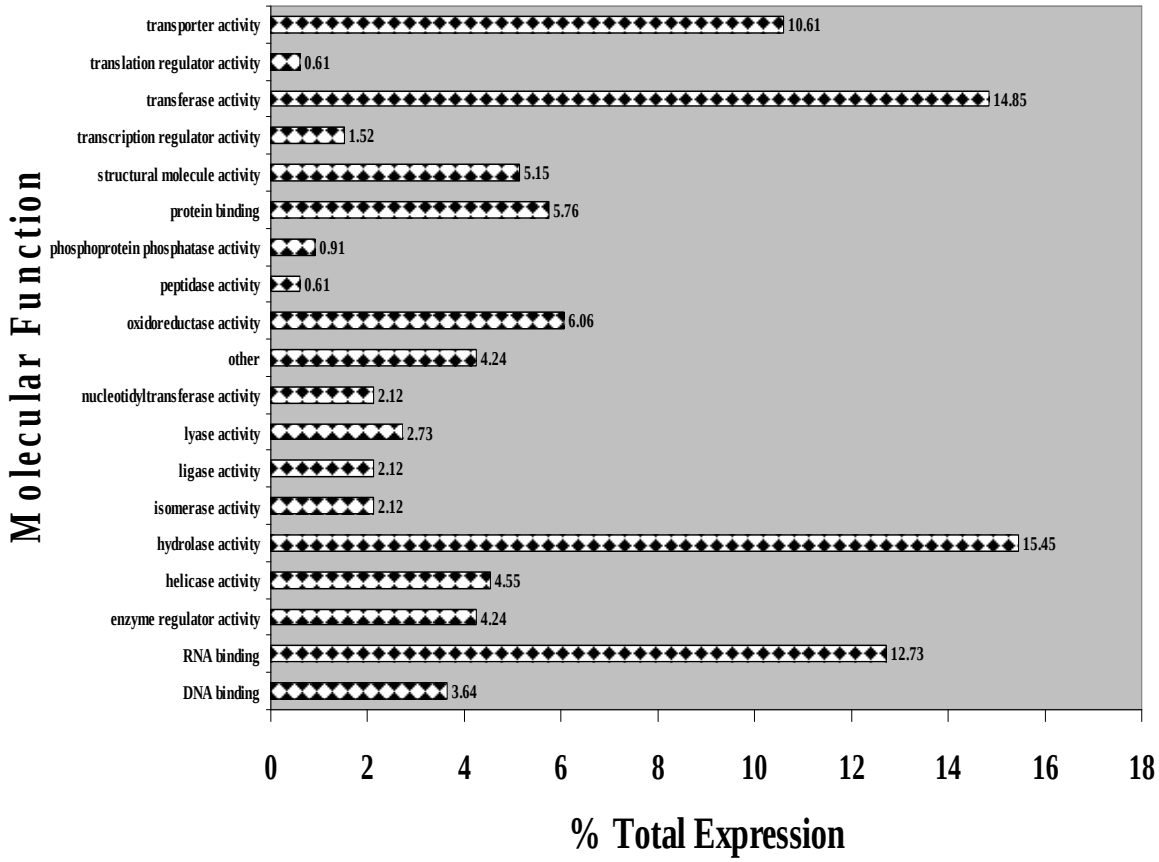

Figure 4.68 The percentage of each molecular function category (200 µM GdnHCl + 20 µM TA 1 hr upregulated genes). Genes upregulated more than two-fold were assigned molecular function categories. The number of genes in each category was expressed as a percentage of the number of total genes.

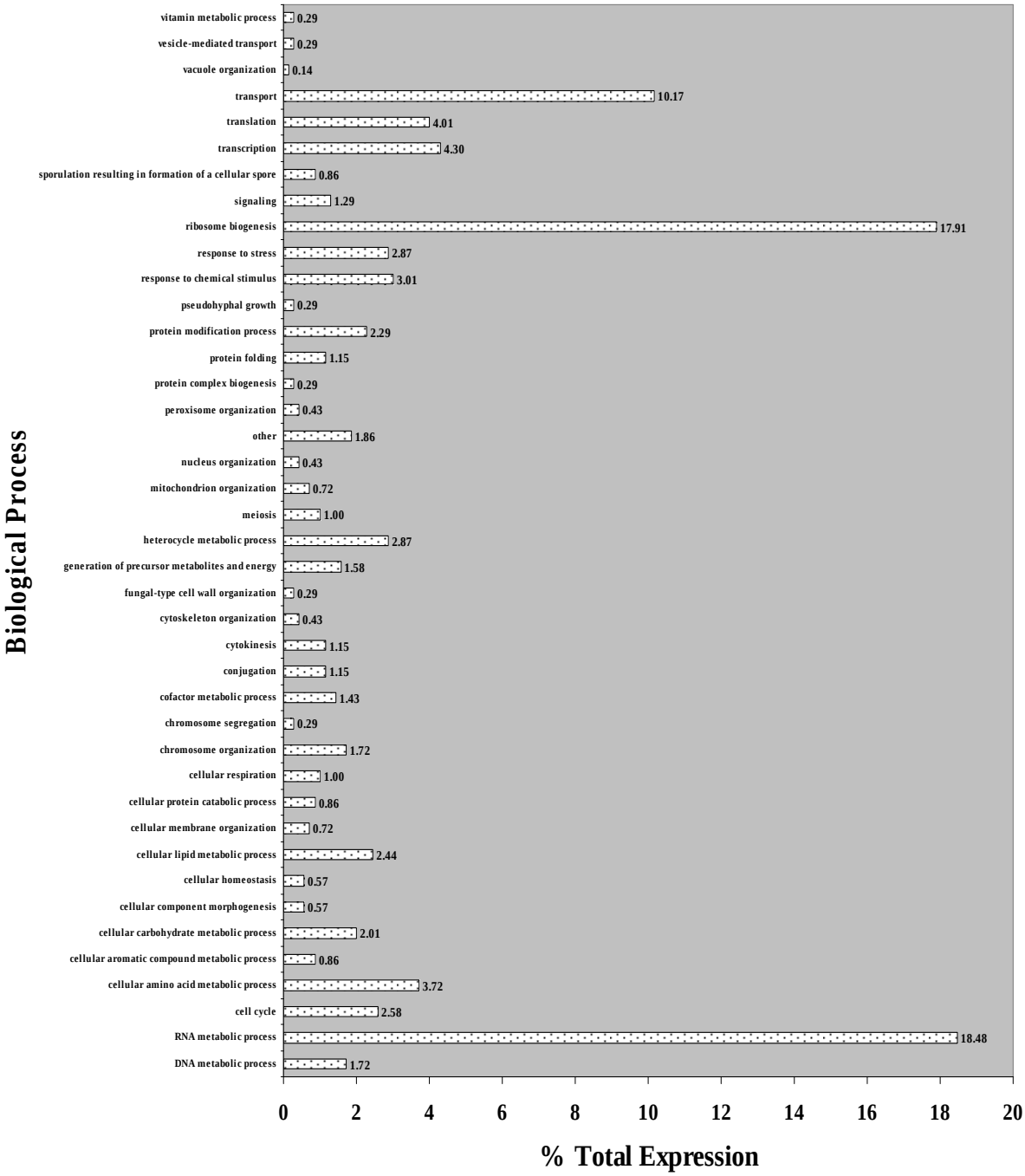

Figure 4.69 The percentage of each biological process category (200 µM GdnHCl + 20 µM TA 1 hr upregulated genes). Genes upregulated more than two-fold were assigned biological process categories. The number of genes in each category was expressed as a percentage of the number of total genes.

The five biological processes, molecular functions and associated cellular components most highly stimulated by exposure to 200 µM GdnHCl + 20 µM TA for 1 hr were further grouped. These are illustrated in figures 4.70-4.72.

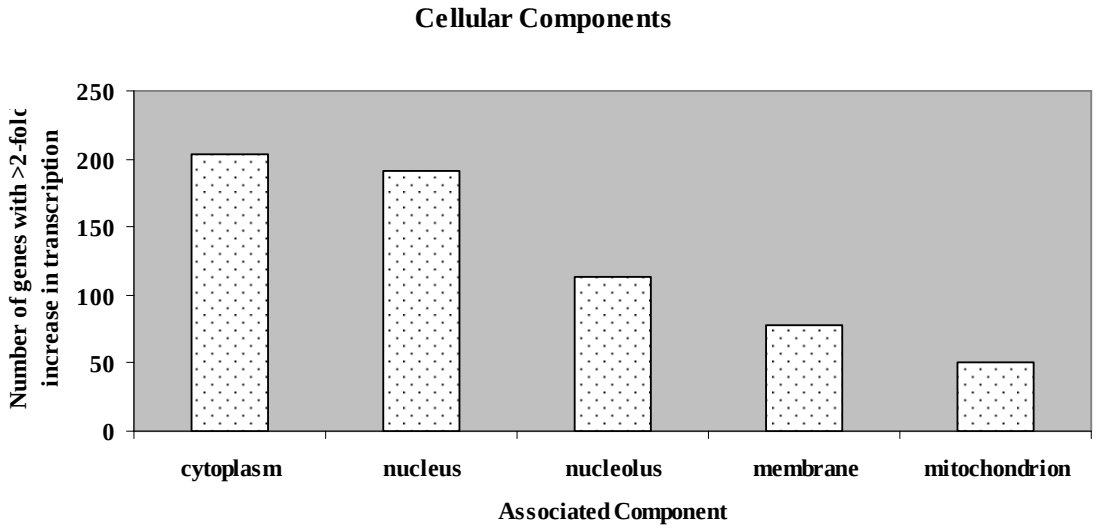

Figure 4.70 The five associated cellular components most highly upregulated by exposure to 200 µM GdnHCl + 20 µM TA for 1 hr.

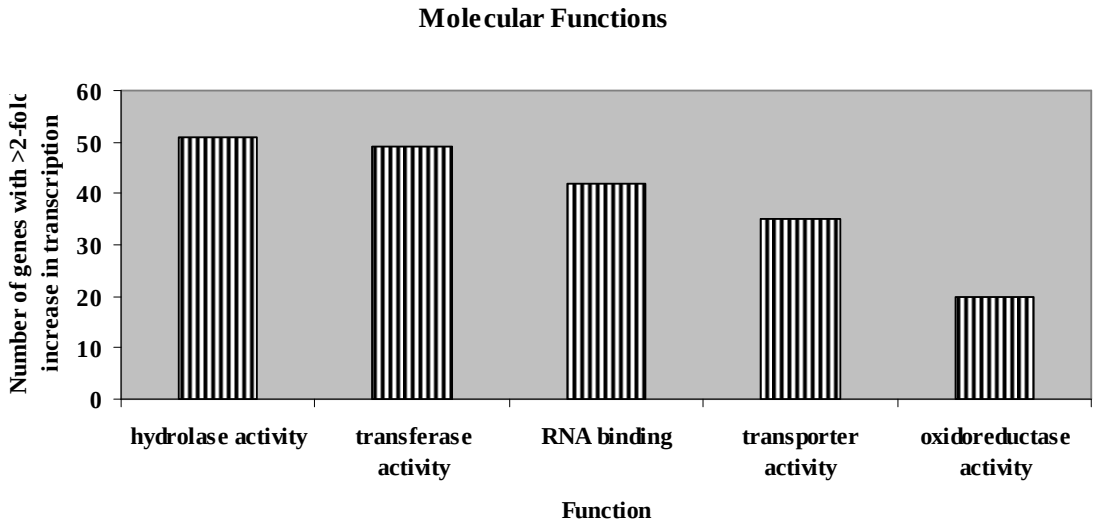

Figure 4.71 The five molecular functions most highly upregulated by exposure to 200 µM GdnHCl + 20 µM TA for 1 hr.

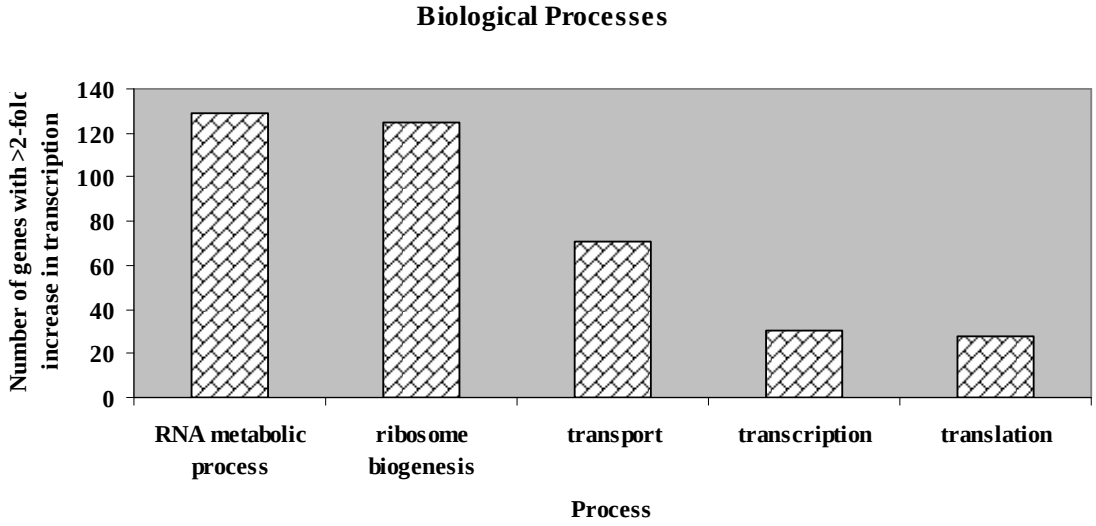

Figure 4.72 The five biological processes most highly upregulated by exposure to 200 µM GdnHCl + 20 µM TA for 1 hr.

Table 4.8 lists the fifty individual genes, and their respective functions, that underwent the highest level of transcriptional upregulation in response to 200 µM GdnHCl + 20 µM TA exposure for 1 hr.

Table 4.8 The fifty genes most highly upregulated in response to 200 µM GdnHCl + 20 µM TA exposure for 1 hr. Gene functions were obtained from www.yeastgenome.org (SGD).

Gene	Fold Change	Gene Function
CUP1-2	17.54	Metallothionein, binds copper and mediates resistance to high concentrations of copper and cadmium; locus is variably amplified in different strains, with two copies, CUP1-1 and CUP1-2, in the genomic sequence reference strain S288C
CUP1-1	17.54	Metallothionein, binds copper and mediates resistance to high concentrations of copper and cadmium; locus is variably amplified in different strains, with two copies, CUP1-1 and CUP1-2, in the genomic sequence reference strain S288C
PCL1	7.63	Cyclin, interacts with cyclin-dependent kinase Pho85p; member of the Pcl1,2-like subfamily, involved in the regulation of polarized growth and morphogenesis and progression through the cell cycle; localizes to sites of polarized cell growth
MF(ALPHA)1	7.16	Mating pheromone alpha-factor, made by alpha cells; interacts with mating type a cells to induce cell cycle arrest and other responses leading to mating; also encoded by MF(ALPHA)2, although MF(ALPHA)1 produces most alpha-factor
CLN1	6.22	G1 cyclin involved in regulation of the cell cycle; activates Cdc28p kinase to promote the G1 to S phase transition; late G1 specific expression depends on transcription factor complexes, MBF (Swi6p-Mbp1p) and SBF (Swi6p-Swi4p)
CWP2	5.99	Covalently linked cell wall mannoprotein, major constituent of the cell wall; plays a role in stabilizing the cell wall; involved in low pH resistance; precursor is GPI-anchored
HTB2	5.51	Histone H2B, core histone protein required for chromatin assembly

		and chromosome function; nearly identical to HTB1; Rad6p-Bre1p-Lge1p mediated ubiquitination regulates transcriptional activation, meiotic DSB formation and H3 methylation
IMD2	5.51	Inosine monophosphate dehydrogenase, catalyzes the rate-limiting step in GTP biosynthesis, expression is induced by mycophenolic acid resulting in resistance to the drug, expression is repressed by nutrient limitation
MAL12	5.50	Maltase (alpha-D-glucosidase), inducible protein involved in maltose catabolism; encoded in the MAL1 complex locus; hydrolyzes the disaccharides maltose, turanose, maltotriose, and sucrose
CTT1	5.08	Cytosolic catalase T, has a role in protection from oxidative damage by hydrogen peroxide
SRL1	5.01	Mannoprotein that exhibits a tight association with the cell wall, required for cell wall stability in the absence of GPI-anchored mannoproteins; has a high serine-threonine content; expression is induced in cell wall mutants
NRM1	4.87	Transcriptional co-repressor of MBF (MCB binding factor)-regulated gene expression; Nrm1p associates stably with promoters via MBF to repress transcription upon exit from G1 phase
KNH1	4.72	Protein with similarity to Kre9p, which is involved in cell wall beta 1,6-glucan synthesis; overproduction suppresses growth defects of a kre9 null mutant; required for propionic acid resistance
YDR246W-A	4.68	Putative protein of unknown function; identified by fungal homology and RT-PCR
PMA2	4.64	Plasma membrane H+-ATPase, isoform of Pma1p, involved in pumping protons out of the cell; regulator of cytoplasmic pH and plasma membrane potential
YNR073C	4.32	Putative mannitol dehydrogenase
MAL32	4.25	Maltase (alpha-D-glucosidase), inducible protein involved in maltose catabolism; encoded in the MAL3 complex locus; functional in genomic reference strain S288C; hydrolyzes the disaccharides maltose, turanose, maltotriose, and sucrose
YFR032C	4.13	Putative protein of unknown function; non-essential gene identified in a screen for mutants with increased levels of rDNA transcription; expressed at high levels during sporulation
HHF2	3.95	Histone H4, core histone protein required for chromatin assembly and chromosome function; one of two identical histone proteins (see also HHF1); contributes to telomeric silencing; N-terminal domain involved in maintaining genomic integrity
DSF1	3.84	Deletion suppressor of mpt5 mutation
CYC1	3.79	Cytochrome c, isoform 1; electron carrier of the mitochondrial intermembrane space that transfers electrons from ubiquinone-cytochrome c oxidoreductase to cytochrome c oxidase during cellular respiration
YHR126C	3.76	Putative protein of unknown function; transcription dependent upon Azf1p
SIM1	3.74	Protein of the SUN family (Sim1p, Uth1p, Nca3p, Sun4p) that may participate in DNA replication, promoter contains SCB regulation box at -300 bp indicating that expression may be cell cycle-regulated
YHP1	3.65	One of two homeobox transcriptional repressors (see also Yox1p), that bind to Mcm1p and to early cell cycle box (ECB) elements of cell cycle regulated genes, thereby restricting ECB-mediated transcription to the M/G1 interval
HHF1	3.61	Histone H4, core histone protein required for chromatin assembly and chromosome function; one of two identical histone proteins (see also HHF2); contributes to telomeric silencing; N-terminal domain involved in maintaining genomic integrity
SCW4	3.61	Cell wall protein with similarity to glucanases; scw4 scw10 double mutants exhibit defects in mating
CCW12	3.57	Cell wall mannoprotein, mutants are defective in mating and agglutination, expression is downregulated by alpha-factor

CLB1	3.52	B-type cyclin involved in cell cycle progression; activates Cdc28p to promote the transition from G2 to M phase; accumulates during G2 and M, then targeted via a destruction box motif for ubiquitin-mediated degradation by the proteasome
YGR107W	3.50	Dubious open reading frame unlikely to encode a protein, based on available experimental and comparative sequence data
ALD3	3.44	Cytoplasmic aldehyde dehydrogenase, involved in beta-alanine synthesis; uses NAD+ as the preferred coenzyme; very similar to Ald2p; expression is induced by stress and repressed by glucose
YEL007W	3.43	Putative protein with sequence similarity to S. pombe gti1+ (gluconate transport inducer 1)
ENO1	3.38	Enolase I, a phosphopyruvate hydratase that catalyzes the conversion of 2-phosphoglycerate to phosphoenolpyruvate during glycolysis and the reverse reaction during gluconeogenesis; expression is repressed in response to glucose
GAS3	3.37	Putative 1,3-beta-glucanosyltransferase, has similarity to Gas1p; localizes to the cell wall
ADH4	3.35	Alcohol dehydrogenase isoenzyme type IV, dimeric enzyme demonstrated to be zinc-dependent despite sequence similarity to iron-activated alcohol dehydrogenases; transcription is induced in response to zinc deficiency
YHL018W	3.33	Putative protein of unknown function; green fluorescent protein (GFP)-fusion protein localizes to mitochondria and is induced in response to the DNA-damaging agent MMS
PDS1	3.26	Securin, inhibits anaphase by binding separin Esp1p; blocks cyclin destruction and mitotic exit, essential for meiotic progression and mitotic cell cycle arrest; localization is cell-cycle dependent and regulated by Cdc28p phosphorylation
HXK1,YFR052C-A	3.21	Hexokinase isoenzyme 1, a cytosolic protein that catalyzes phosphorylation of glucose during glucose metabolism; expression is highest during growth on non-glucose carbon sources; glucose-induced repression involves the hexokinase Hxk2p
YMR144W	3.20	Putative protein of unknown function; localized to the nucleus; YMR144W is not an essential gene
GPD1	3.19	NAD-dependent glycerol-3-phosphate dehydrogenase, key enzyme of glycerol synthesis, essential for growth under osmotic stress; expression regulated by high-osmolarity glycerol response pathway; homolog of Gpd2p
WSC4	3.19	ER membrane protein involved in the translocation of soluble secretory proteins and insertion of membrane proteins into the ER membrane; may also have a role in the stress response but has only partial functional overlap with WSC1-3
YPL014W	3.17	Putative protein of unknown function; green fluorescent protein (GFP)-fusion protein localizes to the cytoplasm and to the nucleus
YOX1	3.15	Homeodomain-containing transcriptional repressor, binds to Mcm1p and to early cell cycle boxes (ECBs) in the promoters of cell cycle-regulated genes expressed in M/G1 phase; expression is cell cycle-regulated; potential Cdc28p substrate
SWI5	3.12	Transcription factor that activates transcription of genes expressed at the M/G1 phase boundary and in G1 phase; localization to the nucleus occurs during G1 and appears to be regulated by phosphorylation by Cdc28p kinase
GDH1	3.09	NADP(+)-dependent glutamate dehydrogenase, synthesizes glutamate from ammonia and alpha-ketoglutarate; rate of alpha-ketoglutarate utilization differs from Gdh3p; expression regulated by nitrogen and carbon sources
YMR003W	3.00	Protein of unknown function; GFP-fusion protein localizes to the mitochondria; null mutant is viable and displays reduced frequency of mitochondrial genome loss
ALD2	2.00	Cytoplasmic aldehyde dehydrogenase, involved in ethanol oxidation and beta-alanine biosynthesis; uses NAD+ as the preferred coenzyme; expression is stress induced and glucose repressed; very similar to Ald3p

YOS1	2.00	Integral membrane protein required for ER to Golgi transport; localized to the Golgi, the ER, and COPII vesicles; interacts with Yip1p and Yif1p
ECO1	2.00	Acetyltransferase required for sister chromatid cohesion; modifies Smc3p at DNA replication forks during S-phase; modifies Mcd1p in response to double-strand DNA breaks during G2/M; mutations in human homolog ESCO2 cause Roberts syndrome
MSN4	2.00	Transcriptional activator related to Msn2p; activated in stress conditions, which results in translocation from the cytoplasm to the nucleus; binds DNA at stress response elements of responsive genes, inducing gene expression
SGO1	2.02	Component of the spindle checkpoint, involved in sensing lack of tension on mitotic chromosomes; protects centromeric Rec8p at meiosis I; required for accurate chromosomal segregation at meiosis II and for mitotic chromosome stability

Summary of the overall effects of gene downregulation on cells

Figures 4.73-4.75 depict the overall effects on cells induced by genes downregulated more than 2-fold in response to 200 µM GdnHCl + 20 µM TA exposure for 1 hr.

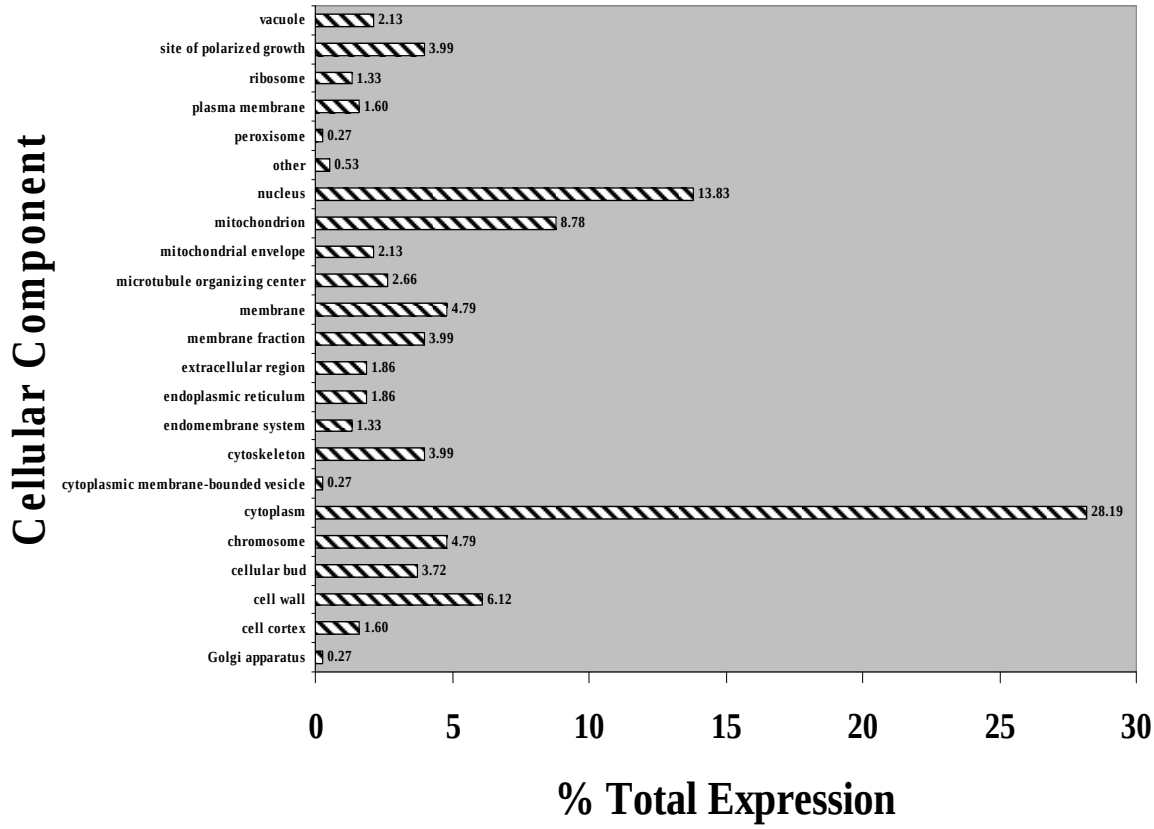

Figure 4.73 The percentage of each cellular component category (200 µM GdnHCl + 20 µM TA 1 hr downregulated genes). Genes downregulated more than two-fold were assigned cellular component categories. The number of genes in each category was expressed as a percentage of the number of total genes.

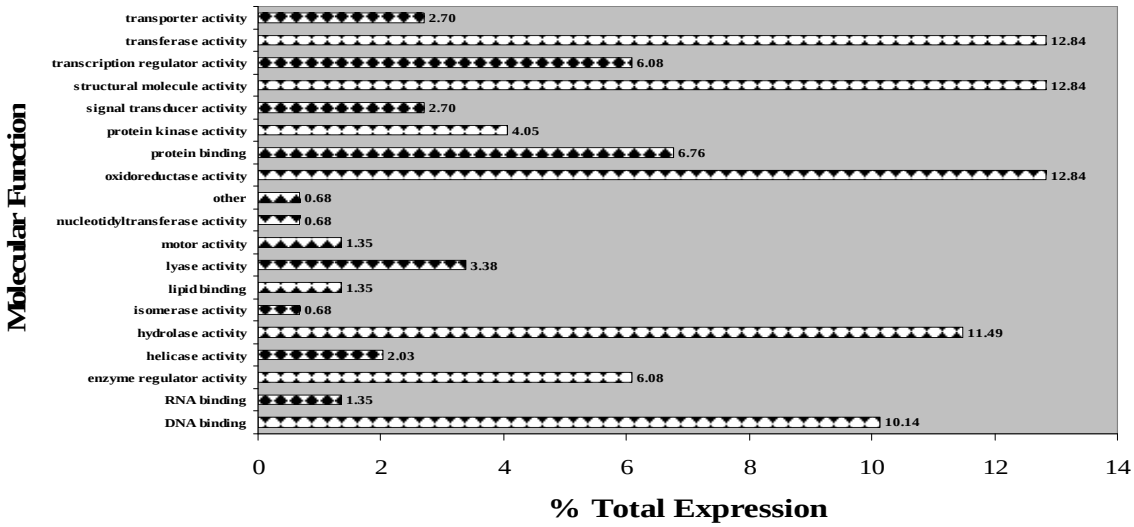

Figure 4.74 The percentage of each molecular function category (200 µM GdnHCl + 20 µM TA 1 hr downregulated genes). Genes downregulated more than two-fold were assigned molecular function categories. The number of genes in each category was expressed as a percentage of the number of total genes.

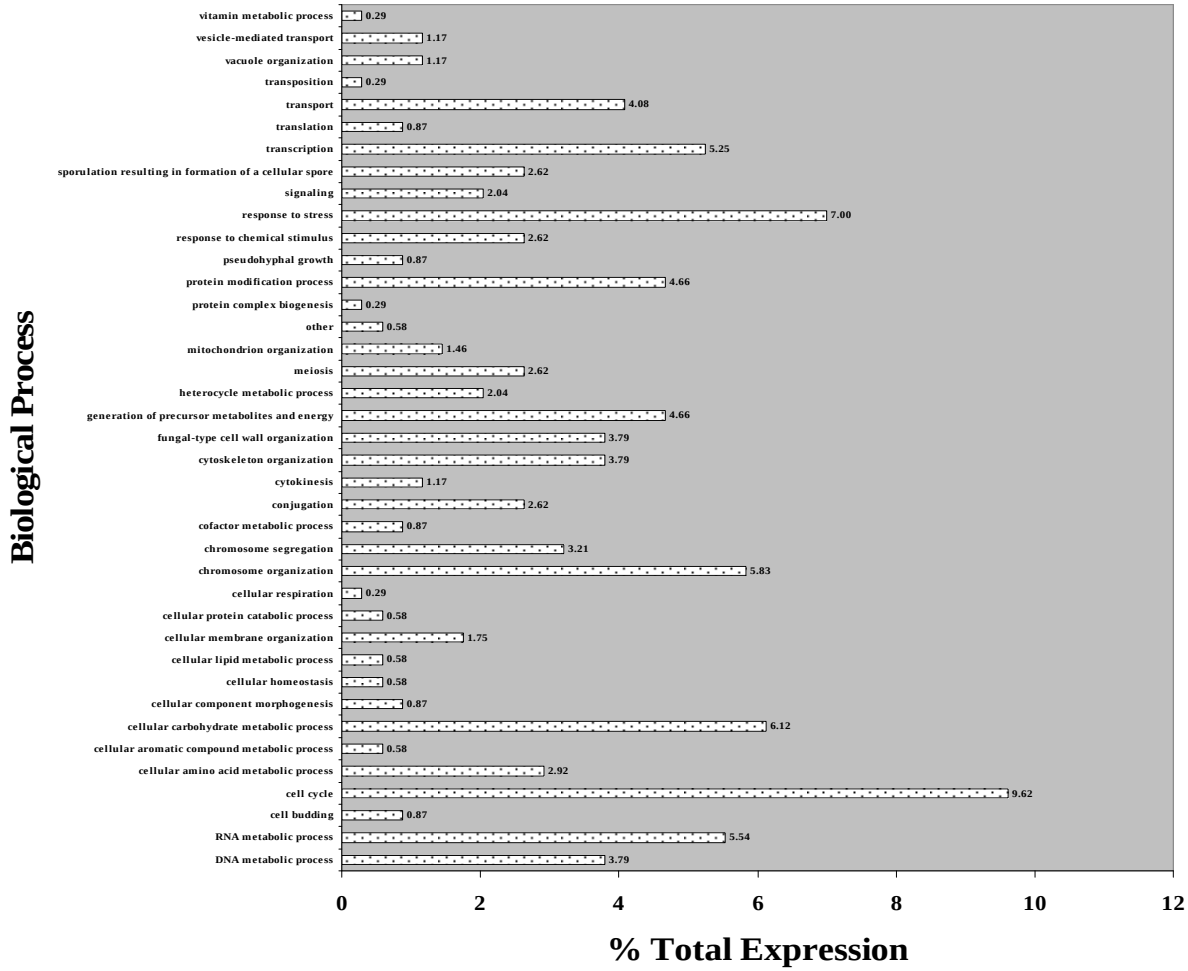

Figure 4.75 The percentage of each biological process category (200 µM GdnHCl + 20 µM TA 1 hr downregulated genes). Genes downregulated more than two-fold were assigned biological process categories. The number of genes in each category was expressed as a percentage of the number of total genes.

The five biological processes, molecular functions and associated cellular components most downregulated by exposure to 200 µM GdnHCl + 20 µM TA for 1 hr were further grouped. These are illustrated in figures 4.76-4.78.

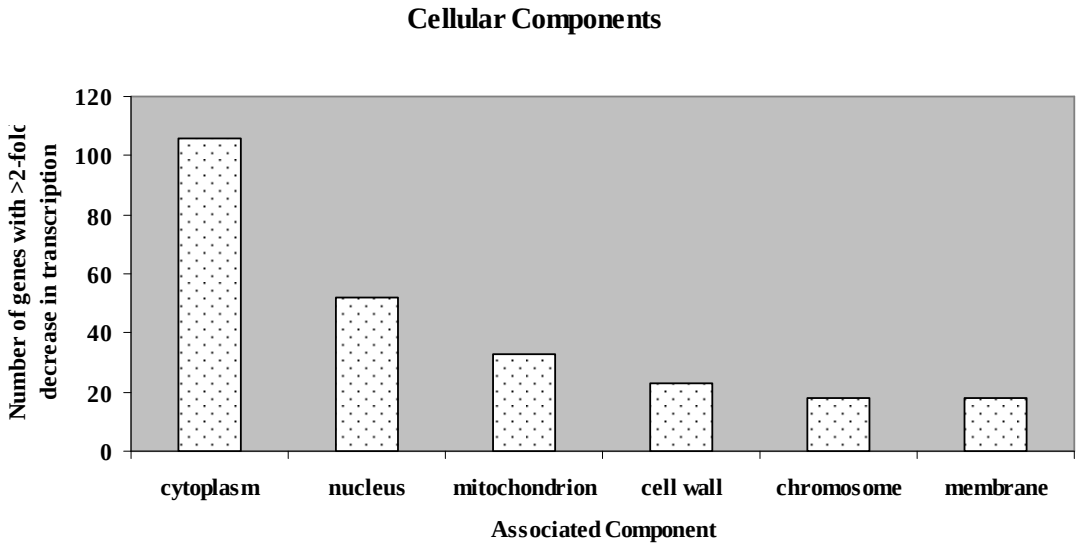

**Figure 4.76 The *five associated cellular components most highly downregulated by exposure to 200 µM GdnHCl + 20 µM TA for 1 hr. ***The 5th and 6th most repressed associated cellular components are represented by the same number of genes and are thus both included.

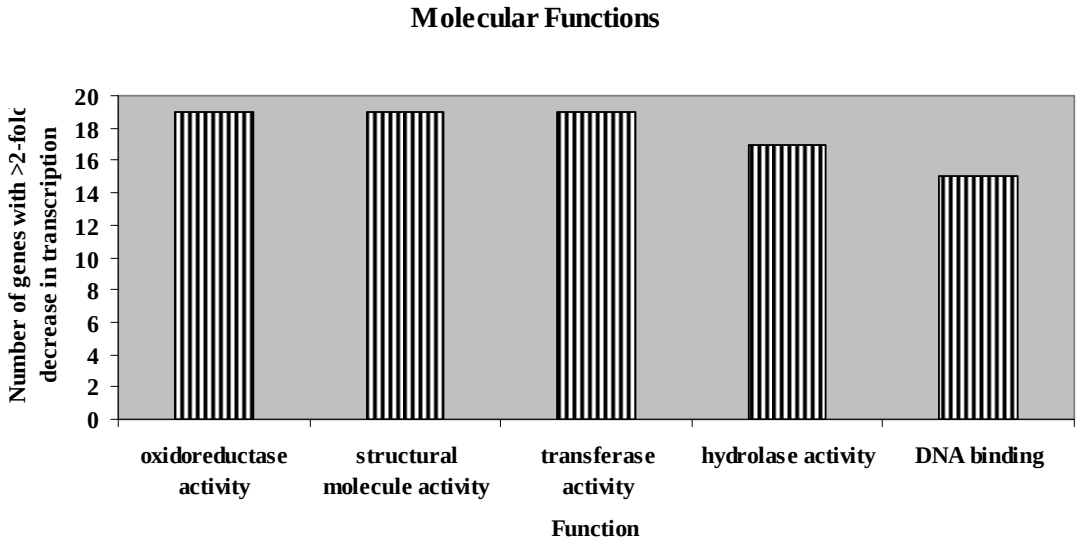

Figure 4.77 The five molecular functions most highly downregulated by exposure to 200 µM GdnHCl + 20 µM TA for 1 hr.

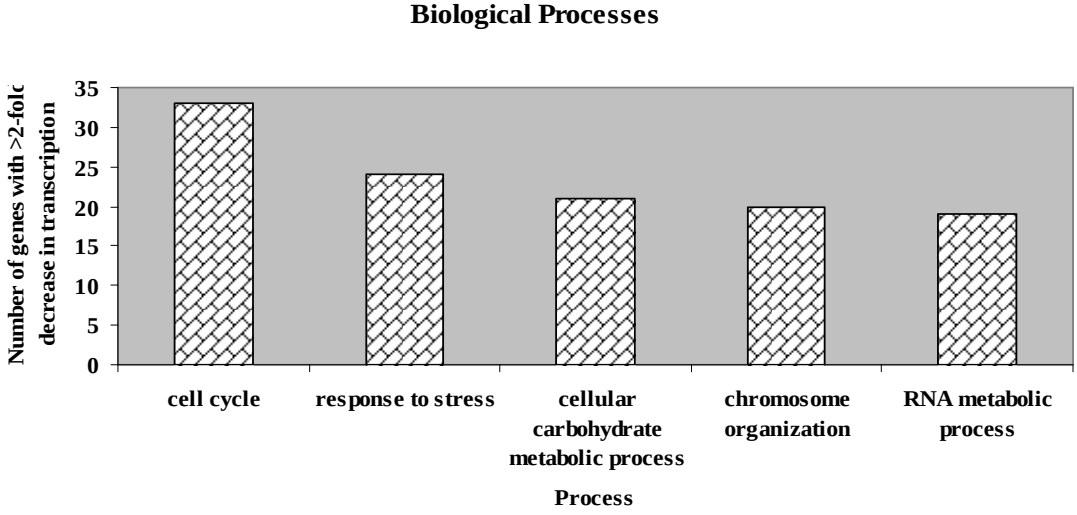

Figure 4.78 The five biological processes most highly downregulated by exposure to 200 µM GdnHCl + 20 µM TA for 1 hr.

Table 4.9 lists the fifty individual genes, and their respective functions, that underwent the most acute transcriptional downregulation in response to 200 µM GdnHCl + 20 µM TA exposure for 1 hr.

Table 4.9 The fifty genes most highly downregulated in response to 200 µM GdnHCl + 20 µM TA exposure for 1 hr. Gene functions were obtained from www.yeastgenome.org (SGD).

Gene	Fold Change	Gene Function
ADY2	-22.82	Acetate transporter required for normal sporulation; phosphorylated in mitochondria
FRM2	-21.65	Protein of unknown function, involved in the integration of lipid signaling pathways with cellular homeostasis; expression induced in cells treated with the mycotoxin patulin; has similarity to bacterial nitroreductases
BSC1	-12.31	Protein of unconfirmed function, similar to cell surface flocculin Muc1p; ORF exhibits genomic organization compatible with a translational readthrough-dependent mode of expression
COX2	-11.51	Subunit II of cytochrome c oxidase, which is the terminal member of the mitochondrial inner membrane electron transport chain; one of three mitochondrially-encoded subunits
SAM1	-11.25	S-adenosylmethionine synthetase, catalyzes transfer of the adenosyl group of ATP to the sulfur atom of methionine; one of two differentially regulated isozymes (Sam1p and Sam2p)
JJJ3	-9.53	Protein of unknown function, contains a J-domain, which is a region with homology to the E. coli DnaJ protein
DBP2	-9.52	Essential ATP-dependent RNA helicase of the DEAD-box protein family, involved in nonsense-mediated mRNA decay and rRNA processing
CIT2	-9.14	Citrate synthase, catalyzes the condensation of acetyl coenzyme A and oxaloacetate to form citrate, peroxisomal isozyme involved in glyoxylate cycle; expression is controlled by Rtg1p

		and Rtg2p transcription factors
SPL2	-8.90	Protein with similarity to cyclin-dependent kinase inhibitors; downregulates low-affinity phosphate transport during phosphate limitation; overproduction suppresses a plc1 null mutation; GFP-fusion protein localizes to the cytoplasm
SFC1	-8.40	Mitochondrial succinate-fumarate transporter, transports succinate into and fumarate out of the mitochondrion; required for ethanol and acetate utilization
DLD3	-7.74	D-lactate dehydrogenase, part of the retrograde regulon which consists of genes whose expression is stimulated by damage to mitochondria and reduced in cells grown with glutamate as the sole nitrogen source, located in the cytoplasm
CHA1	-7.71	Catabolic L-serine (L-threonine) deaminase, catalyzes the degradation of both L-serine and L-threonine; required to use serine or threonine as the sole nitrogen source, transcriptionally induced by serine and threonine
GUA1	-7.04	GMP synthase, an enzyme that catalyzes the second step in the biosynthesis of GMP from inosine 5'-phosphate (IMP); transcription is not subject to regulation by guanine but is negatively regulated by nutrient starvation
YIL057C	-6.51	Protein of unknown function involved in energy metabolism under respiratory conditions; expression induced under carbon limitation and repressed under high glucose
PCK1	-6.48	Phosphoenolpyruvate carboxykinase, key enzyme in gluconeogenesis, catalyzes early reaction in carbohydrate biosynthesis, glucose represses transcription and accelerates mRNA degradation, regulated by Mcm1p and Cat8p, located in the cytosol
CGR1	-6.43	Protein involved in nucleolar integrity and processing of the pre-rRNA for the 60S ribosome subunit; transcript is induced in response to cytotoxic stress but not genotoxic stress
YPR036W-A	-6.39	Protein of unknown function; transcription is regulated by Pdr1p
RKI1	-6.33	Ribose-5-phosphate ketol-isomerase, catalyzes the interconversion of ribose 5-phosphate and ribulose 5-phosphate in the pentose phosphate pathway; participates in pyridoxine biosynthesis
DSE1	-6.21	Daughter cell-specific protein, may regulate cross-talk between the mating and filamentation pathways; deletion affects cell separation after division and sensitivity to alpha-factor and drugs affecting the cell wall
LTV1	-6.16	Component of the GSE complex, which is required for proper sorting of amino acid permease Gap1p; required for ribosomal small subunit export from nucleus; required for growth at low temperature
ERO1	-6.07	Thiol oxidase required for oxidative protein folding in the endoplasmic reticulum
MLS1	-6.03	Malate synthase, enzyme of the glyoxylate cycle, involved in utilization of non-fermentable carbon sources; expression is subject to carbon catabolite repression; localizes in peroxisomes during growth in oleic acid medium
PHO89	-6.01	Na+/Pi cotransporter, active in early growth phase; similar to phosphate transporters of Neurospora crassa; transcription regulated by inorganic phosphate concentrations and Pho4p
RMT2	-5.74	Arginine N5 methyltransferase; methylates ribosomal protein Rpl12 (L12) on Arg67
OSW1	-5.44	Protein involved in sporulation; required for the construction of the outer spore wall layers; required for proper localization of Spo14p
NCE103	-5.36	Carbonic anhydrase; poorly transcribed under aerobic conditions and at an undetectable level under anaerobic conditions; involved in non-classical protein export pathway
YAT2	-5.27	Carnitine acetyltransferase; has similarity to Yat1p, which is a

		carnitine acetyltransferase associated with the mitochondrial outer membrane
YGR067C	-5.19	Putative protein of unknown function; contains a zinc finger motif similar to that of Adr1p
SSF1	-5.15	Constituent of 66S pre-ribosomal particles, required for ribosomal large subunit maturation; functionally redundant with Ssf2p; member of the Brix family
AAC3	-5.09	Mitochondrial inner membrane ADP/ATP translocator, exchanges cytosolic ADP for mitochondrially synthesized ATP; expressed under anaerobic conditions; similar to Pet9p and Aac1p; has roles in maintenance of viability and in respiration
UTP6	-5.00	Nucleolar protein, component of the small subunit (SSU) processome containing the U3 snoRNA that is involved in processing of pre-18S rRNA
YGR272C	-4.96	Essential protein required for maturation of 18S rRNA; null mutant is sensitive to hydroxyurea and is delayed in recovering from alpha-factor arrest; green fluorescent protein (GFP)-fusion protein localizes to the nucleolus
MRD1	-4.86	Essential conserved protein that is part of the 90S preribosome; required for production of 18S rRNA and small ribosomal subunit; contains five consensus RNA-binding domains
NOP15	-4.85	Constituent of 66S pre-ribosomal particles, involved in 60S ribosomal subunit biogenesis; localizes to both nucleolus and cytoplasm
YOR338W	-4.85	Putative protein of unknown function; YOR338W transcription is regulated by Azf1p and its transcript is a specific target of the G protein effector Scp160p; identified as being required for sporulation in a high-throughput mutant screen
ENA1	-4.81	P-type ATPase sodium pump, involved in Na+ and Li+ efflux to allow salt tolerance
YBL028C	-4.78	Protein of unknown function that may interact with ribosomes; green fluorescent protein (GFP)-fusion protein localizes to the nucleolus; predicted to be involved in ribosome biogenesis
NOP14	-4.75	Nucleolar protein, forms a complex with Noc4p that mediates maturation and nuclear export of 40S ribosomal subunits; also present in the small subunit processome complex, which is required for processing of pre-18S rRNA
HCA4	-4.75	Putative nucleolar DEAD box RNA helicase; high-copy number suppression of a U14 snoRNA processing mutant suggests an involvement in 18S rRNA synthesis
DIP5	-4.58	Dicarboxylic amino acid permease, mediates high-affinity and high-capacity transport of L-glutamate and L-aspartate; also a transporter for Gln, Asn, Ser, Ala, and Gly
DSE2	-4.49	Daughter cell-specific secreted protein with similarity to glucanases, degrades cell wall from the daughter side causing daughter to separate from mother; expression is repressed by cAMP
PUT1	-4.45	Proline oxidase, nuclear-encoded mitochondrial protein involved in utilization of proline as sole nitrogen source; PUT1 transcription is induced by Put3p in the presence of proline and the absence of a preferred nitrogen source
RPF1	-4.43	Nucleolar protein involved in the assembly and export of the large ribosomal subunit; constituent of 66S pre-ribosomal particles; contains a sigma(70)-like motif, which is thought to bind RNA
HIT1	-4.36	Protein of unknown function, required for growth at high temperature
NIP7	-4.32	Nucleolar protein required for 60S ribosome subunit biogenesis, constituent of 66S pre-ribosomal particles; physically interacts with Nop8p and the exosome subunit Rrp43p
FAL1	-4.27	Nucleolar protein required for maturation of 18S rRNA, member of the eIF4A subfamily of DEAD-box ATP-dependent RNA helicases

OLI1	-4.18	F0-ATP synthase subunit c (ATPase-associated proteolipid), encoded on the mitochondrial genome; mutation confers oligomycin resistance; expression is specifically dependent on the nuclear genes AEP1 and AEP2
YGR271C-A	-4.18	Essential protein required for maturation of 18S rRNA; null mutant is sensitive to hydroxyurea and is delayed in recovering from alpha-factor arrest; green fluorescent protein (GFP)-fusion protein localizes to the nucleolus
DRS1	-4.18	Nucleolar DEAD-box protein required for ribosome assembly and function, including synthesis of 60S ribosomal subunits; constituent of 66S pre-ribosomal particles
FAF1	-4.14	Protein required for pre-rRNA processing and 40S ribosomal subunit assembly

4.18.1.5 Analysis of the effect of 3 hr 200 µM GdnHCl + 20 µM TA exposure on yeast cells

In response to 200 µM GdnHCl + 20 µM TA exposure for 3 hr, 175 *S. cerevisiae* genes were upregulated more than 2-fold, 50 of these over 3-fold. The same treatment led to 571 genes being downregulated more than 2-fold, 163 of these more than 3-fold.

Summary of the overall effects of gene upregulation on cells

Figures 4.79-4.81 depict the overall effects on cells induced by genes upregulated more than 2-fold in response to 200 µM GdnHCl + 20 µM TA exposure for 3 hr.

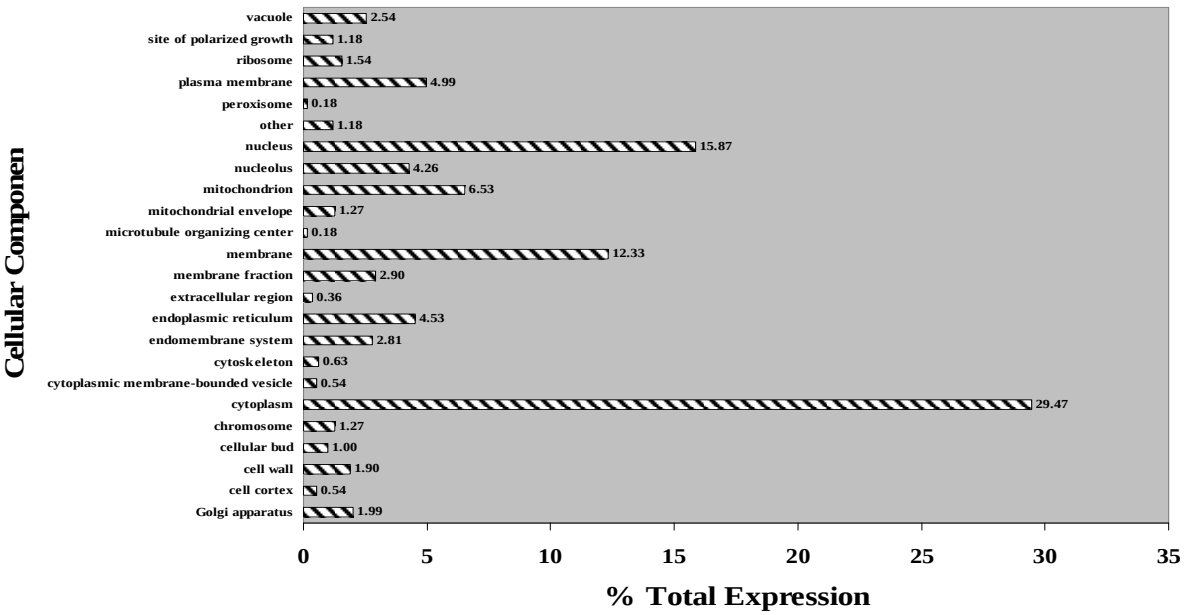

Figure 4.79 The percentage of each cellular component category (200 µM GdnHCl + 20 µM TA 3 hr upregulated genes). Genes upregulated more than two-fold were assigned cellular component categories. The number of genes in each category was expressed as a percentage of the number of total genes.

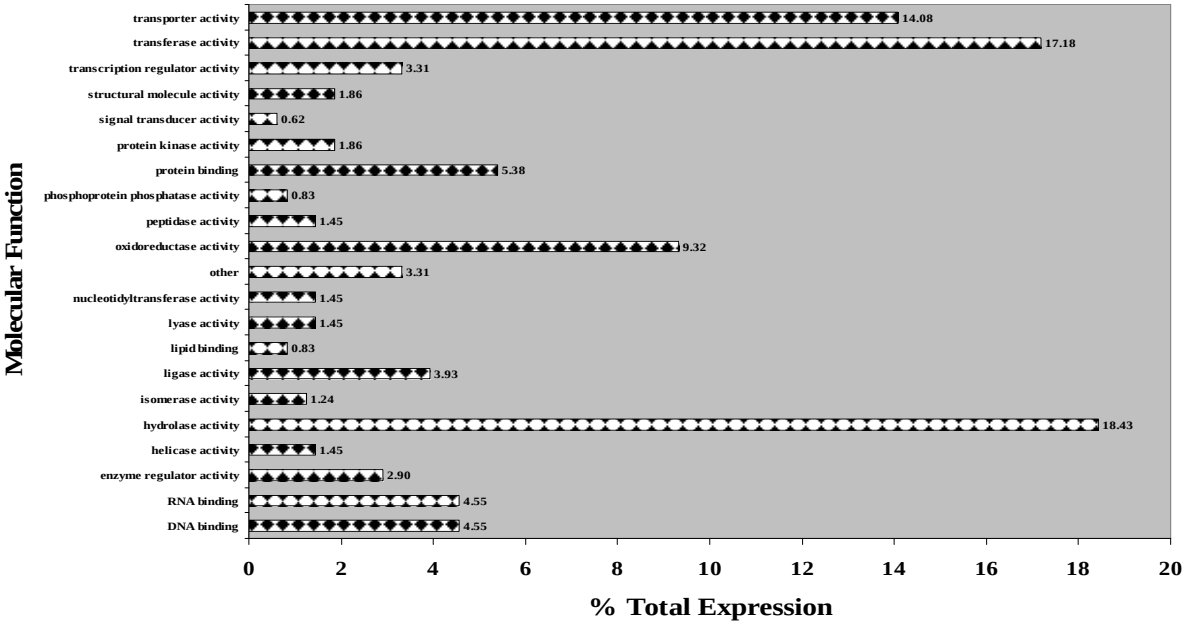

Figure 4.80 The percentage of each molecular function category (200 µM GdnHCl + 20 µM TA 3 hr upregulated genes). Genes upregulated more than two-fold were assigned molecular function categories. The number of genes in each category was expressed as a percentage of the number of total genes.

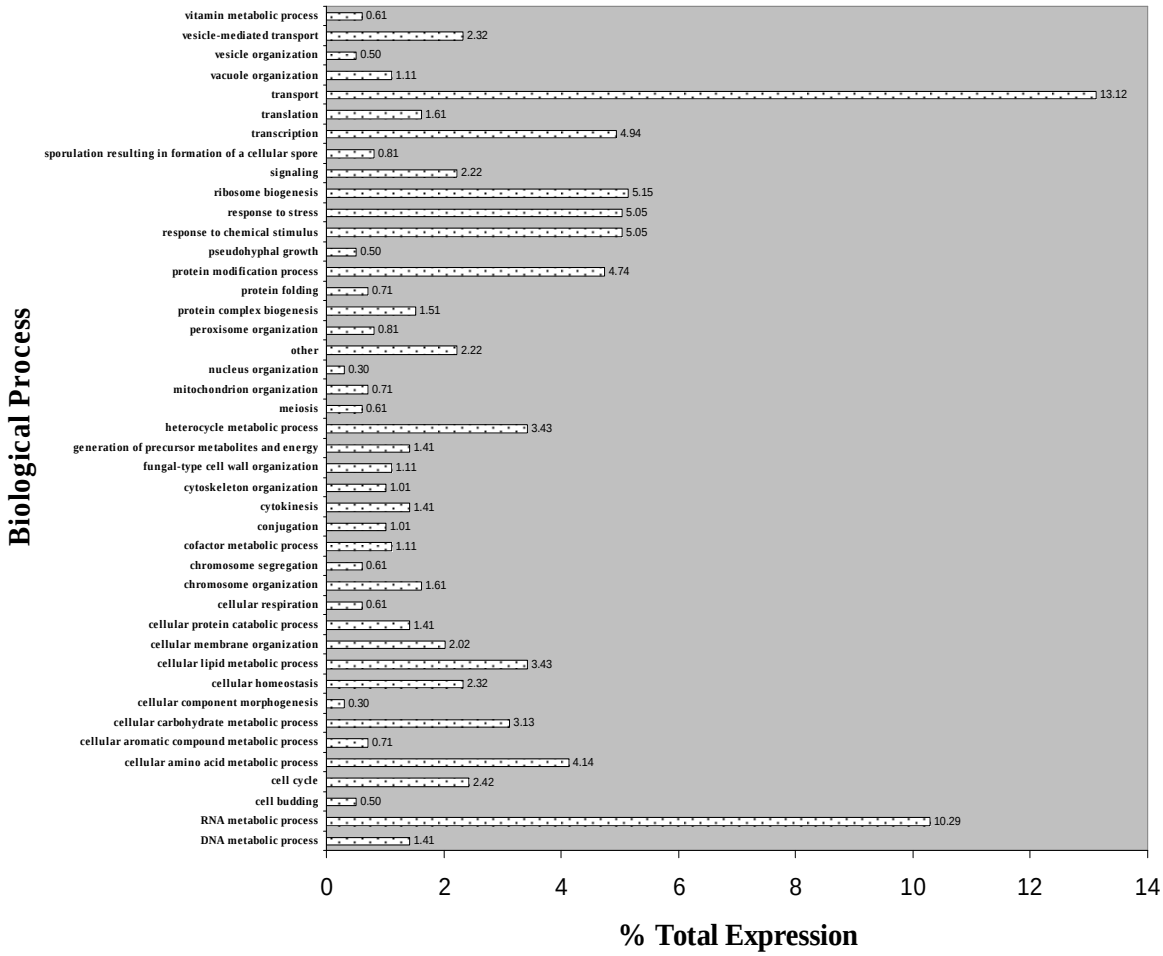

Figure 4.81 The percentage of each biological process category (200 µM GdnHCl + 20 µM TA 3 hr upregulated genes). Genes upregulated more than two-fold were assigned biological process categories. The number of genes in each category was expressed as a percentage of the number of total genes.

The five biological processes, molecular functions and associated cellular components most induced by exposure to 200 µM GdnHCl + 20 µM TA for 3 hr were further explored. These are illustrated in figures 4.82-4.84.

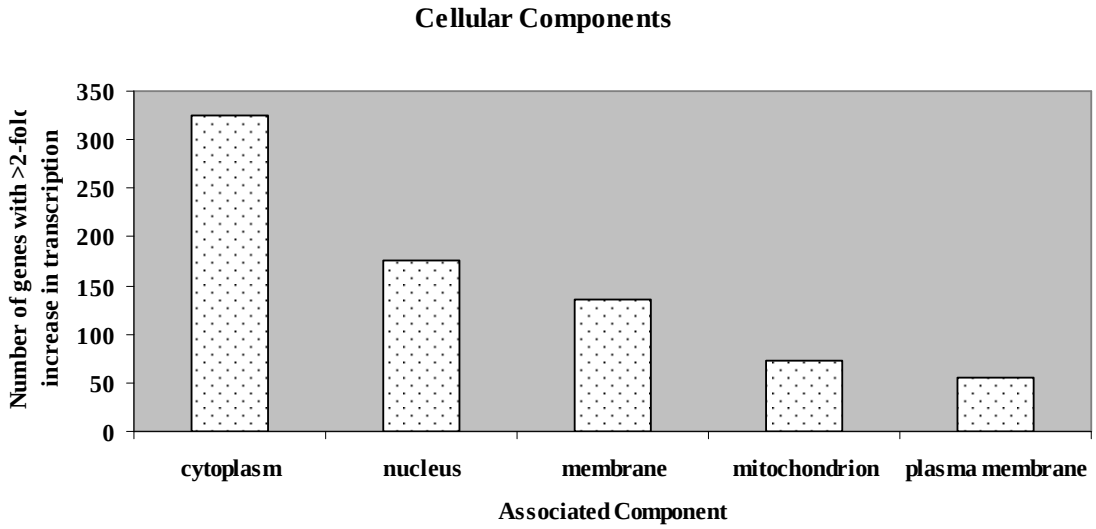

Figure 4.82 The five associated cellular components most highly upregulated by exposure to 200 µM GdnHCl + 20 µM TA for 3 hr.

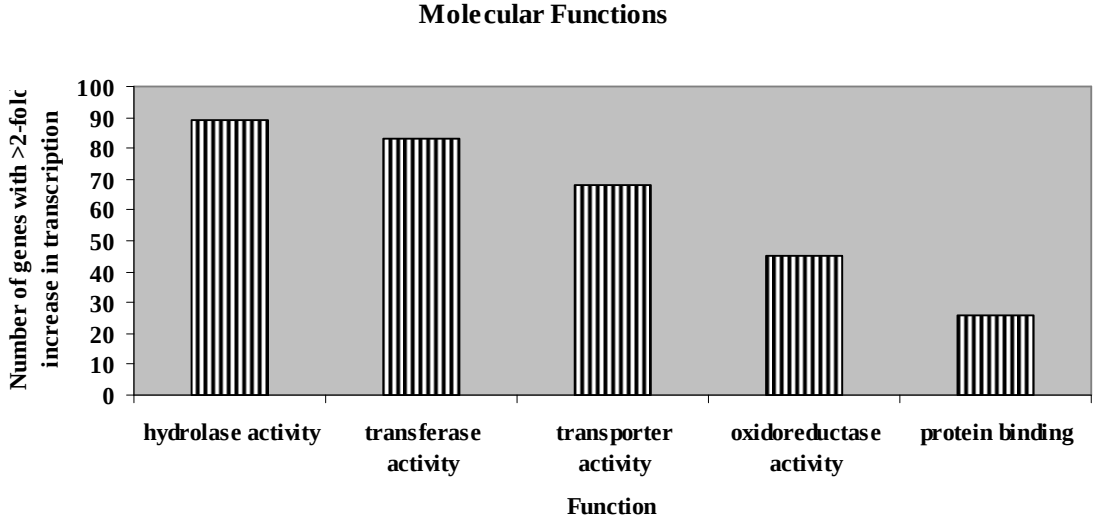

Figure 4.83 The five molecular functions most highly upregulated by exposure to 200 µM GdnHCl + 20 µM TA for 3 hr.

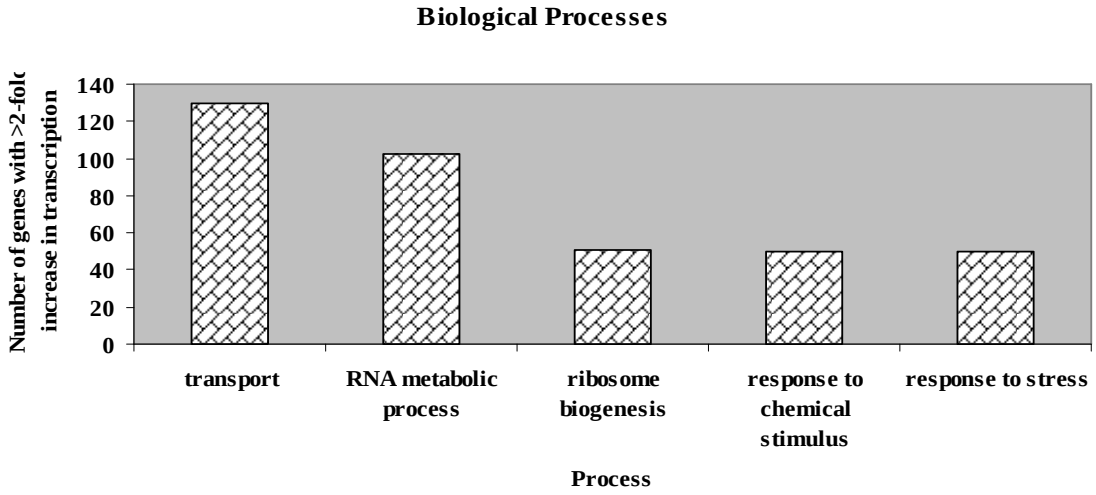

Figure 4.84 The five biological processes most highly upregulated by exposure to 200 µM GdnHCl + 20 µM TA for 3 hr.

Table 4.10 lists the fifty individual genes, and their respective functions, that underwent the highest level of transcriptional upregulation in response to 200 µM GdnHCl + 20 µM TA exposure for 3 hr.

Table 4.10 The fifty genes most highly upregulated in response to 200 µM GdnHCl + 20 µM TA exposure for 3 hr. Gene functions were obtained from www.yeastgenome.org (SGD).

Gene	Fold Change	Gene Function
MF(ALPHA)1	18.97	Mating pheromone alpha-factor, made by alpha cells; interacts with mating type a cells to induce cell cycle arrest and other responses leading to mating; also encoded by MF(ALPHA)2, although MF(ALPHA)1 produces most alpha-factor
ARO10	14.35	Phenylpyruvate decarboxylase, catalyzes decarboxylation of phenylpyruvate to phenylacetaldehyde, which is the first specific step in the Ehrlich pathway
ICL1	9.97	Isocitrate lyase, catalyzes the formation of succinate and glyoxylate from isocitrate, a key reaction of the glyoxylate cycle; expression of ICL1 is induced by growth on ethanol and repressed by growth on glucose
MLS1	8.17	Malate synthase, enzyme of the glyoxylate cycle, involved in utilization of non-fermentable carbon sources; expression is subject to carbon catabolite repression; localizes in peroxisomes during growth in oleic acid medium
PMA2	7.89	Plasma membrane H+-ATPase, isoform of Pma1p, involved in pumping protons out of the cell; regulator of cytoplasmic pH and plasma membrane potential
YJL045W	6.83	Minor succinate dehydrogenase isozyme; homologous to Sdh1p, the major isozyme reponsible for the oxidation of succinate and transfer of electrons to ubiquinone; induced during the diauxic shift in a Cat8p-dependent manner
KNH1	6.59	Protein with similarity to Kre9p, which is involved in cell wall beta 1,6-glucan synthesis; overproduction suppresses growth defects of a kre9 null mutant; required for propionic acid

		resistance
MDH2	6.22	Cytoplasmic malate dehydrogenase, one of three isozymes that catalyze interconversion of malate and oxaloacetate; involved in the glyoxylate cycle and gluconeogenesis during growth on two-carbon compounds; interacts with Pck1p and Fbp1
PDC6	5.73	Minor isoform of pyruvate decarboxylase, decarboxylates pyruvate to acetaldehyde, involved in amino acid catabolism; transcription is glucose- and ethanol-dependent, and is strongly induced during sulfur limitation
FBP1	5.50	Fructose-1,6-bisphosphatase, key regulatory enzyme in the gluconeogenesis pathway, required for glucose metabolism; undergoes either proteasome-mediated or autophagy-mediated degradation depending on growth conditions; interacts with Vid30p
ADH2	5.41	Glucose-repressible alcohol dehydrogenase II, catalyzes the conversion of ethanol to acetaldehyde; involved in the production of certain carboxylate esters; regulated by ADR1
ARO9	5.26	Aromatic aminotransferase II, catalyzes the first step of tryptophan, phenylalanine, and tyrosine catabolism
CYC1	5.21	Cytochrome c, isoform 1; electron carrier of the mitochondrial intermembrane space that transfers electrons from ubiquinone-cytochrome c oxidoreductase to cytochrome c oxidase during cellular respiration
PCK1	5.14	Phosphoenolpyruvate carboxykinase, key enzyme in gluconeogenesis, catalyzes early reaction in carbohydrate biosynthesis, glucose represses transcription and accelerates mRNA degradation, regulated by Mcm1p and Cat8p, located in the cytosol
YER158C	4.99	Protein of unknown function, has similarity to Afr1p; potentially phosphorylated by Cdc28p
ACS1	4.89	Acetyl-coA synthetase isoform which, along with Acs2p, is the nuclear source of acetyl-coA for histone acetlyation; expressed during growth on nonfermentable carbon sources and under aerobic conditions
CWP2	4.63	Covalently linked cell wall mannoprotein, major constituent of the cell wall; plays a role in stabilizing the cell wall; involved in low pH resistance; precursor is GPI-anchored
PIR3	4.44	O-glycosylated covalently-bound cell wall protein required for cell wall stability; expression is cell cycle regulated, peaking in M/G1 and also subject to regulation by the cell integrity pathway
SIP18	4.29	Phospholipid-binding protein; expression is induced by osmotic stress
ACO1	4.21	Aconitase, required for the tricarboxylic acid (TCA) cycle and also independently required for mitochondrial genome maintenance; phosphorylated; component of the mitochondrial nucleoid; mutation leads to glutamate auxotrophy
CWP1	4.11	Cell wall mannoprotein that localizes specifically to birth scars of daughter cells, linked to a beta-1,3- and beta-1,6-glucan heteropolymer through a phosphodiester bond; required for propionic acid resistance
TMA7	4.02	Protein of unknown that associates with ribosomes; null mutant exhibits translation defects, altered polyribosome profiles, and resistance to the translation inhibitor anisomcyin
CIT3	4.00	Dual specificity mitochondrial citrate and methylcitrate synthase; catalyzes the condensation of acetyl-CoA and oxaloacetate to form citrate and that of propionyl-CoA and oxaloacetate to form 2-methylcitrate
RPL28	3.99	Ribosomal protein of the large (60S) ribosomal subunit, has similarity to E. coli L15 and rat L27a ribosomal proteins; may have peptidyl transferase activity; can mutate to cycloheximide resistance
ALD6	3.93	Cytosolic aldehyde dehydrogenase, activated by Mg2+ and

		utilizes NADP+ as the preferred coenzyme; required for conversion of acetaldehyde to acetate; constitutively expressed; locates to the mitochondrial outer surface upon oxidative stress
SPS100	3.84	Protein required for spore wall maturation; expressed during sporulation; may be a component of the spore wall; expression also induced in cells treated with the mycotoxin patulin
ATO3	3.84	Plasma membrane protein, regulation pattern suggests a possible role in export of ammonia from the cell; phosphorylated in mitochondria; member of the TC 9.B.33 YaaH family of putative transporters
ACS2	3.80	Acetyl-coA synthetase isoform which, along with Acs1p, is the nuclear source of acetyl-coA for histone acetylation; mutants affect global transcription; required for growth on glucose; expressed under anaerobic conditions
OLE1	3.65	Delta(9) fatty acid desaturase, required for monounsaturated fatty acid synthesis and for normal distribution of mitochondria
NCA3	3.62	Protein that functions with Nca2p to regulate mitochondrial expression of subunits 6 (Atp6p) and 8 (Atp8p) of the Fo-F1 ATP synthase; member of the SUN family; expression induced in cells treated with the mycotoxin patulin
SIP4	3.60	C6 zinc cluster transcriptional activator that binds to the carbon source-responsive element (CSRE) of gluconeogenic genes; involved in the positive regulation of gluconeogenesis; regulated by Snf1p protein kinase; localized to the nucleus
YLR162W	3.44	Putative protein of unknown function; overexpression confers resistance to the antimicrobial peptide MiAMP1
PST1	3.40	Cell wall protein that contains a putative GPI-attachment site; secreted by regenerating protoplasts; up-regulated by activation of the cell integrity pathway, as mediated by Rlm1p; upregulated by cell wall damage via disruption of FKS1
CUP1-1	3.38	Metallothionein, binds copper and mediates resistance to high concentrations of copper and cadmium; locus is variably amplified in different strains, with two copies, CUP1-1 and CUP1-2, in the genomic sequence reference strain S288C
CUP1-2	3.38	Metallothionein, binds copper and mediates resistance to high concentrations of copper and cadmium; locus is variably amplified in different strains, with two copies, CUP1-1 and CUP1-2, in the genomic sequence reference strain S288C
YGL260W	3.34	Putative protein of unknown function; transcription is significantly increased in a NAP1 deletion background; deletion mutant has increased accumulation of nickel and selenium
ARG1	3.31	Arginosuccinate synthetase, catalyzes the formation of L-argininosuccinate from citrulline and L-aspartate in the arginine biosynthesis pathway; potential Cdc28p substrate
YLR164W	3.30	Mitochondrial inner membrane of unknown function; similar to Tim18p and Sdh4p; expression induced by nitrogen limitation in a GLN3, GAT1-dependent manner
ICS2	3.23	Protein of unknown function; null mutation does not confer any obvious defects in growth, spore germination, viability, or carbohydrate utilization
SPO19	3.18	Meiosis-specific prospore protein; required to produce bending force necessary for proper assembly of the prospore membrane during sporulation; identified as a weak high-copy suppressor of the spo1-1 ts mutation
YAT1	3.18	Outer mitochondrial carnitine acetyltransferase, minor ethanol-inducible enzyme involved in transport of activated acyl groups from the cytoplasm into the mitochondrial matrix; phosphorylated
RNH203	3.16	Ribonuclease H2 subunit, required for RNase H2 activity; related to human AGS3 that causes Aicardi-Goutieres syndrome
PDH1	3.15	Mitochondrial protein that participates in respiration, induced by diauxic shift; homologous to E. coli PrpD, may take part in the conversion of 2-methylcitrate to 2-methylisocitrate

SSA3	3.15	ATPase involved in protein folding and the response to stress; plays a role in SRP-dependent cotranslational protein-membrane targeting and translocation; member of the heat shock protein 70 (HSP70) family; localized to the cytoplasm
CDA1	3.15	Chitin deacetylase, together with Cda2p involved in the biosynthesis ascospore wall component, chitosan; required for proper rigidity of the ascospore wall
PUT4	3.12	Proline permease, required for high-affinity transport of proline; also transports the toxic proline analog azetidine-2-carboxylate (AzC); PUT4 transcription is repressed in ammonia-grown cells
ASH1	3.12	Zinc-finger inhibitor of HO transcription; mRNA is localized and translated in the distal tip of anaphase cells, resulting in accumulation of Ash1p in daughter cell nuclei and inhibition of HO expression; potential Cdc28p substrate
MMR1	3.04	Phosphorylated protein of the mitochondrial outer membrane, localizes only to mitochondria of the bud; interacts with Myo2p to mediate mitochondrial distribution to buds; mRNA is targeted to the bud via the transport system involving She2p
SPS4	3.029	Protein whose expression is induced during sporulation; not required for sporulation; heterologous expression in E. coli induces the SOS response that senses DNA damage
RPP1B	3.00	Ribosomal protein P1 beta, component of the ribosomal stalk, which is involved in interaction of translational elongation factors with ribosome; accumulation is regulated by phosphorylation and interaction with the P2 stalk component

Summary of the overall effects of gene downregulation on cells

Figures 4.85-4.87 depict the overall effects on cells induced by genes downregulated more than 2-fold in response to 200 µM GdnHCl + 20 µM TA exposure for 3 hr.

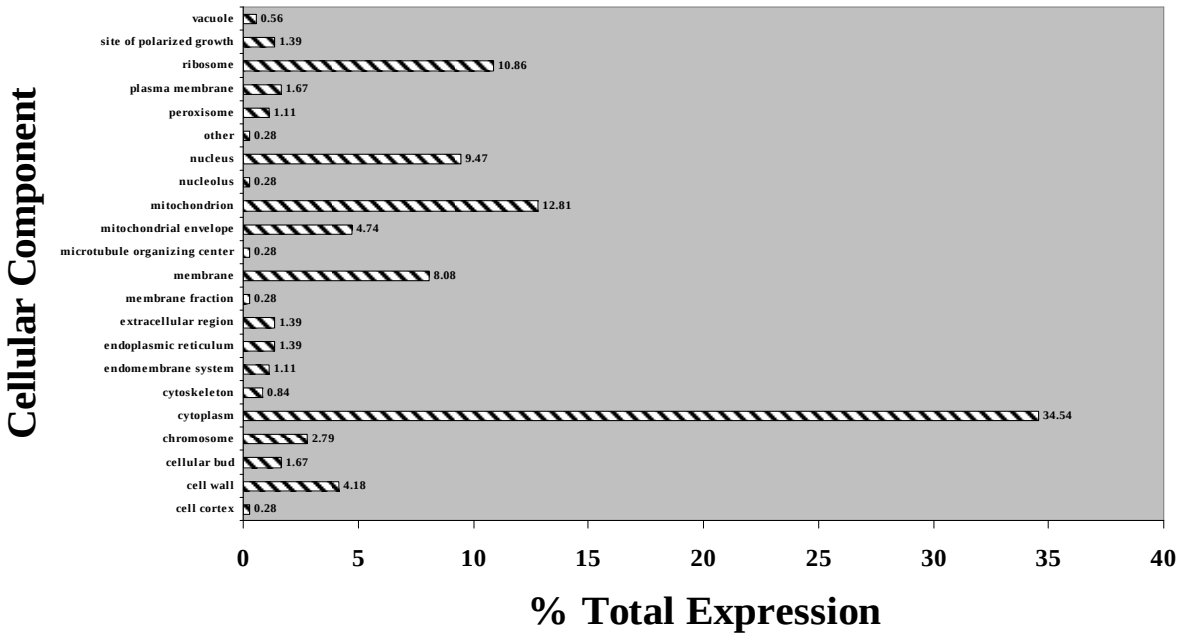

Figure 4.85 The percentage of each cellular component category (200 µM GdnHCl + 20 µM TA 3 hr downregulated genes). Genes downregulated more than two-fold were assigned cellular component categories. The number of genes in each category was expressed as a percentage of the number of total genes.

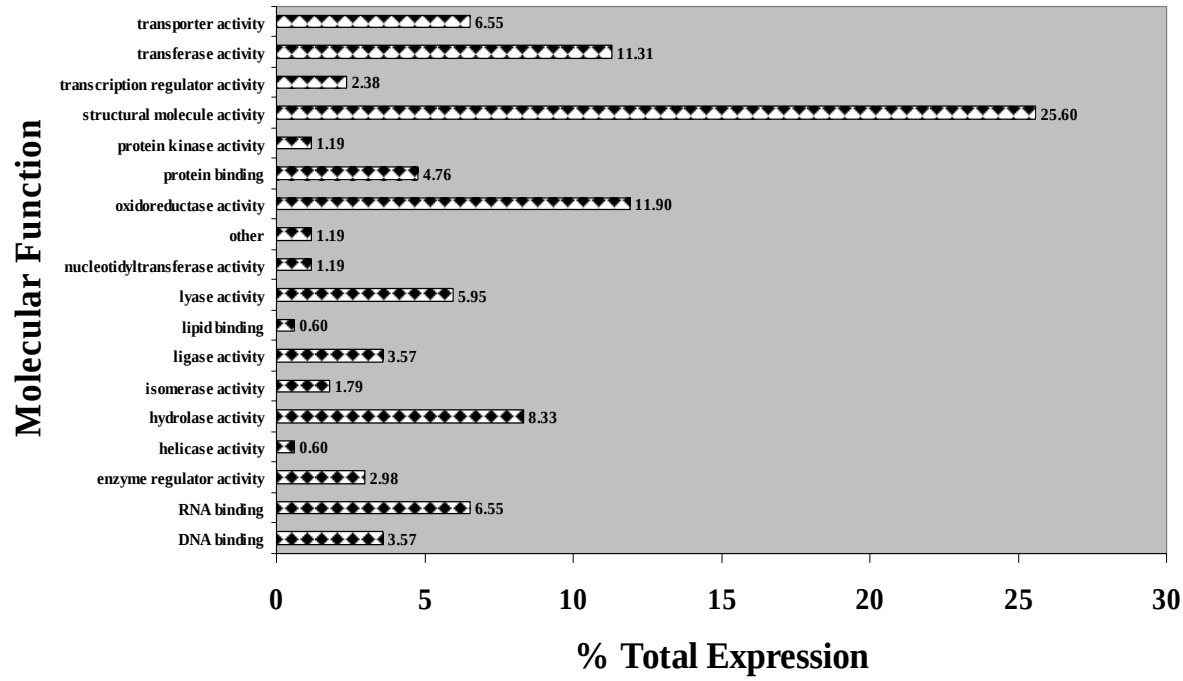

Figure 4.86 The percentage of each molecular function category (200 µM GdnHCl + 20 µM TA 3 hr downregulated genes). Genes downregulated more than two-fold were assigned molecular function categories. The number of genes in each category was expressed as a percentage of the number of total genes.

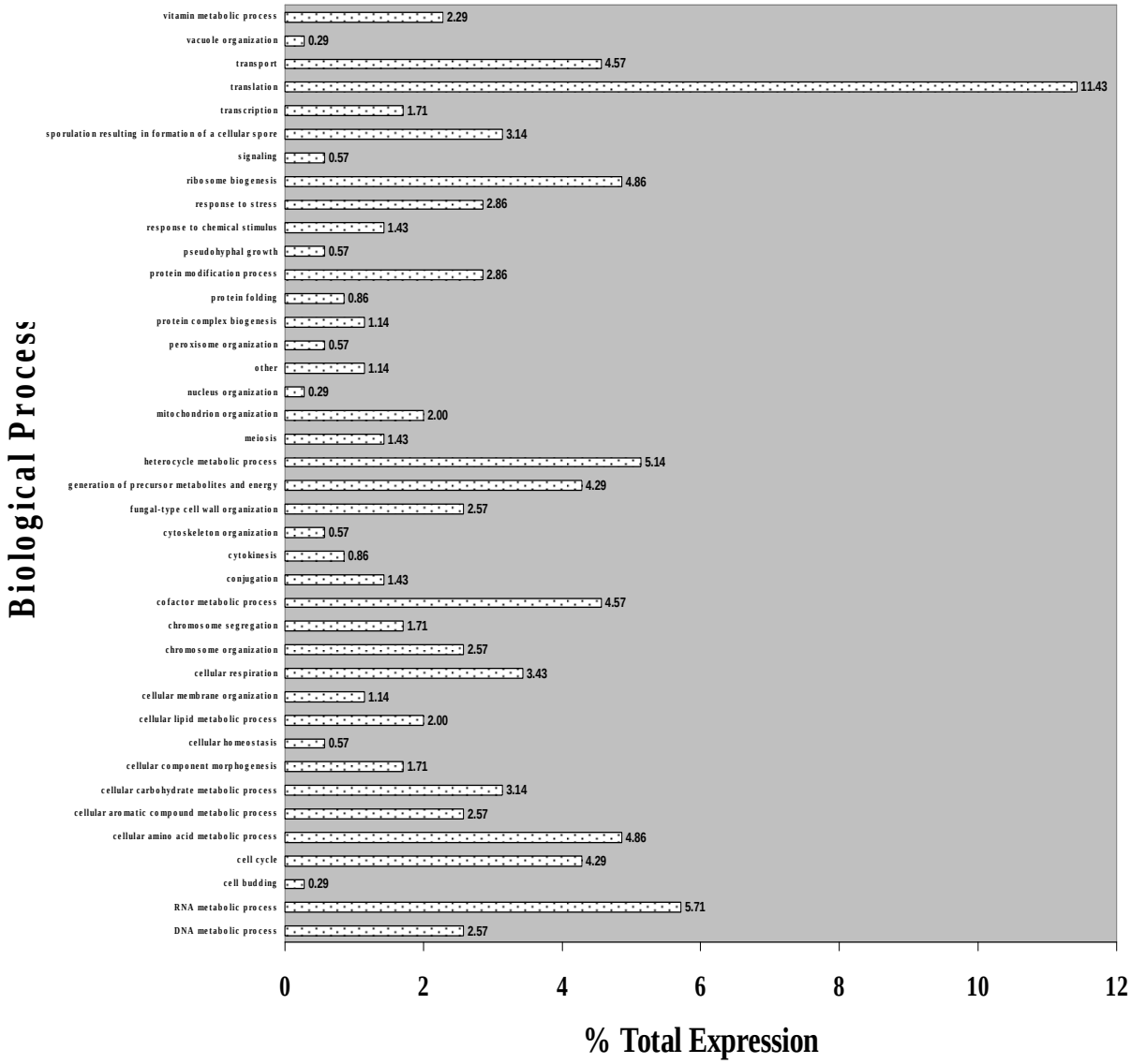

Figure 4.87 The percentage of each biological process category (200 µM GdnHCl + 20 µM TA 3 hr downregulated genes). Genes downregulated more than two-fold were assigned biological process categories. The number of genes in each category was expressed as a percentage of the number of total genes.

The five biological processes, molecular functions and associated cellular components most repressed by exposure to 200 µM GdnHCl + 20 µM TA for 3 hr were further graphed. These are illustrated in figures 4.88-4.90.

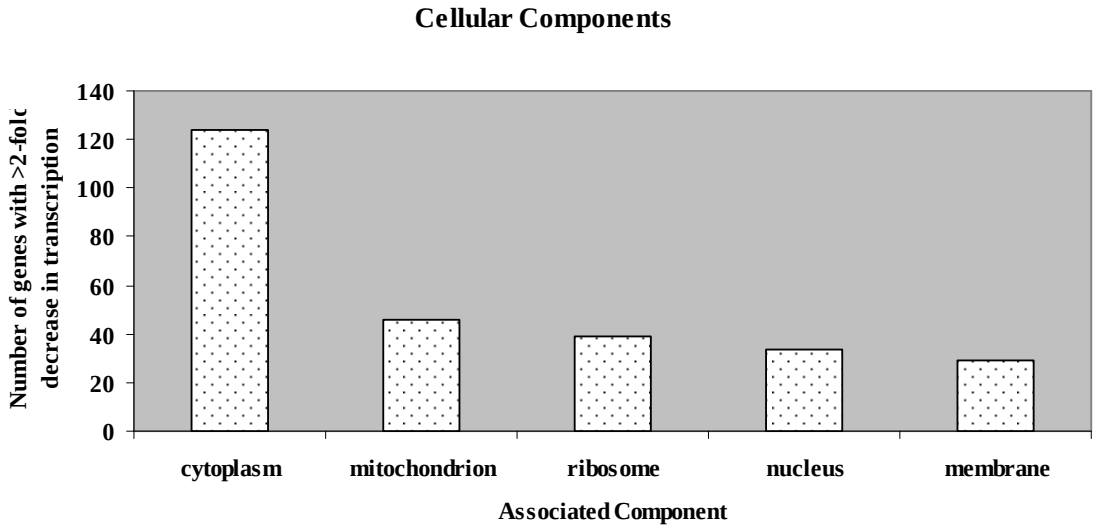

Figure 4.88 The five associated cellular components most highly downregulated by exposure to 200 µM GdnHCl + 20 µM TA for 3 hr.

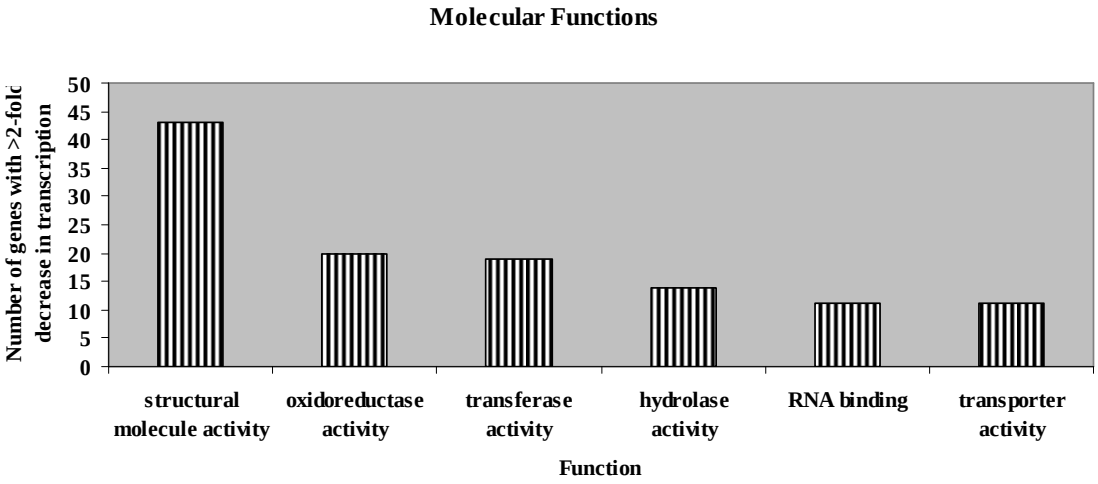

Figure 4.89 The *five molecular functions most highly downregulated by exposure to 200 µM GdnHCl + 20 µM TA for 3 hr. * The 5th and 6th most repressed molecular functions are represented by the same number of genes and are thus both included.

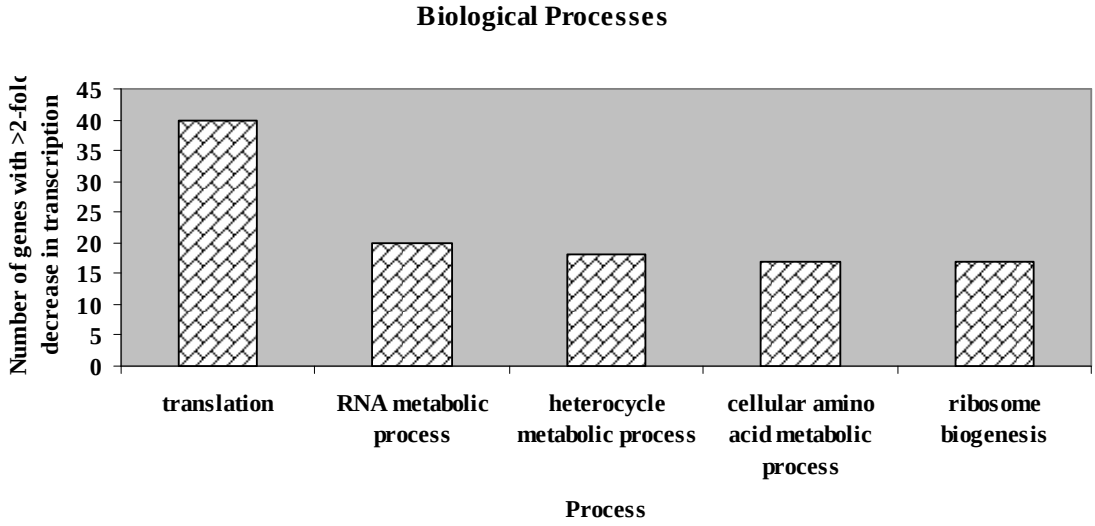

Figure 4.90 The five biological processes most highly downregulated by exposure to 200 µM GdnHCl + 20 µM TA for 3 hr.

Table 4.11 lists the fifty genes, and their respective functions, that were the most transcriptionally downregulated in response to 200 µM GdnHCl + 20 µM TA exposure for 3 hr.

Table 4.11 The fifty genes most highly downregulated in response to 200 µM GdnHCl + 20 µM TA exposure for 3 hr. Gene functions were obtained from www.yeastgenome.org (SGD).

Gene	Fold Change	Gene Function
FRM2	-30.67	Protein of unknown function, involved in the integration of lipid signaling pathways with cellular homeostasis; expression induced in cells treated with the mycotoxin patulin; has similarity to bacterial nitroreductases
HXT4	-28.61	High-affinity glucose transporter of the major facilitator superfamily, expression is induced by low levels of glucose and repressed by high levels of glucose
SAM1	-19.10	S-adenosylmethionine synthetase, catalyzes transfer of the adenosyl group of ATP to the sulfur atom of methionine; one of two differentially regulated isozymes (Sam1p and Sam2p)
CHA1	-13.31	Catabolic L-serine (L-threonine) deaminase, catalyzes the degradation of both L-serine and L-threonine; required to use serine or threonine as the sole nitrogen source, transcriptionally induced by serine and threonine
AAD6	-11.68	Putative aryl-alcohol dehydrogenase with similarity to P. chrysosporium aryl-alcohol dehydrogenase, involved in the oxidative stress response; expression induced in cells treated with the mycotoxin patulin
ERO1	-11.53	Thiol oxidase required for oxidative protein folding in the endoplasmic reticulum
AAD16	-10.86	Putative aryl-alcohol dehydrogenase with similarity to P. chrysosporium aryl-alcohol dehydrogenase; mutational analysis

		has not yet revealed a physiological role
CYC7	-10.73	Cytochrome c isoform 2, expressed under hypoxic conditions; electron carrier of the mitochondrial intermembrane space that transfers electrons from ubiquinone-cytochrome c oxidoreductase to cytochrome c oxidase during cellular respiration
AQR1	-10.47	Plasma membrane multidrug transporter of the major facilitator superfamily, confers resistance to short-chain monocarboxylic acids and quinidine; involved in the excretion of excess amino acids
YBR238C	-9.91	Mitochondrial membrane protein with similarity to Rmd9p; not required for respiratory growth but causes a synthetic respiratory defect in combination with rmd9 mutations; transcriptionally up-regulated by TOR; deletion increases life span
SER2	-8.63	Phosphoserine phosphatase of the phosphoglycerate pathway, involved in serine and glycine biosynthesis, expression is regulated by the available nitrogen source
OYE3	-8.29	Conserved NADPH oxidoreductase containing flavin mononucleotide (FMN), homologous to Oye2p with different ligand binding and catalytic properties; has potential roles in oxidative stress response and programmed cell death
DAN1	-8.18	Cell wall mannoprotein with similarity to Tir1p, Tir2p, Tir3p, and Tir4p; expressed under anaerobic conditions, completely repressed during aerobic growth
MUP1	-7.97	High affinity methionine permease, integral membrane protein with 13 putative membrane-spanning regions; also involved in cysteine uptake
HXT3	-7.96	Low affinity glucose transporter of the major facilitator superfamily, expression is induced in low or high glucose conditions
ATX2	-7.60	Golgi membrane protein involved in manganese homeostasis; overproduction suppresses the sod1 (copper, zinc superoxide dismutase) null mutation
HBN1	-7.32	Putative protein of unknown function; similar to bacterial nitroreductases; green fluorescent protein (GFP)-fusion protein localizes to the cytoplasm and nucleus; protein becomes insoluble upon intracellular iron depletion
OYE2	-7.24	Conserved NADPH oxidoreductase containing flavin mononucleotide (FMN), homologous to Oye3p with different ligand binding and catalytic properties; may be involved in sterol metabolism, oxidative stress response, and programmed cell death
VID24	-6.99	Peripheral membrane protein located at Vid (vacuole import and degradation) vesicles; regulates fructose-1,6-bisphosphatase (FBPase) targeting to the vacuole; promotes proteasome-dependent catabolite degradation of FBPase
AAC3	-6.76	Mitochondrial inner membrane ADP/ATP translocator, exchanges cytosolic ADP for mitochondrially synthesized ATP; expressed under anaerobic conditions; similar to Pet9p and Aac1p; has roles in maintenance of viability and in respiration
HXK2	-6.69	Hexokinase isoenzyme 2 that catalyzes phosphorylation of glucose in the cytosol; predominant hexokinase during growth on glucose; functions in the nucleus to repress expression of HXK1 and GLK1 and to induce expression of its own gene
YGL157W	-6.13	NADPH-dependent aldehyde reductase, utilizes aromatic and alophatic aldehyde substrates; member of the short-chain dehydrogenase/reductase superfamily
GSH1	-6.05	Gamma glutamylcysteine synthetase catalyzes the first step in glutathione (GSH) biosynthesis; expression induced by oxidants, cadmium, and mercury
ATR1	-6.04	Multidrug efflux pump of the major facilitator superfamily, required for resistance to aminotriazole and 4-nitroquinoline-N-

		oxide
MUP3	-5.80	Low affinity methionine permease, similar to Mup1p
FLR1	-5.67	Plasma membrane multidrug transporter of the major facilitator superfamily, involved in efflux of fluconazole, diazaborine, benomyl, methotrexate, and other drugs; expression induced in cells treated with the mycotoxin patulin
ADE4	-5.63	Phosphoribosylpyrophosphate amidotransferase (PRPPAT; amidophosphoribosyltransferase), catalyzes first step of the 'de novo' purine nucleotide biosynthetic pathway
GRC3	-5.60	Polynucleotide kinase present on rDNA that is required for efficient transcription termination by RNA polymerase I; required for cell growth; mRNA is cell-cycle regulated
SCW11	-5.59	Cell wall protein with similarity to glucanases; may play a role in conjugation during mating based on its regulation by Ste12p
YFL054C	-5.54	Putative channel-like protein; similar to Fps1p; mediates passive diffusion of glycerol in the presence of ethanol
YGR035C	-5.47	Putative protein of unknown function, potential Cdc28p substrate; transcription is activated by paralogous transcription factors Yrm1p and Yrr1p along with genes involved in multidrug resistance
AAD4	-5.37	Putative aryl-alcohol dehydrogenase with similarity to P. chrysosporium aryl-alcohol dehydrogenase, involved in the oxidative stress response; expression induced in cells treated with the mycotoxin patulin
GTT2	-5.32	Glutathione S-transferase capable of homodimerization; functional overlap with Gtt2p, Grx1p, and Grx2p
INM1	-5.16	Inositol monophosphatase, involved in biosynthesis of inositol and in phosphoinositide second messenger signaling; INM1 expression increases in the presence of inositol and decreases upon exposure to antibipolar drugs lithium and valproate
PFK27	-5.15	6-phosphofructo-2-kinase, catalyzes synthesis of fructose-2,6-bisphosphate; inhibited by phosphoenolpyruvate and sn-glycerol 3-phosphate, expression induced by glucose and sucrose, transcriptional regulation involves protein kinase A
YNL024C	-4.97	Putative protein of unknown function with seven beta-strand methyltransferase motif; green fluorescent protein (GFP)-fusion protein localizes to the cytoplasm; YNL024C is not an essential gene
YLR301W	-4.94	Protein of unknown function that interacts with Sec72p
MIG1	-4.93	Transcription factor involved in glucose repression; sequence specific DNA binding protein containing two Cys2His2 zinc finger motifs; regulated by the SNF1 kinase and the GLC7 phosphatase
JJJ3	-4.89	Protein of unknown function, contains a J-domain, which is a region with homology to the E. coli DnaJ protein
STE14	-4.77	Farnesyl cysteine-carboxyl methyltransferase, mediates the carboxyl methylation step during C-terminal CAAX motif processing of a-factor and RAS proteins in the endoplasmic reticulum, localizes to the ER membrane
HOR2	-4.74	One of two redundant DL-glycerol-3-phosphatases (RHR2/GPP1 encodes the other) involved in glycerol biosynthesis; induced in response to hyperosmotic stress and oxidative stress, and during the diauxic transition
YKL071W	-4.66	Putative protein of unknown function; expression induced in cells treated with the mycotoxin patulin, and also the quinone methide triterpene celastrol; green fluorescent protein (GFP)-fusion protein localizes to the cytoplasm
PMP2	-4.61	Proteolipid associated with plasma membrane H(+)-ATPase (Pma1p); regulates plasma membrane H(+)-ATPase activity; nearly identical to PMP1
PGA3	-4.60	Putative cytochrome b5 reductase, localized to the plasma membrane; may be involved in regulation of lifespan; required for maturation of Gas1p and Pho8p, proposed to be involved in

		protein trafficking
AGA1	-4.57	Anchorage subunit of a-agglutinin of a-cells, highly O-glycosylated protein with N-terminal secretion signal and C-terminal signal for addition of GPI anchor to cell wall, linked to adhesion subunit Aga2p via two disulfide bonds
CST26	-4.57	Protein required for incorporation of stearic acid into phosphatidylinositol; affects chromosome stability when overexpressed
COX5B	-4.53	Subunit Vb of cytochrome c oxidase, which is the terminal member of the mitochondrial inner membrane electron transport chain; predominantly expressed during anaerobic growth while its isoform Va (Cox5Ap) is expressed during aerobic growth
GPX2	-4.45	Phospholipid hydroperoxide glutathione peroxidase induced by glucose starvation that protects cells from phospholipid hydroperoxides and nonphospholipid peroxides during oxidative stress
SPI1	-4.44	GPI-anchored cell wall protein involved in weak acid resistance; basal expression requires Msn2p/Msn4p; expression is induced under conditions of stress and during the diauxic shift; similar to Sed1p
YNL134C	-4.40	Putative protein of unknown function with similarity to dehydrogenases from other model organisms; green fluorescent protein (GFP)-fusion protein localizes to both the cytoplasm and nucleus and is induced by the DNA-damaging agent MMS

4.18.1.6 Investigation into the differential effects of GdnHCl and TA exposure time on yeast cells

I was interested at this point in assessing the effects induced by GdnHCl and TA under different lengths of exposure. RNA sequencing data was compared from cells exposed to 200 µM GdnHCl + 20 µM TA for 1 hr, 3 hr and 14 generations, as summarised in previous sections. The five most commonly stimulated and repressed molecular functions, biological processes and associated cellular components were compared and contrasted. This provides insight into the ways in which different exposure times affect the *S. cerevisiae* drug response.

Figures 4.91-4.93 depict comparisons of the biological processes, cellular components and molecular functions stimulated by GdnHCl and TA upon 1 hr., 3 hr. and 14 generation exposures. It appears that there are differences in responses induced by cellular exposure to GdnHCl and TA for 1 hr. and 3 hr. As shown in figure 4.91, RNA metabolic process, ribosome biogenesis and transport are all some of the most highly stimulated processes under 1 hr., 3 hr. and 14 generation exposures. Genes

involved in translation are greatly stimulated by GdnHCl and TA exposure for 1 hr and 14 generations, but not 3 hr. Transcription and cell cycle appear to be induced upon 1 hr. and 14 generation exposure respectively, while genes involved in the response to stress and chemical stimulus are stimulated only under 3 hr. exposure.

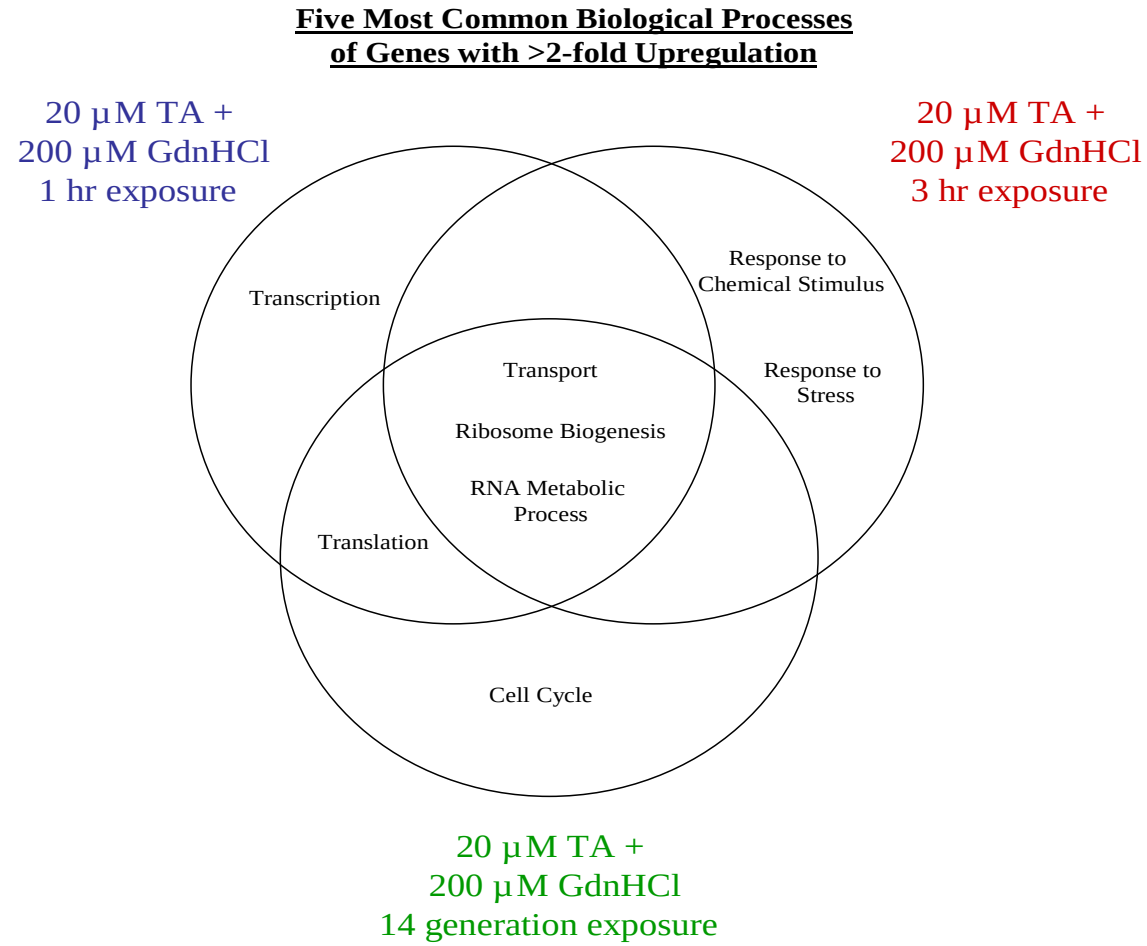

Figure 4.91 Comparison of the five most common biological processes of genes with >2-fold upregulation.

Genes associated with the cytoplasm, nucleus and membrane are all some of those most highly expressed upon 1 hr., 3 hr. and 14 generation exposure to GdnHCl and TA, as illustrated in figure 4.92. Genes associated with the nucleolus are highly upregulated under the 1 hr. and 14 generation exposures only, while plasma membrane-associated genes are acutely induced solely under 3 hr exposure. The high upregulation of mitochondrion-associated genes occurs only upon 1 hr. and 3 hr. exposures, while

genes involved in ribosome function are only acutely expressed upon 14 generation treatment.

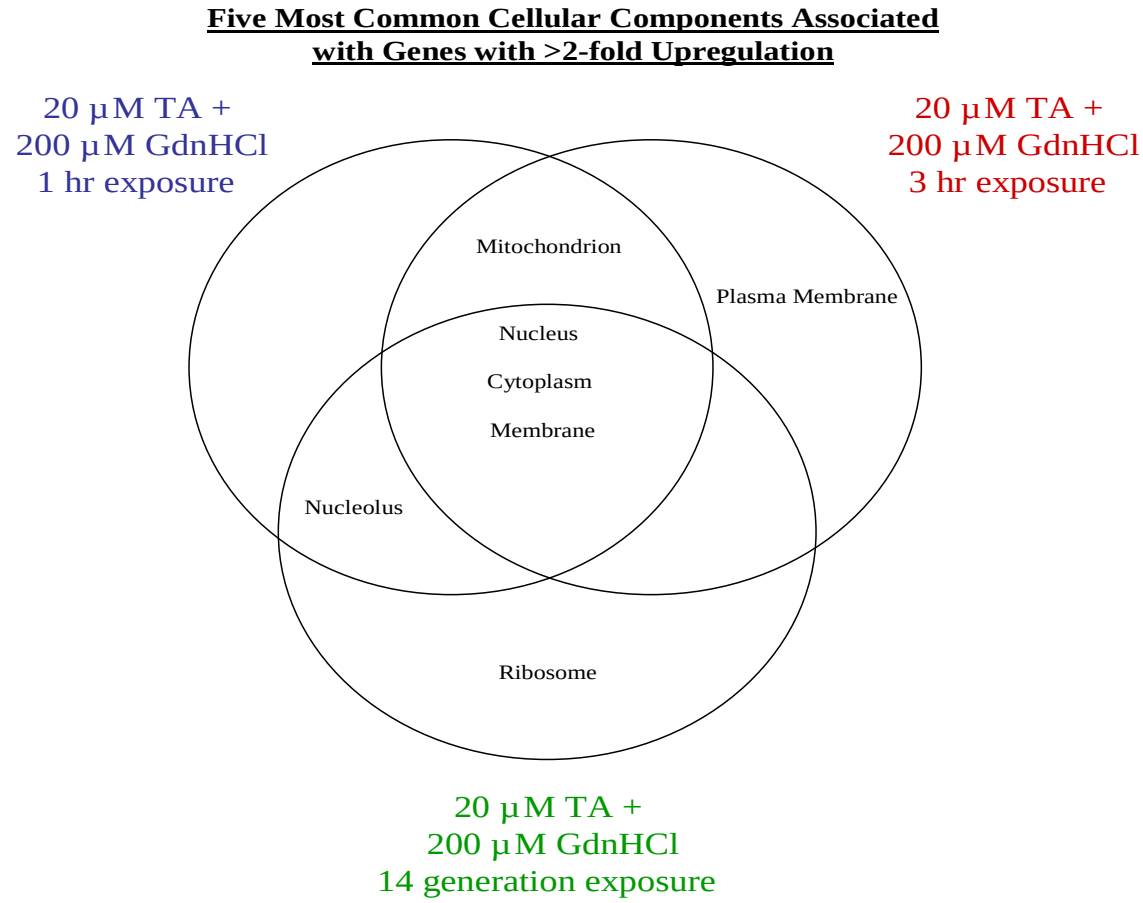

Figure 4.92 Comparison of the five most common associated cellular components of genes with >2-fold upregulation.

Transferase and hydrolase activity are among the most induced functions when cells are treated to these agents for 1 hr., 3 hr. and 14 generations (figure 4.93). Oxidoreductase and transporter activity are most highly stimulated under the two shorter exposure times. Genes involved in RNA binding are highly upregulated upon 1 hr. and 14 generation treatments, while those that play a role in protein binding are acutely induced in response to 3 hr. and 14 generation exposures. Structural molecule activity is only highly stimulated under treatment for 14 generations.

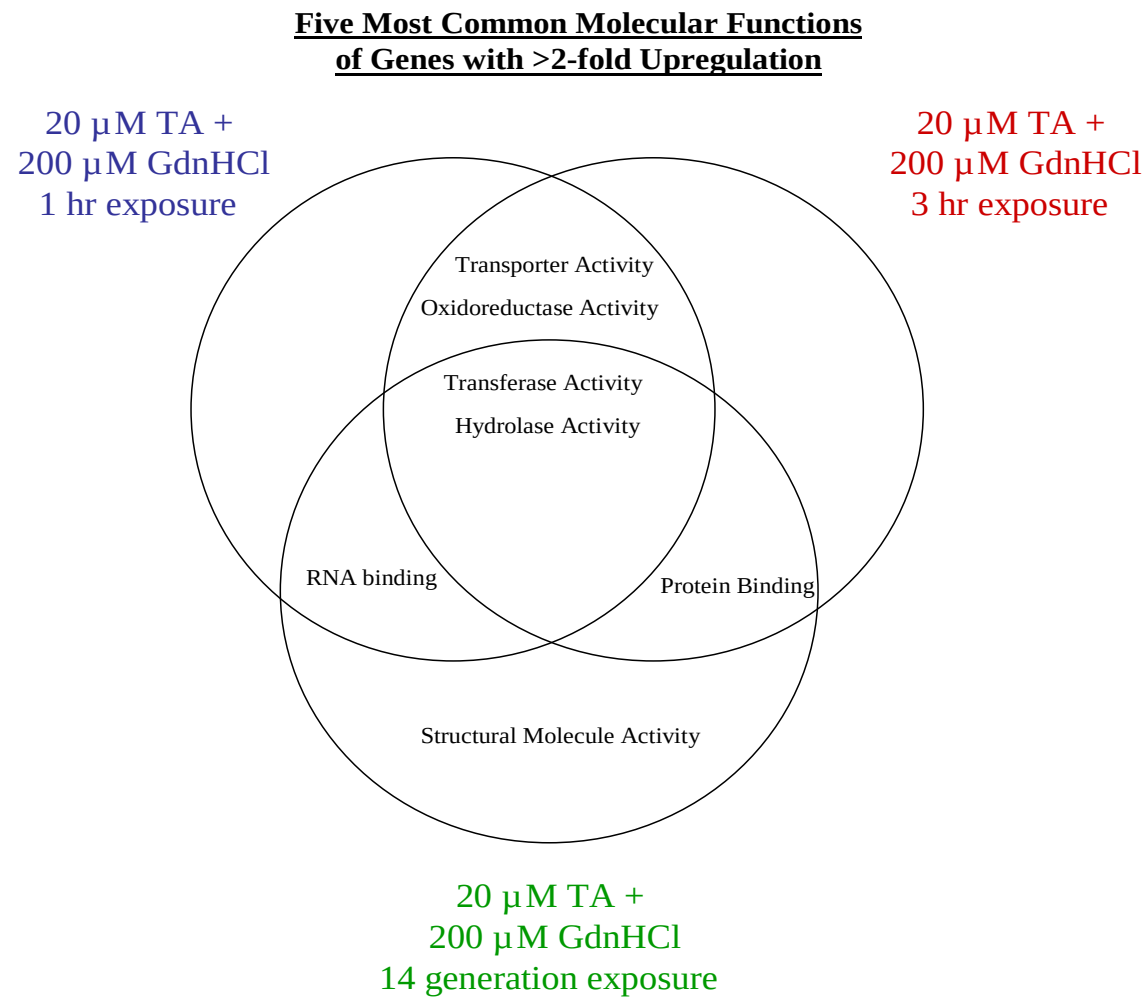

Figure 4.93 Comparison of the five most common molecular functions of genes with >2-fold upregulation.

Downregulated gene GO identities were also compared and contrasted, as illustrated in figures 4.94-4.96. Figure 4.94 depicts the great difference in genes that are repressed upon 1 hr., 3 hr. and 14 generation exposure to GdnHCl and TA. RNA metabolic process is the only biological process greatly inhibited in response to all exposure times. Response to stress, cellular carbohydrate metabolic process, chromosome organisation and cell cycle are all inhibited upon 1 hr. exposure. Heterocycle metabolic process, ribosome biogenesis, cellular amino acid metabolic process and translation are the most repressed processes upon treatment for 3 hr. In contrast, genes involved in transport, transcription, generation of precursor metabolites

and energy, response to chemical stimulus and mitochondrion organistaion are all acutely repressed under 14 generation treatment.

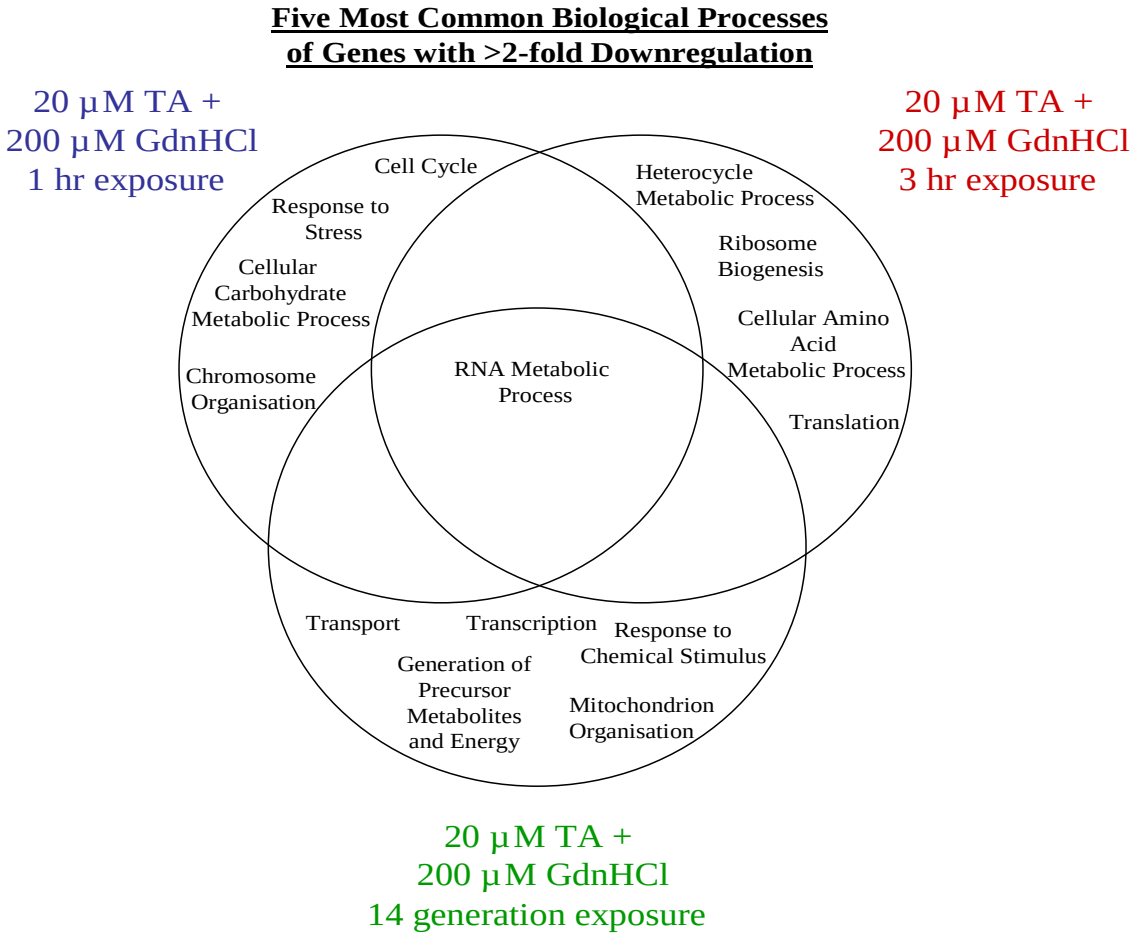

Figure 4.94 Comparison of the *five most common biological processes of genes with >2-fold downregulation. * In response to 14 generation exposure the 5th and 6th most repressed biological processes are represented by the same number of genes and are thus both included.

Upon comparison of the cellular components associated with the most acutely donwregulated genes, it was found that those associated with the cytoplasm, nucleus, mitochondrion and membrane are common to all three exposure times (figure 4.95).

Cell wall- and chromosome-associated genes are only highly repressed under drug treatment for 1 hr. Ribosome-associated genes are only highly inhibited under exposure for 3 hr., while genes involved in the mitochondrial envelope are only those most repressed under the 14 generation treatment.

Five Most Common Cellular Components Associated with Genes with >2-fold Downregulation

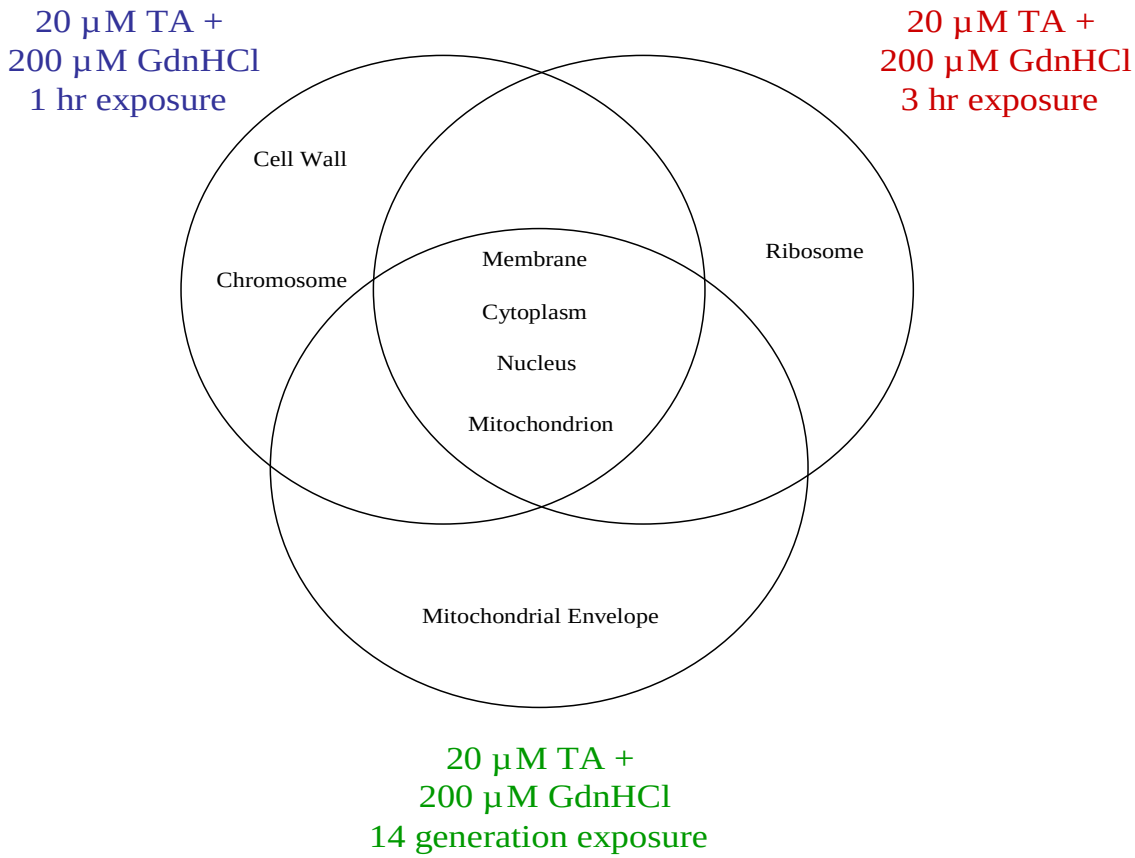

Figure 4.95 Comparison of the *five most common associated cellular components of genes with >2-fold downregulation. *In response to 1 hr exposure the 5th and 6th most repressed associated cellular components are represented by the same number of genes and are thus both included.

As illustrated in figure 4.96, oxidoreductase and transferase activity are both some of the most repressed functions under drug exposure for 1 hr., 3 hr. and 14 generations. Upon 1 hr. yeast cell treatment, DNA binding is most inhibited, which is also common to 14 generation exposure. Other molecular functions inhibited under this treatment are transcription regulator activity and protein binding. Upon drug exposure for 3 hr., RNA binding and transporter activity are those most hindered, in addition to hydrolase and structural molecule activity, which are both also acutely inhibited under 1 hr. exposure.

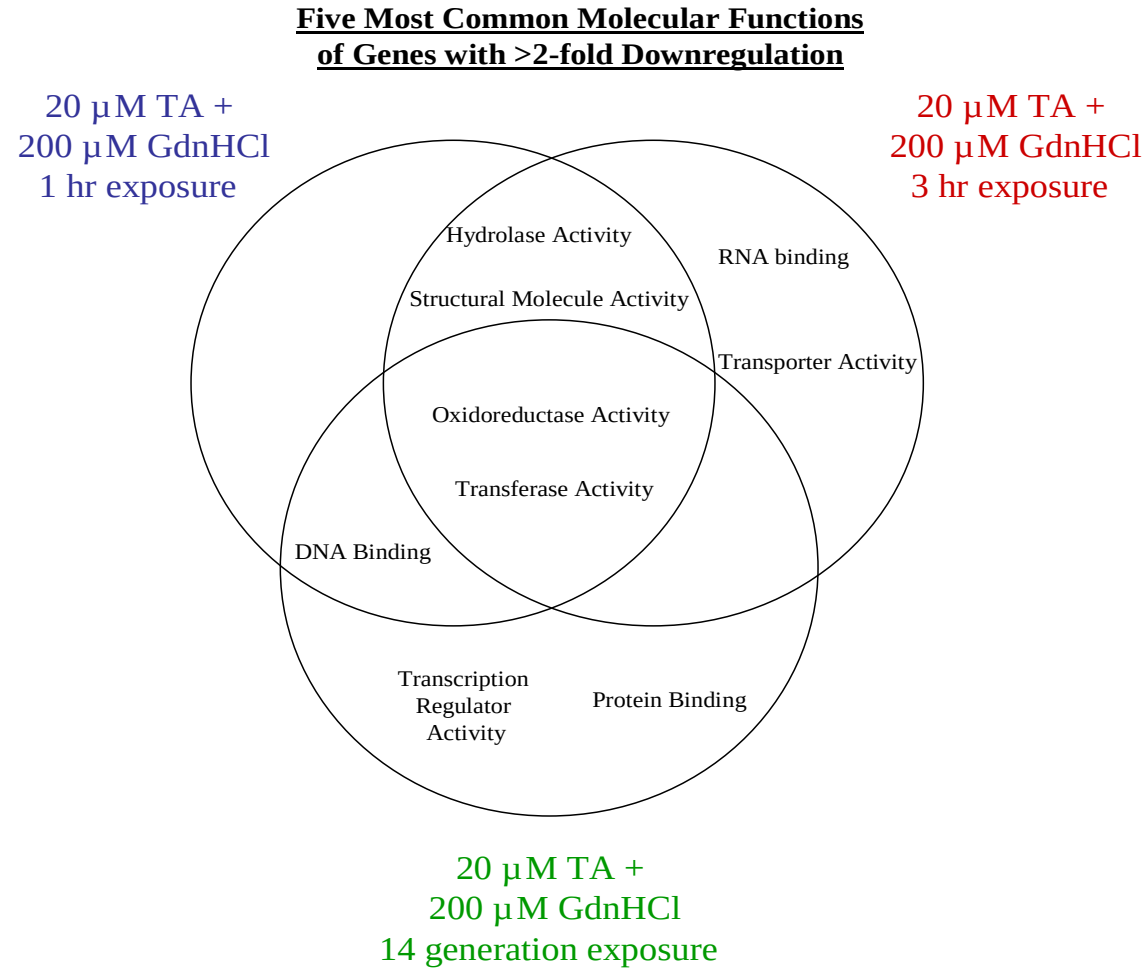

Figure 4.96 Comparison of the *five most common molecular functions of genes with >2-fold downregulation. * In response to 3 hr. exposure the 5th and 6th most repressed molecular functions are represented by the same number of genes and are thus both included.

4.18.1.7 Assessing the effects of TA on heatshock and related genes using transcriptomics

It is known that heatshock proteins and related co-chaperones are involved in prion propagation (Jones and Tuite, 2005). Disruption of normal chaperone protein activity, particularly that of Hsp70p can disturb prion propagation (Jung *et al.*, 2000, Jones and Masison, 2003, Jones *et al.*, 2004). It was thus considered that the curing of [*PSI*$^{+}$] by TA may involve alterations in chaperone function or chaperone expression levels. Further to this, the expression levels of a number of genes encoding proteins with chaperone-related function were assessed under GdnHCl and TA exposure (table 4.12).

The majority of the genes in the table below have been previously discussed. *CDC37*, like *STI1* encodes a Hsp90p co-chaperone and the two are known to interact with one another (Kimura *et al.*, 1997, Abbas-Terki *et al.*, 2002). Cells deleted for *HSP26* and *HSP42* have been shown to accumulate protein aggregates (Petko and Lindquist, 1986, Haslbeck *et al.*, 2004). Hsp26p and Hsp42p encoded by these genes are small heatshock proteins (sHSPs) that are involved in the suppression of cytosolic protein aggregation (Haslbeck *et al.*, 2004). It has been reported that Hsp26p co-aggregates with misfolded proteins, thereby facilitating their disaggregation and reactivation by Hsp104p, Hsp70p and Hsp40p (Cashikar *et al.*, 2005). This provides a possible link for sHSPs and prion propagation.

Table 4.12 Expression levels of a number of genes possibly involved in [*PSI*$^+$] propagation in the presence of GdnHCl and TA.

Gene	Control	14 gen Gdn	14 gen Gdn + TA	1hr Gdn + TA	3hr Gdn + TA
APJ1	44.18	90.23	75.54	36.59	56.82
CDC37	104.68	54.10	49.93	113.45	65.76
CNS1	40.76	19.94	12.85	10.77	16.42
CPR7	19.77	4.977	3.85	16.64	11.28
ECM10	N/A	N/A	N/A	N/A	N/A
FES1	76.61	63.44	46.11	48.53	112.31
HSP104	705.00	224.57	382.18	860.98	798.13
HSP26	6677.16	2513.75	5033.54	7950.32	13825.5
HSP42	672.22	586.49	726.93	830.18	764.81
HSP82	772.31	235.18	370.91	543.59	817.02
KAR2	570.35	138.76	116.47	186.38	235.16
LHS1	53.31	18.19	17.93	24.94	23.65
SSA1	1214.19	168.49	319.47	1373.99	1396.94
SSA2	799.88	88.80	176.41	20.27	725.72
SSA3	300.07	129.80	214.15	297.10	945.95
SSA4	233.94	59.69	79.36	245.03	138.58
SSB1	326.94	85.72	47.05	224.71	357.90
SSB2	336.71	139.75	76.53	282.77	461.26
SSC1	1497.55	2658.25	2913.65	1332.14	1440.8
SSE1	360.65	167.19	127.61	164.28	241.92
SSE2	301.94	217.88	N/A	455.17	340.52
SSQ1	63.24	N/A	78.93	60.81	42.41
SSZ1	122.36	63.92	51.38	76.31	N/A
STI1	392.04	194.60	227.42	N/A	482.27
YDJ1	214.95	55.35	38.51	93.22	192.82

Hsp82p and Hsc82p are the two *S. cerevisiae* Hsp90 proteins (Borkovich *et al.*, 1989, Gross *et al.*, 1990). As previously described, Hsp90 proteins work in conjunction with Hsp70 members to carry out correct protein folding and maintain cell viability (Wegele *et al.*, 2004). The fact that Hsp70p and Hsp90p closely cooperate and many co-chaperones are common to both families of heatshock proteins suggests that Hsp90p may also have a regulatory function linked to prion propagation. Kar2p and Lhs1p are endoplasmic reticulum-associated Hsp70 proteins (Rose *et al.*, 1989, Craven *et al.*, 1996) and the mammalian Bip protein, homologous to Kar2p has been shown to prevent PrP aggregation and facilitate PrP^{Sc} proteosomal degradation (Normington *et al.*, 1989, Jin *et al.*, 2000).

4.18.2 Using two-dimensional gel electrophoresis to assess the *S. cerevisiae* response to TA

In addition to analysing the global transcriptional response of yeast to TA, the proteomic response was explored. 2D gel electrophoresis was employed to achieve this. Protein was extracted, precipitated and quantified, from untreated control cells, cells exposed to 200 µM GdnHCl and cells exposed to 200 µM GdnHCl + 20 µM TA. The cells were exposed to the compounds for 14 generations as we knew this to be enough time to fully cure [PSI^{+}].

Proteins were separated based on their isoelectric point, followed by their mass and coomassie stained. Progenesis™ same spot software was used to identify proteins differentially expressed. Protein expression patterns were sought that depicted differential expression upon the two treatments. 15 protein spots of interest, illustrated in figure 4.97 were selected, extracted and identified using Liquid Chromatography Mass Spectrometry (LC-MS).

Table 4.13 lists the 15 proteins identified that were expressed at different levels in response to treatment with GdnHCl alone and in combination with TA.

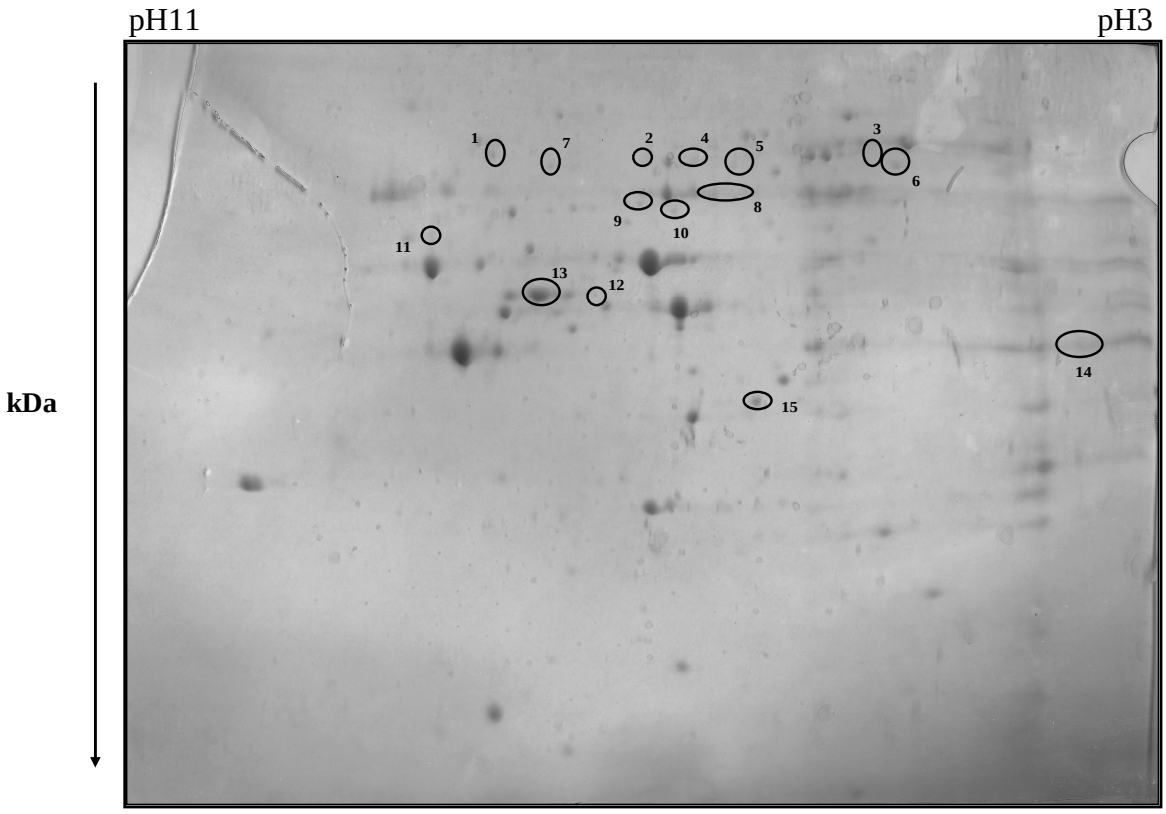

Figure 4.97 Separated proteins from G600 cells. Spots circled represent proteins that undergo an increase or decrease in level of expression in response to 200 µM GdnHCl and 200 µM GdnHCl + 20 µM TA exposure.

Spot no. 1, Ilv2p is downregulated in response to GdnHCl alone, but upregulated in the presence of both GdnHCl and TA (figure 4.98).

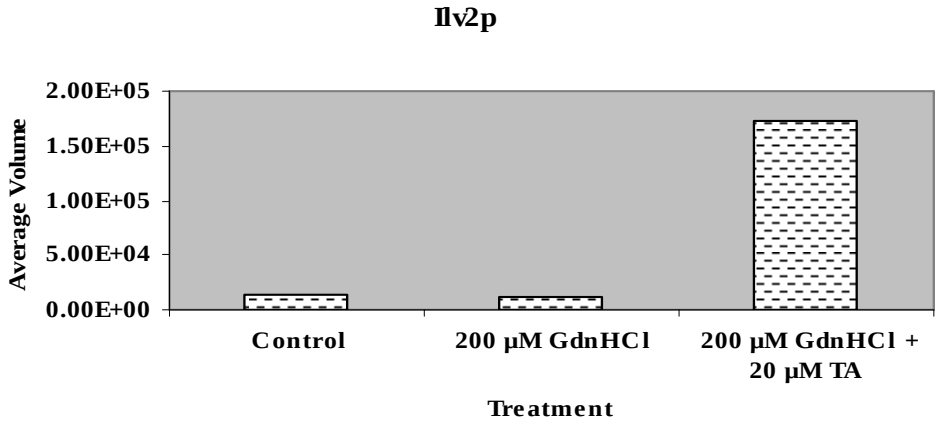

Figure 4.98 Ilv2p expression in response to GdnHCl and TA. Progenesis™ calculated p = 7.215e-004.

Spot no. 2, Ssb1p follows the same pattern of expression as Ilv2p whereby expression decreases under exposure to GdnHCl alone and increases in the presence of both GdnHCl and TA (figure 4.99).

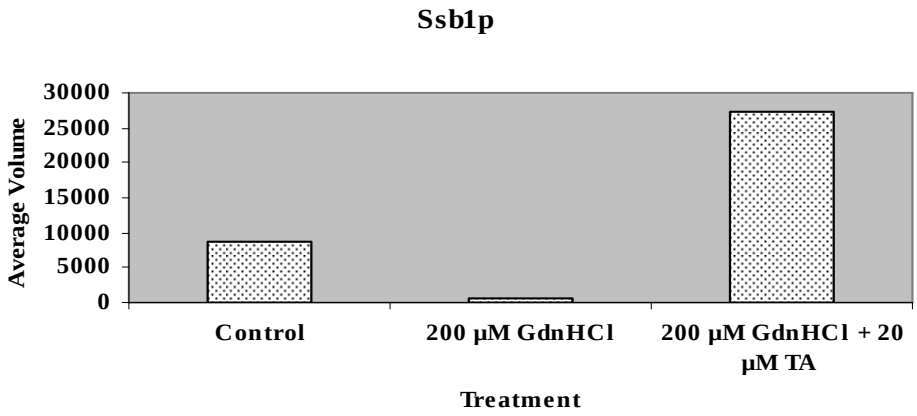

Figure 4.99 Ssb1p expression in response to GdnHCl and TA. Progenesis^{TM} calculated p = 0.014.

Spot no. 3, Ssa2p was found to be upregulated in response to GdnHCl and further increased in when TA was present (figure 4.100).

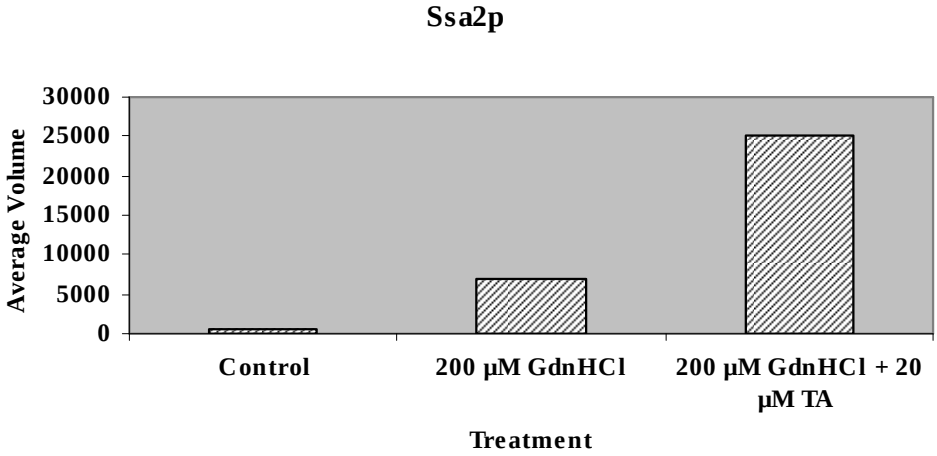

Figure 4.100 Ssa2p expression in response to GdnHCl and TA. Progenesis^{TM} calculated p = 0.013.

Table 4.13 Yeast proteins identified as undergoing an increase or decrease in expression under GdnHCl and TA treatment. * Fold change is the sum of changes between the control and GdnHCl alone, and GdnHCl alone and with the addition of TA.

Spot No.	Protein Name	Sum of fold changes*	Change C-GdnHCl	Change Gdn-TA	PI Value	Molecular Mass (Da)	Peptides Matched	Mascot Score	Coverage (%)	Protein Function
1	Ilv2	15.6	Down-	Up-	8.95	75064	10(3)	420	12	Acetolactate synthase, catalyses the first common step in isoleucine and valine biosynthesis and is the target of several classes of inhibitors, localizes to the mitochondria; expression of the gene is under general amino acid control
2	Ssb1	50.7	Down-	Up-	5.32	42078	5(0)	195	9	Cytoplasmic ATPase that is a ribosome-associated molecular chaperone, functions with J-protein partner Zuo1p; may be involved in folding of newly-made polypeptide chains; member of the HSP70 family; interacts with phosphatase subunit Reg1p
3	Ssa2	42.1	Up-	Up-	4.95	69601	5(1)	256	10	ATP binding protein involved in protein folding and vacuolar import of proteins; member of heat shock protein 70 (HSP70) family; associated with the chaperonin-containing T-complex; present in the cytoplasm, vacuolar membrane and cell wall
4	Ssb1	16.5	Down-	Up-	5.32	66735	4(0)	199	5	Cytoplasmic ATPase that is a ribosome-associated molecular chaperone, functions with J-protein partner Zuo1p; may be involved in folding of newly-made polypeptide chains; member of the HSP70 family; interacts with phosphatase subunit Reg1p
5	Asn2	6.6	Down-	Up-	5.48	65085	5(0)	168	5	Asparagine synthetase, isozyme of Asn1p; catalyzes the synthesis of L-asparagine from L-aspartate in the asparagine biosynthetic pathway

6	Ssa2	21.4	Up-	Up-	4.95	69601	10(2)	413	12	ATP binding protein involved in protein folding and vacuolar import of proteins; member of heat shock protein 70 (HSP70) family; associated with the chaperonin-containing T-complex; present in the cytoplasm, vacuolar membrane and cell wall
7	Ade17	9.4	Down-	Down-	6.12	65571	3(1)	201	5	Enzyme of 'de novo' purine biosynthesis containing both 5-aminoimidazole-4-carboxamide ribonucleotide transformylase and inosine monophosphate cyclohydrolase activities, isozyme of Ade16p; ade16 ade17 mutants require adenine and histidine
8	Pdc1	5.8	Up-	Up-	5.8	61689	4(1)	146	4	Major of three pyruvate decarboxylase isozymes, key enzyme in alcoholic fermentation, decarboxylates pyruvate to acetaldehyde; subject to glucose-, ethanol-, and autoregulation; involved in amino acid catabolism
9	Pdc1	11.8	Down-	Up-	5.8	61689	2(0)	89	3	Major of three pyruvate decarboxylase isozymes, key enzyme in alcoholic fermentation, decarboxylates pyruvate to acetaldehyde; subject to glucose-, ethanol-, and autoregulation; involved in amino acid catabolism
10	Aro8	13.3	Up-	Up-	5.68	56375	2(0)	83	4	Aromatic aminotransferase I, expression is regulated by general control of amino acid biosynthesis
11	Imd3	17.7	Down-	Up-	7.04	56955	2(0)	78	3	Inosine monophosphate dehydrogenase, catalyzes the first step of GMP biosynthesis, member of a four-gene family in S. cerevisiae, constitutively expressed

12	Adh1	93.9	Down-	Up-	5.94	37290	2(0)	90	4	Alcohol dehydrogenase, fermentative isozyme active as homo- or heterotetramers; required for the reduction of acetaldehyde to ethanol, the last step in the glycolytic pathway
13	Adh1	14.1	Up-	Up-	5.94	37290	8(0)	304	15	Alcohol dehydrogenase, fermentative isozyme active as homo- or heterotetramers; required for the reduction of acetaldehyde to ethanol, the last step in the glycolytic pathway
14	Tdh3		Up-	Up-	6.46	35840	2(0)	77	5	Glyceraldehyde-3-phosphate dehydrogenase, isozyme 3, involved in glycolysis and gluconeogenesis; tetramer that catalyzes the reaction of glyceraldehyde-3-phosphate to 1,3 bis-phosphoglycerate; detected in the cytoplasm and cell wall
15	Rhr2		Up-	Up-	5.35	28103	5(1)	255	20	Constitutively expressed isoform of DL-glycerol-3-phosphatase; involved in glycerol biosynthesis, induced in response to both anaerobic and, along with the Hor2p/Gpp2p isoform, osmotic stress

Spot no. 4, another Ssb1p isoform, is downregulated in response to GdnHCl alone and under cellular exposure to both GdnHCl and TA in combination it is highly upregulated (figure 4.101).

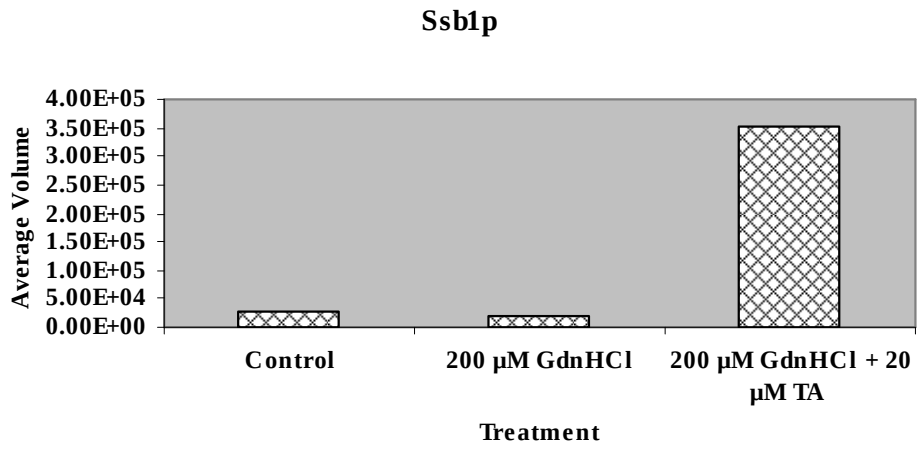

Figure 4.101 Ssb1p expression in response to GdnHCl and TA. Progenesis^{TM} calculated p = 0.012.

Spot no. 5, identified as Asn2p is downregulated in the presence of GdnHCl and upregulated under GdnHCl and TA combined exposure (figure 4.102).

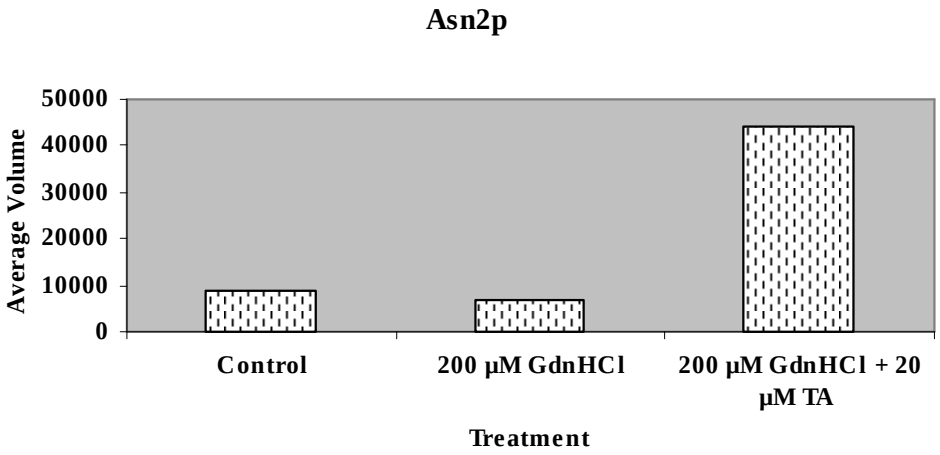

Figure 4.102 Asn2p expression in response to GdnHCl and TA. Progenesis^{TM} calculated p = 0.009.

Spot no. 6, Ssa2p is upregulated under exposure to both treatments (figure 4.103).

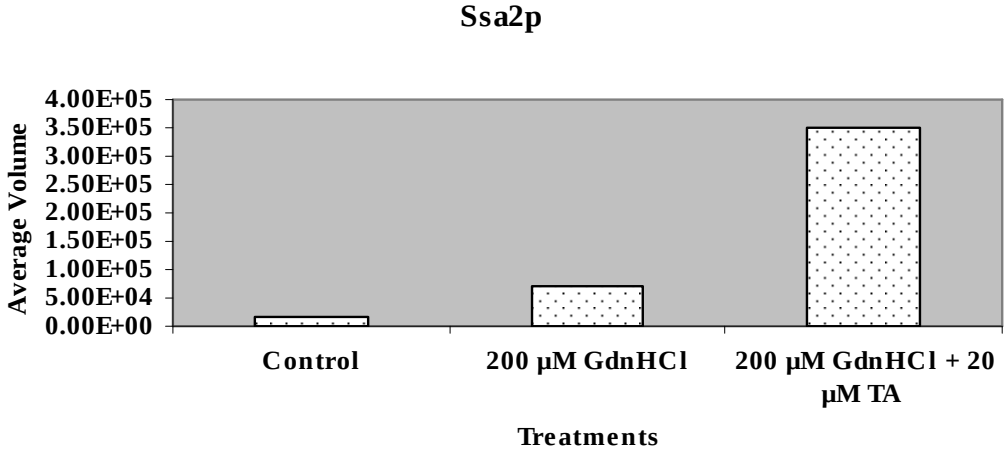

Figure 4.103 Ssa2p expression in response to GdnHCl and TA. Progenesis^{TM} calculated p = 0.043.

Ade17p was found to be represented by spot no. 7, and the expression of this protein is repressed in the presence of GdnHCl alone and further inhibited in the presence of a combination of GdnHCl and TA (figure 4.104).

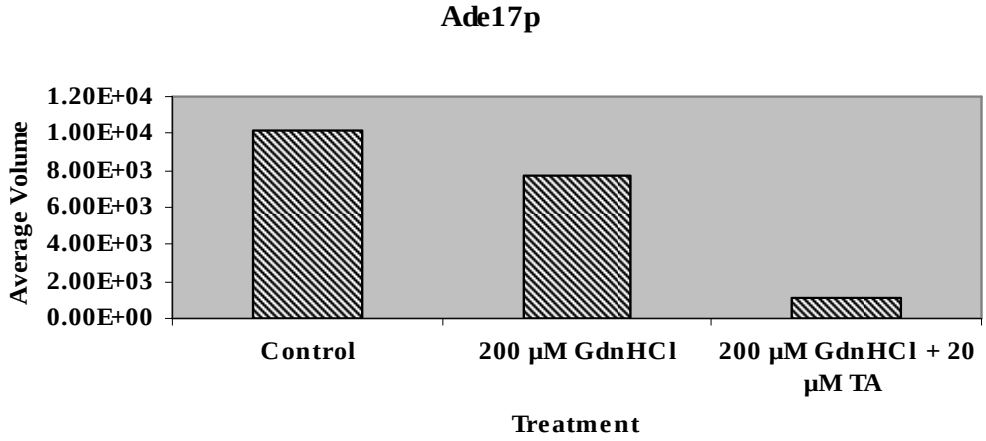

Figure 4.104 Ade17p expression in response to GdnHCl and TA. Progenesis^{TM} calculated p = 0.034

Spot no. 8, identified as Pdc1p is upregulated upon GdnHCl exposure and its expression increases further upon TA addition (figure 4.105).

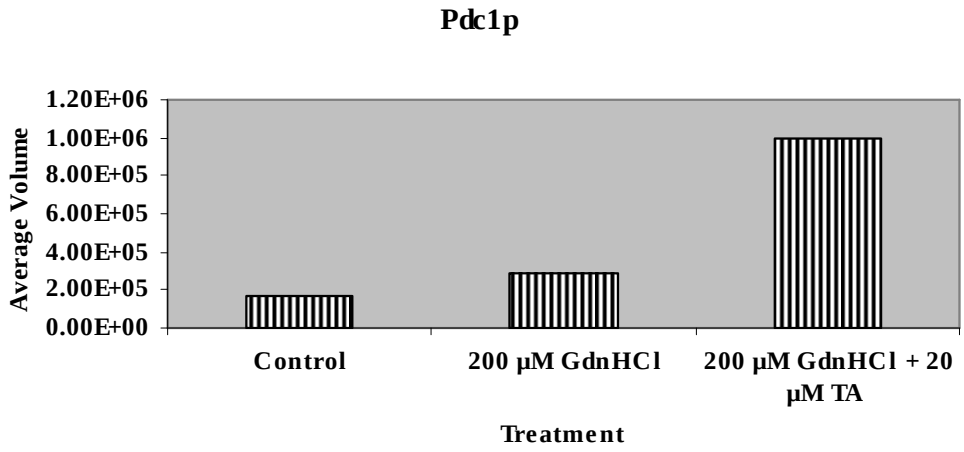

Figure 4.105 Pdc1p expression in response to GdnHCl and TA. Progenesis^{TM} calculated p = 0.020.

Protein spot no. 9 was also identified as Pdc1p. In this instance, Pdc1p was seen to be downregulated in the presence of GdnHCl alone and highly upregulated with the addition of TA (figure 4.106).

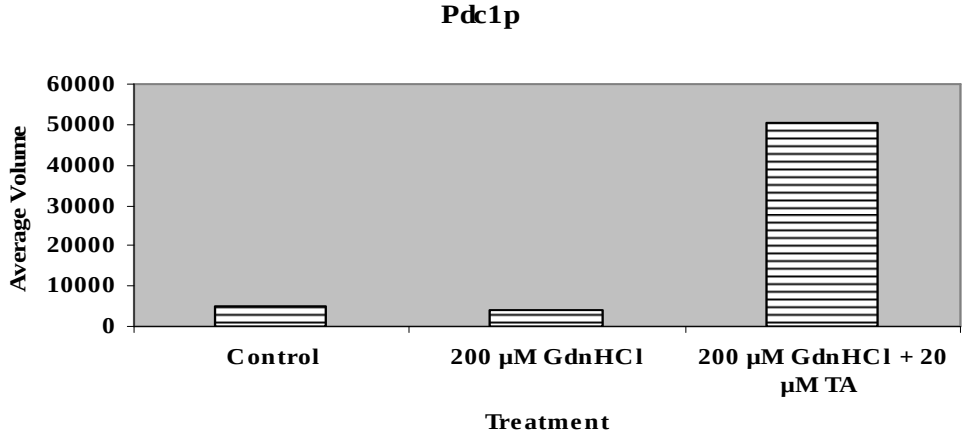

Figure 4.106 Pdc1p expression in response to GdnHCl and TA. Progenesis^{TM} calculated p = 0.043.

The protein represented by spot no. 10 was identified as Aro8p. Proteomic study demonstrated that this protein is upregulated under exposure to GdnHCl alone and then furthermore in the presence of a combination of both GdnHCl and TA (figure 4.107).

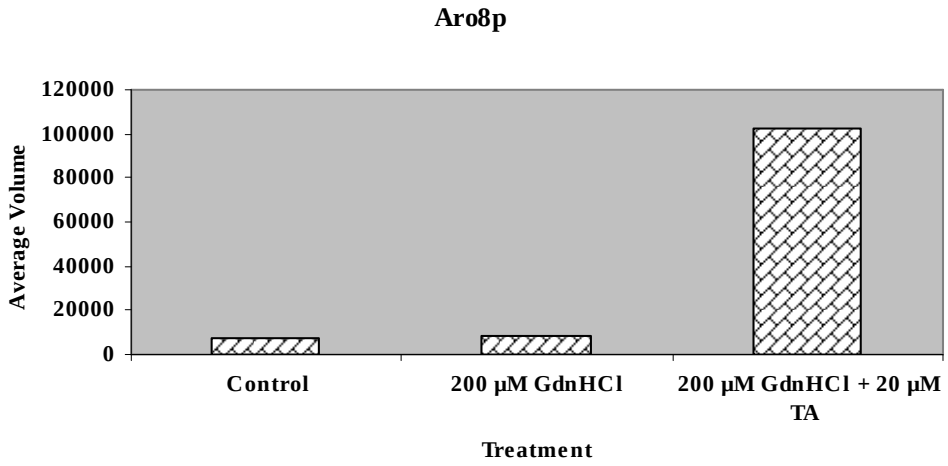

Figure 4.107 Aro8p expression in response to GdnHCl and TA. Progenesis^{TM} calculated p = 0.032.

The expression of protein spot no. 11, Imd3p decreases upon exposure to GdnHCl but is highly stimulated under the addition of TA (figure 4.108).

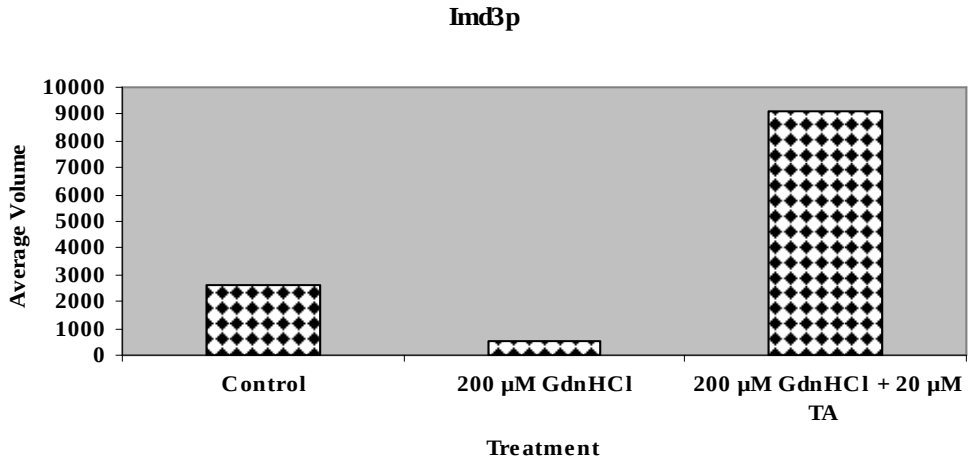

Figure 4.108 Imd3p expression in response to GdnHCl and TA. Progenesis^{TM} calculated p = 0.007.

The expression of Adh1p, represented by spot no. 12 is heavily repressed in the presence of GdnHCl alone but highly induced under exposure to both GdnHCl and TA (figure 4.109).

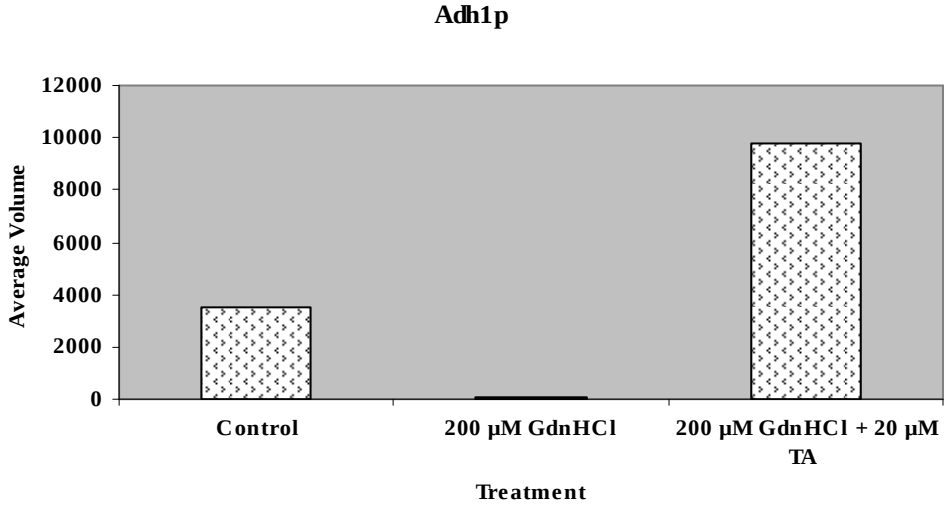

Figure 4.109 Adh1p expression in response to GdnHCl and TA. Progenesis^{TM} calculated p = 0.003.

Spot no. 13 was also identified as Adh1p. As for spot 12, this was found to be highly expressed in the presence of a combination of GdnHCl and TA. Unlike spot 12, expression was upregulated under exposure to GdnHCl alone (figure 4.110).

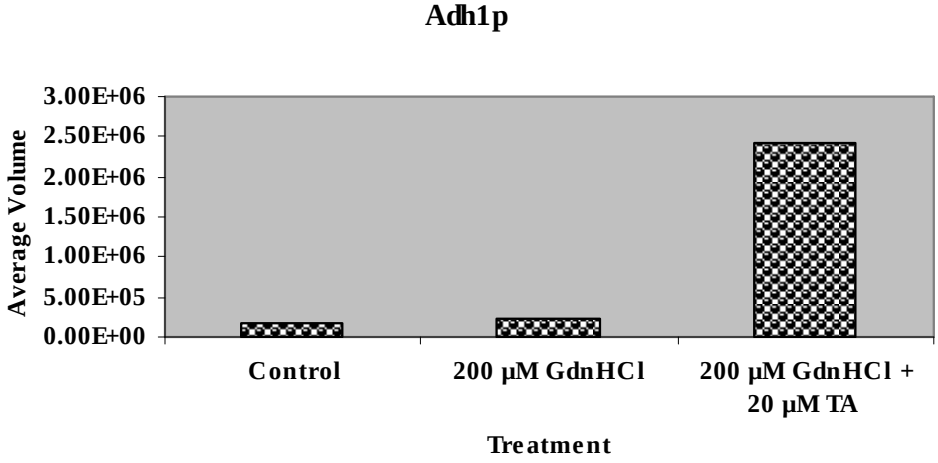

Figure 4.110 Adh1p expression in response to GdnHCl and TA. Progenesis^{TM} calculated p = 0.040.

Tdh3p, found to be represented by spot no. 14 is upregulated upon GdnHCl exposure and furthermore with the addition of TA (figure 4.111).

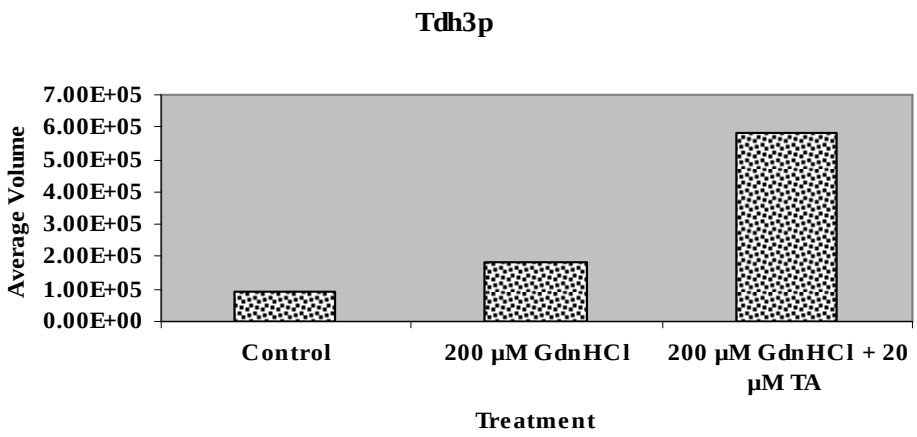

Figure 4.111 Tdh3p expression in response to GdnHCl and TA. Progenesis™ calculated p = 0.042.

Spot no. 15 was identified as Rhr2p. This appears to be stimulated in the presence of GdnHCl alone and induced to a higher level under exposure GdnHCl and TA in combination (figure 4.112).

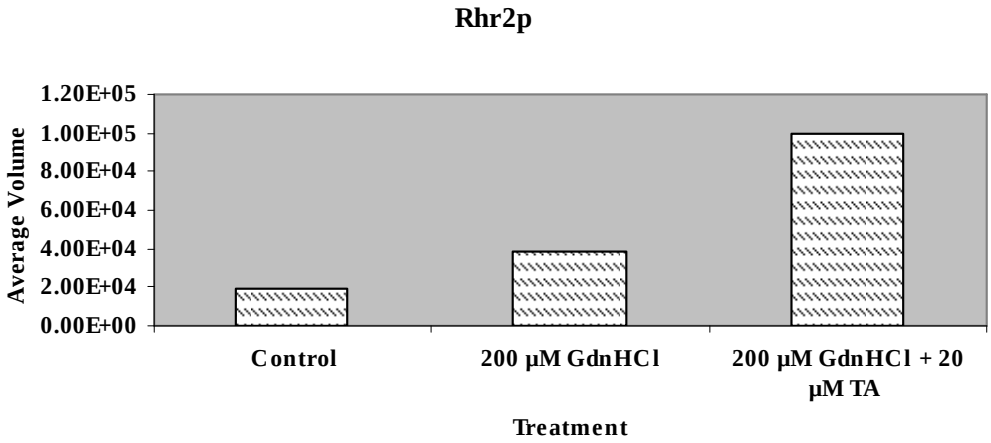

Figure 4.112 Rhr2p expression in response to GdnHCl and TA. Progenesis™ calculated p = 0.046.

Figure 4.113 below presents gels containing separated proteins from cells that were untreated, exposed to 200 µM GdnHCl and treated with 200 µM GdnHCl + 20 µM TA.

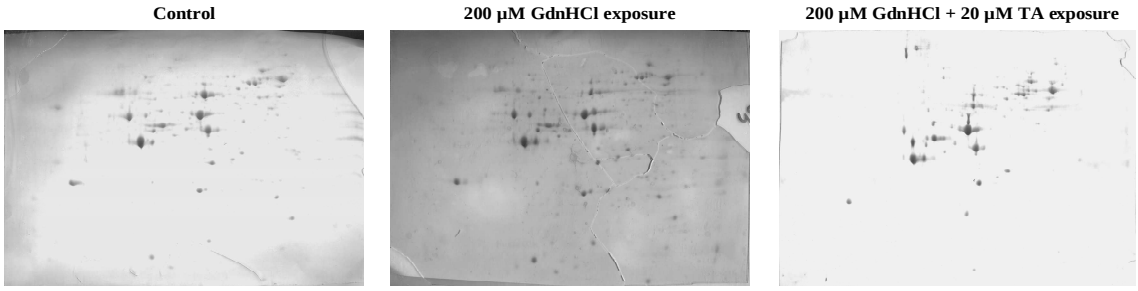

Figure 4.113 Comparison of gels containing separated proteins from untreated cells, and cells exposed to GdnHCl and TA.

Figure 4.114 provides an example of proteins found to be differentially expressed upon drug exposure.

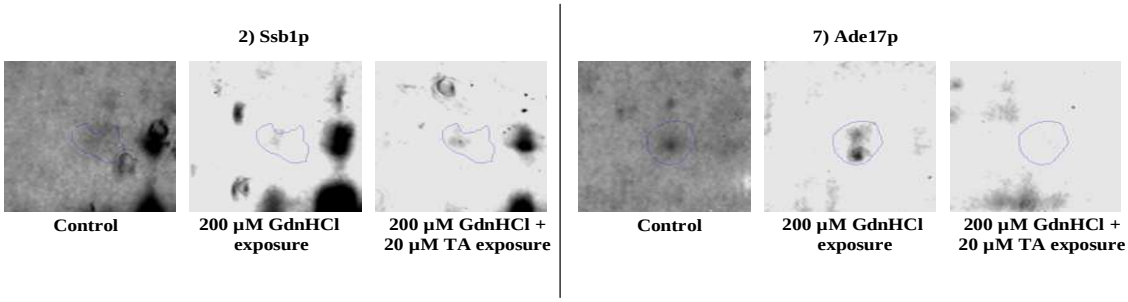

Figure 4.114 Illustration of differential Ssb1p and Ade17p expression in response to GdnHCl and TA exposure.

Protein spot no. 2 Ssb1p as depicted in figure 4.114 is downregulated in the presence of GdnHCl alone and upregulated under exposure to a combination of GdnHCl and TA. The figure above illustrates the visible difference in spot intensity. Ade17p is repressed under cellular exposure to GdnHCl alone and further decreased with the addition of TA.

4.19 Discussion

Much of the work described in this chapter was carried out to learn more about the mode of action of TA. Although commonly prescribed for decades to treat Alzheimer's Disease (Summers, 2006), TA was recently identified as an agent displaying prion-curing capacity in yeast (Tribouillard-Tanvier *et al.*, 2008a). Unlike

two other drugs 6AP and GA identified in a similar screen, TA was found to be inactive against mammalian prions (Bach *et al.*, 2003, Tribouillard-Tanvier *et al.*, 2008a, Tribouillard-Tanvier *et al.*, 2008b). It was thus hypothesised that the yeast TA target may be too far diverged in the mammalian system for the drug to be effective (Tribouillard-Tanvier *et al.*, 2008b).

In this study, it was demonstrated that TA, 6AP and GA all have the ability to cure [*PSI*$^+$] in wild-type *S. cerevisiae*, but only in the presence of GdnHCl. It therefore appears that a certain level of background curing by GdnHCl is required before the anti-prion effects of the drugs can be observed in wild-type. Importantly, the concentration of GdnHCl that facilitates [*PSI*$^+$] curing by the drugs does not cure the prion when supplied alone. This can be seen in figures 4.3, 4.5 and 4.6. It was noted that relatively low concentrations, such as 5 µM, of all three drugs is sufficient to elicit effects.

When [*PSI*$^+$] cells are treated wth an effective level of GdnHCl, the cleavage of new propagons by Hsp104p is prevented, halting priongenesis, and the remaining prion seeds are diluted out over time (Paushkin *et al.*, 1996, Eaglestone *et al.*, 2000, Ferreira *et al.*, 2001). Based on the curing curves constructed in this study, it appears that 6AP, GA and TA function in a similar manner, preventing prion propagation, allowing residual propagons to be diluted out over subsequent generations. Although it is thought that 6AP and GA cure [*PSI*$^+$] through a different mode of action to TA, methods may be similar in this respect. Like GdnHCl, the way in which these three drugs cure [*PSI*$^+$] may also be a result of chaperone function inhibition. It is already known that 6AP and GA decrease the level of ribosomal chaperone activity. Although structurally unrelated, 6AP and GA cure prions through a similar in *trans* mode of action (Reis *et al.*, 2011). Both compete with unfolded protein for the domain V of the large rRNA of the large ribosomal subunit and inhibit ribosomal-mediated protein folding (Tribouillard-Tanvier *et al.*, 2008b, Reis *et al.*, 2011). The analogous TA curing curve implies this agent may

also inhibit chaperone activity, hindering prion propagation. Perhaps TA is inhibiting a chaperone that is diverged or undiscovered in mammals, as suggested by Tribouillard-Tanvier *et al.* (2008a). To date, no Hsp104p homologue has been discovered in mammals (Jones and Tuite, 2005), it was thus hypothesised that TA may target Hsp104p, as GdnHCl does, and like TA, GdnHCl does not cure mammalian prions. The TA curing curve data correlates well with the result from another assay demonstrating that growth is required for TA to cure [*PSI*$^{+}$]. Cell cultures exposed to TA (in combination with GdnHCl) in which cells did not grow remained [*PSI*$^{+}$], while cells that underwent growth began to cure (figure 4.7). Data from both assays depicted TA prion curing over time, associated with cell growth.

Although similarities were observed in 6AP, GA and TA curing curves, some differences were also seen. Both 6AP and GA appear to cure [*PSI*$^{+}$] in the wild-type background faster than TA, suggesting that they are more potent prion-curing agents than TA. However, when comparing the level of curing after 11 generations, TA exposure results in a greater percentage of cured cells than 6AP or GA. These discrepancies in drug curing patterns highlights a probable difference in the way in which 6AP and GA cure [*PSI*$^{+}$], in comparison to TA. This difference may simply be a disparity in the chaperone activity targeted by the respective drugs.

Further to these results, thermotolerance assays were carried out. Hsp104p is key in enabling cells to withstand heatshock (Sanchez and Lindquist, 1990). It was reasoned that if TA does target Hsp104p, inhibiting its function, this may be reflected in the level of cellular thermotolerance. After Hsp104p induction by incubation at 39ºC and subsequent heatshock at 52ºC, a clear growth gradient was observed for wild-type cells on YPD (figure 4.11). Prolonged heatshock resulted in increased cell death. Exposure to 3 mM GdnHCl following heatshock strongly inhibited cell growth, illustrating inhibition of Hsp104p activity by GdnHCl, thus hindering thermotolerance. Neither 20

µM TA nor 200 µM GdnHCl alone effected wild-type cellular thermotolerance, demonstrating the neither alone exert any considerable influence on Hsp104p. However, growth of heatshocked cells exposed to a combination of both is hindered. This implies that TA may inhibit Hsp104p, as it enhances the effect of a low, ineffective level of GdnHCl. It may be the case that together, TA and GdnHCl have an accumulative effect on Hsp104p, resulting in clear inhibition.

Thermotolerance assays using G600 Δ*hsp104* showed no difference in growth of heat-shocked cells, regardless of drug exposure (figure 4.12). Due to the absence of *HSP104*, drugs cannot take effect, supporting the hypothesis that TA targets Hsp104p.

Thermotolerance assays were also performed using 6AP and GA. This allowed comparisons to be made to the inhibitory effects of TA on Hsp104p. In contrast to TA, a combination of 20 µM 6AP/GA and 200 µM GdnHCl did not appear to result in the inhibition of Hsp104p (figure 4.15). This suggests that 6AP and GA do not amplify the effects of GdnHCl, and do not target Hsp104p and again highlights a difference in the modes of action of 6AP/GA and TA.

Following thermotolerance assay results that demonstrated an apparent accumulative effect of GdnHCl and TA on Hsp104p, it was hypothesised that TA may function in increasing the rate of GdnHCl uptake by cells. An attempt was made to monitor the uptake of [^{14}C]-labelled GdnHCl in the presence and absence of TA. Unfortunately, the assay was unsuccessful.

Upon environmental stress, Hsp104p works through collaboration with Hsp70p and Hsp40p to rescue denatured, aggregated proteins (Glover and Lindquist, 1998). Taking into account that TA appears to cure [*PSI*$^{+}$] in a similar manner to GdnHCl, the effects of this drug on Hsp70p activity was also investigated. Hsp70 protein family members have a peptide-binding domain (PBD) which maintains tight association with its substrate when ADP is bound to the adjacent ATPase-binding

domain (ABP). In contrast, when ATP is bound, rapid substrate exchange takes place (Masison *et al.*, 2009). This ATPase binding cycle is regulated by a number of co-chaperones and NEFs such as Ydj1p, Sis1p, Fes1p, Sse1p, Sti1p, Cns1p and Cpr7p (Cyr *et al.*, 1992, Dolinski *et al.*, 1998, Lu and Cyr, 1998, Kabani *et al.*, 2002, Wegele *et al.*, 2003, Hainzl *et al.*, 2004, Jones *et al.*, 2004, Raviol *et al.*, 2006). The importance of Hsp70p and the ATPase binding cycle in prion propagation has been demonstrated and is of particular interest due to the high level of conservation between yeast and mammals (Chernoff *et al.*, 1995, Newnam *et al.*, 1999, Jones *et al.*, 2004). In this study, wild-type and mutant strains lacking genes involved in the Hsp70p ATPase binding cycle were exposed to TA alone and in the presence of GdnHCl (figure 4.17). As expected, it was seen that TA alone does not cure [*PSI*$^+$] in wild-type G600, but clear zones of TA curing were seen in the presence of 200 µM and 500 µM background GdnHCl. Very different results were obtained for Hsp70p-associated mutants. TA cures Δ*ssa1* [*PSI*$^+$] in the absence of background GdnHCl, however 3 mM GdnHCl appears to have the same effect as 10 mM TA. When 200 µM and 500 µM GdnHCl are present TA curing is enhanced. Similar results were seen for Δ*cpr7*, Δ*sti1* and Δ*fes1*, however that for the double mutant Δ*sti1*Δ*cpr7* was somewhat different. In the presence of 500 µM background GdnHCl, the TA zone of Δ*sti1*Δ*cpr7* [*PSI*$^+$] curing was greater than that for either of the single mutants. This suggests that an exacerbated disruption of the Hsp70p ATPase binding cycle renders cells more sensitive to curing by TA.

The same experiment was performed using 6AP and GA, so that the effects of these drugs could be compared to that of TA (figures 4.18 and 4.19). Comparable results were obtained for 6AP curing of [*PSI*$^+$] in these strains. In the absence of background GdnHCl, 6AP did not cure [*PSI*$^+$] in wild-type G600 but it did in the mutant strains. It does appear however that 6AP is to a small degree more potent than TA in curing prions in Hsp70p-related mutant strains. The [*PSI*$^+$] curing capacity of GA

in these strains was also observed. Interestingly, GA seemed to be the weakest anti-prion agent as the curing zones induced in both wild-type and mutant strains was considerably smaller than those for TA and 6AP. The fact that all three drugs alone have the ability to cure [*PSI*$^{+}$] in these mutant strains suggests that any of these drugs might target Hsp70p or the ATPase binding cycle. It may be the case that the drugs are inhibiting an already weakend ATPase binding cycle and exhibiting intensified [*PSI*$^{+}$] curing. The fact that 6AP and GA alone cure [*PSI*$^{+}$] in Hsp70p-related mutants may indicate a possible link between Hsp70p- and ribosomal-mediated protein folding. Importantly, it was clearly demonstrated in these assays that in a suitable background strain, TA, 6AP and GA have the ability to cure [*PSI*$^{+}$]. Following the observation that TA has the ability to cure [*PSI*$^{+}$] in the absence of GdnHCl, it can be assumed that this drug does not solely function through enhancing the uptake of GdnHCl, as was previously hypothesised.

To further investigate if any of these drugs target Hsp104p or Hsp70p, Western blot analysis was performed. The expression levels of Ssa1p and Hsp104p under drug exposure was assessed. Untreated wild-type cells express the same level of both Ssa1p and Hsp104p as those treated with GdnHCl alone and in combination with TA, 6AP and GA. This indicates that TA, 6AP and GA do not directly affect the level of these chaperone proteins and correlates with results published by Lahiri *et al.* (1994), who showed that TA does not induce changes in the expression level of mammalian Hsp70p. If any of these drugs do induce [*PSI*$^{+}$] curing through targeting Hsp70p or Hsp104p, they may do so by altering chaperone protein activity rather than direct expression levels.

Additional investigation into the mode of action of TA involved assessing the genes that are up- and downregulated in response to exposure. RNA sequencing data was analysed and the cellular transcriptomic responses to 200 µM GdnHCl and 200 µM

GdnHCl + 20 µM TA were compared (exposure for 14 generations). Genes that underwent more than 2-fold increase or decrease in transcription were assessed. It must be noted that many more genes are downregulated than upregulated in response to both treatments.

It appears that whether the cells are exposed to 200 µM GdnHCl alone, or in combination with 20 µM TA, the cells respond in the same way at a general biological level. The five most highly induced biological processes are common to both treatments (4.61). The RNA metabolic process is stimulated, to increase the amount of RNA available, prerequisite to protein production, presumably as a general response to the above described compounds. The fact that ribosome biogenesis and translation are stimulated adds weight to this hypothesis, increasing potential for augmented protein production. Transport, also seen to be provoked, is important subsequently for carriage of synthesised proteins to regions where function might occur. The importance of the cell cycle becomes clear at this point, as it is necessary for cells to undergo duplication to increase the opportunity to respond to both TA and GdnHCl.

The cellular response at the molecular function level to both treatments is also quite similar (4.63). Transferase activity involves the transfer of a functional group from one molecule to another, e.g. transfer of a phosphate group to a molecule from ATP by a kinase (Parson, 1993). The fact that transferase activity is upregulated could denote that GdnHCl and TA are creating stressful conditions for the cell. Kinases have previously been shown to be transcriptionally upregulated in response to osmotic, oxidative and heavy metal stress in *Candida albicans* (Enjalbert *et al.*, 2006) and environmental stress in *Schizosaccharomyces pombe* (Berlanga *et al.*, 2010). It is already known that GdnHCl is toxic to yeast at concentrations of above 3-5 mM and thus causes an inhibition of growth (Jung *et al.*, 2002). The 200 µM concentration, albeit 15-25 times lower that that found by others to be toxic, could bring about stress

that would precede cell death in cultures exposed to 3-5 mM GdnHCl. As illustrated by figures 4.61 and 4.63**,** it is difficult to assess the impact TA has on the cell, as TA and GdnHCl combined at these concentrations don't initiate biological or molecular responses that aren't seen under GdnHCl exposure alone.

Genes associated with the cytoplasm, nucleus, membrane and ribosome are some of the most highly induced in the presence of GdnHCl alone and combined wih TA. However, GdnHCl alone stimulates genes associated with the mitochondrion, while GdnHCl and TA together stimulate nucleolus-associated genes (figure 4.62). rRNA is transcribed and assembled within the nucleolus (Parson, 1993). The fact that under exposure to GdnHCl and TA combined, nucleolus-associated genes are most highly upregulated, suggests the cells strive to respond to those compounds by increasing protein production, be it proteins involved in regular housekeeping functions or specific proteins that enable survival in the presence of the drugs.

When comparing the biological processes carried out by the most acutely downregulated genes, a greater difference was observed. Genes associated with transport, RNA metabolic process and transcription are highly downregulated under exposure to both GdnHCl alone and in combination with TA. However, cellular lipid and heterocycle metabolic processes are only acutely repressed in the presence of GdnHCl alone. In contrast, the response to chemical stimulus, generation of precursor metabolites and energy and mitochondrion organisation are all greatly inhibited when TA is added to GdnHCl. Heterocycle metabolism involves 'chemical reactions and pathways involving heterocyclic compounds, those with a cyclic molecular structure' (SGD www.yeastgenome.org). However GdnHCl does not possess a cyclic structure.

A high degree of overlap was observed from expression data in genes that are up- and downregulated in response to GdnHCl alone and in combination with TA for 14 generations. For example, three of the four genes most upregulated in response to

GdnHCl exposure are also some of the four genes most stimulated in the presence of GdnHCl and TA combined.

It was important not only to look at the cellular response to GdnHCl and TA after 14 generations, when [PSI^+] cells have been completely cured by a combination of the two. Cellular responses after 1 hr. and 3 hr. exposures provides insight into the way in which yeast initially react to the presence of the drugs. The RNA sequencing data depicting the complete yeast cellular response to GdnHCl and TA combined for 14 generations was also used in assessing the differential effects induced by various exposure times. Comparisons were made of the genes differentially expressed under exposure to 200 µM GdnHCl + 20 µM TA for 1 hr., 3 hr. and 14 generations. All three exposure times induced an increase in the expression of genes involved in RNA metabolic process, ribosome biogenesis and transport. The shortest exposure time caused an upregulation in transcription- and translation-associated genes, the latter also common to the 14 generation treatment, while the 3 hr. exposure induced genes that play a role in response to chemical stimulus and stress. Uniquely, the 14 generation exposure acutely induced genes involved in the cell cycle (4.91).

Genes associated with the nucleolus were only highly upregulated upon 1 hr. and 14 generation exposure, while those associated with the plasma membrane where only highly stimulated under 3 hr. exposure, as shown in figure 4.92. Cytoplasm-, nucleus-, and membrane-associated genes were some of the most highy upregulated genes in response to all treatments. Conversely, genes associated with the mitochondrion were only highly stimulated under the two shorter exposures, while those involved with ribosome function were found to be most induced upon 14 generation treatment.

As regards molecular function, transferase and hydrolase activity were commonly induced under the three different exposures. Oxidoreductase and transporter

activity were stimulated under 1 hr. and 3 hr. exposures, while RNA binding was acutely induced upon 1 hr. and 14 generation exposures. Protein binding was commonly upregulated upon 3 hr. and 14 generation treatments and structural molecule activity was uniquely one of the most highly stimulated functions under the longest exposure (figure 4.93).

Interestingly, very little correlation was observed in biological processes repressed upon GdnHCl + TA exposure for 1 hr., 3 hr. and 14 generations (figure 4.94). Only RNA metabolic process was highly inhibited in response to all treatments. Genes most heavily downregulated upon 1 hr. treatment function in the response to stress, cellular carbohydrate metabolic process, chromosome organisation and cell cycle. Those downregulated upon 3 hr. exposure play a role in heterocycle metabolic process, ribosome biogenesis, cellular amino acid metabolic process and translation. The processes most hindered under exposure for 14 generations were transport, transcription, generation of precursor metabolites and energy, response to chemical stimulus and mitochondrial organisation.

A higher degree of correlation was observed in the comparison of cellular components associated with genes highly repressed upon exposure 1 hr., 3 hr. and 14 generation exposure. Genes associated with the cytoplasm, nucleus, mitochondrion and membrane were heavily downregulated under all exposures (figure 4.95). Cell wall- and chromosome-associated genes were among those most repressed during the shortest exposure, while ribosome-associated genes were seen to be inhibited most heavily during the 3 hr. exposure. Conversely, genes involved with the mitochondrial envelope were acutely downregulated upon the 14 generation treatment.

In response to GdnHCl + TA exposure for 1 hr., 3 hr. and 14 generations, genes involved in oxidoreductase and transferase activity were all highly repressed (figure 4.96). Hydrolase and structural molecule activity were severely inhibited under the two

shorter treatments, while DNA binding genes were acutely downregulated upon 1 hr. and 14 generation exposures. Specific to the 3 hr. treatment, genes related to RNA binding and transporter activity were transcriptionally repressed. Transcription regulator activity and protein binding-associated genes were severly downregulated upon 14 generation exposure only.

Taking these results together, it appears that exposure to GdnHCl and TA combined may be conferring some kind of cellular stress. The biological process termed response to stress is acutely stimulated under 3 hr. exposure. Individual genes involved in the stress response can be some of the most highly upregulated genes in the presence of these agents. For example, *CUP1-1* and *CUP1-2* are upregulated almost 18-fold under the 1 hr. treatment (table 4.8). *CUP1-1* and *CUP1-2* are two copies of a gene encoding a metallothionein that confers resistance to cells against copper and cadmium (Winge *et al.*, 1985, Jeyaprakash *et al.*, 1991). In response to 3 hr. exposure, these genes are again among the 50 most highly upregulated genes. However, after exposure for 14 generations, these genes do not fall into the 50 most highly upregulated gene category. This may imply that when cells are initially exposed to GdnHCl and TA combined, they are subjected to stress on some level, which they begin to respond to and eventually adapt to. The fact that the concentrations of these agents used elicit effects but do not kill cells may facilitate this response and adaptation.

Examining the expression levels of a number of genes involved or related in some way to prion propagation yielded interesting results (table 4.12). Ydj1p is a member of the Hsp40 protein family (Cyr *et al.*, 1994). It interacts with Hsp70p and plays a role in regulating the ATPase binding cycle, thus facilitating Hsp70p activity and prion propagation (Cyr *et al.*, 1992, Masison *et al.*, 2009). When cells are exposed to 200 µM GdnHCl alone for 14 generations, *YDJ1* is downregulated 3.9-fold. With the addition of 20 µm TA, it is further repressed 1.4-fold. Similar patterns were observed

for other genes encoding Hsp70p ATPase cycle regulators. The *CNS1* gene product acts as a co-chaperone for both Hsp90p and Hsp70p, stimulating ATPase activity of the latter (Dolinski et al., 1998, Hainzl et al., 2004). *CNS1* was found to be downregulated 2-fold under exposure to GdnHCl alone and downregulated 1.6-fold further in the presence of GdnHCl and TA combined. Similar patterns of transcriptional repression were observed for other genes *CPR7*, *FES1* and *SSE1*, which act as Hsp70p ATPase binding cycle regulators (Kabani *et al.*, 2002, Raviol *et al.*, 2006, Masison *et al.*, 2009). The fact that these genes are all heavily downregulated upon GdnHCl exposure alone can perhaps be explained. GdnHCl is known to inhibit Hsp104p-mediated prion propagation (Ferreira *et al.*, 2001). Moosavi *et al.* (2010) demonstrated that [PSI^{+}] curing by Hsp104p overexpression requires Hsp70p co-chaperones and suggested that these proteins regulate Hsp104p activity or alter its binding ability. It may be the case that in this study, when Hsp104p activity was inhibited by GdnHCl, the cells responded by downregulating the expression of Hsp70p co-chaperones as they were not required for Hsp104p regulation. If TA does target Hsp104p, this response may be enhanced with the addition of TA. Alternatively, the exacerbated decrease in *YDJ1*, *CNS1*, *CPR7*, *FES1* and *SSE1* expression under GdnHCl + TA exposure may be indicative that TA targets the Hsp70p ATPase binding cycle.

Following two-dimensional gel electrophoresis and LC-MS, analysis of proteins differentially expressed under 200 µM GdnHCl and 20 µM TA exposure led to the identification of a number of proteins displaying similar patterns of expression. A number of spots determined to be Ssa2p (two spots), Pdc1p, Aro8p, Adh1p, Tdh3p and Rhr2p were shown to be upregulated in response to GdnHCl exposure alone and further elevated in the presence of GdnHCl and TA combined (figures 4.100, 4.103, 4.105, 4.107, 4.110-4.112). Ssa2p as described above is a member of the Hsp70 Stress Seventy subclass A (Craig *et al.*, 1993), and the fact that expression of this protein is upregulated

in this manner may suggest that TA cures [*PSI*$^{+}$] by targeting Hsp70p expression in combination with GdnHCl. It may be the case that TA and GdnHCl negatively affect Hsp70p and in response to this the cells increase Ssa2p production.

Pdc1p is a pyruvate decarboxylase, and along with the alcohol dehydrogenease Adh1p and the glyceraldehyde-3-phosphate dehydrogenase Tdh3p, plays a role in the glucose fermentation pathway (Lutstorf and Megnet, 1968, Bennetzen and Hall, 1982, Schmitt and Zimmermann, 1982, McAlister and Holland, 1985, Pronk *et al.*, 1996). The increases in expression of these proteins in response to GdnHCl alone and in combination with TA suggest that glucose fermentation may be stimulated in response to these agents. As was discussed in chapter 3, the increased activation of this process may be a result of cellular oxidative stress.

Rhr2p, which was shown to be upregulated in response to GdnHCl and TA, is a glycerol-3-phosphatase that is involved in yeast stress responses (Norbeck *et al.*, 1996, Pahlman *et al.*, 2001). The fact that this protein is increasingly expressed in response to these agents supports the hypothesis that they may induce cellular stress. Interestingly, this protein has been shown to physically interact with other Hsp70 family members Ssa1p, Ssb1p and Sse1p (Gong *et al.*, 2009). If TA and GdnHCl exposure does result in an alteration of Hsp70p expression, the upregulation of Rhr2p may be implicated in the differential chaperone expression.

Aro8p is an aminotransferase (Iraqui *et al.*, 1998) that undergoes an increase in expression in response to GdnHCl and TA. This protein is also known to interact physically with Sse1p (Gong *et al.*, 2009) and may be thus involved somehow in [*PSI*$^{+}$]-curing by GdnHCl and TA.

Other proteins were also found to undergo interesting patterns of differential expression. Ade17p is responsible for catalysing part of the *de novo* purine biosynthesis pathway (Tibbetts and Appling, 2000) and was the only protein downregulated upon

GdnHCl exposure and furthermore with the addition of TA (figure 4.104). A number of proteins were downregulated in the presence of GdnHCl alone and then upregulated under exposure to GdnHCl and TA combined. Protein spots representing Ilv2p, Ssb1p (two spots), Asn2p, Pdc1p, Imd3p and Adh1p all followed this pattern of expression (figures 4.98, 4.99, 4.101, 4.102, 4.106, 4.108, 4.109). Ilv2p plays a role in isoleucine and valine biosynthesis and physically interacts with Ssb2p, a Stress Seventy B Hsp70 subclass member (Falco *et al.*, 1985, Craig *et al.*, 1993, Krogan *et al.*, 2006). Interestingly, the second member of the Ssb Hsp70 subfamily, Ssb1p (Craig *et al.*, 1993), was found to exhibit the same expression pattern as Ilv2p under GdnHCl and TA exposure. These results suggest that in response to GdnHCl alone, the Hsp70 Ssa proteins are generally upregulated and the Ssb proteins downregulated, and with the addition of TA, expression of both subfamilies is upregulated. Thus, it appears that exposure to GdnHCl alone induces differential expression of Stress Seventy proteins but in combination with TA, these proteins are largely upregulated.

Asn2p is a synthetase required in the asparagine biosynthesis pathway (Dang *et al.*, 1996), while Imd3p is an inosine monophosphate dehydrogenase (Escobar-Henriques and Daignan-Fornier, 2001). Both are downregulated under exposure to GdnHCl alone and upregulated in the presence of GdnHCl and TA combined. Although protein spots consistently upregulated were identified as Pdc1p and Adh1p, additional spots displaying the same expression pattern as Asn2p were determined to be Pdc1p and Adh1p. Although these patterns do not fully correlate, both demonstrate that Pdc1p and Adh1p are highly stimulated in the presence of GdnHCl and TA combined.

Additional work performed to investigate possible targets of TA involved ethyl methanesulfonate (EMS) mutagenesis, whereby the G600 genome was randomly mutagenised in an attempt to identify gene(s) that when disrupted alter [*PSI*$^{+}$]-curing by TA. A high-copy plasmid screen was also carried out with the aim of identifying gene(s)

that when overexpressed alter [*PSI*$^+$]-curing by TA. More than 500 colonies were screened in each of these experiments but no genes of interest were identified.

In investigating the mode of action of TA, four mutant strains lacking *LTV1*, *YAR1*, *RPL8A* and *RPL8B*, deficient in ribosomal stability and reported to display [*PSI*$^+$] instability were employed (M. Blondel, personal communication). Exposure of these strains to 6AP or GA has been shown to confer stability to the weak [*PSI*$^+$] prion (M. Blondel, personal communication). The fact that ribosomal imbalance is stabilised by 6AP and GA supports the findings that these drugs target ribosomal chaperone activity (Tribouillard-Tanvier *et al.*, 2008b), and further implicates ribosome function in prion propagation. As for wild-type 74D strain, [*PSI*$^+$] curing by TA, 6AP and GA in Δ*ltv1*, Δ*yar1*, Δ*rpl8a* and Δ*rpl8b* requires the presence of a relatively low concentration of GdnHCl (figures 4.22-4.24). Drug-mediated [*PSI*$^+$] curing in these strains is not enhanced and similar zones of curing to wild-type were observed in disc assays. It did however appear that [*PSI*$^+$] in the Δ*ltv1* background did not cure as efficiently as the other strains tested, particularly under 6AP exposure. Therefore, it appears that 6AP stabilises the prion to the greatest extent in the absence of *LTV1*.

The fact that Hsp104p- and ribosomal-mediated chaperone activity are both involved in prion propagation has been previously discussed. Further to this, it was of interest to assess if their roles in maintaing [*PSI*$^+$] overlap, and analyse the effects of both *HSP104* and *LTV1*/*YAR1* deletion on the yeast phenotype. In this study only Δ*ltv1* and Δ*yar1* were found to exhibit weak [*PSI*$^+$] and the spontanaeous appearance of [*psi*$^-$] colonies (figure 4.21), and were thus the only strains used for further investigation. To learn more, the question of whether these functions overlap in relation to acquired thermotolerance was addressed. 74D Δ*hsp104* displayed an identical phenotype to wild-type upon 3 mM GdnHCl exposure (figures 4.25-4.26). This demonstrates that in the 74D background strain 3 mM GdnHCl inhibits Hsp104p activity to the same extent as if

the *HSP104* gene were absent. Δ*ltv1* exhibited a higher level of induced thermotolerance than Δ*hsp104*, although a certain level of this was attributed to Hsp104p as when the cells were treated with 3 mM GdnHCl, growth was inhibited mimicking the Δ*hsp104* phenotype (figure 4.28). Exposure to 200 µM GdnHCl and 20 µM TA combined also inhibits Δ*ltv1* thermotolerance while either drug alone at these concentrations does not. In the absence of both *LTV1* and *HSP104*, cells do not survive at all after a 10 minute heatshock, illustrating the severly low level of acquired thermotolerance (figure 4.29). Neither TA nor GdnHCl had any effect of the virtually absent induced thermotolerance of the Δ*ltv1*Δ*hsp104* strain. This suggests that *LTV1* and *HSP104* exhibit an accumulative effect in conferring thermotolerance to *S. cerevisiae*. The fact that Δ*ltv1*Δ*hsp104* did not grow to the same extent as Δ*ltv1* exposed to 3 mM, as was expected, raises the possibility that Ltv1p and Hsp104p synergy is required for a comprehensive acquired heatshock response.

The phenotype of Δ*yar1* was somewhat different to that of Δ*ltv1*, demonstrating that although both mutants exhibit ribosome instability, the cells appear to be affected differently. Δ*yar1* was unable to grow after the 10 min. heatshock, displaying an acute lack of acquired thermotolerance, even though *HSP104* was present (figure 4.30). 3 mM GdnHCl exposure appeared to be the only treatment that affected the growth of this strain and was seen to inhibit cell growth further, resulting in only a small level of cell growth prior to heatshock. Interestingly, the deletion of *HSP104* in Δ*yar1* appears to induce a positive genetic effect, as in the absence of *HSP104*, Δ*yar1* appears to grow better (figure 4.31). There is a small amount of Δ*yar1*Δ*hsp104* growth after the 10 minute heatshock on YPD, although not upon drug exposure. Also when exposed to 3 mM GdnHCl, Δ*yar1*Δ*hsp104* undergoes a much higher level of growth than Δ*yar1*. This is accounted for by the absence of Hsp104p, the GdnHCl target (Ferreira *et al.*, 2001). Although it seems that Ltv1p and Hsp104p work in union with one another to facilitate

thermotolerance, Yar1p and Hsp104p may not. Ultimately, it appears that in the absence of Yar1p, Hsp104p in some way renders the cells more vulnerable to heatshock.

Due to ambiguity surrounding thermotolerance assay results, luciferase assays were performed that enabled further investigation into the effects of *LTV1* and *YAR1* deletion on heatshock recovery. In contrast to results from thermotolerance assays, luciferase assays suggested that the absence of *YAR1* and *LTV1* facilitates a much more rapid recovery of luciferase, following denaturation (figure 4.32). Following heatshock, the cells that demonstrated the fastest luciferase activity recovery, representative of chaperone activity, were Δ*yar1* cells. These cells exhibited more than 100% of their initial pre-heatshock luciferase activity after 60 min. As Hsp104p plays an essential role in heatshock recovery and acquired thermotolerance (Sanchez and Lindquist, 1990), this implies that the absence of *YAR1* allows exacerbated Hsp104p activity. Δ*yar1*Δ*hsp104* was in fact the strain that displayed the lowest level of luciferase activity recovery following heatshock, suggesting that it is uniquely Hsp104p that facilitates the rapid recovery observed for Δ*yar1*. Similar results were obtained for Δ*ltv1* and Δ*ltv1*Δ*hsp104*. After Δ*yar1*, Δ*ltv1* was the second most rapidly recovering strain with regards to luciferase activity, exhibiting restored chaperone activity considerably faster than wild-type, while Δ*ltv1*Δ*hsp104* was the second slowest recovering strain. This again is suggestive of ribosomal imbalance facilitating accelerated chaperone recovery and in turn allowing refolding of proteins into their functional state, but only in the presence of Hsp104p. These results are more consistent than those obtained from the thermotolerance assays, however there is confliction. Returning to the initial model illustrated in figure 4.1, the luciferase assay results may be explained. Ribosomal imbalance may lead to excess chaperone activity which increases the rate of luciferase recovery. Perhaps this activity enhances Hsp104p function either directly or indirectly. Further to this, the absence of both *YAR1*/*LTV1* and *HSP104* may then severely hinder

the ability of cells to recover following heatshock, which is subsequently exemplified by the low level of luciferase activity.

While assessing the effects of *LTV1* and *YAR1* absence on functional chaperone activity and prion propagation, it was observed that the wild-type 74D background strain phenotypically differed from G600 in some respects. 74D is substantially more TS than G600 and unlike the latter, does not survive following incubation at 39ºC for 48 hr (figure 4.33). As Hsp104p and Hsp70p are heavily implicated in enabling cells to withstand thermostress (Sanchez and Lindquist, 1990, Glover and Lindquist, 1998), it was hypothesised that 74D may produce a lower basal level of these chaperone proteins than G600. Western blot analysis was thus performed to investigate the expression levels of these proteins upon cellular incubation at 30ºC, 37ºC and 39ºC (figure 4.36). For both strains, it was found that 1 hr. incubation at 37ºC caused an increase in expression of both Hsp104p and Ssa1p. 1 hr. incubation at 39ºC induced a further increase in the level of these proteins. Thus, it appears that both strains are able to acquire thermotolerance through pre-incubation at 37ºC and 39ºC, however 74D cannot survive prolonged exposure to the latter temperature. This experiment also demonstrated that 74D does indeed produce a somewhat lower basal level of both Hsp104p and Ssa1p than G600, which may contribute to temperature sensitivity.

To further investigate, the 74D genome was sequenced and compared with that of the S288C reference strain. Approximately 5, 500 non-synonymous amino acid changes were identified in the 74D genome, a number of them in genes encoding chaperones and cochaperones, including *SSA1*, *CPR7*, and *STI1* (tables 4.1-4.2). Although no non-synonymous amino acid changes were found in *HSP104*, which is of great importance in acquired thermotolerance (Sanchez and Lindquist, 1990), changes were found in the Hsp70p family *SSA1* gene, that is required for Hsp104p-mediated protein folding (Glover and Lindquist, 1998).

Additionally, a high-copy plasmid screen was performed with the aim of identifying gene(s) that when overexpressed reduce 74D temperature sensitivity. A number of genes were found whose overexpression resulted in similar 74D growth to that of G600 (figure 4.34). It was anticipated at this point that a certain level of overlap would be observed and that a number of genes might encode products involved in the same pathway or process. However, when the identity of these genes were revealed, there appeared to be no overlap and thus no specific function could be said to be responsible in part for 74D temperature sensitivity.

In overall conclusion, differences in the TA mode of action compared to that of 6AP and GA are highlighted in this chapter. While results suggest that TA may target Hsp104p, as GdnHCl does (Ferreira *et al.*, 2001), they suggest that 6AP and GA do not. The hypothesis that TA functions solely through enhancing GdnHCl uptake also appears to be invalidated. Disruption of Hsp70p activity enhances [*PSI*$^{+}$] curing by all drugs and eliminates the requirement for background GdnHCl curing, suggesting that any one of the three drugs may target Hsp70p and its regulators. TA and GdnHCl combined appear to induce cellular stress, implying that cells must adapt when treated with these drugs to enable survival. There are differences in results relating to the effects of *LTV1* and *YAR1* absence on acquired cellular thermotolerance. Regardless, *LTV1* or *YAR1* deletion alone and in combination with *HSP104* deletion severely impacts upon the way in which cells recover and survive following heatshock. Thus it can be concluded that ribosomal imbalance has an acute affect on heatshock and chaperone activity, which may subsequently have implications for prion-propagation.

Chapter 5 Discussion and future work

Part 1 Using *Saccharomyces cerevisiae* as a model organism to investigate the eukaryotic response to the toxic fungal metabolite gliotoxin

As a secondary metabolite that assists in facilitating host colonisation by a number of fungal species, including *A. fumigatus* (Weindling and Emerson, 1936, Müllbacher and Eichner, 1984), gliotoxin is an interesting toxin. In this study, *S. cerevisiae*, a commonly used model organism, was employed to investigate the eukaryotic response to gliotoxin. The detrimental effects of gliotoxin were clearly evident as it inhibited the growth of yeast strains in both solid and liquid culture. As this distinct consequence of gliotoxin exposure was observed, RNA sequencing and proteomic analysis were utilised to investigate the eukaryotic cellular response induced as a result of exposure to gliotoxin.

To our knowledge, analysis of the yeast global response to gliotoxin had not been performed prior to this study, although Chamilos *et al.* (2008) had previously carried out a genomewide screen to identify *S. cerevisiae* genes associated with gliotoxin resistance or sensitivity.

Previous work has indicated that the presence of gliotoxin gives rise to OS in mammalian cells, particularly as the toxin can undergo redox cycling (Trown and Bilello, 1972, Eichner *et al.*, 1988, Orr *et al.*, 2004). The findings discussed here have supported these observations as wild-type *S. cerevisiae* increased the expression of a large number of proteins that play a role in the OS response. This stimulation often occured at both the transcription level and the proteomic level. For example, genes involved in the sulfur amino acid biosynthesis pathway, both directly and through its regulation, were upregulated considerably in response to two concentrations of gliotoxin, as demonstrated by RNA sequencing analysis. This led to increased protein expression in some cases which was possible to detect using 2-dimensional gel electrophoresis. This sulfur amino acid biosynthesis pathway must be fully functional before glutathione

can be produced which has been significantly implicated in protection against OS (Williamson *et al.*, 1982, Dormer *et al.*, 2000, Mosharov *et al.*, 2000, Penninckx, 2000). Moreover, mutant analysis also demonstrated the importance of the OS response in resistance to gliotoxin. In agreement with Chamilos *et al.* (2008), Δ*cys3* was seen to be hyper-sensitive to gliotoxin, due to disruption of the transsulfuration pathway, a subsection of the sulfur amino acid biosynthesis pathway that generates cysteine (Ono *et al.*, 1992, Cherest *et al.*, 1993). Δ*sod1* and Δ*yap1* also displayed increased sensitivity to gliotoxin, Δ*yap1* more acutely than Δ*sod1*, due to the absence of cytosolic superoxide dismutase and important transcriptional regulation of a wide range of OS responses (Bermingham-McDonogh *et al.*, 1988, Schnell *et al.*, 1992, Lee *et al.*, 1999). These mutants also exhibited increased sensitivity to H_2O_2, highlighting the possible similarity in deleterious effects imposed on cells by both gliotoxin and H_2O_2. The fact that cysteine and glutathione suppress the uptake of O_2 in the presence of glucose, favouring fermentation (Quastel and Wheatley, 1932) may be one of the reasons why many proteins involved in glucose fermentation were found to be upregulated in response to gliotoxin. Alternatively, it may be the requirement of the thioredoxin and glutaredoxin OS defence systems for NADPH produced during the process (Holmgren, 1989), that drives the system.

GSH is one of the most important proteins in preventing cellular oxidative damage (Penninckx, 2002). However, the absence of *GSH1*, encoding a protein that catalyses the first step in yeast GSH biosynthesis (Ohtake and Yabuuchi, 1991, Wu and Moye-Rowley, 1994) has afforded elevated cellular resistance to gliotoxin. As discussed previously, this may be due to rapid efflux of gliotoxin from the cells in the absence of GSH. The Δ*cys3* mutant, producing much lower levels of GSH than wild-type may synthesise enough GSH to allow retention of gliotoxin within the cell, yet not

enough to confer efficient protection to cells. This proposed model is illustrated in figure 5.1.

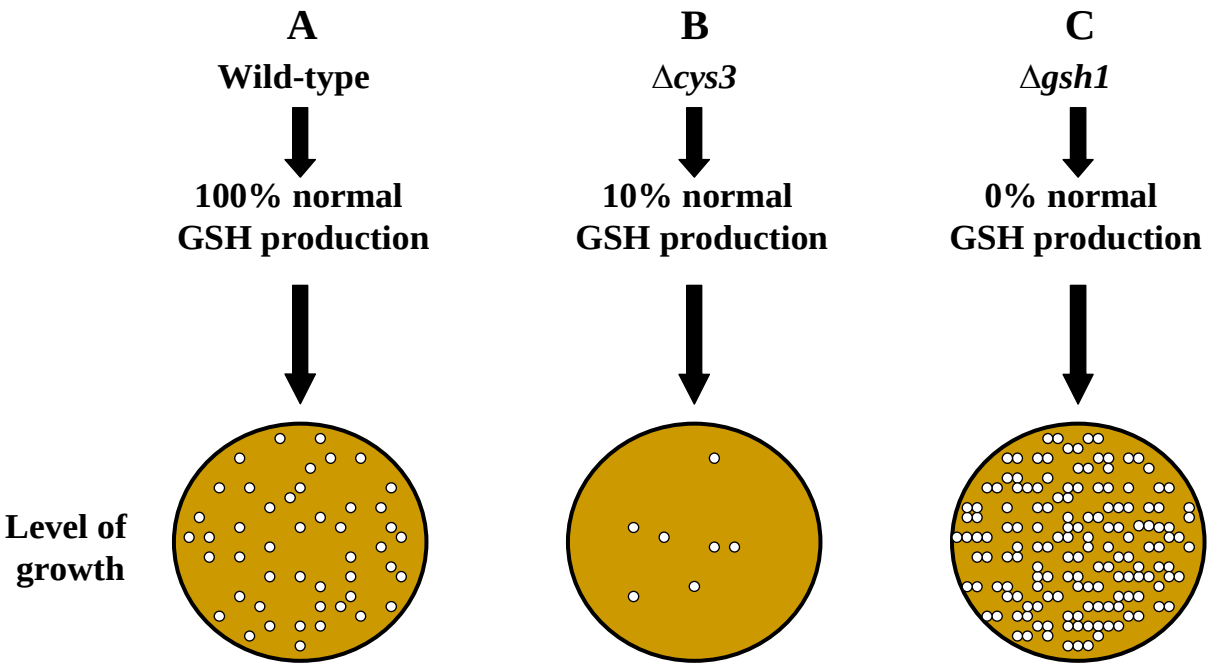

Figure 5.1 Proposed model demonstrating how changes in GSH levels affect yeast growth in the presence of gliotoxin. A) When normal levels of GSH are produced, gliotoxin enters the cell and is reduced by GSH, becoming cell membrane impermeable and thus causing damage. However, the high levels of GSH assist in protecting the cells against the deleterious toxin effects. B) When the transsulfuration pathway is disrupted, less GSH is produced, yet there is enough to retain gliotoxin intracellularly, facilitating damage. The decrease in GSH results in less cellular protection against gliotoxin. C) In the absence of Δ*gsh1*, no GSH is produced. Therefore, gliotoxin cannot be retained in the cell and no deleterious effects can be elicited.

Taking all results into account, the yeast response elicited by gliotoxin in this study is largely characteristic of cellular OS and the majority of mutant analyses have supported this finding. Thus, we come to the conclusion that gliotoxin exposure is likely to impose OS on *S. cerevisiae*. Importantly, the damaging effects caused by the toxin which result in yeast growth inhibition can be arrested by the constitutive expression of the *A. fumigatus GliT* gene (figure 5.2).

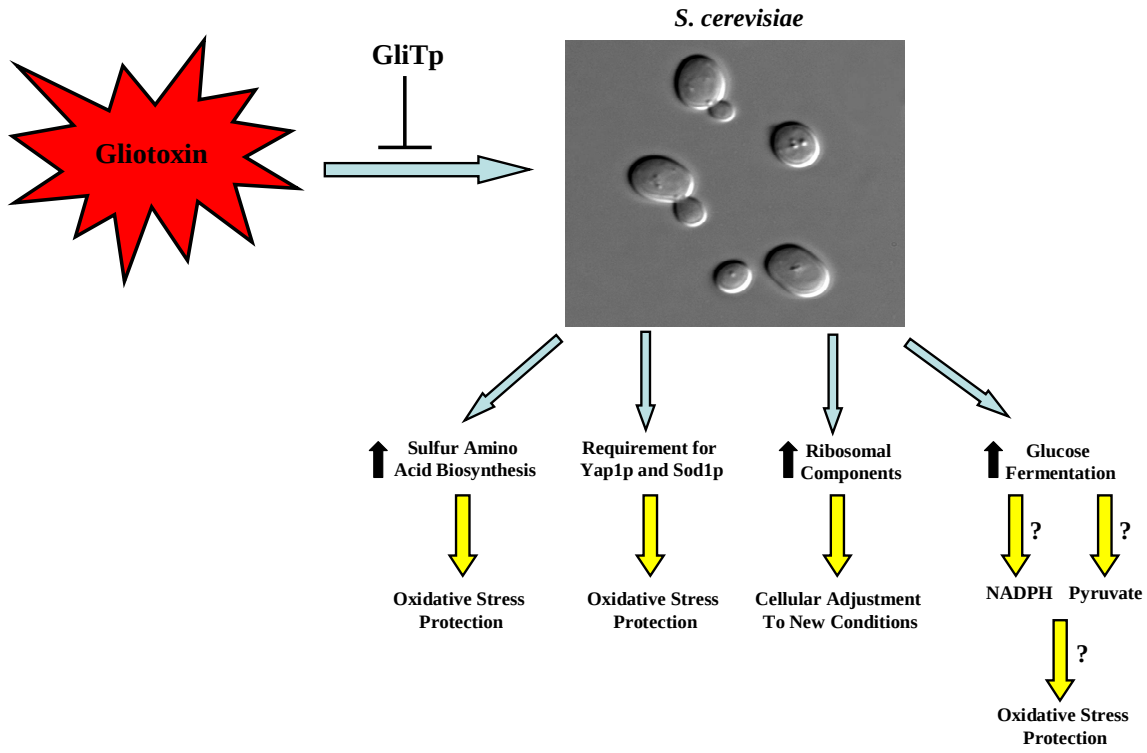

Figure 5.2 Principal effects of gliotoxin on *S. cerevisiae*.

To further validate the conclusion that gliotoxin induces conditions of OS in yeast cultures, additional advanced genetics must be applied. To extensively elucidate the proteins required by *S. cerevisiae* to withstand gliotoxin exposure it would be necessary to create double mutants deficient in more than one OS defence system. It has been demonstrated in this study that Δ*sod1* displays increased sensitivity to gliotoxin, emphasising the importance of superoxide dismutase in protection against the toxin. Sod1p is involved in the dismutation of the superoxide anion O_2^- to the less damaging H_2O_2 and O_2 (McCord and Fridovich, 1968, McCord and Fridovich, 1969a). Yeast deleted for the *CTT1* gene in this study did not appear to display increased sensitivity to gliotoxin. As the catalase T protein encoded by this gene catalyses the decomposition of H_2O_2 to O_2 and H_2O (Loew, 1900, Hartig and Ruis, 1986), which may be viewed as the next step of detoxification after SOD activity, it would be of interest to assess the

growth of Δ*sod1*Δ*ctt1* in the presence of gliotoxin, compared to wild-type and the single mutants.

A number of mutants deleted for genes involved in the sulfur amino acid biosynthesis pathway have exhibited a wild-type growth rate in the presence of gliotoxin. However, Δ*cys3* displayed increased sensitivity.

As the sulfur amino acid biosynthesis and glucose fermentation pathways are both highly stimulated by gliotoxin exposure, disruption of both pathways followed by mutant analysis would be interesting. This would determine if stimulation of the glucose fermentation pathway is a direct consequence of gliotoxin exposure or if it is a result of increased sulfur amino acid biosynthesis.

To further advance our understanding of the way in which *S. cerevisiae* responds to gliotoxin, it might be of interest to investigate gliotoxin-induced apoptosis. It has been reported that gliotoxin induces apoptosis in immune cells, while the garlic-derivative allicin achieves a similar result in yeast cells (Waring *et al.*, 1988, Zhou *et al.*, 2000, Stanzani *et al.*, 2005, Gruhlke *et al.*, 2010). It is known that ROS act as apoptosis-regulators in yeast (Madeo *et al.*, 1999), thus much of the data illustrating the yeast response to gliotoxin may be indicative of Programmed Cell Death due to OS. A comparison of the yeast cellular response to gliotoxin and allicin could potentially yield some interesting results and provide insight into gliotoxin-induced apoptosis in yeast.

To test the hypothesis depicted in figure 5.1, it would be of interest to measure the levels of intracellular GSH. Subsequent to this, the location of oxidised gliotoxin in these strains could be monitored and compared, perhaps using [^{14}C]-labelled gliotoxin. This could provide evidence for the requirement for GSH in facilitating gliotoxin-induced cellular OS.

Part 2 Investigation into the mode of action of the prion-curing drug Tacrine

One of the main aims of this study was to gain further insight into the mode of action of TA. Along with this drug, 6AP and GA have been shown to exhibit prion-curing activity in yeast (Bach *et al.*, 2006, Tribouillard-Tanvier *et al.*, 2008a, Tribouillard-Tanvier *et al.*, 2008b). Due to the fact that 6AP and GA have been studied in more detail than TA, these drugs were utilised to compare the effects of TA with.

The work discussed here provides support for previous findings identifying TA, 6AP and GA as yeast prion-curing agents. Although a certain level of background curing by GdnHCl is required for any of these drugs to cure wild-type [PSI^+] in yeast, it has been demonstrated in this study that in a suitable background strain, the effects of TA, 6AP and GA alone can be seen.

Unlike 6AP and GA, TA is known to be inactive against mammalian prions (Tribouillard-Tanvier *et al.*, 2008a), highlighting the fact that its mode of action differs to that of 6AP and GA and the results obtained in this study comply. It appears that all three drugs cure [PSI^+] through chaperone activity inhibition. While it has been reported that 6AP and GA inhibit ribosomal-mediated protein folding (Tribouillard-Tanvier *et al.*, 2008b), the work presented here suggests that TA may also function through targeting chaperone activity, specifically that of Hsp104p. GdnHCl is known to prevent [PSI^+] propagation through inhibition of Hsp104p activity (Chernoff *et al.*, 1995, Ferreira *et al.*, 2001). Thermotolerance assays have illustrated that a combination of GdnHCl and TA, at concentrations that are alone ineffective at inhibiting Hsp104p activity, clearly have the capacity to inhibit the chaperone. This implies that TA may also hinder Hsp104p activity, in a similar manner to GdnHCl. Interestingly, these results were not observed upon performing the same assay using 6AP and GA, suggesting that the ability to enhance the effects of GdnHCl is unique to TA.

The difference in modes of action of 6AP and GA compared to that of TA is supported by results from curing curve analysis. The curing curves indicate that all drugs prevent prion propagation, and similarly to GdnHCl, facilitate the dilution of the prion out of cells over time. However, the curing patterns of 6AP and GA are different to that of TA. TA effects only appear after 7 generations, while 6AP and GA seem to have a direct effect after 5 generations. This implies that although 6AP and GA may have different targets to TA, they are more potent agents. No further results dispute that 6AP is more potent that TA, however disc assays suggest that GA is the least potent compound as the smallest zone of curing was observed for this drug.

Despite the fact that the results discussed here and published by other groups suggest that 6AP and GA, and TA target ribosomal and Hsp104p chaperone function respectively, disc assays propose that any or all of these drugs may also target Hsp70p or its ATPase binding cycle. This is apparent as disruption (through gene deletion) of the ATPase binding cycle magnifies the curing capacities of all 3 drugs. The fact that the expression of many Hsp70p cochaperone genes is downregulated upon TA exposure adds weight to this hypothesis. Perhaps the presence of TA disrupts the regulation of the Hsp70p ATPase binding cycle. If it is the case that TA, 6AP, or GA cure [*PSI*$^{+}$] through targeting Hsp104p or Hsp70p, they do not mediate their effects through altering the expression levels of these proteins. Western blot analysis has demonstrated that the expression levels of these proteins remain stable under drug exposure.

Results obtained from investigating the *S. cerevisiae* response to 20 µM TA combined with 200 µM GdnHCl suggests that a combination of the two imposes cellular stress upon yeast cells. After 1 hr. exposure to TA and GdnHCl combined, the cells mount a stress response, which decreases after 3 hr. exposure and furthermore under treatment for 14 generations. This implies that these concentrations of TA and GdnHCl induce cellular stress, to which cells adapt over time. Support is provided by

the fact 2-dimensional gel electrophoresis illustrates that the glucose fermentation pathway appears to be stimulated in the presence of TA and GdnHCl combined. As discussed in chapter 3, stimulation of glucose fermentation may be linked to conditions of OS.

Prion-curing drugs such as 6AP and GA function through targeting ribosomal activity (Tribouillard-Tanvier *et al.*, 2008b). Ribosomal instability caused by the deletion of *YAR1* or *LTV1* does not cure [PSI^+] but destabilises it, leading to the appearance of spontaneous [psi^-] colonies (M. Blondel, personal communication). The results under discussion here show that Δ*ltv1* [PSI^+] is less sensitive to curing by all three drugs, supporting the previous findings that exposure of this strain to 6AP and GA stabilises the weakened prion (M. Blondel, personal communication). In this study, it was demonstrated that the absence of *LTV1* and *YAR1* (alone and in combination with *HSP104*) severely alters chaperone activity and cellular recovery and survival post heatshock. It appears that Hsp104p acts synergistically with both Ltv1p and Yar1p to facilitate induced thermotolerance, and that Yar1p plays a more important role than Ltv1p in allowing cellular survival following heatshock. Interestingly, the recovery of luciferase activity occurs more rapidly when cells are deleted for *YAR1* or *LTV1*. However, when these genes are deleted in the Δ*hsp104* background the luciferase recovery rate is lower than even that for Δ*hsp104*. Despite the apparent confliction of results from thermotolerance and luciferase assays, the results cannot be compared. Thermotolerance assays involve the assessment of the whole cellular response, leading to cell survival. Thus, it must be considered that a range of proteins contribute to the observed result. Conversely, luciferase assays examine the refolding activity of one protein, thus, the two assays do not equate.

It is reasonable to believe that TA may target Hsp104p and mediate its effects through regulation of Hsp104p activity. The fact that in a suitable background strain,

TA has been shown to cure [*PSI*$^{+}$] in the absence of GdnHCl suggests that this drug does not function solely through enhancing the uptake of GdnHCl. Ideally, the [^{14}C]-labelled GdnHCl assay should be attempted again to confirm this, perhaps using fresh materials. If the assay procedure is perfected and fully functional, TA could be utilised and its ability to enhance the uptake of GdnHCl could be tested.

It would be interesting to investigate whether or not TA interacts with Hsp104p. To accomplish this, and also to assess the molecular basis of TA-mediated effects through protein interaction, a relatively new technique could be applied. West *et al.* (2010) described a method involving protein chemical modification and mass spectrometry, which they employed to identify the complete set of targets of the immunosuppressant cyclosporin A. This technique could potentially be utilised to identify the yeast targets of TA and could provide great insight into the drug's mode of action. Following this, mutant analyses could be performed, to assess the ability of TA to cure [*PSI*$^{+}$] cells in the absence of possible TA targets. This would potentially give a similar result to that which would have been achieved had EMS mutagenesis been successful.

Regarding Δ*ltv1* and Δ*yar1* mutant studies, future work should involve performing Western Blot analysis to assess the expression levels of Hsp70p and Hsp104p in these mutant strains under TA, 6AP and GA exposure. Additionally, the viability of the double mutant Δ*ltv1*Δ*yar1* requires consideration. If this strain is shown to be viable, it should be employed in luciferase and thermotolerance assay performance.

References

ABBAS-TERKI, T., BRIAND, P. A., DONZÉ, O. & PICARD, D. 2002. The Hsp90 co-chaperones Cdc37 and Sti1 interact physically and genetically. *Biol Chem,* 383**,** 1335-42.

ALDHOUS, P. 1990. BSE: spongiform encephalopathy found in cat. *Nature,* 345**,** 194.

ALFAFARA, C., KANDA, A., SHIOI, T., SHIMIZU, H., SHIOYA, S. & SUGA, K. 1992. Effect of amino acids on glutathione production by *Saccharomyces cerevisiae*. *Appl Microbiol Biotechnol,* 36**,** 538-540.

ALJOFAN, M., SGANGA, M. L., LO, M. K., ROOTES, C. L., POROTTO, M., MEYER, A. G., SAUBERN, S., MOSCONA, A. & MUNGALL, B. A. 2009. Antiviral activity of gliotoxin, gentian violet and brilliant green against Nipah and Hendra virus in vitro. *Virol J,* 6**,** 187.

ALLEN, K. D., WEGRZYN, R. D., CHERNOVA, T. A., MÜLLER, S., NEWNAM, G. P., WINSLETT, P. A., WITTICH, K. B., WILKINSON, K. D. & CHERNOFF, Y. O. 2005. Hsp70 chaperones as modulators of prion life cycle: novel effects of Ssa and Ssb on the Saccharomyces cerevisiae prion [PSI+]. *Genetics,* 169**,** 1227-42.

ANDERSON, M. E. 1998. Glutathione: an overview of biosynthesis and modulation. *Chem Biol Interact,* 111-112**,** 1-14.

ANKRI, S. & MIRELMAN, D. 1999. Antimicrobial properties of allicin from garlic. *Microbes Infect,* 1**,** 125-9.

AREVALO, S. G. & WARNER, J. R. 1990. Ribosomal protein L4 of Saccharomyces cerevisiae: the gene and its protein. *Nucleic Acids Res,* 18**,** 1447-9.

ARNÉR, E. S. & HOLMGREN, A. 2000. Physiological functions of thioredoxin and thioredoxin reductase. *Eur J Biochem,* 267**,** 6102-9.

ARRICK, B. A., NATHAN, C. F., GRIFFITH, O. W. & COHN, Z. A. 1982. Glutathione depletion sensitizes tumor cells to oxidative cytolysis. *J Biol Chem,* 257**,** 1231-7.

ARÉVALO-RODRÍGUEZ, M., PAN, X., BOEKE, J. D. & HEITMAN, J. 2004. FKBP12 controls aspartate pathway flux in Saccharomyces cerevisiae to prevent toxic intermediate accumulation. *Eukaryot Cell,* 3**,** 1287-96.

AVERY, A. M. & AVERY, S. V. 2001. Saccharomyces cerevisiae expresses three phospholipid hydroperoxide glutathione peroxidases. *J Biol Chem,* 276**,** 33730-5.

AXELSSON, V., PIKKARAINEN, K. & FORSBY, A. 2006. Glutathione intensifies gliotoxin-induced cytotoxicity in human neuroblastoma SH-SY5Y cells. *Cell Biol Toxicol,* 22**,** 127-36.

BACH, S., TALAREK, N., ANDRIEU, T., VIERFOND, J. M., METTEY, Y., GALONS, H., DORMONT, D., MEIJER, L., CULLIN, C. & BLONDEL, M. 2003. Isolation of drugs active against mammalian prions using a yeast-based screening assay. *Nat Biotechnol,* 21**,** 1075-81.

BACH, S., TRIBOUILLARD, D., TALAREK, N., DESBAN, N., GUG, F., GALONS, H. & BLONDEL, M. 2006. A yeast-based assay to isolate drugs active against mammalian prions. *Methods,* 39**,** 72-7.

BALIBAR, C. J. & WALSH, C. T. 2006. GliP, a multimodular nonribosomal peptide synthetase in Aspergillus fumigatus, makes the diketopiperazine scaffold of gliotoxin. *Biochemistry,* 45**,** 15029-38.

BARBOSA-TESSMANN, I. P., CHEN, C., ZHONG, C., SCHUSTER, S. M., NICK, H. S. & KILBERG, M. S. 1999. Activation of the unfolded protein response pathway induces human asparagine synthetase gene expression. *J Biol Chem,* 274**,** 31139-44.

BARDANA, E. J., SOBTI, K. L., CIANCIULLI, F. D. & NOONAN, M. J. 1975. Aspergillus antibody in patients with cystic fibrosis. *Am J Dis Child,* 129**,** 1164-7.

BARONI, M., LIVIAN, S., MARTEGANI, E. & ALBERGHINA, L. 1986. Molecular cloning and regulation of the expression of the MET2 gene of Saccharomyces cerevisiae. *Gene,* 46**,** 71-8.

BATEMAN, E. D. 1994. A new look at the natural history of Aspergillus hypersensitivity in asthmatics. *Respir Med,* 88**,** 325-7.

BAUM, S., BITTINS, M., FREY, S. & SEEDORF, M. 2004. Asc1p, a WD40-domain containing adaptor protein, is required for the interaction of the RNA-binding protein Scp160p with polysomes. *Biochem J,* 380**,** 823-30.

BAUMANN, F., MILISAV, I., NEUPERT, W. & HERRMANN, J. M. 2000. Ecm10, a novel hsp70 homolog in the mitochondrial matrix of the yeast Saccharomyces cerevisiae. *FEBS Lett,* 487**,** 307-12.

BEAUDET, A. L. & CASKEY, C. T. 1971. Mammalian peptide chain termination. II. Codon specificity and GTPase activity of release factor. *Proc Natl Acad Sci U S A,* 68**,** 619-24.

BEAUVAIS, A. & MÜLLER, F. M. 2009. Biofilm formation in *Aspergillus fumigatus*. *In:* LATGE, J. P. & STEINBACH, W. J. (eds.) *Aspergillus fumigatus and Aspergillosis.* Washington, DC: American Society for Microbiology Press.

BEAVER, J. P. & WARING, P. 1994. Lack of correlation between early intracellular calcium ion rises and the onset of apoptosis in thymocytes. *Immunol Cell Biol,* 72**,** 489-99.

BELAZZI, T., WAGNER, A., WIESER, R., SCHANZ, M., ADAM, G., HARTIG, A. & RUIS, H. 1991. Negative regulation of transcription of the Saccharomyces cerevisiae catalase T (CTT1) gene by cAMP is mediated by a positive control element. *EMBO J,* 10**,** 585-92.

BENNETT, J. W. & KLICH, M. 2003. Mycotoxins. *Clin Microbiol Rev,* 16**,** 497-516.

BENNETZEN, J. L. & HALL, B. D. 1982. The primary structure of the Saccharomyces cerevisiae gene for alcohol dehydrogenase. *J Biol Chem,* 257**,** 3018-25.

BERGLUND, O., KARLSTRÖM, O. & REICHARD, P. 1969. A new ribonucleotide reductase system after infection with phage T4. *Proc Natl Acad Sci U S A,* 62**,** 829-35.

BERLANGA, J. J., RIVERO, D., MARTÍN, R., HERRERO, S., MORENO, S. & DE HARO, C. 2010. Role of mitogen-activated protein kinase Sty1 in regulation of eukaryotic initiation factor 2alpha kinases in response to environmental stress in Schizosaccharomyces pombe. *Eukaryot Cell,* 9**,** 194-207.

BERMINGHAM-MCDONOGH, O., GRALLA, E. B. & VALENTINE, J. S. 1988. The copper, zinc-superoxide dismutase gene of Saccharomyces cerevisiae: cloning, sequencing, and biological activity. *Proc Natl Acad Sci U S A,* 85**,** 4789-93.

BERNARDO, P. H., BRASCH, N., CHAI, C. L. & WARING, P. 2003. A novel redox mechanism for the glutathione-dependent reversible uptake of a fungal toxin in cells. *J Biol Chem,* 278**,** 46549-55.

BERNARDO, P. H., CHAI, C. L., DEEBLE, G. J., LIU, X. M. & WARING, P. 2001. Evidence for gliotoxin-glutathione conjugate adducts. *Bioorg Med Chem Lett,* 11**,** 483-5.

BERNDT, C., LILLIG, C. H., WOLLENBERG, M., BILL, E., MANSILLA, M. C., DE MENDOZA, D., SEIDLER, A. & SCHWENN, J. D. 2004. Characterization and reconstitution of a 4Fe-4S adenylyl sulfate/phosphoadenylyl sulfate reductase from Bacillus subtilis. *J Biol Chem,* 279**,** 7850-5.

BERTLING, A., NIEMANN, S., UEKÖTTER, A., FEGELER, W., LASS-FLÖRL, C., VON EIFF, C. & KEHREL, B. E. 2010. Candida albicans and its metabolite

gliotoxin inhibit platelet function via interaction with thiols. *Thromb Haemost,* 104**,** 270-8.

BISSINGER, P. H., WIESER, R., HAMILTON, B. & RUIS, H. 1989. Control of Saccharomyces cerevisiae catalase T gene (CTT1) expression by nutrient supply via the RAS-cyclic AMP pathway. *Mol Cell Biol,* 9**,** 1309-15.

BLAISEAU, P. L., ISNARD, A. D., SURDIN-KERJAN, Y. & THOMAS, D. 1997. Met31p and Met32p, two related zinc finger proteins, are involved in transcriptional regulation of yeast sulfur amino acid metabolism. *Mol Cell Biol,* 17**,** 3640-8.

BOK, J. W., BALAJEE, S. A., MARR, K. A., ANDES, D., NIELSEN, K. F., FRISVAD, J. C. & KELLER, N. P. 2005. LaeA, a regulator of morphogenetic fungal virulence factors. *Eukaryot Cell,* 4**,** 1574-82.

BOK, J. W., CHUNG, D., BALAJEE, S. A., MARR, K. A., ANDES, D., NIELSEN, K. F., FRISVAD, J. C., KIRBY, K. A. & KELLER, N. P. 2006. GliZ, a transcriptional regulator of gliotoxin biosynthesis, contributes to Aspergillus fumigatus virulence. *Infect Immun,* 74**,** 6761-8.

BOK, J. W. & KELLER, N. P. 2004. LaeA, a regulator of secondary metabolism in Aspergillus spp. *Eukaryot Cell,* 3**,** 527-35.

BOLTON, D. C., MEYER, R. K. & PRUSINER, S. B. 1985. Scrapie PrP 27-30 is a sialoglycoprotein. *J Virol,* 53**,** 596-606.

BONGERS, R. S., HOEFNAGEL, M. H. & KLEEREBEZEM, M. 2005. High-level acetaldehyde production in Lactococcus lactis by metabolic engineering. *Appl Environ Microbiol,* 71**,** 1109-13.

BORCHELT, D. R., SCOTT, M., TARABOULOS, A., STAHL, N. & PRUSINER, S. B. 1990. Scrapie and cellular prion proteins differ in their kinetics of synthesis and topology in cultured cells. *J Cell Biol,* 110**,** 743-52.

BORKOVICH, K. A., FARRELLY, F. W., FINKELSTEIN, D. B., TAULIEN, J. & LINDQUIST, S. 1989. hsp82 is an essential protein that is required in higher concentrations for growth of cells at higher temperatures. *Mol Cell Biol,* 9**,** 3919-30.

BOTSTEIN, D., CHERVITZ, S. A. & CHERRY, J. M. 1997. Yeast as a model organism. *Science,* 277**,** 1259-60.

BOWDISH, K. S. & MITCHELL, A. P. 1993. Bipartite structure of an early meiotic upstream activation sequence from Saccharomyces cerevisiae. *Mol Cell Biol,* 13**,** 2172-81.

BOYER, J., MICHAUX, G., FAIRHEAD, C., GAILLON, L. & DUJON, B. 1996. Sequence and analysis of a 26.9 kb fragment from chromosome XV of the yeast Saccharomyces cerevisiae. *Yeast,* 12**,** 1575-86.

BROWN, D. R., CLIVE, C. & HASWELL, S. J. 2001. Antioxidant activity related to copper binding of native prion protein. *J Neurochem,* 76**,** 69-76.

BROWN, D. R., WONG, B. S., HAFIZ, F., CLIVE, C., HASWELL, S. J. & JONES, I. M. 1999. Normal prion protein has an activity like that of superoxide dismutase. *Biochem J,* 344 Pt 1**,** 1-5.

BROWNING, C. H. & CRAWFORD, A. B. 1951. The Acridines. *BMJ,* 2**,** 1386.

BRUNMARK, A. & CADENAS, E. 1989. Redox and addition chemistry of quinoid compounds and its biological implications. *Free Radic Biol Med,* 7**,** 435-77.

BRUNS, S., SEIDLER, M., ALBRECHT, D., SALVENMOSER, S., REMME, N., HERTWECK, C., BRAKHAGE, A. A., KNIEMEYER, O. & MÜLLER, F. M. 2010. Functional genomic profiling of Aspergillus fumigatus biofilm reveals enhanced production of the mycotoxin gliotoxin. *Proteomics,* 10**,** 3097-107.

BRZYWCZY, J. & PASZEWSKI, A. 1993. Role of O-acetylhomoserine sulfhydrylase in sulfur amino acid synthesis in various yeasts. *Yeast,* 9**,** 1335-42.

BUKAU, B. & HORWICH, A. L. 1998. The Hsp70 and Hsp60 chaperone machines. *Cell,* 92**,** 351-66.

BYRNE, E. J. & ARIE, T. 1994. Tetrahydroaminoacridine and Alzheimer's disease. *BMJ,* 308**,** 868-9.

BYRNE, L., COX, B., COLE, D., RIDOUT, M., MORGAN, B. & TUITE, M. 2007. Cell division is essential for elimination of the yeast [PSI+] prion by guanidine hydrochloride. *Proc Natl Acad Sci U S A,* 104**,** 11688-93.

CAMPBELL, M. G. & KARBSTEIN, K. 2011. Protein-protein interactions within late pre-40S ribosomes. *PLoS One,* 6**,** e16194.

CAPLAN, A. J., CYR, D. M. & DOUGLAS, M. G. 1992. YDJ1p facilitates polypeptide translocation across different intracellular membranes by a conserved mechanism. *Cell,* 71**,** 1143-55.

CARBERRY, S. 2008. *Proteomic investigation of gliotoxin metabolism in Aspergillus fumigatus.* . PhD, National University of Ireland, Maynooth.

CARBERRY, S., NEVILLE, C. M., KAVANAGH, K. A. & DOYLE, S. 2006. Analysis of major intracellular proteins of Aspergillus fumigatus by MALDI mass spectrometry: identification and characterisation of an elongation factor 1B protein with glutathione transferase activity. *Biochem Biophys Res Commun,* 341**,** 1096-104.

CARRICO, R. J. & DEUTSCH, H. F. 1970. The presence of zinc in human cytocuprein and some properties of the apoprotein. *J Biol Chem,* 245**,** 723-7.

CASHIKAR, A. G., DUENNWALD, M. & LINDQUIST, S. L. 2005. A chaperone pathway in protein disaggregation. Hsp26 alters the nature of protein aggregates to facilitate reactivation by Hsp104. *J Biol Chem,* 280**,** 23869-75.

CAÑIZARES, P., GRACIA, I., GÓMEZ, L. A., GARCÍA, A., MARTÍN DE ARGILA, C., BOIXEDA, D. & DE RAFAEL, L. 2004. Thermal degradation of allicin in garlic extracts and its implication on the inhibition of the in-vitro growth of Helicobacter pylori. *Biotechnol Prog,* 20**,** 32-7.

CHAE, H. Z., CHUNG, S. J. & RHEE, S. G. 1994. Thioredoxin-dependent peroxide reductase from yeast. *J Biol Chem,* 269**,** 27670-8.

CHAMILOS, G., LEWIS, R., LAMARIS, G., ALBERT, N. & KONTOYIANNIS, D. 2008. Genomewide screening for genes associated with gliotoxin resistance and sensitivity in Saccharomyces cerevisiae. *Antimicrob Agents Chemother,* 52**,** 1325-9.

CHANG, E. C., CRAWFORD, B. F., HONG, Z., BILINSKI, T. & KOSMAN, D. J. 1991. Genetic and biochemical characterization of Cu,Zn superoxide dismutase mutants in Saccharomyces cerevisiae. *J Biol Chem,* 266**,** 4417-24.

CHATELLIER, G. & LACOMBLEZ, L. 1990. Tacrine (tetrahydroaminoacridine; THA) and lecithin in senile dementia of the Alzheimer type: a multicentre trial. Groupe Français d'Etude de la Tetrahydroaminoacridine. *BMJ,* 300**,** 495-9.

CHEFFER, A. & ULRICH, H. 2011. Inhibition mechanism of rat α_3 β_4 nicotinic acetylcholine receptor by the Alzheimer therapeutic tacrine. *Biochemistry,* 50**,** 1763-70.

CHELIKANI, P., FITA, I. & LOEWEN, P. C. 2004. Diversity of structures and properties among catalases. *Cell Mol Life Sci,* 61**,** 192-208.

CHEREST, H., EICHLER, F. & ROBICHON-SZULMAJSTER, H. 1969. Genetic and regulatory aspects of methionine biosynthesis in Saccharomyces cerevisiae. *J Bacteriol,* 97**,** 328-36.

CHEREST, H., KERJAN, P. & SURDIN-KERJAN, Y. 1987. The Saccharomyces cerevisiae MET3 gene: nucleotide sequence and relationship of the 5' non-coding region to that of MET25. *Mol Gen Genet,* 210**,** 307-13.

CHEREST, H., NGUYEN, N. T. & SURDIN-KERJAN, Y. 1985. Transcriptional regulation of the MET3 gene of Saccharomyces cerevisiae. *Gene,* 34**,** 269-81.

CHEREST, H. & SURDIN-KERJAN, Y. 1978. S-adenosyl methionine requiring mutants in Saccharomyces cerevisiae: evidences for the existence of two methionine adenosyl transferases. *Mol Gen Genet,* 163**,** 153-67.

CHEREST, H. & SURDIN-KERJAN, Y. 1992. Genetic analysis of a new mutation conferring cysteine auxotrophy in Saccharomyces cerevisiae: updating of the sulfur metabolism pathway. *Genetics,* 130**,** 51-8.

CHEREST, H., THOMAS, D. & SURDIN-KERJAN, Y. 1993. Cysteine biosynthesis in Saccharomyces cerevisiae occurs through the transsulfuration pathway which has been built up by enzyme recruitment. *J Bacteriol,* 175**,** 5366-74.

CHEREST, H., THOMAS, D. & SURDIN-KERJAN, Y. 2000. Polyglutamylation of folate coenzymes is necessary for methionine biosynthesis and maintenance of intact mitochondrial genome in Saccharomyces cerevisiae. *J Biol Chem,* 275**,** 14056-63.

CHERNOFF, Y. O., LINDQUIST, S. L., ONO, B., INGE-VECHTOMOV, S. G. & LIEBMAN, S. W. 1995. Role of the chaperone protein Hsp104 in propagation of the yeast prion-like factor [psi+]. *Science,* 268**,** 880-4.

CHERNOFF, Y. O., NEWNAM, G. P., KUMAR, J., ALLEN, K. & ZINK, A. D. 1999. Evidence for a protein mutator in yeast: role of the Hsp70-related chaperone ssb in formation, stability, and toxicity of the [PSI] prion. *Mol Cell Biol,* 19**,** 8103-12.

CHIANG, P. K. & CANTONI, G. L. 1977. Activation of methionine for transmethylation. Purification of the S-adenosylmethionine synthetase of bakers' yeast and its separation into two forms. *J Biol Chem,* 252**,** 4506-13.

CHOI, H. S., SHIM, J. S., KIM, J. A., KANG, S. W. & KWON, H. J. 2007. Discovery of gliotoxin as a new small molecule targeting thioredoxin redox system. *Biochem Biophys Res Commun,* 359**,** 523-8.

CLARK, R. A. 1990. The human neutrophil respiratory burst oxidase. *J Infect Dis,* 161**,** 1140-7.

COHEN, G., FESSL, F., TRACZYK, A., RYTKA, J. & RUIS, H. 1985. Isolation of the catalase A gene of Saccharomyces cerevisiae by complementation of the cta1 mutation. *Mol Gen Genet,* 200**,** 74-9.

COHEN, G., RAPATZ, W. & RUIS, H. 1988. Sequence of the Saccharomyces cerevisiae CTA1 gene and amino acid sequence of catalase A derived from it. *Eur J Biochem,* 176**,** 159-63.

CONN, E. E. & VENNESLAND, B. 1951. Glutathione reductase of wheat germ. *J Biol Chem,* 192**,** 17-28.

COSTA, V., QUINTANILHA, A. & MORADAS-FERREIRA, P. 2007. Protein oxidation, repair mechanisms and proteolysis in Saccharomyces cerevisiae. *IUBMB Life,* 59**,** 293-8.

COUSTOU, V., DELEU, C., SAUPE, S. & BEGUERET, J. 1997. The protein product of the het-s heterokaryon incompatibility gene of the fungus Podospora anserina behaves as a prion analog. *Proc Natl Acad Sci U S A,* 94**,** 9773-8.

COX, B. 1965. [PSI], a cytoplasmic suppressor of super-suppression in yeast. *Heredity,* 20**,** 505-521.

COX, B. S. 1971. A recessive lethal super-suppressor mutation in yeast and other psi phenomena. *Heredity,* 26**,** 211-32.

COX, B. S., TUITE, M. F. & MCLAUGHLIN, C. S. 1988. The psi factor of yeast: a problem in inheritance. *Yeast,* 4**,** 159-78.

CRAIG, E. A., GAMBILL, B. D. & NELSON, R. J. 1993. Heat shock proteins: molecular chaperones of protein biogenesis. *Microbiol Rev,* 57**,** 402-14.

CRAIG, E. A. & JACOBSEN, K. 1984. Mutations of the heat inducible 70 kilodalton genes of yeast confer temperature sensitive growth. *Cell,* 38**,** 841-9.

CRAIG, E. A. & JACOBSEN, K. 1985. Mutations in cognate genes of Saccharomyces cerevisiae hsp70 result in reduced growth rates at low temperatures. *Mol Cell Biol,* 5**,** 3517-24.

CRAIG, E. A., KRAMER, J. & KOSIC-SMITHERS, J. 1987. SSC1, a member of the 70-kDa heat shock protein multigene family of Saccharomyces cerevisiae, is essential for growth. *Proc Natl Acad Sci U S A,* 84**,** 4156-60.

CRAIG, E. A., KRAMER, J., SHILLING, J., WERNER-WASHBURNE, M., HOLMES, S., KOSIC-SMITHERS, J. & NICOLET, C. M. 1989. SSC1, an essential member of the yeast HSP70 multigene family, encodes a mitochondrial protein. *Mol Cell Biol,* 9**,** 3000-8.

CRAMER, R. A., GAMCSIK, M. P., BROOKING, R. M., NAJVAR, L. K., KIRKPATRICK, W. R., PATTERSON, T. F., BALIBAR, C. J., GRAYBILL, J. R., PERFECT, J. R., ABRAHAM, S. N. & STEINBACH, W. J. 2006. Disruption of a nonribosomal peptide synthetase in Aspergillus fumigatus eliminates gliotoxin production. *Eukaryot Cell,* 5**,** 972-80.

CRAVEN, R. A., EGERTON, M. & STIRLING, C. J. 1996. A novel Hsp70 of the yeast ER lumen is required for the efficient translocation of a number of protein precursors. *EMBO J,* 15**,** 2640-50.

CSAIKL, U. & CSAIKL, F. 1986. Molecular cloning and characterization of the MET6 gene of Saccharomyces cerevisiae. *Gene,* 46**,** 207-14.

CUTLER, R. R. & WILSON, P. 2004. Antibacterial activity of a new, stable, aqueous extract of allicin against methicillin-resistant Staphylococcus aureus. *Br J Biomed Sci,* 61**,** 71-4.

CYR, D. M., LANGER, T. & DOUGLAS, M. G. 1994. DnaJ-like proteins: molecular chaperones and specific regulators of Hsp70. *Trends Biochem Sci,* 19**,** 176-81.

CYR, D. M., LU, X. & DOUGLAS, M. G. 1992. Regulation of Hsp70 function by a eukaryotic DnaJ homolog. *J Biol Chem,* 267**,** 20927-31.

D'ANDREA, R., SURDIN-KERJAN, Y., PURE, G. & CHEREST, H. 1987. Molecular genetics of met 17 and met 25 mutants of Saccharomyces cerevisiae: intragenic complementation between mutations of a single structural gene. *Mol Gen Genet,* 207**,** 165-70.

DAGENAIS, T. R. & KELLER, N. P. 2009. Pathogenesis of Aspergillus fumigatus in Invasive Aspergillosis. *Clin Microbiol Rev,* 22**,** 447-65.

DANG, V. D., VALENS, M., BOLOTIN-FUKUHARA, M. & DAIGNAN-FORNIER, B. 1996. Cloning of the ASN1 and ASN2 genes encoding asparagine synthetases in Saccharomyces cerevisiae: differential regulation by the CCAAT-box-binding factor. *Mol Microbiol,* 22**,** 681-92.

DAS, D., DAS, A., SAMANTA, D., GHOSH, J., DASGUPTA, S., BHATTACHARYA, A., BASU, A., SANYAL, S. & DAS GUPTA, C. 2008. Role of the ribosome in protein folding. *Biotechnol J,* 3**,** 999-1009.

DAVIS, C., CARBERRY, S., SCHRETTL, M., SINGH, I., STEPHENS, J. C., BARRY, S. M., KAVANAGH, K., CHALLIS, G. L., BROUGHAM, D. & DOYLE, S. 2011. The role of glutathione S-transferase GliG in gliotoxin biosynthesis in Aspergillus fumigatus. *Chem Biol,* 18**,** 542-52.

DAVIS, K. L. & POWCHIK, P. 1995. Tacrine. *Lancet,* 345**,** 625-30.

DAVIS, K. L., THAL, L. J., GAMZU, E. R., DAVIS, C. S., WOOLSON, R. F., GRACON, S. I., DRACHMAN, D. A., SCHNEIDER, L. S., WHITEHOUSE, P. J. & HOOVER, T. M. 1992. A double-blind, placebo-controlled multicenter study of tacrine for Alzheimer's disease. The Tacrine Collaborative Study Group. *N Engl J Med,* 327**,** 1253-9.

DE OLIVEIRA, I. M., ZANOTTO-FILHO, A., MOREIRA, J. C., BONATTO, D. & HENRIQUES, J. A. 2010. The role of two putative nitroreductases, Frm2p and Hbn1p, in the oxidative stress response in Saccharomyces cerevisiae. *Yeast,* 27**,** 89-102.

DENNING, D. W. 1996. Therapeutic outcome in invasive aspergillosis. *Clin Infect Dis,* 23**,** 608-15.

DENNING, D. W. 1998. Invasive aspergillosis. *Clin Infect Dis,* 26**,** 781-803; quiz 804-5.

DERKATCH, I. L., BRADLEY, M. E., ZHOU, P., CHERNOFF, Y. O. & LIEBMAN, S. W. 1997. Genetic and environmental factors affecting the de novo appearance of the [PSI+] prion in Saccharomyces cerevisiae. *Genetics,* 147**,** 507-19.

DERKATCH, I. L., CHERNOFF, Y. O., KUSHNIROV, V. V., INGE-VECHTOMOV, S. G. & LIEBMAN, S. W. 1996. Genesis and variability of [PSI] prion factors in Saccharomyces cerevisiae. *Genetics,* 144**,** 1375-86.

DESAGHER, S., GLOWINSKI, J. & PRÉMONT, J. 1997. Pyruvate protects neurons against hydrogen peroxide-induced toxicity. *J Neurosci,* 17**,** 9060-7.

DESOUZA, L., SHEN, Y. & BOGNAR, A. L. 2000. Disruption of cytoplasmic and mitochondrial folylpolyglutamate synthetase activity in Saccharomyces cerevisiae. *Arch Biochem Biophys,* 376**,** 299-312.

DETWILER, L. A. 1992. Scrapie. *Rev Sci Tech,* 11**,** 491-537.

DEVE, F. 1938. Une Nouvelle Forme Anatomoradiologicque de Mycose Pulmonaire Primitive. Le Megamycatom Intra Bronchiectasique. *Arch. Med. Chir. Appar. Repir.,* 13**,** 337.

DEWITTE-ORR, S. J. & BOLS, N. C. 2005. Gliotoxin-induced cytotoxicity in three salmonid cell lines: cell death by apoptosis and necrosis. *Comp Biochem Physiol C Toxicol Pharmacol,* 141**,** 157-67.

DICKINSON, D. A. & FORMAN, H. J. 2002. Glutathione in defense and signaling: lessons from a small thiol. *Ann N Y Acad Sci,* 973**,** 488-504.

DOLEZAL, V., LISÁ, V. & TUCEK, S. 1997. Effect of tacrine on intracellular calcium in cholinergic SN56 neuronal cells. *Brain Res,* 769**,** 219-24.

DOLINSKI, K. J., CARDENAS, M. E. & HEITMAN, J. 1998. CNS1 encodes an essential p60/Sti1 homolog in Saccharomyces cerevisiae that suppresses cyclophilin 40 mutations and interacts with Hsp90. *Mol Cell Biol,* 18**,** 7344-52.

DORMER, U. H., WESTWATER, J., MCLAREN, N. F., KENT, N. A., MELLOR, J. & JAMIESON, D. J. 2000. Cadmium-inducible expression of the yeast GSH1 gene requires a functional sulfur-amino acid regulatory network. *J Biol Chem,* 275**,** 32611-6.

DU, Z., PARK, K. W., YU, H., FAN, Q. & LI, L. 2008. Newly identified prion linked to the chromatin-remodeling factor Swi1 in Saccharomyces cerevisiae. *Nat Genet,* 40**,** 460-5.

DUJON, B. 1989. Group I introns as mobile genetic elements: facts and mechanistic speculations--a review. *Gene,* 82**,** 91-114.

DUTCHER, J. D. 1941. The chemical nature of gliotoxin: A microbicidal compound produced by the fungus *Gliocladium fimbriatum*.: *J. Bact.*

EAGLESTONE, S. S., RUDDOCK, L. W., COX, B. S. & TUITE, M. F. 2000. Guanidine hydrochloride blocks a critical step in the propagation of the prion-like determinant [PSI(+)] of Saccharomyces cerevisiae. *Proc Natl Acad Sci U S A,* 97**,** 240-4.

ECKERS, E., BIEN, M., STROOBANT, V., HERRMANN, J. M. & DEPONTE, M. 2009. Biochemical characterization of dithiol glutaredoxin 8 from Saccharomyces cerevisiae: the catalytic redox mechanism redux. *Biochemistry,* 48**,** 1410-23.

EICHNER, R. D., AL SALAMI, M., WOOD, P. R. & MÜLLBACHER, A. 1986. The effect of gliotoxin upon macrophage function. *Int J Immunopharmacol,* 8**,** 789-97.

EICHNER, R. D., WARING, P., GEUE, A. M., BRAITHWAITE, A. W. & MÜLLBACHER, A. 1988. Gliotoxin causes oxidative damage to plasmid and cellular DNA. *J Biol Chem,* 263**,** 3772-7.

ENJALBERT, B., SMITH, D. A., CORNELL, M. J., ALAM, I., NICHOLLS, S., BROWN, A. J. & QUINN, J. 2006. Role of the Hog1 stress-activated protein kinase in the global transcriptional response to stress in the fungal pathogen Candida albicans. *Mol Biol Cell,* 17**,** 1018-32.

ERCAL, N., GURER-ORHAN, H. & AYKIN-BURNS, N. 2001. Toxic metals and oxidative stress part I: mechanisms involved in metal-induced oxidative damage. *Curr Top Med Chem,* 1**,** 529-39.

ERJAVEC, N., LARSSON, L., GRANTHAM, J. & NYSTRÖM, T. 2007. Accelerated aging and failure to segregate damaged proteins in Sir2 mutants can be suppressed by overproducing the protein aggregation-remodeling factor Hsp104p. *Genes Dev,* 21**,** 2410-21.

ESCOBAR-HENRIQUES, M. & DAIGNAN-FORNIER, B. 2001. Transcriptional regulation of the yeast gmp synthesis pathway by its end products. *J Biol Chem,* 276**,** 1523-30.

FALCO, S. C., DUMAS, K. S. & LIVAK, K. J. 1985. Nucleotide sequence of the yeast ILV2 gene which encodes acetolactate synthase. *Nucleic Acids Res,* 13**,** 4011-27.

FARR, S. B., D'ARI, R. & TOUATI, D. 1986. Oxygen-dependent mutagenesis in Escherichia coli lacking superoxide dismutase. *Proc Natl Acad Sci U S A,* 83**,** 8268-72.

FERREIRA, P., NESS, F., EDWARDS, S., COX, B. & TUITE, M. 2001. The elimination of the yeast [PSI+] prion by guanidine hydrochloride is the result of Hsp104 inactivation. *Mol Microbiol,* 40**,** 1357-69.

FILIPIC, M. & HEI, T. K. 2004. Mutagenicity of cadmium in mammalian cells: implication of oxidative DNA damage. *Mutat Res,* 546**,** 81-91.

FINKELSTEIN, J. D. 1998. The metabolism of homocysteine: pathways and regulation. *Eur J Pediatr,* 157 Suppl 2**,** S40-4.

FITTEN, L. J., FLOOD, J. F., BAXTER, C. F., TACHIKI, K. H. & PERRYMAN, K. 1987. Long-term oral administration of memory-enhancing doses of tacrine in mice: a study of potential toxicity and side effects. *J Gerontol,* 42**,** 681-5.

FLAHERTY, K. M., DELUCA-FLAHERTY, C. & MCKAY, D. B. 1990. Three-dimensional structure of the ATPase fragment of a 70K heat-shock cognate protein. *Nature,* 346**,** 623-8.

FLINT, D. H., TUMINELLO, J. F. & EMPTAGE, M. H. 1993. The inactivation of Fe-S cluster containing hydro-lyases by superoxide. *J Biol Chem,* 268**,** 22369-76.

FORSYTH, D. R., SURMON, D. J., MORGAN, R. A. & WILCOCK, G. K. 1989. Clinical experience with and side-effects of tacrine hydrochloride in Alzheimer's disease: a pilot study. *Age Ageing,* 18**,** 223-9.

FRAGA, C. G. & OTEIZA, P. I. 2002. Iron toxicity and antioxidant nutrients. *Toxicology,* 180**,** 23-32.

FREEMAN, B. A. & CRAPO, J. D. 1982. Biology of disease: free radicals and tissue injury. *Lab Invest,* 47**,** 412-26.

FRIDOVICH, I. 1978. The biology of oxygen radicals. *Science,* 201**,** 875-80.

FROLOVA, L., LE GOFF, X., RASMUSSEN, H. H., CHEPEREGIN, S., DRUGEON, G., KRESS, M., ARMAN, I., HAENNI, A. L., CELIS, J. E. & PHILIPPE, M. 1994. A highly conserved eukaryotic protein family possessing properties of polypeptide chain release factor. *Nature,* 372**,** 701-3.

FÅHRAEUS, R. & BLONDEL, M. 2008. RNA-assisted protein folding. *Biotechnol J,* 3**,** 967-9.

GAJDUSEK, D. C., GIBBS, C. J. & ALPERS, M. 1966. Experimental transmission of a Kuru-like syndrome to chimpanzees. *Nature,* 209**,** 794-6.

GALIAZZO, F., SCHIESSER, A. & ROTILIO, G. 1987. Glutathione peroxidase in yeast. Presence of the enzyme and induction by oxidative conditions. *Biochem Biophys Res Commun,* 147**,** 1200-5.

GAN, Z. R., POLOKOFF, M. A., JACOBS, J. W. & SARDANA, M. K. 1990. Complete amino acid sequence of yeast thioltransferase (glutaredoxin). *Biochem Biophys Res Commun,* 168**,** 944-51.

GARDINER, D. M., COZIJNSEN, A. J., WILSON, L. M., PEDRAS, M. S. & HOWLETT, B. J. 2004. The sirodesmin biosynthetic gene cluster of the plant pathogenic fungus Leptosphaeria maculans. *Mol Microbiol,* 53**,** 1307-18.

GARDINER, D. M. & HOWLETT, B. J. 2005. Bioinformatic and expression analysis of the putative gliotoxin biosynthetic gene cluster of Aspergillus fumigatus. *FEMS Microbiol Lett,* 248**,** 241-8.

GARDINER, D. M., WARING, P. & HOWLETT, B. J. 2005. The epipolythiodioxopiperazine (ETP) class of fungal toxins: distribution, mode of action, functions and biosynthesis. *Microbiology,* 151**,** 1021-32.

GAUTSCHI, M., LILIE, H., FÜNFSCHILLING, U., MUN, A., ROSS, S., LITHGOW, T., RÜCKNAGEL, P. & ROSPERT, S. 2001. RAC, a stable ribosome-associated complex in yeast formed by the DnaK-DnaJ homologs Ssz1p and zuotin. *Proc Natl Acad Sci U S A,* 98**,** 3762-7.

GAUTSCHI, M., MUN, A., ROSS, S. & ROSPERT, S. 2002. A functional chaperone triad on the yeast ribosome. *Proc Natl Acad Sci U S A,* 99**,** 4209-14.

GAVÍN, R., BRAUN, N., NICOLAS, O., PARRA, B., UREÑA, J. M., MINGORANCE, A., SORIANO, E., TORRES, J. M., AGUZZI, A. & DEL RÍO, J. A. 2005. PrP(106-126) activates neuronal intracellular kinases and Egr1 synthesis through activation of NADPH-oxidase independently of PrPc. *FEBS Lett,* 579**,** 4099-106.

GERSTMANN, J., STRÄUSSLER, E. & SCHEINKER, I. 1936. Über eine eigenartige hereditär-familiäre Erkrankung des Zentralnervensystems. Zugleich ein Beitrag zur Frage des vorzeitigen lokalen Alterns. *Z. Neurol.,* 154**,** 736–762.

GIMBEL, D. A., NYGAARD, H. B., COFFEY, E. E., GUNTHER, E. C., LAURÉN, J., GIMBEL, Z. A. & STRITTMATTER, S. M. 2010. Memory impairment in transgenic Alzheimer mice requires cellular prion protein. *J Neurosci,* 30**,** 6367-74.

GLOVER, J. R., KOWAL, A. S., SCHIRMER, E. C., PATINO, M. M., LIU, J. J. & LINDQUIST, S. 1997. Self-seeded fibers formed by Sup35, the protein determinant of [PSI+], a heritable prion-like factor of S. cerevisiae. *Cell,* 89**,** 811-9.

GLOVER, J. R. & LINDQUIST, S. 1998. Hsp104, Hsp70, and Hsp40: a novel chaperone system that rescues previously aggregated proteins. *Cell,* 94**,** 73-82.

GLÄSER, H. U., THOMAS, D., GAXIOLA, R., MONTRICHARD, F., SURDIN-KERJAN, Y. & SERRANO, R. 1993. Salt tolerance and methionine biosynthesis in Saccharomyces cerevisiae involve a putative phosphatase gene. *EMBO J,* 12**,** 3105-10.

GODON, C., LAGNIEL, G., LEE, J., BUHLER, J. M., KIEFFER, S., PERROT, M., BOUCHERIE, H., TOLEDANO, M. B. & LABARRE, J. 1998. The H2O2 stimulon in Saccharomyces cerevisiae. *J Biol Chem,* 273**,** 22480-9.

GONG, Y., KAKIHARA, Y., KROGAN, N., GREENBLATT, J., EMILI, A., ZHANG, Z. & HOURY, W. A. 2009. An atlas of chaperone-protein interactions in

Saccharomyces cerevisiae: implications to protein folding pathways in the cell. *Mol Syst Biol,* 5**,** 275.

GONZALEZ PORQUÉ, P., BALDESTEN, A. & REICHARD, P. 1970. The involvement of the thioredoxin system in the reduction of methionine sulfoxide and sulfate. *J Biol Chem,* 245**,** 2371-4.

GONZÁLEZ, J. C., BANERJEE, R. V., HUANG, S., SUMNER, J. S. & MATTHEWS, R. G. 1992. Comparison of cobalamin-independent and cobalamin-dependent methionine synthases from Escherichia coli: two solutions to the same chemical problem. *Biochemistry,* 31**,** 6045-56.

GRALLA, E. B. & KOSMAN, D. J. 1992. Molecular genetics of superoxide dismutases in yeasts and related fungi. *Adv Genet,* 30**,** 251-319.

GRANT, C. M. 2001. Role of the glutathione/glutaredoxin and thioredoxin systems in yeast growth and response to stress conditions. *Mol Microbiol,* 39**,** 533-41.

GRANT, C. M., COLLINSON, L. P., ROE, J. H. & DAWES, I. W. 1996. Yeast glutathione reductase is required for protection against oxidative stress and is a target gene for yAP-1 transcriptional regulation. *Mol Microbiol,* 21**,** 171-9.

GRANT, C. M., MACIVER, F. H. & DAWES, I. W. 1997. Glutathione synthetase is dispensable for growth under both normal and oxidative stress conditions in the yeast Saccharomyces cerevisiae due to an accumulation of the dipeptide gamma-glutamylcysteine. *Mol Biol Cell,* 8**,** 1699-707.

GRANT, C. M., PERRONE, G. & DAWES, I. W. 1998. Glutathione and catalase provide overlapping defenses for protection against hydrogen peroxide in the yeast Saccharomyces cerevisiae. *Biochem Biophys Res Commun,* 253**,** 893-8.

GREGERSEN, N. 2006. Protein misfolding disorders: pathogenesis and intervention. *J Inherit Metab Dis,* 29**,** 456-70.

GRIFFITH, J. S. 1967. Self-replication and scrapie. *Nature,* 215**,** 1043-4.

GROSS, D. S., ADAMS, C. C., ENGLISH, K. E., COLLINS, K. W. & LEE, S. 1990. Promoter function and in situ protein/DNA interactions upstream of the yeast HSP90 heat shock genes. *Antonie Van Leeuwenhoek,* 58**,** 175-86.

GROSS, U., NIEGER, M. & BRÄSE, S. 2010. A Unified Strategy Targeting the Thiodiketopiperazine Mycotoxins Exserohilone, Gliotoxin, the Epicoccins, the Epicorazines, Rostratin A and Aranotin. *Chemistry*.

GRUHLKE, M. C., PORTZ, D., STITZ, M., ANWAR, A., SCHNEIDER, T., JACOB, C., SCHLAICH, N. L. & SLUSARENKO, A. J. 2010. Allicin disrupts the cell's electrochemical potential and induces apoptosis in yeast. *Free Radic Biol Med,* 49**,** 1916-24.

GÜNTHERBERG, H. & ROST, J. 1966. The true oxidized glutathione content of red blood cells obtained by new enzymic and paper chromatographic methods. *Anal Biochem,* 15**,** 205-10.

HAASS, C. & SELKOE, D. J. 1993. Cellular processing of beta-amyloid precursor protein and the genesis of amyloid beta-peptide. *Cell,* 75**,** 1039-42.

HAINZL, O., WEGELE, H., RICHTER, K. & BUCHNER, J. 2004. Cns1 is an activator of the Ssa1 ATPase activity. *J Biol Chem,* 279**,** 23267-73.

HALLIWELL, B. 1991. Reactive oxygen species in living systems: source, biochemistry, and role in human disease. *Am J Med,* 91**,** 14S-22S.

HALLIWELL, B. 1994. Free radicals, antioxidants, and human disease: curiosity, cause, or consequence? *Lancet,* 344**,** 721-4.

HALLSTROM, T. C., KATZMANN, D. J., TORRES, R. J., SHARP, W. J. & MOYE-ROWLEY, W. S. 1998. Regulation of transcription factor Pdr1p function by an Hsp70 protein in Saccharomyces cerevisiae. *Mol Cell Biol,* 18**,** 1147-55.

HANSEN, J., CHEREST, H. & KIELLAND-BRANDT, M. C. 1994. Two divergent MET10 genes, one from Saccharomyces cerevisiae and one from

Saccharomyces carlsbergensis, encode the alpha subunit of sulfite reductase and specify potential binding sites for FAD and NADPH. *J Bacteriol,* 176**,** 6050-8.

HANSEN, J. & JOHANNESEN, P. F. 2000. Cysteine is essential for transcriptional regulation of the sulfur assimilation genes in Saccharomyces cerevisiae. *Mol Gen Genet,* 263**,** 535-42.

HARDING, H. P., ZHANG, Y., ZENG, H., NOVOA, I., LU, P. D., CALFON, M., SADRI, N., YUN, C., POPKO, B., PAULES, R., STOJDL, D. F., BELL, J. C., HETTMANN, T., LEIDEN, J. M. & RON, D. 2003. An integrated stress response regulates amino acid metabolism and resistance to oxidative stress. *Mol Cell,* 11**,** 619-33.

HARSHMAN, K. D., MOYE-ROWLEY, W. S. & PARKER, C. S. 1988. Transcriptional activation by the SV40 AP-1 recognition element in yeast is mediated by a factor similar to AP-1 that is distinct from GCN4. *Cell,* 53**,** 321-30.

HARTIG, A. & RUIS, H. 1986. Nucleotide sequence of the Saccharomyces cerevisiae CTT1 gene and deduced amino-acid sequence of yeast catalase T. *Eur J Biochem,* 160**,** 487-90.

HASLBECK, M., BRAUN, N., STROMER, T., RICHTER, B., MODEL, N., WEINKAUF, S. & BUCHNER, J. 2004. Hsp42 is the general small heat shock protein in the cytosol of Saccharomyces cerevisiae. *EMBO J,* 23**,** 638-49.

HAYNES, C. M., TITUS, E. A. & COOPER, A. A. 2004. Degradation of misfolded proteins prevents ER-derived oxidative stress and cell death. *Mol Cell,* 15**,** 767-76.

HERFARTH, H., BRAND, K., RATH, H. C., ROGLER, G., SCHÖLMERICH, J. & FALK, W. 2000. Nuclear factor-kappa B activity and intestinal inflammation in dextran sulphate sodium (DSS)-induced colitis in mice is suppressed by gliotoxin. *Clin Exp Immunol,* 120**,** 59-65.

HERRERO, E., ROS, J., BELLÍ, G. & CABISCOL, E. 2008. Redox control and oxidative stress in yeast cells. *Biochim Biophys Acta,* 1780**,** 1217-35.

HINNEBUSCH, A. G. 1984. Evidence for translational regulation of the activator of general amino acid control in yeast. *Proc Natl Acad Sci U S A,* 81**,** 6442-6.

HINSON, K. F., MOON, A. J. & PLUMMER, N. S. 1952. Broncho-pulmonary aspergillosis; a review and a report of eight new cases. *Thorax,* 7**,** 317-33.

HIRATA, D., YANO, K. & MIYAKAWA, T. 1994. Stress-induced transcriptional activation mediated by YAP1 and YAP2 genes that encode the Jun family of transcriptional activators in Saccharomyces cerevisiae. *Mol Gen Genet,* 242**,** 250-6.

HOFFMANN, B., MÖSCH, H. U., SATTLEGGER, E., BARTHELMESS, I. B., HINNEBUSCH, A. & BRAUS, G. H. 1999. The WD protein Cpc2p is required for repression of Gcn4 protein activity in yeast in the absence of amino-acid starvation. *Mol Microbiol,* 31**,** 807-22.

HOLMGREN, A. 1976. Hydrogen donor system for Escherichia coli ribonucleoside-diphosphate reductase dependent upon glutathione. *Proc Natl Acad Sci U S A,* 73**,** 2275-9.

HOLMGREN, A. 1979. Glutathione-dependent synthesis of deoxyribonucleotides. Characterization of the enzymatic mechanism of Escherichia coli glutaredoxin. *J Biol Chem,* 254**,** 3672-8.

HOLMGREN, A. 1985. Thioredoxin. *Annu Rev Biochem,* 54**,** 237-71.

HOLMGREN, A. 1989. Thioredoxin and glutaredoxin systems. *J Biol Chem,* 264**,** 13963-6.

HOLT, T. A. & PHILLIPS, J. 1988. Bovine spongiform encephalopathy. *Br Med J (Clin Res Ed),* 296**,** 1581-2.

HUNG, G. & MASISON, D. 2006. N-terminal domain of yeast Hsp104 chaperone is dispensable for thermotolerance and prion propagation but necessary for curing prions by Hsp104 overexpression. *Genetics,* 173**,** 611-20.

HURNE, A. M., CHAI, C. L. & WARING, P. 2000. Inactivation of rabbit muscle creatine kinase by reversible formation of an internal disulfide bond induced by the fungal toxin gliotoxin. *J Biol Chem,* 275**,** 25202-6.

IMLAY, J. A. 2003. Pathways of oxidative damage. *Annu Rev Microbiol,* 57**,** 395-418.

INGOLIA, T. D., SLATER, M. R. & CRAIG, E. A. 1982. Saccharomyces cerevisiae contains a complex multigene family related to the major heat shock-inducible gene of Drosophila. *Mol Cell Biol,* 2**,** 1388-98.

INOUE, Y., MATSUDA, T., SUGIYAMA, K., IZAWA, S. & KIMURA, A. 1999. Genetic analysis of glutathione peroxidase in oxidative stress response of Saccharomyces cerevisiae. *J Biol Chem,* 274**,** 27002-9.

INOUE, Y., SUGIYAMA, K., IZAWA, S. & KIMURA, A. 1998. Molecular identification of glutathione synthetase (GSH2) gene from Saccharomyces cerevisiae. *Biochim Biophys Acta,* 1395**,** 315-20.

IRAQUI, I., VISSERS, S., CARTIAUX, M. & URRESTARAZU, A. 1998. Characterisation of Saccharomyces cerevisiae ARO8 and ARO9 genes encoding aromatic aminotransferases I and II reveals a new aminotransferase subfamily. *Mol Gen Genet,* 257**,** 238-48.

IWAHASHI, H., KITAGAWA, E., SUZUKI, Y., UEDA, Y., ISHIZAWA, Y. H., NOBUMASA, H., KUBOKI, Y., HOSODA, H. & IWAHASHI, Y. 2007. Evaluation of toxicity of the mycotoxin citrinin using yeast ORF DNA microarray and Oligo DNA microarray. *BMC Genomics,* 8**,** 95.

IWAHASHI, Y., HOSODA, H., PARK, J. H., LEE, J. H., SUZUKI, Y., KITAGAWA, E., MURATA, S. M., JWA, N. S., GU, M. B. & IWAHASHI, H. 2006. Mechanisms of patulin toxicity under conditions that inhibit yeast growth. *J Agric Food Chem,* 54**,** 1936-42.

IZAWA, S., MAEDA, K., MIKI, T., MANO, J., INOUE, Y. & KIMURA, A. 1998. Importance of glucose-6-phosphate dehydrogenase in the adaptive response to hydrogen peroxide in Saccharomyces cerevisiae. *Biochem J,* 330 (Pt 2)**,** 811-7.

IZQUIERDO, A., CASAS, C., MÜHLENHOFF, U., LILLIG, C. H. & HERRERO, E. 2008. Saccharomyces cerevisiae Grx6 and Grx7 are monothiol glutaredoxins associated with the early secretory pathway. *Eukaryot Cell,* 7**,** 1415-26.

JAMIESON, D. J. 1998. Oxidative stress responses of the yeast Saccharomyces cerevisiae. *Yeast,* 14**,** 1511-27.

JANG, Y. K., WANG, L. & SANCAR, G. B. 1999. RPH1 and GIS1 are damage-responsive repressors of PHR1. *Mol Cell Biol,* 19**,** 7630-8.

JEPPESEN, M. G., ORTIZ, P., SHEPARD, W., KINZY, T. G., NYBORG, J. & ANDERSEN, G. R. 2003. The crystal structure of the glutathione S-transferase-like domain of elongation factor 1Bgamma from Saccharomyces cerevisiae. *J Biol Chem,* 278**,** 47190-8.

JEYAPRAKASH, A., WELCH, J. W. & FOGEL, S. 1991. Multicopy CUP1 plasmids enhance cadmium and copper resistance levels in yeast. *Mol Gen Genet,* 225**,** 363-8.

JIN, T., GU, Y., ZANUSSO, G., SY, M., KUMAR, A., COHEN, M., GAMBETTI, P. & SINGH, N. 2000. The chaperone protein BiP binds to a mutant prion protein and mediates its degradation by the proteasome. *J Biol Chem,* 275**,** 38699-704.

JOHANNESSEN, L. N., NILSEN, A. M. & LØVIK, M. 2005. The mycotoxins citrinin and gliotoxin differentially affect production of the pro-inflammatory cytokines tumour necrosis factor-alpha and interleukin-6, and the anti-inflammatory cytokine interleukin-10. *Clin Exp Allergy,* 35**,** 782-9.

JONES, G. & MASISON, D. 2003. Saccharomyces cerevisiae Hsp70 mutations affect [PSI+] prion propagation and cell growth differently and implicate Hsp40 and tetratricopeptide repeat cochaperones in impairment of [PSI+]. *Genetics,* 163**,** 495-506.

JONES, G., SONG, Y., CHUNG, S. & MASISON, D. 2004. Propagation of Saccharomyces cerevisiae [PSI+] prion is impaired by factors that regulate Hsp70 substrate binding. *Mol Cell Biol,* 24**,** 3928-37.

JONES, G., SONG, Y. & MASISON, D. 2003. Deletion of the Hsp70 chaperone gene SSB causes hypersensitivity to guanidine toxicity and curing of the [PSI+] prion by increasing guanidine uptake in yeast. *Mol Genet Genomics,* 269**,** 304-11.

JONES, G. W. & TUITE, M. F. 2005. Chaperoning prions: the cellular machinery for propagating an infectious protein? *Bioessays,* 27**,** 823-32.

JUNG, G., JONES, G. & MASISON, D. 2002. Amino acid residue 184 of yeast Hsp104 chaperone is critical for prion-curing by guanidine, prion propagation, and thermotolerance. *Proc Natl Acad Sci U S A,* 99**,** 9936-41.

JUNG, G., JONES, G., WEGRZYN, R. D. & MASISON, D. C. 2000. A role for cytosolic hsp70 in yeast [PSI(+)] prion propagation and [PSI(+)] as a cellular stress. *Genetics,* 156**,** 559-70.

JUNG, G. & MASISON, D. C. 2001. Guanidine hydrochloride inhibits Hsp104 activity in vivo: a possible explanation for its effect in curing yeast prions. *Curr Microbiol,* 43**,** 7-10.

KABANI, M. 2009. Structural and functional diversity among eukaryotic Hsp70 nucleotide exchange factors. *Protein Pept Lett,* 16**,** 623-60.

KABANI, M., BECKERICH, J. M. & BRODSKY, J. L. 2002. Nucleotide exchange factor for the yeast Hsp70 molecular chaperone Ssa1p. *Mol Cell Biol,* 22**,** 4677-89.

KADIISKA, M. B., HANNA, P. M., JORDAN, S. J. & MASON, R. P. 1993. Electron spin resonance evidence for free radical generation in copper-treated vitamin E- and selenium-deficient rats: in vivo spin-trapping investigation. *Mol Pharmacol,* 44**,** 222-7.

KALININA, E. V., CHERNOV, N. N. & SAPRIN, A. N. 2008. Involvement of thio-, peroxi-, and glutaredoxins in cellular redox-dependent processes. *Biochemistry (Mosc),* 73**,** 1493-510.

KAMEI, K. & WATANABE, A. 2005. Aspergillus mycotoxins and their effect on the host. *Med Mycol,* 43 Suppl 1**,** S95-9.

KANG, S. W., CHAE, H. Z., SEO, M. S., KIM, K., BAINES, I. C. & RHEE, S. G. 1998. Mammalian peroxiredoxin isoforms can reduce hydrogen peroxide generated in response to growth factors and tumor necrosis factor-alpha. *J Biol Chem,* 273**,** 6297-302.

KAPLOWITZ, N. 1981. The importance and regulation of hepatic glutathione. *Yale J Biol Med,* 54**,** 497-502.

KAPPUS, H. 1987. Oxidative stress in chemical toxicity. *Arch Toxicol,* 60**,** 144-9.

KAWANISHI, S., INOUE, S. & YAMAMOTO, K. 1989. Hydroxyl radical and singlet oxygen production and DNA damage induced by carcinogenic metal compounds and hydrogen peroxide. *Biol Trace Elem Res,* 21**,** 367-72.

KEELE, B. B., MCCORD, J. M. & FRIDOVICH, I. 1970. Superoxide dismutase from escherichia coli B. A new manganese-containing enzyme. *J Biol Chem,* 245**,** 6176-81.

KHODAVANDI, A., ALIZADEH, F., AALA, F., SEKAWI, Z. & CHONG, P. P. 2010. In vitro investigation of antifungal activity of allicin alone and in combination with azoles against Candida species. *Mycopathologia,* 169**,** 287-95.

KIM, S. Y. & CRAIG, E. A. 2005. Broad sensitivity of Saccharomyces cerevisiae lacking ribosome-associated chaperone ssb or zuo1 to cations, including aminoglycosides. *Eukaryot Cell,* 4**,** 82-9.

KIMURA, Y., RUTHERFORD, S. L., MIYATA, Y., YAHARA, I., FREEMAN, B. C., YUE, L., MORIMOTO, R. I. & LINDQUIST, S. 1997. Cdc37 is a molecular chaperone with specific functions in signal transduction. *Genes Dev,* 11**,** 1775-85.

KING, C. Y., TITTMANN, P., GROSS, H., GEBERT, R., AEBI, M. & WÜTHRICH, K. 1997. Prion-inducing domain 2-114 of yeast Sup35 protein transforms in vitro into amyloid-like filaments. *Proc Natl Acad Sci U S A,* 94**,** 6618-22.

KINZY, T. G., RIPMASTER, T. L. & WOOLFORD, J. L. 1994. Multiple genes encode the translation elongation factor EF-1 gamma in Saccharomyces cerevisiae. *Nucleic Acids Res,* 22**,** 2703-7.

KORCH, C., MOUNTAIN, H. A. & BYSTRÖM, A. S. 1991. Cloning, nucleotide sequence, and regulation of MET14, the gene encoding the APS kinase of Saccharomyces cerevisiae. *Mol Gen Genet,* 229**,** 96-108.

KREMS, B., CHARIZANIS, C. & ENTIAN, K. D. 1995. Mutants of Saccharomyces cerevisiae sensitive to oxidative and osmotic stress. *Curr Genet,* 27**,** 427-34.

KRETZSCHMAR, H. A., STOWRING, L. E., WESTAWAY, D., STUBBLEBINE, W. H., PRUSINER, S. B. & DEARMOND, S. J. 1986. Molecular cloning of a human prion protein cDNA. *DNA,* 5**,** 315-24.

KROGAN, N. J., CAGNEY, G., YU, H., ZHONG, G., GUO, X., IGNATCHENKO, A., LI, J., PU, S., DATTA, N., TIKUISIS, A. P., PUNNA, T., PEREGRÍN-ALVAREZ, J. M., SHALES, M., ZHANG, X., DAVEY, M., ROBINSON, M. D., PACCANARO, A., BRAY, J. E., SHEUNG, A., BEATTIE, B., RICHARDS, D. P., CANADIEN, V., LALEV, A., MENA, F., WONG, P., STAROSTINE, A., CANETE, M. M., VLASBLOM, J., WU, S., ORSI, C., COLLINS, S. R., CHANDRAN, S., HAW, R., RILSTONE, J. J., GANDI, K., THOMPSON, N. J., MUSSO, G., ST ONGE, P., GHANNY, S., LAM, M. H., BUTLAND, G., ALTAF-UL, A. M., KANAYA, S., SHILATIFARD, A., O'SHEA, E., WEISSMAN, J. S., INGLES, C. J., HUGHES, T. R., PARKINSON, J., GERSTEIN, M., WODAK, S. J., EMILI, A. & GREENBLATT, J. F. 2006. Global landscape of protein complexes in the yeast Saccharomyces cerevisiae. *Nature,* 440**,** 637-43.

KRYNDUSHKIN, D. S., SMIRNOV, V. N., TER-AVANESYAN, M. D. & KUSHNIROV, V. V. 2002. Increased expression of Hsp40 chaperones, transcriptional factors, and ribosomal protein Rpp0 can cure yeast prions. *J Biol Chem,* 277**,** 23702-8.

KUGE, S. & JONES, N. 1994. YAP1 dependent activation of TRX2 is essential for the response of Saccharomyces cerevisiae to oxidative stress by hydroperoxides. *EMBO J,* 13**,** 655-64.

KUGE, S., JONES, N. & NOMOTO, A. 1997. Regulation of yAP-1 nuclear localization in response to oxidative stress. *EMBO J,* 16**,** 1710-20.

KUPFAHL, C., HEINEKAMP, T., GEGINAT, G., RUPPERT, T., HÄRTL, A., HOF, H. & BRAKHAGE, A. A. 2006. Deletion of the gliP gene of Aspergillus fumigatus results in loss of gliotoxin production but has no effect on virulence of the fungus in a low-dose mouse infection model. *Mol Microbiol,* 62**,** 292-302.

KUPFAHL, C., MICHALKA, A., LASS-FLÖRL, C., FISCHER, G., HAASE, G., RUPPERT, T., GEGINAT, G. & HOF, H. 2008. Gliotoxin production by clinical and environmental Aspergillus fumigatus strains. *Int J Med Microbiol,* 298**,** 319-27.

KUSHNIROV, V. V., TER-AVANESYAN, M. D., TELCKOV, M. V., SURGUCHOV, A. P., SMIRNOV, V. N. & INGE-VECHTOMOV, S. G. 1988. Nucleotide sequence of the SUP2 (SUP35) gene of Saccharomyces cerevisiae. *Gene,* 66**,** 45-54.

KWEON, Y. O., PAIK, Y. H., SCHNABL, B., QIAN, T., LEMASTERS, J. J. & BRENNER, D. A. 2003. Gliotoxin-mediated apoptosis of activated human hepatic stellate cells. *J Hepatol,* 39**,** 38-46.

LAABS, T. L., MARKWARDT, D. D., SLATTERY, M. G., NEWCOMB, L. L., STILLMAN, D. J. & HEIDEMAN, W. 2003. ACE2 is required for daughter cell-specific G1 delay in Saccharomyces cerevisiae. *Proc Natl Acad Sci U S A,* 100**,** 10275-80.

LAGADIC-GOSSMANN, D., RISSEL, M., LE BOT, M. A. & GUILLOUZO, A. 1998. Toxic effects of tacrine on primary hepatocytes and liver epithelial cells in culture. *Cell Biol Toxicol,* 14**,** 361-73.

LAHIRI, D. K. 1994. Reversibility of the effect of tacrine on the secretion of the beta-amyloid precursor protein in cultured cells. *Neurosci Lett,* 181**,** 149-52.

LAHIRI, D. K. & FARLOW, M. R. 1996. Differential effect of tacrine and physostigmine on the secretion of the beta-amyloid precursor protein in cell lines. *J Mol Neurosci,* 7**,** 41-9.

LAHIRI, D. K., LEWIS, S. & FARLOW, M. R. 1994. Tacrine alters the secretion of the beta-amyloid precursor protein in cell lines. *J Neurosci Res,* 37**,** 777-87.

LANDOLFO, S., POLITI, H., ANGELOZZI, D. & MANNAZZU, I. 2008. ROS accumulation and oxidative damage to cell structures in Saccharomyces cerevisiae wine strains during fermentation of high-sugar-containing medium. *Biochim Biophys Acta,* 1780**,** 892-8.

LANDOLFO, S., ZARA, G., ZARA, S., BUDRONI, M., CIANI, M. & MANNAZZU, I. 2010. Oleic acid and ergosterol supplementation mitigates oxidative stress in wine strains of Saccharomyces cerevisiae. *Int J Food Microbiol,* 141**,** 229-35.

LANSBURY, P. T. 1999. Evolution of amyloid: what normal protein folding may tell us about fibrillogenesis and disease. *Proc Natl Acad Sci U S A,* 96**,** 3342-4.

LARIN, N. M., COPPING, M. P., HERBST-LAIER, R. H., ROBERTS, B. & WENHAM, R. B. 1965. Antiviral activity of gliotoxin. *Chemotherapy,* 10**,** 12-23.

LATGÉ, J. P. 1999. Aspergillus fumigatus and aspergillosis. *Clin Microbiol Rev,* 12**,** 310-50.

LAUFER, P., FINK, J. N., BRUNS, W. T., UNGER, G. F., KALBFLEISCH, J. H., GREENBERGER, P. A. & PATTERSON, R. 1984. Allergic bronchopulmonary aspergillosis in cystic fibrosis. *J Allergy Clin Immunol,* 73**,** 44-8.

LAURENT, T. C., MOORE, E. C. & REICHARD, P. 1964. ENZYMATIC SYNTHESIS OF DEOXYRIBONUCLEOTIDES. IV. ISOLATION AND CHARACTERIZATION OF THIOREDOXIN, THE HYDROGEN DONOR FROM ESCHERICHIA COLI B. *J Biol Chem,* 239**,** 3436-44.

LAURÉN, J., GIMBEL, D. A., NYGAARD, H. B., GILBERT, J. W. & STRITTMATTER, S. M. 2009. Cellular prion protein mediates impairment of synaptic plasticity by amyloid-beta oligomers. *Nature,* 457**,** 1128-32.

LAUTERBURG, B. H., SMITH, C. V., HUGHES, H. & MITCHELL, J. R. 1984. Biliary excretion of glutathione and glutathione disulfide in the rat. Regulation and response to oxidative stress. *J Clin Invest,* 73**,** 124-33.

LEE, J., GODON, C., LAGNIEL, G., SPECTOR, D., GARIN, J., LABARRE, J. & TOLEDANO, M. B. 1999. Yap1 and Skn7 control two specialized oxidative stress response regulons in yeast. *J Biol Chem,* 274**,** 16040-6.

LEVINE, L., GORDON, J. A. & JENCKS, W. P. 1963. The relationship of structure to the effectiveness of denaturing agents for deoxyribonucleic acid. *Biochemistry,* 2**,** 168-75.

LEWINSKA, A., WNUK, M., GRZELAK, A. & BARTOSZ, G. 2010. Nucleolus as an oxidative stress sensor in the yeast Saccharomyces cerevisiae. *Redox Rep,* 15**,** 87-96.

LEWIS, R. E., WIEDERHOLD, N. P., LIONAKIS, M. S., PRINCE, R. A. & KONTOYIANNIS, D. P. 2005. Frequency and species distribution of gliotoxin-producing Aspergillus isolates recovered from patients at a tertiary-care cancer center. *J Clin Microbiol,* 43**,** 6120-2.

LI, B. Z. & YUAN, Y. J. 2010. Transcriptome shifts in response to furfural and acetic acid in Saccharomyces cerevisiae. *Appl Microbiol Biotechnol,* 86**,** 1915-24.

LIANG, G., LIAO, X., DU, G. & CHEN, J. 2008. Elevated glutathione production by adding precursor amino acids coupled with ATP in high cell density cultivation of Candida utilis. *J Appl Microbiol,* 105**,** 1432-40.

LIBEREK, K., SKOWYRA, D., ZYLICZ, M., JOHNSON, C. & GEORGOPOULOS, C. 1991. The Escherichia coli DnaK chaperone, the 70-kDa heat shock protein eukaryotic equivalent, changes conformation upon ATP hydrolysis, thus triggering its dissociation from a bound target protein. *J Biol Chem,* 266**,** 14491-6.

LIEBMAN, S. W., STEWART, J. W. & SHERMAN, F. 1975. Serine substitutions caused by an ochre suppressor in yeast. *J Mol Biol,* 94**,** 595-610.

LINDQUIST, S. 1997. Mad cows meet psi-chotic yeast: the expansion of the prion hypothesis. *Cell,* 89**,** 495-8.

LIU, B., LARSSON, L., CABALLERO, A., HAO, X., OLING, D., GRANTHAM, J. & NYSTRÖM, T. 2010. The polarisome is required for segregation and retrograde transport of protein aggregates. *Cell,* 140**,** 257-67.

LIU, J. J., SONDHEIMER, N. & LINDQUIST, S. L. 2002. Changes in the middle region of Sup35 profoundly alter the nature of epigenetic inheritance for the yeast prion [PSI+]. *Proc Natl Acad Sci U S A,* 99 Suppl 4**,** 16446-53.

LIU, X. F., ELASHVILI, I., GRALLA, E. B., VALENTINE, J. S., LAPINSKAS, P. & CULOTTA, V. C. 1992. Yeast lacking superoxide dismutase. Isolation of genetic suppressors. *J Biol Chem,* 267**,** 18298-302.

LOAR, J. W., SEISER, R. M., SUNDBERG, A. E., SAGERSON, H. J., ILIAS, N., ZOBEL-THROPP, P., CRAIG, E. A. & LYCAN, D. E. 2004. Genetic and biochemical interactions among Yar1, Ltv1 and Rps3 define novel links between environmental stress and ribosome biogenesis in Saccharomyces cerevisiae. *Genetics,* 168**,** 1877-89.

LOEW, O. 1900. A NEW ENZYME OF GENERAL OCCURRENCE IN ORGANISMIS. *Science,* 11**,** 701-2.

LOOVERS, H. M., GUINAN, E. & JONES, G. W. 2007. Importance of the Hsp70 ATPase domain in yeast prion propagation. *Genetics,* 175**,** 621-30.

LOURIDAS, G. 1976. Bronchopulmonary aspergillosis. An epidemiological study in a hospital population. *Respiration,* 33**,** 281-8.

LU, Z. & CYR, D. M. 1998. Protein folding activity of Hsp70 is modified differentially by the hsp40 co-chaperones Sis1 and Ydj1. *J Biol Chem,* 273**,** 27824-30.

LUIKENHUIS, S., PERRONE, G., DAWES, I. W. & GRANT, C. M. 1998. The yeast Saccharomyces cerevisiae contains two glutaredoxin genes that are required for protection against reactive oxygen species. *Mol Biol Cell,* 9**,** 1081-91.

LUSHCHAK, V. I. 2011. Adaptive response to oxidative stress: Bacteria, fungi, plants and animals. *Comp Biochem Physiol C Toxicol Pharmacol,* 153**,** 175-90.

LUTSTORF, U. & MEGNET, R. 1968. Multiple forms of alcohol dehydrogenase in Saccharomyces cerevisiae. I. Physiological control of ADH-2 and properties of ADH-2 and ADH-4. *Arch Biochem Biophys,* 126**,** 933-44.

LYCAN, D. E., STAFFORD, K. A., BOLLINGER, W. & BREEDEN, L. L. 1996. A new Saccharomyces cerevisiae ankyrin repeat-encoding gene required for a normal rate of cell proliferation. *Gene,* 171**,** 33-40.

MABEY, J. E., ANDERSON, M. J., GILES, P. F., MILLER, C. J., ATTWOOD, T. K., PATON, N. W., BORNBERG-BAUER, E., ROBSON, G. D., OLIVER, S. G. & DENNING, D. W. 2004. CADRE: the Central Aspergillus Data REpository. *Nucleic Acids Res,* 32**,** D401-5.

MACHADO, A. K., MORGAN, B. A. & MERRILL, G. F. 1997. Thioredoxin reductase-dependent inhibition of MCB cell cycle box activity in Saccharomyces cerevisiae. *J Biol Chem,* 272**,** 17045-54.

MADEO, F., FRÖHLICH, E., LIGR, M., GREY, M., SIGRIST, S. J., WOLF, D. H. & FRÖHLICH, K. U. 1999. Oxygen stress: a regulator of apoptosis in yeast. *J Cell Biol,* 145**,** 757-67.

MARISAVLJEVIĆ, D., ROLOVIĆ, Z., BUKUMIROVIĆ, K., BOSKOVIĆ, D. & ELEZOVIĆ, I. 1989. [Invasive pulmonary aspergillosis during the treatment of acute leukaemia (3 case report)]. *Srp Arh Celok Lek,* 117**,** 679-88.

MARTINS, M. B. & CARVALHO, I. 2007. Diketopiperazines: biological activity and synthesis. *Tetrahedron,* 63**,** 9923-9932.

MARX, J. L. 1988. FDA queries Alzheimer's trial results. *Science,* 239**,** 969.

MASISON, D., KIRKLAND, P. & SHARMA, D. 2009. Influence of Hsp70s and their regulators on yeast prion propagation. *Prion,* 3**,** 65-73.

MASSELOT, M. & DE ROBICHON-SZULMAJSTER, H. 1975. Methionine biosynthesis in Saccharomyces cerevisiae. I. Genetical analysis of auxotrophic mutants. *Mol Gen Genet,* 139**,** 121-32.

MATITYAHU, I., KACHAN, L., BAR ILAN, I. & AMIR, R. 2006. Transgenic tobacco plants overexpressing the Met25 gene of Saccharomyces cerevisiae exhibit enhanced levels of cysteine and glutathione and increased tolerance to oxidative stress. *Amino Acids,* 30**,** 185-94.

MAYER, C. & GRUMMT, I. 2005. Cellular stress and nucleolar function. *Cell Cycle,* 4**,** 1036-8.

MAYER, M. P. & BUKAU, B. 2005. Hsp70 chaperones: cellular functions and molecular mechanism. *Cell Mol Life Sci,* 62**,** 670-84.

MAYER, M. P., SCHRÖDER, H., RÜDIGER, S., PAAL, K., LAUFEN, T. & BUKAU, B. 2000. Multistep mechanism of substrate binding determines chaperone activity of Hsp70. *Nat Struct Biol,* 7**,** 586-93.

MAYR, C., RICHTER, K., LILIE, H. & BUCHNER, J. 2000. Cpr6 and Cpr7, two closely related Hsp90-associated immunophilins from Saccharomyces cerevisiae, differ in their functional properties. *J Biol Chem,* 275**,** 34140-6.

MCALISTER, L. & HOLLAND, M. J. 1985. Differential expression of the three yeast glyceraldehyde-3-phosphate dehydrogenase genes. *J Biol Chem,* 260**,** 15019-27.

MCCARTHY, S., SOMAYAJULU, M., SIKORSKA, M., BOROWY-BOROWSKI, H. & PANDEY, S. 2004. Paraquat induces oxidative stress and neuronal cell death; neuroprotection by water-soluble Coenzyme Q10. *Toxicol Appl Pharmacol,* 201**,** 21-31.

MCCORD, J. M. & FRIDOVICH, I. 1968. The reduction of cytochrome c by milk xanthine oxidase. *J Biol Chem,* 243**,** 5753-60.

MCCORD, J. M. & FRIDOVICH, I. 1969a. Superoxide dismutase. An enzymic function for erythrocuprein (hemocuprein). *J Biol Chem,* 244**,** 6049-55.

MCCORD, J. M. & FRIDOVICH, I. 1969b. The utility of superoxide dismutase in studying free radical reactions. I. Radicals generated by the interaction of sulfite, dimethyl sulfoxide, and oxygen. *J Biol Chem,* 244**,** 6056-63.

MCDOUGALL, J. K. 1969. Antiviral action of gliotoxin. *Arch Gesamte Virusforsch,* 27**,** 255-67.

MCKINLEY, M. P., BOLTON, D. C. & PRUSINER, S. B. 1983. A protease-resistant protein is a structural component of the scrapie prion. *Cell,* 35**,** 57-62.

MCMAHON, F. G., COLE, P. A., BOYLES, P. W. & VANOV SK: 1974. Study of a new antihypertensive (guanabenz). *Curr Ther Res Clin Exp,* 16**,** 389-97.

MCMINN, P. C., HALLIDAY, G. M. & MULLER, H. K. 1990. Effects of gliotoxin on Langerhans' cell function: contact hypersensitivity responses and skin graft survival. *Immunology,* 71**,** 46-51.

MEISTER, A. 1988. Glutathione metabolism and its selective modification. *J Biol Chem,* 263**,** 17205-8.

MELDRUM, N. U. & TARR, H. L. 1935. The reduction of glutathione by the Warburg-Christian system. *Biochem J,* 29**,** 108-15.

MENZEL, A. E. O., WINTERSTEINER, O. & HOOGERHEIDE, J. C. 1944. THE ISOLATION OF GLIOTOXIN AND FUMIGACIN FROM
CULTURE FILTRATES OF ASPERGILLUS FUMIGATUS. J. Biol.Chem.

MESECKE, N., SPANG, A., DEPONTE, M. & HERRMANN, J. M. 2008. A novel group of glutaredoxins in the cis-Golgi critical for oxidative stress resistance. *Mol Biol Cell,* 19**,** 2673-80.

MEUNIER-CARPENTIER, F. 1983. Treatment of mycoses in cancer patients. *Am J Med,* 74**,** 74-9.

MILLER, P. A., MILSTREY, K. P. & TROWN, P. W. 1968. Specific inhibition of viral ribonucleic acid replication by Gliotoxin. *Science,* 159**,** 431-2.

MILLS, G. C. 1957. Hemoglobin catabolism. I. Glutathione peroxidase, an erythrocyte enzyme which protects hemoglobin from oxidative breakdown. *J Biol Chem,* 229**,** 189-97.

MIYASAKI, K. T., WILSON, M. E., BRUNETTI, A. J. & GENCO, R. J. 1986. Oxidative and nonoxidative killing of Actinobacillus actinomycetemcomitans by human neutrophils. *Infect Immun,* 53**,** 154-60.

MOLLOY, D. W., GUYATT, G. H., WILSON, D. B., DUKE, R., REES, L. & SINGER, J. 1991. Effect of tetrahydroaminoacridine on cognition, function and behaviour in Alzheimer's disease. *CMAJ,* 144**,** 29-34.

MOMOSE, Y. & IWAHASHI, H. 2001. Bioassay of cadmium using a DNA microarray: genome-wide expression patterns of Saccharomyces cerevisiae response to cadmium. *Environ Toxicol Chem,* 20**,** 2353-60.

MOOSAVI, B., WONGWIGKARN, J. & TUITE, M. F. 2010. Hsp70/Hsp90 co-chaperones are required for efficient Hsp104-mediated elimination of the yeast [PSI(+)] prion but not for prion propagation. *Yeast,* 27**,** 167-79.

MORGAN, B. A., BANKS, G. R., TOONE, W. M., RAITT, D., KUGE, S. & JOHNSTON, L. H. 1997. The Skn7 response regulator controls gene expression in the oxidative stress response of the budding yeast Saccharomyces cerevisiae. *EMBO J,* 16**,** 1035-44.

MOSHAROV, E., CRANFORD, M. R. & BANERJEE, R. 2000. The quantitatively important relationship between homocysteine metabolism and glutathione synthesis by the transsulfuration pathway and its regulation by redox changes. *Biochemistry,* 39**,** 13005-11.

MOUNTAIN, H. A., BYSTRÖM, A. S., LARSEN, J. T. & KORCH, C. 1991. Four major transcriptional responses in the methionine/threonine biosynthetic pathway of Saccharomyces cerevisiae. *Yeast,* 7**,** 781-803.

MOYE-ROWLEY, W. S., HARSHMAN, K. D. & PARKER, C. S. 1988. YAP1 encodes a yeast homolog of mammalian transcription factor AP-1. *Cold Spring Harb Symp Quant Biol,* 53 Pt 2**,** 711-7.

MOYE-ROWLEY, W. S., HARSHMAN, K. D. & PARKER, C. S. 1989. Yeast YAP1 encodes a novel form of the jun family of transcriptional activator proteins. *Genes Dev,* 3**,** 283-92.

MUKAI, H., KUNO, T., TANAKA, H., HIRATA, D., MIYAKAWA, T. & TANAKA, C. 1993. Isolation and characterization of SSE1 and SSE2, new members of the yeast HSP70 multigene family. *Gene,* 132**,** 57-66.

MULLER, E. G. 1991. Thioredoxin deficiency in yeast prolongs S phase and shortens the G1 interval of the cell cycle. *J Biol Chem,* 266**,** 9194-202.

MULLER, E. G. 1992. Thioredoxin genes in Saccharomyces cerevisiae: map positions of TRX1 and TRX2. *Yeast,* 8**,** 117-20.

MULLINS, J., HARVEY, R. & SEATON, A. 1976. Sources and incidence of airborne Aspergillus fumigatus (Fres). *Clin Allergy,* 6**,** 209-17.

MUNDAY, R. 1982. Studies on the mechanism of toxicity of the mycotoxin, sporidesmin. I. Generation of superoxide radical by sporidesmin. *Chem Biol Interact,* 41**,** 361-74.

MURGUÍA, J. R., BELLÉS, J. M. & SERRANO, R. 1995. A salt-sensitive 3'(2'),5'-bisphosphate nucleotidase involved in sulfate activation. *Science,* 267**,** 232-4.

MÜLLBACHER, A. & EICHNER, R. D. 1984. Immunosuppression in vitro by a metabolite of a human pathogenic fungus. *Proc Natl Acad Sci U S A,* 81**,** 3835-7.

MÜLLBACHER, A., WARING, P., TIWARI-PALNI, U. & EICHNER, R. D. 1986. Structural relationship of epipolythiodioxopiperazines and their immunomodulating activity. *Mol Immunol,* 23**,** 231-5.

MÜLLER, F. M., SEIDLER, M. & BEAUVAIS, A. 2011. Aspergillus fumigatus biofilms in the clinical setting. *Med Mycol,* 49 Suppl 1**,** S96-S100.

NAKANO, M. 1992. [Free radicals and their biological significance: present and future]. *Hum Cell,* 5**,** 334-40.

NATARAJAN, K., MEYER, M. R., JACKSON, B. M., SLADE, D., ROBERTS, C., HINNEBUSCH, A. G. & MARTON, M. J. 2001. Transcriptional profiling shows that Gcn4p is a master regulator of gene expression during amino acid starvation in yeast. *Mol Cell Biol,* 21**,** 4347-68.

NATH, K. A., NGO, E. O., HEBBEL, R. P., CROATT, A. J., ZHOU, B. & NUTTER, L. M. 1995. alpha-Ketoacids scavenge H2O2 in vitro and in vivo and reduce menadione-induced DNA injury and cytotoxicity. *Am J Physiol,* 268**,** C227-36.

NEEDHAM, P. G. & MASISON, D. C. 2008. Prion-impairing mutations in Hsp70 chaperone Ssa1: effects on ATPase and chaperone activities. *Arch Biochem Biophys,* 478**,** 167-74.

NELSON, R. J., ZIEGELHOFFER, T., NICOLET, C., WERNER-WASHBURNE, M. & CRAIG, E. A. 1992. The translation machinery and 70 kd heat shock protein cooperate in protein synthesis. *Cell,* 71**,** 97-105.

NESS, F., FERREIRA, P., COX, B. & TUITE, M. 2002. Guanidine hydrochloride inhibits the generation of prion "seeds" but not prion protein aggregation in yeast. *Mol Cell Biol,* 22**,** 5593-605.

NEWNAM, G. P., WEGRZYN, R. D., LINDQUIST, S. L. & CHERNOFF, Y. O. 1999. Antagonistic interactions between yeast chaperones Hsp104 and Hsp70 in prion curing. *Mol Cell Biol,* 19**,** 1325-33.

NISAMEDTINOV, I., KEVVAI, K., ORUMETS, K., RAUTIO, J. J. & PAALME, T. 2010. Glutathione accumulation in ethanol-stat fed-batch culture of Saccharomyces cerevisiae with a switch to cysteine feeding. *Appl Microbiol Biotechnol,* 87**,** 175-83.

NORBECK, J., PÂHLMAN, A. K., AKHTAR, N., BLOMBERG, A. & ADLER, L. 1996. Purification and characterization of two isoenzymes of DL-glycerol-3-phosphatase from Saccharomyces cerevisiae. Identification of the corresponding GPP1 and GPP2 genes and evidence for osmotic regulation of Gpp2p expression by the osmosensing mitogen-activated protein kinase signal transduction pathway. *J Biol Chem,* 271**,** 13875-81.

NORDBERG, J. & ARNÉR, E. S. 2001. Reactive oxygen species, antioxidants, and the mammalian thioredoxin system. *Free Radic Biol Med,* 31**,** 1287-312.

NORMINGTON, K., KOHNO, K., KOZUTSUMI, Y., GETHING, M. J. & SAMBROOK, J. 1989. S. cerevisiae encodes an essential protein homologous in sequence and function to mammalian BiP. *Cell,* 57**,** 1223-36.

O'BRIEN, J. T., EAGGER, S. & LEVY, R. 1991. Effects of tetrahydroaminoacridine on liver function in patients with Alzheimer's disease. *Age Ageing,* 20**,** 129-31.

OESCH, B., WESTAWAY, D., WÄLCHLI, M., MCKINLEY, M. P., KENT, S. B., AEBERSOLD, R., BARRY, R. A., TEMPST, P., TEPLOW, D. B. & HOOD, L. E. 1985. A cellular gene encodes scrapie PrP 27-30 protein. *Cell,* 40**,** 735-46.

OHBA, M. 1997. Modulation of intracellular protein degradation by SSB1-SIS1 chaperon system in yeast S. cerevisiae. *FEBS Lett,* 409**,** 307-11.

OHTAKE, Y. & WICKNER, R. B. 1995. KRB1, a suppressor of mak7-1 (a mutant RPL4A), is RPL4B, a second ribosomal protein L4 gene, on a fragment of Saccharomyces chromosome XII. *Genetics,* 140**,** 129-37.

OHTAKE, Y. & YABUUCHI, S. 1991. Molecular cloning of the gamma-glutamylcysteine synthetase gene of Saccharomyces cerevisiae. *Yeast,* 7**,** 953-61.

OLAREWAJU, O., ORTIZ, P. A., CHOWDHURY, W. Q., CHATTERJEE, I. & KINZY, T. G. 2004. The translation elongation factor eEF1B plays a role in the oxidative stress response pathway. *RNA Biol,* 1**,** 89-94.

ONO, B., KIJIMA, K., INOUE, T., MIYOSHI, S., MATSUDA, A. & SHINODA, S. 1994. Purification and properties of Saccharomyces cerevisiae cystathionine beta-synthase. *Yeast,* 10**,** 333-9.

ONO, B., SHIRAHIGE, Y., NANJOH, A., ANDOU, N., OHUE, H. & ISHINO-ARAO, Y. 1988. Cysteine biosynthesis in Saccharomyces cerevisiae: mutation that confers cystathionine beta-synthase deficiency. *J Bacteriol,* 170**,** 5883-9.

ONO, B., SURUGA, T., YAMAMOTO, M., YAMAMOTO, S., MURATA, K., KIMURA, A., SHINODA, S. & OHMORI, S. 1984. Cystathionine accumulation in Saccharomyces cerevisiae. *J Bacteriol,* 158**,** 860-5.

ONO, B., TANAKA, K., NAITO, K., HEIKE, C., SHINODA, S., YAMAMOTO, S., OHMORI, S., OSHIMA, T. & TOH-E, A. 1992. Cloning and characterization of the CYS3 (CYI1) gene of Saccharomyces cerevisiae. *J Bacteriol,* 174**,** 3339-47.

ONO, B. I., STEWART, J. W. & SHERMAN, F. 1979. Yeast UAA suppressors effective in psi+ strains serine-inserting suppressors. *J Mol Biol,* 128**,** 81-100.

ORCIUOLO, E., STANZANI, M., CANESTRARO, M., GALIMBERTI, S., CARULLI, G., LEWIS, R., PETRINI, M. & KOMANDURI, K. V. 2007. Effects of Aspergillus fumigatus gliotoxin and methylprednisolone on human neutrophils: implications for the pathogenesis of invasive aspergillosis. *J Leukoc Biol,* 82**,** 839-48.

ORR, J. G., LEEL, V., CAMERON, G. A., MAREK, C. J., HAUGHTON, E. L., ELRICK, L. J., TRIM, J. E., HAWKSWORTH, G. M., HALESTRAP, A. P. & WRIGHT, M. C. 2004. Mechanism of action of the antifibrogenic compound gliotoxin in rat liver cells. *Hepatology,* 40**,** 232-42.

OZCAN, S. & JOHNSTON, M. 1999. Function and regulation of yeast hexose transporters. *Microbiol Mol Biol Rev,* 63**,** 554-69.

PAHL, H. L., KRAUSS, B., SCHULZE-OSTHOFF, K., DECKER, T., TRAENCKNER, E. B., VOGT, M., MYERS, C., PARKS, T., WARRING, P., MÜHLBACHER, A., CZERNILOFSKY, A. P. & BAEUERLE, P. A. 1996. The immunosuppressive fungal metabolite gliotoxin specifically inhibits transcription factor NF-kappaB. *J Exp Med,* 183**,** 1829-40.

PAHLMAN, A. K., GRANATH, K., ANSELL, R., HOHMANN, S. & ADLER, L. 2001. The yeast glycerol 3-phosphatases Gpp1p and Gpp2p are required for glycerol biosynthesis and differentially involved in the cellular responses to osmotic, anaerobic, and oxidative stress. *J Biol Chem,* 276**,** 3555-63.

PALMQVIST, E., GRAGE, H., MEINANDER, N. Q. & HAHN-HÄGERDAL, B. 1999. Main and interaction effects of acetic acid, furfural, and p-hydroxybenzoic acid on growth and ethanol productivity of yeasts. *Biotechnol Bioeng,* 63**,** 46-55.

PAN, K. M., BALDWIN, M., NGUYEN, J., GASSET, M., SERBAN, A., GROTH, D., MEHLHORN, I., HUANG, Z., FLETTERICK, R. J. & COHEN, F. E. 1993. Conversion of alpha-helices into beta-sheets features in the formation of the scrapie prion proteins. *Proc Natl Acad Sci U S A,* 90**,** 10962-6.

PANNUNZIO, N. R., MANTHEY, G. M. & BAILIS, A. M. 2008. RAD59 is required for efficient repair of simultaneous double-strand breaks resulting in translocations in Saccharomyces cerevisiae. *DNA Repair (Amst),* 7**,** 788-800.

PARSELL, D. A., KOWAL, A. S., SINGER, M. A. & LINDQUIST, S. 1994. Protein disaggregation mediated by heat-shock protein Hsp104. *Nature,* 372**,** 475-8.

PARSON, W. W. 1993. Enzyme Kinetics. *In:* KANE, K. (ed.) *Biochemistry.* Wm. C. Brown Publishers.

PATEL, B. K., GAVIN-SMYTH, J. & LIEBMAN, S. W. 2009. The yeast global transcriptional co-repressor protein Cyc8 can propagate as a prion. *Nat Cell Biol,* 11**,** 344-9.

PATINO, M. M., LIU, J. J., GLOVER, J. R. & LINDQUIST, S. 1996. Support for the prion hypothesis for inheritance of a phenotypic trait in yeast. *Science,* 273**,** 622-6.

PAUSHKIN, S. V., KUSHNIROV, V. V., SMIRNOV, V. N. & TER-AVANESYAN, M. D. 1996. Propagation of the yeast prion-like [psi+] determinant is mediated by oligomerization of the SUP35-encoded polypeptide chain release factor. *EMBO J,* 15**,** 3127-34.

PEDRAJAS, J. R., KOSMIDOU, E., MIRANDA-VIZUETE, A., GUSTAFSSON, J. A., WRIGHT, A. P. & SPYROU, G. 1999. Identification and functional characterization of a novel mitochondrial thioredoxin system in Saccharomyces cerevisiae. *J Biol Chem,* 274**,** 6366-73.

PEMBERTON, L. F. & BLOBEL, G. 1997. Characterization of the Wtm proteins, a novel family of Saccharomyces cerevisiae transcriptional modulators with roles in meiotic regulation and silencing. *Mol Cell Biol,* 17**,** 4830-41.

PENNINCKX, M. 2000. A short review on the role of glutathione in the response of yeasts to nutritional, environmental, and oxidative stresses. *Enzyme Microb Technol,* 26**,** 737-742.

PENNINCKX, M. J. 2002. An overview on glutathione in Saccharomyces versus non-conventional yeasts. *FEMS Yeast Res,* 2**,** 295-305.

PERRIN, A., BUCKLE, M. & DUJON, B. 1993. Asymmetrical recognition and activity of the I-SceI endonuclease on its site and on intron-exon junctions. *EMBO J,* 12**,** 2939-47.

PETERSEN, J. G. & HOLMBERG, S. 1986. The ILV5 gene of Saccharomyces cerevisiae is highly expressed. *Nucleic Acids Res,* 14**,** 9631-51.

PETKO, L. & LINDQUIST, S. 1986. Hsp26 is not required for growth at high temperatures, nor for thermotolerance, spore development, or germination. *Cell,* 45**,** 885-94.

PETROVA, V. Y., DRESCHER, D., KUJUMDZIEVA, A. V. & SCHMITT, M. J. 2004. Dual targeting of yeast catalase A to peroxisomes and mitochondria. *Biochem J,* 380**,** 393-400.

PETUKHOVA, G., STRATTON, S. A. & SUNG, P. 1999. Single strand DNA binding and annealing activities in the yeast recombination factor Rad59. *J Biol Chem,* 274**,** 33839-42.

PITT, J. I. 1994. The current role of Aspergillus and Penicillium in human and animal health. *J Med Vet Mycol,* 32 Suppl 1**,** 17-32.

PLANTA, R. J. & MAGER, W. H. 1998. The list of cytoplasmic ribosomal proteins of Saccharomyces cerevisiae. *Yeast,* 14**,** 471-7.

PLUMMER, P. J. 1946. Scrapie-A Disease of Sheep: A Review of the literature. *Can J Comp Med Vet Sci,* 10**,** 49-54.

POMPELLA, A., VISVIKIS, A., PAOLICCHI, A., DE TATA, V. & CASINI, A. F. 2003. The changing faces of glutathione, a cellular protagonist. *Biochem Pharmacol,* 66**,** 1499-503.

POWELL, S. R. 2000. The antioxidant properties of zinc. *J Nutr,* 130**,** 1447S-54S.

PRONK, J. T., YDE STEENSMA, H. & VAN DIJKEN, J. P. 1996. Pyruvate metabolism in Saccharomyces cerevisiae. *Yeast,* 12**,** 1607-33.

PRUSINER, S. B. 1982. Novel proteinaceous infectious particles cause scrapie. *Science,* 216**,** 136-44.

PRUSINER, S. B. 1991. Molecular biology of prion diseases. *Science,* 252**,** 1515-22.

PRUSINER, S. B. 1997. Prion diseases and the BSE crisis. *Science,* 278**,** 245-51.

PRUSINER, S. B. 1998. Prions. *Proc Natl Acad Sci U S A,* 95**,** 13363-83.

PRUSINER, S. B., MCKINLEY, M. P., BOWMAN, K. A., BOLTON, D. C., BENDHEIM, P. E., GROTH, D. F. & GLENNER, G. G. 1983. Scrapie prions aggregate to form amyloid-like birefringent rods. *Cell,* 35**,** 349-58.

PUJOL-CARRION, N., BELLI, G., HERRERO, E., NOGUES, A. & DE LA TORRE-RUIZ, M. A. 2006. Glutaredoxins Grx3 and Grx4 regulate nuclear localisation of Aft1 and the oxidative stress response in Saccharomyces cerevisiae. *J Cell Sci,* 119**,** 4554-64.

PUJOL-CARRION, N. & DE LA TORRE-RUIZ, M. A. 2010. Glutaredoxins Grx4 and Grx3 of Saccharomyces cerevisiae play a role in actin dynamics through their Trx domains, which contributes to oxidative stress resistance. *Appl Environ Microbiol,* 76**,** 7826-35.

QIZILBASH, N., WHITEHEAD, A., HIGGINS, J., WILCOCK, G., SCHNEIDER, L. & FARLOW, M. 1998. Cholinesterase inhibition for Alzheimer disease: a meta-analysis of the tacrine trials. Dementia Trialists' Collaboration. *JAMA,* 280**,** 1777-82.

QUASTEL, J. H. & WHEATLEY, A. H. 1932. The relation of thiol compounds to glucose fermentation. *Biochem J,* 26**,** 2169-76.

RABINKOV, A., MIRON, T., KONSTANTINOVSKI, L., WILCHEK, M., MIRELMAN, D. & WEINER, L. 1998. The mode of action of allicin: trapping of radicals and interaction with thiol containing proteins. *Biochim Biophys Acta,* 1379**,** 233-44.

RABINKOV, A., MIRON, T., MIRELMAN, D., WILCHEK, M., GLOZMAN, S., YAVIN, E. & WEINER, L. 2000. S-Allylmercaptoglutathione: the reaction product of allicin with glutathione possesses SH-modifying and antioxidant properties. *Biochim Biophys Acta,* 1499**,** 144-153.

RAFALSKI, J. A. & FALCO, S. C. 1988. Structure of the yeast HOM3 gene which encodes aspartokinase. *J Biol Chem,* 263**,** 2146-51.

RAGHUNANDANA RAO, R., SRINIVASA RAO, S. & VENKATARAMAN, P. R. 1946. Investigations on plant antibiotics; studies on allicin, the antibacterial principle of Allium sativum (garlic). *J Sci Ind Res (1942),* 5**,** 31-5.

RAVINDRANATH, S. D. & FRIDOVICH, I. 1975. Isolation and characterization of a manganese-containing superoxide dismutase from yeast. *J Biol Chem,* 250**,** 6107-12.

RAVIOL, H., SADLISH, H., RODRIGUEZ, F., MAYER, M. P. & BUKAU, B. 2006. Chaperone network in the yeast cytosol: Hsp110 is revealed as an Hsp70 nucleotide exchange factor. *EMBO J,* 25**,** 2510-8.

REIDY, M. & MASISON, D. C. 2010. Sti1 regulation of Hsp70 and Hsp90 is critical for curing of Saccharomyces cerevisiae [PSI+] prions by Hsp104. *Mol Cell Biol,* 30**,** 3542-52.

REIS, S. D., PANG, Y., VISHNU, N., VOISSET, C., GALONS, H., BLONDEL, M. & SANYAL, S. 2011. Mode of action of the antiprion drugs 6AP and GA on ribosome assisted protein folding. *Biochimie,* 93**,** 1047-54.

RICHARD, J. L., DEBEY, M. C., CHERMETTE, R., PIER, A. C., HASEGAWA, A., LUND, A., BRATBERG, A. M., PADHYE, A. A. & CONNOLE, M. D. 1994. Advances in veterinary mycology. *J Med Vet Mycol,* 32 Suppl 1**,** 169-87.

RIGHTSEL, W. A., SCHNEIDER, H. G., SLOAN, B. J., GRAF, P. R., MILLER, F. A., BARTZ, O. R., EHRLICH, J. & DIXON, G. J. 1964. Antiviral activity of gliotoxin and gliotoxin acetate. *Nature,* 204**,** 1333-4.

ROBERTS, G. W., LOFTHOUSE, R., ALLSOP, D., LANDON, M., KIDD, M., PRUSINER, S. B. & CROW, T. J. 1988. CNS amyloid proteins in neurodegenerative diseases. *Neurology,* 38**,** 1534-40.

RODRIGUEZ, P. L. & CARRASCO, L. 1992. Gliotoxin: inhibitor of poliovirus RNA synthesis that blocks the viral RNA polymerase 3Dpol. *J Virol,* 66**,** 1971-6.

RODRÍGUEZ-ARRONDO, F., IRIBARREN, J. A., ARRIZABALAGA, J., GROCIN, A. I., VON WICHMANN, M. A. & GARDE, C. 1991. [Invasive aspergillosis in patients infected by the human immunodeficiency virus]. *Enferm Infecc Microbiol Clin,* 9**,** 477-83.

RODRÍGUEZ-MANZANEQUE, M. T., ROS, J., CABISCOL, E., SORRIBAS, A. & HERRERO, E. 1999. Grx5 glutaredoxin plays a central role in protection against protein oxidative damage in Saccharomyces cerevisiae. *Mol Cell Biol,* 19**,** 8180-90.

ROGOZA, T., GOGINASHVILI, A., RODIONOVA, S., IVANOV, M., VIKTOROVSKAYA, O., RUBEL, A., VOLKOV, K. & MIRONOVA, L. 2010. Non-Mendelian determinant [ISP+] in yeast is a nuclear-residing prion form of the global transcriptional regulator Sfp1. *Proc Natl Acad Sci U S A,* 107**,** 10573-7.

ROOS, D., WEENING, R. S., WYSS, S. R. & AEBI, H. E. 1980. Protection of human neutrophils by endogenous catalase: studies with cells from catalase-deficient individuals. *J Clin Invest,* 65**,** 1515-22.

ROSE, M. D., MISRA, L. M. & VOGEL, J. P. 1989. KAR2, a karyogamy gene, is the yeast homolog of the mammalian BiP/GRP78 gene. *Cell,* 57**,** 1211-21.

RUOPPOLO, M., LUNDSTRÖM-LJUNG, J., TALAMO, F., PUCCI, P. & MARINO, G. 1997. Effect of glutaredoxin and protein disulfide isomerase on the glutathione-dependent folding of ribonuclease A. *Biochemistry,* 36**,** 12259-67.

SANCHEZ, Y. & LINDQUIST, S. L. 1990. HSP104 required for induced thermotolerance. *Science,* 248**,** 1112-5.

SANTOSO, A., CHIEN, P., OSHEROVICH, L. Z. & WEISSMAN, J. S. 2000. Molecular basis of a yeast prion species barrier. *Cell,* 100**,** 277-88.

SCHARF, D. H., REMME, N., HEINEKAMP, T., HORTSCHANSKY, P., BRAKHAGE, A. A. & HERTWECK, C. 2010. Transannular disulfide formation in gliotoxin biosynthesis and its role in self-resistance of the human pathogen Aspergillus fumigatus. *J Am Chem Soc,* 132**,** 10136-41.

SCHILKE, B., FORSTER, J., DAVIS, J., JAMES, P., WALTER, W., LALORAYA, S., JOHNSON, J., MIAO, B. & CRAIG, E. 1996. The cold sensitivity of a mutant of Saccharomyces cerevisiae lacking a mitochondrial heat shock protein 70 is suppressed by loss of mitochondrial DNA. *J Cell Biol,* 134**,** 603-13.

SCHIRMAIER, F. & PHILIPPSEN, P. 1984. Identification of two genes coding for the translation elongation factor EF-1 alpha of S. cerevisiae. *EMBO J,* 3**,** 3311-5.

SCHMID, D., BAICI, A., GEHRING, H. & CHRISTEN, P. 1994. Kinetics of molecular chaperone action. *Science,* 263**,** 971-3.

SCHMITT, H. D. & ZIMMERMANN, F. K. 1982. Genetic analysis of the pyruvate decarboxylase reaction in yeast glycolysis. *J Bacteriol,* 151**,** 1146-52.

SCHMITT-ULMS, G., LEGNAME, G., BALDWIN, M. A., BALL, H. L., BRADON, N., BOSQUE, P. J., CROSSIN, K. L., EDELMAN, G. M., DEARMOND, S. J., COHEN, F. E. & PRUSINER, S. B. 2001. Binding of neural cell adhesion molecules (N-CAMs) to the cellular prion protein. *J Mol Biol,* 314**,** 1209-25.

SCHNELL, N., KREMS, B. & ENTIAN, K. D. 1992. The PAR1 (YAP1/SNQ3) gene of Saccharomyces cerevisiae, a c-jun homologue, is involved in oxygen metabolism. *Curr Genet,* 21**,** 269-73.

SCHRETTL, M., CARBERRY, S., KAVANAGH, K., HAAS, H., JONES, G., O'BRIEN, J., NOLAN, A., STEPHENS, J., FENELON, O. & DOYLE, S. 2010. Self-protection against gliotoxin--a component of the gliotoxin biosynthetic cluster, GliT, completely protects Aspergillus fumigatus against exogenous gliotoxin. *PLoS Pathog,* 6**,** e1000952.

SCHRIEK, U. & SCHWENN, J. D. 1986. Properties of the purified APS-kinase from Escherichia coli and Saccharomyces cerevisiae. *Arch Microbiol,* 145**,** 32-8.

SCHULZ, J. B., LINDENAU, J., SEYFRIED, J. & DICHGANS, J. 2000. Glutathione, oxidative stress and neurodegeneration. *Eur J Biochem,* 267**,** 4904-11.

SCHÄFER, T., STRAUSS, D., PETFALSKI, E., TOLLERVEY, D. & HURT, E. 2003. The path from nucleolar 90S to cytoplasmic 40S pre-ribosomes. *EMBO J,* 22**,** 1370-80.

SCHÜLLER, C., BREWSTER, J. L., ALEXANDER, M. R., GUSTIN, M. C. & RUIS, H. 1994. The HOG pathway controls osmotic regulation of transcription via the stress response element (STRE) of the Saccharomyces cerevisiae CTT1 gene. *EMBO J,* 13**,** 4382-9.

SEAH, T. C., BHATTI, A. R. & KAPLAN, J. G. 1973. Novel catalatic proteins of bakers' yeast. I. An atypical catalase. *Can J Biochem,* 51**,** 1551-5.

SEIDLER, M. J., SALVENMOSER, S. & MÜLLER, F. M. 2008. Aspergillus fumigatus forms biofilms with reduced antifungal drug susceptibility on bronchial epithelial cells. *Antimicrob Agents Chemother,* 52**,** 4130-6.

SEISER, R. M., SUNDBERG, A. E., WOLLAM, B. J., ZOBEL-THROPP, P., BALDWIN, K., SPECTOR, M. D. & LYCAN, D. E. 2006. Ltv1 is required for efficient nuclear export of the ribosomal small subunit in Saccharomyces cerevisiae. *Genetics,* 174**,** 679-91.

SETYA, A., MURILLO, M. & LEUSTEK, T. 1996. Sulfate reduction in higher plants: molecular evidence for a novel 5'-adenylylsulfate reductase. *Proc Natl Acad Sci U S A,* 93**,** 13383-8.

SHAH, D. T. & LARSEN, B. 1991. Clinical isolates of yeast produce a gliotoxin-like substance. *Mycopathologia,* 116**,** 203-8.

SHAULIAN, E. & KARIN, M. 2001. AP-1 in cell proliferation and survival. *Oncogene,* 20**,** 2390-400.

SHELTON, M. D., CHOCK, P. B. & MIEYAL, J. J. 2005. Glutaredoxin: role in reversible protein s-glutathionylation and regulation of redox signal transduction and protein translocation. *Antioxid Redox Signal,* 7**,** 348-66.

SIES, H. & DE GROOT, H. 1992. Role of reactive oxygen species in cell toxicity. *Toxicol Lett,* 64-65 Spec No**,** 547-51.

SKONECZNA, A., MICIAŁKIEWICZ, A. & SKONECZNY, M. 2007. Saccharomyces cerevisiae Hsp31p, a stress response protein conferring protection against reactive oxygen species. *Free Radic Biol Med,* 42**,** 1409-20.

SKONECZNY, M., CHEŁSTOWSKA, A. & RYTKA, J. 1988. Study of the coinduction by fatty acids of catalase A and acyl-CoA oxidase in standard and mutant Saccharomyces cerevisiae strains. *Eur J Biochem,* 174**,** 297-302.

SLUMP, P. & SCHREUDER, H. A. 1973. Oxidation of methionine and cystine in foods treated with hydrogen peroxide. *J Sci Food Agric,* 24**,** 657-61.

SONG, J. J., RHEE, J. G., SUNTHARALINGAM, M., WALSH, S. A., SPITZ, D. R. & LEE, Y. J. 2002. Role of glutaredoxin in metabolic oxidative stress. Glutaredoxin as a sensor of oxidative stress mediated by H2O2. *J Biol Chem,* 277**,** 46566-75.

SONG, Y., WU, Y., JUNG, G., TUTAR, Y., EISENBERG, E., GREENE, L. & MASISON, D. 2005. Role for Hsp70 chaperone in Saccharomyces cerevisiae prion seed replication. *Eukaryot Cell,* 4**,** 289-97.

SOUBANI, A. O. & CHANDRASEKAR, P. H. 2002. The clinical spectrum of pulmonary aspergillosis. *Chest,* 121**,** 1988-99.

SPEVAK, W., FESSL, F., RYTKA, J., TRACZYK, A., SKONECZNY, M. & RUIS, H. 1983. Isolation of the catalase T structural gene of Saccharomyces cerevisiae by functional complementation. *Mol Cell Biol,* 3**,** 1545-51.

SPEVAK, W., HARTIG, A., MEINDL, P. & RUIS, H. 1986. Heme control region of the catalase T gene of the yeast Saccharomyces cerevisiae. *Mol Gen Genet,* 203**,** 73-8.

SPIELBERG, S. P., BOXER, L. A., OLIVER, J. M., ALLEN, J. M. & SCHULMAN, J. D. 1979. Oxidative damage to neutrophils in glutathione synthetase deficiency. *Br J Haematol,* 42**,** 215-23.

STADTMAN, E. R. 1990. Metal ion-catalyzed oxidation of proteins: biochemical mechanism and biological consequences. *Free Radic Biol Med,* 9**,** 315-25.

STAHL, N., BORCHELT, D. R., HSIAO, K. & PRUSINER, S. B. 1987. Scrapie prion protein contains a phosphatidylinositol glycolipid. *Cell,* 51**,** 229-40.

STANZANI, M., ORCIUOLO, E., LEWIS, R., KONTOYIANNIS, D. P., MARTINS, S. L., ST JOHN, L. S. & KOMANDURI, K. V. 2005. Aspergillus fumigatus suppresses the human cellular immune response via gliotoxin-mediated apoptosis of monocytes. *Blood,* 105**,** 2258-65.

STEPHEN, D. W. & JAMIESON, D. J. 1996. Glutathione is an important antioxidant molecule in the yeast Saccharomyces cerevisiae. *FEMS Microbiol Lett,* 141**,** 207-12.

SUHADOLNIK, R. J. & CHENOWITH, R. G. 1958. Biosynthesis of gliotoxin. I. Incorporation of phenylalanine-1- and -2-C14. *J. Am. Chem. Soc.,* 80**,** 4391-4392.

SULIMAN, H. S., SAWYER, G. M., APPLING, D. R. & ROBERTUS, J. D. 2005. Purification and properties of cobalamin-independent methionine synthase from

Candida albicans and Saccharomyces cerevisiae. *Arch Biochem Biophys,* 441**,** 56-63.

SUMMERS, W. K. 2006. Tacrine, and Alzheimer's treatments. *J Alzheimers Dis,* 9**,** 439-45.

SUMMERS, W. K., MAJOVSKI, L. V., MARSH, G. M., TACHIKI, K. & KLING, A. 1986. Oral tetrahydroaminoacridine in long-term treatment of senile dementia, Alzheimer type. *N Engl J Med,* 315**,** 1241-5.

SUMMERS, W. K., VIESSELMAN, J. O., MARSH, G. M. & CANDELORA, K. 1981. Use of THA in treatment of Alzheimer-like dementia: pilot study in twelve patients. *Biol Psychiatry,* 16**,** 145-53.

SUSANI, M., ZIMNIAK, P., FESSL, F. & RUIS, H. 1976. Localization of catalase A in vacuoles of Saccharomyces cerevisiae: evidence for the vacuolar nature of isolated "yeast peroxisomes". *Hoppe Seylers Z Physiol Chem,* 357**,** 961-70.

SWEENEY, M. J. & DOBSON, A. D. 1998. Mycotoxin production by Aspergillus, Fusarium and Penicillium species. *Int J Food Microbiol,* 43**,** 141-58.

SÖDERBERG, B. O., SJÖBERG, B. M., SONNERSTAM, U. & BRÄNDÉN, C. I. 1978. Three-dimensional structure of thioredoxin induced by bacteriophage T4. *Proc Natl Acad Sci U S A,* 75**,** 5827-30.

TAMAI, K. T., GRALLA, E. B., ELLERBY, L. M., VALENTINE, J. S. & THIELE, D. J. 1993. Yeast and mammalian metallothioneins functionally substitute for yeast copper-zinc superoxide dismutase. *Proc Natl Acad Sci U S A,* 90**,** 8013-7.

TER-AVANESYAN, M. D., DAGKESAMANSKAYA, A. R., KUSHNIROV, V. V. & SMIRNOV, V. N. 1994. The SUP35 omnipotent suppressor gene is involved in the maintenance of the non-Mendelian determinant [psi+] in the yeast Saccharomyces cerevisiae. *Genetics,* 137**,** 671-6.

THAUER, R. K., JUNGERMANN, K. & DECKER, K. 1977. Energy conservation in chemotrophic anaerobic bacteria. *Bacteriol Rev,* 41**,** 100-80.

THOMAS, D., BARBEY, R., HENRY, D. & SURDIN-KERJAN, Y. 1992a. Physiological analysis of mutants of Saccharomyces cerevisiae impaired in sulphate assimilation. *J Gen Microbiol,* 138**,** 2021-8.

THOMAS, D., BARBEY, R. & SURDIN-KERJAN, Y. 1990. Gene-enzyme relationship in the sulfate assimilation pathway of Saccharomyces cerevisiae. Study of the 3'-phosphoadenylylsulfate reductase structural gene. *J Biol Chem,* 265**,** 15518-24.

THOMAS, D., CHEREST, H. & SURDIN-KERJAN, Y. 1991. Identification of the structural gene for glucose-6-phosphate dehydrogenase in yeast. Inactivation leads to a nutritional requirement for organic sulfur. *EMBO J,* 10**,** 547-53.

THOMAS, D., JACQUEMIN, I. & SURDIN-KERJAN, Y. 1992b. MET4, a leucine zipper protein, and centromere-binding factor 1 are both required for transcriptional activation of sulfur metabolism in Saccharomyces cerevisiae. *Mol Cell Biol,* 12**,** 1719-27.

THOMAS, D., KURAS, L., BARBEY, R., CHEREST, H., BLAISEAU, P. L. & SURDIN-KERJAN, Y. 1995. Met30p, a yeast transcriptional inhibitor that responds to S-adenosylmethionine, is an essential protein with WD40 repeats. *Mol Cell Biol,* 15**,** 6526-34.

THOMAS, D. & SURDIN-KERJAN, Y. 1989. Structure of the HOM2 gene of Saccharomyces cerevisiae and regulation of its expression. *Mol Gen Genet,* 217**,** 149-54.

THOMAS, D. & SURDIN-KERJAN, Y. 1991. The synthesis of the two S-adenosyl-methionine synthetases is differently regulated in Saccharomyces cerevisiae. *Mol Gen Genet,* 226**,** 224-32.

THOMAS, D. & SURDIN-KERJAN, Y. 1997. Metabolism of sulfur amino acids in Saccharomyces cerevisiae. *Microbiol Mol Biol Rev,* 61**,** 503-32.

TIBBETTS, A. S. & APPLING, D. R. 2000. Characterization of two 5-aminoimidazole-4-carboxamide ribonucleotide transformylase/inosine monophosphate cyclohydrolase isozymes from Saccharomyces cerevisiae. *J Biol Chem,* 275**,** 20920-7.

TOMLINSON, J. R. & SAHN, S. A. 1987. Aspergilloma in sarcoid and tuberculosis. *Chest,* 92**,** 505-8.

TREVITT, C. R. & COLLINGE, J. 2006. A systematic review of prion therapeutics in experimental models. *Brain,* 129**,** 2241-65.

TRIBOUILLARD-TANVIER, D., BÉRINGUE, V., DESBAN, N., GUG, F., BACH, S., VOISSET, C., GALONS, H., LAUDE, H., VILETTE, D. & BLONDEL, M. 2008a. Antihypertensive drug guanabenz is active in vivo against both yeast and mammalian prions. *PLoS One,* 3**,** e1981.

TRIBOUILLARD-TANVIER, D., DOS REIS, S., GUG, F., VOISSET, C., BÉRINGUE, V., SABATE, R., KIKOVSKA, E., TALAREK, N., BACH, S., HUANG, C., DESBAN, N., SAUPE, S., SUPATTAPONE, S., THURET, J., CHÉDIN, S., VILETTE, D., GALONS, H., SANYAL, S. & BLONDEL, M. 2008b. Protein folding activity of ribosomal RNA is a selective target of two unrelated antiprion drugs. *PLoS One,* 3**,** e2174.

TRINGE, S. G., WILLIS, J., LIBERATORE, K. L. & RUBY, S. W. 2006. The WTM genes in budding yeast amplify expression of the stress-inducible gene RNR3. *Genetics,* 174**,** 1215-28.

TROTTER, E. W. & GRANT, C. M. 2002. Thioredoxins are required for protection against a reductive stress in the yeast Saccharomyces cerevisiae. *Mol Microbiol,* 46**,** 869-78.

TROWN, P. W. & BILELLO, J. A. 1972. Mechanism of action of gliotoxin: elimination of activity by sulfhydryl compounds. *Antimicrob Agents Chemother,* 2**,** 261-6.

TRULL, A. K., PARKER, J. & WARREN, R. E. 1985. IgG enzyme linked immunosorbent assay for diagnosis of invasive aspergillosis: retrospective study over 15 years of transplant recipients. *J Clin Pathol,* 38**,** 1045-51.

TSUNAWAKI, S., YOSHIDA, L. S., NISHIDA, S., KOBAYASHI, T. & SHIMOYAMA, T. 2004. Fungal metabolite gliotoxin inhibits assembly of the human respiratory burst NADPH oxidase. *Infect Immun,* 72**,** 3373-82.

TUITE, M. F., COX, B. S. & MCLAUGHLIN, C. S. 1987. A ribosome-associated inhibitor of in vitro nonsense suppression in [psi-] strains of yeast. *FEBS Lett,* 225**,** 205-8.

TUITE, M. F., MUNDY, C. R. & COX, B. S. 1981. Agents that cause a high frequency of genetic change from [psi+] to [psi-] in Saccharomyces cerevisiae. *Genetics,* 98**,** 691-711.

VALKO, M., MORRIS, H. & CRONIN, M. T. 2005. Metals, toxicity and oxidative stress. *Curr Med Chem,* 12**,** 1161-208.

VAN LOON, A. P., PESOLD-HURT, B. & SCHATZ, G. 1986. A yeast mutant lacking mitochondrial manganese-superoxide dismutase is hypersensitive to oxygen. *Proc Natl Acad Sci U S A,* 83**,** 3820-4.

VEENHUIS, M., MATEBLOWSKI, M., KUNAU, W. H. & HARDER, W. 1987. Proliferation of microbodies in Saccharomyces cerevisiae. *Yeast,* 3**,** 77-84.

WAKSMAN, S. A. & GEIGER, W. B. 1944. The Nature of the Antibiotic Substances Produced by Aspergillus fumigatus. *J Bacteriol,* 47**,** 391-7.

WALSH, P., BURSAĆ, D., LAW, Y. C., CYR, D. & LITHGOW, T. 2004. The J-protein family: modulating protein assembly, disassembly and translocation. *EMBO Rep,* 5**,** 567-71.

WARING, P. 1990. DNA fragmentation induced in macrophages by gliotoxin does not require protein synthesis and is preceded by raised inositol triphosphate levels. *J Biol Chem,* 265**,** 14476-80.

WARING, P. & BEAVER, J. 1996. Gliotoxin and related epipolythiodioxopiperazines. *Gen Pharmacol,* 27**,** 1311-6.

WARING, P., EICHNER, R. D., MÜLLBACHER, A. & SJAARDA, A. 1988. Gliotoxin induces apoptosis in macrophages unrelated to its antiphagocytic properties. *J Biol Chem,* 263**,** 18493-9.

WARING, P., SJAARDA, A. & LIN, Q. H. 1995. Gliotoxin inactivates alcohol dehydrogenase by either covalent modification or free radical damage mediated by redox cycling. *Biochem Pharmacol,* 49**,** 1195-201.

WATKINS, P. B., ZIMMERMAN, H. J., KNAPP, M. J., GRACON, S. I. & LEWIS, K. W. 1994. Hepatotoxic effects of tacrine administration in patients with Alzheimer's disease. *JAMA,* 271**,** 992-8.

WEGELE, H., HASLBECK, M., REINSTEIN, J. & BUCHNER, J. 2003. Sti1 is a novel activator of the Ssa proteins. *J Biol Chem,* 278**,** 25970-6.

WEGELE, H., MÜLLER, L. & BUCHNER, J. 2004. Hsp70 and Hsp90--a relay team for protein folding. *Rev Physiol Biochem Pharmacol,* 151**,** 1-44.

WEGRZYN, R. D., BAPAT, K., NEWNAM, G. P., ZINK, A. D. & CHERNOFF, Y. O. 2001. Mechanism of prion loss after Hsp104 inactivation in yeast. *Mol Cell Biol,* 21**,** 4656-69.

WEI, M., FABRIZIO, P., MADIA, F., HU, J., GE, H., LI, L. M. & LONGO, V. D. 2009. Tor1/Sch9-regulated carbon source substitution is as effective as calorie restriction in life span extension. *PLoS Genet,* 5**,** e1000467.

WEILAND, D., FERGUSON, R. M., PETERSON, P. K., SNOVER, D. C., SIMMONS, R. L. & NAJARIAN, J. S. 1983. Aspergillosis in 25 renal transplant patients. Epidemiology, clinical presentation, diagnosis, and management. *Ann Surg,* 198**,** 622-9.

WEINDLING, R. & EMERSON, O. H. 1936. The isolation of a toxic substance from the culture filtrate of *Trichoderma*. *Phytopathology,* 26**,** 1068-1070.

WEINSTOCK, M. 1995. The pharmacotherapy of Alzheimer's disease based on the cholinergic hypothesis: an update. *Neurodegeneration,* 4**,** 349-56.

WERNER-WASHBURNE, M., BECKER, J., KOSIC-SMITHERS, J. & CRAIG, E. A. 1989. Yeast Hsp70 RNA levels vary in response to the physiological status of the cell. *J Bacteriol,* 171**,** 2680-8.

WERNER-WASHBURNE, M., STONE, D. E. & CRAIG, E. A. 1987. Complex interactions among members of an essential subfamily of hsp70 genes in Saccharomyces cerevisiae. *Mol Cell Biol,* 7**,** 2568-77.

WEST, G. M., TUCKER, C. L., XU, T., PARK, S. K., HAN, X., YATES, J. R. & FITZGERALD, M. C. 2010. Quantitative proteomics approach for identifying protein-drug interactions in complex mixtures using protein stability measurements. *Proc Natl Acad Sci U S A,* 107**,** 9078-82.

WICKNER, R. B. 1994. [URE3] as an altered URE2 protein: evidence for a prion analog in Saccharomyces cerevisiae. *Science,* 264**,** 566-9.

WICKNER, R. B. 1997. A new prion controls fungal cell fusion incompatibility. *Proc Natl Acad Sci U S A,* 94**,** 10012-4.

WILCOCK, G. K., ASHWORTH, D. L., LANGFIELD, J. A. & SMITH, P. M. 1994. Detecting patients with Alzheimer's disease suitable for drug treatment: comparison of three methods of assessment. *Br J Gen Pract,* 44**,** 30-3.

WILLIAMS, E. S. & YOUNG, S. 1980. Chronic wasting disease of captive mule deer: a spongiform encephalopathy. *J Wildl Dis,* 16**,** 89-98.

WILLIAMSON, J. M., BOETTCHER, B. & MEISTER, A. 1982. Intracellular cysteine delivery system that protects against toxicity by promoting glutathione synthesis. *Proc Natl Acad Sci U S A,* 79**,** 6246-9.

WINGE, D. R., NIELSON, K. B., GRAY, W. R. & HAMER, D. H. 1985. Yeast metallothionein. Sequence and metal-binding properties. *J Biol Chem,* 260**,** 14464-70.

WINSTEAD, J. A. & SUHADOLNIK, R. J. 1960. Biosynthesis of gliotoxin. II. Further studies on the incorporation of carbon-14 and tritium-labeled precursors. *J. Am. Chem. Soc.,* 82**,** 1644-1647.

WITTUNG-STAFSHEDE, P., GUIDRY, J., HORNE, B. E. & LANDRY, S. J. 2003. The J-domain of Hsp40 couples ATP hydrolysis to substrate capture in Hsp70. *Biochemistry,* 42**,** 4937-44.

WU, A. L. & MOYE-ROWLEY, W. S. 1994. GSH1, which encodes gamma-glutamylcysteine synthetase, is a target gene for yAP-1 transcriptional regulation. *Mol Cell Biol,* 14**,** 5832-9.

WU, Y., GREENE, L., MASISON, D. & EISENBERG, E. 2005. Curing of yeast [PSI+] prion by guanidine inactivation of Hsp104 does not require cell division. *Proc Natl Acad Sci U S A,* 102**,** 12789-94.

YAMAGATA, S., TAKESHIMA, K. & NAIKI, N. 1975. O-acetylserine and O-acetylhomoserine sulfhydrylase of yeast; studies with methionine auxotrophs. *J Biochem,* 77**,** 1029-36.

YON, J., GIALLONGO, A. & FRIED, M. 1991. The organization and expression of the Saccharomyces cerevisiae L4 ribosomal protein genes and their identification as the homologues of the mammalian ribosomal protein gene L7a. *Mol Gen Genet,* 227**,** 72-80.

YOSHIDA, L. S., ABE, S. & TSUNAWAKI, S. 2000. Fungal gliotoxin targets the onset of superoxide-generating NADPH oxidase of human neutrophils. *Biochem Biophys Res Commun,* 268**,** 716-23.

YOSHITAKE, S., NANRI, H., FERNANDO, M. R. & MINAKAMI, S. 1994. Possible differences in the regenerative roles played by thioltransferase and thioredoxin for oxidatively damaged proteins. *J Biochem,* 116**,** 42-6.

YOST, F. J. & FRIDOVICH, I. 1973. An iron-containing superoxide dismutase from Escherichia coli. *J Biol Chem,* 248**,** 4905-8.

YOUN, H. D., KIM, E. J., ROE, J. H., HAH, Y. C. & KANG, S. O. 1996. A novel nickel-containing superoxide dismutase from Streptomyces spp. *Biochem J,* 318 (Pt 3)**,** 889-96.

YU, L., GUO, N., MENG, R., LIU, B., TANG, X., JIN, J., CUI, Y. & DENG, X. 2010. Allicin-induced global gene expression profile of Saccharomyces cerevisiae. *Appl Microbiol Biotechnol,* 88**,** 219-29.

YUMOTO, N., KAWATA, Y., NODA, S. & TOKUSHIGE, M. 1991. Rapid purification and characterization of homoserine dehydrogenase from Saccharomyces cerevisiae. *Arch Biochem Biophys,* 285**,** 270-5.

ZELENAYA-TROITSKAYA, O., PERLMAN, P. S. & BUTOW, R. A. 1995. An enzyme in yeast mitochondria that catalyzes a step in branched-chain amino acid biosynthesis also functions in mitochondrial DNA stability. *EMBO J,* 14**,** 3268-76.

ZELLER, C. E., PARNELL, S. C. & DOHLMAN, H. G. 2007. The RACK1 ortholog Asc1 functions as a G-protein beta subunit coupled to glucose responsiveness in yeast. *J Biol Chem,* 282**,** 25168-76.

ZHANG, M., EDDY, C., DEANDA, K., FINKELSTEIN, M. & PICATAGGIO, S. 1995. Metabolic Engineering of a Pentose Metabolism Pathway in Ethanologenic Zymomonas mobilis. *Science,* 267**,** 240-3.

ZHOU, X., ZHAO, A., GOPING, G. & HIRSZEL, P. 2000. Gliotoxin-induced cytotoxicity proceeds via apoptosis and is mediated by caspases and reactive oxygen species in LLC-PK1 cells. *Toxicol Sci,* 54**,** 194-202.

ZHOURAVLEVA, G., FROLOVA, L., LE GOFF, X., LE GUELLEC, R., INGE-VECHTOMOV, S., KISSELEV, L. & PHILIPPE, M. 1995. Termination of translation in eukaryotes is governed by two interacting polypeptide chain release factors, eRF1 and eRF3. *EMBO J,* 14**,** 4065-72.

ZHU, X., ZHAO, X., BURKHOLDER, W. F., GRAGEROV, A., OGATA, C. M., GOTTESMAN, M. E. & HENDRICKSON, W. A. 1996. Structural analysis of substrate binding by the molecular chaperone DnaK. *Science,* 272**,** 1606-14.